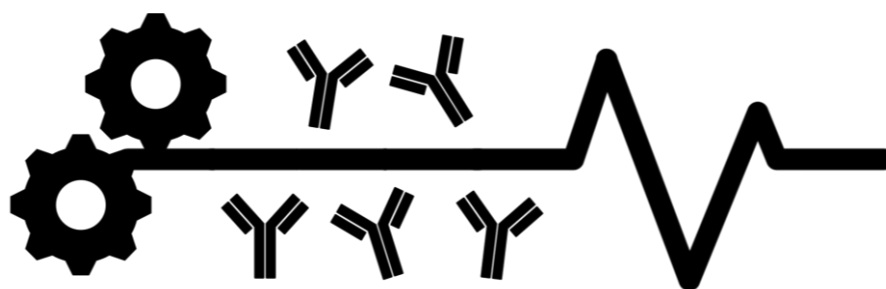Emanuel Augusto
Vieira Capela

Plataformas inovadoras e sustentáveis para o processamento a jusante de biofármacos baseados em anticorpos

Innovative and sustainable platforms for the downstream processing of antibody-based biopharmaceuticals

Emanuel Augusto Vieira Capela

Plataformas inovadoras e sustentáveis para o processamento a jusante de biofármacos baseados em anticorpos

Innovative and sustainable platforms for the downstream processing of antibody-based biopharmaceuticals

Tese apresentada à Universidade de Aveiro para cumprimento dos requisitos necessários à obtenção do grau de Doutor em Engenharia Química, realizada sob a orientação científica da Doutora Mara Guadalupe Freire Martins, Investigadora Coordenadora no Departamento de Química, CICECO, da Universidade de Aveiro, e coorientação do Professor Doutor João Manuel da Costa e Araújo Pereira Coutinho, Professor Catedrático no Departamento de Química, CICECO, da Universidade de Aveiro, e da Professora Doutora Ana Margarida Nunes da Mata Pires de Azevedo, Professora Auxiliar no Departamento de Bioengenharia, Instituto de Bioengenharia e Biociências, do Instituto Superior Técnico da Universidade de Lisboa.

"Sê todo em cada coisa. Põe quanto és
No mínimo que fazes."
- Ricardo Reis

o júri

presidente

Prof. Dr. Óscar Emanuel Chaves Mealha
Professor Catedrático no Departamento de Comunicação e Arte da Universidade de Aveiro

Prof. Dra. Isabel Maria Delgado Jana Marrucho Ferreira
Professora Catedrática no Departamento de Engenharia Química do Instituto Superior Técnico da Universidade de Lisboa

Prof. Dr. João Manuel da Costa e Araújo Pereira Coutinho
Professor Catedrático no Departamento de Química da Universidade de Aveiro

Prof. Dra. Fani Pereira de Sousa
Professora Associada no Departamento de Ciências Médicas da Universidade da Beira Interior

Prof. Dr. Jorge Fernando Brandão Pereira
Professor Auxiliar no Departamento de Engenharia Química da Universidade de Coimbra

Dra. Ana Mafalda Rodrigues Almeida Rocha
Investigadora Doutorada no Departamento de Química da Universidade de Aveiro

palavras-chave

Biofármacos, anticorpos, imunoglobulina G, soro humano, sobrenadantes de culturas celulares, processamento a jusante, líquidos iónicos, extração, purificação, sistemas aquosos bifásicos, partição trifásica, líquidos iónicos suportados.

resumo

Os anticorpos, e em particular a imunoglobulina G (IgG), são considerados uma das pontas de lança da indústria biofarmacêutica, apresentando elevada relevância para o tratamento de várias doenças e sendo, por vezes, a única terapia disponível para algumas patologias. Apesar do seu amplo potencial, a extração e purificação destas biomoléculas a partir dos seus meios biológicos complexos com elevada qualidade e pureza é ainda baseada em abordagens com várias etapas e com elevado custo associado. Portanto, o desenvolvimento de processos a jusante alternativos, económicos e eficientes, capazes de fornecer elevadas quantidades de anticorpos terapêuticos a um custo reduzido é altamente necessário. Novas estratégias baseadas em líquidos iónicos (LIs) foram então investigadas nesta tese de Doutoramento para o processamento a jusante de anticorpos. Os LIs foram escolhidos principalmente devido ao seu carácter de solventes customizáveis. Esta característica dos LIs permite adequar a polaridade, interações e seletividade dos processos desenvolvidos, permitindo superar algumas limitações técnicas dos processos convencionais.

Três tipos de plataformas baseadas em LIs foram investigadas para o processamento a jusante de anticorpos, nomeadamente sistemas aquosos bifásicos (SAB), partição trifásica e líquidos iónicos suportados. SAB contendo LIs como adjuvantes foram investigados, permitindo a extração e purificação de anticorpos humanos (anticorpos policlonais e monoclonais) com um bom desempenho em uma única etapa. LIs mais biocompatíveis e sustentáveis foram também estudados como compostos formadores de fases de SAB, demonstrando em simultâneo a possibilidade de utilizar abordagens de partição trifásica baseadas em SAB para a purificação e recuperação de anticorpos humanos. Finalmente, foram propostas novas matrizes cromatográficas baseadas em líquidos iónicos suportados, capazes de capturar e/ou purificar anticorpos a partir dos seus meios biológicos complexos através de dois mecanismos distintos, nomeadamente através dos modos negativo e positivo.

Em suma, nesta tese de Doutoramento foi demonstrado que os LIs, se adequadamente concebidos, podem ser aplicados com sucesso na extração, purificação e/ou recuperação de anticorpos humanos, sendo plataformas alternativas promissoras para o processamento a jusante de biofármacos baseados em anticorpos.

keywords

abstract

Antibodies, and in particular immunoglobulin G (IgG), are considered as one of the spearheads of the biopharmaceutical industry, presenting high relevance for the treatment of several diseases and being sometimes the only available therapy for some pathologies. Despite their wide potential, the extraction and purification of these biomolecules from their complex biological media with high quality and purity is still based on multi-step approaches and is of high cost. Therefore, the development of alternative and cost-effective downstream processes able to provide high amounts of therapeutic antibodies at lower cost is highly demanded. Novel ionic-liquid-based (IL-based) strategies for the downstream processing of antibodies were investigated in this PhD thesis. ILs were chosen mainly due to their designer solvents character. This feature of ILs allows to tailor the polarity, interactions and selectivity of the developed processes, allowing to overcome some technical limitations of the conventional ones.

Three types of IL-based platforms for antibodies downstream processing were investigated, namely aqueous biphasic systems (ABS), three-phase partitioning (TPP) and supported ionic liquids (SILs). ABS containing ILs as adjuvants were investigated, allowing the extraction and purification of human antibodies (polyclonal and monoclonal antibodies) with good performance in a single-step. More biocompatible and sustainable ILs were also studied as phase-forming compounds of ABS, while showing the possibility of using TPP approaches based on ABS for the purification and recovery of human antibodies. Finally, new chromatographic matrices were proposed based on SILs materials, able to capture and/or purify antibodies from their complex biological media through two different mechanisms, namely through the flowthrough-like and bind-and-elute-like modes.

In summary, in this PhD thesis it is shown that ILs, if properly designed, can be successfully applied in the extraction, purification and/or recovery of human antibodies, being promising alternative platforms for the downstream processing of antibody-based biopharmaceuticals.

CONTENTS

List of tables

List of figures

Notation

List of symbols

%Aggregation	aggregation percentage
%EE	extraction efficiency
%Purity	percentage purity
%Yield	recovery yield
[IgG]	IgG concentration
A	area
Dp	mean pore diameter
K	partition coefficient
PF	purification factor
R^2	correlation coefficient
S:L ratio	solid:liquid ratio
t	contact time
V	volume
β	hydrogen-bond basicity
θ	ellipticity
λ	wavelength
S_{BET}	specific surface area (Brunauer-Emmett-Teller)
VR	volume ratio

List of abbreviations

$[Bu_3NC_4]Br$	tri(*n*-butyl)[4-ethoxy-4-oxobutyl]ammonium bromide
$[C_4\text{-}4mpy]Cl$	1-butyl-4-methylpyridinium chloride
$[C_4mim][CH_3CO_2]$	1-butyl-3-methylimidazolium acetate
$[C_4mim][HSO_4]$	1-butyl-3-methylimidazolium hydrogen sulphate
$[C_4mim]Br$	1-butyl-3-methylimidazolium bromide
$[C_4mim]Cl$	1-butyl-3-methylimidazolium chloride
$[Ch][Ac]$	cholinium acetate
$[Ch]Cl$	cholinium chloride
$[Et_3NC_4]Br$	triethyl[4-ethoxy-4-oxobutyl]ammonium bromide
$[MepyrNC_4]Br$	*N*-(1-methylpyrrolidyl-4-ethoxy-4-oxobutyl)ammonium bromide
$[N_{1111}]Cl$	tetramethylammonium chloride
$[N_{4444}]Br$	tetra(*n*-butyl)ammonium bromide
$[N_{4444}]Cl$	tetrabutylammonium chloride
$[P_{4444}]Br$	tetra(*n*-butyl)phosphonium bromide
$[P_{4444}]Cl$	tetra(*n*-butyl)phosphonium chloride
$[Pr_3NC_4]Br$	tri(*n*-propyl)[4-ethoxy-4-oxobutyl]ammonium bromide
$[Si][C_3]Cl$	3-chloropropylsilane
$[Si][C_3mim]Cl$	1-methyl-3-propylimidazolium-based supported silica with chloride
$[Si][N_{3444}]Cl$	propyltributylammonium-based supported silica with chloride
$[Si][N_{3888}]Cl$	propyltrioctylammonium-based supported silica with chloride
7TM	7-transmembrane
ABC	activated B-cell
ABS	aqueous biphasic system
ACE2	angiotensin-converting enzyme 2
ACR	American College of Rheumatology
AEX	anion exchange chromatography
AGB	glycine-betaine analogue
AGB-ILs	glycine-betaine analogues ionic liquids
ALL	acute lymphoblastic leukemia
AMD	age-related macular degeneration
AMTPS	aqueous micellar two-phase systems

anti-HCV	anti-hepatitis C virus
anti-IL-8	anti-interleukin-8
anti-TNF	anti-tumor necrosis factor
APS	ammonium persulfate
AQP4-IgG	aquaporin-4 IgG
ATPS	aqueous two-phase system
ATR-FTIR	attenuated total reflectance Fourier-transform infrared
BSA	bovine serum albumin
bsAbs	bispecific antibody
CAGR	compound annual growth rate
cAMP	cyclic adenosine monophosphate
CD	circular dichroism
CD31	cluster of differentiation 31
CDI	*Clostridium difficile* infection
CDR	complementary-determining region
CEX	cation exchange chromatography
CHO	Chinese Hamster Ovary
CLC	cardiotrophin-like cytokine
CLR	C-type lectin receptor
cMcAr	cadherin-mediated cell adhesion receptor
CNTF	ciliary neurotrophic factor
COG	cost of goods
COVID-19	coronavirus disease 2019
CoVs	Coronavirus
CPMAS	cross-polarization magic-angle spinning
CR	complete response
CT-1	cardiotropin-1
CXCL8	chemokine ligand 8
DAMP	damage associated molecular pattern
dextran 500k	dextran with a molecular weight of 500,000 $g \cdot mol^{-1}$
DF	diafiltration
DHFR	dihydrofolate reductase
DLBCL	diffuse large B-cell lymphoma

DMEM	Dulbecco's modified Eagle's medium
DoE	design of experiment
DOR	duration of response
DTT	dithiothreitol
EF	edema factor
ELISA	enzyme-linked immunosorbent assay
EMA	European Medicines Agency
EpCAM	epithelial cell-adhesion molecule
ER	endoplasmic reticulum
EU	European Union
Fab	antigen-binding fragment
FBS	fetal bovine serum
FDA	Food and Drug Administration
FT	flowthrough
GAPDH	glyceraldehyde-3-phosphate dehydrogenase
GDP	guanosine diphosphate
GPCR	G-protein-coupled receptor
GPLR	G protein-linked receptors
GS	glutamine synthase
GTP	guanosine triphosphate
H.C.	heavy chain
HAMA	human anti-mouse-antibodies
HAT	hypoxanthine, aminopterin and thymidine
HCIC	hydrophobic charge induction chromatography
HCP	host cell protein
HHV-8	human herpesvirus-8
HIC	hydrophobic interaction chromatography
HIV	human immunodeficiency virus
HMW	high molecular weight
HPS	hydroxypropyl starch
HPTFF	high performance tangential flow filtration
HSA	human serum albumin
ICAM-1	intercellular Adhesion Molecule-1

IDA	iminodiacetate
IEF	isoelectric focusing
IEX	ion exchange chromatography
Ig	immunoglobulin
IG	intramuscular immunoglobulin
IGF-1R	insulin-like growth factor-1 receptor
IgG	immunoglobulin G
IgMcAr	immunoglobulin superfamily-mediated cell adhesion receptor
IgY	immunoglobulin Y
IL	ionic liquid
IL-1	interleukin- 1
IL-6	interleukin- 6
IL-6R	interleukin- 6 receptor
IL-8	interleukin- 8
ILTPP	ionic liquid-based three-phase partitioning
IMAC	immobilized metal affinity chromatography
iMcAr	integrin-mediated cell adhesion receptor
IP10	induced protein 10
IP_3	inositol trisphosphate
IPCR	immuno-polymerase chain reaction
IPS-1	IFN-b-promoter stimulator 1
ITAM	immunoreceptor tyrosine-based activation motif
IVIG	intravenous immunoglobulin
L.C.	light chain
LF	lethal factor
LFA-1	lymphocyte function-associated antigen 1
LIF	leukemia inhibitory factor
LMW	low molecular weight
LYTAG-Z	choline binding polypeptide tag fused to antibody binding Z-domain
mAb	monoclonal antibody
Mac-1	macrophage-1 antigen
MAPK	mitogen-activated protein kinase
MCP-1	monocyte chemoattractant protein-1

MERS	Middle East respiratory syndrome
MMAE	monomethyl auristatin E
MMC	multimodal chromatography
MPO	myeloperoxidase
MSX	methionine sulphoximine
MuLV	Murine Leukemia Virus
MyD88	Myeloid differentiation primary response gene 88
N.A.	not applicable
NF-kB	nuclear factor-κB
NLR	nucleotide-binding and oligomerization domain-like receptor
NMOSD	neuromyelitis optica spectrum disorder
NMR	nuclear magnetic resonance
NOD	nucleotide-binding and oligomerization domain
NP	neuropoietin
NS5B	non-structural protein 5B
NTA	nitrilotriacetate
OSM	oncostatin M
PA	protective antigen
pAb	polyclonal antibody
PAMP	pathogen associated molecular pattern
PASI	Psoriasis Area and Severity Index
PBA	phenylboronic acid
PBS	phosphate buffered saline
PDMS	polydimethylsiloxane
PECAM-1	platelet endothelial cell adhesion molecule
PEG	polyethelyneglycol
PEG 1000	polyethylene glycol with a molecular weight of 1000 $g \cdot mol^{-1}$
PEG 1500	polyethylene glycol with a molecular weight of 1500 $g \cdot mol^{-1}$
PEG 2000	polyethylene glycol with a molecular weight of 2000 $g \cdot mol^{-1}$
PEG 3350	polyethylene glycol with a molecular weight of 3350 $g \cdot mol^{-1}$
PEG 600	polyethylene glycol with a molecular weight of 600 $g \cdot mol^{-1}$
PET-CT	Positron Emission Tomography – Computed Tomography
pI	isoelectric point

PIP$_2$	phosphatidylinositol 4,5-bisphosphate
PIP$_3$	phosphatidylinositol (3,4,5)-trisphosphate
PIPK	phosphatidylinositol 4-phosphate kinase
PPG	poly(propylene) glycol
proA	protein A
PRR	pattern recognition receptor
PZC	point zero charge
RA	rheumatoid arthritis
RIG	retinoic acid-inducible gene
RLR	retinoic acid-inducible gene-I-like receptor
RNS	reactive nitrogen species
ROS	reactive oxygen specie
RSV	respiratory syncytial virus
SARM	sterile-α and armadillo motif-containing protein
SARS	severe acute respiratory syndrome
scFv	single-chain antibody fragment
SDS	sodium dodecyl sulfate
SDS-PAGE	sodium dodecyl sulphate-polyacrylamide gel electrophoresis
SEC	size-exclusion chromatography
SE-HPLC	size-exclusion high-performance liquid chromatography
SEM	scanning electron microscopy
SIL	supported ionic liquid
sMcAr	selectin-mediated cell adhesion receptor
TED	tris(carboxymethyl)ethylenediamine
TEG-AG	triethylene glycol-diglutaric acid
TEMED	*N,N,N',N'*-tetramethylethylenediamine
TGF- β	transforming growth factor β
TIRAP	TIR domain-containing adaptor protein
TL	tie-line
TLL	tie-line length
TLR	toll-like receptor
TNF	tumor necrosis factor
tPA	tissue plasminogen activator

TPP	three-phase partitioning
TRAM	Trif-related adaptor molecule
TRIF	TIR-domain-containing adaptor inducing IFNβ
TSHR	thyroid-stimulating hormone receptor
UF	ultrafiltration
VCAM-1	vascular cell adhesion molecule-1

"nanos gigantum humeris insidentes"

General Introduction 1

1.1. Contextualization, scopes and objectives

All lives are important. However, there is a large range of diseases that negatively affect people's lives; unfortunately, not all therapies are currently accessible to everyone. Among these are biopharmaceuticals, which have gained significant relevance in recent years since they largely improved the treatment of many diseases, being sometimes the only approved therapies available for a particular disorder [1]. Antibodies are the largest class of biopharmaceuticals [2], currently dominating the biopharmaceuticals approvals and being the most lucrative single product class (representing more than 65 % of the total biopharmaceuticals global sales) [3]. Among these, there are polyclonal antibodies (pAbs) taken from mammal's serum and monoclonal antibodies (mAbs), the last ones covering the highest market share. mAbs were first discovered in 1975, and since then have proven to be relevant therapeutic agents in a myriad of diseases, with more than 90 mAbs approved by the US Food and Drug Administration (FDA) for the treatment of several diseases, such as cancer (breast cancer, leukemia and prostate cancer), auto-immune disorders, asthma, cardiovascular and infectious diseases [4]. Despite their advantages and therapeutic potential, the costs of producing/obtaining these therapeutics with high quality and purity level are still high due to the absence of simpler and cost-effective extraction/purification methods. The upstream processing of mAbs has gone through several improvements in recent years, by using alternative expression systems or by optimizing the medium formulations and feeding strategies [5]. On the contrary, the downstream processing has not evolved at the same rate and is nowadays considered the bottleneck in the manufacturing of mAbs for therapeutic purposes at reliable costs, representing up to 80 % of their total production costs [6].

Based on the aforementioned information, the main objective of this PhD work consisted on the development of alternative cost-effective purification techniques for antibodies using different ionic-liquid-based strategies, aiming to contribute towards a reduction in the antibodies production costs while allowing their widespread use as recurrent therapies. Accordingly, the current PhD thesis starts with a literature overview (**chapter 1**), divided in two main topics: (i) biopharmaceuticals market, main characteristics, features and applications of mAbs, evolution of their upstream processing, and challenges and bottlenecks associated with their downstream processing – **subchapter 1.2**; and (ii) relevance of mAbs for therapeutic purposes, using the case of inflammatory diseases as main example – **subchapter 1.3**.

After introducing the relevance of antibodies for human society, as well as the challenges related with the downstream processing of these biopharmaceuticals, this thesis follows with the

chapters in which are presented the efforts carried out to tackle the presented challenges, using ionic-liquid-based strategies. In **chapter 2** are provided the works focusing the extraction and purification of antibodies by liquid-liquid extraction, namely by aqueous biphasic systems comprising ILs. **Subchapter 2.1** reports the results obtained with ABS composed of a wide range of conventional ILs as adjuvants, allowing the screening of the performance of several systems for the extraction and further purification of antibodies from human serum samples. In **subchapter 2.2** it is reported the successful application of the best ABS/ILs identified in the previous subchapter, for the capture and purification of two different mAbs (anti-interleukin-8 (anti-IL-8) and anti-hepatitis C virus (anti-HCV)) from cell culture supernatants with different complexity degrees (serum-containing and serum-free Chinese Hamster Ovary (CHO) cell culture supernatants), being possible to prove the robustness of the developed platform. In addition, it is suggested the possibility of using such ABS in miniaturized and continuous mode, for massive parallelization (scale-out) at the preparative scale. **Subchapter 2.3** follows the same line of research, yet moving towards the development of more sustainable ABS, i.e. by the use of biocompatible ILs derived from renewal resources as phase-forming components, namely glycine-betaine analogue (AGB) ILs. Besides the characterization of the novel ternary phase diagrams, these IL-based ABS were successfully applied in the recovery and purification of mAbs from cell culture supernatants. However, in this work, some evidence on the potential of IL-based three-phase partitioning (ILTPP) systems to purify mAbs was disclosed as well. In this work, it was proved that the biological activity of mAbs is maintained after the several purification and recovery steps involving ILs.

The findings obtained in **subchapter 2.3** on the possibility to create TPP systems for the simultaneous purification and recovery of antibodies, motivated to proceed with the work presented in **chapter 3**, in which the TPP concept based on ABS was comprehensively investigated to maximize the technique potential to purify antibodies. **Subchapter 3.1** focus on the purification and recovery of antibodies using TPP approaches based on ABS containing ILs as adjuvants. The ABS phase-forming components were selected according to the characteristics required to act as TPP systems, and several representative ILs were studied as additives, allowing to tailor the selectivity and performance of the developed platform. This process was successfully applied to the processing of both human serum samples and cell cultures supernatants, being possible to easily recover the purified antibodies in a third solid layer in the interphase of the system, with high purity and, in the case of mAbs from cell culture supernatants, with an almost complete removal of host cell proteins (HCPs).

Finally, taking into account the enormous potential of ILs in the development of more sustainable and cost-effective downstream strategies and also on the fact that chromatography is the gold-standard technique used (and often expensive) by the (bio)pharmaceutical industry, **chapter 4** focus on purification of antibodies using supported ionic liquids (SILs) as alternative materials/chromatographic matrices. In **subchapter 4.1** it is presented a work in which different SILs were investigated, containing similar chemical structures to those of the ILs that performed best in the previous chapters. These novel SILs were synthesized, characterized and investigated as novel materials for the adsorption and purification of antibodies from complex biological matrices. Several operating conditions were optimized, and by an appropriate manipulation of the chemical structure of the SIL, it was possible to successfully purify antibodies by two different mechanisms: by the flowthrough-like or bind-and-elute-like modes. The developed platform proved to be effective in the processing of different biological matrices.

In conclusion, the current thesis comprises a set of works that present the same goal – the development of more sustainable and cost-effective IL-based strategies to extract and purify high-value antibodies from their complex biological matrices. To a better understanding of the organization of the current thesis, a graphical layout that summarizes all the information herein provided is given in **Figure 1.1.1.**
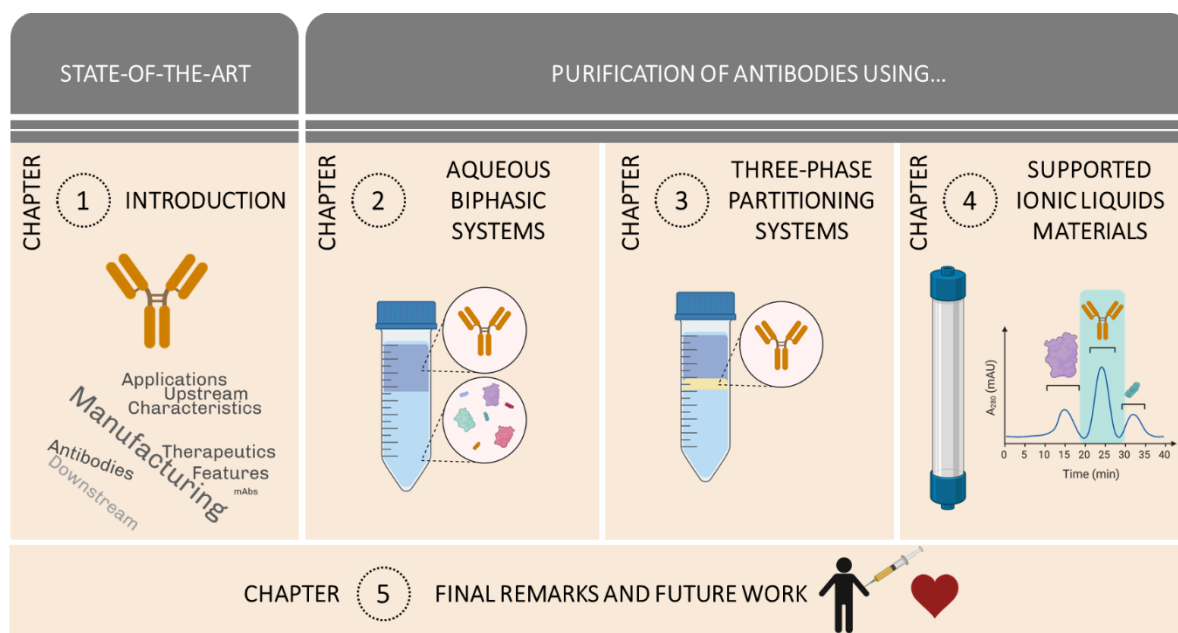
Figure 1.1.1. Graphical layout of the information presented in each chapter of the current thesis. Part of this figure was created with a paid subscription of BioRender (https://biorender.com).

1.1.1. References

1.   P. Rosa, I. Ferreira, A. Azevedo, and M. Aires-Barros, *Aqueous two-phase systems: a viable platform in the manufacturing of biopharmaceuticals.* Journal of Chromatography A, 2010. **1217**(16): p. 2296-2305.

2.   M. Kesik-Brodacka, *Progress in biopharmaceutical development.* Biotechnology and Applied Biochemistry, 2018. **65**(3): p. 306-322.

3.   G. Walsh, *Biopharmaceutical benchmarks 2018.* Nature Biotechnology, 2018. **36**(12): p. 1136-1145.

4.   R.-M. Lu, Y.-C. Hwang, I.-J. Liu, C.-C. Lee, H.-Z. Tsai, H.-J. Li, and H.-C. Wu, *Development of therapeutic antibodies for the treatment of diseases.* Journal of Biomedical Science, 2020. **27**(1): p. 1-30.

5.   P. Gronemeyer, R. Ditz, and J. Strube, *Trends in upstream and downstream process development for antibody manufacturing.* Bioengineering, 2014. **1**(4): p. 188-212.

6.   O. Yang, M. Qadan, and M. Ierapetritou, *Economic analysis of batch and continuous biopharmaceutical antibody production: a review.* Journal of Pharmaceutical Innovation, 2019. **15**: p. 182–200.

1.2. Monoclonal antibodies – addressing the challenges on the manufacturing processing of an advanced class of therapeutic agents

1.2.1. Abstract

Monoclonal antibodies (mAbs) were firstly described by Köhler and Milstein in 1975, and their potential as powerful therapeutic agents recognized in the following years. Currently, the US Food and Drug Administration (FDA) has already approved 56 monoclonal antibodies for the treatment of several diseases, including cancer (e.g. breast cancer, leukemia and prostate cancer), auto-immune disorders (rheumatoid arthritis and Crohn's disease), asthma, and cardiovascular and infectious diseases. Despite their advantages and therapeutic potential, the costs of manufacturing these therapeutics with high quality and purity level is still extremely high due to the absence of current cost-effective extraction/purification methods, and which has also impaired their widespread application as recurrent therapeutic agents. The upstream processing of mAbs has gone through several improvements in recent years, by using alternative expression systems or by optimizing the medium formulations and feeding strategies. On the contrary, the downstream processing is considered the bottleneck in the manufacturing of mAbs for therapeutic purposes at reliable costs, representing up to 80 % of their total production costs – which is a frontier in clinical drug research. In the past years, several chromatographic and non-chromatographic alternatives have been explored for this purpose, resulting in the development of efficient platforms for the purification of mAbs, and that are overviewed and discussed in this chapter. In summary, this chapter provides a vision on the current state of the art of the biopharmaceuticals market, on the production and use of mAbs as valuable therapeutic agents, including their use for the treatment of infectious diseases, while summarizing the mAbs-based products already approved by regulatory agencies.

New insights concerning the development of new and alternative platforms for the extraction and purification of mAbs are also discussed, while envisaging the adoption of the most relevant techniques by the pharmaceutical industry to allow the widespread use of biopharmaceuticals in the near future.

1.2.2. Introductory aspects

In recent years, human society has been facing several issues concerning the exponential emergence of drug-resistant microorganisms, diseases that are unresponsive to common drug therapies and the appearance of individuals with impaired immune systems who are unable to respond to conventional vaccines. These events fomented the search on effective alternative therapeutics, that is a crucial goal to be achieved within the next few years [1]. In this context, biopharmaceuticals have considerably improved the treatment of several diseases and are in many cases the only available therapies approved for a particular disorder [2]. By definition, biopharmaceuticals are biological-based products, with high-molecular weight and complex molecular composition, obtained from heterogeneous mixtures from living beings, cells, animals or plants [3, 4]. Recombinant proteins, antibodies and nucleic-acid-based products are examples of biopharmaceuticals with application in several medicinal areas, such as in vaccination/immunization, oncology, cardiology, neurology and infectious diseases [2]. In what concerns antibodies, although being in many cases the only available therapy, the production cost of antibodies with high quality/purity for therapeutic applications still remains very high due to the absence of a cost-effective purification method, which has conditioned its application on a large scale and as a recurrent therapy [5].

Monoclonal antibodies (mAbs) are the most prevalent class of therapeutic recombinant proteins, used in the treatment of several diseases, including cancer (*e.g.* breast cancer, non-Hodgkin's lymphoma, leukemia, colorectal and prostate cancer), auto-immune disorders (rheumatoid arthritis and Crohn's disease), transplant rejection, asthma, and cardiovascular and infectious diseases [6]. Regarding the production of therapeutic mAbs, one of the most challenging aspects within the biopharmaceutical market is related with the need of quite high therapeutic doses, resulting in a crucial need of obtaining high amounts of pure mAbs [7]. These antibodies are biological products that can be produced by cell lines and extracted from their extracellular supernatant, thus exhibiting a high content of impurities. The current production process of therapeutic mAbs typically comprises two main steps: (i) the upstream processing, that relies on the production of antibodies by cell lines derived from mammalian cells; and (ii) the downstream

Monoclonal antibodies – addressing the challenges on the manufacturing processing of an advanced class of therapeutic agents

1

processing, which consists on the recovery, purification and isolation of mAbs from cells and cell debris, processing medium and other impurities [15]. In the last few years, the upstream processing of mAbs has greatly improved; however, the downstream processing has not evolved at the same pace and is considered the bottleneck in the production of therapeutic mAbs – representing, at least, up to 80 % of the total production costs [8, 9]. At low product titers, upstream manufacturing is more expensive than the downstream, but higher titers shift the main manufacturing costs towards the downstream processing [10], and lead to a non-linear increase of overall costs for the manufacturing process [11]. Since these antibodies should be obtained from the complex matrix with an exceptional purification degree, the downstream process is the critical step in the overall process [12]. In this context, the downstream processing of mAbs represents a frontier in clinical drug research that should be overcome, so that their widespread use as valuable therapeutic agents could become a reality.

This chapter aims to review the current state of the art of the biopharmaceuticals market, the use of mAbs as powerful therapeutic agents for several therapeutic applications, and the description of the mAbs-based products already approved by regulatory agencies. New insights concerning the development of new and alternative chromatographic and non-chromatographic platforms for the extraction and purification of mAbs, including their advantages and limitations, are also reviewed and discussed.

1.2.3. Biopharmaceuticals market

The biopharmaceuticals market has been growing since the human recombinant insulin Humulin®, produced by *Escherichia coli*, was approved by the Food and Drug Administration (FDA) in 1982, for the treatment of Diabetes Mellitus [13]. Later, in 1986, the human protein tissue plasminogen activator (tPA) became the first therapeutic protein obtained from mammalian cells approved in the market. During the same year, FDA also approved the first therapeutic monoclonal antibody (mAb), Orthoclone OKT3 (muromonab-CD3), produced *in vivo* by hybridoma cell technology [14]. Currently, there are more than 150 therapeutic proteins approved in the USA/EU, demonstrating their importance in the treatment of several diseases [15]. In addition, more than 500 recombinant proteins with potential as biopharmaceuticals are currently under clinical trials. This increasing number of dugs candidates is being essentially driven by the biotechnological advances registered in relevant areas, such as genomics and proteomics, that allowed to discover new candidates [16].

The global market of biopharmaceutical products, estimated in US$ 199.7 billion in 2013, was projected to achieve US$ 497.9 billion in 2020 [17]. In the last 10 years, the commercial importance of antibodies has been growing, being the most used type of biopharmaceuticals in different medical and scientific areas, mainly because of their capacity to bind to antigens with high affinity and specificity [18]. Medicine is now moving into an era of personalized medicine and therapies, where monoclonal antibodies fit within as powerful therapeutic agents to treat a wide variety of diseases. For instance, mAbs represent the largest production segment in the global biopharmaceuticals market, accounting with US$ 75 billion in 2013, and was expected to reach US$ 125 billion in 2020 [19]. In the period between 2010 and 2015, it was expected that mAbs were able to generate itself US$ 25 billion, as presented in **Table 1.2.1**, thus enticing a growing number of companies to expand in this field [20]. During 2014, 36 of the top 50 pharmaceutical companies (excluding generics companies) had presence in the mAbs therapeutic sector.

Table 1.2.1. Combined global prescription for the top 50 pharmaceutical companies (excluding generic-drugs companies) by molecule type (2010 – 2015) [20].

Molecule type	Sales (US$ billion)						Differences in sales between 2010 and 2015
	2010	2011	2012	2013	2014	2015	
Small molecules	413	414	402	398	399	401	-12
Therapeutic proteins	70	73	76	79	81	81	11
Monoclonal antibodies	46	52	57	62	67	71	25
Vaccines	24	25	28	30	31	32	8

Due to this robust market demand, the global mAbs market size will ascend by more than 12 % in 2013-2017, reaching US$ 141 billion in 2017 [21]. By November of 2016, a total of 56 therapeutic mAbs were already approved by FDA and 6 were still under revision. In **Table 1.2.2** are summarized the mAbs-based products already approved by regulatory agencies.

Taking into account the high value of the biopharmaceuticals market, the advances in mAb technologies, and patents expiration of several mAb products (e.g. infliximab, Remicade® from Johnson & Johnson, that will expire in the US in September 2018 and has expired in Europe in February 2015; trastuzumab, Herceptin® from Roche, that will expire in the US in September 2019 and has expired in Europe in February 2014; and adalimumab, Humira® from Abbott, expired in the US in 2016), it is expected a strong market competition in this field in the near future [21].

Monoclonal antibodies – addressing the challenges on the manufacturing processing of an advanced class of therapeutic agents

1

Table 1.2.2. Therapeutic mAbs approved or in review in the EU and US by regulatory agencies. Data collected from The Antibody Society (www.antibodysociety.org).

International non-proprietary name	Brand name	Target; Format	Indication (first approved or reviewed)	First approval year	
				EU	US
Avelumab	(Pending)	PD-L1; Human IgG1	Merkel cell carcinoma	In review	NA
Sirukumab	(Pending)	IL-6; Human IgG1	Rheumatoid arthritis	In review	In review
Dupilumab	Dupixent	IL-4R alpha; Human IgG4	Atopic dermatitis	NA	In review
Romosozumab	(Pending)	Sclerostin; Humanized IgG2	Osteoporosis in postmenopausal women at increased risk of fracture	NA	In review
Inotuzumab ozogamicin	(Pending)	CD22; Humanized IgG4; ADC	Hematological malignancy	In review	NA
Ocrelizumab	OCREVUS	CD20; Humanized IgG1	Multiple sclerosis	In review	In review
(Pending)	Xilonix	IL-1 alpha; Human IgG1	Advanced colorectal cancer	In review	NA
Bezlotoxumab	Zinplava	*Clostridium difficile* enterotoxin B; Human IgG1	Prevention of *Clostridium difficile* infection recurrence	In review	2016
Brodalumab	(Pending)	IL-17R; Human IgG2	Immune-mediated disorders	In review	In review
Sarilumab	(Pending)	IL-6R; Human IgG1	Rheumatoid arthritis	In review	In review
Olaratumab	(Pending)	PDGFRα; Human IgG1	Soft tissue sarcoma	In review	2016
Atezolizumab	Tencentriq	PD-L1; Humanized IgG1	Bladder cancer	In review	2016
Reslizumab	Cinqair	IL-5; Humanized IgG4	Asthma	2016	2016
Obiltoxaximab	Anthim	Protective antigen of B. anthracis exotoxin; Chimeric IgG1	Prevention of inhalational anthrax	NA	2016

Ixekizumab	Taltz	IL-17a; Humanized IgG4	Psoriasis	2016	2016
Daratumumab	Darzalex	CD38; Human IgG1	Multiple myeloma	2016	2015
Elotuzumab	Empliciti	SLAMF7; Humanized IgG1	Multiple myeloma	2016	2015
Necitumumab	Portrazza	EGFR; Human IgG1	Non-small cell lung cancer	2015	2015
Idarucizumab	Praxbind	Dabigatran; Humanized Fab	Reversal of dabigatran-induced anticoagulation	2015	2015
Mepolizumab	Nucala	IL-5; Humanized IgG1	Severe eosinophilic asthma	2015	2015
Alirocumab	Praluent	PCSK9; Human IgG1	High cholesterol	2015	2015
Evolocumab	Repatha	PCSK9; Human IgG2	High cholesterol	2015	2015
Dinutuximab	Unituxin	GD2; Chimeric IgG1	Neuroblastoma	2015	2015
Secukinumab	Cosentyx	IL-17a; Human IgG1	Psoriasis	2015	2015
Nivolumab	Opdivo	PD1; Human IgG4	Melanoma, non-small cell lung cancer	2015	2014
Blinatumomab	Blincyto	CD19, CD3; Murine bispecific tandem scFv	Acute lymphoblastic leukemia	2015	2014
Pembrolizumab	Keytruda	PD1; Humanized IgG4	Melanoma	2015	2014
Ramucirumab	Cyramza	VEGFR2; Human IgG1	Gastric cancer	2014	2014
Vedolizumab	Entyvio	α4β7 integrin; humanized IgG1	Ulcerative colitis, Crohn disease	2014	2014
Siltuximab	Sylvant	IL-6; Chimeric IgG1	Castleman disease	2014	2014
Obinutuzumab	Gazyva	CD20; Humanized IgG1; Glycoengineered	Chronic lymphocytic leukemia	2014	2013
Adotrastuzumab emtansine	Kadcyla	HER2; humanized IgG1; ADC	Breast cancer	2013	2013

Raxibacumab	(Pending)	*B. anthrasis* PA; Human IgG1	Anthrax infection	NA	2012
Pertuzumab	Perjeta	HER2; humanized IgG1	Breast cancer	2013	2012
Brentuximab vedotin	Adcetris	CD30; Chimeric IgG1; ADC	Hodgkin lymphoma, systemic anaplastic large cell lymphoma	2012	2011
Belimumab	Benlysta	BLyS; Human IgG1	Systemic lupus erythematosus	2011	2011
Ipilimumab	Yervoy	CTLA-4; Human IgG1	Metastatic melanoma	2011	2011
Denosumab	Prolia	RANK-L; Human IgG2	Bone loss	2010	2010
Tocilizumab	RoActemra, Actemra	IL-6R; Humanized IgG1	Rheumatoid arthritis	2009	2010
Ofatumumab	Arzerra	CD20; Human IgG1	Chronic lymphocytic leukemia	2010	2009
Canakinumab	Ilaris	IL-1β; Human IgG1	Muckle-Wells syndrome	2009	2009
Golimumab	Simponi	TNF; Human IgG1	Rheumatoid and psoriatic arthritis, ankylosing spondylitis	2009	2009
Ustekinumab	Stelara	IL-12/23; Human IgG1	Psoriasis	2009	2009
Certolizumab pegol	Cimzia	TNF; Humanized Fab, pegylated	Crohn disease	2009	2008
Catumaxomab	Removab	EPCAM/CD3; Rat/mouse bispecific mAb	Malignant ascites	2009	NA
Eculizumab	Soliris	C5; Humanized IgG2/4	Paroxysmal nocturnal hemoglobinuria	2007	2007
Ranibizumab	Lucentis	VEGF; Humanized IgG1 Fab	Macular degeneration	2007	2006
Panitumumab	Vectibix	EGFR; Human IgG2	Colorectal cancer	2007	2006
Natalizumab	Tysabri	a4 integrin; Humanized IgG4	Multiple sclerosis	2006	2004
Bevacizumab	Avastin	VEGF; Humanized IgG1	Colorectal cancer	2005	2004
Cetuximab	Erbitux	EGFR; Chimeric IgG1	Colorectal cancer	2004	2004

Efalizumab	Raptiva	CD11a; Humanized IgG1	Psoriasis	2004#	2003#
Omalizumab	Xolair	IgE; Humanized IgG1	Asthma	2005	2003
Tositumomab-I131	Bexxar	CD20; Murine IgG2a	Non-Hodgkin lymphoma	NA	2003#
Ibritumomab tiuxetan	Zevalin	CD20; Murine IgG1	Non-Hodgkin lymphoma	2004	2002
Adalimumab	Humira	TNF; Human IgG1	Rheumatoid arthritis	2003	2002
Alemtuzumab	MabCampat h, Campath1H; Lemtrada	CD52; Humanized IgG1	Chronic myeloid leukemia#; multiple sclerosis	2001#; 2013	2001#; 2014
Gemtuzumab ozogamicin	Mylotarg	CD33; Humanized IgG4; ADC	Acute myeloid leukemia	NA	2000#
Trastuzumab	Herceptin	HER2; Humanized IgG1	Breast cancer	2000	1998
Infliximab	Remicade	TNF; Chimeric IgG1	Crohn disease	1999	1998
Palivizumab	Synagis	RSV; Humanized IgG1	Prevention of respiratory syncytial virus infection	1999	1998
Basiliximab	Simulect	IL-2R; Chimeric IgG1	Prevention of kidney transplant rejection	1998	1998
Daclizumab	Zenapax; Zinbryta	IL-2R; Humanized IgG1	Prevention of kidney transplant rejection; multiple sclerosis	1999#; 2016	1997#; 2016
Rituximab	MabThera, Rituxan	CD20; Chimeric IgG1	Non-Hodgkin lymphoma	1998	1997
Abciximab	Reopro	GPIIb/IIIa; Chimeric IgG1 Fab	Prevention of blood clots in angioplasty	1995*	1994
Muromonab-CD3	Orthoclone Okt3	CD3; Murine IgG2a	Reversal of kidney transplant rejection	1986*	1986#

* - Country-specific approval. # - Withdrawn or marketing discontinued for the first approved indication. NA - not approved or in review in the EU; information on review status in US not available.

Antibodies have proven an important role in the biopharmaceutical market, both economically and in terms of improving the efficiency of the treatment of various pathologies. Despite the effectiveness and safety of mAbs for human administration, particularly when they present high degree of purity and retain their specific activities, the access to this type of therapy

Monoclonal antibodies – addressing the challenges on the manufacturing processing of an advanced class of therapeutic agents

1

has been hampered by high manufacturing costs, making it imperative to develop effective and economical methods to purify antibodies [22, 23].

1.2.4. Structural and functional characteristics of antibodies

Antibodies are glycoproteins that are found in plasma and extracellular fluids [18]. They are the major effectors of the adaptive immune system, and they are produced in response to molecules and organisms (such as bacteria, viruses, foreign molecules and other agents) which are neutralized and/or eliminated by these. This response is a key mechanism used by a host organism to protect itself against the action of foreign molecules or organisms. They are secreted by specialized B-lymphocytes (plasma cells) and may also be called immunoglobulins (Ig) since they contain a structural domain found in various proteins. There are several Ig populations that can be found on the surface of lymphocytes in exocrine secretions and extravascular fluids [24]. Each animal can produce millions of different antibodies, and each antibody is able to bind specifically to a particular foreign substance known as an antigen [18]. B-lymphocytes carrying specific receptors, recognize and bind the antigenic determinants of the antigen and induce a process of division and differentiation, which transforms the B-lymphocytes into plasma cells that predominantly synthesize antibodies.

Antibodies comprise four polypeptide chains, namely two heavy chains (approximately 55 kDa each) and two identical light chains (about 25 kDa each), organized in "Y"-shape format. Each of these chains contains one variable region and multiple constant regions, associated by disulfide bonds and non-covalent bonds, resulting in a molecule with a molecular weight of approximately 150 kDa, as can be seen in **Figure 1.2.1**. The antibody binding to the antigen occurs in the antigen-binding fragment (Fab) region through complementary-determining regions (CDR). CDRs are composed of different sequences of amino acids according to the type of antigen to which are associated, and are therefore referred as hypervariable regions [25]. The heavy chains are associated by disulfide bonds, located in a flexible hinge region, with approximately 12 amino acids (essentially proline, threonine, serine and cysteine), and are highly sensitive to enzymatic or chemical cleavage [24]. Each globular region, comprised by the folding of the polypeptide chains, is designated by domain.

In mammals, there are five classes of Ig (IgG, IgM, IgA, IgD and IgE) that depend on their primary sequence of amino acids and differ on the functions performed in the immune system. Both IgA and IgG are subdivided in subclasses – isotypes – due to the polymorphisms verified in constant regions of the heavy chain [18].

Antigen-binding site

Fab region

Fc region

Variable domains

Light chain

Heavy chain

Constant domain
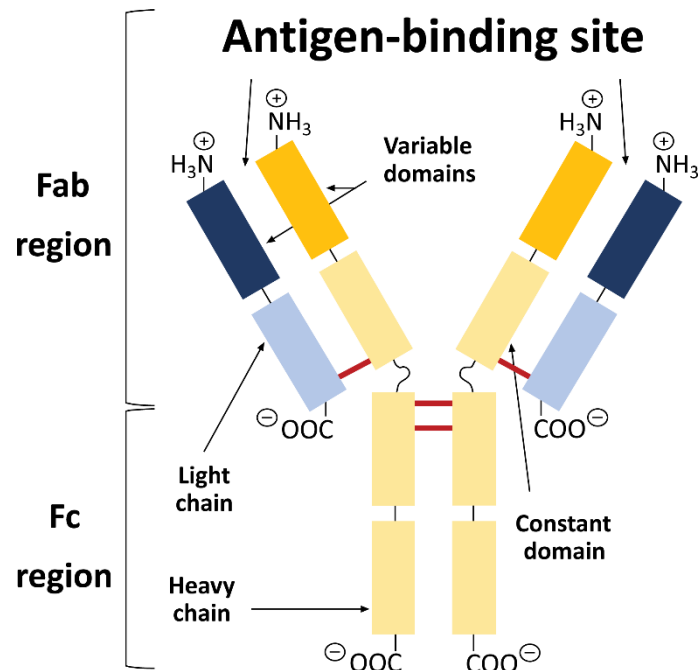
Figure 1.2.1. Schematic representation of a conventional antibody. It comprises two identical heavy (yellow) and light (blue) chains of antibodies, joined by disulphide bonds (red). Each chain contains a constant and variable region (colored darker), where the antigen-binding site is located.

Each Ig class determines a type and temporal nature of the immune response. Currently, two isotypes of IgA – IgA1 and IgA2 – are known, and four isotypes of IgG are known – IgG1, IgG2, IgG3 and IgG4. In a biotechnology perspective, IgG is the most important class of antibodies, since they are the most abundant Ig in the blood (representing 75 % of the antibodies) [26].

1.2.5. Applications of antibodies

Monoclonal antibodies (mAbs) have been the subject of intense investigation since their production was first achieved [27]. Their high specificity is an excellent advantage therapeutic purposes since mAbs can only interact with a specific substance [18]. This specificity is also very attractive for numerous clinical trials and laboratory diagnostic tests, such as the detection and identification of analytes, cell markers, pathogens, among others [28]. However, their monospecificity may also be considered a limitation, since the occurrence of minor changes in the structure of an epitope may affect the function of the antibody. Finally, an additional advantage of mAbs is related with the fact that, once the desired hybridoma has been generated, mAbs can be produced through a constant and renewable source, allowing a continuous and reproducible delivery of antibodies. Due to all these factors, mAbs, and in particular IgG, represent the most used

type of antibodies for a large plethora of scientific and therapeutic applications. Below we describe some of the main applications of this biomolecule for such purposes.

At the diagnostic level, IgG antibodies are ideal biological recognition agents, and have thus been used in numerous analytical techniques, such as Western Blotting (immunoblotting), immunohistochemistry, immunocytochemistry, immunoprecipitation, enzyme-linked immunosorbent assay (ELISA), microarrays of antibodies, immunoscintigraphy, radioimmunological assays, flow cytometry analysis, immunosensors, immuno-polymerase chain reactions (IPCRs) and real-time IPCRs [29]. These antibodies are also used as important tools in immunoaffinity chromatography [30], in the identification and localization of intracellular and extracellular proteins [18], and used for the detection of pathogens, adulterants, toxins, and/or other residues (drugs, chemicals or pesticides) in food products and in environmental analysis/monitoring [30].

Concerning their therapeutic applications, mAbs present a large potential for use in passive immunotherapy. Passive immunity is conferred by transferring specific antibodies against a particular pathogen to a host, and is distinguished from the active immunity because, in the last case, the immunity is conferred by the host's response to a given pathogen antigen, as depicted in **Figure 1.2.2**.
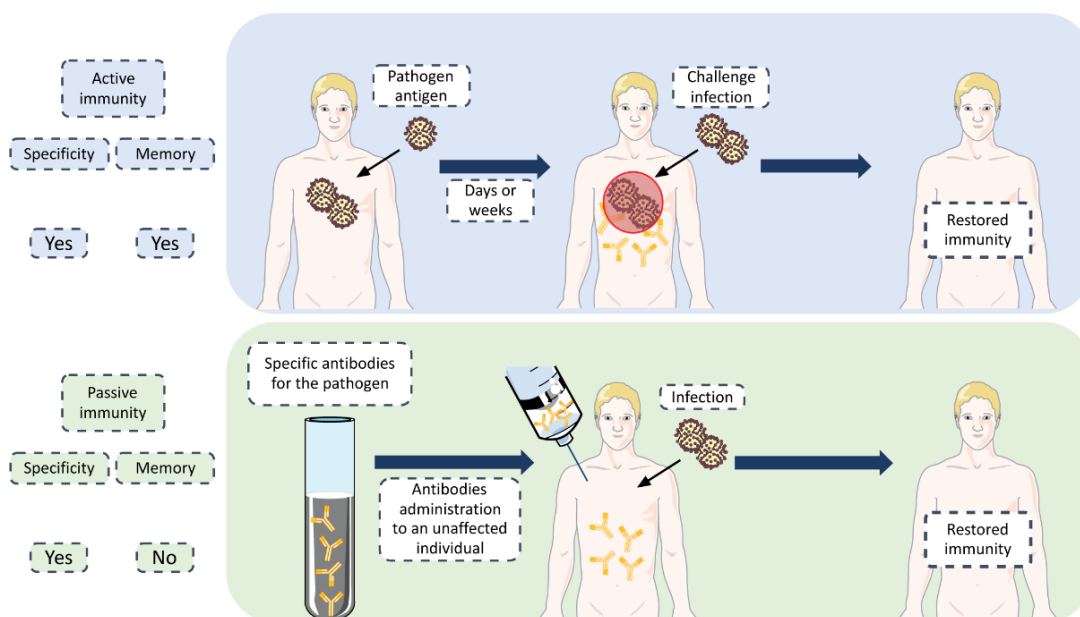
Figure 1.2.2. Active immunity vs. Passive immunity.

Antibodies can be administered as: (i) human or animal plasma or serum; (ii) pooled human immunoglobulin for intravenous (IVIG) or intramuscular (IG) use; (iii) high-titer human IVIG or IG from immunized or convalescing donors; and (iv) as monoclonal antibodies (mAbs) [31]. In

particular, intravenous immunoglobulin (IVIG) is used as a replacement therapy in immunodeficient individuals, who are unable to create their own effective immune responses [32]. IVIG can also be used to suppress the pathological immune responses that occur in patients with autoimmunity [33]. IVIG formulations are prepared from the human serum IgG fraction, which is pooled from a minimum of 1000 up to 60,000 donors [34].

The therapeutic potential of antibodies in infectious diseases has also been investigated, since some of the biopharmaceuticals-based therapies presented on **Table 1.2.2** refer to anti-infectives mAbs. Respiratory syncytial virus (RSV) infection is classified into the subfamily Pneumovirinae within the *Paramyxoviridae* family of enveloped, single-stranded, and negative-sense RNA viruses [35]. This infection can result in a severe lower respiratory tract disease, and represents the leading cause of hospitalization of young children with respiratory tract diseases. Since previous vaccine attempts have failed to provide a long-lived protective immune response and since there is no currently approved vaccine against RSV, this is considered an important target for antiviral development [36]. Therefore, passive antibody therapies are used in high-risk infants to prevent and modify RSV infection [31]. The treatment for RSV infection has been limited to RSV-IVIG derived from plasma donors with high RSV neutralizing antibodies [31], and ribavirin, a non-specific antiviral that interferes with virus transcription [37]. However, side effects associated to the use of ribavirin and the historical debate surrounding its efficacy illustrate the need for more potent and safe therapeutics to treat RSV infection. Palivizumab was the first mAb commercially available for immunoprophylactic use to prevent an infectious disease, and consists in a humanized mouse IgG1 against the RSV surface F glycoprotein [38]. Although the indications for RSV-IGIV and palivizumab are similar, palivizumab is preferred because of its lower cost and its easiest administration (intramuscular *versus* intravenous administration for RSV-IVIG). Further, palivizumab does not interfere with measles and varicella vaccines and is less likely to transmit an infectious agent since it is not prepared from plasma. Motavizumab, an affinity-optimized monoclonal antibody developed from palivizumab, has also been under clinical trials [39]. Palivizumab was the first mAb commercially available (in 1999) in the EU for immunoprophylactic use to prevent an infectious disease, and consists in a humanized mouse IgG1 against the respiratory syncytial virus (RSV) surface F glycoprotein [38]. *Bacillus anthracis* causes inhalational anthrax, and its endospores have been developed to be a highly lethal bioterrorism threat [40]. After the bioterrorist attacks of September 2001, which resulted in eleven confirmed cases of inhalational anthrax and five fatalities, the US government enacted new regulations to encourage the pharmaceutical industry towards the development of medical countermeasures against

Monoclonal antibodies – addressing the challenges on the manufacturing processing of an advanced class of therapeutic agents

1

bioterrorist threats [41]. The anthrax toxin is a tripartite toxin that contains enzymatic and binding moieties. Lethal factor (LF) and edema factor (EF) have enzymatic activities. Protective antigen (PA) is the gatekeeper moiety that binds to cell receptors and then binds and translocates LF and EF into the cell [42]. In December 2012, the United States Food and Drug Administration (FDA) approved raxibacumab for the treatment and prophylaxis against inhalational anthrax [43]. Raxibacumab is a fully human IgG1 mAb that binds PA, thus blocking the binding of PA to its cell receptors, the binding of LF and EF, and the internalization of anthrax toxin [44]. So, the neutralization of PA appeared as an effective treatment and prevention strategy of the pathogenesis of inhalational anthrax. More recently, in 2016, another antitoxin therapy was licensed under the US FDA – obiltoxaximab – a chimeric IgG1(κ) mAb that prevents binding of PA to the cellular receptors [45, 46]. Also in 2016, bezlotoxumab was also approved as anti-infective mAb for the prevention of *Clostridium difficile* infection recurrence. The debilitating symptoms of *C. difficile* infection (CDI) are caused by two exotoxins – *C. difficile* toxins A and B. Clinical trials have shown that the neutralisation of these toxins can prevent recurrence of infection, offering an antibacterial-sparing treatment option [47]. Bezlotoxumab consists in a human monoclonal antibody against *C. difficile* toxin B developed by Merck & Co, for reduction of CDI recurrence in adults who are receiving antibacterial drug treatment of CDI and are at a high risk for CDI recurrence [48, 49].

Besides mAbs, two biopharmaceuticals given in **Table 1.2.2**, based on bispecific antibodies (bsAbs) - blinatumomab and catumaxomab – should be also highlighted. A bispecific antibody is based on a conventional monoclonal antibody; yet, it can recognizes and binds to two different antigens or epitopes simultaneously. Thus, bsAbs show some advantages as therapeutic agents since they can potentially increase binding specificity by interacting with two different cell-surface antigens, further enabling the simultaneous blocking of two different pathways that exert unique or overlapping functions in pathogenesis, among others [50]. Their potential as new agents for therapeutic can be supported by the example of blinatumomab, that consists in a novel, bispecific T-cell engaging antibody that targets both tumour-associated antigens CD19 (expressed on B cells) and CD3 (a receptor on T cells) [51, 52], and was approved through an accelerated pathway for the treatment of acute lymphoblastic leukemia (ALL). Blinatumomab consists of two single-chain recombinant antibodies with a small distance between the two that joins CD19 and CD3 by a flexible, non-glycosylated five-amino acid non-immunogenic linker [53]. On the other hand, catumaxomab was approved in the European Union (EU) in April 2009 for the intraperitoneal treatment of malignant ascites in patients with epithelial cell-adhesion molecule (EpCAM)-positive carcinomas [53]. Catumaxomab is a targeted immunotherapy characterized by its binding to three

different cell types – tumour cells, T-cells and accessory cells – presenting two antigen-binding specificities – one for EpCAM on tumour cells and one for the CD3 antigen on T-cells [53, 54]. Despite these features, traditional combination therapies using mAbs can also modulate multiple therapeutic targets achieving similar effects, and in fact, the majority of the biopharmaceuticals going to clinical trials are still based on mAbs.

1.2.6. Upstream processing of monoclonal antibodies

The clinical and commercial success of mAbs has led to the need of a large-scale production in mammalian cell cultures. This has resulted in a rapid expansion of the global manufacturing capacity, an increase in the size of reactors and to an increased effort to improve the process efficiency with a concomitant manufacturing cost reduction [55]. For this purpose, genetic engineering and cell engineering had allied themselves to develop new media and reactors that lead to the optimization of mammalian cell culture conditions at a larger scale. Hybridoma technology was the first technology that made possible the production of large quantities of mAbs from murine origin, but latter new and very efficient expression systems were developed in order to allow the full exploitation of the antibodies potential.

1.2.6.1. Hybridoma technology

Monoclonal antibodies were first recognized in the serum of patients with multiple myeloma, in whom clonal expansion of malignant plasma cells led to the production of high levels of identical antibodies, resulting in a monoclonal gammopathy [18]. The discovery of monoclonal antibodies produced by these tumours led to the idea that it may be possible to produce similar mAbs of any desired specificity by immortalizing individual antibody-secreting cells from an animal immunized with a known antigen [27].

In 1975, Georges Köhler and Cesar Milstein [27] developed a technique named hybridoma technology, that relies on fusing B-lymphocytes from an immunized animal (typically a mouse) with a myeloma cell line, and growing the cells under conditions in which the unfused normal and tumour cells cannot survive. In this procedure, spleen cells from a mouse that has been immunized with a known antigen or mixture of antigens are fused with an enzyme-deficient partner myeloma cell line [25]. The myeloma partner used does not secrete its own Igs. The cells are then placed in a selection medium containing hypoxanthine, aminopterin and thymidine (HAT medium) that allows only the survival of the immortalized hybrid cells. These hybridomas are then grown as single cell clones and tested for the secretion of the antibody of interest. The clones with the desired

specificity are selected and further expanded. Each hybridoma produces only one Ig and the antibodies secreted by each hybridoma clone are monoclonal antibodies which are specific for a single epitope on the antigen or antigen mixture used to identify antibody secreting clones.

In the late 80s, murine mAbs started their clinical development, however suffering from a large number of drawbacks. Murine mAbs exhibit a relatively short serum half-life when compared to human IgG and induced the development of human anti-mouse-antibodies (HAMA) in the patients, especially when repeated administrations were necessary. Also, murine mAbs are relatively poor recruiters of effector functions, which is critical for their efficacy, especially in oncology indications [56, 57]. In order to overcome these problems, Boulianne *et al.* (1984) and Morrison *et al.* (1984) developed mouse-human chimeric antibodies by genetic engineering techniques, through grafting the murine variable domain, specific for a given antigen, with the constant domains of the human antibodies [58, 59]. This new technique allowed to obtain molecules that were approximately 66 % human, which consequently present a superior half-life in humans and a lower immunogenicity. Later, Jones *et al.* (1986) proposed changes and improvements to these antibodies by grafting only the murine hypervariable regions into the human framework, resulting in molecules that were approximately 95 % human [60].

Whilst humanized mAbs appeared to overcome the inherent immunogenic problems of murine and chimeric mAbs, humanization has however some additional limitations, since it requires a laborious, complex and time-costing process. In order to obtain fully human mAbs, new techniques have emerged in the last years. One of these techniques is phage display, in which a library of bacteriophage expressing the antibody variable domains are screened against an immobilized target antigen in order to capture the phages that specifically bind to the antigen. Unbounded phage are washed away while bounded phage are eluted, propagated in *E. coli* cells and further used in another round of selection. At the end of the panning procedure, *E.coli* cells are further infected with the phage from the last round and the individual clones correspond to individual monoclonal variable domains. An additional alternative technology consist on the creation of transgenic mice expressing repertoires of human antibody gene sequences, which allow the production of fully human monoclonal antibodies through the hybridoma technology, with low immunogenic potential and properties similar to the human endogenous antibodies [61, 62]. In **Figure 1.2.3** is depicted the several types of antibodies possible of being obtained through genetic engineering, as well as their classification according to the origin of their primary sequence.

In clinical terms, there are no apparent differences between the monoclonal antibodies obtained using phage display techniques or transgenic mice. However, the detection process of an

antibody by phage display allows a more direct isolation and also a higher control under the specificity and affinity of the antibody.
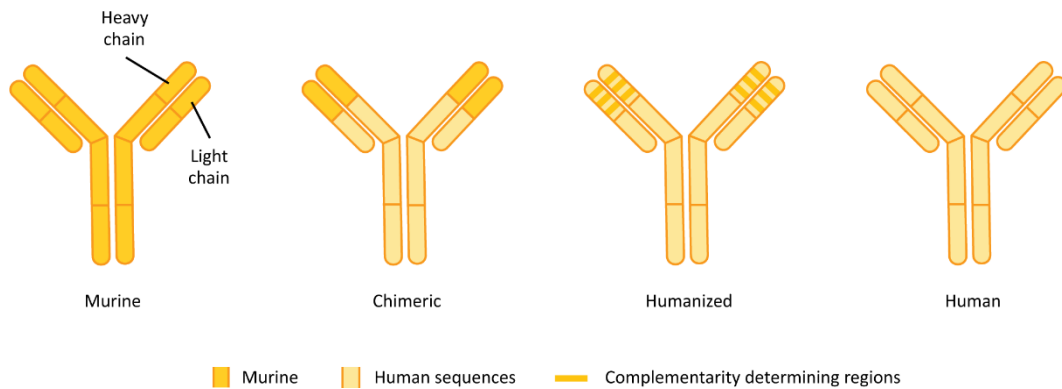
Figure 1.2.3. Humanization of antibodies through genetic engineering. Therapeutic mAbs can be murine (100 % murine protein) [suffix: -omab], chimeric (composed of approximately 35 % murine sequences) [suffix: -ximab], humanized (only possess 5-10 % of murine regions) [suffix: -zumab] or fully human (100 % human protein) [suffix: -umab].

1.2.6.2. Recombinant DNA technology

The development of very efficient expression systems is essential to the full exploitation of the antibodies therapeutic potential, both in terms of therapeutic efficiency and cost/widespread application [63]. The expression of functional, correctly folded antibodies or antibody fragments and its scale up to commercial levels is a major goal in the therapeutic antibodies development. Since antibody therapies may require large doses over a long period of time, the manufacturing capacity becomes an issue because the drug substance must be produced in large quantities at a cost and time efficiency which meet the clinical requirements. In response to the strong demand, companies have built large scale manufacturing plants containing multiple 10,000 L or larger cell culture bioreactors [64].

Therapeutic antibodies are mainly produced in mammalian cell expression systems due to their ability to produce large amounts of mAbs with a consistent quality and to adapt well to culture in large-scale suspension bioreactors [65]. Another reason, and probably the most important for the dominance of mammalian cells, is their capability to perform the required protein folding, assembly and post-translational modifications, such as glycosylation, so that the produced mAbs would be chemically similar to human forms for increased product efficacy and safety. In particular, the cell line obtained from Chinese Hamster Ovary (CHO) is the most widely used cell line for the production of large-scale mAbs [66]. This cell line was first isolated in 1957 by Dr. Theodore T. Puck

Monoclonal antibodies – addressing the challenges on the manufacturing processing of an advanced class of therapeutic agents

1

from a female Chinese hamster, and quickly gained recognition due to their ease and rapid growth/culture time and high expression [67]. Currently, this cell line appears as the production host of approximately 70 % of total recombinant therapeutic proteins [68]. It is widely used as the main vehicle for the production of mAbs due the advantages summarized below:

1. CHO cells have proven a track record of producing safe, biocompatible and bioactive mAbs, enabling products from these cells to gain a more easily regulatory approval [69, 70];

2. Genetic modification techniques such as the use of dihydrofolate reductase (DHFR) or glutamine synthase (GS) can be used to attenuate the low specific productivity that hinders the production of recombinant proteins in mammalian cells [68, 71];

3. CHO cells present the appropriate molecular repertoire for the occurrence of native-like post-translational modifications with glycoforms comparable to those of humans, thus exhibiting similar molecular activity [72];

4. They grow in serum-free suspension cultures, often in stainless steel bioreactors or even disposable bioreactors [73];

5. Their scale-up is possible [72];

6. Human pathogenic viruses, such as HIV, influenza and polio, do not replicate in CHO cells, enhancing the safety of the produced mAbs [74];

7. They are easily genetic modified to optimize the production process [70].

Close to the CHO cells, the most commonly used cell lines for mAbs production are the murine lymphoid cells NS0 and SP2/0, since they are originated from differentiated B-lymphocytes that produce high amounts of immunoglobulins. However, these are not the preferred cell culture for mAbs production because the produced antibodies may contain immunogenic residues, resulting in a reduced half-life *in vivo* [75].

The use of cells from human sources is an option that allow to overcome the presence of antigenic groups in the antibodies produced. There are currently several possibilities being studied, namely human embryonic cells derived from the kidney HEK293, immortalized human amniocytes from CEVEC, and human embryonic cells derived from retinoblasts PER.C6 from Crucell [76]. Although HEK293 and human amniocytes are reported to be the most suitable for protein production, PER.C6 are considered the most promising candidates since they are the most productive and can reach cell densities considerably higher than CHO cells, producing more than 27 g·L^{-1} of protein in reactors [76, 77]. Despite of human cell lines being still subject to regulatory problems due to their low resistance against adventitious agents, several products derived from PER.C6 are currently in the clinical trials phase [76].

Highly productive cell lines result from a host cell line that has the desired characteristics, an appropriate expression system, and a good transfection and selection protocol. The selection of the appropriate expression system is determined by its ability to produce high titers, to consistently produce antibodies with the desired characteristics (e.g. the glycosylation pattern), to reach a high yielding cell line rapidly, and to grow in suspension. The process for the development of highly expressing cell lines begins with the transfection of mammalian cells with plasmid vectors carrying the heavy and light chain genes of the antibody of interest, and also selection marker genes, which allow the selection of the transfected cells conferring resistance to certain antibiotics or advantages in growth/development under certain deficient nutrition conditions [69]. In the case of CHO DG44 or DXB11 cells deficient in the enzyme dihydrofolate reductase (DHFR), a DHFR label is used, which confers the ability to reduce dihydrofolate to tetrahydrofolate, a metabolite required for nucleic acid metabolism, thereby allowing only cells that incorporated the vector with the DHFR gene to survive in a medium without hypoxanthine and thymidine [69, 78]. Amplification of the product can also be achieved by the addition of methotrexate to the medium, which inhibits the activity of DHFR, forcing cells to begin the amplification of the DHFR gene to ensure their survival, resulting in a simultaneous amplification of the mAb genes [79]. Another example is the glutamine synthetase (GS) marker, an enzyme that catalyses the formation of glutamine from glutamate and ammonia, allowing the successfully transfected cells to survive in media lacking in glutamine. The use of this system with mammalian cells with endogenous levels of GS requires the use of methionine sulphoximine (MSX), a GS inhibitor. Similar to using MTX with DHFR, using MSX with GS forces cells to co-amplify the GS gene and the product gene [80]. The GS system has a time advantage over the DHFR system during development, and requires fewer copies of the recombinant gene per cell, allowing a faster selection of high-producing cell lines.

After the selection of transfectants and amplification, single clones are chosen for the scale-up and characterization of product quality and long-term expression. It is important to remark that the integration and random amplification originate several heterogeneous products, making the process of production and selection of clones time-costly and very laborious [69]. In this context, recent developments have emerged for the selection of clones with high production efficiency using automation, particularly to reduce the time dispended and to improve the consistency of the process. Flow cytometry applied to fluorescence-activated cell sorting allows a rapid monitoring of millions of cells to isolate specific subpopulations of several heterogenous products, and can be applied to the separation of surface-labelled antibody-producing cells, since the levels of excreted proteins are proportional to the levels of proteins found on the surface of the cell [81].

1.2.7. Downstream processing of monoclonal antibodies

As mentioned above, the upstream processing of mAbs has undergone numerous advances in the last years, namely in cell culture technologies that allow higher expression levels and higher cell densities [82]. However, the downstream processing has not evolved at the same pace, being currently considered as the bottleneck in the production of therapeutic mAbs [83]. This type of processing depends on chemical and physical interactions, which make it difficult to select a generic method, so they must be modelled, tested and developed from primary principles [8]. The main aspects that should be taken into consideration during the development of a purification process are the speed, and the total yield and purity of the target product. In addition, the process should fulfil several production criteria, such as robustness, reliability and capability to be scaled-up [12].

The explosion in the number of mAbs that went under clinical trial processes, created the need to apply a standard approach for their purification [84]. The purification process should produce mAbs suitable for human use, in which impurities such as host cell proteins, DNA, endogenous and adventitious viruses, endotoxins, aggregates and other species should be removed. Moreover, it is important to note that any treatment performed during the purification steps exerts stress on the protein, due to drastic changes in pH values, salt or protein concentrations, buffers, solvents, among others [85]. This stress can result in denaturation or aggregation of the antibody, with losses in recovery yields; therefore, the monitoring of the quality and functionality of the product is essential during all the processing steps using fast and appropriate analytical tools. Taken all together, the isolation and purification of the final mAbs products requires numerous and complex steps. All these steps represent a high contribution to the final costs of downstream processing, estimated to range between 50 and 80 % of the total production cost of mAbs [4, 86]. With the increased antibody titer achievable through the upstream processing, higher amount of chromatographic resins, buffers and membranes will be consequently required, thus leading to higher costs associated to the downstream processing stage. Strube *et al*. [11] presented a comprehensive study on the cost distributions in downstream processing according to product concentrations. Based on the assumption of a constant spectrum of impurities, the overall cost of goods (COG) decrease with increasing product titers. Therefore, downstream costs will have a higher impact on the overall production costs with increasing titer. In this context, all the efforts should be centered in the creation of a robust and generic process, with a limited number of steps, suitable for all mAbs candidates, by reducing the time and resources required, while fulfilling criteria of purity, quality, efficacy and safety of the therapeutic antibodies for therapeutic applications.

1.2.7.1. Standard downstream processing platform

Figure 1.2.4 depicts a general scheme of a typical downstream platform for the purification of mAbs, based in a common sequence of unit operations that have been developed and integrated aiming to accelerate the entry of these biopharmaceuticals into the clinical trials phase. This platform comprises 6 main steps: 1) clarification; 2) capture of mAbs; 3) viral inactivation; 4) polishing steps; 5) viral removal; and 6) final formulation of the bioproduct.
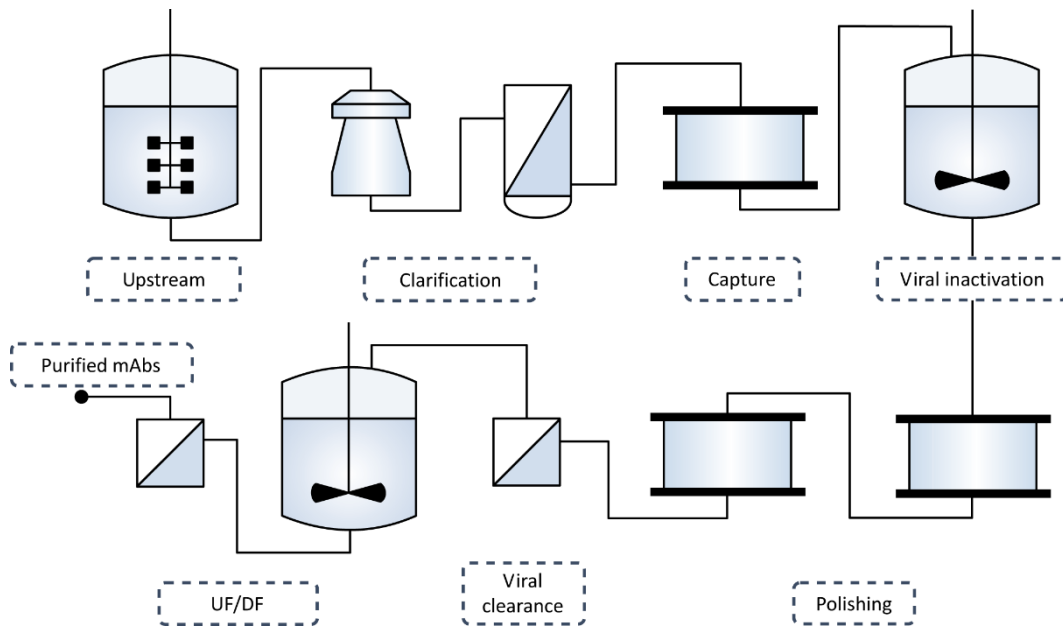
Figure 1.2.4. Standard downstream platform for the purification of mAbs.

The first step in the recovery of an antibody from a mammalian cell culture is the **clarification step**. Since mAbs are typically produced using high density mammalian cell cultures, the removal of cells and cell debris from culture broth to yield a clarified fluid suitable for chromatography is required [84]. Typically, the concentration of solids in mammalian cell culture broths ranges between 40 and 50 %; by the end of the clarification process the presence of solids is expected to be negligible, despite some residual turbidity. This step is generally accomplished through the use of centrifugation, depth filtration and sterile filtration, although other approaches may be applied. Centrifugation is typically preferred over other clarification technologies, such as tangential flow microfiltration, due to its easy application at an industrial scale and ability to operate with large volumes (typically between 2-15,000L per batch) [12]. Clarification operations, in terms of capital cost and energy consumption, can account for up to 25 % of the cost of the entire downstream process [87].

Monoclonal antibodies – addressing the challenges on the manufacturing processing of an advanced class of therapeutic agents

1

After a successful clarification, the medium containing the desired mAbs is subjected to a **capture step**, with protein A (proA) affinity chromatography being the gold standard in most industrial processes [88]. ProA is a naturally occurring polypeptide found anchored in the wall of the bacteria Staphylococcus aureus [89]. The molecular weight of the intact native molecule is 54 kDa. However, typically a recombinant proA is used for IgG purification, produced as a secreted extracellular protein in E. coli, devoided of its domain responsible for binding to cell wall, and with a molecular weight of 42 kDa [87]. The natural high affinity of proA for the Fc region of IgG-type antibodies is the basis of the purification of IgG, IgG fragments and subclasses [84]. In particular, IgG binds to proA at the junction between the heavy chain constant region 2 (CH2) and 3 (CH3) [90]. In **Figure 1.2.5**, a schematic representation of this purification step using proA affinity chromatography is provided.
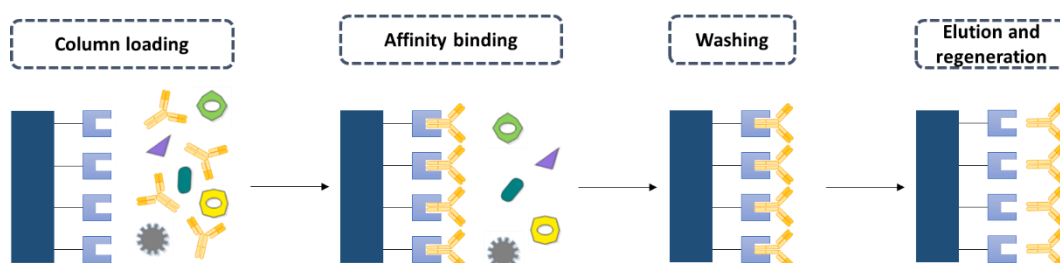
Figure 1.2.5. Schematic representation of the mAbs capture step by protein A affinity chromatography.

This step typically involves the passage of the clarified cell culture supernatant over the column at pH 6-8, conditions under which the antibodies bind and unwanted components such as host cell proteins and cell culture media components and putative viruses flow through the column. An optional intermediated wash step may be carried out to remove non-specifically bounded impurities from the column, followed by the final elution of the product with a low pH elution buffer, ranging between 2.5 and 4. The IgG-proA binding mechanism primarily consists of hydrophobic interactions related to specific hydrogen bonds that are established as a function of the pH. At alkaline pH values, histidyl residues on the binding site of IgG–protein remain uncharged. At more acidic pH values, both histidyl residues in proA and on IgG become positively charged, and as they are close in the binding area, they mutually repel each other, thereby providing an easy way for the dissociation of the IgG from proA [87].

The last step consists in the regeneration of the proA column that is performed to allow its further reuse, while extending its life span (usually < 200 chromatographic cycles) [91, 92]. The regeneration is usually performed using acidic solutions (pH < 3), solutions containing chaotropic

species, such as guanidine chloride or urea, or with a sodium hydroxide aqueous solution (< 100 mM) to completely remove proteins and impurities [12].

ProA affinity chromatography is reported to be highly selective for mAbs, resulting in purity levels higher than 99 % obtained from complex cell culture supernatants [12]. Therefore, proA chromatography is widely used as the first stage of antibody purification due to its high selectivity and high removal capacity of impurities, namely host cell proteins (HCP), host DNA, virus, among others [84]. After this step, antibodies are found with high purity and more stable due to the elimination of proteases and other components of the culture medium which may cause the degradation of the product. Nevertheless, this step displays several disadvantages that should be taken into consideration [12]. The ligand used is prone to proteolysis and the cleaved domains can adhere to product molecules creating an additional separation challenge. Conventional proA ligands cannot be exposed to alkaline conditions that are commonly employed to sanitize other column modes, thus requiring the use of high concentrations of chaotropes, such as urea, for column regeneration and sanitization. The use of high concentrations of chaotropes creates a cost issue as well as a disposal challenge. The need to elute the column at a low pH can induce product aggregation for some mAbs. Finally, and most significantly, the cost of proA resins is nearly an order of magnitude higher than conventional chromatographic resins.

Subsequently, a **viral inactivation step** is always required to remove endogenous retroviruses and adventitious viruses produced by the mammalian cells during the upstream processing stage [87]. All regulatory agencies impose a viral safety threshold for final formulations, although they generally do not state any preferred or recommended method for virus removal/inactivation. To achieve this purpose, it is necessary to use two steps based on two different mechanisms in order to reduce the viral load and to ensure the safety of the products produced by mammalian cells. Most industrial purification processes use inactivation at low pH values, taking advantage of the acidic pH used in the elution during proA chromatography [87]. Other approaches are based on the use of heat, solvents, detergents or ultraviolet radiation [93-95], albeit presenting some limitations of robustness and scale-up.

Polishing steps are further addressed for a final removal of trace impurities of the solution containing the target mAbs [87]. The characteristics of the product and the impurities determine the nature of the polishing steps, but usually one or two additional chromatography polishing steps are applied. Most mAb purification processes include at least one ion exchange chromatography step, for reducing high molecular weight aggregates, charge-variants, residual DNA and host cell proteins, leached ProA and viral particles. The use of anion exchange chromatography (AEX) is more

common than the cation exchange chromatography (CEX), as this resin is often used in the flowthrough mode (in which the product does not bind to the column whereas impurities are retained) [96]. Its operational pH is generally below the protein pI. This ensures that the mAb is positively charged and, therefore, easily washed away from the AEX matrix while negatively charged impurities remain attached. AEX can be used to remove impurities, such as the ones removed by CEX, but will also remove leached proA, HCP, endotoxins, and even viruses, which are bounded to the AEX column [97].

The efficiency of **viral clearance** is determined by the evaluation of the viral load before and after the removal step, typically using a model virus – *e.g.* Murine Leukemia Virus (MuLV) – that is incorporated in the culture medium [87]. According to safety guidelines, products obtained from mammalian cells may contain less than one virus particle per million doses, which represents approximately a clearance of 12-18 $\log_{10}$ for endogenous retrovirus and of 6 $\log_{10}$ clearance for adventitious virus [84]. Filtration is a relatively insensitive technique to small variations in operational parameters, which make it quite suitable for implementation in a standardized process, and is therefore a recommended choice for viral clearance [87]. Filters are typically used at constant pressure and the volumetric charge may range from 200 to 400 $L \cdot m^{-2}$ before a substantial flow decay is perceptible [98].

Finally, the purification process is completed when the product is placed in a predefined formulation buffer, which is usually accomplished with a final **ultrafiltration step in the diafiltration mode** (UF/DF) [87]. There are some parameters that can be standardized for almost all mAbs: type of membrane, transmembrane pressure, and tangential flow velocity. Membranes composed of regenerated cellulose are the most commonly used, mainly due to their attractive characteristics, such as low cost, bio-based nature, and low tendency to fouling and easiness of cleaning. These can be used in different configurations, from plate-and-frame to hollow fiber modules. In general, hollow fibers are the most appropriate to process viscous solutions and/or shear-stress-sensitive products. Since mAb-based drugs are usually administered in high doses, their concentration in a final product represents a critical aspect, being dependent on this last unit operation while reinforcing its relevance. The final formulation should contain a high concentration of mAbs, reinforcing the fundamental role of the concentration step. To prevent physical degradation of mAbs some additives like sugars or surfactants are frequently added to the final formulation [85].

1.2.7.2. Alternative downstream processing platforms

Downstream processing would never have developed as an individual sector of the bioprocessing industry without chromatography, whose inherent selectivity has made of it a key enabling technology in all bioseparation processes [8]. However, chromatography has been the major cost center, derived mainly from the high resin costs and relatively long processing times. Hence, lower cost alternatives have also been pursued [2]. Two viable options have been proposed for the downstream processing of mAbs: (i) the replacement of the proA affinity chromatography by other chromatographic processes; and (ii) the elimination at all of chromatography by non-chromatographic methods. In fact, a large number of alternative platforms for the IgG purification has been reported, which are summarized and compared concerning the recovery yields and purity levels in **Table 1.2.3**.

Table 1.2.3. Most used chromatographic and non-chromatographic methods for the purification of IgG, compared in terms of recovery yield and purity level of IgG.

Purification method	Ligand	Recovery Yield (%)	Purity level (%)	Reference
Chromatographic platforms				
CEX, AEX, HIC (3 chromatographic steps)	-	85	> 99	[99]
CEX	Phosphonate	92-98	95	[100]
	Heparin	90	83	[101]
	Capto™ S	81-83	80-84	[102]
AEX	Advective Hydrogel Membrane	> 90	> 85	[103]
HIC	PVDF membranes	> 97	> 97	[104]
Multimodal chromatography	Capto™ MMC	92-93	95-96	[102]
	MEP-Hypercel™	76	69	[105]
	Phenylboronic acid	98	83	[106]
Affinity chromatography	Epitope imprinted macroporous membrane (5 cycles)	80-90	88	[107]

	Membranes based on Nylon 66 coated with low-molar-mass dextran or poly(vinylalcohol), pre-activated polysulfone (Ultrabind®) and regenerated cellulose (Sartobind®) membranes, carrying Protein-A ligands.	-	-	[108]
Immobilized metal affinity chromatography	Metal ions	-	-	[109]
Expanded bed adsorption chromatography	ProA	92	98	[110]
Continuous annular chromatography	ProA	77-82	-	[111]
	Hydroxyapatite	87-92	-	[111]
Non-chromatographic platforms				
Preparative electrophoresis	-	80	-	[112]
	-	80-90	-	[113]
Affinity precipitation	Eudragit S-100	68	PF = 8	[114]
	GAPDH	98	PF = 1,8	[115]
	Bivalent peptidic hapten	> 85	> 97	[116]
Magnetic separation	Protein A coated magnetic particles	-	-	[117]
	Stimuli-responsive magnetic nanoparticles	64	> 98	[118]
	Starch-coated magnetic nanoparticles	69	> 99	[119]
High performance tangential flow filtration	Composite regenerated cellulose membranes, Biomax™ modified polyethersulfone membranes and conventional regenerated cellulose membranes	-	-	[120]
	Ultracell™ composite regenerated cellulose membranes chemically modified with bromo-propyl-trimethylammonium bromide	98	PF = 10	[121]

AEX – anion exchange chromatography; CEX – cation exchange chromatography; GAPDH – glyceraldehyde 3-phosphate dehydrogenase; HIC – hydrophobic interaction chromatography; PF – purification factor; ProA – protein A; PVDF – polyvinylidene fluoride.

Regarding the chromatographic alternatives to the ProA affinity chromatography, **cation exchange chromatography (CEX)** was one of the first techniques to be recognized with high potential to carry out the primary adsorption step in the downstream processing of mAbs. Indeed, CEX is already used in several commercial processes, including for instance the mAb-product Humira® (adalimumab) [122]. Interesting dynamic binding capacities have been reported for CEX (> 100 g of protein/L of resin), being these values higher than those reported for Protein A resin (usually ≤ 40 g of protein/L of resin) [123]. Furthermore, this type of chromatography allows the removal of host cell proteins to comparable levels to those obtained with the traditional process, allied to the use of a chromatographic matrix an order of magnitude cheaper than proA resin [84, 87]. This alternative may be relevant also because proA chromatography requires the use of an acidic pH during the elution step, which may promote product aggregation and proA leaching from the column, as opposed to cation exchange chromatography which does not require an eluent with low pH values. In fact, the successful use of appropriate cation exchange columns has been already reported to resolve downstream bottlenecks, sustain cost-effective production, and manage large quantities, with remarkable advances om the use of phosphonates bound to Zirconia particles [100] in the development of new ligands such as heparin [101] or sulfonate [102]. It was already demonstrated the potential of a platform constituted by 3 chromatographic steps for the purification of IgG, without the use of proA chromatography [99].

It has also been highlighted the use of other chromatographic variants, such as the anion exchange chromatography (AEX) [103] and hydrophobic interaction chromatography (HIC) [104]. However, it is notorious that the use of a platform consisting of 3 chromatographic steps (combining CEX, AEX and HIC) allows the achievement of an exceptional purity level (> 99 %) [99], which is not achieved by any of the techniques alone (CEX – 95 % [124]; AEX – 85 % [103]; HIC – 97 % [104]). A major drawback in the use of CEX is that it requires samples with low ionic strength prior to loading, and furthermore, due to the high amounts of salts used in the elution buffer, the corrosion of the metal instruments of the equipment may also be a problem. Furthermore, since cell culture supernatants present moderate/high conductivities, they do not allow good binding capacities to be achieved when directly applied to cation exchange resins. To overcome this issue, a previous diafiltration step of the supernatant or its dilution is required before loading into the column. Moreover, the lack of pH control during elution may also affect protein stability causing

precipitation. However, the lower cost of the CEX resin and the high selectivity and purity values obtained offsets the increase on the time spent and number of unit operations.
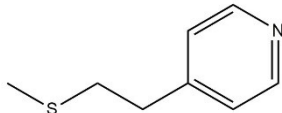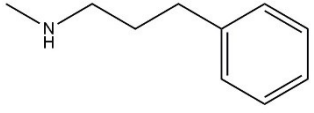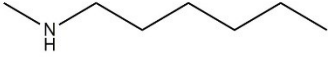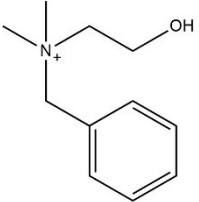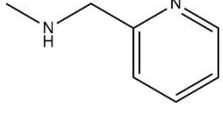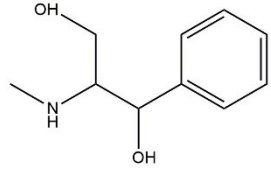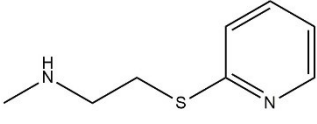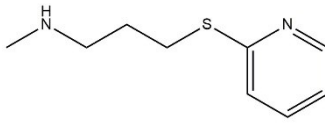
Hydrophobic interaction chromatography (HIC) is a useful tool for separating proteins based on their hydrophobicity, and is complementary to other techniques that separate proteins based on charge, size or affinity. HIC is a well-studied major polishing step in the purification of IgG-based products and is known for its capability to remove aggregated forms of the antibody [125-128]. HIC resins containing phenyl or butyl ligands [125, 129], and more recently these hydrophobic ligands have been used in combination with convective adsorbents, such as membranes and monoliths [104]. However, due to the high efficiency of proA affinity chromatography, HIC is mostly used as an intermediate purification step after the proA step or as a polishing step after ion exchange chromatography [84]. HIC in flowthrough (FT) mode is efficient in removing a large percentage of aggregates with a relatively high yield. HIC in bind-and-elute mode normally provides effective separation of process-related and product-related impurities from the antibody product. The majority of host cell proteins, DNA and aggregates can be removed from the target antibody through the selection of a suitable salt concentration in the elution buffer or by the use of a gradient elution method. For instance, Ghosh *et al.* [104] achieved the separation of humanized monoclonal antibodies from cell culture media using HIC with membranes composed of polyvinylidene, with a pore size of 0.1μm, obtaining a purity and recovery higher than 97 %. Although HIC is a very powerful tool in mAbs purification processes, there are two main limitations when used in the bind-elution mode. In general, HIC resins have relatively lower binding capacity and lower step yield compared to the other chromatography steps used in mAbs purification. Furthermore, sufficient binding of mAb proteins to HIC resins is usually achieved with increasing salt concentrations in the binding buffers, and the elution product pool from the HIC step purification may still contain large amounts of salt, which often complicates sample manipulations and process flow transitions during large-scale manufacture. Efforts have been done in this context, for instance by Ghose *et al.* [130] who reported an unconventional way of operating HIC in the FT mode, just by using sodium citrate and modulating the pH of the mobile phase to alter the surface charge of the protein, and thereby influence selectivity [130]. Future trends will pass through the improvement of the properties of HIC resins on two main areas: resin pore size optimization to facilitate mass transport of mAb molecules towards the ligand binding sites to increase the binding capacity, and hydrophobic charge induction (HCIC) chromatography design to allow the mAb molecules binding to the resin at lower salt conditions.
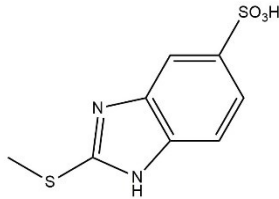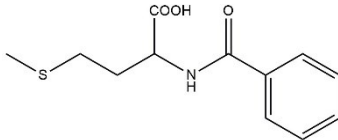
In the last decade, **multimodal chromatography** (MMC) has been receiving considerable attention [86]. MMC is a type of chromatography that involves multiple types of interactions between the stationary and mobile phases, comprising typically ion exchange, hydrogen bonding and hydrophobic interactions [131]. Nevertheless, other specific type of interactions (e.g., thiophilic, charge transfer, cation $\cdots \pi$) may be considered, and each of these individual interactions can be manipulated in accordance. MMC can be seen as a versatile chromatographic tool capable to lead to different selectivities and specificities when compared to chromatographic techniques based on more traditional ligands [86]. However, since multiple types of interaction can be promoted, the optimization of the best conditions for the chromatographic cycle that allow the purification of a target biomolecule can be indeed a complex process. Therefore, a screening of the most appropriate conditions is usually first performed, using design of experiments (DoE) [132, 133] and Monte Carlo simulations [134]. More recently, a microfluidic lab-on-a-chip has been proposed to screen binding and adsorption condition in less than 3 min and using only 210 nL of resin.

The most appropriate ligand should be selected for a specific purification approach. Thus, the knowledge of both protein and ligand structures and interactions can facilitate this task [86]. Two different moieties can be typically distinguished in multimodal ligands: an hydrophobic moiety (*e.g.* an aromatic or aliphatic group), and an ionic moiety (*e.g.* amino, carboxyl and sulfonic groups) [135]. The balance between the different moieties and possible interactions are crucial to define the capacity and recovery obtained in a given purification process. In particular, hydrophobicity can be promoted by including linear or heterocyclic groups that interact with proteins by aromatic, aliphatic, π-π stacking or cation-π interactions, allowing adsorption at moderate/high ionic strengths [136]. This can be seen as an advantage since it can be used to directly process cell culture supernatants. The ionic moiety contains either a positively or a negatively charged group, or both as in the case of hydroxyapatite, and its efficiency is highly associated to the pKa of the ionic group. The degree of dissociation of the ionic groups allows to predict the type of interaction that will occur between the protein and the ligand, namely attraction if both bear opposite charges or repulsion if they bear the same charge, which can be used to derive either adsorption or elution strategies. Other type of moieties can be found in the multimodal ligands, including hydrogen bond or electron-pair donor and acceptor groups. These also have been demonstrated to play a role in the process performance [137]. Furthermore, thiophilic interactions can also be considered, providing some advantages when dealing with the purification of immunoglobulins, particularly due to the high affinity of antibodies/proteins towards sulfur-containing ligands [138, 139]. The most

Monoclonal antibodies – addressing the challenges on the manufacturing processing of an advanced class of therapeutic agents

1

studied/used multimodal ligands were reviewed by Pinto et al. [86], and are summarized in **Table 1.2.4**.

Table 1.2.4. Examples of ligands employed in multimodal chromatography [86].

	Ligands	pKa	Chemical structure
Ligands positively charged	4-mercaptoethylpyridine (MEP HyperCel™)	4.85	
	Phenylpropylamine (PPA HyperCel™)	6.0 - 7.0	
	Hexylamine (HEA HyperCel™)	≈ 10	
	N-benzyl-N-methyl ethanolamine (Capto™ adhere)	-	
	2-aminomethylpyridine	pKa1 = 2.2 pKa2 = 8.5	
	Aminophenylpropanediol	9.0	
	2-(pyridin-2'-ylsulfanyl) ethanamine	-	
	3-(pyridin-2'-ylsulfanyl) propanamine	-	

35

Ligands negatively charged	2-mercapto-5-benzimidazole sulfonic acid (MBI HyperCel™)	-	
	2-benzamido-4-mercaptobutanoic acid (Capto™ MMC)	3.3	

One of the most studied ligands is Capto™ MMC (**Figure 1.2.6**), a weak cation exchanger containing in its structure a phenyl, an amide, and a thioether group, that is also able to establish hydrophobic, hydrogen-bonding and thiophilic interactions.

Hydrophobic interaction

Electrostatic interaction

Thiophilic interaction

Hydrogen bonding
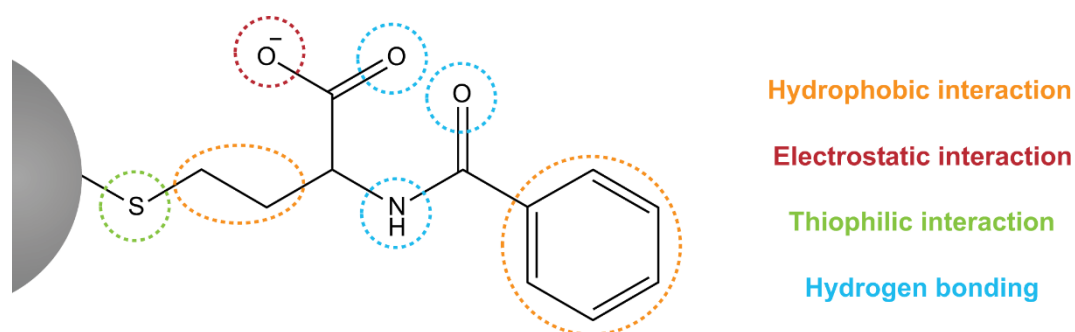
Figure 1.2.6. Molecular structure of a multimodal ligand commercialized for monoclonal antibodies purification (Capto™ MMC), evidencing the several interactions that could be integrated.

This hydrophobic multimodal ligand is able to maintain a high dynamic binding capacities at moderate/high values of ionic strength, being labelled as a "salt-tolerant" ligand [140]. Due to its advantages, it was recently patented for the direct capture of mAbs from cell culture supernatants [86]. Several studies have been reported in the literature reinforcing the potential of Capto™ MMC for the capture of antibodies from CHO cell cultures [102], with extraction yields ranging between 92 and 93 % and a purity level of ranging between 95 and 96 %.

Another multimodal ligand widely studied is the MEP Hypercel™ ligand, which yields comparable binding capacities to proA adsorbents, without ligand contamination/instability [86]. This ligand has shown to be successful in the capture and purification of mAbs from a protein-free cell culture, with an extraction yield ranging from 83 to 98 % and a purity level higher than 95 %, with a combined decrease of the viral load and DNA [141]. The best operational conditions in this

work were found to be neutral pH and physiological ionic strength. Furthermore, the elution can be easily performed by changing the pH, since it turns the ligand charged resulting in the desorption of the protein [142]. In the same line, it was reported the direct capture of antibodies from a fetal bovine serum (FBS)-containing cell culture supernatant, with a purity level of 69 %, and being further improved to values higher than 98 % using a second step of hydroxyapatite chromatography [105].

A more recent study relied on the use of phenylboronic acid (PBA) silica-based resins as a multimodal chromatography, and the authors proved a successful 100-fold scale-up with a recovery yield of 98 % and a protein purity of 83 % [106]. In summary, several characteristics that make these ligands attractive for application on an industrial scale can be highlighted, namely they are synthetic binders with a defined composition, they display enhanced chemical and physical stability, and can be modified or tailored to provide adequate selectivities allied to cost–effectiveness (resins can cost 5-10 times less than proA resin). However, it is difficult to predict the promoted interactions and to optimize the operating window, and it is also laborious and expensive to perform the screening studies and to use high-throughput screening platforms. Although the results are not as good as the obtained with proA chromatography, this technique is seen as a promising alternative for the established platform.

Affinity chromatography, introduced in 1968, by Cuatrecasas and co-workers [143], is based on a biochemical separation that relies on a reversible specific interaction occurring between the protein and the ligand, e.g. binding of an antigen to its specific antibody. The specificity of binding provided by the ligand to the target protein present in a complex mixture is behind the good results that can be obtained. The target protein is then eluted either by using competitive analogs, denaturing agents or by changing the pH, ionic strength or polarity of the eluent. Essentially due to the improved results that can be obtained, this type of chromatography has been the most used for antibodies purification [29]. Most efforts in this arena envisaged the improvement of the purification process, comprising issues such as specificity, selectivity, reproducibility, recovery, and packaging. In this context, the identification and design of novel affinity ligands and matrices for immobilization played a major role, in which the optimization of the process always depends on the type of antibody and its ability to recognize the ligand. Recently, a type of affinity chromatography was proposed by Schwark *et al.* [107], where epitope-imprinted membranes targeting the C-terminal fragment of IgG heavy chain was developed and used for the purification of a commercial monoclonal antibody. Yields of extraction ranging between 80 - 90 % were achieved from a cell culture broth after production of anti-IL-8 antibody, and the depletion of host cell proteins using

the best performing imprinted membrane under low-salt conditions reached 88 % (0.7–1.2 log units), implying an effective removal of impurities from the cell culture supernatant. Castilho *et al.* [108] showed the potentiality of three affinity membranes as adsorbents for the purification of IgG, namely membranes based on Nylon 66 coated with low-molar-mass dextran or poly(vinylalcohol), as well as commercial pre-activated polysulfone (Ultrabind®) and regenerated cellulose (Sartobind®) membranes, carrying Protein-A ligands, demonstrating high affinity for human IgG. Besides the high association constants, Protein-A adsorbers based on polysulfone and regenerated cellulose membranes showed also enhanced charge-to-charge consistency, simpler preparation procedure, membrane sterilizability, good selectivity for IgG purification from cell culture supernatants and good stability throughout repeated adsorption–elution cycles.

Immobilized metal affinity chromatography (IMAC) is also a widely used method for the purification of antibodies, since biomolecules with exposed His, Cys, Ser, Glu, Asp and Trp have affinity towards metal ions [144-146]. This feature is exploited in designing ligands for IMAC, which are attached to a matrix via a covalently linked chelating compound and spacer group [130]. Commonly used chelating compounds are iminodiacetate (IDA) and nitrilotriacetate (NTA) which are classified as tri and tetradentate ligands based on the number of coordination sites that are available to each transition metal ion used in IMAC, such as Ni^{2+}, Cu^{2+}, Co^{2+}, Zn^{2+}, Fe^{3+} and Ga^{3+} [147]. The number of electron pair donor atoms (e.g. nitrogen, oxygen and sulfur) on the chelating compound determines the strength and the binding stability of the metal-chelate complex. **Figure 1.2.7** exemplifies the interaction mechanism in IMAC, where a tridentate chelating agent IDA coordinates with the nickel atom, which also interacts with the histidine tail present in a random protein.
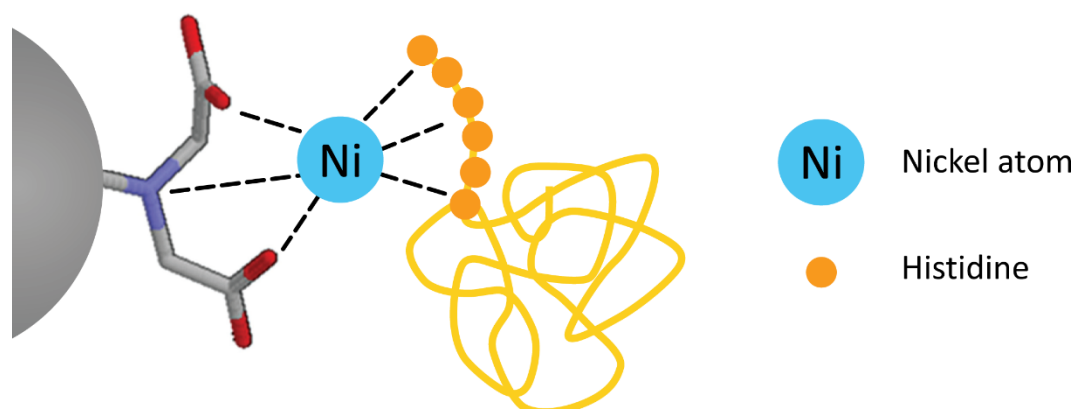
Figure 1.2.7. Schematic representation of the interaction mechanism in immobilized metal affinity chromatography. The tridentate chelating agent IDA (iminodiacetic acid) coordinates with the nickel atom, which also interacts with the histidine tail present in the protein.

It should be remarked that this histidine tail is not commonly present in antibodies; however, IMAC can be used to purify antibodies due to the presence of accessible histidine residues on the surface of the biomolecules that allow a similar interaction. Vançan and co-workers [109] compared four metal ions and buffer systems for the purification of IgG from human plasma and showed high purity absorption of IgG for all metals irrespective of the buffer system used. The ligands (metal chelates) in IMAC are of low cost and have high stability, capacity, simplicity, and selectivity. It is a versatile technique since the same ligand can be used for the purification of different proteins and the same chelating resin can be used to chelate different metal ions [148-150]. An important aspect in IMAC method is the occasional leakage of metal ions from the resin, leading to metal ions contamination of the final product. In this case, a column packed with metal-free matrix derivatized with a strong chelating ligand, such as TED (Tris(carboxymethyl)ethylenediamine), could be used to trap any metal ions present in the eluate without altering the chromatographic time or the purification effectiveness [149]. Despite the IMAC potential as a less expensive alternative to biological affinity, a note of caution is in order: polynucleotides, endotoxin, and virus, have all been shown to bind to various immobilized metals. On the other hand, IMAC has also been used to selectively bind antibody fragments while endotoxins were removed by washing with a surfactant solution [151].

Regarding the chromatography-based methods, it is possible to highlight the work developed by González *et al.* [110] using **expanded-bed affinity chromatography**, allowing them to obtain extraction yields of 92 % with a purity level of 98 %. Finally, it is still possible to emphasize **continuous annular chromatography** as a viable alternative for IgG purification, as reported by Giovannini *et al.* [111] using proA as ligand, obtaining extraction yields ranging from 77 % to 82 %, and with the substitution of this ligand by hydroxyapatite, the extraction yields increased for the range between 87 % and 92 %.

Taking into account that most of the production costs of a biological product rely in the chromatographic steps, there is a great need for efficient, effective and economical (non-)chromatographic bioseparation techniques, capable of being scalable and that simultaneously lead to a high yield and purity degree, while maintaining the biological activity of the molecule. In this context, new non-chromatographic technologies have been developed as alternative strategies. The main techniques used in this field include preparative electrophoresis [112, 113], affinity precipitation [114-116], magnetic separation [117-119], membrane filtration [108, 152], and aqueous two-phase systems (ATPS) [153]. This last technique was not previously mentioned in

Table 1.2.3. However, due to their promising character, the main studied ATPS will be summarized and discussed below.

    Preparative electrophoresis has proved to be a viable strategy for the purification of IgG, based on charge and size phenomena. Lim *et al.* [112] reported the use of gradiflow technology, by using a set of polyacrylamide separation membranes to separate molecules based on their size and charge. By tailoring the pH and pore size, the researchers [112] were able to separate IgG with 80 % of recovery yield. Thomas *et al.* [113] developed a similar study, using the same gradiflow technology, through which they reported yields of IgG extraction ranging from 80 % to 90 %. This technology proved to be a viable alternative since in addition to lead to acceptable recovery yields of antibodies, it is a method that does not depend on a variable binding interaction, it is applicable to a broad species spectrum, presents low cost and can be applied on an industrial scale.

    Affinity precipitation has also been considered as an alternative for the conventional chromatography column. Precipitation consists in a simple and low-cost fractionation technology, in which proteins are precipitated and further resuspended, while restoring their functional characteristics [2]. This methodology can be used in two different strategies: 1) to remove impurities; or 2) to isolate the target protein. The first case leads to a precipitate containing the impurities that are discarded during the recovery step, whereas in the second approach, the target protein is precipitated and then resuspended in a small volume of a buffered aqueous solution. This step also allows to decrease the sample volume and to concentrate the target protein. However, the major drawbacks of this technology are related with its low resolution, low specificity, the cost of the precipitating agents, and the environmental impact when these agents are discarded, particularly when scaled-up processes are envisioned. In order to overcome the selectivity limitation, affinity ligands can be used. As demonstrated by Taipa *et al.* [114], IgG can be isolated from cell culture supernatants by precipitation of affinity with a heterobifunctional ligand derived from Eudragit S-100, yielding 68 % of IgG with a 8-fold purification factor. Dainiak *et al.* [115] also studied IgG affinity precipitation, but using the glyceraldehyde-3-phosphate dehydrogenase ligand (GAPDH), with extraction yields higher than 98 %, albeit with a purification factor of only 1.8 times. More recently, Handlogten *et al.* [116] have shown to greatly improve the affinity precipitation process using a bivalent peptidic hapten, with a yield higher than 85 % and a purity level higher than 97 %. In summary, the target protein adsorbs to the polymer and the affinity complex precipitates by a proper manipulation of the operational conditions. This affinity complex is then separated from the impurities by centrifugation. Finally, the target protein can be dissociated from the affinity

complex under appropriate conditions, allowing the recovery of the target protein and the reuse of the ligand [153].

Magnetic separation also consists in a versatile non-chromatographic method, capable to purify target biomolecules from crude extracts. The process is based on the use of magnetic adsorbents in combination with a magnetic concentrator, and an example of a magnetic separation process is depicted in **Figure 1.2.8**.
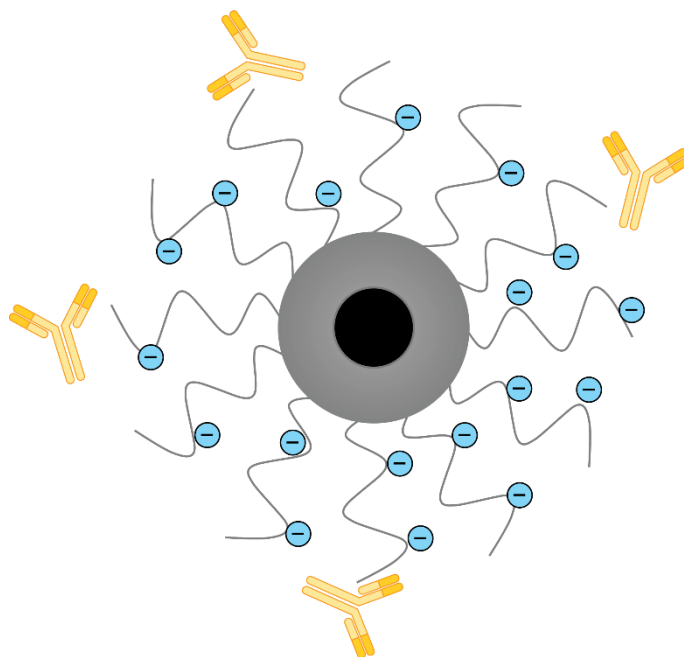
Figure 1.2.8. Schematic representation of a magnetic separation process exemplifying the adsorption of antibodies on a modified magnetic nanoparticle with a negatively charged polymer.

Holschuh *et al.* [117] demonstrated the feasibility of protein A coated magnetic particles in the preparative purification of a monoclonal antibody from a 100 L cell culture supernatant. The separation process was performed with a separation efficiency of more than 99 % at a flow rate of 150 L·h^{-1}. In comparison with conventional column and expanded bed chromatography, similar yields and purities were achieved but with much faster processing times. Later, Borlido *et al.* [154] used commercially available silica magnetic particles functionalized with phenylboronic acid (SiMAG-Boronic acid) to selectively capture mAbs directly from CHO supernatant with an overall yield of 86 % while removing 88 % of the CHO host cell proteins (HCP) and more than 97 % of the CHO genomic DNA. In a different approach, thermo-responsive magnetic particles composed of a poly(methylmethacrylate) magnetic core with a N-isoproylacrylamide-co-acrylic acid polymeric shell were used as cationic exchangers for the purification of mAbs from a dialyzed CHO supernatant

[118]. The antibody was able to be recovered with an overall yield of 64 % and an HCP removal higher than 98 %.

More recently, Gagnon *et al.* [119] reported 69 % of IgG recovery with more than 99 % removal of HCP using magnetic starch-coated nanoparticles. Taking into account all the information mentioned before, it can be concluded that magnetic separation consists in a fast and smooth process, which combines the capability of scale-up with the possibility of automation, allows the separation and purification of mAbs in few minutes, and once the contaminants are tolerated, there is no need to perform any filtration or centrifugation prior to sample loading, which supports the potential of this technique for mAbs purification. However, the lack of large scale magnetic separators and the high cost of commercially available magnetic particles are the major challenges faced by this technology [155].

High performance tangential flow filtration (HPTFF) is a technique based on electrostatic interactions between proteins and charged ultrafiltration membranes [151]. Although potential exists for solutes to be retained by these interactions, antibody selectivity is mediated by ion exclusion. A positively charged ultrafiltration membrane repels (rejects) positively charged proteins such as IgG, despite them being small enough to pass through the pores. This permits their selective retention and concentration in the retentate, while weakly alkaline, neutral, and weakly acidic contaminants pass through the membrane, being collected in the permeate. **Figure 1.2.9** depicts a schematic representation of a HPTFF process using ultrafiltration (UF) membranes positively charged.
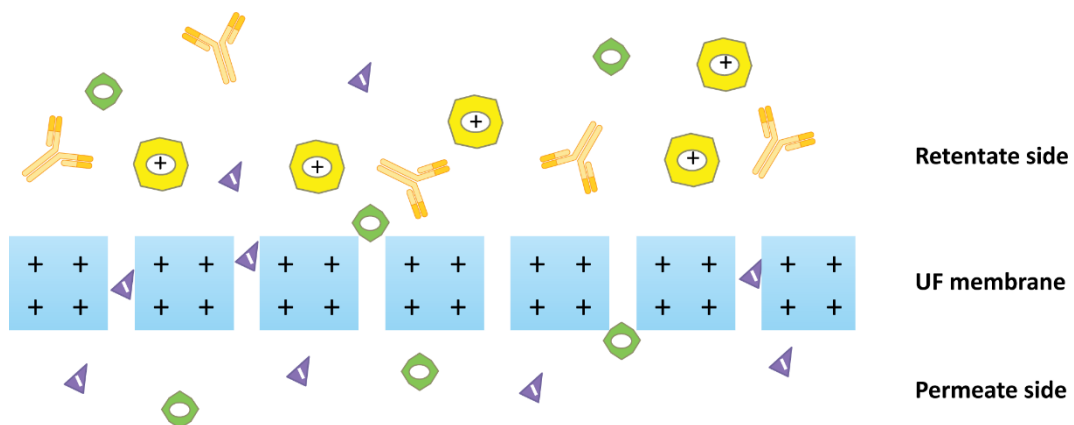
Figure 1.2.9. Schematic representation of HPTFF process illustrated for the specific case of antibody purification using positively charged ultrafiltration (UF) membranes.

Concerning this technique, van Reis *et al.* [120, 121, 156] published several works concerning the use of membranes. In a first study [120], the authors were able to demonstrate that HPTFF

using composite regenerated cellulose membranes, Biomax™ modified polyethersulfone membranes, and conventional regenerated cellulose membranes, leads to purification factors and yields for IgG-BSA separations comparable to those of a range of commercial protein separation processes. In a further work, although the authors [156] did not focus on the purification of monoclonal antibodies, they proved that this technique is a powerful tool for the purification of proteins. The authors [156] reported an HPTFF-based process at pH 8.4 with a Biomax™ 100 negative membrane, which resulted in 94 % BSA recovery yield with a 990-fold increase in the purification in linear scale-down systems representative of existing industrial scale systems. More recently, a scheme for the purification of a human pharmaceutical antibody fragment expressed in *E. coli*, using positively charged cellulosic membranes (Ultracell™ composite regenerated cellulose membranes chemically modified *in situ* using bromo-propyl-trimethylammonium bromide) was proposed [121]. HPTFF was shown to successfully enable the concentration, purification and formulation in a single unit operation, with a 10-fold removal of *E. coli* host cell proteins (HCP) and an overall process yield of 98 %. The HPTFF performance was shown to be robust and reproducible, and the authors regenerated and re-used the membrane for seven times without loss of selectivity or throughput [121].

Finally, there is a classical technology, quite established in the pharmaceutical industry, named liquid-liquid extraction, that recurs to the use of organic solvents for purification purposes from aqueous media [2]. However, these organic solvents are in most cases very volatile, flammable and toxic, and proteins, in particular, present low solubility and high propensity for denaturation in the presence of these type of solvents [157]. Thus, their use in biotechnological processes is limited only to the recovery of low molecular weight products, such as antibiotics and organic acids from fermentation media [158]. Within liquid-liquid extraction techniques, **aqueous two-phase systems (ATPS)** can be considered. They have demonstrated an enormous potential and versatility for the downstream processing of biopharmaceuticals, such as monoclonal antibodies, hormones, cytokines, growth factors, and plasmid DNA [2]. Due to their potential as a non-chromatographic alternative technique for the extraction and purification of mAbs, they are discussed below in more detail.

1.2.8. Aqueous biphasic systems

Aqueous biphasic systems (ABS), also known as aqueous two-phase systems (ATPS) fall within the liquid-liquid extraction techniques since they allow the extraction/migration of (bio)molecules from one liquid phase to another, in which both phases are mainly composed of water. In 1896,

Beijerinck reported for the first time the incompatibility and formation of two aqueous phases of solutions of agar with starch or soluble gelatin [159]. However, it was only in 1955 that ATPS were reported as a separation technique by Albertsson, who demonstrated that polyethylene glycol (PEG), phosphate salts and water, as well as PEG, dextran and water formed two immiscible aqueous phases aqueous above given concentration [160]. One of the phases is enriched in one of the solutes, while the other phase is enriched in the second phase-forming component. These solutes may be two polymers (for example PEG and dextran), a polymer and a salt (for example PEG and sodium phosphate) or other type of combinations [161]. The main advantages inherent to ATPS are related with the fact that it is a relatively simple technique, with a low cost associated, easy to operate and to apply on an industrial scale, with a high resolution capacity [2]. In addition, ATPS provide a highly biocompatible environment since both phases have a high water content and the majority of the polymers used can have a stabilization effect on the tertiary structure of proteins and on their biological activity [162].

The selective partition of a given product between the two coexisting phases represents the basis of the separation using an ATPS system [2]. This partition is controlled by several parameters, related with the properties of the system, the target solute, and the interactions between both. Concerning the system properties, several factors that influence the partition can be highlighted, namely the chemical nature of the phase-forming components, their molecular weight and concentration, system pH and ionic strength; regarding the properties of the target solute involved in the partition, it is possible to emphasize the charge, molecular weight, hydrophobicity and conformational characteristics. The complexity of the interactions involved (chemical and physical) in the partitioning process make these systems quite powerful contrary to other established purification methodologies, since it is possible to achieve a high resolution only by manipulating the intrinsic properties of the system [163]. However, all this complexity of ATPS coupled with the fact that partition mechanisms are still poorly understood, undermine the prediction of the effectiveness of a particular ATPS [164].

Each ATPS has a single phase diagram under a particular set of conditions, such as temperature and pH [162]. As shown in **Figure 1.2.10**, the binodal curve (ABCD) divides two regions: the monophasic region (below the curve), where the system presents only one phase, and the biphasic region (above the curve), that represents the solutes concentrations at which the system forms two aqueous immiscible phases [161].
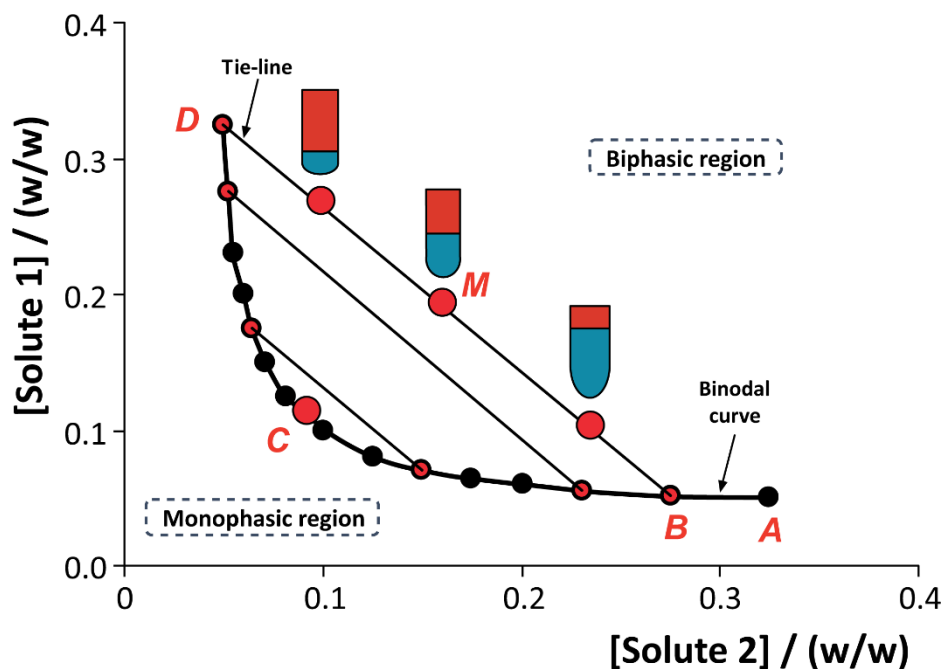
Figure 1.2.10. Schematic representation of a phase diagram of an ATPS composed of two different solutes, in weight fraction, and where the concentration of water is omitted.

In this figure it is also possible to identify the M point, which corresponds to a mixture point in the biphasic region, and whose composition of each phase acquires the designation B and D, since they are the end-points (nodes) of a specific tie-line (TL) where the mixture point is comprised. It is possible to select several mixing points along the same TL, differing only in the total system composition and volume ratio of the phases, while keeping the exact composition of the two coexistent phases (B and D) [162]. The tie-line length (TLL) is a numerical indicator of the composition difference between the two phases and is generally used to correlate trends in the partitioning of solutes between both phases [161].

One of the most common polymers used in the formation of ATPS is PEG [165]. PEG is a polyether diol, commercially available in a wide variety of molecular weights [166]. This polymer is widely used mainly due to its interesting characteristics, namely its high biodegradability, low toxicity, low volatility, low melting temperature, high miscibility in water and low cost [167]. Moreover, PEG significantly accelerates the renaturation of proteins, allowing the recovery of their biological activity, and consequently presenting a stabilizing role in their structure [168]. However, there are other polymers that can be used in the formation of ATPS, such as dextran. This is a more expensive hydrophilic polymer when compared to PEG, although also commercially available in a wide variety of molecular weights [2, 169]. Regarding the separation of the phases in a solution containing a mixture of polymers, the phenomenon has been treated from a more fundamental

point of view through the application of several theories that involve the thermodynamic properties of the polymers in solution [162].

In **Figure 1.2.11** is represented an example of a process based on the use of ATPS for the extraction and purification of antibodies from a complex matrix containing several impurities, where the antibodies are extracted to the upper phase, while the other impurities are retained in the opposite layer of the system.
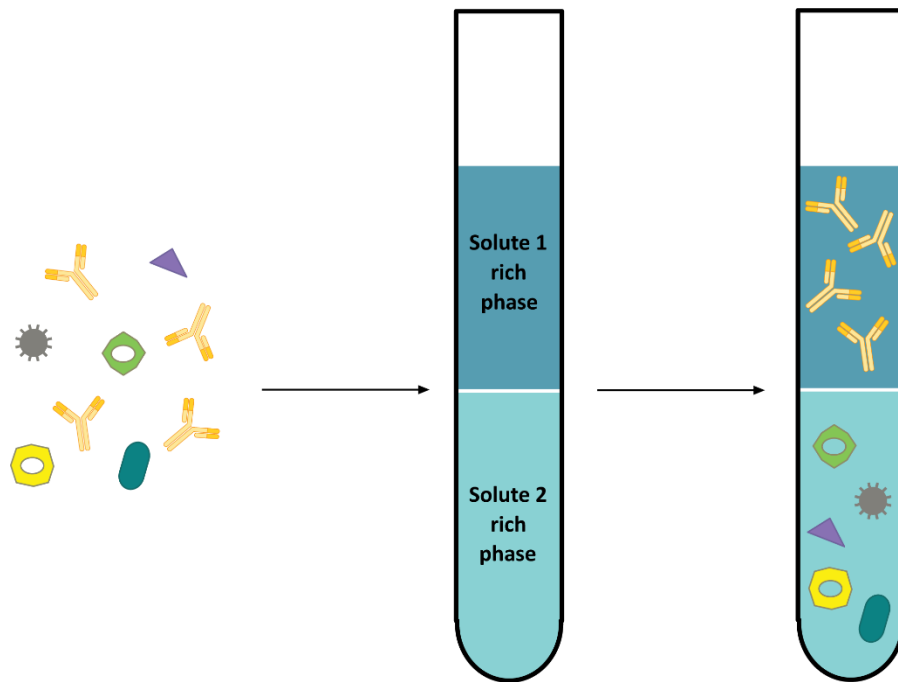
Figure 1.2.11. Schematic representation of the extraction/purification of antibodies using ATPS.

The first study that suggested the use of ATPS for antibody purification was conducted by Andrews *et al.* [170], in 1990, using a proA-modified PEG molecule. However, the costs of this ligand impeded the approach proposed to be used on a wider scale [170]. Later, in 1992, Sulk *et al.* [171] proposed an extraction procedure using an ATPS consisting of 5 % of PEG 1540 and 22 % of phosphate buffer coupled to a final purification step using thiophilic absorption chromatography. The IgG1 monoclonal antibody against horseradish peroxidase from hybridoma cell culture supernatant was recovered in the PEG-rich top phase, with a process overall yield of 71 %, with 90 % recovery in the ATPS step and a purification factor of 6.2. Later, Andrews *et al.* [172] described a polymer-salt ATPS that allowed the recovery of a mouse antibody from a hybridoma cell supernatant in two step process. The extraction of IgG to the PEG-rich phase was performed with an ATPS composed of 15 % of PEG 1500, with a low concentration of phosphate and NaCl (14 and 12 %, respectively) and at pH 5.5, with a recovery yield of 90 % and a purification factor of 2.7. IgG

was subsequently re-extracted to a fresh phosphate solution, and the most hydrophobic compounds, which partitioned alongside with IgG, were further removed by hydrophobic interaction chromatography, using an ammonium sulfate solution as the mobile phase. In the same line, Ziljstra *et al.* [173, 174] coupled a triazine mimetic-dye to PEG molecules to recover IgG from hybridoma cells grown in the dextran-rich phase. More recently, in 2015, Muendges *et al.* [175, 176] published two studies on the extraction and purification of IgG from CHO cell lines through a single-stage and by using a multi-stage aqueous two-phase extraction. In the single-stage approach, the authors [176] were able to extract IgG1 from a CHO cell culture supernatant with a system composed of PEG 2000 and sodium phosphate at pH 6 with an yield higher than 90 % and purification factor up to 3.1. However, the authors found that it is necessary to carry out a multi-stage approach to achieve a higher purity of IgG1 [177].

More recently, Aires-Barros and co-workers [17, 155, 163, 178-191] reported the successful use of ATPS for the purification of antibodies from distinct supernatants of cell lines, namely hybridoma and CHO cells. **Table 1.2.5** presents a comparison between the performance of different ATPS in terms of recovery yields and purity levels studied by Aires-Barros and co-workers [17, 155, 163, 178-191]. ATPS based on PEG/phosphate [163, 178-181, 190], PEG/sodium citrate [182, 183], PEG/dextran [17, 155, 184-188, 191], and UCON/dextran [189], have been used for the extraction and purification of antibodies from real matrices.

The addition of NaCl to a PEG/phosphate-based ATPS allowed the separation of IgG from an artificial mixture of albumin and myoglobin [163], and the purification of IgG from both hybridoma and CHO cell supernatants [178]. Using this type of systems the authors simulated a countercurrent chromatography process to separate IgG from the remaining impurities [179]. In addition, this type of ATPS has already been tested on a pilot scale and showed to be equally efficient [180]. On the other hand, this ATPS was also incorporated into a microfluidic platform proving its reduction to the microscale [181]. The use of a battery of mixer-settlers separators to carry out a continuous multi-stage extraction of IgG from supernatants of two different types of cell lines was also investigated, and where promising results were obtained [190]. Essentially due to the concerns associated with the use of phosphate salts, other alternatives have been studied, namely ATPS consisting of PEG and sodium citrate, in the presence and absence of NaCl, for the recovery of human antibodies from a hybridoma and a CHO cell supernatants [182, 183]. The authors [182] demonstrated that ATPS can be integrated in a process involving HIC and size-exclusion chromatography (SEC), and that it is also possible to apply a back-extraction/purification step that

allows not only an improvement on the IgG purification but also allows the separation of the antibody from the polymer [183].

In order to improve the IgG specificity to the PEG-rich phase in PEG/dextran ATPS, PEG functionalized with various ligands [185-187] or including some additives, such as triethylene glycol-diglutaric acid (TEG-AG) or a choline binding polypeptide tag fused to the synthetic antibody binding Z-domain (LYTAG-Z), have been studied [184, 188, 191]. With this approach, an increase the systems selectivity for IgG and higher yields of extraction have been obtained. Included in the versatility of the techniques applied for the purification of IgG, a hybrid process combining ATPS with magnetic separation was also developed [155].

Table 1.2.5. ATPS investigated by Aires-Barros and co-workers for the extraction and purification of antibodies, compared in terms of system performance, namely IgG recovery yield and purity level.

Composition of ATPS	IgG origin	Recovery yield (%)	Purity level (%)	Ref.
8 % PEG 3350 + 10 % phosphate + 15 % NaCl, pH 6	AM	76	100	[163]
12 % PEG 6000 + 10 % phosphate + 15 % NaCl, pH 6	CHO	88	PF = 4,3	[178]
12 % PEG 6000 + 10 % phosphate + 15 % NaCl, pH 6	HYB	90	PF = 4,1	[178]
8 % PEG 3350 + 10 % phosphate + 10 % NaCl, pH 6 5 steps: ATPS + 4 countercurrent steps	CHO	89	75	[179]
PEG 3350 + phosphate Pilot scale with continuous extraction using ATPS in countercurrent	CHO	85	50	[180]
PEG 3350 + phosphate + NaCl, pH 6 3 steps: extraction, re-extraction and washing	CHO	80	97	[190]
PEG 3350 + phosphate + NaCl, pH 6 3 steps: extraction, re-extraction and washing	PER.C6	100	97	[190]
10 % PEG 3350 + 12 % sodium citrate, pH 6 3 steps: ATPS + HIC + SEC	CHO	90	100	[182]
8 % PEG 3350 + 8 % sodium citrate + 15 % NaCl, pH 6 2 steps: extraction, back-extraction	HYB	99	76	[183]
PEG 150-GA + dextran 500000	CHO	93	PF = 1,9	[185]
10 % PEG 3350-GA + 5 % dextran 500000 2 steps: ATPS + CEX	CHO	73	91	[187]

8 % PEG 3350-GA + 5 % dextran 500000 + 10mM potassium phosphate, pH 7	CHO	97	94	[186]
8 % UCON 2000 + 6 % dextran 500000 + 20 % TEG-GA 2 steps: extraction and re-extraction	CHO	85	88	[184]
7 % PEG 3350 + 5 % dextran 500000 + 1.3 % TEG-GA, pH 4	CHO	96	43	[188]
7 % PEG 3350 + 5 % dextran 500000 + 1.3 % TEG-GA, pH 4 5 steps: ATPS + 4 countercurrent steps	CHO	95	85	[188]
8 % UCON 50HB-3520 + 5 % dextran 500000, pH 5 2 steps: extraction and re-extraction	-	82	-	[189]
7 % PEG 3350 + 5 % dextran 500000 + 300 mM NaCl, pH 3	HYB	72	-	[17]
7 % PEG 6000 + 5 % dextran 500000 + 150 mM NaCl, pH 3	HYB	84	-	[17]
8 % PEG 3350 + 5 % dextran 500000 + 200 mM NaCl + GA-APBA-MP	CHO	92	98	[155]
7 % PEG 3350 + 5 % dextran 500000 + LYTAG-Z	HYB	89	42	[191]

ATPS – aqueous two-phase system; AEX – anion exchange chromatography; AM – artificial mixture; CEX – cation exchange chromatography; CHO – Chinese hamster ovary cells; GA – diglutaric acid (COOH); GA-APBA-MP – gum arabic coated particles modified with aminophenyl boronic acid; HIC – hydrophobic interaction chromatography; HYB – hybridoma cells; LYTAG-Z – choline binding polypeptide tag fused to the synthetic antibody binding Z-domain; PEG – polyethylene glycol; PER.C6 – human embryonic cells derived from retinoblasts; PF – purification factor; SEC – size-exclusion chromatography; TEG-GA – triethylene glycol diglutaric acid; UCON – ethylene oxide/propylene oxide.

In order to be applied and administered to humans, the extracted and purified antibodies must have an exceptional purity degree. According to the CFR-Code of Federal Regulations, purity means the relative freedom of foreign matter in the final product, not being harmful to human use or harmful to the product [192]. Therefore, impurities must be kept to minimum levels in order to minimize the associated risks, in particular immunogenic problems that may arise from the presence of those contaminants. The systems composed of 8 % of PEG 3350, 10 % of phosphate buffer with 15 % of NaCl [163], and 10 % of PEG 3350 with 12 % of sodium citrate [182], are quite relevant in this line since they allow to obtain 100 % purity of IgG. However, it is important to note that the first system [163] aimed at purifying IgG from an artificial mixture containing IgG, albumin and myoglobin (the major protein impurities present in serum-containing cell culture supernatants), so it is difficult to extrapolate this result to the reality, since a real matrix is much more complex. In the second system [182], 100 % purity was reached as the result of 3 extraction

steps: 1 step with ATPS and 2 subsequent chromatographic steps (HIC and SEC). This result, when compared to the 3-step chromatographic platform [99] presented in **Table 1.2.3**, which allowed the recovery of 85 % of IgG with a purity higher than 99 %, is more promising since it reduces one chromatographic step, allowing even higher yields of IgG (90 %) with a comparable purity level. Comparing these results with the isolated use of HIC [104], it is found that it is not possible to reach the same level of purity, since the authors have shown only 97 %, and, despite being a high purity level, it is not able to compete with the current established platform. In this context, ATPS appears to be an interesting alternative that deserves to be explored in more detail, since excellent results were already achieved.

Another advantage of ATPS is that clarification, purification and concentration can be integrated in a single step. In fact, the productivity, yield and economy of bioprocesses can be considerably improved by process integration, facilitating the development of scalable and efficient bioprocesses [193]. Thus, there is nowadays a strong demand for intensification and integration of process steps to increase yield, reduce the process time and cut down in running costs and capital expenditure. Besides these advantages, integrated processes still wait for broad industrial application, since it has a complex development, and there is a need for detailed process knowledge of the applicant [194]. Efforts have been made in this line, and there are already several works described in the literature that report the integration of clarification, capture, purification and concentration in one ATPS step [17, 191, 195, 196]. Platis *et al.* [196] successfully developed and optimized an ATPS composed of 12 % of PEG 1500 and 13 % of phosphate buffer at pH 5 for the purification of mAb 2F5. Through the incorporation of this system in a downstream processing protocol, the authors [196] achieved a clarification of the plant extract, removal of the plant derived compounds, such as phenolics and alkaloids, and partial purification of the antibody (3–4-fold purification, with 95 % recovery at the bottom phase). Later, the same authors [195] used a system composed of 13.1 % of PEG 1500 and 12.5 % of phosphate buffer at pH 5 for the purification of anti-HIV mAbs 2G12 and 4E10 from unclarified transgenic tobacco crude extracts. Both mAbs partitioned to the bottom salt-rich phase with 85 and 84 % yield and 2.4- and 2.1-fold purification factor, respectively. Furthermore, the ATPS was integrated in an affinity-based purification protocol, using proA, yielding antibodies of high purity and yield [195]. Therefore, a simple and effective way for the bioprocessing of therapeutic antibodies in two steps (ATPS + affinity chromatography) was proposed by the authors, suitable for analytical or clinical purposes. Also Silva *et al.* [17] proposed an ATPS composed of 7 % of PEG 6000, 5 % of dextran 500,000 and 150 mM of NaCl at pH 3, able to recover approximately 84 % of IgG with only 0.1 % of cells in the top phase,

Monoclonal antibodies – addressing the challenges on the manufacturing processing of an advanced class of therapeutic agents

1

phase in which the antibody was retained, and with a clearance of cells higher than 99.8 % . More recently, Campos-Pinto *et al.* [191] proposed a strategy to integrate the clarification and the primary recovery of mAbs from a complex medium containing Hybridoma cells, based on the use of a single-step ATPS composed of 7 % of PEG 3350 and 6 % of dextran 500,000 and the dual tag ligand LYTAG-Z. Based on the capacity of this system to tolerate solid components/impurities, allowing the simultaneous clarification of the media, purification and concentration, ATPS are thus promising downstream processed when compared, for example, with chromatography, that requires a limpid and clear solution to be loaded.

Other researchers have also recently suggested new methods for the separation and purification of IgG from various non-conventional matrices. Rito-Palomares *et al.* [197] studied ATPS consisting of PEG 1000 and phosphate buffer at pH 9 for bovine blood processing in an approach comprising two steps: extraction and re-extraction. Through this approach, the authors [197] verified that soluble proteins such as bovine serum albumin (BSA), haemoglobin and IgG partition into the PEG-rich top phase, while the cell debris (such as clotting factors and blood cells) are partitioned mostly into the salt-rich bottom phase. A back extraction of the soluble protein into a second phosphate-rich bottom phase resulted in a maximum overall protein recovery of 62 %, and the authors [197] proved the recycling of the PEG-rich phase up to 5 cycles. It is also possible to highlight the investigations of Vargas *et al.* [198] that reported a new method of plasma fractionation using an ATPS formed by PEG 3350, potassium phosphate and NaCl at pH 6. Wu *et al.* [199] found that the system consisting of 12 % of PEG 4000, 18 % of hydroxypropyl starch (HPS) and 10 % of NaCl at pH 8 is promising for the primary recovery of IgG from a HSA containing feedstock, attaining an yield of 99.2 % with a purification factor of 5.28 in a single step. With the addition of a back extraction step the authors [199] reported a 84.0 % yield with a purification factor of 5.73. More recently, Freire and co-workers [200] investigated the use of ATPS formed by bio-based ionic liquids (ILs), composed of ions derived from natural sources, and biocompatible polymers for the extraction and purification of IgG from rabbit serum. The authors [200] reported the recovery of *ca.* 85 % of antibodies with a 58 % enhancement in the IgG purity when compared with its purity in serum samples. The same research group [201] also reported the use of ILs as adjuvants in the formation of ATPS composed of polyethylene glycol and a buffered salt. The best results were achieved with a system composed of 25 % of PEG 400, 25 % of $C_6H_5K_3O_7$/$C_6H_8O_7$ and 5 % of 1-butyl-3-methylimidazolium acetate ($[C_4mim][CH_3CO_2]$) where the complete extraction of IgG in a single-step was achieved with the purity in the polymer-rich phase enhanced by *ca.* 37 % as compared to the IL-free ATPS.

One of the major research groups that works directly within the monoclonal antibody purification area using ATPS is the Platis and Laubrou research group in Athens, which study transgenic plants, more specifically the tobacco plant [195, 196, 202]. Plant biotechnology has demonstrated that transgenic plants are suitable hosts for expressing recombinant biomolecules. Several reagent-grade recombinant proteins from transgenic corn (trypsin and avidin) [203, 204] and rice (lysozyme and lactoferrin) [205, 206] have been commercialized, while clinical trials for plant-derived therapeutic proteins (e.g. interferon alpha-2b) are underway [207]. Future progress in utilizing transgenic plants for biopharmaceuticals production will depend on the efficiency of the purification methods, since in those cases, purification steps also play the most significant fraction of the final products [208]. The tobacco plant has the same glycosylation pattern as humans, whereby the production of humanized monoclonal antibodies through this plant is possible and viable. The main benefits are the low production costs and the low risk of human contamination, since they are of plant origin. ATPS proved to be a beneficial system for the purification of plant proteins, which would otherwise have to resort to several chromatographic steps, namely ion exchange chromatography (IEX), molecular exclusion and affinity chromatography [202]. The authors [196] studied systems composed of PEG 1500 and phosphate buffer, which allowed the removal of potentially harmful secondary metabolites of the tobacco plant. Moreover, it was possible to couple this purification method, essentially for the removal of polyphenols, with CEX and metal affinity chromatography, increasing even more the purification levels [202], and there is already evidence of the selective partition of mAbs and plant cells fragments to opposite phases [195]. The purified mAbs were always analyzed by protein electrophoresis, ELISA and western blot, demonstrating the activity of mAbs and proving their purity concerning degraded variants, polyphenols and alkaloids [195, 196, 202].

In summary, some promising results have been achieved in the extraction/purification of IgG from various complex matrices, in particular from biological matrices, such as bovine blood, hybridoma and CHO cell culture supernatants, rabbit serum or even transgenic plants. The differences obtained with the various studies are related with the modification of the ATPS phase-forming components, their concentration, pH, presence or absence of additional ligands, addition of electrolytes and use of additional or combined/hybrid purification steps. It is however important to note that the need to resort to additional extraction/purification steps makes the process more complex and less cost-effective. In general, it is noticeable that one of the most used phase-forming components of ATPS is PEG, possibly due to its previously discussed biocompatibility characteristics. Nevertheless, the search on new affinity ligands, electrolytes and phase-forming components is

Monoclonal antibodies – addressing the challenges on the manufacturing processing of an advanced class of therapeutic agents

1

very important since it can lead to significant improvements on the selectivity of ATPS for target biomolecules.

1.2.9. Conclusions

This chapter provides a global vision on the current state-of-the-art regarding the manufacturing and possible applications of monoclonal antibodies, while highlighting new trends to improve their purification process. The most used technologies for the production of mAbs were presented and discussed, with the mammalian cell technology established as the golden standard for the upstream processing of mAbs. In the downstream side, new and alternative process strategies are still under development, in order to reduce the number of steps in the isolation and purification process of mAbs aiming at turning the biotechnological process more competitive for the biopharmaceutical industries. Attempts to replace the golden-standard and expensive proA affinity chromatography from the process have been made, with the major goal of reducing the costs associated to the downstream processing of mAbs. Several chromatographic and non-chromatographic methods have been proposed to embrace the challenge of obtaining mAbs at a lower cost. Non-chromatographic techniques appear to be the most promising group of alternatives, since they generally allow to achieve high recovery yields and high purity levels, allied with simplicity, robustness, and lower energy consumption. In particular, ATPS can be highlighted as a promising non-chromatographic approach, since they are a simple technique, with a low cost associated, easy to operate and to apply on an industrial scale, with a high resolution capacity and able to provide a biocompatible environment. This technology allows the intensification of the downstream process, as clarification, purification and concentration can be integrated in a single step. Several promising works have already proved the efficiency of this technique concerning the extraction and/or purification of mAbs directly from biological matrices; however, it is evident that the study of new systems aiming the selective extraction and consequent purification of IgG should be performed by manipulating the ATPS components, the extraction conditions or the exploration of different electrolytes/ligands. It has been reported that using ATPS, the purification costs can be reduced by at least 39 %, which emphasizes the potential of this technique [209]. All the works discussed in this chapter correspond to strategies proposed in recent years to overcome the major bottleneck in the processing of cost-effective mAbs. This information should encourage both the search on new and more efficient alternatives and the improvement of the existent technologies in order to boost the manufacturing process and the widespread use of mAbs as conventional therapies.

1.2.10. References

1.   J. Kovacs-Nolan and Y. Mine, *Egg yolk antibodies for passive immunity.* Annual review of food science and technology, 2012. **3**: p. 163-182.

2.   P. Rosa, I. Ferreira, A. Azevedo, and M. Aires-Barros, *Aqueous two-phase systems: a viable platform in the manufacturing of biopharmaceuticals.* Journal of Chromatography A, 2010. **1217**(16): p. 2296-2305.

3.   G. Guiochon and L.A. Beaver, *Separation science is the key to successful biopharmaceuticals.* Journal of Chromatography A, 2011. **1218**(49): p. 8836-8858.

4.   A.M. Azevedo, P.A. Rosa, I.F. Ferreira, and M.R. Aires-Barros, *Chromatography-free recovery of biopharmaceuticals through aqueous two-phase processing.* Trends in Biotechnology, 2009. **27**(4): p. 240-247.

5.   J. Kovacs-Nolan and Y. Mine, *Avian egg antibodies: basic and potential applications.* Avian and Poultry Biology Reviews, 2004. **15**(1): p. 25-46.

6.   S.S. Farid, *Process economics of industrial monoclonal antibody manufacture.* Journal of Chromatography B, 2007. **848**(1): p. 8-18.

7.   S.D. Jones, F.J. Castillo, and H.L. Levine, *Advances in the Development of Therapeutic Monoclonal Antibodies.* BioPharm International, 2007. **20**(10): p. 96-114.

8.   U. Gottschalk, *Bioseparation in antibody manufacturing: the good, the bad and the ugly.* Biotechnology progress, 2008. **24**(3): p. 496-503.

9.   J. Thömmes and M. Etzel, *Alternatives to chromatographic separations.* Biotechnology progress, 2007. **23**(1): p. 42-45.

10.   P. Gronemeyer, R. Ditz, and J. Strube, *Trends in upstream and downstream process development for antibody manufacturing.* Bioengineering, 2014. **1**(4): p. 188-212.

11.   J. Strube, F. Grote, and R. Ditz, *Bioprocess design and production technology for the future.* Biopharmaceutical Production Technology, Volume 1 & Volume 2, 2012: p. 657-705.

12.   A.A. Shukla, B. Hubbard, T. Tressel, S. Guhan, and D. Low, *Downstream processing of monoclonal antibodies—application of platform approaches.* Journal of Chromatography B, 2007. **848**(1): p. 28-39.

13.   G. Kretzmer, *Industrial processes with animal cells.* Applied Microbiology and Biotechnology, 2002. **59**(2-3): p. 135-142.

14.   G. Goldstein, A.J. Fuccello, D.J. Norman, C.F. Shield III, R.B. Colvin, and A.B. Cosimi, *OKT3 monoclonal antibody plasma levels during therapy and the subsequent development of host antibodies to OKT3.* Transplantation, 1986. **42**(5): p. 507-510.

15.   G. Walsh, *Biopharmaceuticals: biochemistry and biotechnology*. 2013: John Wiley & Sons.

16.   G. Walsh, *Biopharmaceutical benchmarks.* Nature biotechnology, 2000. **18**(8): p. 829-834.

17.   M.F. Silva, A. Fernandes-Platzgummer, M.R. Aires-Barros, and A.M. Azevedo, *Integrated purification of monoclonal antibodies directly from cell culture medium with aqueous two-phase systems.* Separation and Purification Technology, 2014. **132**: p. 330-335.

18.   N.S. Lipman, L.R. Jackson, L.J. Trudel, and F. Weis-Garcia, *Monoclonal versus polyclonal antibodies: distinguishing characteristics, applications, and information resources.* ILAR journal, 2005. **46**(3): p. 258-268.

19.   D.M. Ecker, S.D. Jones, and H.L. Levine. *The therapeutic monoclonal antibody market*. in *MAbs*. 2015. Taylor & Francis.

20.   Datamonitor, *Prescription Pharmaceutical Sales Overview – Analysis of forecast sales in the major pharmaceutical markets.*

21.   ResearchandMarkets, *Global and Chinese Monoclonal Antibody Industry Report, 2013-2017, China.* 2013.

22.   E. Jain and A. Kumar, *Upstream processes in antibody production: evaluation of critical parameters.* Biotechnology advances, 2008. **26**(1): p. 46-72.

23.   M.D. Costioli, C. Guillemot-Potelle, C. Mitchell-Logean, and H. Broly, *Cost of goods modeling and quality by design for developing cost-effective processes.* BioPharm International, 2010. **23**(6).

24.   A. Biosciences, *Antibody purification handbook.* Edition AC, 2002: p. 10-18.

25.   A.K. Abbas, A.H. Lichtman, and S. Pillai, *Cellular and Molecular Immunology: with STUDENT CONSULT Online Access*. 2014: Elsevier Health Sciences.

26.   S.J. Kim, Y. Park, and H.J. Hong, *Antibody engineering for the development of therapeutic antibodies.* Mol Cells, 2005. **20**(1): p. 17-29.

27.   G. Köhler and C. Milstein, *Derivation of specific antibody-producing tissue culture and tumor lines by cell fusion.* European journal of immunology, 1976. **6**(7): p. 511-519.

28.   P. Nelson, G. Reynolds, E. Waldron, E. Ward, K. Giannopoulos, and P. Murray, *Demystified…: monoclonal antibodies.* Molecular Pathology, 2000. **53**(3): p. 111.

29.   B.V. Ayyar, S. Arora, C. Murphy, and R. O'Kennedy, *Affinity chromatography as a tool for antibody purification.* Methods, 2012. **56**(2): p. 116-129.

30.   A. Subramanian, *Immunoaffinity chromatography.* Molecular Biotechnology, 2002. **20**(1): p. 41-47.

31.   M.A. Keller and E.R. Stiehm, *Passive immunity in prevention and treatment of infectious diseases.* Clinical microbiology reviews, 2000. **13**(4): p. 602-614.

32. I. Schwab and F. Nimmerjahn, *Intravenous immunoglobulin therapy: how does IgG modulate the immune system?* Nature Reviews Immunology, 2013. **13**(3): p. 176-189.

33. L. Dézsi, Z. Horváth, and L. Vécsei, *Intravenous immunoglobulin: pharmacological properties and use in polyneuropathies.* Expert Opinion on Drug Metabolism & Toxicology, 2016: p. 1-16.

34. A.M. Buehler, U.P. Flato, C.P. Ferri, and J.G. Fernandes, *Is there evidence for recommending specific intravenous immunoglobulin formulations? A systematic review of head-to-head randomized controlled trials.* European journal of pharmacology, 2015. **747**: p. 96-104.

35. K. Huang, L. Incognito, X. Cheng, N.D. Ulbrandt, and H. Wu, *Respiratory syncytial virus-neutralizing monoclonal antibodies motavizumab and palivizumab inhibit fusion.* Journal of virology, 2010. **84**(16): p. 8132-8140.

36. E.M. Castilow and S.M. Varga, *Overcoming T-cell-mediated immunopathology to achieve safe respiratory syncytial virus vaccination.* 2008.

37. R.W. Sidwell and D.L. Barnard, *Respiratory syncytial virus infections: recent prospects for control.* Antiviral research, 2006. **71**(2): p. 379-390.

38. G.A. Storch, *Humanized Monoclonal Antibody for Prevention of Respiratory Syncytial Virus Infection.* Pediatrics, 1998. **102**(3): p. 648-651.

39. H. Wu, D. Pfarr, G. Losonsky, and P. Kiener, *Immunoprophylaxis of RSV infection: advancing from RSV-IGIV to palivizumab and motavizumab*, in *Human Antibody Therapeutics for Viral Disease*. 2008, Springer. p. 103-123.

40. T.-S. Migone, S. Bolmer, J. Zhong, A. Corey, D. Vasconcelos, M. Buccellato, and G. Meister, *Added benefit of raxibacumab to antibiotic treatment of inhalational anthrax.* Antimicrobial agents and chemotherapy, 2015. **59**(2): p. 1145-1151.

41. P.K. Russell, *Project BioShield: what it is, why it is needed, and its accomplishments so far.* Clinical Infectious Diseases, 2007. **45**(Supplement 1): p. S68-S72.

42. T.V. Inglesby, T. O'toole, D.A. Henderson, J.G. Bartlett, M.S. Ascher, E. Eitzen, A.M. Friedlander, J. Gerberding, J. Hauer, and J. Hughes, *Anthrax as a biological weapon, 2002: updated recommendations for management.* Jama, 2002. **287**(17): p. 2236-2252.

43. C.E. Kummerfeldt, *Raxibacumab: potential role in the treatment of inhalational anthrax.* Infection and drug resistance, 2014. **7**: p. 101.

44. G.M. Subramanian, P.W. Cronin, G. Poley, A. Weinstein, S.M. Stoughton, J. Zhong, Y. Ou, J.F. Zmuda, B.L. Osborn, and W.W. Freimuth, *A phase 1 study of PAmAb, a fully human monoclonal antibody against Bacillus anthracis protective antigen, in healthy volunteers.* Clinical infectious diseases, 2005. **41**(1): p. 12-20.

45.   B.J. Yamamoto, A.M. Shadiack, S. Carpenter, D. Sanford, L.N. Henning, E. O'Connor, N. Gonzales, J. Mondick, J. French, and G.V. Stark, *Obiltoxaximab for inhalational anthrax: efficacy projection across a range of disease severity.* Antimicrobial Agents and Chemotherapy, 2016: p. AAC. 00972-16.

46.   B.J. Yamamoto, A.M. Shadiack, S. Carpenter, D. Sanford, L.N. Henning, N. Gonzales, E. O'Connor, L.S. Casey, and N.V. Serbina, *Obiltoxaximab Prevents Disseminated Bacillus anthracis Infection and Improves Survival during Pre-and Postexposure Prophylaxis in Animal Models of Inhalational Anthrax.* Antimicrobial Agents and Chemotherapy, 2016. **60**(10): p. 5796-5805.

47.   A. Markham, *Bezlotoxumab: First Global Approval.* Drugs, 2016. **76**(18): p. 1793-1798.

48.   J.M. Reichert. *Antibodies to watch in 2017*. in *MAbs*. 2016. Taylor & Francis.

49.   R.W. Chapin, T. Lee, C. McCoy, C.D. Alonso, and M.V. Mahoney, *Bezlotoxumab: Could This B the Answer for Clostridium difficile Recurrence?* Annals of Pharmacotherapy, 2017: p. 1060028017706374.

50.   X. Zhang, Y. Yang, D. Fan, and D. Xiong, *The development of bispecific antibodies and their applications in tumor immune escape.* Experimental Hematology & Oncology, 2017. **6**(1): p. 12.

51.   M.B. May and A. Glode, *Blinatumomab: A novel, bispecific, T-cell engaging antibody.* American Journal of Health-System Pharmacy, 2016. **73**(1).

52.   X. Thomas, *Blinatumomab: a new era of treatment for adult ALL?* The Lancet Oncology, 2015. **16**(1): p. 6-7.

53.   L. Hoffman and L. Gore, *Blinatumomab, a bi-specific anti-CD19/CD3 BiTE® antibody for the treatment of acute lymphoblastic leukemia: perspectives and current pediatric applications.* Frontiers in oncology, 2014. **4**: p. 63.

54.   D. Seimetz, *Novel monoclonal antibodies for cancer treatment: the trifunctional antibody catumaxomab (removab).* J Cancer, 2011. **2**: p. 309-316.

55.   M.C. Flickinger, *Upstream industrial biotechnology, 2 volume Set*. 2013: John Wiley & Sons.

56.   N.A. Buss, S.J. Henderson, M. McFarlane, J.M. Shenton, and L. de Haan, *Monoclonal antibody therapeutics: history and future.* Current opinion in pharmacology, 2012. **12**(5): p. 615-622.

57.   M. Stern and R. Herrmann, *Overview of monoclonal antibodies in cancer therapy: present and promise.* Critical reviews in oncology/hematology, 2005. **54**(1): p. 11-29.

58.   G.L. Boulianne, N. Hozumi, and M.J. Shulman, *Production of functional chimaeric mouse/human antibody.* 1984.

59.   S.L. Morrison, M.J. Johnson, L.A. Herzenberg, and V.T. Oi, *Chimeric human antibody molecules: mouse antigen-binding domains with human constant region domains.* Proceedings of the National Academy of Sciences, 1984. **81**(21): p. 6851-6855.

60.   P.T. Jones, P.H. Dear, J. Foote, M.S. Neuberger, and G. Winter, *Replacing the complementarity-determining regions in a human antibody with those from a mouse.* 1986.

61.   M. Yamashita, Y. Katakura, and S. Shirahata, *Recent advances in the generation of human monoclonal antibody.* Cytotechnology, 2007. **55**(2-3): p. 55-60.

62.   C. Chan, A. Chan, B. Hanson, and E. Ooi, *The use of antibodies in the treatment of infectious diseases.* Singapore medical journal, 2009. **50**(7): p. 663-72; quiz 673.

63.   E. Laffly and R. Sodoyer, *Monoclonal and recombinant antibodies, 30 years after.* Human antibodies, 2005. **14**(1/2): p. 33.

64.   F. Li, N. Vijayasankaran, A. Shen, R. Kiss, and A. Amanullah. *Cell culture processes for monoclonal antibody production*. in *MAbs*. 2010. Taylor & Francis.

65.   J.R. Birch and A.J. Racher, *Antibody production.* Advanced drug delivery reviews, 2006. **58**(5): p. 671-685.

66.   M. Butler and A. Meneses-Acosta, *Recent advances in technology supporting biopharmaceutical production from mammalian cells.* Applied microbiology and biotechnology, 2012. **96**(4): p. 885-894.

67.   J.-H. Tjio and T.T. Puck, *Genetics of somatic mammalian cells: II. Chromosomal constitution of cells in tissue culture.* The Journal of experimental medicine, 1958. **108**(2): p. 259.

68.   F.M. Wurm, *Production of recombinant protein therapeutics in cultivated mammalian cells.* Nature biotechnology, 2004. **22**(11): p. 1393-1398.

69.   S.C. Ho, Y.W. Tong, and Y. Yang, *Generation of monoclonal antibody-producing mammalian cell lines.* Pharmaceutical bioprocessing, 2013. **1**(1): p. 71-87.

70.   K.P. Jayapal, K.F. Wlaschin, W. Hu, and M.G. Yap, *Recombinant protein therapeutics from CHO cells-20 years and counting.* Chemical Engineering Progress, 2007. **103**(10): p. 40.

71.   L. Fan, I. Kadura, L.E. Krebs, J.L. Larson, D.M. Bowden, and C.C. Frye, *Development of a highly-efficient CHO cell line generation system with engineered SV40E promoter.* Journal of biotechnology, 2013. **168**(4): p. 652-658.

72.   A.R. Costa, M.E. Rodrigues, M. Henriques, J. Azeredo, and R. Oliveira, *Guidelines to cell engineering for monoclonal antibody production.* European Journal of Pharmaceutics and Biopharmaceutics, 2010. **74**(2): p. 127-138.

73.   M.M. Zhu, A. Goyal, D.L. Rank, S.K. Gupta, T.V. Boom, and S.S. Lee, *Effects of Elevated pCO2 and Osmolality on Growth of CHO Cells and Production of Antibody-Fusion Protein B1: A Case Study.* Biotechnology progress, 2005. **21**(1): p. 70-77.

74.   M. Wiebe, F. Becker, R. Lazar, L. May, B. Casto, M. Semense, and C. Fautz, *A multifaceted approach to assure that recombinant tPA is free of adventitious virus.* 1989.

75.   K.N. Baker, M.H. Rendall, A.E. Hills, M. Hoare, R.B. Freedman, and D.C. James, *Metabolic control of recombinant protein N-glycan processing in NS0 and CHO cells.* Biotechnology and bioengineering, 2001. **73**(3): p. 188-202.

76.   K. Swiech, V. Picanço-Castro, and D.T. Covas, *Human cells: new platform for recombinant therapeutic protein production.* Protein expression and purification, 2012. **84**(1): p. 147-153.

77.   M. Kuczewski, E. Schirmer, B. Lain, and G. Zarbis-Papastoitsis, *A single-use purification process for the production of a monoclonal antibody produced in a PER. C6 human cell line.* Biotechnology journal, 2011. **6**(1): p. 56-65.

78.   G. Urlaub and L.A. Chasin, *Isolation of Chinese hamster cell mutants deficient in dihydrofolate reductase activity.* Proceedings of the National Academy of Sciences, 1980. **77**(7): p. 4216-4220.

79.   J. Chusainow, Y.S. Yang, J.H. Yeo, P.C. Toh, P. Asvadi, N.S. Wong, and M.G. Yap, *A study of monoclonal antibody-producing CHO cell lines: What makes a stable high producer?* Biotechnology and bioengineering, 2009. **102**(4): p. 1182-1196.

80.   M. Brown, G. Renner, R. Field, and T. Hassell, *Process development for the production of recombinant antibodies using the glutamine synthetase (GS) system.* Cytotechnology, 1992. **9**(1-3): p. 231-236.

81.   N. Kumar and N. Borth, *Flow-cytometry and cell sorting: an efficient approach to investigate productivity and cell physiology in mammalian cell factories.* Methods, 2012. **56**(3): p. 366-374.

82.   I.F. Pinto, S.A. Rosa, M.R. Aires-Barros, and A.M. Azevedo, *Exploring the use of heparin as a first capture step in the purification of monoclonal antibodies from cell culture supernatants.* Biochemical Engineering Journal, 2015.

83.   B. Kelley. *Industrialization of mAb production technology: the bioprocessing industry at a crossroads*. in *MAbs*. 2009. Taylor & Francis.

84.   H.F. Liu, J. Ma, C. Winter, and R. Bayer. *Recovery and purification process development for monoclonal antibody production*. in *MAbs*. 2010. Taylor & Francis.

85.   A. Jacobi, B. Enenkel, P. Garidel, C. Eckermann, M. Knappenberger, I. Presser, and H. Kaufmann, *Process development and manufacturing of therapeutic antibodies.* Handbook of Therapeutic Antibodies, 2014: p. 601-664.

86.   I.F. Pinto, M.R. Aires-Barros, and A.M. Azevedo, *Multimodal chromatography: debottlenecking the downstream processing of monoclonal antibodies.* Pharmaceutical Bioprocessing, 2015. **3**(3): p. 263-279.

87.   P. Marichal-Gallardo and M. Alvarez, *State-of-the-art in downstream processing of monoclonal antibodies: Process trends in design and validation.* Biotechnology progress, 2012. **28**(4): p. 899-916.

88.   K. Swinnen, A. Krul, I. Van Goidsenhoven, N. Van Tichelt, A. Roosen, and K. Van Houdt, *Performance comparison of protein A affinity resins for the purification of monoclonal antibodies.* Journal of Chromatography B, 2007. **848**(1): p. 97-107.

89.   H. Hjelm, K. Hjelm, and J. Sjöquist, *Protein A from Staphylococcus aureus. Its isolation by affinity chromatography and its use as an immunosorbent for isolation of immunoglobulins.* FEBS letters, 1972. **28**(1): p. 73-76.

90.   J. Deisenhofer, *Crystallographic refinement and atomic models of a human Fc fragment and its complex with fragment B of protein A from Staphylococcus aureus at 2.9-and 2.8-. ANG. resolution.* Biochemistry, 1981. **20**(9): p. 2361-2370.

91.   R.M. O'Leary, D. Feuerhelm, D. Peers, Y. Xu, and G.S. Blank, *Determining the useful lifetime chromatography resins-Prospective small-scale studies.* BIOPHARM-THE APPLIED TECHNOLOGIES OF BIOPHARMACEUTICAL DEVELOPMENT, 2001. **14**(9): p. 10-+.

92.   J. Curling, *The development of antibody purification technologies.* Process Scale Purification of Antibodies, 2009: p. 25-52.

93.   G. Bolton, J. Cormier, M. Krishnan, J. Lewnard, and H. Lutz, *Integrity testing of normal flow parvovirus filters using air-liquid based tests.* BIOPROCESSING JOURNAL, 2006. **5**(1): p. 50.

94.   D.M. Strauss, J. Gorrell, M. Plancarte, G.S. Blank, Q. Chen, and B. Yang, *Anion exchange chromatography provides a robust, predictable process to ensure viral safety of biotechnology products.* Biotechnology and bioengineering, 2009. **102**(1): p. 168-175.

95.   L. Connell-Crowley, T. Nguyen, J. Bach, S. Chinniah, H. Bashiri, R. Gillespie, J. Moscariello, P. Hinckley, H. Dehghani, and S. Vunnum, *Cation exchange chromatography provides effective retrovirus clearance for antibody purification processes.* Biotechnology and bioengineering, 2012. **109**(1): p. 157-165.

96.   G. Ferreira, J. Dembecki, K. Patel, and A. Arunakumari, *A two-column process to purify antibodies without Protein A.* Biopharm international, 2007. **20**(5).

97.   Y. Yigzaw, R. Piper, M. Tran, and A.A. Shukla, *Exploitation of the adsorptive properties of depth filters for host cell protein removal during monoclonal antibody purification.* Biotechnology progress, 2006. **22**(1): p. 288-296.

98.   M.W. Phillips, G. Bolton, M. Krishnan, J.J. Lewnard, and B. Raghunath, *11 Virus Filtration Process Design and Implementation.* Process Scale Bioseparations for the Biopharmaceutical Industry, 2007: p. 333.

99.   D.K. Follman and R.L. Fahrner, *Factorial screening of antibody purification processes using three chromatography steps without protein A.* Journal of Chromatography A, 2004. **1024**(1): p. 79-85.

100.   A.M. Clausen, A. Subramanian, and P.W. Carr, *Purification of monoclonal antibodies from cell culture supernatants using a modified zirconia based cation-exchange support.* Journal of Chromatography A, 1999. **831**(1): p. 63-72.

101.   I.F. Pinto, S.A. Rosa, M.R. Aires-Barros, and A.M. Azevedo, *Exploring the use of heparin as a first capture step in the purification of monoclonal antibodies from cell culture supernatants.* Biochemical Engineering Journal, 2015. **104**: p. 27-33.

102.   G. Joucla, C. Le Senechal, M. Begorre, B. Garbay, X. Santarelli, and C. Cabanne, *Cation exchange versus multimodal cation exchange resins for antibody capture from CHO supernatants: identification of contaminating Host Cell Proteins by mass spectrometry.* Journal of Chromatography B, 2013. **942**: p. 126-133.

103.   Y. Hou, M. Brower, D. Kanani, R. Jacquemart, B. Kachuik, D. Pollard, and J. Stout, *Advective Hydrogel Membrane Chromatography for Monoclonal Antibody Purification in Bioprocessing.* Biotechnology Progress, 2015.

104.   R. Ghosh and L. Wang, *Purification of humanized monoclonal antibody by hydrophobic interaction membrane chromatography.* Journal of Chromatography A, 2006. **1107**(1-2): p. 104-109.

105.   L. Guerrier, I. Flayeux, and E. Boschetti, *A dual-mode approach to the selective separation of antibodies and their fragments.* Journal of Chromatography B: Biomedical Sciences and Applications, 2001. **755**(1-2): p. 37-46.

106.   S.A. Rosa, R. dos Santos, M.R. Aires-Barros, and A.M. Azevedo, *Phenylboronic acid chromatography provides a rapid, reproducible and easy scalable multimodal process for the capture of monoclonal antibodies.* Separation and Purification Technology, 2016. **160**: p. 43-50.

107.   S. Schwark, W. Sun, J. Stute, D. Lütkemeyer, M. Ulbricht, and B. Sellergren, *Monoclonal antibody capture from cell culture supernatants using epitope imprinted macroporous membranes.* RSC Advances, 2016. **6**(58): p. 53162-53169.

108.   L.R. Castilho, F.B. Anspach, and W.-D. Deckwer, *Comparison of affinity membranes for the purification of immunoglobulins.* Journal of Membrane Science, 2002. **207**(2): p. 253-264.

109.   S. Vançan, E.A. Miranda, and S.M.A. Bueno, *IMAC of human IgG: studies with IDA-immobilized copper, nickel, zinc, and cobalt ions and different buffer systems.* Process Biochemistry, 2002. **37**(6): p. 573-579.

110.   Y. González, N. Ibarra, H. Gómez, M. Gonzalez, L. Dorta, S. Padilla, and R. Valdés, *Expanded bed adsorption processing of mammalian cell culture fluid: comparison with packed bed affinity chromatography.* Journal of Chromatography B, 2003. **784**(1): p. 183-187.

111.   R. Giovannini and R. Freitag, *Isolation of a recombinant antibody from cell culture supernatant: continuous annular versus batch and expanded-bed chromatography.* Biotechnology and Bioengineering, 2001. **73**(6): p. 522-529.

112.   S. Lim, H. Manusu, A. Gooley, K. Williams, and D. Rylatt, *Purification of monoclonal antibodies from ascitic fluid using preparative electrophoresis.* Journal of Chromatography A, 1998. **827**(2): p. 329-335.

113.   T. Thomas, E. Shave, I. Bate, S. Gee, S. Franklin, and D. Rylatt, *Preparative electrophoresis: a general method for the purification of polyclonal antibodies.* Journal of Chromatography A, 2002. **944**(1): p. 161-168.

114.   M.Â. Taipa, R.-H. Kaul, B. Mattiasson, and J.M. Cabral, *Recovery of a monoclonal antibody from hybridoma culture supernatant by affinity precipitation with Eudragit S-100.* Bioseparation, 2000. **9**(5): p. 291-298.

115.   M. Dainiak, V. Izumrudov, V. Muronetz, I.Y. Galaev, and B. Mattiasson, *Affinity precipitation of monoclonal antibodies by nonstoichiometric polyelectrolyte complexes.* Bioseparation, 1998. **7**(4-5): p. 231-240.

116.   M.W. Handlogten, J.F. Stefanick, P.E. Deak, and B. Bilgicer, *Affinity-based precipitation via a bivalent peptidic hapten for the purification of monoclonal antibodies.* Analyst, 2014. **139**(17): p. 4247-4255.

117.   K. Holschuh and A. Schwämmle, *Preparative purification of antibodies with protein A—an alternative to conventional chromatography.* Journal of magnetism and magnetic materials, 2005. **293**(1): p. 345-348.

118.   L. Borlido, L. Moura, A.M. Azevedo, A.C. Roque, M.R. Aires-Barros, and J.P.S. Farinha, *Stimuli-Responsive magnetic nanoparticles for monoclonal antibody purification.* Biotechnology journal, 2013. **8**(6): p. 709-717.

119.   P. Gagnon, P. Toh, and J. Lee, *High productivity purification of immunoglobulin G monoclonal antibodies on starch-coated magnetic nanoparticles by steric exclusion of polyethylene glycol.* Journal of Chromatography A, 2014. **1324**: p. 171-180.

120.   R. van Reis, S. Gadam, L.N. Frautschy, S. Orlando, E.M. Goodrich, S. Saksena, R. Kuriyel, C.M. Simpson, S. Pearl, and A.L. Zydney, *High performance tangential flow filtration.* Biotechnology and bioengineering, 1997. **56**(1): p. 71-82.

121.   B. Lebreton, A. Brown, and R. van Reis, *Application of high-performance tangential flow filtration (HPTFF) to the purification of a human pharmaceutical antibody fragment expressed in Escherichia coli.* Biotechnology and bioengineering, 2008. **100**(5): p. 964-974.

122.   B. Lain, M.A. Cacciuttolo, and G. Zarbis-Papastoitsis, *Development of a high-capacity Mab capture step based on cation-exchange chromatography.* BioProcess Int, 2009. **7**(5): p. 26-34.

123.   M. Urmann, H. Graalfs, M. Joehnck, L.R. Jacob, and C. Frech. *Cation-exchange chromatography of monoclonal antibodies: Characterisation of a novel stationary phase designed for production-scale purification*. in *MAbs*. 2010. Taylor & Francis.

124.   T. Müller-Späth, L. Aumann, G. Ströhlein, and M. Morbidelli, *Improvement of specific monoclonal antibody (mAb) activity by reduction of the mAb heterogeneity using continuous chromatography (MCSGP).* New Biotechnology, 2009. **25**: p. S187.

125.   A. Guse, A. Milton, H. Schulze-Koops, B. Müller, E. Roth, B. Simmer, H. Wächter, E. Weiss, and F. Emmrich, *Purification and analytical characterization of an anti-CD4 monoclonal antibody for human therapy.* Journal of chromatography A, 1994. **661**(1): p. 13-23.

126.   I. Tornøe, I.L. Titlestad, K. Kejling, K. Erb, H.J. Ditzel, and J.C. Jensenius, *Pilot scale purification of human monoclonal IgM (COU-1) for clinical trials.* Journal of immunological methods, 1997. **205**(1): p. 11-17.

127.   P. Gagnon, *Purification tools for monoclonal antibodies.* 1996.

128.   E.H. Rinderknecht and G.A. Zapata, *Antibody purification*. 2006, Google Patents.

129.   Y. Kato, K. Nakamura, T. Kitamura, M. Hasegawa, and H. Sasaki, *Hydrophobic interaction chromatography at low salt concentration for the capture of monoclonal antibodies.* Journal of Chromatography A, 2004. **1036**(1): p. 45-50.

130.   S. Ghose, Y. Tao, L. Conley, and D. Cecchini. *Purification of monoclonal antibodies by hydrophobic interaction chromatography under no-salt conditions*. in *MAbs*. 2013. Taylor & Francis.

131. P. Gagnon, *Purification of Monoclonal Antibodies by Mixed-Mode Chromatography.* Process Scale Purification of Antibodies, 2009: p. 125-143.

132. M. Toueille, A. Uzel, J.-F. Depoisier, and R. Gantier, *Designing new monoclonal antibody purification processes using mixed-mode chromatography sorbents.* Journal of Chromatography B, 2011. **879**(13): p. 836-843.

133. J. Pezzini, G. Joucla, R. Gantier, M. Toueille, A.-M. Lomenech, C. Le Sénéchal, B. Garbay, X. Santarelli, and C. Cabanne, *Antibody capture by mixed-mode chromatography: A comprehensive study from determination of optimal purification conditions to identification of contaminating host cell proteins.* Journal of Chromatography A, 2011. **1218**(45): p. 8197-8208.

134. A. Forss, G. Rodrigo, J. Liderfelt, K. Torstensson, and K. Eriksson, *Optimization, robustness, and scale-up of MAb purification.* BioProcess Int, 2011. **9**(9).

135. G. Zhao, X.-Y. Dong, and Y. Sun, *Ligands for mixed-mode protein chromatography: principles, characteristics and design.* Journal of biotechnology, 2009. **144**(1): p. 3-11.

136. D. Gao, D.-Q. Lin, and S.-J. Yao, *Mechanistic analysis on the effects of salt concentration and pH on protein adsorption onto a mixed-mode adsorbent with cation ligand.* Journal of Chromatography B, 2007. **859**(1): p. 16-23.

137. R.-Z. Wang, D.-Q. Lin, H.-F. Tong, H.-L. Lu, and S.-J. Yao, *Evaluation of mixed-mode chromatographic resins for separating IgG from serum albumin containing feedstock.* Journal of Chromatography B, 2013. **936**: p. 33-41.

138. E. Boschetti, *The use of thiophilic chromatography for antibody purification: a review.* Journal of biochemical and biophysical methods, 2001. **49**(1): p. 361-389.

139. V.B. Brochier, H. Chabre, A. Lautrette, V. Ravault, M.-N. Couret, A. Didierlaurent, and P. Moingeon, *High throughput screening of mixed-mode sorbents and optimisation using pre-packed lab-scale columns for the purification of the recombinant allergen rBet v 1a.* Journal of Chromatography B, 2009. **877**(24): p. 2420-2427.

140. F. Oehme and J. Peters, *Mixed-mode chromatography in downstream process development.* BioPharm International, 2010: p. 12-19.

141. W. Schwartz, D. Judd, M. Wysocki, L. Guerrier, E. Birck-Wilson, and E. Boschetti, *Comparison of hydrophobic charge induction chromatography with affinity chromatography on protein A for harvest and purification of antibodies.* Journal of Chromatography A, 2001. **908**(1): p. 251-263.

142. L. Guerrier, P. Girot, W. Schwartz, and E. Boschetti, *New method for the selective capture of antibodies under physiolgical conditions.* Bioseparation, 2000. **9**(4): p. 211-221.

143. P. Cuatrecasas, M. Wilchek, and C.B. Anfinsen, *Selective enzyme purification by affinity chromatography.* Proceedings of the National Academy of Sciences, 1968. **61**(2): p. 636-643.

144. S. Storcksdieck, G. Bonsmann, and R. Hurrell, *Iron-binding properties, amino acid composition, and structure of muscle tissue peptides from in vitro digestion of different meat sources.* Journal of Food Science, 2007. **72**(1): p. S019-S029.

145. P.G. Taylor, C. Martinez-Torres, E.L. Romano, and M. Layrisse, *The effect of cysteine-containing peptides released during meat digestion on iron absorption in humans.* The American journal of clinical nutrition, 1986. **43**(1): p. 68-71.

146. J.H. Swain, L.B. Tabatabai, and M.B. Reddy, *Histidine content of low-molecular-weight beef proteins influences nonheme iron bioavailability in Caco-2 cells.* The Journal of nutrition, 2002. **132**(2): p. 245-251.

147. J.J. Winzerling, P. Berna, and J. Porath, *How to use immobilized metal ion affinity chromatography.* Methods, 1992. **4**(1): p. 4-13.

148. J. Porath, *Immobilized metal ion affinity chromatography.* Protein expression and purification, 1992. **3**(4): p. 263-281.

149. E. Ueda, P. Gout, and L. Morganti, *Current and prospective applications of metal ion–protein binding.* Journal of Chromatography A, 2003. **988**(1): p. 1-23.

150. V. Gaberc-Porekar and V. Menart, *Potential for using histidine tags in purification of proteins at large scale.* Chemical engineering & technology, 2005. **28**(11): p. 1306-1314.

151. P. Gagnon, *Technology trends in antibody purification.* Journal of chromatography A, 2012. **1221**: p. 57-70.

152. G. Serpa, E.F.P. Augusto, W.M.S.C. Tamashiro, M.B. Ribeiro, E.A. Miranda, and S.M.A. Bueno, *Evaluation of immobilized metal membrane affinity chromatography for purification of an immunoglobulin G 1 monoclonal antibody.* Journal of Chromatography B, 2005. **816**(1): p. 259-268.

153. A.C. Roque, C.S. Silva, and M.Â. Taipa, *Affinity-based methodologies and ligands for antibody purification: advances and perspectives.* Journal of Chromatography A, 2007. **1160**(1): p. 44-55.

154. L. Borlido, A. Azevedo, A. Sousa, P. Oliveira, A. Roque, and M. Aires-Barros, *Fishing human monoclonal antibodies from a CHO cell supernatant with boronic acid magnetic particles.* Journal of Chromatography B, 2012. **903**: p. 163-170.

155. V.L. Dhadge, S.A. Rosa, A. Azevedo, R. Aires-Barros, and A.C. Roque, *Magnetic aqueous two phase fishing: a hybrid process technology for antibody purification.* Journal of Chromatography A, 2014. **1339**: p. 59-64.

156. R. Van Reis, J. Brake, J. Charkoudian, D. Burns, and A. Zydney, *High-performance tangential flow filtration using charged membranes.* Journal of Membrane Science, 1999. **159**(1): p. 133-142.

157. K. Raghavarao, N. Rastogi, M. Gowthaman, and N. Karanth, *Aqueous two-phase extraction for downstream processing of enzymes/proteins.* Advances in applied microbiology, 1995. **41**: p. 97-171.

158. B. Sivasankar, *Biosperations: Principles and Techniques*. 2005: PHI Learning Pvt. Ltd.

159. M. Beijerinck, *Kulturversuche mit Amoeben auf festem Substrate.* Centralb. f. Bakteriol., Orig, 1896. **19**: p. 257-267.

160. P.-Å. Albertsson, *Partition of cell particles and macromolecules: separation and purification of biomolecules, cell organelles, membranes, and cells in aqueous polymer two-phase systems and their use in biochemical analysis and biotechnology*. Vol. 346. 1986: Wiley New York etc.

161. M.G. Freire, A.F.M. Claudio, J.M.M. Araújo, J.A.P. Coutinho, I.M. Marrucho, J.N.C. Lopes, and L.P.N. Rebelo, *Aqueous biphasic systems: a boost brought about by using ionic liquids.* Chemical Society Reviews, 2012. **41**(14): p. 4966-4995.

162. R. Hatti-Kaul, *Aqueous two-phase systems: methods and protocols*. Vol. 11. 2000: Springer Science & Business Media.

163. P.A. Rosa, A.M. Azevedo, and M.R. Aires-Barros, *Application of central composite design to the optimisation of aqueous two-phase extraction of human antibodies.* Journal of Chromatography A, 2007. **1141**(1): p. 50-60.

164. M. Bensch, B. Selbach, and J. Hubbuch, *High throughput screening techniques in downstream processing: preparation, characterization and optimization of aqueous two-phase systems.* Chemical engineering science, 2007. **62**(7): p. 2011-2021.

165. J.A. Asenjo and B.A. Andrews, *Aqueous two-phase systems for protein separation: phase separation and applications.* Journal of Chromatography A, 2012. **1238**: p. 1-10.

166. M.G. Freire, J.F.B. Pereira, M. Francisco, H. Rodríguez, L.P.N. Rebelo, R.D. Rogers, and J.A.P. Coutinho, *Insight into the interactions that control the phase behaviour of new aqueous biphasic systems composed of polyethylene glycol polymers and ionic liquids.* Chemistry-A European Journal, 2012. **18**(6): p. 1831-1839.

167. S. Raja, V.R. Murty, V. Thivaharan, V. Rajasekar, and V. Ramesh, *Aqueous two phase systems for the recovery of biomolecules–a review.* Science and Technology, 2011. **1**(1): p. 7-16.

168. J.L. Cleland, C. Hedgepeth, and D. Wang, *Polyethylene glycol enhanced refolding of bovine carbonic anhydrase B. Reaction stoichiometry and refolding model.* Journal of Biological Chemistry, 1992. **267**(19): p. 13327-13334.

Monoclonal antibodies – addressing the challenges on the manufacturing processing of an advanced class of therapeutic agents

1

169.   A.L. Grilo, M.R. Aires-Barros, and A.M. Azevedo, *Partitioning in Aqueous Two-Phase Systems: fundamentals, applications and trends.* Separation & Purification Reviews, 2014(just-accepted).

170.   B. Andrews, D. Head, P. Dunthorne, and J. Asenjo, *PEG activation and ligand binding for the affinity partitioning of proteins in aqueous two-phase systems.* Biotechnology techniques, 1990. **4**(1): p. 49-54.

171.   B. Sulk, G. Birkenmeier, and G. Kopperschläger, *Application of phase partitioning and thiophilic adsorption chromatography to the purification of monoclonal antibodies from cell culture fluid.* Journal of immunological methods, 1992. **149**(2): p. 165-171.

172.   B. Andrews, S. Nielsen, and J. Asenjo, *Partitioning and purification of monoclonal antibodies in aqueous two-phase systems.* Bioseparation, 1995. **6**(5): p. 303-313.

173.   G. Zijlstra, M. Michielsen, C. De Gooijer, L. Van der Pol, and J. Tramper, *Separation of hybridoma cells from their IgG product using aqueous two-phase systems.* Bioseparation, 1996. **6**(4): p. 201-210.

174.   G. Zijlstra, M. Michielsen, C. De Gooijer, L. Van der Pol, and J. Tramper, *IgG and hybridoma partitioning in aqueous two-phase systems containing a dye-ligand.* Bioseparation, 1998. **7**(2): p. 117-126.

175.   J. Mündges, J. Zierow, and T. Zeiner, *Experiment and Simulation of an Aqueous Two-Phase Extraction Process for the Purification of a Monoclonal Antibody.* Chemical Engineering and Processing: Process Intensification, 2015.

176.   J. Muendges, I. Stark, S. Mohammad, A. Górak, and T. Zeiner, *Single stage aqueous two-phase extraction for monoclonal antibody purification from cell supernatant.* Fluid Phase Equilibria, 2015. **385**: p. 227-236.

177.   J. Muendges, A. Zalesko, A. Górak, and T. Zeiner, *Multistage aqueous two-phase extraction of a monoclonal antibody from cell supernatant.* Biotechnology progress, 2015. **31**(4): p. 925-936.

178.   A.M. Azevedo, P.A. Rosa, I.F. Ferreira, and M.R. Aires-Barros, *Optimisation of aqueous two-phase extraction of human antibodies.* Journal of Biotechnology, 2007. **132**(2): p. 209-217.

179.   P. Rosa, A. Azevedo, S. Sommerfeld, M. Mutter, M. Aires-Barros, and W. Bäcker, *Application of aqueous two-phase systems to antibody purification: a multi-stage approach.* Journal of biotechnology, 2009. **139**(4): p. 306-313.

180.   P. Rosa, A. Azevedo, S. Sommerfeld, W. Bäcker, and M. Aires-Barros, *Continuous aqueous two-phase extraction of human antibodies using a packed column.* Journal of Chromatography B, 2012. **880**: p. 148-156.

181.   D. Silva, A. Azevedo, P. Fernandes, V. Chu, J. Conde, and M. Aires-Barros, *Design of a microfluidic platform for monoclonal antibody extraction using an aqueous two-phase system.* Journal of Chromatography A, 2012. **1249**: p. 1-7.

182.   A. Azevedo, P. Rosa, I. Ferreira, and M. Aires-Barros, *Integrated process for the purification of antibodies combining aqueous two-phase extraction, hydrophobic interaction chromatography and size-exclusion chromatography.* Journal of Chromatography A, 2008. **1213**(2): p. 154-161.

183.   A.M. Azevedo, A.G. Gomes, P.A. Rosa, I.F. Ferreira, A.M. Pisco, and M.R. Aires-Barros, *Partitioning of human antibodies in polyethylene glycol–sodium citrate aqueous two-phase systems.* Separation and Purification Technology, 2009. **65**(1): p. 14-21.

184.   I.F. Ferreira, A.M. Azevedo, P.A. Rosa, and M.R. Aires-Barros, *Purification of human immunoglobulin G by thermoseparating aqueous two-phase systems.* Journal of Chromatography A, 2008. **1195**(1): p. 94-100.

185.   P. Rosa, A. Azevedo, I. Ferreira, J. De Vries, R. Korporaal, H. Verhoef, T. Visser, and M. Aires-Barros, *Affinity partitioning of human antibodies in aqueous two-phase systems.* Journal of Chromatography A, 2007. **1162**(1): p. 103-113.

186.   A. Azevedo, P. Rosa, I. Ferreira, A. Pisco, J. De Vries, R. Korporaal, T. Visser, and M. Aires-Barros, *Affinity-enhanced purification of human antibodies by aqueous two-phase extraction.* Separation and Purification Technology, 2009. **65**(1): p. 31-39.

187.   A.M. Azevedo, P.A. Rosa, I.F. Ferreira, J. De Vries, T. Visser, and M.R. Aires-Barros, *Downstream processing of human antibodies integrating an extraction capture step and cation exchange chromatography.* Journal of Chromatography B, 2009. **877**(1-2): p. 50-58.

188.   P. Rosa, A. Azevedo, I. Ferreira, S. Sommerfeld, W. Bäcker, and M. Aires-Barros, *Downstream processing of antibodies: Single-stage versus multi-stage aqueous two-phase extraction.* Journal of Chromatography A, 2009. **1216**(50): p. 8741-8749.

189.   L. Borlido, A.M. Azevedo, and M.R. Aires-Barros, *Extraction of human IgG in thermo-responsive aqueous two-phase systems: assessment of structural stability by circular dichroism.* Separation Science and Technology, 2010. **45**(15): p. 2171-2179.

190.   P.A. Rosa, A.M. Azevedo, S. Sommerfeld, M. Mutter, W. Bäcker, and M.R. Aires-Barros, *Continuous purification of antibodies from cell culture supernatant with aqueous two-phase systems: From concept to process.* Biotechnology journal, 2013. **8**(3): p. 352-362.

191.   I. Campos-Pinto, E. Espitia-Saloma, S.A. Rosa, M. Rito-Palomares, O. Aguilar, M. Arévalo-Rodríguez, M.R. Aires-Barros, and A.M. Azevedo, *Integration of cell harvest with affinity-enhanced*

purification of monoclonal antibodies using aqueous two-phase systems with a dual tag ligand. Separation and Purification Technology, 2017. **173**: p. 129-134.

192.   Food and D. Administration, *CFR-Code of Federal Regulations Title 21.* Part 860--Medical Device Classification Procedures, 2015.

193.   M. Rito-Palomares, *Practical application of aqueous two-phase partition to process development for the recovery of biological products.* Journal of Chromatography B, 2004. **807**(1): p. 3-11.

194.   K. Schügerl and J. Hubbuch, *Integrated bioprocesses.* Current Opinion in Microbiology, 2005. **8**(3): p. 294-300.

195.   D. Platis and N.E. Labrou, *Application of a PEG/salt aqueous two-phase partition system for the recovery of monoclonal antibodies from unclarified transgenic tobacco extract.* Biotechnology journal, 2009. **4**(9): p. 1320-1327.

196.   D. Platis and N.E. Labrou, *Development of an aqueous two-phase partitioning system for fractionating therapeutic proteins from tobacco extract.* Journal of chromatography A, 2006. **1128**(1): p. 114-124.

197.   M. Rito-Palomares, C. Dale, and A. Lyddiatt, *Generic application of an aqueous two-phase process for protein recovery from animal blood.* Process Biochemistry, 2000. **35**(7): p. 665-673.

198.   M. Vargas, Á. Segura, M. Herrera, M. Villalta, Y. Angulo, J.M. Gutiérrez, G. León, and T. Burnouf, *Purification of IgG and albumin from human plasma by aqueous two phase system fractionation.* Biotechnology Progress, 2012. **28**(4): p. 1005-1011.

199.   Q. Wu, D.-Q. Lin, and S.-J. Yao, *Evaluation of poly (ethylene glycol)/hydroxypropyl starch aqueous two-phase system for immunoglobulin G extraction.* Journal of Chromatography B, 2013. **928**: p. 106-112.

200.   D. Mondal, M. Sharma, M.V. Quental, A.P. Tavares, K. Prasad, and M.G. Freire, *Suitability of bio-based ionic liquids for the extraction and purification of IgG antibodies.* Green Chemistry, 2016. **18**(22): p. 6071-6081.

201.   A.M. Ferreira, V.F. Faustino, D. Mondal, J.A.P. Coutinho, and M.G. Freire, *Improving the extraction and purification of immunoglobulin G by the use of ionic liquids as adjuvants in aqueous biphasic systems.* Journal of biotechnology, 2016. **236**: p. 166-175.

202.   D. Platis, J. Drossard, R. Fischer, J.-C. Ma, and N. Labrou, *New downstream processing strategy for the purification of monoclonal antibodies from transgenic tobacco plants.* Journal of Chromatography A, 2008. **1211**(1): p. 80-89.

203.   E.E. Hood, A. Kusnadi, Z. Nikolov, and J.A. Howard, *Molecular farming of industrial proteins from transgenic maize*, in *Chemicals via higher plant bioengineering*. 1999, Springer. p. 127-147.

204.   S.L. Woodard, J.M. Mayor, M.R. Bailey, D.K. Barker, R.T. Love, J.R. Lane, D.E. Delaney, J.M. McComas-Wagner, H.D. Mallubhotla, and E.E. Hood, *Maize (Zea mays)-derived bovine trypsin: characterization of the first large-scale, commercial protein product from transgenic plants.* Biotechnology and Applied Biochemistry, 2003. **38**(2): p. 123-130.

205.   Y.A. Suzuki, S.L. Kelleher, D. Yalda, L. Wu, J. Huang, N. Huang, and B. Lönnerdal, *Expression, characterization, and biologic activity of recombinant human lactoferrin in rice.* Journal of pediatric gastroenterology and nutrition, 2003. **36**(2): p. 190-199.

206.   D. Yang, F. Guo, B. Liu, N. Huang, and S.C. Watkins, *Expression and localization of human lysozyme in the endosperm of transgenic rice.* Planta, 2003. **216**(4): p. 597-603.

207.   P.A. Arlen, R. Falconer, S. Cherukumilli, A. Cole, A.M. Cole, K.K. Oishi, and H. Daniell, *Field production and functional evaluation of chloroplast-derived interferon-α2b.* Plant biotechnology journal, 2007. **5**(4): p. 511-525.

208.   S. Hassan, C.J. Van Dolleweerd, F. Ioakeimidis, E. Keshavarz-Moore, and J.K.C. Ma, *Considerations for extraction of monoclonal antibodies targeted to different subcellular compartments in transgenic tobacco plants.* Plant biotechnology journal, 2008. **6**(7): p. 733-748.

209.   P. Rosa, A. Azevedo, S. Sommerfeld, W. Bäcker, and M. Aires-Barros, *Aqueous two-phase extraction as a platform in the biomanufacturing industry: economical and environmental sustainability.* Biotechnology advances, 2011. **29**(6): p. 559-567.

1.3. Monoclonal antibodies as therapeutic agents for inflammatory diseases

This chapter is based on the submitted book chapter

Jéssica Bairos[§], Emanuel V. Capela[§], Ana P.M. Tavares, Mara G. Freire*

in Frontiers in Clinical Drug Research – Anti Infectives (FCDR-AI), Edited by Atta-ur-Rahman,

Bentham Science Publishers (2021). [§]Equal Contribution. [*]Corresponding author.

1.3.1. Abstract

Inflammation is a physiological process caused when an agent (chemical, biological or physical) transcends the primary defence barrier of an organism, setting a series of biological reactions to restore the integrity of such organism, thus playing a central role in the fight against those pathogens. Uncontrolled amplification of these events may lead to undesirable pathological manifestations such as cancer, diabetes, and cardiovascular, neurological and chronic inflammatory diseases. Monoclonal antibodies (mAbs) were first described in 1975, and since then they have proven to be relevant therapeutic agents in a myriad of diseases. The US Food and Drug Administration (FDA) has already approved more than 90 mAbs for the treatment of several diseases, from which approximately 26 % were specifically approved for the treatment of inflammatory diseases, for instance rheumatoid arthritis, Crohn's disease, ulcerative colitis, psoriasis, psoriatic arthritis and palmoplantar pustulosis. This chapter provides an overview on the inflammation process and main biochemical mechanisms, together with a vision on the current state of the art of the mAbs-based biopharmaceuticals market and their application as powerful therapeutic agents for inflammatory diseases.

1.3.2. Introductory aspects

As reviewed in the previous subchapter, monoclonal antibodies (mAbs) have been gaining high relevance for several different applications, from which the therapeutic applications were highlighted. In fact, from the more than 90 mAbs already approved by the US Food and Drug Administration (FDA), approximately 26 % were specifically approved for the treatment of inflammatory diseases.

This fact in particular, encouraged the comprehensive literature review presented in the current subchapter, that aims to remark the importance of mAbs in a specific group of disorders – the inflammatory ones.

Inflammation consists in the natural protective response of body to injury. It occurs when an agent (chemical, physical or biological) transcends the primary defence barrier of the organism [1, 2]. It plays a central role in the fight against pathogens and can set biochemical reactions to restore homeostasis through the activation of specific components, which act through the destruction or isolation of the aggressor agent [3, 4]. Inflammation can be manifested as an acute process, comprising three main events: i) increased blood flow; ii) development of edema, and iii) migration of leukocytes to the inflammatory focus [2]. Uncontrolled amplification of these events may lead to a chronic process, which is of long-term and associated with the presence of lymphocytes fibrosis and tissue necrosis [5, 6]. This phenomenon causes undesirable pathological manifestations such as cancer, diabetes, and cardiovascular, neurological, and chronic inflammatory diseases [5, 6]. Therefore, this type of diseases' progression fostered the search for effective alternative therapies, which is a crucial objective to be achieved in the coming years.

In recent decades, technological advances in bioprocess engineering have increased the interest in the development of alternative therapies for inflammation treatment, particularly recurring to biopharmaceuticals [7]. Biopharmaceuticals are biological macromolecules or cellular components that can be used in vaccines or as therapeutic agents. They are obtained by biological processes (*in vitro* or *in vivo*), and are extracted from biological sources, for example tissues and organs, microorganisms, fluids of animals, from mammalian cell cultures, insects, and also plants [7]. Main examples comprise recombinant proteins (monoclonal antibodies) and nucleic-acid-based products, which can be applied in the treatment of several inflammatory diseases, for instance in Crohn's disease, ulcerative colitis, rheumatoid arthritis, psoriasis, psoriatic arthritis and palmoplantar pustulosis [8]. Among them, monoclonal antibodies are the most used biopharmaceuticals, representing 53 % of all biopharmaceuticals approved [9].

Monoclonal antibodies (mAbs) were firstly described by Köhler and Milstein in 1975 [10] and since then, they have become the new backbone of the pharmaceutical industry since they have exquisite target selectivity and specificity [10]. mAbs offer the most promising prospects for new therapeutic approaches for inflammatory diseases [11, 12]. The most successful applications of mAbs is in autoimmune and inflammatory conditions [13]. Furthermore, as a wide range of mAb-based agents target several cytokines, chemokines, adhesion molecules, receptors and various

types of cells, it is expected that these therapeutic "magic bullets" [14] will greatly expand in the future, while providing better personalized treatment for a wide range of diseases.

In this sub-chapter, the most important aspects and main biochemical mechanisms of the inflammation process are overviewed, followed by a current review on the mAbs-based biopharmaceuticals market and approved mAbs product/therapies for inflammatory diseases. The action mechanisms and features of some relevant mAbs are also discussed, highlighting the advantages of mAbs-based therapies, together with the steps required for their increased adoption and widespread use.

1.3.3. Inflammation overview

Inflammation occurs in vascularized connective tissues, involving the capillary beds, plasma, circulating cells, sensory neurons, and cellular and extracellular constituents of this type of tissue. It is a physiological process caused when a chemical, physical and/or biological invader agent transcends the primary defence barrier of the organism, the epithelial and/or endothelial layer, and its specialized structures [1, 2]. Its role is to restore the homeostasis of the damaged tissue through the activation of the specific components that generate the effector cells and their products (cytokines and antibodies) and non-specific components of immunity, which act through the destruction or isolation of the aggressor agent, involving the action of phagocytic cells and mediators as well as their migration to the lesion site [3, 4]. Inflammation can manifest as an acute or chronic process. During the acute inflammatory process there are several events mediated by cellular and vascular components that induce morphological and biochemical changes [5]. Among them, three main events are highlighted: i) increased caliber of arterioles, capillaries and venules, which cause increased blood flow; ii) exudation of plasma proteins, complement factors and antibodies, which contribute for the development of edema; and iii) migration of leukocytes from the intravascular space to the inflammatory focus [2]. Together, these events characterize the classic signs of inflammation: flushing, heat, tumour, pain, and loss of function [15]. On the other hand, the chronic inflammatory process is of long-term and associated with the presence of lymphocytes and macrophages, proliferation of blood vessels, fibrosis and tissue necrosis [5, 6].

Before an injury, epithelial tissue separates the external environment or a body cavity from the underlying and more delicate connective tissue and body organs. The connective tissue is nurtured by blood vessels and mast cells. Both the inflammatory response and wound healing occur simultaneously, but consisting in separate processes that begin immediately after the injury [16]. After aggression, the inflammatory response is triggered and the accumulation of cells from the

immune system (leukocytes, macrophages and lymphocytes) occurs, secreting various cytokines and chemokines [16]. Leukocytes express several types of receptors in their surface that recognize external stimulus and release activating signals. Those receptors can be G-protein-coupled receptors (GPCRs) [17], adhesion receptors (selectins and integrins) [18], pattern recognition receptors (PRRs) [19], Fc-receptors [20] and cytokine receptors [21, 22].

1.3.3.1 G-protein-coupled receptors

GPCRs, known as G protein-linked receptors (GPLR) or serpentine receptors (**Figure 1.3.1**), are coupled to G proteins.
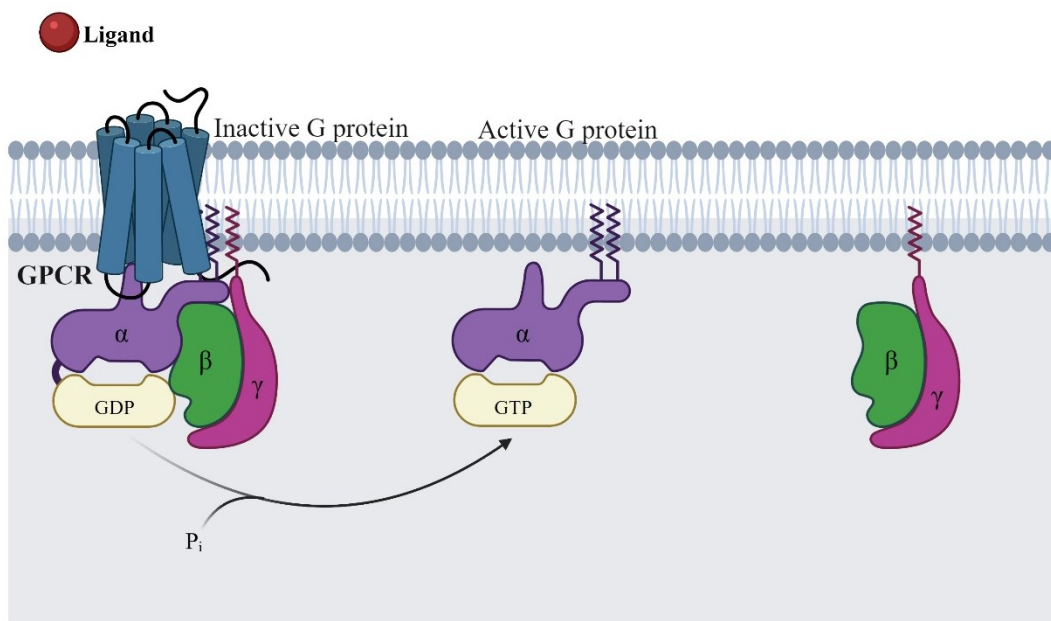
Figure 1.3.1. Representation of the G-protein-coupled receptors (GPCR) and G protein subunits (GDP: G_{alpha} (α), G_{beta} (β) and G_{gamma} (γ)). The G protein is attached to the inside of the cell membrane but is able to move along it. When GDP is attached to the G protein, it is inactive. The ligand activates the GPCR, inducing a conformational change in the receptor that allows it to function as a guanine nucleotide exchange factor (GEF) that exchanges GDP for GTP – thus turning "on" the GPCR. Created with a paid subscription of BioRender (https://biorender.com).

They belong to a large family of protein receptors that distinguish molecules outside the cell and activate internal signal transduction pathways (the cyclic adenosine monophosphate (cAMP) signal and the phosphatidylinositol signal) and finally, cellular responses [17, 23, 24]. They are found in neutrophils and macrophages and participate in host defence and inflammation. These include formyl-peptide receptors [17, 23, 24] that sense bacterial products and tissue injury, receptors for

leukotriene B4, platelet activating factor and complement fragment [24-27], as well as α-chemokines and β-chemokines receptors [28-30]. All of these strongly activate the chemotactic migration of leukocytes and trigger other responses, such as the production of reactive oxygen species (ROS), exocytosis of intracellular granules and vesicles, and are able to augment the responses of leukocytes to subsequent stimulation by other agonists [31].

GPCRs are formed by seven transmembrane domains, with the amino terminal at the extracellular medium and the carboxyl terminal in the intracellular medium and interact with G proteins. In the moment that an external signalling molecule binds to a GPCR, a conformational change in the GPCR occurs. This change then triggers the interaction between the GPCR and a nearby G protein [17, 23, 24]. The bond promotes a conformational change in the intracellular domain of the receptor, which allows its interaction with a second protein (stimulatory G protein). The occupied receptor causes replacement of guanosine diphosphate (GDP) bound to the Gα subunit by guanosine triphosphate (GTP), activating the Gα subunit. This subunit dissociates from the Gβγ dimer and an intracellular signalling cascades is started [17, 23, 24]. It results in the activation of adenylate cyclase, small GTPases, phospholipases and kinases, eventually being capable to control the expression of genes that are involved in survival, proliferation and differentiation [17, 23, 24].

1.3.3.2 Adhesion receptors

Adhesion receptors (**Figure 1.3.2**) are responsible for the initial stabilized binding of leukocytes to the blood vessel wall and their succeeding transendothelial migration to the perivascular tissue, either during normal recirculation and or the inflammation process [18].

Most of them belong to the four protein families: selectins, integrins, cadherins and the Ig superfamily (IgCAMs). The two major groups involved in the inflammation process are selectins and integrins. The first are single-chain transmembrane glycoproteins that are able to recognize carbohydrate moieties and mediate transient interactions between leukocytes and the vessel wall [18]. Selectins and selectin ligands are mandatory for the rolling phase of the leukocyte adhesion and transmigration cascade [18, 32]. On the other hand, integrins can be defined as heterodimeric transmembrane glycoproteins that are present on all mammalian cells [33]. The most important integrins expressed on leukocytes belong to the β2 integrin [34]. Lymphocyte function-associated antigen 1 (LFA-1) is expressed on all circulating leukocytes while macrophage-1 antigen (Mac-1) is primarily expressed on myeloid cells such as neutrophils, monocytes, and macrophages. LFA-1 and

Mac-1 bind to endothelial intercellular Adhesion Molecule-1 (ICAM-1) and are involved in different phases of leukocyte adhesion and transendothelial migration [35].
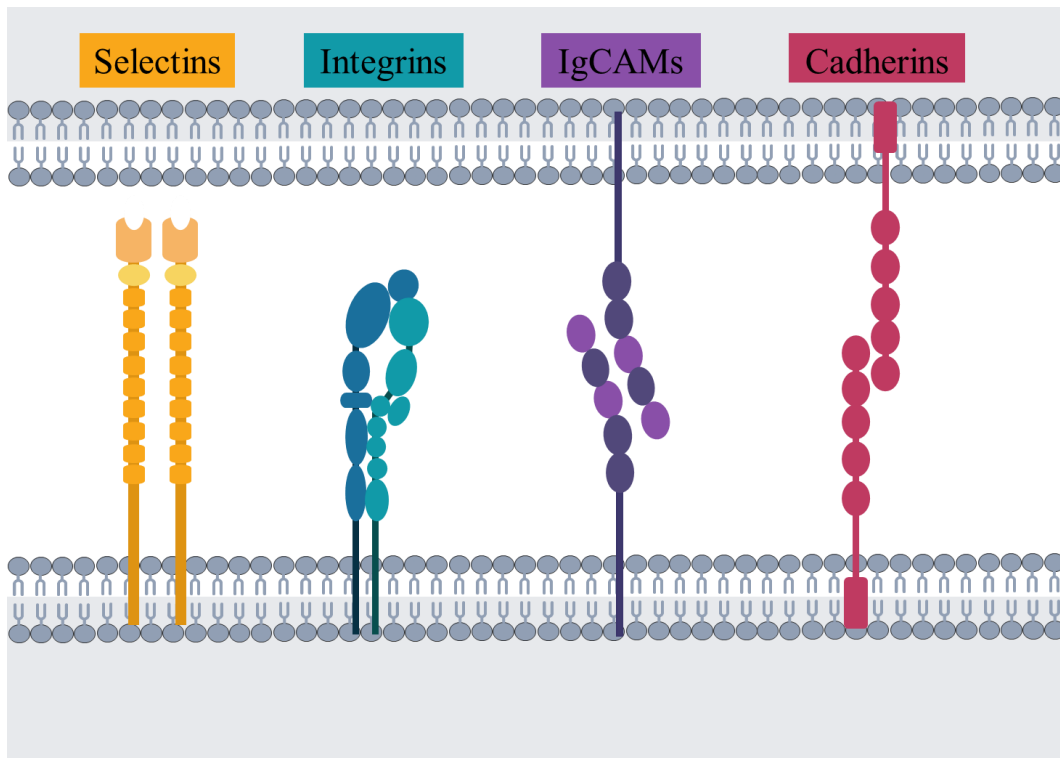
Figure 1.3.2. Different types of cell adhesion receptors, form the left to right: selectin-mediated cell adhesion receptor (sMcAr); integrin-mediated cell adhesion receptor (iMcAr) immunoglobulin superfamily-mediated cell adhesion receptor (IgMcAr) and cadherin-mediated cell adhesion receptor (cMcAr). Part of this figure was created with Servier medical art (https://smart.servier.com).

1.3.3.3 Pattern recognition receptors

Pattern recognition receptors (PRRs) (**Figure 1.3.3**) are important in the innate immune response by recognizing the pathogen associated molecular patterns (PAMPs) and the endogenous molecules released from damaged cells, called damage associated molecular patterns (DAMPs) [19, 36]. Those pathogens can be bacteria, viruses, parasites, fungi, and protozoa. They are expressed in macrophages, dendritic cells and in various nonprofessional immune cells (such as epithelial cells, endothelial cells, and fibroblasts) [19, 36].

The PRRs are either localized on the cell surface, to perceive extracellular pathogens, or within the endosomes. These receptors are involved in triggering pro-inflammatory signalling pathways, stimulating phagocytic responses or binding to microbes as secreted proteins [19, 36]. They can also be classified into four different classes of PRR families: transmembrane proteins like

toll-like receptors (TLRs); C-type lectin receptors (CLRs); cytoplasmic proteins like retinoic acid-inducible gene (RIG)-I-like receptors (RLRs) and nucleotide-binding and oligomerization domain (NOD)-like receptors (NLRs) [19]. The TLRs function through kinases to stimulate the production of microbicidal substances and cytokines by leukocytes [37]. These proteins have an important relationship with the interleukin- 1 (IL-1) receptor. Several studies [19, 31, 36] have demonstrated that these proteins activate the nuclear factor-κB (NF-kB) and mitogen-activated protein kinase (MAPK) pathway. Furthermore, they regulate the expression of cytokines through various adaptors such as TIR domain-containing adaptor protein (TIRAP), Myeloid differentiation primary response gene 88 (MyD88), TIR-domain-containing adaptor inducing IFNβ (TRIF), Trif-related adaptor molecule (TRAM), and Sterile-α and Armadillo motif-containing protein (SARM).
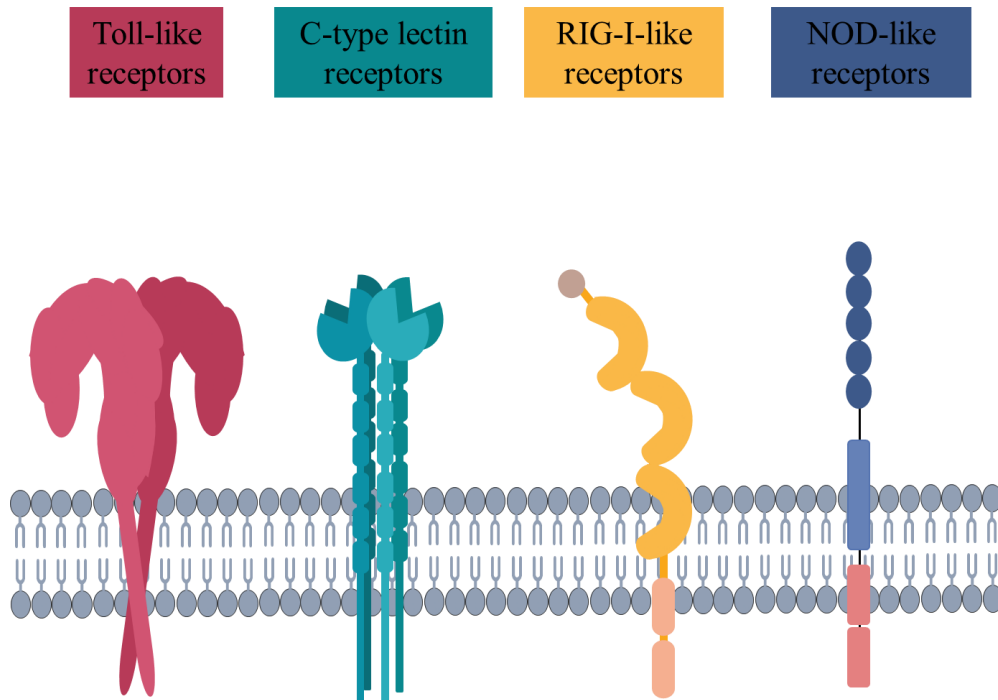
Figure 1.3.3. Major pattern recognition receptors (PRRs) presented from the left to right: Toll-like receptors (TLRs), C-type lectin receptors (CLRs), cytoplasmic proteins like Retinoic acid-inducible gene (RIG)-I-like receptors (RLRs) and NOD-like receptors (NLRs). Part of this figure was created with Servier medical art (https://smart.servier.com).

The activation of the NF-kB pathway initiates an immune adaptive response by the production of inflammatory cytokines such as IL-1, IL-6, IL-8, TNF-α, IL-12 [19, 31, 36]. The CLRs through the recognition of carbohydrates interact with some microorganisms, for instance, viruses, fungi, and bacteria. CLRs are also involved in the modulation of the innate immune response. These recognitions allow the internalization of the pathogen, subsequent degradation and then antigen

presentation. CLRs can stimulate the production of proinflammatory cytokines or inhibit TLR-mediated immune complexes. Most of these receptors signal through an immunoreceptor tyrosine-based activation motifs (ITAM)-based mechanism like Fc-receptors or through the activation of protein kinases or phosphatases. CLR-induced signal transduction seems to mainly activate or modulate NF-κB functions [19, 31, 38, 39]. RLRs are a family of RNA helicases that recognize genomic RNA of dsRNA viruses and dsRNA generated as the replication intermediate of ssRNA viruses [19, 31, 36]. After detection of a viral infection, RIG-I and MDA5 cooperate with the adaptor IFN-b-promoter stimulator 1 (IPS-1 also called VISA, CARDIF and MAVS) via CARD-CARD interactions. IPS-1 activates the release of cytokines and the IKK-related kinase, which activates IRF3/IRF7, resulting in the transcription of type I interferons. IPS-1 also activates NF-κB through recruitment of TRADD, FADD, caspase-8, and caspase-10 [19, 31, 36]. The NLRs are cytoplasmic sensors of PAMPs, DAMPs and danger signals that lead to transcriptional changes or activate cytokine-processing caspases. They can work together with Toll receptors and regulate the inflammatory and apoptotic response. The protein receptor NOD1 and NOD2 which port CARDs domain, activate NF-κB and MAP-kinase pathways via an adapter (RIP2/RICK). NF-κB then activates the expression of inflammatory cytokines [19, 31].

1.3.3.4 Fc-receptors

Fc-receptors (**Figure 1.3.4**) are proteins found on the surface of B lymphocytes, follicular dendritic cells, NK cells, macrophages, neutrophils, eosinophils, basophils, and mast cells [20]. They have the ability to bind to antibodies in their Fc region and are involved in the recognition of Ig-opsonized pathogens, participating as well in immune complex-mediated inflammatory processes [20].

These receptors promote phagocytic or cytotoxic cells to destroy microbes or cells which were infected by antibody-mediated phagocytosis or ADCC. Some viruses (e.g. flaviviruses) use Fc receptors to help them infect cells, by a mechanism known as enhancement of antibody-dependent infection [20]. The most important Fc-receptors in neutrophils are the low-affinity Fcγ-receptors [40]. These receptors present important roles in immune complex mediated activation of neutrophils. The activation of leukocytes by immune complexes requires synergistic ligation of both FcγRIIA and FcγRIIIB [41]. They also express the high-affinity FcγRI molecule [42, 43] and FcαRI, which can mediate IgA-induced inflammatory processes, tumour cell killing [44, 45], and may participate in allergic responses [46, 47] or as pathogenic factors in certain infectious diseases [48]. It is important to remark that signalling usually starts by crosslinking of the Fc receptor. This

crosslinking leads to an engagement with other receptors, that activate a signalling cascade [49-51].
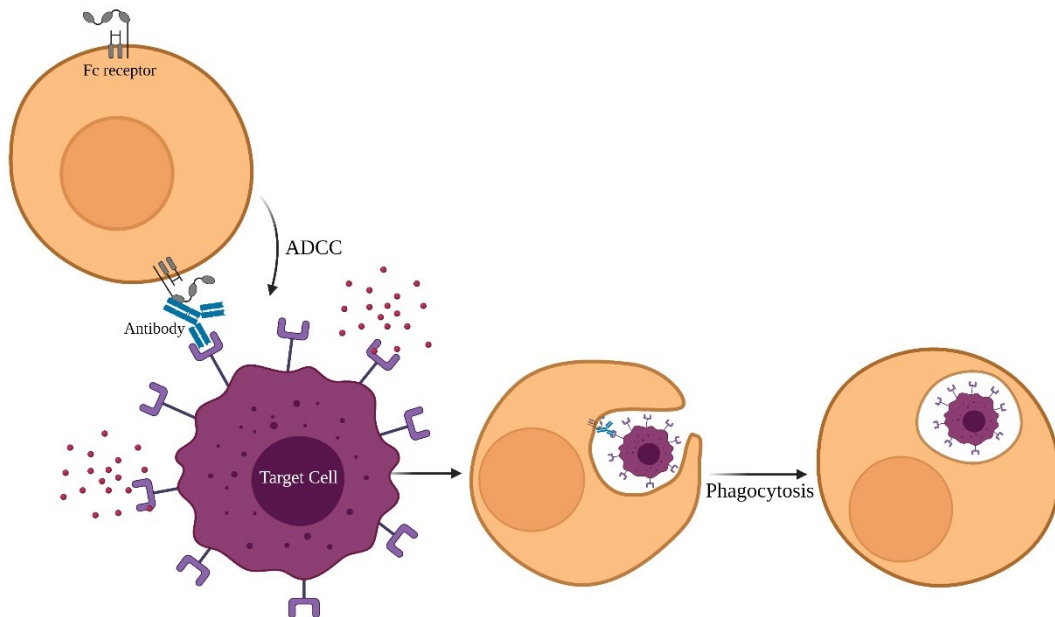
Figure 1.3.4. Schematic illustration of an Fc receptor and its interaction with an Ab-coated target. Fc receptor binds to the antibodies in their Fc region, triggering the recognition of Ig-opsonized pathogens. After contact, a process called phagocytosis occurs, where foreign substances are ingested or engulfed in a defensive reaction against infection and invasion of the body. Created with a paid subscription of BioRender (https://biorender.com).

1.3.3.5 Cytokine receptors

Cytokine receptors (**Figure 1.3.5**) are cell surface glycoproteins that, when linked to cytokines, transduce a signal. These receptors permit the communication between the cells and the extracellular environment, responding to signals produced in the body [21]. Therefore, the first binding of cytokines to their receptors is a crucial event that is fast, in low concentrations, generally irreversible and leads to intracellular changes, resulting in a biological response [21]. They comprise six group members, based on their three-dimensional structure, namely type I, type II, Ig superfamily, tumour necrosis factor (TNF) receptor family, chemokine receptor and transforming growth factor β (TGF- β) receptor family.

Conventional cytokine receptors are grouped into type I and type II. Those types of receptors are involved in a few neutrophil functions. Type I receptors consists in transmembrane receptors expressed on the surface of cells, recognizing and responding to cytokines with four α-helical strands [21]. G-CSF and GM-CSF guide the differentiation, survival and activation of neutrophils

[21]. IL-4, IL-6, and IL-15 are involved as well in activation of neutrophils and in the coordination of the inflammatory response.
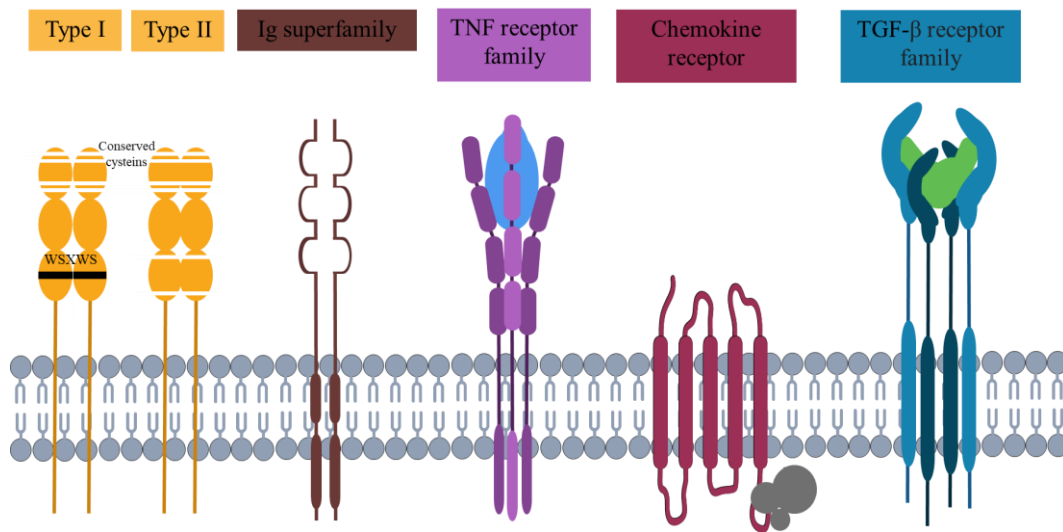
Figure 1.3.5. Types of cytokine receptors: type I and type II families possess extracellular fibronectin like domains, only differing in the WSXWS motif present in the type I, that are not present in type II receptors. The Ig superfamily shares extracellular regions structural homology with immunoglobulin domains. The TNF receptor family has cysteine-rich motifs in their extracellular regions able to bind ligands. Chemokine receptor are G protein coupled receptors and TGF- β receptor family are Serine/threonine kinase receptors. Part of this figure was created with Servier medical art (https://smart.servier.com).

Type II are similar to type I cytokine receptors, except they do not possess the signature sequence of common amino acid motif. IFNα/β delay apoptosis of neutrophils [22], whereas IFNγ which is secreted by NK cells reacting to antigens and activated T lymphocytes during adaptive immune responses. IFN-γ is a major macrophage activating cytokine [52]. IL-10 presents an inhibitory effect on various functional responses of neutrophils, namely chemokine and cytokine production [53]. Type I and type II cytokine receptors trigger the activation of the JAK-STAT pathway [54-56], Src-family kinases [57-60], the PI3-kinase-Akt pathway [58, 60-62], the ERK and p38 MAPK [63, 64], and the inhibitory SOCS molecules [65-67]. Ig superfamily are involved in the recognition, binding, or adhesion processes of cells. They all possess a domain known as an immunoglobulin domain or fold. Included in this group are molecules involved in the presentation of antigen to lymphocytes, cell adhesion molecules, cell surface antigen receptors, co-receptors and co-stimulatory molecules of the immune system [21, 28]. TNF receptors are characterized by the ability to bind tumour necrosis factors (TNFs) via an extracellular cysteine-rich domain. They are engaged in apoptosis and inflammation phenomena, but also participate in other signal transduction

pathways, such as proliferation, survival and differentiation [28]. The chemokine receptor interacts with a type of cytokine called a chemokine. Each has a rhodopsin-like 7-transmembrane (7TM) structure that allows to couple to G-protein for signal transduction within a cell, making them members of the large protein family of GPCR. After interaction with their specific chemokine ligands, the chemokine receptors trigger a flux in intracellular calcium (Ca^{2+}) ions. This event causes cell responses, including the onset of a process known as chemotaxis that traffics the cell to a desired location within the organism [28]. TGF-β receptors are serine/threonine kinase involved in cell growth, cell differentiation, apoptosis and cellular homeostasis [21, 22]. TGFβ ligands bind to a type II receptor, which recruits and phosphorylates the type I receptor. Then it phosphorylates the receptor-regulated SMADs (R-SMADs) which bind the coSMAD SMAD. The complex R-SMAD/coSMAD accrue in the nucleus where they join in the regulation of target gene expression, acting as a transcription factor [21, 22].

After accumulation, mast cells are stimulated by the chemokine alarm chemicals to release histamine. Adhesion of neutrophils (first leukocyte to respond) is mediated by adhesion molecules, whose expression is enhanced by secreted proteins known as cytokines (**Figure 1.3.6**) [68, 69]. These are secreted by cells in response to microorganisms and other harmful agents, ensuring that neutrophils are recruited into the tissues. The initial interactions of bearing are mediated by selectins [70, 71], which are divided into three types: one expressed in leukocytes (L-selectin), one in the endothelium (E-selectin) and one in platelets (P-selectin). Its expression is regulated by cytokines produced in response to inflammation and injury. Leukocytes (neutrophils and monocytes) express L-selectin at their surface, and as a result they roll along the endothelial surface. This rolling is regulated by TNF [72] and IL-1 [73], which induce the endothelial expression of integrin ligands, especially vascular cell adhesion molecule-1 (VCAM-1) and intercellular adhesion molecule-1 (ICAM- 1). The expression of integrin ligands induced by the chemoattractants like cytokines, and the activation of the integrins in the leukocytes results in a firm adhesion to the endothelium [33]. Due to the chemoattractant gradients in the tissue, leukocytes are able to migrate to the interstitial tissue fluid, via chemoattractant receptor–mediated chemotaxis [74]. Through the receptor in the surface of the leukocytes are initiated signals, that result in the activation of a second messenger that increase cytosolic Ca^{2+}, activate enzymes such as protein kinase C and phospholipase A_2, and induce polymerization of actin, ensuing in increased quantities in direction of the cell border and localization of myosin filaments. In the intercellular junctions there are adhesion molecules called platelet endothelial cell adhesion molecule (PECAM-1) or cluster of differentiation 31 (CD31) that aid in transmigration [68, 75]. The leukocytes migrate in

the direction of the locally produced chemoattractant gradient. After crossing the endothelium, the leukocytes leave the circulation and migrate to the tissues towards the lesion site by chemotaxis [76]. When leukocytes reach the site of inflammation, they are activated to perform their functions, recognition of aggressive agents, which release signals and these signals activate the leukocytes to ingest and destroy the hostile agents and amplify the inflammatory reaction [77].

The functional responses which are the most important for the destruction of microbes and other harmful agents are phagocytosis and intracellular killing. Phagocytosis involves three sequential steps: i) recognition and binding of the particle to be ingested by the leukocyte; ii) its intake, with subsequent formation of the phagocytic vacuole; and iii) death or degradation of the ingested material [78, 79].
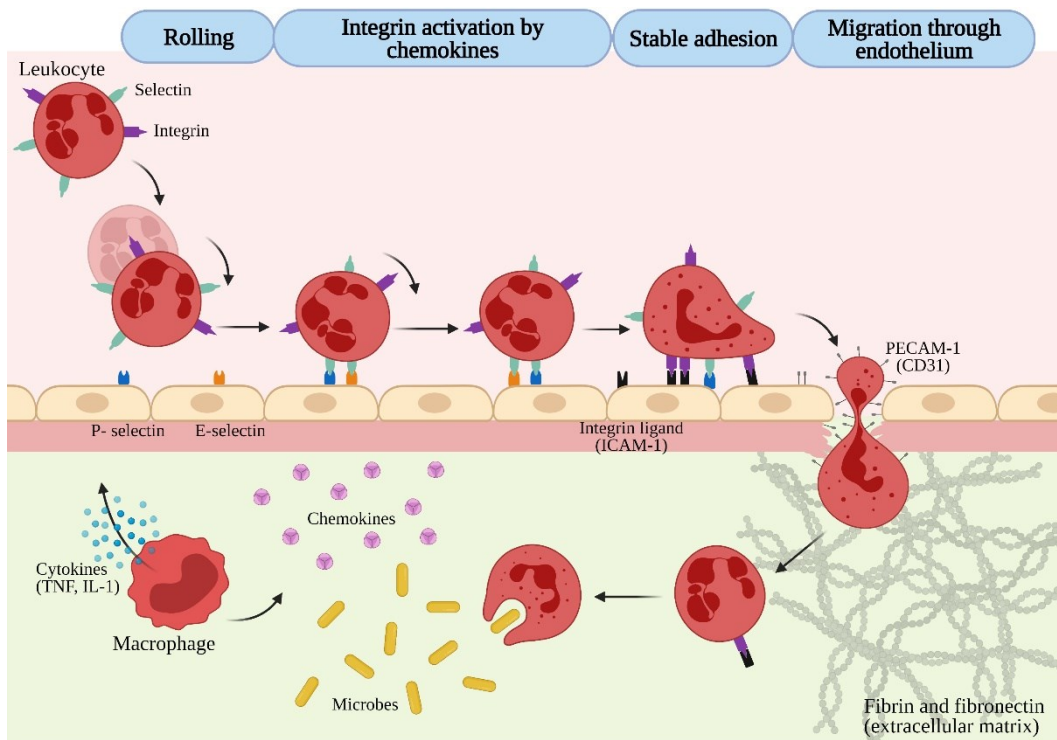
Figure 1.3.6. Firstly, leukocytes roll and then become activated, adhering to the endothelium. Following occurs their penetration in the basement membrane and migration towards the chemoattractants released at the source of the injury. Different molecules have important roles in different phases – selectin in the scroll; chemokines activated neutrophils; integrins in firm adhesion and CD31 (PECAM-1) in transmigration. Adapted from Kumar *et al*. [77]. Created with a paid subscription of BioRender (https://biorender.com).

Phagocytosis depends on the polymerization of actin filaments and is increased when the microbes are opsonized by specific proteins, opsonin, for which phagocytes express high affinity receptors [80]. After binding of the microorganisms to the receptors, extensions of the cytoplasm

flow around them and the plasma membrane closes in a vesicle, called the phagosome. It fuses with the lysosome, resulting in discharge of the bead content into the phagolysosome [80]. The last step in the removal of infectious agents and necrotic cells is death and degradation within neutrophils and macrophages. The microbial death is carried out by ROS and reactive nitrogen species (RNS) [78, 79]. The generation of ROS is catalysed by the action of NADPH oxidase, that oxidizes NADPH and reduces oxygen to the superoxide anion ($O_2^{\bullet-}$). $O_2^{\bullet-}$ is converted to hydrogen peroxide (H_2O_2), whichever cannot efficiently destroy microbes. However, H_2O_2 can be converted to the hydroxyl radical ($OH^{\bullet}$), or through the enzyme myeloperoxidase (MPO), converted to hypochlorite ($OCl^{\bullet}$), both potent antimicrobial agents that destroy microbes by halogenation or oxidation of proteins and lipids [81]. NO also participates in microbial death. It reacts with $O_2^{\bullet-}$ to generate the peroxynitrite radical ($ONOO^{\bullet}$). These free radicals attack and damage the lipids, proteins and nucleic acids of microbes [82]. The elimination of microbes and dead cells activated leukocytes have other roles in the defence of the host. After this "cleansing", macrophages produce growth factors that stimulate endothelial cell proliferation, fibroblasts and collagen synthesis, that remodel connective tissues, allowing healing and the end of the inflammatory process [83].

It can be concluded that inflammation plays a central role in the fight against pathogens and can set biological reactions to restore the integrity of the organism. Hysterical amplification of the events may lead to undesirable pathological manifestations such as neoplastic transformations due to the oxidation of DNA, cancer, diabetes, and cardiovascular, neurological, and chronic inflammatory diseases. Therefore, it is necessary to limit the inflammatory process by eliminating the cellular infiltrate and its potentially toxic products [5, 6].

As shown and discussed throughout this section, inflammatory mediators (e.g., cytokines) present complex signalling pathways [84]. Thus, depending on the disease's scenarios, sometimes it would be more beneficial to target the ligand rather than the receptor, or vice-versa. Several factors contributed for the increased importance of soluble ligands as mAbs targets, such as the growing understanding of their role in the immune system, the easier access to ligands than their receptors and the easier mapping of epitopes in protein ligands [84]. However, some challenges may appear, for instance the possibility of a mAb to target a ligand but not inhibiting its interaction with the intended receptor, or the challenges associated to the targeting of GPCRs or other membrane proteins. GPCRs or other membrane proteins are highly challenging for antibodies development since most of the receptor protein is embedded in the lipid bilayer [85]. Thus, in the specific case of GPCRs, only the N-terminal domain and the extracellular loop regions are accessible as immunogenic epitopes, while the transmembrane components present no inherent therapeutic

interest. It is of upmost importance to understand the biological features of each target, in order to assure that the mAb biopharmaceutical is correctly targeted according to the desired treatment. In the next section, an overview on the most relevant/recent mAbs-based therapeutics targeted for the treatment of inflammatory diseases is presented.

1.3.4. Monoclonal antibody-based therapies for the treatment of inflammation

1.3.4.1 Interleukin-8 and interleukin-6

There are more than 40 different chemokines that can be classified according to the location of the cysteine residues at the amine terminus [86]. One of the most widely studied chemokine is interleukin-8 (IL-8), also called chemokine ligand 8 (CXCL8) (**Figure 1.3.7**) [87].
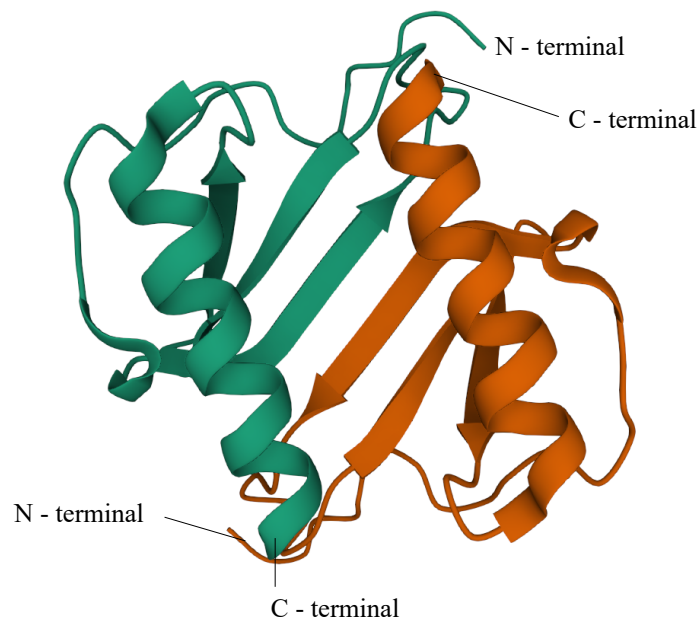
Figure 1.3.7. 3D structure of interleukin-8 dimer (image from the Protein Data Bank website (http://rcsb.org/pdb) of PDB ID 1IL8 [88]). N- and C-terminals are also identified.

Based on a chain of biochemical reactions, IL-8 is produced by leukocytes and epithelial and endothelial cells [87]. IL-8 is initially produced as a 99 amino acid precursor peptide, and then undergoes cleavage to create various active IL-8 isoforms. The peptide containing 72 amino acids, possess a molecular weight of 8.4 kDa and a isoelectric point > 8.5, is the mature form secreted by macrophages [89]. IL-8 is a key mediator associated with inflammation, mediating the recruitment and activation of neutrophils through complex signalling mechanisms and extracellular adhesion molecules [90]. Its receptors are found on the surface membrane of various cells of the immune

system. The most important are the G protein-coupled receptors, which after binding to IL-8 activate the intracellular signalling cascades and triggers a conformational change, resulting in the activation of G protein [90]. G protein subunits stimulate phosphatidylinositol 4-phosphate kinase (PIPK) which in turn synthesizes phosphatidylinositol 4,5-bisphosphate (PIP_2), being the source of inositol trisphosphate (IP_3) and phosphatidylinositol (3,4,5)-trisphosphate (PIP_3). IP_3 leads to the release of Ca^{2+} that induces chemotaxis, oxidative burst, exocytosis and eventually the release of more inflammatory mediators [90]. PIP_3 activates ras/raf/MAPK pathways, inducing the expression of adhesion molecules, such as integrin, fundamental for chemotaxis [90].

One highly relevant pro-inflammatory cytokine is interleukin-6 (IL-6) (**Figure 1.3.8**). It was originally discovered in 1986 by Hirano *et al.* [91], as a T cell–derived B cell stimulatory factor-2, promoting Ig synthesis by activated B-cells. Its production is associated with monocytes, macrophages, lymphocytes, endothelial cells and fibroblasts, and can be stimulated by interleukin-1 (IL-1) and TNF [92, 93].
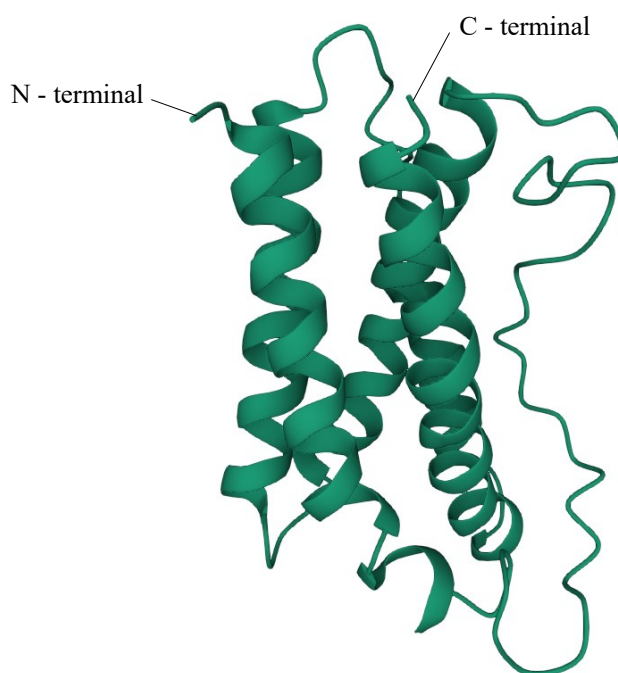
Figure 1.3.8. 3D structure of interleukin-6 (image from the Protein Data Bank website (http://rcsb.org/pdb) of PDB ID 1IL6 [94]). N- and C-terminals are also identified.

Human IL-6 consist of a polypeptide cytokine with a four–α-helix structure and is composed of 212 amino acids, including a 28-amino-acid signal peptide, and its gene has been mapped to chromosome 7p21. Even though the core protein possess 20 kDa, glycosylation is responsible for the size of 21 − 26 kDa of natural IL-6 [92, 93]. IL-6 family cytokines are a group of cytokines

consisting of IL-6, oncostatin M (OSM), leukemia inhibitory factor (LIF), ciliary neurotrophic factor (CNTF), cardiotropin-1 (CT-1), cardiotrophin-like cytokine (CLC), neuropoietin (NP), IL-11, IL-27, and IL-31. In the receptor complexes, all of them contain a common receptor signal transducer subunit (gp130), except IL-31 [93].

IL-6 is a pleiotropic cytokine which play a part in the short-term defence against infection or injury, warning the immune system against the source of inflammation [95]. Upon being secreted during an acute inflammatory response, IL-6 forms a protein complex with its specific α-receptor (IL-6R) and the ubiquitously expressed 130 kDa transmembrane protein mentioned before – gp130 – which encourages the transition from neutrophil to monocyte in inflammation, initiating the signal transduction [96]. This binding induces the homodimerization of gp130 that triggers cellular events, including activation of the JAK/STAT3 pathway. Then, STAT3 and SHP2 are phosphorylated and activated by the activated JAK. SHP2 links the cytokine receptor to the Ras/MAPK pathway and it also links the Grb2-SOS complex and Gab1 to gp130 [92, 96-98]. Then, the phosphorylated STAT3 forms a dimer and translocate into the nucleus in order to activate the transcription of genes comprising STAT3 response elements. STAT3 induces as well the expression of the suppressor of cytokine signalling 1 and 3, that binds to phosphorylated JAK and gp130, respectively, leading to the cessation of IL-6 signalling via a negative feedback loop [92, 96-98]. Nevertheless, IL-6 can also signal through its soluble form, sIL-6R, which is present in human serum. After binding IL-6 to sIL-6R, the complex binds to gp130, consequently stimulating cells that do not express transmembrane IL-6R, for example smooth and endothelial muscle cells. This form of IL-6 signalling is known as IL-6 trans signalling, while transmembrane IL-6R signalling is known as classical IL-6 signalling [97].

1.3.4.2 Anti-interleukin-8 and anti-interleukin-6 mAbs

Interleukin-8 induces morphologic change of neutrophils and release activated substances under ischemic and hypoxic conditions. On the other hand, it is an important neutrophilic granulocyte chemotactic regulator and endorses infiltration of neutrophils into the vascular wall, causing its destruction and hyperplasia [90, 99]. IL-8 accelerates proliferation, migration and incrassation of smooth muscle cells, exacerbating vasospasm and vasogenic edema [90, 99]. Generation of IL-8 can be expected upon infection, trauma, ischemia and other disturbances of tissues, since IL-1 and TNF levels are increased [89]. Studies presented by Alcorn *et al.* [100] reported high IL-8 levels in asthma, obstructive lung disease and acute respiratory distress syndrome. Also, as the inflammatory response represents a major component of the tumour microenvironment, being responsible for the mediation of the biological communication network

and the molecular signalling flow, it is important to observe the levels of this interleukin in this situation. A study by Abdollahi *et al.* [101] showed that overexpression of IL-8 and/or its receptors increases tumour growth and angiogenesis, a critical step for tumour metastasis [101].

Taking into account the overproduction of IL-8 and aiming its reduction, it was revealed in 1989 by a study in rheumatoid synovial membrane cultures that the use of anti-tumour necrosis factor (anti-TNF) mAbs inhibited the local production of proinflammatory mediators, such as interleukins (IL-1, IL-6, IL-8) [13, 102]. During the inflammatory process, the activation of cells took place after binding to IL-8 receptors, which are expressed in immune system cells such as neutrophils, monocytes, endothelial cells, astrocytes and microglia [103, 104]. The accumulation of active neutrophils in the injured areas and the overproduction of IL-8 can lead to chronic inflammatory conditions [103, 104]. The overproduction of IL-8 has been proposed to significantly contribute to all these pathologies, characterized by the accumulation of activated neutrophils in injured areas [103, 104].

Tests using mAbs against IL-8 in animal models with acute inflammation showed inhibition or reduction of neutrophil function and partially solved inflammation [103, 104]. Several studies [103-105] have shown that anti-IL-8 significantly reduces neutrophil infiltration in the early stage of the inflammation event and that anti-IL-8 treatment also reduced redness and sagging of the joints and prevented membrane damage synovial [103, 104]. In the study conducted by Yang *et al.* [106], it was found that among all fully human IgG2κ anti-IL-8 mAbs studied, K4.3 and K2.2 (derived from Xeno-Mouse strains) blocked IL-8 binding to human neutrophils, as well as the activation of neutrophils and chemotaxis of neutrophils. Skov *et al.* [103] provided an *in vivo* proof of concept of the application of an anti-human IL-8 antibody (HuMab 10F8) for the treatment of inflammatory diseases, such as palmoplantar pustulosis [103]. Mahler *et al.* [107] demonstrated that the use of anti-IL-8 antibody (ABX-IL8) in the treatment of chronic obstructive pulmonary disease was well tolerated and safe, once the neutralization of IL-8 led to small but significant reducing of the severity of dyspnea, the major symptom of this disease, which evidences a reduction in the number of neutrophils in the blood [107]. Investigations have also been conducted with HIV, where Guha *et al.* [108] found that anti-IL-8 restored 38 % and 22 % of neuronal death. As there are inflammation situations in cancer, this IL-8 mAbs is starting to be used in the treatment of cancer, being however under development [109]. An important finding in this field was reported by Huang *et al.* [109], showing promising results with the use of this therapy in a melanoma case. The results revealed that ABX-IL8 does not inhibit the proliferation of melanoma cells *in vitro*, but increases the number of apoptotic tumour cells and significantly suppressed tumorigenicity *in vivo* [109]. Using a more

complex model system of metastatic primary tumours, histochemical analysis confirmed that anti-IL-8 therapy results in a significant reduction of Matrix Metalloproteinase-9-neutrophils, associated with reduced levels of angiogenesis [110].

Interleukin-6 elicits acute phase reactions, but also the development of specific cellular and humoral immune responses, namely end-stage B cell differentiation, immunoglobulin secretion and T cell activation. It is produced at low levels, but there is an increase in its expression in the presence of inflammation or trauma [92, 93, 95]. After its production in the inflammatory region, it reaches the liver through the bloodstream. Following occurs a rapid induction of the secretion of vascular endothelium growth factor (VEGF), leading to the increased growth of blood vessels and vascular permeability in inflammation. It also induces high concentrations of SAA for a long time, that leads to the development of amyloid A amyloidosis – a severe complication of chronic inflammatory diseases [92, 93, 95].

The dysregulated overproduction of IL-6 has been implicated in the development of several autoimmune and chronic inflammatory diseases (rheumatoid arthritis, systemic juvenile arthritis and Crohn's disease) [111]. This association of IL-6 with inflammatory diseases was first shown in 1988 in a case of rheumatoid arthritis, where the patients were detected with high levels in synovial fluids [112]. Subsequent studies [92] have shown that this dysregulation also occurred in swollen lymph nodes of Castleman's disease, myeloma cells and peripheral blood cells or involved tissues in various other chronic inflammatory diseases. Consequently, it is extremely important to regulate the magnitude and duration of the response of this unregulated IL-6 production. One of the first approved mAbs for the treatment of inflammatory diseases was tocilizumab (trade name, Actemra) in 2010 [113]. This humanized anti-IL-6R mAb binds both soluble and transmembrane receptor of IL-6 (IL-6R), blocking the action of IL-6 without increasing its half-life [114]. Clinical studies [111, 114-116] demonstrated its outstanding efficacy for the treatment of rheumatoid arthritis and Castleman's disease. For the treatment of rheumatoid arthritis, tocilizumab was quite effective with > 80 % and > 30 % of patients achieving ACR20 and ACR50 responses (clinical response parameter established by the American College of Rheumatology (ACR)), respectively [114]. Tocilizumab can be used as a monotherapy or in combination with disease-modifying antirheumatic drugs, and it has significantly suppressed the disease activity and radiographically detected progression of joint deformity, allowing to improve daily functional activity [111, 114-116]. Later, in 2014, siltuximab (trade name Sylvant) [117], anti-IL-6 chimeric (made from human and mouse proteins) mAb, was approved for the treatment of patients with Castleman's disease who do not have human immunodeficiency virus (HIV) or human herpesvirus-8 (HHV-8). Van Rhee *et al.* [118] studied the

assess treatment of long-term safety and activity of siltuximab for 6 years, and concluded that in 97 % of patients idiopathic multicentric Castleman disease was controlled, supporting the use of this anti-IL-6 mAb as a first-line therapeutic in this disease. Sarilumab (trade name Kevzara, 2017), a humanized anti-IL-6R mAb, is able to inhibit IL-6 signalling, which otherwise would upregulate the release of rheumatoid arthritis-related factors from hepatocytes [119]. Sarilumab was approved by FDA for the treatment of moderately to severely active rheumatoid arthritis in people who do not respond or tolerate more conventional treatments. The biopharmaceutical can be used alone or in combination with methotrexate or other disease-modifying antirheumatic drugs [119]. Fleischmann *et al.* [120] showed a reduction of the absolute neutrophil counts (<1000 cells.mm^{-3}) for 13 % and 15 % of patients treated with combination therapy and only sarilumab, allowing to confirm its long-term safety profile. Also, a humanized anti-IL-6R mAb, satralizumab-mwge (trade name Enspryng), was the last one to be approved so far, in 2020. It is indicated for the treatment of neuromyelitis optica spectrum disorder (NMOSD) in adults with a particular antibody (anti-aquaporin-4 positive) [121]. Traboulsee *et al.* [122] proved that the monotherapy with satralizumab-mwge reduces the risk of relapse by 55 % for all NMOSD patients and by 74 % in anti-aquaporin-4 positive-IgG seropositive patients, suggesting it as a safe and effective alternative for all NMOSD patients. Yet, there are many clinical studies underway on anti-IL-6 mAbs, such as sirukumab (CNTO136), olokizumab (CP6038), elsilimomab (BE-8), clazakizumab (BMS945429) and MEDI5117 which are in different phases of clinical trials to ascertain their efficacy and safety [123].

All previously reported studies here discussed suggest that anti-IL-8 and anti-IL-6 mAb-based therapy, if proven effective in clinical trials, could be used to treat a broad spectrum of disorders, with particular interest for inflammatory diseases.

1.3.4.3 Role of anti- IL-6 mAbs in the case of Severe Acute Respiratory Syndrome-2

Inflammation is a stereotyped response [124]; so, it is reflected as a mechanism of innate immunity, as compared to adaptive immunity that is specific for each pathogen [124]. The inflammation response turns out to be transversal to several diseases, not only the inflammatory ones, but also infectious diseases for example. Infections are a frequent cause of inflammation and are caused by an infectious agent. The inflammation they cause depends on the type of infectious agent and the location of the organism where it is installed [125]. A known example of this is the coronavirus (CoVs), which contain a large group of viruses and is one of the main pathogens directed mainly to the human respiratory system. In the past decade, two new viruses have revealed to be highly pathogenic infectious agents for humans, causing potentially lethal infections. They are the

coronaviruses responsible for Severe Acute Respiratory Syndrome (SARS-CoV) and the coronaviruses of the Middle East Respiratory Syndrome (MERS-CoV) [126-128]. Genetic analysis carried out to date have shown that the new CoVs belong to the same group that includes SARS-CoV, identified 10 years ago [126-128]. The designation of the new coronavirus as 2019-nCoV has been replaced by SARS-CoV-2, which means that it is the second coronavirus in the SARS group.

The SARS-CoV-2 was first identified in humans in December 2019 in the city of Wuhan, China, causing an infection disease, called Coronavirus Disease 2019 (COVID-19) that had spread worldwide [126-129]. This infection can be asymptomatic, but even in these cases, infected individuals can transmit the virus to other people, especially during the first days after the infection, when the viral replication in the upper respiratory tract is particularly productive [126-129]. The clinical signs and symptoms that characterize COVID-19 are very diverse, including fever, cough, illness and breathing difficulties, with invasive lesions in lungs that appear after an incubation period that can vary between 2 to 14 days [127]. In more severe cases, the infection can cause pneumonia, SARS, kidney failure and even death [127]. Although the virus can infect people of all ages, it appears to be particularly aggressive for individuals over the age of 65 with co-morbidities (example diabetes, hypertension, liver problems or immunosuppression due to cancer) [126-129].

SARS-CoV-2 is easily transmitted from person to person in two ways, through droplets and aerosols emitted with coughing, sneezing or during conversation at small distances. Its replication (**Figure 1.3.9**) on host cells occurs when the S glycoprotein on the virion binds to cellular receptor angiotensin-converting enzyme 2 (ACE2) and enters the target cells via an endosomal pathway [128, 130]. Following the entry, the viral RNA is unveiled in the cytoplasm and some RNA is translated into polyproteins, which are cleaved by proteases. Some of these proteins form a replication complex to produce more RNA. After the production of SARS-CoV-2 structural proteins, nucleocapsids are assembled in the cytoplasm and followed by budding into the lumen of the endoplasmic reticulum (ER)–Golgi intermediate compartment. The virions are then released from the infected cell via exocytosis [128, 130].

There are several approaches to the treatment of viruses, but is important to recognize that, at the moment, there are few available antiviral treatments. Considering the most recent pandemic, the approaches involved convalescent plasma therapy and antiviral therapies, with the aim of reducing viral replication, which is the main pathogenic mechanism. Another possible approach is immunomodulatory therapies, which are directed at the inflammatory response that leads to ARDS [131].

According to the pathogenesis of SARS-CoV-2, several studies evidenced that inflammatory cytokines and chemokines, including IL-6, IL-12, induced protein 10 (IP10), monocyte chemoattractant protein-1 (MCP-1) and TNF-α are considerable released in COVID-19 patients, creating a "cytokine storm" [132-134]. Thus, these released cytokines can be seen as important targets for the development of a therapeutic treatment. *Post-mortem* pathological analysis revealed tissue necrosis, interstitial macrophage and monocyte infiltrations in the lung, heart, and gastrointestinal mucosa [132-134]. These analysis are in accordance with IL-6 overproduction, which leads to an excessive signalling pathway and contribute to organ damage, including the maturation of naive T cells into effector T cells, induction of VEGF expression in epithelial cells, increased vessel permeability and reduced myocardium contractility [132].
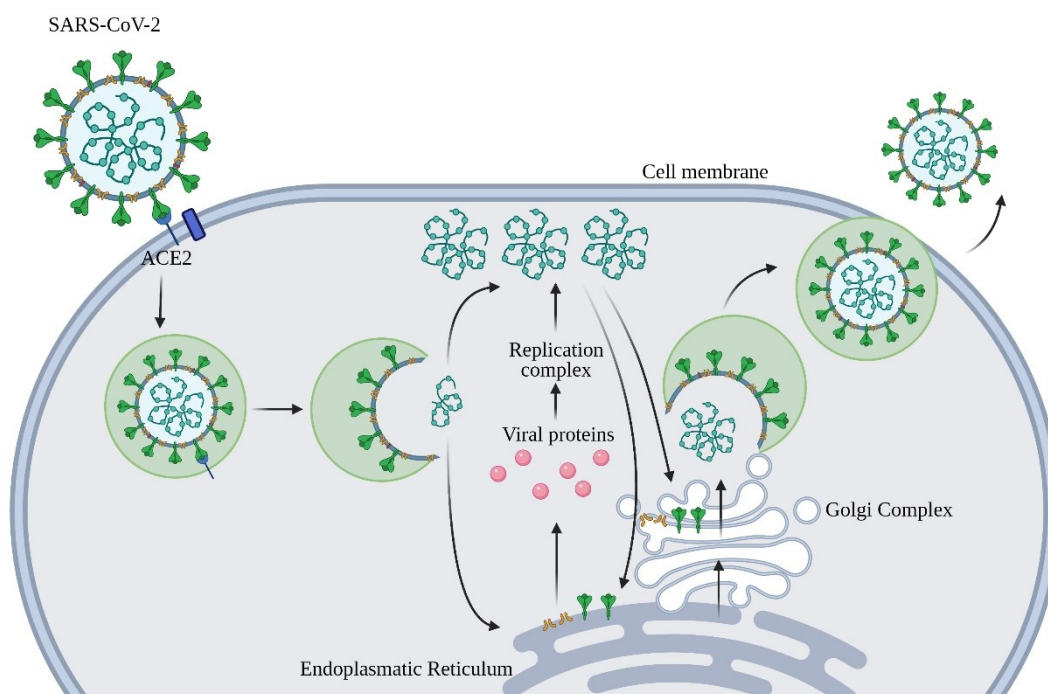
Figure 1.3.9. Life cycle of SARS-CoV-2 in the host cells. S glycoprotein on the virion binds to ACE2. The virion then releases its RNA, some being translated into proteins by the cell's machinery. Proteins and RNA are assembled into a new virion in the Golgi complex and released from the cell. Created with a paid subscription of BioRender (https://biorender.com).

Therefore, targeting IL-6 and its receptor (IL6R) using mAbs, such as tocilizumab, could mitigate cytokine storm-related symptoms in severe COVID-19 patients [135]. In 2017, tocilizumab was approved by FDA for severe life-threatening cytokine release syndrome [136]. Moreover, Xu et al. [137] observed, with repeated doses of tocilizumab 4 mg·kg^{-1} Intravenous (maximum dose 400 mg), a recovery of 91 % of patients with severe respiratory symptoms. Also with the same dosage,

Buonaguro et al. [133] observed that most patients experienced a 75 % improvement in the need for lower oxygen, an increase in lymphocyte levels, decreased fever and improvement in chest tightness. Taking these results into account, since March 2020, tocilizumab has been officially included in the treatment program for COVID-19 (7th edition) of the National Health Commission of China for patients with increased levels of IL-6, extensive opacity of bilateral lung injuries or in critically ill [138].

Based on the exposed, it seems that anti-IL6R mAb presents a protective role in COVID-19, and in particular tocilizumab, that demonstrated to be an effective therapeutic strategy in severe disease. What conveys a lot of hope is that in the past two months in China, clinical treatment with tocilizumab has shown remarkable efficacy and safety, promoting a certain expectation of benefiting other countries that are currently fighting the pandemic. However, it should be remarked that anti-IL6R may only be controlling the "cytokine storm" with no deleterious effect on virus replication [133, 138].

1.3.4.4 Other recently approved monoclonal antibodies for the case of inflammatory diseases

By December 2020, 96 therapeutic mAbs had been approved by the FDA; still, there is a significant growth potential associated to these biopharmaceuticals [119]. Only during 2019 and 2020, 20 new mAbs were approved in the US and started to be commercialized by several known pharmaceutical companies, such as Genentech®, Roche®, Novartis®, Alder BioPharmaceuticals®, Immunomedics®, Chugai Pharmaceutical®, AstraZeneca®, Viela Bio® and MedImmune®. These new mAbs were approved for the treatment of several disorders, for instance: thrombotic thrombocytopenic purpura (caplacizumab-yhdp), moderate-to-severe plaque psoriasis (risankizumab-rzaa), diffuse large B-cell lymphoma (polatuzumab vedotin-piiq and tafasitamab-cxix), osteoporosis (romosozumab-aqqg), macular degeneration (brolucizumab-dbll), sickle cell disease (crizanlizumab-tmca), urothelial cancer (enfortumab vedotin-ejfv), HER2+ metastatic breast cancer (fam-trastuzumab deruxtecan-nxki and margetuximab-cmkb), migraine prevention (eptinezumab-jjmr), multiple myeloma (isatuximab-irfc and belantamab mafodotin-blmf), thyroid eye disease (teprotumumab-trbw), triple-negative breast cancer (sacituzumab govitecan-hziy), neuromyelitis optica spectrum disorder (inebilizumab-cdon and satralizumab-mwge), Ebola virus infection (atoltivimab, maftivimab, and odesivimab-ebgn [mixture of 3 human IgG1] and ansuvimab-zykl), high-risk neuroblastoma and refractory osteomedullary disease (naxitamab-gqgk).

Among the 20 approved mAbs, 3 were suggested to be used in the treatment of inflammatory diseases, such as plaque psoriasis (risankizumab-rzaa [139]) and neuromyelitis optica spectrum disorder (satralizumab-mwge [121] and inebilizumab-cdon [140]). Nevertheless, it should be remarked that inflammation appears also as a condition with an important role in several other type of diseases pathogenesis and progression. Therefore, several mAbs have been approved throughout the years for such disorders, namely in the prevention of respiratory syncytial virus infection (palivizumab [141]), treatment of macular degeneration (ranibizumab [142] and brolucizumab-dbll [143]), chronic lymphocytic leukemia (alemtuzumab [144], ofatumumab [102] and obinutuzumab [145]), Non-Hodgkin lymphoma (ibritumomab tiuxetan [146]), Hodgkin lymphoma and systemic anaplastic large cell lymphoma (brentuximab vedotin [147]), giant lymph node hyperplasia and Castleman's disease (siltuximab [117]), acute lymphoblastic leukemia (blinatumomab [148], gemtuzumab ozogamicin [149] and inotuzumab ozogamicin [150]), hairy cell leukemia (moxetumomab pasudotox-tdfk [151]), thrombotic thrombocytopenic purpura (caplacizumab-yhdp [152]), diffuse large B-cell lymphoma (polatuzumab vedotin-piiq [153]) and thyroid eye disease (teprotumumab-trbw [154]).

The FDA-approved mAbs for the treatment of inflammatory diseases are summarized in **Table 1.3.1**, being the 3 most recent approved mAbs for inflammatory diseases and the 3 most recent approved for diseases with relevant inflammation indication highlighted in bold and further discussed in detail. For some of the mentioned diseases, there are also small molecule therapeutics [155] available and often prescribed (e.g., rheumatoid arthritis [156], psoriasis [157]). However, such class of molecules are not under the scope of the present chapter, and thus only mAbs-based biopharmaceuticals are mentioned and discussed.

Table 1.3.1. FDA-approved mAbs for the treatment of inflammatory diseases.

International non-proprietary name	Brand name	Type	Disease	Approval year	Ref.
Rituximab	Rituxan	Chimeric	RA	1997#; for RA in 2006	[102]
Infliximab	Remicade	Chimeric	Crohn's disease	1998	[158]
Adalimumab	Humira	Fully Human	RA	2002	[102, 158]

Omalizumab	Xolair	Humanized	Asthma	2003	[158]
Certolizumab-pegol	Cimzia	Humanized	RA, Crohn's disease	2008	[117, 158]
Golimumab	Simponi	Fully Human	RA, psoriatic arthritis, and ankylosing spondylitis	2009	[117, 158]
Canakinumab	Ilaris	Fully Human	Cryopyrin-associated periodic syndrome	2009	[158]
Ustekinumab	Stelara	Fully Human	Psoriasis, plaque psoriasis, psoriatic arthritis, Crohn's disease	2009	[117, 158, 159]
Tocilizumab	Actemra	Humanized	RA	2010	[102, 117 , 158 , 159]
Belimumab	Benlysta	Fully Human	Systemic lupus erythematosus	2011	[160]
Vedolizumab	Entyvio	Humanized	Ulcerative colitis and Crohn's disease	2014	[158, 159]
Secukinumab	Cosentyx	Fully Human	Arthritis, psoriatic psoriasis, ankylosing spondylitis	2015	[161]
Mepolizumab	Nucala	Humanized	Severe eosinophilic asthma	2015	[162]
Ixekizumab	Taltz	Humanized	Plaque psoriasis	2016	[117]
Reslizumab	Cinqair	Humanized	Asthma	2016	[163]
Sarilumab	Kevzara	Fully Human	RA	2017	[117]
Guselkumab	Tremfya	Fully Human	Plaque psoriasis	2017	[117]
Ocrelizumab	Ocrevus	Humanized	RA and systemic lupus erythematosus	2017	[102, 158]
Brodalumab	Siliq	Chimeric	Plaque psoriasis	2017	[164]
Benralizumab	Fasenra	Humanized	Asthma	2017	[165]
Tildrakizumab-asmn	Ilumya	Humanized	Plaque psoriasis	2018	[166]
Ibalizumab-uiyk	Trogarzo	Humanized	HIV	2018	[167]

Risankizumab-rzaa	Skyrizi	Humanized	Moderate-to-severe Plaque psoriasis	2019	[139]
Polatuzumab vedotin-piiq*	Polivy	Humanized	Diffuse large B-cell lymphoma	2019	[153]
Brolucizumab-dbll*	BEOVU	Humanized	Macular degeneration	2019	[143]
Teprotumumab-trbw*	Tepezza	Fully Human	Thyroid eye disease	2020	[154]
Satralizumab-mwge	Enspryng	Humanized	Neuromyelitis optica spectrum disorder	2020	[121]
Inebilizumab-cdon	Uplizna	Humanized	Neuromyelitis optica spectrum disorder	2020	[140]

HIV - human immunodeficiency virus; RA - rheumatoid arthritis; # - first approved for the treatment of Non-Hodgkin's lymphoma and chronic lymphocytic leukemia; * - recently approved mAbs for other diseases with relevant inflammation indication.

Risankizumab-rzaa

Psoriasis is a skin disease that causes red and itchy scaly patches on the knees, elbows and scalp [168]. This condition has an increased expression of pro-inflammatory cytokines, namely IFN-γ, TNFα, IL-1, IL-6, and the chemokine IL-8. This overproduction is consistent with the inflammatory markers found in lesioned psoriatic skin [168, 169]. Also, IL-23 is produced by antigen-presenting cells and induces and maintains the differentiation of T-helper cells (Th17 and Th22), which are a primary cellular source of proinflammatory cytokines [170]. Such cytokines mediate the keratinocyte immune activation, epidermal hyperplasia and tissue inflammation in psoriasis [170]. About 90 % of the cases of psoriasis correspond to a chronic illness situation without cure. However, a promising therapeutic was recently proposed, namely risankizumab-rzaa [168, 169]. Risankizumab-rzaa (brand name SKYRIZI) is a humanized IgG1 mAb that was developed in partnership between AbbVie and Boehringer Ingelheim, for the treatment of immunological and inflammatory disorders. This biopharmaceutical binds with high affinity to and neutralizes the p19 subunit of IL-23, thereby inhibiting the proinflammatory effects of IL-23 [139, 143]. IL-23 regulates the inflammation in the peripheral tissues, especially in type 1-polarized T-cell-driven disease. *In vitro*, risankizumab was able to inhibit IL-23-dependent phosphorylation of STAT3 in human B-lymphoblastoid cell lines originated from human diffuse large cell lymphoma, whereas *in vivo* (in mouse splenocytes) it inhibited the induction of IL-17 production from human IL-23 stimulation

[139]. The recommended dosage of this biopharmaceutical is 150 mg (two 75 mg subcutaneous injections), but it carried out some risks of infections, including the activation of tuberculosis sepsis, cellulitis, and pneumonia. In the phase I of clinical trials, patients received a single dose of this mAb, where some of them received via intravenous, subcutaneous and a control group received the placebo (solution of 0.9 % NaCl). At the end of the 12th week, 87 % of patients achieved a decrease of 75 % in the Psoriasis Area and Severity Index (PASI), while 58 % and 16 % of the patients achieved a decrease of 90 % and 100 %, respectively [171, 172]. In phase II, several patients received subcutaneous injections of risankizumab-rzaa or ustekinumab and also the placebo. At week 12, 77 % and 40 % of the patients achieved a decrease of 90 % or higher in the PASI, for risankizumab-rzaa or ustekinumab, respectively [172]. To evaluate the efficacy, safety and tolerability, a third phase program, with four random clinical trials (IMMvent (NCT02694523), IMMhance (NCT02672852), ultIMMA-1 (NCT02684370), and ultIMMa-2 (NCT02684357)) was conducted in Asia, Canada, Europe, Mexico, South America, and the United States, comparing risankizumab-rzaa to ustekinumab, adalimumab and placebo in the indication of plaque psoriasis [139, 143, 171]. In the end of these 4 trials, risankizumab-rzaa showed more efficacy than placebo and more tolerability. On 26th March 2019, it was first approved in Japan for the treatment of plaque psoriasis, generalized pustular psoriasis, erythrodermic psoriasis and psoriatic arthritis, and on 23rd April 2019, FDA approved the treatment of moderate to severe plaque psoriasis. By the end of April 2019, this mAb had been granted approvals in Canada, US, and EU. Nevertheless, there are still many clinical trials ongoing, namely in Brazil and Russia, for the treatment of psoriatic arthritis, Crohn's disease, ulcerative colitis and atopic dermatitis [139, 143, 171].

Polatuzumab vedotin-piiq

Polatuzumab vedotin-piiq (brand name Polivy) is a humanized IgG1 conjugated to the antimitotic agent monomethyl auristatin E (MMAE) that was developed by Genentech and Roche as an antibody-drug conjugate designed for the treatment of haematological malignancies. Its target is CD79b, which is a B-cell receptor component, moderately to strongly expressed in lymphoma covalently conjugated via a cleavable linker to the MMAE. After the internalization and linker cleavage of Polivy, the released MMAE inhibits cell division and promotes apoptosis [143, 153]. Polatuzumab vedotin-piiq displayed activity against most diffuse large B-cell lymphoma cell lines evaluated *in vitro*, regardless of whether they were of the activated B-cell-like (ABC) or germinal center-like cell-of-origin subtype or harboured mutations in CD79B known to be associated with poor survival in diffuse large B-cell lymphoma. *In vivo* (mouse xenograft models),

polatuzumab vedotin-piiq enhanced the apoptosis and reduced the proliferation of mature CD79b+ B-cell NHL cell lines, increasing the overall survival [153]. Its recommended dosage is an intravenous infusion of 1.8 mg·kg^{-1} in combination with bendamustine plus rituximab, but included common side effects - cytopenia [143, 153, 173, 174]. There were several clinical trials to test the use of polatuzumab vedotin-piiq in combination with immunotherapy, immunomodulating therapy, chemotherapy and as monotherapy. However, its approval by the FDA was based on evidence from one study GO29365 (NCT02257567), an open-label, multicenter clinical trial that included a cohort of patients with relapsed or refractory diffuse large B-cell lymphoma (DLBCL), that was steered in the US, Canada, Europe, and Asia [143, 153]. The phase Ib safety run-in included 6 Polivy combined with bendamustine and rituximab (P+BR)–treated patients, where the best response by the independent review committee was a complete response (CR) rate of 50.0 % and an overall response of 50.0 % [153, 173, 174]. In a phase Ib/II expansion it was evaluated Polivy plus bendamustine and obinutuzumab (P+BG)-treated patients, and the best results by the independent review committee was a CR rate of 37.0 %, an overall response of 48.1 % and an average survival of 10.8 months [143, 153, 173, 174]. In phase II, patients were randomized to receive an intravenous therapy of Polivy (1.8 mg·kg^{-1}) with bendamustine (90 mg·m^{-2}) and rituximab (375 mg·m^{-2}) (P+BR) or BR alone, during 21 days for 6 cycles. Efficacy was founded on CR rate and duration of response (DOR), established as the time the disease stays in remission. At the end of the treatment, by PET-CT (Positron Emission Tomography – Computed Tomography) scans, the best responses by the independent review committee was a CR rate of 50.0 % with P+BR and 22.5 % with BR alone, an overall response of 62.5 % with P+BR compared with 25.0 % with BR and a median overall survival of 12.4 and 4.7 months, respectively [143, 153, 173, 174]. In 10th June 2019, polatuzumab vedotin-piiq was approved in the US by FDA in combination with the chemotherapy bendamustine and a rituximab product for the treatment of relapsed/refractory diffuse large B-cell lymphoma – a rare type of white blood cells cancer. In the end of January 2020 it was approved for medical use in EU, by EMA [143, 153]. Despite this approval there are still numerous clinical trials enduring, for instance a phase Ib/II with Polivy in combination with an immunomodulating agent, a phase III comparing polatuzumab vedotin-piiq plus rituximab-CHP with rituximab-CHOP and a phase Ib/II trials which are evaluating polatuzumab vedotin-piiq in combination with other immunochemotherapy [153].

Brolucizumab-dbll

Brolucizumab-dbll (brand name BEOVU) consists in a humanized single-chain antibody fragment (scFv) that was industrialized by ESBATech, Alcon Laboratories, and Novartis for the treatment of exudative (wet) age-related macular degeneration (AMD), diabetic macular edema and macular edema secondary to retinal vein occlusion [175]. In AMD, a process called choroidal neovascularization occurs, in which new atypical blood vessels develop under the retina [176]. Due to this phenomenon, a localized macular edema or haemorrhage may elevate the area of the macula. In such situation, it is shown that high levels of VEGF and IL-10, 12 and 6 are present [176]. Brolucizumab-dbll is a biopharmaceutical that binds to the 3 major isoforms of human VEGF-A (VEGF110, VEGF121, and VEGF165), thereby interfering with their interaction with receptors VEGFR-1 and VEGFR-2, leading to the suppression of endothelial cell proliferation, neovascularization, and vascular permeability. By blocking VEGF-A, brolucizumab-dbll reduces the blood vessels growth and controls the leakage and swelling [143, 175]. *In vitro* BEOVU achieved a Ka of 28.4 pmol/L and an IC_{50} of 0.86 for the biding between VEGF165 and VEGFR2, which induced proliferation of human umbilical vein endothelial cells. *In vivo* (cynomolgus monkeys), after one intravitreal injection parallel clearance from all ocular compartments was observed [175]. The recommended dosage regime is 6 mg (0.05 ml of a 120 mg·ml^{-1} solution) via intravitreal injection monthly, despite that hoard side effects, as blurred vision, cataract, conjunctival haemorrhage, increased intraocular pressure, among others [175]. In a SEE study: phase I/II, a single dose of an intravitreal injection of brolucizumab-dbll (0.5, 3, 4.5, or 6 mg) was compared with ranibizumab 0.5 mg, which consisted in dose-escalation phase of brolucizumab-dbll to the maximum feasible dose [143, 175, 177]. In the OWL study: phase II (NCT01849692) brolucizumab-dbll was compared once again with ranibizumab, using microvolume injections (1.2 mg·10 μL^{-1} and 0.6 mg·10 μL^{-1}) and infusions (1.0 mg·8.3 μL^{-1} and 0.5 mg·8.3 μL^{-1}) and both stages demonstrated an effective comeback to BEOVU injection, with 70 % and 80 % rates in stages 1 and 2, respectively, and a rate of 60 % in the brolucizumab-dbll infusion [143, 175, 177]. In the OSPREY study: phase II (NCT01796964), several patients were randomized to compare the intravitreal injection between brolucizumab-dbll (6 mg·50 μL^{-1}) and aflibercept (2 mg·50 μL^{-1}). The treatment regime encompassed 3 treatment periods, week 8, week 32 and week 44 for brolucizumab-dbll, with the aflibercept group maintained on q8-week dosing. At week 40 (q12-week), this study demonstrated that a 61 % of brolucizumab-dbll-treated eyes had a non-appearance of intraretinal fluid and subretinal fluid and these results gave crucial information for the study design and end points of the Phase III studies [143, 175, 177]. The optimal treatment and dosing regimen for patients (q8 weeks or q12 weeks) were determined

by HAWK and HARRIER Studies: Phase III. In HAWK (NCT02307682) and HARRIER (NCT02434328) studies, brolucizumab-dbll and aflibercept were administered through intravitreal injection at weeks 0, 4, and 8, then once every 12 weeks unless disease activity was exhibited. Brolucizumab-dbll successfully finalized phase III, demonstrating its efficacy and safety, while reducing treatment burden associated with regular IVT injections by achieving a result of 55.6 % and 51.0 %, maintained in the dose range of q-12 week afterwards the loading phase until week 48 in HAWK and HARRIER, respectively [143, 175, 177]. On 9th October 2019 it received its first approval by FDA for the treatment of wet AMD. BEOVU was the first anti-VEGF approved that offered greater fluid resolution versus aflibercept and also the ability to maintain eligible wet AMD patients on a three-month dosing interval immediately after a three-month loading phase. By the end of February 2020 its use was approved in the European Union [143, 175, 177]. Several phase III studies comparing brolucizumab-dbll and aflibercept in patients with diabetic macular edema and retinal vein occlusion are undergoing [175].

Teprotumumab-trbw

Teprotumumab-trbw (brand name Tepezza) is a fully human IgG1 developed by the Horizon Therapeutics and used for the treatment of thyroid eye disease. Thyroid eye disease is a condition in which the eye muscles, eyelids, tear glands and fatty tissues behind the eye become inflamed [178]. In this condition, there is the trigger of autoantibodies that activates the thyroid-stimulating hormone receptor (TSHR) and leads to the overproduction of thyroid hormones by thyroid follicular cells. Autoantibodies that activate the insulin-like growth factor-1 receptor (IGF-1R) signalling are also produced, ultimately stimulating cytokine production and extracellular matrix [178]. In this specific disease, there is up-regulation of TNF-α and IL-6 cytokine production [178]. In order to tackle this disorder, teprotumumab-trbw was recently approved. This biopharmaceutical targets IGF-1R and blocks its activation and signalling; however, the exact mechanism of its actuation as a drug has not been fully strongminded and no official studies have been conducted [154]. The recommended prescription is an initial dose of 10 mg·kg^{-1} intravenous infusion and then a dose of 20 mg·kg^{-1} every three weeks for 7 additional infusions. Similarly to any other drug, it has some risks associated, like muscle spasms, nausea, alopecia, diarrhea and fatigue [154]. In 2016, a phase I trial in patients with diabetic macular edema was completed [143, 154, 179]. Tepezza was approved based on the results of two clinical trials, Trial I/ NCT01868997 and Trial II/ NCT03298867. The phase II trial was a multicenter, double-mask and placebo-controlled study, where teprotumumab-trbw was administered intravenously to patients (10 mg·kg^{-1} for the first infusion and 20 mg·kg^{-1}

thereafter) and placebo (8 infusions), during 3 weeks. At week 24, it showed a greater than two-millimeter reduction in proptosis (eye protrusion) in 71.4 % of the teprotumumab-treated patients, as compared with 20 % of the placebo-treated ones [143, 154, 179]. In the phase III trial, patients with active thyroid eye disease were randomized the same way they were in phase II. At week 24 (primary outcome) a reduction in proptosis was observed in 83.0 % of teprotumumab patients versus 10.0 % of placebo patients. Moreover, the results from orbital imaging, made in patients treated with teprotumumab, revealed reductions of the orbital fat volume and in the extraocular muscle [143, 154, 179]. On 21st January 2020, teprotumumab received its first approval in US by FDA for the treatment of thyroid eye disease. A specific clinical trial is currently ongoing, consisting in an extension of the phase III OPTIC trial, OPTIC-X (NCT03461211), with the purpose to provide access of this biopharmaceutical for patients with thyroid eye disease when no satisfactory alternative therapy is available [154].

Satralizumab-mwge

Satralizumab-mwge (brand name Enspryng) is a humanized immunoglobulin G2 and was developed by Chugai Pharmaceutical and Roche for the treatment of neuromyelitis optica spectrum disorder (NMOSD). NMOSD is a chronic inflammation disorder of the brain and spinal cord, associated with serum aquaporin-4 IgG antibodies (AQP4-IgG) [180]. There are indications of high levels of T helper 17 (Th 17) cells-related cytokines, including IL-21, IL-23, IL-17, and IL-6, in NMO sera [180]. In this sense, a very recent mAb – Satralizumab-mwge – was developed; however, the exact mechanism of its action is still unknown. Although, it is believed that it binds to the IL-6 receptor, blocking IL-6 signalling paths, reducing inflammation and IL-6 mediated autoimmune T- and B-cell activation, preventing differentiation of B cells into anti-aquaporin-4-IgG secreting plasma blasts [121, 143]. *In vitro*, Enspryng allowed a reduction of NMO-induced BBB dysfunction. *In vivo*, subcutaneously administered Enspryng, inhibited in a significant way the IL-6 receptor signalling for four weeks, with increases in soluble IL-6 receptor levels observed in Japanese and Caucasian healthy volunteers and patients with rheumatoid arthritis or with NMOSD [121, 143]. A dosage of 120 mg is recommended at week 0, 2 and 4 as loading doses, followed by a maintenance dose of 120 mg every 4 weeks [121]. In phase I of the clinical trial, two studies were performed. SA-001JP was a single dose study in healthy volunteers, where the doses ranged from 30 to 240 mg [181].

Rheumatoid arthritis (RA) is a chronic autoimmune and inflammatory disorder, that primarily affects joints. It is a complex disease, involving many types of cells, macrophages, T and B cells,

fibroblast, dendritic cells, among others [182]. RA results in the body's immune system attacking the tissues of the joints, causing extremely pain and inflammation [112, 182]. The inflammatory process is characterized by infiltration of cytokines, like TGF- β, IL-1β, IL-6, IL-21, and IL-23, that suppress production of regulatory T cells and shift the homeostatic balance, and lead to proliferation of synoviocytes and destruction of cartilage and bone [112, 182]. SA-105JP was a multiple dose study in patients with rheumatoid arthritis, where they received a loading dose of 120 mg of satralizumab-mwge at weeks 0, 2, and 4, followed by three further doses of either 120 mg, 60 mg, or 30 mg, also at four week intervals [181]. Within the first 28 days of SA-001JP, serum C-reactive protein levels were underneath the limit in all participants who received 120 mg and 240 mg, suggesting the efficient IL-6R blocking. In SA-105JP, the results showed that a loading dose of 120 mg at Weeks 0, 2 and 4, followed by 120 mg, resulted in a stable IL-6R concentration for the duration of treatment in patients with rheumatoid arthritis [181]. Enspryng's approval was based on robust data from a two phase III of clinical trials, SAkuraStar (NCT02073279) and SAkuraSky (NCT02028884), in patients with anti-aquaporin-4-IgG seropositive and seronegative [121, 143, 181]. Patients were randomized to receive satralizumab-mwge subcutaneously (120 mg) or saline placebo at weeks 0, 2, 4, and every 4 weeks thereafter for a maximum duration of 1-5 years [121, 143, 181].   The monotherapy study, SAkuraStar, demonstrated that satralizumab-mwge considerably reduced the risk of relapse versus placebo by 55 % in all representative NMOSD's patients [121, 122, 143, 181]. The baseline immunosuppressant therapy, SAkuraSky, included azathioprine, mycophenolate mofetil or oral corticosteroids at stable doses. Satralizumab-mwge lowered the risk of relapse versus placebo by 62 % in NMOSD's patients, including anti-aquaporin-4-IgG positive and negative patients. The proportion of relapse free at weeks 48 and 96 was 89 % and 78 % with satralizumab-mwge and 66 % and 59 % with placebo, respectively. The threat of relapse in patients who received satralizumab-mwge added to immunosuppressant treatment was lower in comparison with those that received the placebo [121, 122, 143, 181, 183]. Based on the two phase III trials, satralizumab-mwge showed to have a favorable safety profile and to be generally well tolerated when administered as a monotherapy or as an add-on therapy to baseline immunosuppressant therapy in patients with NMOSD [121, 122]. Despite all promising results, it should be remarked that satralizumab-mwge reported adverse effects, including headache, arthralgia and injection related reactions [121]. On 17th August 2020, satralizumab-mwge was approved in the US by FDA for the treatment of NMOSD in adult patients who are anti-aquaporin-4-IgG positive. The open-label extension periods of phase III SAkuraStar (NCT02073279) and SAkuraSky (NCT02028884) trials are currently ongoing [121, 143].

Given the aforementioned information, during 2020 many mAbs have been approved for the treatment of a wide range of diseases, especially inflammatory ones. In addition to the approved mAbs, there are still many FDA and EMA clinical studies underway, for instance narsoplimab (Omeros Corporation), tanezumab (Pfizer, Eli Lilly and Company), etrolizumab (Roche) and netakimab (BIOCAD) [143].

1.3.5. Conclusions

Antibodies are proteins produced by vertebrates to help the immune system to fight viruses, bacteria, or other pathogens by recognizing a specific antigen. Due to advances on biotechnology and biomedicine it became possible to produce mAbs in high titers using mammalian cell technology. The development of new technologies and all characteristics associated to mAbs (specificity, selectivity, and affinity) result in their recognition as important tools for therapeutic purposes, covering a wide range of diseases, with *ca.* 26 % developed to target inflammatory disorders. Inflammation is part of the body's natural immune response; however, an excessive response can last for months and years, causing tissue damage and leading to undesirable pathological manifestations such as cancer, diabetes, and cardiovascular, neurological, and chronic inflammatory diseases. Therefore, it is crucial to have available biopharmaceuticals to treat long-term inflammation without (or with reduced) side effects – such as mAbs.

In the current chapter, it is provided the state-of-the-art related with the characteristics, features, and possible applications of mAbs, focusing on inflammatory diseases. The molecular mechanisms and molecules/mediators involved in the inflammatory process were overviewed, while presenting some of the most recently approved mAbs-based treatments. There are over 150 mAbs currently being evaluated in clinical trials or as candidates for approval, and more than 90 mAbs are already approved by FDA (and/or EMA). Several studies demonstrated mAb-based therapies approved by FDA for the treatment of inflammatory diseases, such as sarilumab and brodalumab for rheumatoid arthritis and plaque psoriasis, respectively. More recent mAbs approved in this field comprise risankizumab-rzaa for the treatment of plaque psoriasis, and satralizumab-mwge and inebilizumab-cdon for neuromyelitis optica spectrum disorder. It is also important to highlight anti-IL6 and anti-IL6R mAbs that were already approved by FDA, such as tocilizumab, siltuximab and sarilumab, since they show high potential to fight inflammation. Tocilizumab has been of particular interest in the last months by the scientific and medical community due to its possible application for the treatment of severe patients with COVID-19.

All the works discussed in this chapter allow to understand that the mAbs field is constantly evolving and gaining visibility, with several new/recently approved mAbs showing very promising results for the treatment of inflammatory diseases and/or diseases with relevant inflammation indication. Overall, in the field of biopharmaceuticals, it is estimated that mAb-based products will continue to dominate the market in the next years.

Even though it is clearly stated the effectiveness of mAbs as powerful therapeutic agents, their current high cost, mainly arising from difficulties on their purification from the complex/biological medium in which they are produced, still limits their widespread use. Thus, several treatments usually resort to the use of cheaper small molecules with reduced target selectivity and high toxicity. Based on the exposed, and to tackle the accessibility challenge of mAbs, significant efforts are still required, particularly to reduce production time and costs through the development of cost-effective downstream strategies. Furthermore, the information here presented should encourage both the testing and clinical trials of already existing mAbs that can have a positive effect in the treatment of several diseases (including inflammatory disorders), but also the search on new and more efficient alternatives to boost the widespread use of mAbs as conventional therapies for a wide range of diseases.

1.3.6. References

1. M.G. Netea, F. Balkwill, M. Chonchol, F. Cominelli, M.Y. Donath, E.J. Giamarellos-Bourboulis, D. Golenbock, M.S. Gresnigt, M.T. Heneka, and H.M. Hoffman, *A guiding map for inflammation.* Nature Immunology, 2017. **18**(8): p. 826-831.

2. W. Spector and D. Willoughby, *The inflammatory response.* Bacteriological Reviews, 1963. **27**(2): p. 117.

3. D. Laveti, M. Kumar, R. Hemalatha, R. Sistla, V. Gm Naidu, V. Talla, V. Verma, N. Kaur, and R. Nagpal, *Anti-inflammatory treatments for chronic diseases: a review.* Inflammation & Allergy-Drug Targets, 2013. **12**(5): p. 349-361.

4. G. Schett and M.F. Neurath, *Resolution of chronic inflammatory disease: universal and tissue-specific concepts.* Nature Communications, 2018. **9**(1): p. 1-8.

5. B.B. Aggarwal, S. Shishodia, S.K. Sandur, M.K. Pandey, and G. Sethi, *Inflammation and cancer: how hot is the link?* Biochemical Pharmacology, 2006. **72**(11): p. 1605-1621.

6. F. Balkwill and L.M. Coussens, *An inflammatory link.* Nature, 2004. **431**(7007): p. 405-406.

7. S. Fekete, A. Goyon, J.-L. Veuthey, and D. Guillarme, *Size exclusion chromatography of protein biopharmaceuticals: past, present and future.* American Pharmaceutical Review, 2018: p. 1-4.

8. L.E. Crowell, A.E. Lu, K.R. Love, A. Stockdale, S.M. Timmick, D. Wu, Y.A. Wang, W. Doherty, A. Bonnyman, and N. Vecchiarello, *On-demand manufacturing of clinical-quality biopharmaceuticals.* Nature Biotechnology, 2018. **36**(10): p. 988-995.

9. G. Walsh, *Biopharmaceutical benchmarks 2018.* Nature Biotechnology, 2018. **36**(12): p. 1136-1145.

10. G. Köhler and C. Milstein, *Continuous cultures of fused cells secreting antibody of predefined specificity.* Nature, 1975. **256**(5517): p. 495-497.

11. F. Darrouzain, S. Bian, C. Desvignes, C. Bris, H. Watier, G. Paintaud, and A. de Vries, *Immunoassays for measuring serum concentrations of monoclonal antibodies and anti-biopharmaceutical antibodies in patients.* Therapeutic Drug Monitoring, 2017. **39**(4): p. 316-321.

12. B. Gencer, R. Laaksonen, A. Buhayer, and F. Mach, *Use and role of monoclonal antibodies and other biologics in preventive cardiology.* Swiss Medical Weekly, 2015. **145**: p. w14179.

13. E. Andreakos, P.C. Taylor, and M. Feldmann, *Monoclonal antibodies in immune and inflammatory diseases.* Current Opinion in Biotechnology, 2002. **13**(6): p. 615-620.

14. K. Strebhardt and A. Ullrich, *Paul Ehrlich's magic bullet concept: 100 years of progress.* Nature Reviews Cancer, 2008. **8**(6): p. 473-480.

15. R.P. Tracy, *The five cardinal signs of inflammation: calor, dolor, rubor, tumor… and penuria (apologies to Aulus Cornelius Celsus, De medicina, c. AD 25).* The Journals of Gerontology Series A: Biological Sciences and Medical Sciences, 2006. **61**(10): p. 1051-1052.

16. B. Johnston and E.C. Butcher, *Chemokines in rapid leukocyte adhesion triggering and migration.* Seminars in Immunology, 2002. **14**(2): p. 83-92.

17. I. Migeotte, D. Communi, and M. Parmentier, *Formyl peptide receptors: a promiscuous subfamily of G protein-coupled receptors controlling immune responses.* Cytokine & Growth Factor Reviews, 2006. **17**(6): p. 501-519.

18. M. Sperandio, C.A. Gleissner, and K. Ley, *Glycosylation in immune cell trafficking.* Immunological Reviews, 2009. **230**(1): p. 97-113.

19. O. Takeuchi and S. Akira, *Pattern recognition receptors and inflammation.* Cell, 2010. **140**(6): p. 805-820.

20. M. Raghavan and P.J. Bjorkman, *Fc receptors and their interactions with immunoglobulins.* Annual Review of Cell and Developmental Biology 1996. **12**(1): p. 181-220.

21. D.R. Barreda, P.C. Hanington, and M. Belosevic, *Regulation of myeloid development and function by colony stimulating factors.* Developmental & Comparative Immunology, 2004. **28**(5): p. 509-554.

22. D. Scheel-Toellner, K. Wang, N.V. Henriquez, P.R. Webb, R. Craddock, D. Pilling, A.N. Akbar, M. Salmon, and J.M. Lord, *Cytokine-mediated inhibition of apoptosis in non-transformed T cells and neutrophils can be dissociated from protein kinase B activation.* European Journal of Immunology, 2002. **32**(2): p. 486-493.

23. D.Y. Richard, F. Boulay, J.M. Wang, C. Dahlgren, C. Gerard, M. Parmentier, C.N. Serhan, and P.M. Murphy, *International Union of Basic and Clinical Pharmacology. LXXIII. Nomenclature for the formyl peptide receptor (FPR) family.* Pharmacological Reviews, 2009. **61**(2): p. 119-161.

24. M.-J. Rabiet, E. Huet, and F. Boulay, *The N-formyl peptide receptors and the anaphylatoxin C5a receptors: an overview.* Biochimie, 2007. **89**(9): p. 1089-1106.

25. M. Bäck, S.-E. Dahlén, J.M. Drazen, J.F. Evans, C.N. Serhan, T. Shimizu, T. Yokomizo, and G.E. Rovati, *International Union of Basic and Clinical Pharmacology. LXXXIV: leukotriene receptor nomenclature, distribution, and pathophysiological functions.* Pharmacological Reviews, 2011. **63**(3): p. 539-584.

26. D.M. Stafforini, T.M. McIntyre, G.A. Zimmerman, and S.M. Prescott, *Platelet-activating factor, a pleiotrophic mediator of physiological and pathological processes.* Critical Reviews in Clinical Laboratory Sciences, 2003. **40**(6): p. 643-672.

27. H. Lee, P.L. Whitfeld, and C.R. Mackay, *Receptors for complement C5a. The importance of C5aR and the enigmatic role of C5L2.* Immunology and Cell Biology, 2008. **86**(2): p. 153-160.

28. P.M. Murphy, M. Baggiolini, I.F. Charo, C.A. Hébert, R. Horuk, K. Matsushima, L.H. Miller, J.J. Oppenheim, and C.A. Power, *International union of pharmacology. XXII. Nomenclature for chemokine receptors.* Pharmacological Reviews, 2000. **52**(1): p. 145-176.

29. F. Boulay, N. Naik, E. Giannini, M. Tardif, and L. Brouchon, *Phagocyte chemoattractant receptors.* Annals of the New York Academy of Sciences, 1997. **832**(1): p. 69-84.

30. R. Bonecchi, N. Polentarutti, W. Luini, A. Borsatti, S. Bernasconi, M. Locati, C. Power, A. Proudfoot, T.N. Wells, and C. Mackay, *Up-regulation of CCR1 and CCR3 and induction of chemotaxis to CC chemokines by IFN-γ in human neutrophils.* The Journal of Immunology, 1999. **162**(1): p. 474-479.

31. K. Futosi, S. Fodor, and A. Mócsai, *Reprint of Neutrophil cell surface receptors and their intracellular signal transduction pathways.* International Immunopharmacology, 2013. **17**(4): p. 1185-1197.

32.   D.A. Carlow, K. Gossens, S. Naus, K.M. Veerman, W. Seo, and H.J.J.I.r. Ziltener, *PSGL-1 function in immunity and steady state homeostasis.* Immunological Reviews, 2009. **230**(1): p. 75-96.

33.   R.O. Hynes, *Integrins: bidirectional, allosteric signaling machines.* Cell, 2002. **110**(6): p. 673-687.

34.   J. Schymeinsky, A. Mócsai, and B. Walzog, *Neutrophil activation via β2 integrins (CD11/CD18): molecular mechanisms and clinical implications.* Thrombosis and Haemostasis, 2007. **98**(08): p. 262-273.

35.   T.A. Springer, *Adhesion receptors of the immune system.* Nature, 1990. **346**(6283): p. 425-434.

36.   M.R. Thompson, J.J. Kaminski, E.A. Kurt-Jones, and K.A. Fitzgerald, *Pattern recognition receptors and the innate immune response to viral infection.* Viruses, 2011. **3**(6): p. 920-940.

37.   E. Meylan, J. Tschopp, and M. Karin, *Intracellular pattern recognition receptors in the host response.* Nature, 2006. **442**(7098): p. 39-44.

38.   C. Del Fresno, S. Iborra, P. Saz-Leal, M. Martínez-López, and D. Sancho, *Flexible signaling of myeloid C-type lectin receptors in immunity and inflammation.* Frontiers in Immunology, 2018. **9**: p. 804.

39.   T.B. Geijtenbeek and S.I. Gringhuis, *Signalling through C-type lectin receptors: shaping immune responses.* Nature Reviews Immunology, 2009. **9**(7): p. 465-479.

40.   P. Bruhns, *Properties of mouse and human IgG receptors and their contribution to disease models.* Blood, 2012. **119**(24): p. 5640-5649.

41.   M.-j. Zhou, D.M. Lublin, D.C. Link, and E.J. Brown, *Distinct tyrosine kinase activation and Triton X-100 insolubility upon FcγRII or FcγRIIIB ligation in human polymorphonuclear leukocytes: implications for immune complex activation of the respiratory burst.* Journal of Biological Chemistry, 1995. **270**(22): p. 13553-13560.

42.   P.M. Guyre, A.S. Campbell, W.D. Kniffin, and M.W. Fanger, *Monocytes and polymorphonuclear neutrophils of patients with streptococcal pharyngitis express increased numbers of type I IgG Fc receptors.* The Journal of Clinical Investigation, 1990. **86**(6): p. 1892-1896.

43.   R. Repp, T. Valerius, A. Sendler, M. Gramatzki, H. Iro, J. Kalden, and E. Platzer, *Neutrophils express the high affinity receptor for IgG (Fc gamma RI, CD64) after in vivo application of recombinant human granulocyte colony-stimulating factor.* Blood, 1991. **78**(4): p. 885–889.

44.   L.P. van der Steen, J.E. Bakema, A. Sesarman, F. Florea, C.W. Tuk, G. Kirtschig, J.J. Hage, C. Sitaru, and M. van Egmond, *Blocking Fcα receptor I on granulocytes prevents tissue damage induced by IgA autoantibodies.* The Journal of Immunology, 2012. **189**(4): p. 1594-1601.

45. M.A. Otten, E. Rudolph, M. Dechant, C.W. Tuk, R.M. Reijmers, R.H. Beelen, J.G. van de Winkel, and M. van Egmond, *Immature neutrophils mediate tumor cell killing via IgA but not IgG Fc receptors.* The Journal of Immunology, 2005. **174**(9): p. 5472-5480.

46. A.S. Gounni, B. Lamkhioued, L. Koussih, C. Ra, P.M. Renzi, and Q. Hamid, *Human neutrophils express the high-affinity receptor for immunoglobulin E (FceRI): role in asthma.* The FASEB Journal, 2001. **15**(6): p. 940-949.

47. J. Monteseirin, I. Bonilla, M. Camacho, J. Conde, and F. Sobrino, *IgE-dependent release of myeloperoxidase by neutrophils from allergic patients.* Clinical & Experimental Allergy, 2001. **31**(6): p. 889-892.

48. A. Porcherie, C. Mathieu, R. Peronet, E. Schneider, J. Claver, P.-H. Commere, H. Kiefer-Biasizzo, H. Karasuyama, G. Milon, and M. Dy, *Critical role of the neutrophil-associated high-affinity receptor for IgE in the pathogenesis of experimental cerebral malaria.* Journal of Experimental Medicine, 2011. **208**(11): p. 2225-2236.

49. L. Pfefferkorn and M. Fanger, *Cross-linking of the high affinity Fc receptor for human immunoglobulin G1 triggers transient activation of NADPH oxidase activity: continuous oxidase activation requires continuous de novo receptor cross-linking.* Journal of Biological Chemistry, 1989. **264**(24): p. 14112-14120.

50. P.R. Moody, E.J. Sayers, J.P. Magnusson, C. Alexander, P. Borri, P. Watson, and A.T. Jones, *Receptor crosslinking: a general method to trigger internalization and lysosomal targeting of therapeutic receptor: ligand complexes.* Molecular Therapy, 2015. **23**(12): p. 1888-1898.

51. L. Koenderman, *Inside-out control of Fc-receptors.* Frontiers in Immunology, 2019. **10**: p. 544.

52. T.N. Ellis and B.L. Beaman, *Interferon-γ activation of polymorphonuclear neutrophil function.* Immunology, 2004. **112**(1): p. 2-12.

53. F. Bazzoni, N. Tamassia, M. Rossato, and M.A. Cassatella, *Understanding the molecular mechanisms of the multifaceted IL-10-mediated anti-inflammatory response: lessons from neutrophils.* European Journal of Immunology, 2010. **40**(9): p. 2360-2368.

54. C. Haan, S. Kreis, C. Margue, and I. Behrmann, *Jaks and cytokine receptors — an intimate relationship.* Biochemical Pharmacology, 2006. **72**(11): p. 1538-1546.

55. K. Ghoreschi, A. Laurence, and J.J. O'Shea, *Janus kinases in immune cell signaling.* Immunological Reviews, 2009. **228**(1): p. 273-287.

56. J.J. O'Shea and R. Plenge, *JAK and STAT signaling molecules in immunoregulation and immune-mediated disease.* Immunity, 2012. **36**(4): p. 542-550.

57.   C.H. Mermel, M.L. McLemore, F. Liu, S. Pereira, J. Woloszynek, C.A. Lowell, and D.C. Link, *Src family kinases are important negative regulators of G-CSF-dependent granulopoiesis.* Blood, 2006. **108**(8): p. 2562-2568.

58.   Q.-s. Zhu, L. Xia, G.B. Mills, C.A. Lowell, I.P. Touw, and S.J. Corey, *G-CSF induced reactive oxygen species involves Lyn-PI3-kinase-Akt and contributes to myeloid cell growth.* Blood, 2006. **107**(5): p. 1847-1856.

59.   S.J. Corey, A.L. Burkhardt, J.B. Bolen, R.L. Geahlen, L.S. Tkatch, and D.J. Tweardy, *Granulocyte colony-stimulating factor receptor signaling involves the formation of a three-component complex with Lyn and Syk protein-tyrosine kinases.* Proceedings of the National Academy of Sciences of the United States of America, 1994. **91**(11): p. 4683-4687.

60.   Q.-S. Zhu, L.J. Robinson, V. Roginskaya, and S.J. Corey, *G-CSF-induced tyrosine phosphorylation of Gab2 is Lyn kinase dependent and associated with enhanced Akt and differentiative, not proliferative, responses.* Blood, 2004. **103**(9): p. 3305-3312.

61.   J.L. Eyles, A.W. Roberts, D. Metcalf, and I.P. Wicks, *Granulocyte colony-stimulating factor and neutrophils — forgotten mediators of inflammatory disease.* Nature Clinical Practice Rheumatology, 2006. **2**(9): p. 500-510.

62.   R. Liu, T. Itoh, K.-i. Arai, and S. Watanabe, *Two distinct signaling pathways downstream of Janus kinase 2 play redundant roles for antiapoptotic activity of granulocyte-macrophage colony-stimulating factor.* Molecular Biology of the Cell, 1999. **10**(11): p. 3959-3970.

63.   M. Pelletier, C. Ratthé, and D. Girard, *Mechanisms involved in interleukin-15-induced suppression of human neutrophil apoptosis: role of the anti-apoptotic Mcl-1 protein and several kinases including Janus kinase-2, p38 mitogen-activated protein kinase and extracellular signal-regulated kinases-1/2.* FEBS Letters, 2002. **532**(1-2): p. 164-170.

64.   N. Sato, K. Sakamaki, N. Terada, K.-i. Arai, and A. Miyajima, *Signal transduction by the high-affinity GM-CSF receptor: two distinct cytoplasmic regions of the common beta subunit responsible for different signaling.* The EMBO Journal, 1993. **12**(11): p. 4181-4189.

65.   C. Ratthe, M. Pelletier, S. Chiasson, and D. Girard, *Molecular mechanisms involved in interleukin-4-induced human neutrophils: expression and regulation of suppressor of cytokine signaling.* Journal of Leukocyte Biology, 2007. **81**(5): p. 1287-1296.

66.   M. Hörtner, U. Nielsch, L.M. Mayr, J.A. Johnston, P.C. Heinrich, and S. Haan, *Suppressor of cytokine signaling-3 is recruited to the activated granulocyte-colony stimulating factor receptor and modulates its signal transduction.* The Journal of Immunology, 2002. **169**(3): p. 1219-1227.

67. M.A. Cassatella, S. Gasperini, C. Bovolenta, F. Calzetti, M. Vollebregt, P. Scapini, M. Marchi, R. Suzuki, A. Suzuki, and A. Yoshimura, *Interleukin-10 (IL-10) selectively enhances CIS3/SOCS3 mRNA expression in human neutrophils: evidence for an IL-10–induced pathway that is independent of STAT protein activation.* Blood, 1999. **94**(8): p. 2880-2889.

68. W.A. Muller, *Leukocyte-endothelial cell interactions in the inflammatory response.* Laboratory Investigation, 2002. **82**(5): p. 521-534.

69. A.D. Luster, R. Alon, and U.H. von Andrian, *Immune cell migration in inflammation: present and future therapeutic targets.* Nature Immunology, 2005. **6**(12): p. 1182-1190.

70. R.P. McEver, *Selectins: lectins that initiate cell adhesion under flow.* Current Opinion in Cell Biology, 2002. **14**(5): p. 581-586.

71. M. Sperandio, *Selectins and glycosyltransferases in leukocyte rolling in vivo.* The FEBS Journal, 2006. **273**(19): p. 4377-4389.

72. M.G. Tansey and D.E. Szymkowski, *The TNF superfamily in 2009: new pathways, new indications, and new drugs.* Drug Discovery Today, 2009. **14**(23-24): p. 1082-1088.

73. C.A. Dinarello, *Interleukin-1β.* Critical Care Medicine, 2005. **33**(12): p. S460-S462.

74. B.A. Zabel, A. Rott, and E.C. Butcher, *Leukocyte chemoattractant receptors in human disease pathogenesis.* Annual Review of Pathology: Mechanisms of Disease, 2015. **10**: p. 51-81.

75. C. Weber, L. Fraemohs, and E. Dejana, *The role of junctional adhesion molecules in vascular inflammation.* Nature Reviews Immunology, 2007. **7**(6): p. 467-477.

76. P.J. Van Haastert and P.N. Devreotes, *Chemotaxis: signalling the way forward.* Nature Reviews Molecular Cell Biology, 2004. **5**(8): p. 626-634.

77. V. Kumar, A.K. Abbas, and J.C. Aster, *Robbins basic pathology e-book*. 2017: Elsevier Health Sciences.

78. A.W. Segal, *How neutrophils kill microbes.* Annual Review of Immunology, 2005. **23**: p. 197-223.

79. F.C. Fang, *Antimicrobial reactive oxygen and nitrogen species: concepts and controversies.* Nature Reviews Microbiology, 2004. **2**(10): p. 820-832.

80. D.M. Underhill and A. Ozinsky, *Phagocytosis of microbes: complexity in action.* Annual Review of Immunology, 2002. **20**(1): p. 825-852.

81. B. Pinegin, N. Vorobjeva, M. Pashenkov, and B. Chernyak, *The role of mitochondrial ROS in antibacterial immunity.* Journal of Cellular Physiology, 2018. **233**(5): p. 3745-3754.

82. C. Nathan and M.U. Shiloh, *Reactive oxygen and nitrogen intermediates in the relationship between mammalian hosts and microbial pathogens.* Proceedings of the National Academy of Sciences of the United States of America, 2000. **97**(16): p. 8841-8848.

83. S. Gordon and P.R. Taylor, *Monocyte and macrophage heterogeneity.* Nature Reviews Immunology, 2005. **5**(12): p. 953-964.

84. M.M. Attwood, J. Jonsson, M. Rask-Andersen, and H.B. Schiöth, *Soluble ligands as drug targets.* Nature Reviews Drug Discovery, 2020. **19**(10): p. 695-710.

85. C.J. Hutchings, M. Koglin, and F.H. Marshall, *Therapeutic antibodies directed at G protein-coupled receptors.* MAbs, 2010. **2**(6): p. 594-606.

86. K. Christopherson and R. Hromas, *Chemokine regulation of normal and pathologic immune responses.* Stem Cells, 2001. **19**(5): p. 388-396.

87. X. Long, Y. Ye, L. Zhang, P. Liu, W. Yu, F. Wei, X. Ren, and J. Yu, *IL-8, a novel messenger to cross-link inflammation and tumor EMT via autocrine and paracrine pathways.* International Journal of Oncology, 2016. **48**(1): p. 5-12.

88. G.M. Clore, E. Appella, M. Yamada, K. Matsushima, and A.M. Gronenborn, *Three-dimensional structure of interleukin 8 in solution.* Biochemistry, 1990. **29**(7): p. 1689-1696.

89. M. Baggiolini and I. Clark-Lewis, *Interleukin-8, a chemotactic and inflammatory cytokine.* FEBS letters, 1992. **307**(1): p. 97-101.

90. M.D. Turner, B. Nedjai, T. Hurst, and D.J. Pennington, *Cytokines and chemokines: at the crossroads of cell signalling and inflammatory disease.* Biochimica et Biophysica Acta - Molecular Cell Research, 2014. **1843**(11): p. 2563-2582.

91. T. Hirano, K. Yasukawa, H. Harada, T. Taga, Y. Watanabe, T. Matsuda, S.-i. Kashiwamura, K. Nakajima, K. Koyama, and A. Iwamatsu, *Complementary DNA for a novel human interleukin (BSF-2) that induces B lymphocytes to produce immunoglobulin.* Nature, 1986. **324**(6092): p. 73-76.

92. T. Tanaka, M. Narazaki, and T. Kishimoto, *IL-6 in inflammation, immunity, and disease.* Cold Spring Harbor Perspectives in Biology, 2014. **6**(10): p. a016295.

93. H. Su, C.-T. Lei, and C. Zhang, *Interleukin-6 signaling pathway and its role in kidney disease: an update.* Frontiers in Immunology, 2017. **8**: p. 405.

94. G.-Y. Xu, H.-A. Yu, J. Hong, M. Stahl, T. McDonagh, L.E. Kay, and D.A. Cumming, *Solution structure of recombinant human interleukin-6.* Journal of Molecular Biology, 1997. **268**(2): p. 468-481.

95. T. Kishimoto, *Interleukin-6: discovery of a pleiotropic cytokine.* Arthritis Research & Therapy, 2006. **8**(2): p. 1-6.

96.   C. Gabay, *Interleukin-6 and chronic inflammation.* Arthritis Research & Therapy, 2006. **8**(2): p. 1-6.

97.   G. Schett, *Physiological effects of modulating the interleukin-6 axis.* Rheumatology, 2018. **57**: p. ii43-ii50.

98.   A.P. Costa-Pereira, *Regulation of IL-6-type cytokine responses by MAPKs.* Biochemical Society Transactions, 2014. **42**: p. 59-62.

99.   L. Ye, L. Gao, and H. Cheng, *Inflammatory profiles of the interleukin family and network in cerebral hemorrhage.* Cellular and Molecular Neurobiology, 2018. **38**(7): p. 1321-1333.

100.   M. Alcorn, J. Booth, K. Coggeshall, and J. Metcalf, *Adenovirus type 7 induces interleukin-8 production via activation of extracellular regulated kinase 1/2.* Journal of Virology, 2001. **75**(14): p. 6450-6459.

101.   T. Abdollahi, *Potential for TRAIL as a therapeutic agent in ovarian cancer.* Vitamins & Hormones, 2004. **67**: p. 347-364.

102.   S. Kotsovilis and E. Andreakos, *Therapeutic human monoclonal antibodies in inflammatory diseases*, in *Human Monoclonal Antibodies. Methods in Molecular Biology*. 2014. p. 37-59.

103.   L. Skov, F.J. Beurskens, C.O. Zachariae, S. Reitamo, J. Teeling, D. Satijn, K.M. Knudsen, E.P. Boot, D. Hudson, and O. Baadsgaard, *IL-8 as antibody therapeutic target in inflammatory diseases: reduction of clinical activity in palmoplantar pustulosis.* The Journal of Immunology, 2008. **181**(1): p. 669-679.

104.   A. Harada, N. Sekido, T. Akahoshi, T. Wada, N. Mukaida, and K. Matsushima, *Essential involvement of interleukin-8 (IL-8) in acute inflammation.* Journal of Leukocyte Biology, 1994. **56**(5): p. 559-564.

105.   S.A. Rosa, C. da Silva, M.R. Aires-Barros, A. Dias-Cabral, and A.M. Azevedo, *Thermodynamics of the adsorption of monoclonal antibodies in phenylboronate chromatography: affinity versus multimodal interactions.* Journal of Chromatography A, 2018. **1569**: p. 118-127.

106.   X.D. Yang, J.R. Corvalan, P. Wang, C.M.N. Roy, and C.G. Davis, *Fully human anti-interleukin-8 monoclonal antibodies: potential therapeutics for the treatment of inflammatory disease states.* Journal of Leukocyte Biology, 1999. **66**(3): p. 401-410.

107.   D.A. Mahler, S. Huang, M. Tabrizi, and G.M. Bell, *Efficacy and safety of a monoclonal antibody recognizing interleukin-8 in COPD: a pilot study.* Chest, 2004. **126**(3): p. 926-934.

108.   D. Guha, P. Nagilla, C. Redinger, A. Srinivasan, G.P. Schatten, and V. Ayyavoo, *Neuronal apoptosis by HIV-1 Vpr: contribution of proinflammatory molecular networks from infected target cells.* Journal of Neuroinflammation, 2012. **9**(1): p. 1-15.

109. S. Huang, L. Mills, B. Mian, C. Tellez, M. McCarty, X.-D. Yang, J.M. Gudas, and M. Bar-Eli, *Fully humanized neutralizing antibodies to interleukin-8 (ABX-IL8) inhibit angiogenesis, tumor growth, and metastasis of human melanoma.* The American Journal of Pathology, 2002. **161**(1): p. 125-134.

110. E.M. Bekes, B. Schweighofer, T.A. Kupriyanova, E. Zajac, V.C. Ardi, J.P. Quigley, and E.I. Deryugina, *Tumor-recruited neutrophils and neutrophil TIMP-free MMP-9 regulate coordinately the levels of tumor angiogenesis and efficiency of malignant cell intravasation.* The American Journal of Pathology, 2011. **179**(3): p. 1455-1470.

111. T. Tanaka and T. Kishimoto, *Targeting interleukin-6: all the way to treat autoimmune and inflammatory diseases.* International Journal of Biological Sciences, 2012. **8**(9): p. 1227.

112. T. Hirano, T. Matsuda, M. Turner, N. Miyasaka, G. Buchan, B. Tang, K. Sato, M. Shimi, R. Maid, and M. Feldmann, *Excessive production of interleukin 6/B cell stimulatory factor-2 in rheumatoid arthritis.* European Journal of Immunology, 1988. **18**(11): p. 1797-1802.

113. M. Sheppard, F. Laskou, P.P. Stapleton, S. Hadavi, and B. Dasgupta, *Tocilizumab (Actemra).* Human Vaccines & Immunotherapeutics, 2017. **13**(9): p. 1972-1988.

114. C. Ding, F. Cicuttini, J. Li, and G. Jones, *Targeting IL-6 in the treatment of inflammatory and autoimmune diseases.* Expert Opinion on Investigational Drugs, 2009. **18**(10): p. 1457-1466.

115. T. Tanaka, M. Narazaki, and T. Kishimoto, *Anti-Interleukin-6 receptor antibody therapy against autoimmune inflammatory diseases*, in *Molecular Biology of B Cells*, T.H. Frederick W. Alt, Andreas Radbruch, Michael Reth, Editor. 2015, Elsevier. p. 515-525.

116. N. Nishimoto and T. Kishimoto, *Inhibition of IL-6 for the treatment of inflammatory diseases.* Current Opinion in Pharmacology, 2004. **4**(4): p. 386-391.

117. Y. Lai and C. Dong, *Therapeutic antibodies that target inflammatory cytokines in autoimmune diseases.* International Immunology, 2016. **28**(4): p. 181-188.

118. F. van Rhee, C. Casper, P.M. Voorhees, L.E. Fayad, D. Gibson, K. Kanhai, and R. Kurzrock, *Long-term safety of siltuximab in patients with idiopathic multicentric Castleman disease: a prespecified, open-label, extension analysis of two trials.* The Lancet Haematology, 2020. **7**(3): p. e209-e217.

119. R.-M. Lu, Y.-C. Hwang, I.-J. Liu, C.-C. Lee, H.-Z. Tsai, H.-J. Li, and H.-C. Wu, *Development of therapeutic antibodies for the treatment of diseases.* Journal of Biomedical Science, 2020. **27**(1): p. 1-30.

120. R. Fleischmann, M.C. Genovese, Y. Lin, G. St John, D. van der Heijde, S. Wang, J.J. Gomez-Reino, J.A. Maldonado-Cocco, M. Stanislav, and A.J. Kivitz, *Long-term safety of sarilumab in*

rheumatoid arthritis: an integrated analysis with up to 7 years' follow-up. Rheumatology, 2020. **59**(2): p. 292-302.

121. Y.-A. Heo, *Satralizumab: first approval.* Drugs, 2020. **80**: p. 1477–1482.

122. A. Traboulsee, B.M. Greenberg, J.L. Bennett, L. Szczechowski, E. Fox, S. Shkrobot, T. Yamamura, Y. Terada, Y. Kawata, and P. Wright, *Safety and efficacy of satralizumab monotherapy in neuromyelitis optica spectrum disorder: a randomised, double-blind, multicentre, placebo-controlled phase 3 trial.* The Lancet Neurology, 2020. **19**(5): p. 402-412.

123. S. Kaur, Y. Bansal, R. Kumar, and G. Bansal, *A panoramic review of IL-6: structure, pathophysiological roles and inhibitors.* Bioorganic & Medicinal Chemistry, 2020. **28**(5): p. 115327.

124. A. Signore, *About inflammation and infection.* EJNMMI Research, 2013. **3**(1): p. 8.

125. D. Okin and R. Medzhitov, *Evolution of inflammatory diseases.* Current Biology, 2012. **22**(17): p. R733-R740.

126. G. Novi, M. Mikulska, F. Briano, F. Toscanini, F. Tazza, A. Uccelli, and M. Inglese, *COVID-19 in a MS patient treated with ocrelizumab: does immunosuppression have a protective role?* Multiple Sclerosis and Related Disorders, 2020. **42**: p. 102120.

127. C.-C. Lai, T.-P. Shih, W.-C. Ko, H.-J. Tang, and P.-R. Hsueh, *Severe acute respiratory syndrome coronavirus 2 (SARS-CoV-2) and coronavirus disease-2019 (COVID-19): the epidemic and the challenges.* International Journal of Antimicrobial Agents, 2020. **55**(3): p. 105924.

128. L.a. Alanagreh, F. Alzoughool, and M. Atoum, *The human coronavirus disease COVID-19: its origin, characteristics, and insights into potential drugs and its mechanisms.* Pathogens, 2020. **9**(5): p. 331.

129. R.A. Khailany, M. Safdar, and M. Ozaslan, *Genomic characterization of a novel SARS-CoV-2.* Gene Reports, 2020. **19**: p. 100682.

130. X. Ou, Y. Liu, X. Lei, P. Li, D. Mi, L. Ren, L. Guo, R. Guo, T. Chen, and J. Hu, *Characterization of spike glycoprotein of SARS-CoV-2 on virus entry and its immune cross-reactivity with SARS-CoV.* Nature Communications, 2020. **11**(1): p. 1-12.

131. D.L. Dixon, B.W. Van Tassell, A. Vecchié, A. Bonaventura, A.H. Talasaz, H. Kakavand, F. D'Ascenzo, A. Perciaccante, D. Castagno, and E. Ammirati, *Cardiovascular considerations in treating patients with coronavirus disease 2019 (COVID-19).* Journal of Cardiovascular Pharmacology, 2020. **75**(5): p. 359-367.

132. B. Liu, M. Li, Z. Zhou, X. Guan, and Y. Xiang, *Can we use interleukin-6 (IL-6) blockade for coronavirus disease 2019 (COVID-19)-induced cytokine release syndrome (CRS)?* Journal of Autoimmunity, 2020. **111**: p. 102452.

133.   F.M. Buonaguro, I. Puzanov, and P.A. Ascierto, *Anti-IL6R role in treatment of COVID-19-related ARDS.* Journal of Translational Medicine, 2020. **18: 165**: p. 1-2.

134.   G. Chen, D. Wu, W. Guo, Y. Cao, D. Huang, H. Wang, T. Wang, X. Zhang, H. Chen, and H. Yu, *Clinical and immunological features of severe and moderate coronavirus disease 2019.* The Journal of Clinical Investigation, 2020. **130**(5): p. 2620-2629.

135.   A. AminJafari and S. Ghasemi, *The possible of immunotherapy for COVID-19: a systematic review.* International Immunopharmacology

2020. **83**: p. 106455.

136.   W. Zhang, Y. Zhao, F. Zhang, Q. Wang, T. Li, Z. Liu, J. Wang, Y. Qin, X. Zhang, and X. Yan, *The use of anti-inflammatory drugs in the treatment of people with severe coronavirus disease 2019 (COVID-19): the perspectives of clinical immunologists from China.* Clinical Immunology, 2020. **214**: p. 108393.

137.   X. Xu, M. Han, T. Li, W. Sun, D. Wang, B. Fu, Y. Zhou, X. Zheng, Y. Yang, and X. Li, *Effective treatment of severe COVID-19 patients with tocilizumab.* Proceedings of the National Academy of Sciences of the United States of America, 2020. **117**(20): p. 10970-10975.

138.   B. Fu, X. Xu, and H. Wei, *Why tocilizumab could be an effective treatment for severe COVID-19?* Journal of Translational Medicine, 2020. **18**(1): p. 1-5.

139.   K. McKeage and S. Duggan, *Risankizumab: first global approval.* Drugs, 2019. **79**(8): p. 893-900.

140.   J.E. Frampton, *Inebilizumab: first approval.* Drugs, 2020. **80**: p. 1259–1264.

141.   J.M. Reichert, *New biopharmaceuticals in the USA: trends in development and marketing approvals 1995–1999.* Trends in Biotechnology, 2000. **18**(9): p. 364-369.

142.   R. Narayanan, B.D. Kuppermann, C. Jones, and P. Kirkpatrick, *Ranibizumab.* Nature Reviews Drug Discovery, 2006. **5**(10): p. 815.

143.   H. Kaplon, M. Muralidharan, Z. Schneider, and J.M. Reichert, *Antibodies to watch in 2020.* MAbs, 2020. **12**(1): p. 1703531.

144.   M.J. Keating, S. O'Brien, and A. Ferrajoli, *Alemtuzumab: a novel monoclonal antibody.* Expert Opinion on Biological Therapy, 2001. **1**(6): p. 1059-1065.

145.   F. Cameron and P.L. McCormack, *Obinutuzumab: first global approval.* Drugs, 2014. **74**(1): p. 147-154.

146.   M. Boyiadzis and K.A. Foon, *Approved monoclonal antibodies for cancer therapy.* Expert Opinion on Biological Therapy, 2008. **8**(8): p. 1151-1158.

147. A. Younes, U. Yasothan, and P. Kirkpatrick, *Brentuximab vedotin.* Nature Reviews Drug Discovery, 2012. **11**(1): p. 19-20.

148. M. Sanford, *Blinatumomab: first global approval.* Drugs, 2015. **75**(3): p. 321-327.

149. E.Y. Jen, C.-W. Ko, J.E. Lee, P.L. Del Valle, A. Aydanian, C. Jewell, K.J. Norsworthy, D. Przepiorka, L. Nie, and J. Liu, *FDA approval: gemtuzumab ozogamicin for the treatment of adults with newly diagnosed CD33-positive acute myeloid leukemia.* Clinical Cancer Research, 2018. **24**(14): p. 3242-3246.

150. Y.N. Lamb, *Inotuzumab ozogamicin: first global approval.* Drugs, 2017. **77**(14): p. 1603-1610.

151. S. Dhillon, *Moxetumomab pasudotox: first global approval.* Drugs, 2018. **78**(16): p. 1763-1767.

152. S. Duggan, *Caplacizumab: first global approval.* Drugs, 2018. **78**(15): p. 1639-1642.

153. E.D. Deeks, *Polatuzumab vedotin: first global approval.* Drugs, 2019. **79**(13): p. 1467-1475.

154. A. Markham, *Teprotumumab: First Approval.* Drugs, 2020. **80**(5): p. 509-512.

155. F.D. Makurvet, *Biologics vs. small molecules: drug costs and patient access.* Medicine in Drug Discovery, 2021. **9**: p. 100075.

156. F.M. Meier and I.B. McInnes, *Small-molecule therapeutics in rheumatoid arthritis: scientific rationale, efficacy and safety.* Best Practice & Research Clinical Rheumatology, 2014. **28**(4): p. 605-624.

157. T. Torres and P. Filipe, *Small molecules in the treatment of psoriasis.* Drug Development Research, 2015. **76**(5): p. 215-227.

158. A.C. Chan and P.J. Carter, *Therapeutic antibodies for autoimmunity and inflammation.* Nature Reviews Immunology, 2010. **10**(5): p. 301-316.

159. T. Oude Munnink, M. Henstra, L.I. Segerink, K. Movig, and P. Brummelhuis-Visser, *Therapeutic drug monitoring of monoclonal antibodies in inflammatory and malignant disease: translating TNF-α experience to oncology.* Clinical Pharmacology & Therapeutics, 2016. **99**(4): p. 419-431.

160. I. Sanz, U. Yasothan, and P. Kirkpatrick, *Belimumab.* Nature Reviews Drug Discovery, 2011. **10**(5): p. 335-336.

161. M. Sanford and K. McKeage, *Secukinumab: first global approval.* Drugs, 2015. **75**(3): p. 329-338.

162. G.M. Keating, *Mepolizumab: first global approval.* Drugs, 2015. **75**(18): p. 2163-2169.

163. A. Markham, *Reslizumab: first global approval.* Drugs, 2016. **76**(8): p. 907-911.

164.   S.L. Greig, *Brodalumab: first global approval.* Drugs, 2016. **76**(14): p. 1403-1412.

165.   A. Markham, *Benralizumab: first global approval.* Drugs, 2018. **78**(4): p. 505-511.

166.   A. Markham, *Tildrakizumab: first global approval.* Drugs, 2018. **78**(8): p. 845-849.

167.   A. Markham, *Ibalizumab: first global approval.* Drugs, 2018. **78**(7): p. 781-785.

168.   A. Rendon and K. Schäkel, *Psoriasis pathogenesis and treatment.* International Journal of Molecular Sciences, 2019. **20**(6): p. 1475.

169.   M.-A. Boutet, A. Nerviani, G. Gallo Afflitto, and C. Pitzalis, *Role of the IL-23/IL-17 axis in psoriasis and psoriatic arthritis: the clinical importance of its divergence in skin and joints.* International Journal of Molecular Sciences, 2018. **19**(2): p. 530.

170.   L. Puig, *The role of IL 23 in the treatment of psoriasis.* Expert Review of Clinical Immunology, 2017. **13**(6): p. 525-534.

171.   J.G. Krueger, L.K. Ferris, A. Menter, F. Wagner, A. White, S. Visvanathan, B. Lalovic, S. Aslanyan, E.E. Wang, and D. Hall, *Anti–IL-23A mAb BI 655066 for treatment of moderate-to-severe psoriasis: safety, efficacy, pharmacokinetics, and biomarker results of a single-rising-dose, randomized, double-blind, placebo-controlled trial.* Journal of Allergy and Clinical Immunology, 2015. **136**(1): p. 116-124. e7.

172.   I.M. Haugh, A.K. Preston, D.N. Kivelevitch, and A.M. Menter, *Risankizumab: an anti-IL-23 antibody for the treatment of psoriasis.* Drug Design, Development and Therapy, 2018. **12**: p. 3879.

173.   Y. Choi and C.S. Diefenbach, *Polatuzumab vedotin: a new target for B cell malignancies.* Current Hematologic Malignancy Reports, 2020. **15**(2): p. 125-129.

174.   L.H. Sehn, A.F. Herrera, C.R. Flowers, M.K. Kamdar, A. McMillan, M. Hertzberg, S. Assouline, T.M. Kim, W.S. Kim, and M. Ozcan, *Polatuzumab vedotin in relapsed or refractory diffuse large B-cell lymphoma.* Journal of Clinical Oncology, 2020. **38**(2): p. 155-165.

175.   A. Markham, *Brolucizumab: first approval.* Drugs, 2019. **79**(18): p. 1997-2000.

176.   M.M. Moschos, E. Nitoda, I.P. Chatziralli, and C.A. Demopoulos, *Age-related macular degeneration: pathogenesis, genetic background, and the role of nutritional supplements.* Journal of Chemistry, 2014. **2014**: p. 317536.

177.   Q.D. Nguyen, A. Das, D.V. Do, P.U. Dugel, A. Gomes, F.G. Holz, A. Koh, C.K. Pan, Y.J. Sepah, and N. Patel, *Brolucizumab: evolution through preclinical and clinical studies and the implications for the management of neovascular age-related macular degeneration.* Ophthalmology, 2020. **127**(7): p. 963-976.

178.   S. Gupta and R. Douglas, *The pathophysiology of thyroid eye disease (TED): implications for immunotherapy.* Current Opinion in Ophthalmology, 2011. **22**(5): p. 385.

179.   R.S. Douglas, *Teprotumumab, an insulin-like growth factor-1 receptor antagonist antibody, in the treatment of active thyroid eye disease: a focus on proptosis.* Eye, 2019. **33**(2): p. 183-190.

180.   Y. Wu, L. Zhong, and J. Geng, *Neuromyelitis optica spectrum disorder: pathogenesis, treatment, and experimental models.* Multiple Sclerosis and Related Disorders, 2019. **27**: p. 412-418.

181.   S. Lennon-Chrimes, H.S. Baumann, G. Klingelschmitt, X. Kou, V.G. Anania, H. Ito, and H.-C. von Büdingen, *Characterisation of the PK and PD of satralizumab, a recycling antibody, to support Q4W dosing in patients with NMOSD (1483).* Neurology, 2020. **94**: p. 1483.

182.   A. Gibofsky, *Epidemiology, pathophysiology, and diagnosis of rheumatoid arthritis: a synopsis.* The American Journal of Managed Care, 2014. **20**(7 Suppl): p. S128-35.

183.   T. Yamamura, I. Kleiter, K. Fujihara, J. Palace, B. Greenberg, B. Zakrzewska-Pniewska, F. Patti, C.-P. Tsai, A. Saiz, and H. Yamazaki, *Trial of satralizumab in neuromyelitis optica spectrum disorder.* New England Journal of Medicine, 2019. **381**(22): p. 2114-2124.

Purification of Antibodies using Aqueous Biphasic Systems

2

2.1. Purification of human antibodies from serum samples using aqueous biphasic systems comprising ionic liquids as adjuvants

This chapter is based on the manuscript under preparation with

<u>Emanuel V. Capela</u>, *Alexandra Wagner, João A.P. Coutinho, M. Raquel Aires-Barros, Ana M. Azevedo, Mara G. Freire*

2.1.1. Abstract

Despite the therapeutic potential of human antibodies in the treatment of several diseases, the recovery of these biopharmaceuticals from human sera with high quality and purity is still very complex and expensive. Herein, we propose a novel and high-efficient approach based on the aqueous biphasic systems comprising ionic liquids (ILs) as adjuvants for IgG purification from human serum samples. The process was first optimized by addressing the IgG extraction and yield playing with the IL cation and anion and IL concentration in the ABS composed of polyethelyneglycol (PEG) and dextran. The most promising conditions were then applied and optimized for the extraction and purification of IgG directly from human serum. Overall, IgG is enriched in the PEG-rich phase, the phase for which the IL migrates as well. With the optimized system, containing the IL 1-butyl-3-methylimidazolium bromide ([C$_4$mim]Br) at 35 wt%, a recovery of 93.0 % and a purity level of 93.2 % of polyclonal antibodies was achieved in a single-step. These results reinforce the relevance of having ILs with low hydrogen-bond basicity anions and aromatic cations to improve the selectivity towards IgG. Therefore, a novel approach was proposed as a very promising and powerful tool for the purification of human antibodies in a one-step, very simple, flexible and cost-effective approach, thus contributing for the widespread use of this biopharmaceutical as a recurrent and low-cost therapy. Finally, this work reports promising evidences on the possibility of introducing ILs in the purification of antibodies, giving room for deeper studies on this field.

2.1.2. Introduction

Progress in pharmaceutical sciences led to the dawn of biopharmaceuticals, among which antibodies are the most relevant [1].

Antibodies are host proteins found in plasma and extracellular fluids that serve as the first response and comprise one of the principal effectors of the adaptive immune system [2]. They are generally produced in response to foreign molecules and pathogens, which they ultimately neutralize, being further eliminated by phagocytoses. Immunoglobulin G (IgG) is the most important class of mammal antibodies, since they are the most abundant immunoglobulins in the blood (representing 75 % of the antibodies) [3]. IgG and albumin are the most abundant proteins in plasma (a mean content of 8–12 g·L^{-1} and 35–45 g·L^{-1}, respectively, in plasma pools) and represent, together with various coagulation factors and protease inhibitors, the core products of the plasma fractionation industry [4].

IgG derived from human serum is frequently used as a biopharmaceutical for the prevention and treatment of infections in immunodeficient patients, and also plays an important role in the treatment of autoimmune and inflammatory diseases [5, 6]. Polyvalent intravenous immunoglobulins (IVIGs) are pharmaceutical formulations of IgG obtained from the fractionation of large pools of human plasma from human healthy donors. Besides its importance in the prevention of infectious diseases in primary and acquired immunodeficiencies [7], a growing number of applications has appeared, with IVIG being currently used in the treatment of diverse inflammatory and autoimmune diseases, e.g. autoimmune thrombocytopenic purpura, Kawasaki disease, polymyositis/dermatomyositis, Guillain-Barré syndrome, among others [8]. For safety reasons, clinically used IgG needs to be highly pure, since contaminating serum proteins may cause adverse effects in patients [6, 9]. However, the purification of IgG is challenging due to the large amount of albumin (HSA) present in human serum combined with the complexity of other serum components [10].

The purification of IgG from human serum can be traced back to World War II. Cohn and associates [11] first developed an ethanol-based precipitation technique for IgG fractionation, being this the most commonly used fractionation technique for human IgG, in which IgG with a purity higher than 90 % can be obtained [11]. However, with this technique the recovery of IgG is highly compromised, being of only 40–50 % [7]. Other techniques have been proposed for the same goal, including ammonium sulfate induced precipitation followed by centrifugation [12], caprylic acid based precipitation [13, 14], gradiflow technique [15], carbon nanotubes [16], hydrophobic interaction chromatography [17], hydrophobic charge-induction chromatography [18], membrane chromatography [19, 20], immobilized metal affinity chromatography [21] and affinity chromatography [22-26]. The aforementioned methods if providing high yield tend to give low purity and vice-versa. In addition, most of them require long processing times, whereas certain

Purification of human antibodies from serum samples using aqueous biphasic systems comprising ionic liquids as adjuvants

2

resins and affinity ligands are of high cost. Therefore, efforts have been continuously made to improve plasma fractionation and purification of IgG with high yield and purity.

Aqueous biphasic systems (ABS) can be foreseen as a valuable alternative to the established purification platforms due to their ability for continuous operation and high loading capacity [27]. ABS consist on two immiscible water-rich phases, based on polymer-polymer, polymer-salt or salt-salt combinations dissolved in aqueous media, that may be used in liquid-liquid extraction [28]. Due to their water-rich medium, ABS have been used for the recovery of biological products, such as proteins/enzymes, antibiotics, among other high-value biomolecules [27, 28]. Despite these advantages, few reports are found in the literature on the application of ABS for the extraction and purification of IgG from blood-related products [29-33]. Among these, only one work [29] is related to the extraction of IgG from human plasma, since the others comprised the extraction from animal sources or from mimetic matrices composed of IgG and the most abundant protein, albumin. In these works, to overcome the restricted polarity difference between the phases of traditional polymer-based systems, the addition of salts and multi-stage approaches were investigated. This drawback of restricted polarity can be however overcome by ionic liquids (ILs), which can be used as adjuvants/additives in ABS. Due to their wide diversity of chemical structures and designer solvents ability, they allow the tailoring of the phases' polarities and affinities towards target biomolecules [34]. Despite their advantages, few works are still available on the use of IL-based ABS for IgG extraction/purification [33, 35-37], considering both the IgG recovery from animals serum [33, 35, 37] or from cell culture supernatants [36]. Most of them used ILs as a primary phase-forming components, with only one work [33] referring to the use of ILs as adjuvants in polymer-salt systems, but reporting low IgG purity levels (26 %). Hence, and taking into account the unique properties of ILs, it seems plausible that better ILs can be found to be applied as adjuvants in typical polymer-polymer ABS to overcome their low polarity range, while allowing the purification of high-value biopharmaceuticals, such as antibodies.

In this work, the performance of several ILs used as adjuvants in conventional PEG/dextran ABS was evaluated. Extractions with commercial human IgG were first performed to evaluate the best systems/conditions and ILs to be used. The best systems were further investigated and optimized for the extraction and purification of antibodies directly from human serum samples.

2.1.3. Experimental section

2.1.3.1. Materials

The ABS studied in this work were prepared using an aqueous solution of polyethylene glycol with a molecular weight of 3350 Da (PEG 3350), and an aqueous solution of dextran with a molecular weight of 500,000 Da (dextran 500k). Both polymers were obtained from Sigma-Aldrich (St. Louis, MO, USA) and used without any further purification. Different ILs as adjuvants in the PEG-dextran ABS were investigated, namely: tetramethylammonium chloride ([N_{1111}]Cl, purity > 97 wt%); tetrabutylammonium chloride ([N_{4444}]Cl, purity > 97 wt%); 1-butyl-4-methylpyridinium chloride, ([C_4-4mpy]Cl, purity > 98 wt%); cholinium chloride ([Ch]Cl, purity > 98 wt%); cholinium acetate ([Ch][Ac], purity > 99 wt%); 1-butyl-3-methylimidazolium chloride ([C_4mim]Cl, purity of 99 wt%); 1-butyl-3-methylimidazolium bromide ([C_4mim]Br, purity of 99 wt%); 1-butyl-3-methylimidazolium hydrogen sulfate ([C_4mim][HSO_4], purity of 99 wt%). All ammonium-based ILs were from Sigma-Aldrich, [Ch]Cl was acquired from Acros Organics (Geel, Belgium) and the remaining ILs were acquired from Iolitec (Heilbronn, Germany). Before use, all ILs were purified and dried for a minimum of 24 h, under constant agitation, at moderate temperature of ≈ 50˚C (± 1 °C) and under vacuum (to reduce their volatile impurities to negligible values). After this step, the purity of each IL was confirmed by ^{1}H and ^{13}C NMR spectra and found to be in accordance with the purity levels given by the suppliers. The chemical structures of the investigated ILs are depicted in **Figure 2.1.1**.

The studies using commercial immunoglobulin G (IgG) were performed using human IgG for therapeutic administration (trade name: Gammanorm®), obtained from Octapharma (Lachen, Switzerland), as a 165 mg·mL^{-1} solution containing 95 % of IgG (of which 59 % IgG1, 36 % IgG2, 4.9 % IgG3 and 0.5 % IgG4). The human serum used in this study was from human male AB plasma, USA origin, sterile-filtered, obtained from Sigma Aldrich (H4522 Sigma), with a total protein content ranging between 40-90 mg·mL^{-1}. This product was provided as a liquid and was stored at -20 °C. Phosphate buffered saline (PBS) pellets, from Sigma-Aldrich, were used to dilute human serum previously to its use on each assay. Bovine serum albumin (BSA) standards (2 mg·mL^{-1}), used as model biomolecule for the calibration curve for Bradford protein assays, was purchased from Thermo Scientific Pierce.

The required material for polyacrylamide gel electrophoresis (SDS-PAGE) include: 40 % acrylamide/bis-acrylamide solution, 4x Laemmli Sample Buffer from Bio-Rad and Precision Plus Protein™ Dual Color Standards (Hercules, CA, USA); tris(hydroxymethyl)aminomethane, PA from

Pronalab (Tlalnepantla, Mexico); sodium dodecyl sulfate, (SDS, purity > 98.5 wt%), glycine, ammonium persulfate (APS), *N,N,N',N'*-tetramethylethylenediamine (TEMED), DL-dithiothreitol (DTT) solution 1 mol·L^{-1} in H$_2$O and Coomassie Brilliant Blue R in soluble tablets (commercial name: PhastGel® Blue R) from Sigma-Aldrich; ethanol from Thermo Scientific Pierce (Rockford, IL, USA); acetic acid (purity of 100 %) from Merck Millipore (Darmstadt, Germany).
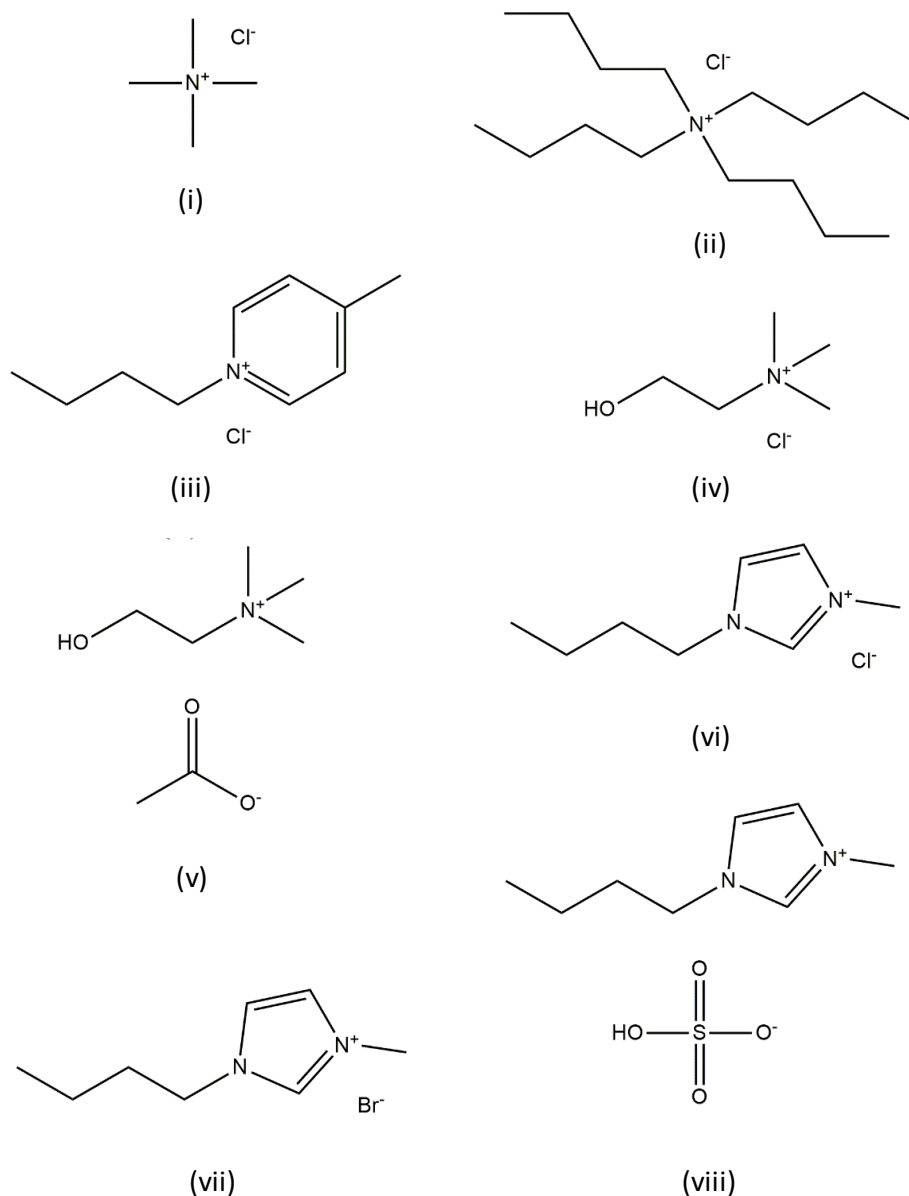
Figure 2.1.1. Chemical structures of the ILs investigated as adjuvants in ABS composed of PEG 3350 + dextran 500k + H$_2$O: (i) [N$_{1111}$]Cl; (ii) [N$_{4444}$]Cl; (iii) [C$_4$-4mpy]Cl; (iv) [Ch]Cl; (v) [Ch][Ac]; (vi) [C$_4$mim]Cl; (vii) [C$_4$mim]Br and (viii) [C$_4$mim][HSO$_4$].

For total protein quantification by Bradford protein assay, Coomassie Plus (Bradford) Protein Assay was purchased from Thermo Scientific Pierce. The water employed along this work was treated with a Milli-Q® Integral water purification apparatus from Merck Millipore.

2.1.3.2. Methods

Extraction/purification of human antibodies using ABS. In the studied ABS, the top phase corresponds to the PEG-rich aqueous phase while the bottom phase is mainly composed of dextran. The ternary mixture composition for the IgG extraction/partition was chosen based on the phase diagram already reported in the literature [38, 39]. In order to have the minimal concentration of both polymers and the maximum concentration of water (more economic and more biocompatible process), the following mixture composition was investigated: 7 wt% PEG 3350 + 5 wt% dextran 500k + 88 wt% H_2O/IgG solution or serum/IL. All partitioning studies of the quaternary systems (comprising the IL) were performed with the same extraction point, where the ILs were introduced as adjuvants in three different concentrations, namely 1, 5 and 10 wt%; for [C_4mim]Br concentrations up to 40 wt% were also tested. The partition behaviour/purification performance of human IgG in aqueous PEG/dextran and PEG/dextran/IL two-phase systems was investigated using IgG stock solution prepared with a concentration at circa 1 $g·L^{-1}$ or human serum 20-fold diluted, both in PBS (phosphate buffered saline at 10 $mmol·L^{-1}$, pH ≈ 7.4, at 25˚C). In each system, the biological sample (IgG aqueous solution or human serum diluted at 1:20 (v:v)) was loaded at 30 wt% to the phase-forming components to reach a total weight of the mixture of 2.0 g. The systems were mixed in a Vortex mixer (Ika, Staufen, Germany), centrifuged for 30 min in a fixed angle rotor bench centrifuge (Eppendorf, Hamburg, Germany) at 1372 × g, and to ensure total phase separation and chemical equilibrium they were settled for 30 min. After the equilibrium conditions were reached, both phases were carefully separated using a micropipette to extract the top phases and a 2.5 mL syringe to take the bottom phases, their volumes were determined and also their pH values at 25 °C (± 1 °C) using a Metrohm 702 SM Titrino (Herisau, Switzerland), with an uncertainty of ± 0.01 in each measurement. Control systems without IL were also prepared to assess their effect in IgG partitioning, as well as blank systems without biological sample to discount the interference of the phase-forming compounds in the analytical methods. IgG was quantified in each phase by affinity chromatography in ÄKTA™ 10 Purifier system from GE Healthcare (Uppsala, Sweden) using an analytical POROS Protein G affinity column (2.1 x 30 mm) from Applied Biosystems (Foster City, CA, USA). Adsorption of IgG to the column was performed in 50 $mmol·L^{-1}$ sodium phosphate (NaH_2PO_4) buffer at pH 7.4 containing 150 $mmol·L^{-1}$ sodium chloride (NaCl) for 1.8 min. Elution was triggered

by decreasing the pH value of the buffer to 2–3, using 12 mmol·L^{-1} chloridric acid (HCl) with 150 mmol·L^{-1} NaCl during 2.5 min. Finally, the column was re-equilibrated with the adsorption buffer for 3.4 min. Samples from top and bottom phases containing IgG were diluted 20 times in the adsorption buffer and 0.5 mL were injected in the column using an Autosampler A-900 from GE Healthcare. Absorbance was monitored at 215 nm. IgG concentration was determined from a daily-fresh calibration curve obtained using Gammanorm IgG as a standard biomolecule, in a concentration ranging between 0.2 to 20 mg·L^{-1}. In the end of each assay, the column was stored in 10 mmol·L^{-1} sodium phosphate (NaH$_2$PO$_4$) buffer at pH 7.4 containing 0.02 % sodium azide. For the assays with the real matrix, total protein content (IgG + remaining proteins) of each phase was also determined using the Bradford protein assay method with a Coomassie Plus kit from Pierce (Rockford, IL, USA) [40]. The assays were set up in 96 well polystyrene microplates and 200 μL of Coomassie reagent were added to 50 μL of samples, previously diluted 4 or 10 times, blanks and standard solutions. A calibration curve with bovine serum albumin (BSA) from 5 to 400 mg·L^{-1} was used as a standard biomolecule for protein calibration. Absorbance was read at 595 nm in a microplate reader from Molecular Devices (Sunnyvale, CA, USA). At least two individual experiments were performed to determine the average in performance parameters, as well as the respective standard deviations.

The IgG partition coefficient into the PEG-rich phase, K_{IgG}, is the ratio between the concentration of IgG in both phases and was determined using Equation 1,

$$K_{IgG} = \frac{[IgG]_{PEG}}{[IgG]_{dextran}} \tag{1}$$

where [IgG]$_{PEG}$ and [IgG]$_{dextran}$ represents the total IgG concentration in the PEG- and dextran-rich phase, respectively.

The IgG recovery yield for the PEG-rich phase, %Yield$_{IgG}$, is the percentage ratio between the amount of protein in the PEG-rich aqueous phase to that added in the initial mixture, and is defined according to Equation 2,

$$\%Yield_{IgG} = \frac{[IgG]_{PEG} \times V_{PEG}}{[IgG]_{initial} \times V_{initial}} \times 100 \tag{2}$$

where [IgG]$_{PEG}$ and [IgG]$_{initial}$ represents the total IgG concentration in the PEG-rich phase and in the initial solution, respectively, and the parameters V_{PEG} and $V_{initial}$ represent the volume of PEG-rich phase and the volume of stock solution added to the ABS, respectively. The percentage purity of IgG was calculated dividing the IgG concentration by the total protein concentration at the PEG-rich phase, according to Equation 3,

$$\%Purity_{IgG} = \frac{[IgG]_{PEG}}{[Total\ proteins]_{PEG}} \tag{3}$$

where [IgG]$_{PEG}$ and [Total proteins]$_{PEG}$ represent the concentration of IgG and total proteins in PEG-rich phase, respectively.

Ionic liquids quantification. The amount of imidazolium-based ILs ([C$_4$mim]Cl, [C$_4$mim]Br and [C$_4$mim][HSO$_4$]) in each phase was quantified by UV-spectroscopy, using a Spectramax 384 Plus from Molecular Devices (Sunnyvale, CA, USA), at a wavelength of 211 nm. Chloride-based ILs ([N$_{1111}$]Cl and [Ch]Cl) were quantified in each phase using a Metrohm 904 Titrando equipped with a chloride-selective electrode. Each sample was 100 times diluted in ultra-pure water and TISAB solution (containing 0.1 mol·L^{-1} potassium nitrate, 0.1 mol·L^{-1} acetic acid and 0.1 mol·L^{-1} sodium acetate) to assure the ionic strength of the samples for further analyses, using the Tiamo™ 2.3 software. Samples were measured under continuous stirring, and after each measurement, the ionic strength of the electrode was re-established in TISAB solution for 5 min. Chloride anion concentration was determined from a calibration curve obtained using potassium chloride (KCl) as a standard, in a concentration ranging between 0.1 to 100 mmol·L^{-1}.

The extraction efficiency of the IL, %EE$_{IL}$, is defined as the quantity of the IL in the PEG-rich to that in the two phases, and is defined according to Equation 4.

$$\%EE_{IL} = \frac{[IL]_{PEG} \times V_{PEG}}{[IL]_{PEG} \times V_{PEG} + [IL]_{dextran} \times V_{dextran}} \times 100 \tag{4}$$

where [IL]$_{PEG}$ and [IL]$_{dextran}$ represents the total IL concentration in PEG- and dextran-rich phase, respectively, and the parameters V$_{PEG}$ and V$_{dextran}$ represent the volume of PEG- and dextran-rich, respectively.

Proteins stability assessment. Sodium dodecyl sulfate polyacrylamide gel electrophoresis (SDS-PAGE) assays were performed to assess the proteins profile and infer on IgG stability and integrity. Samples were prepared and diluted in a sample buffer from Bio-Rad containing 62.5 mmol·L^{-1} Tris–HCl, pH 6.2, 2 % SDS, 0.01 % bromophenol blue and 10 % glycerol, under reducing conditions with 100 mM dithiothreitol (DTT) and then denaturated at 100°C for 10 min. A volume of 25 µL of these samples was applied in a 12 % acrylamide gel, prepared from a 40 % acrylamide/bis-acrylamide stock solution (29:1) from Bio-Rad, and ran at 90 mV using a running buffer containing 192 mmol·L^{-1} glycine, 25 mmol·L^{-1} Tris, and 0.1 % (w/v) SDS at pH 8.3. The molecular weight standard used was Precision Plus Protein™ Dual Color Standards from BioRad. Gels were stained with 0.1 % (w/v) Coomassie Brilliant Blue R-250 from Pharmacia AB Laboratory Separations® (Uppsala, Sweden), 30 % (v/v) ethanol, 10 % (v/v) acetic acid and water, in an orbital shaker at 40 °C and moderate velocity during 1 h. Gels were then distained using a solution

Purification of human antibodies from serum samples using aqueous biphasic systems comprising ionic liquids as adjuvants

2

containing 30 % (v/v) ethanol and 10 % (v/v) acetic acid, in an orbital shaker at 25 °C and moderate velocity, until background color disappeared. Finally, gels were stored in milli-Q water at room temperature, until digital images of the gels were acquired using a calibrated densitometer GS-800 from Bio-Rad and analyzed with the informatics tool Quantity One 4.6 also from Bio-Rad.

2.1.4. Results and discussion

2.1.4.1. Optimization of the extraction process using commercial human IgG

The feasibility of using quaternary ABS composed of PEG 3350 + dextran 500k + H_2O + ILs, at 25 °C, for the extraction of commercial human IgG was initially assessed using a wide range of ILs ([N_{1111}]Cl, [N_{4444}]Cl, [C_4-4mpy]Cl, [Ch]Cl, [Ch][Ac], [C_4mim]Cl, [C_4mim]Br and [C_4mim][HSO_4]), varying both the anion and the cation to understand the effect of each ion and its chemical characteristics in the partition of antibodies. A common mixture composition was used, taking into account the phase diagram of the ternary system: 7 wt% PEG 3350 + 5 wt% dextran 500k + 88 wt% H_2O/IgG solution/IL. ILs were used as adjuvants in the polymer-polymer systems at three different concentrations, namely 1, 5 and 10 wt%. All ILs at the concentrations studied form aqueous two-phase systems; however, the volume ratio of the system changes with the addition of IL (volume of bottom phase in relation to volume of top phase varying from 1:1.64 to 1:3.75), and appears to be highly dependent on the IL used and its concentration [*cf.* **Appendix A (Table A.1)**]. No formation of any precipitated and/or denatured solid protein phase was observed in most cases, with the exception of the systems composed of [C_4mim][HSO_4] in which an intermediate solid layer of protein was observed at the interphase.

Effect of the IL ions

Firstly, the effect of IL cation core and alkyl side chain length on the partitioning of IgG antibodies was assessed using ABS composed of PEG 3350 + dextran 500k + H_2O + 1 wt% ILs with a fixed chloride anion (Cl$^-$) combined with the following cations: [Ch]$^+$, [C_4mim]$^+$, [C_4-4mpy]$^+$, [N_{1111}]$^+$ and [N_{4444}]$^+$. The IL anion effect was also investigated with two different ILs families, namely cholinium-based ILs ([Ch]$^+$) combined with the Cl$^-$ and [Ac]$^-$ anions, and the imidazolium-based ILs ([C_4mim]$^+$) combined with the Cl$^-$, Br$^-$ and [HSO_4]$^-$ anions. The results obtained are shown in **Figure 2.1.2 (A)** and **(B)**, with the respective detailed data reported in **Appendix A (Table A.2)**.

The recovery yield of IgG in the control system (without the addition of IL) is 70.8 %. Remarkably, a low concentration of IL (just 1 wt%) allows the manipulation and enhancement of

the extraction of IgG for the PEG-rich top phase of the system, increasing to values between 76.8 % and 86.7 % (with the exception of $[C_4mim][HSO_4]$ that lowered the yield to 18.9 %). The recovery yield of IgG by the several ABS decreases in the following order of IL cations: $[C_4\text{-}4mpy]^+ > [N_{4444}]^+ \approx [N_{1111}]^+ \approx [C_4mim]^+ > [Ch]^{+,}$ and in the following order of anions: $[Ac]^- > Cl^-$ and $Cl^- > Br^- \gg [HSO_4]^-$, for the cholinium- and imidazolium-based ILs, respectively.

A

B
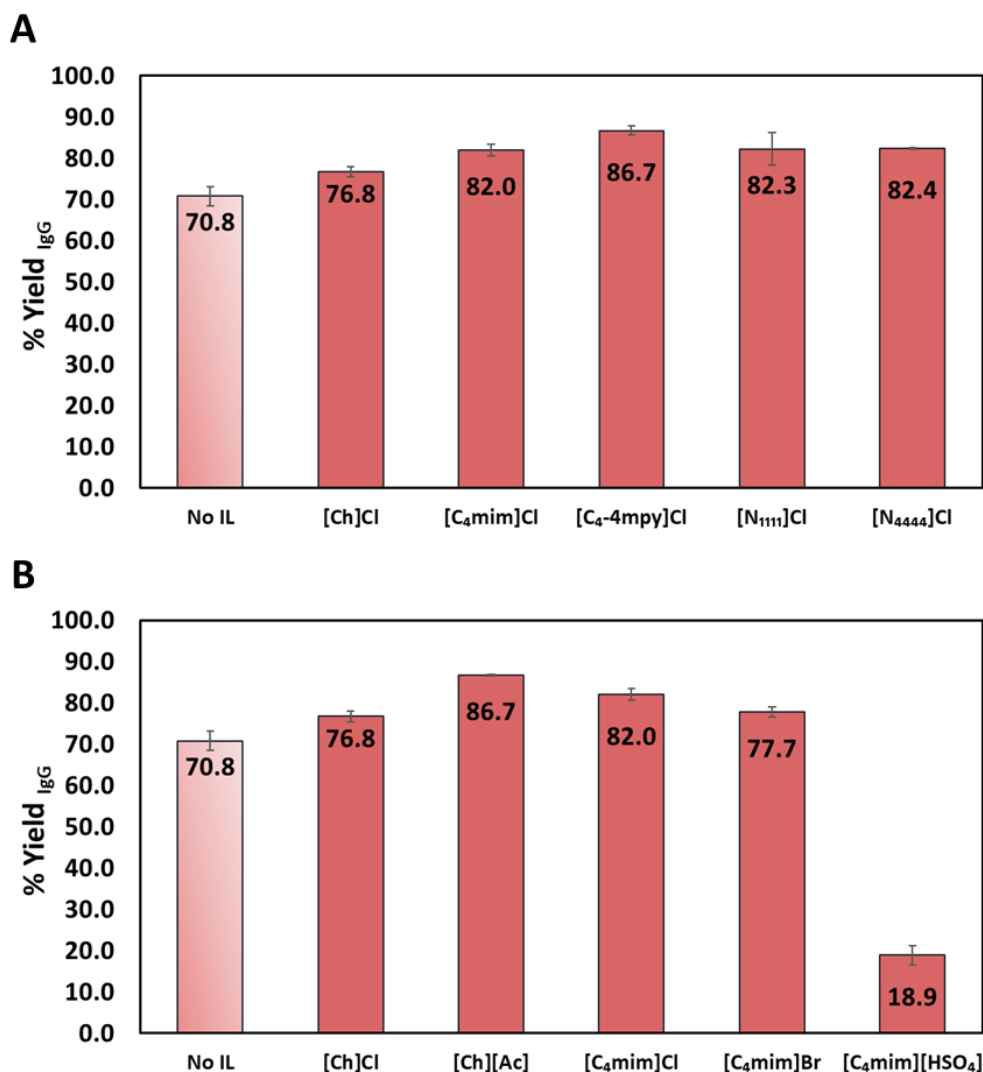
Figure 2.1.2. Percentage recovery yield (%Yield$_{IgG}$ – ■) of human IgG in quaternary ABS formed by PEG 3350 + dextran 500k + H_2O + 1 wt% of different: (A) chloride-based ILs; (B) cholinium- and imidazolium-based ILs, at 25 °C.

The pyridinium-based IL reveals to lead to higher recovery yields of IgG. On the contrary, the cholinium- and phosphonium-based ILs display a lower performance to increase the extraction of IgG. Moreover, it is possible to notice different abilities of tetraalkylammonium- and

Purification of human antibodies from serum samples using aqueous biphasic systems comprising ionic liquids as adjuvants

2

tetraalkylphosphonium-based ILs for IgG extraction, with the first allowing higher recovery yields. No significant differences are observed on the IgG partition as a function of the alkyl side chain length (from methyl to butyl) in tetraalkylammonium-based ILs. These results suggest that no significant dispersive interactions take place between the IL cations and the alkyl outside-oriented groups of the protein.

Regarding the effect of the IL anion, it was macroscopically observed for [C$_4$mim][HSO$_4$] a layer of precipitated protein on the interface of the system, which consequently translates into a decrease on the recovery yield of protein. For the remaining studied anions, it was found that the trend is in accordance with the hydrogen-bond basicity of the studied ILs, since ILs with the [Ac]$^-$, Cl$^-$ and Br$^-$ anions are those with a higher hydrogen-bond basicity: [Ac]$^-$ (β=1.20) > Cl$^-$ (β=0.95) > Br$^-$ (β=0.87) [41]. These ILs appear to be favorable to increase the recovery yield, suggesting that hydrogen-bonding interactions play a role in the extraction process. In addition, the chloride anion in the inorganic salt form (NaCl) has already been reported [42] to be capable to enhance IgG extraction in a concentration of 150 mM in a PEG/phosphate ABS.

The partition coefficient of IgG (K$_{IgG}$) in the studied systems [*cf.* **Appendix A (Table A.2)**] are in accordance to these observations. The control ABS presents a partition coefficient of 0.87 indicating a preferential migration of IgG to the dextran-rich bottom phase of the system, and with the addition of IL we observe the inversion on the partition behavior of the protein, showing then a preferential migration to the PEG-rich top phase, since in all the cases the partition coefficients are higher than 1. It is important to highlight that the PEG-rich phase is also the phase for which the IL preferentially migrates (%EE$_{IL}$ > 66 %), being these results discussed below. Based on all the discussed information, it was possible to conclude that by adding small quantities of IL to this PEG/dextran system it is possible to manipulate the polarities of the coexisting phases and consequently of the partition of antibodies.

Effect of the IL concentration

The effect of the IL concentration was evaluated using three concentrations of IL – 1, 5 and 10 wt%. The gathered recovery yields of IgG are presented in **Figure 2.1.3**, with the respective detailed data reported in **Appendix A (Table A.3)**. The partition coefficients (K$_{IgG}$), extraction efficiency of the IL (%EE$_{IL}$) and extraction pH values are also presented in **Appendix A (Table A.3)**.

In general, the increase in the concentration of IL added to the system is associated with an increase in the yield of IgG recovery towards the PEG-rich phase, that is the same phase for which the IL preferentially partitions, as discussed before [%EE$_{IL}$ = 66 – 77 %, *cf.* **Appendix A (Table A.3)**].

Remarkably, the system containing 10 wt% [Ch][Ac] allowed an IgG recovery yield higher than 97 % in just one extraction step. On the other hand, by using [C₄mim][HSO₄], the opposite was observed. The increase in the concentration of this IL lead to a continuous decrease in the recovery yield of IgG, apparently as a result of the very acidic pH value at which the extraction occurs [lower than 2 – *cf.* **Appendix A (Table A.3)** with pH values]. All remaining systems display a pH at the coexisting phases ranging between 5.7 and 7.8. A better performance of the IL-based ABS is observed between 6.5 and 7.5. This behaviour is in contradiction with a previous report [43] where severe precipitation of IgG (about 50 %) was observed in pH 5 – 8 using PEG/dextran ABS, whereas at more acidic pH values the precipitation was considerably reduced. These results, together with the inversion in the partition behaviour, reinforce the relevance of the IL chemical structure and that specific interactions occurring between the IL and IgG are occurring.
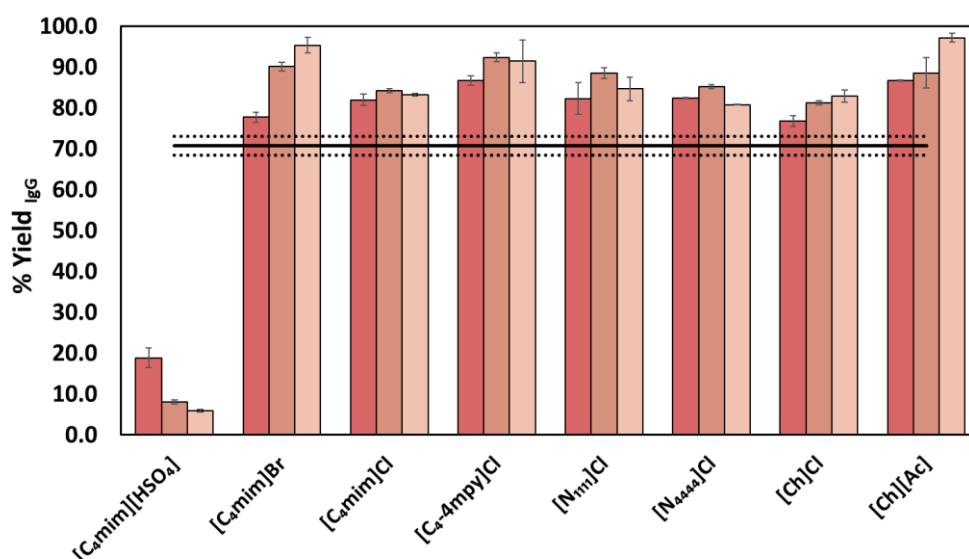
Figure 2.1.3. Percentage recovery yield (%Yield$_{IgG}$) of human IgG and work pH in quaternary ABS formed by PEG 3350 + dextran 500 kDa + H₂O + 1 (■), 5 (■) and 10 (■) wt% of [C₄mim][HSO₄], [C₄mim]Br, [C₄mim]Cl, [C₄-4mpy]Cl, [N₁₁₁₁]Cl, [N₄₄₄₄]Cl, [Ch]Cl and [Ch][Ac] ILs, at 25 °C. The percentage recovery yield obtained by the system with no IL is represented by the black line (▬).

Among all the studied ILs, [C₄mim]Br should be highlighted since it has a highest capacity to increase the recovery yield, increasing with the IL concentration increase. This IL comprises an aromatic cation and the anion with the lowest hydrogen-bond basicity investigated, reinforcing the relevance of the IL chemical nature and specific interactions in ruling the IgG partition between the two phases. These interactions may involve π ⋯ π interactions between the aromatic amino acids of IgG and the aromatic ring of [C₄mim]Br, as well as cation ⋯ π interactions between IgG (which at

Purification of human antibodies from serum samples using aqueous biphasic systems comprising ionic liquids as adjuvants

2

the work pH is positively charged) and the aromatic ring of the IL cation. Since promising results were obtained with 10 wt% of [C$_4$mim]Br, reaching an excellent recovery yield around 95 %, new assays were carried out using 15, 20 and 35 wt% of the same IL aiming at the complete extraction of IgG in a single step. The results obtained are shown in **Figure 2.1.4**, while the detailed data are given in **Appendix A (Table A.3)**.
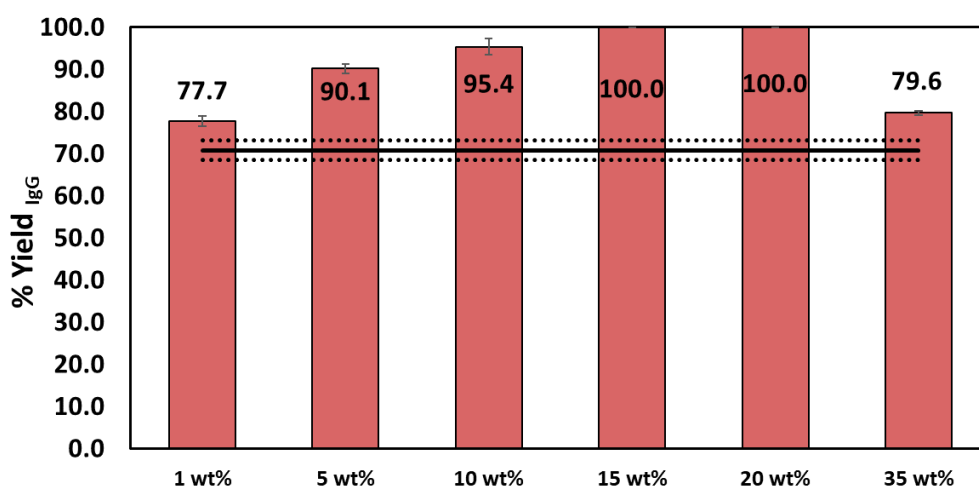
Figure 2.1.4. Percentage recovery yield (%Yield$_{IgG}$ – ■) of human IgG and extraction efficiency (%EE$_{IL}$) of IL in quaternary ABS formed by PEG 3350 + dextran 500 kDa + H$_2$O + 1, 5, 10, 15, 20 and 35 wt% of [C$_4$mim]Br, at 25 °C. The percentage recovery yield obtained by the system with no IL is represented by the black line (─).

According to the gathered results, using 15 and 20 wt% of [C$_4$mim]Br allows the complete extraction of IgG to the upper PEG-rich phase in a single step, with no losses of IgG. However, in the system with 35 wt% of IL a decrease in the recovery yield to about 80 % was observed, possibly related with the denaturation of the protein caused by such high concentration of IL.

Extraction and purification of IgG from human serum samples

The two most promising IL-based ABS identified, composed of [Ch][Ac] and [C$_4$mim]Br as adjuvants, were further evaluated in the purification of polyclonal IgG antibodies directly from human serum samples. The recovery yield and IgG purity level at the PEG-rich upper phase are presented in **Figure 2.1.5 (A)** and **(B)**. Detailed data is reported in **Appendix A (Table A.4)**. The extraction pH values varied between 6.3 and 7.4, and are also given in **Appendix A (Table A.4)**.

With the polymer-polymer ABS with [Ch][Ac] as adjuvant at 1, 5 and 10 wt% (**Figure 2.1.5 (A)**), recovery yields higher than 72 % were obtained, representing a good result when comparing with the control polymer-polymer ABS (without IL) that allowed a recovery yield of *ca.* 68 %. These

recovery yield values are however lower than those obtained with pure IgG using the same ABS, being justified by the increase of the matrix complexity.

A

B
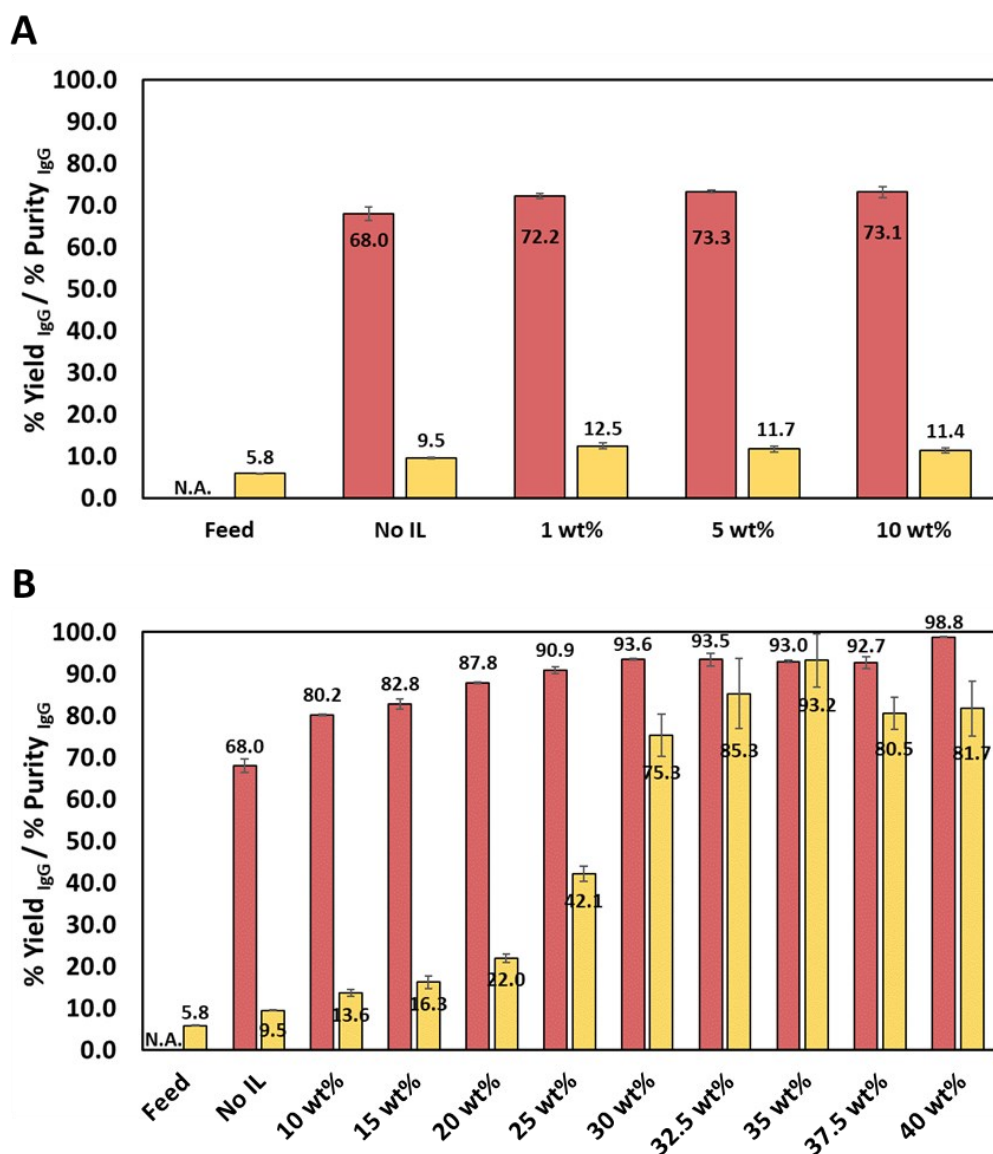
Figure 2.1.5. Percentage recovery yield (%Yield$_{IgG}$ – ■) and purity level (%Purity $_{IgG}$ – ■) of IgG from human serum (diluted at 1:20 (v:v) in quaternary ABS formed by PEG 3350 + dextran 500 kDa + H$_2$O + ILs as adjuvants at different concentrations, at 25 °C – (A) [Ch][Ac]; (B) [C$_4$mim]Br. For the feed, the %Yield$_{IgG}$ is not applicable (N.A.).

Although increasing the purity level of IgG from 5.8 % (in the human serum) to 11.4 - 12.5 %, these values are still very low given the aimed application, Furthermore, the IgG purity decreases with the IL concentration increase, due to the partitioning of human serum albumin (HSA), the main impurity in human serum, to the PEG-rich phase as well. These results allow concluding that this

Purification of human antibodies from serum samples using aqueous biphasic systems comprising ionic liquids as adjuvants

2

ABS comprising a cholinium-based IL has a high ability to extract proteins to the PEG-rich phase, since no significant losses in recovery yields are shown with the serum samples, yet it lacks in selectivity towards IgG.

Contrarily to what observed with aqueous solutions of pure IgG, in the assays with human serum the complete extraction of IgG to the PEG-rich phase of the ABS composed of 15 and 20 wt% of [C$_4$mim]Br (**Figure 2.1.5 (B)**) was not achieved, again probably due to the complexity of the matrix and presence of different proteins and saturation of the phase. Nevertheless, if higher concentrations of this IL are considered, namely 10 - 40 wt%, a significant increase in the IgG recovery yield is obtained, ranging from 80.2 % to 98.8 % in a single-step, revealing a significantly better performance when comparing with the polymer-based system without IL (yield of 68.0 %). These results mean that the presence of IL allows to improve the solubility of proteins in aqueous media. Furthermore, impressive purity levels were achieved at the PEG-rich phase, with values ranging between 13.6 % and 93.2 %, with IL concentrations ranging between 10 wt% and 40 wt%. Remarkably, the best results were obtained for the system composed of 35 wt% [C$_4$mim]Br, that allowed an IgG purity level of 93.2 % in the PEG-rich upper phase, obtained in a single-step, against a purity level of 9.5 % and 5.8 % in the similar system with no IL added and in the feed, respectively. This high level of purity is also due to the precipitation of HSA, the main abundant protein in human serum, at the ABS interphase. By SDS-PAGE gel analysis [**Appendix A (Figure A.1)**] it is confirmed that it was mainly composed of HSA (molecular weight *ca.* 66 kDa), while the presence of the characteristic bands of the heavy (molecular weight *ca.* 50 kDa) and light (molecular weight *ca.* 25 kDa) chains of IgG were not present in this precipitate. These results reinforce the selectivity of the system comprising 35 wt% of [C$_4$mim]Br, both to enrich IgG in the PEG-rich phase and to selectively precipitate HSA at the interphase. This system also allows a recovery yield of 93.0 %. Although similar or higher recovery yields are obtained in the ABS composed of 37.5 wt% and 40 wt% of IL, these represent a compromise in the IgG purity level, that drops down to 80.5 % and 81.7 %, respectively.

The ability of the IL-based ABS to process even higher amounts of proteins was finally addressed, loading human serum directly in the ABS, without any previous dilution step [*cf.* macroscopic aspect in **Appendix A (Figure A.2)**]. Even with a much higher load of total proteins, the IgG yield remains high – 96.2 (± 0.7) %; however, the purification performance of the ABS slightly decreases, allowing a purity level of 72.9 (± 1.8) %. Nevertheless, it should be remarked that this purity level is still higher than those reported up to date in the literature using IL-based ABS, e.g. diluted rabbit serum diluted.

Traditional polymer-polymer ABS have been suggested in the literature as promising approaches to the extraction and purification of IgG, as reviewed by Capela *et al*. [1]. Nevertheless, the restricted polarity of the coexisting phases presented by this type of systems compromises enhanced recovery yields and purity factors to be achieved, thus encouraging the development of other strategies to overcome this bottleneck. Some examples in this field are the addition of salts [44] and affinity ligands [45, 46] and the use of modified phase-forming components [47]. Also, the majority of these works focus on monoclonal antibodies from hybridoma and Chinese Hamster Ovary (CHO) cell cultures supernatants. In what concerns the use of IL-based ABS for extraction/purification of IgG, only few works were reported up to date [33, 35-37], with just one addressing the use of ILs as adjuvants in polymer-salt systems [33], being all carried out with rabbit serum samples or cell culture supernatants. The current work consists in the first report on the use of ILs as adjuvants in polymer-polymer ABS for the extraction and purification of human antibodies from human serum samples, and which results outperform those previously reported using IL-based ABS [33, 35-37]. This is certainly a result of an easier tailoring of the phase polarities by introducing ILs in systems composed of two polymers instead of a polymer and a salt, in which the effect of the usually added salts as a strong salting-out species may mask the IL effect. Indeed, Ferreira *et al*. [33] using commercial ILs as adjuvants in polymer-salt ABS achieved 26 % of IgG purity, with the extraction being carried out from rabbit serum, that contrast with the 93 % of purity achieved in this work with polymer-polymer ABS using ILs as adjuvants, again reinforcing the higher impact that ILs exert in systems composed of two polymers (with no strong salting-out species present). The best obtained results (recovery yield of 93.0 % and purity level of 93.2 %) are also better than those reported in the single work found in whole human plasma to obtain IgG and albumin-enriched fractions, by Vargas *et al.* [29], using a polymer-salt ABS, where for the ABS step the authors reported an IgG recovery of 73 % with a purity of 39 %.

2.1.5. Conclusions

This work addressed the use of ILs as adjuvants in polymer-polymer ABS as an alternative process for the purification of IgG antibodies from human serum. Initial assays with pure IgG were performed in order to select the best IL, allowing to infer the effect of the IL cation, anion and concentration on the recovery yield of the target biomolecule. In all cases, IgG demonstrated a preferential partition towards the PEG-rich phase, that is also the phase for which the ILs preferentially migrate. Under the optimal conditions with pure IgG, [Ch][Ac] and [C_4mim]Br allowed recovery yields of 97.2 % and 100 % in a single step.

After the identification of the two most promising ILs, ABS composed of different concentrations of such ILs were further investigated to extract and purify IgG directly from human serum samples. [C$_4$mim]Br-based ABS at 35 wt% revealed an excellent performance, with an IgG recovery yield of 93.0 % to the PEG-rich upper phase and a purity level of 93.2 %, achieved in a single step. The enhanced performance shown by this system seems to be related to specific interactions occurring between the target biomolecule (IgG) and the IL. Moreover, the depletion of the major impurity on serum (HSA) at the ABS interphase seems to be the main feature behind the IgG purification level, resulting in a decrease on the complexity of the matrix, and allowing outstanding results to be achieved. It should be also highlighted that the results obtained in this work outstands those previously reported in the literature regarding the IgG extraction from human serum samples using IL-based ABS strategies or conventional ABS with no IL added.

Overall, a novel one-step approach based on polymer-polymer ABS comprising ILs as adjuvants is here proposed as a promising and powerful tool for the purification of antibodies from human serum samples, paving the way for the widespread use of this type of biopharmaceuticals as a recurrent and accessible therapy.

2.1.6. References

1.   E.V. Capela, M.R. Aires-Barros, M.G. Freire, and A.M. Azevedo, *Monoclonal Antibodies– Addressing the Challenges on the Manufacturing Processing of an Advanced Class of Therapeutic Agents.* Frontiers in Clinical Drug Research-Anti Infectives: Volume 4, 2017. **4**: p. 142.

2.   N.S. Lipman, L.R. Jackson, L.J. Trudel, and F. Weis-Garcia, *Monoclonal versus polyclonal antibodies: distinguishing characteristics, applications, and information resources.* ILAR journal, 2005. **46**(3): p. 258-268.

3.   S.J. Kim, Y. Park, and H.J. Hong, *Antibody engineering for the development of therapeutic antibodies.* Mol Cells, 2005. **20**(1): p. 17-29.

4.   T. Burnouf, *Modern plasma fractionation.* Transfusion medicine reviews, 2007. **21**(2): p. 101-117.

5.   H.B. Dickler and E.W. Gelfand, *Current perspectives on the use of intravenous immunoglobulin.* Advances in internal medicine, 1996. **41**: p. 641.

6.   U. Katz, A. Achiron, Y. Sherer, and Y. Shoenfeld, *Safety of intravenous immunoglobulin (IVIG) therapy.* Autoimmunity reviews, 2007. **6**(4): p. 257-259.

7.   M. Radosevich and T. Burnouf, *Intravenous immunoglobulin G: trends in production methods, quality control and quality assurance.* Vox sanguinis, 2010. **98**(1): p. 12-28.

8.   S. Kivity, U. Katz, N. Daniel, U. Nussinovitch, N. Papageorgiou, and Y. Shoenfeld, *Evidence for the use of intravenous immunoglobulins—a review of the literature.* Clinical reviews in allergy & immunology, 2010. **38**(2-3): p. 201-269.

9.   A. Farrugia and P. Robert, *Plasma protein therapies: current and future perspectives.* Best Practice & Research Clinical Haematology, 2006. **19**(1): p. 243-258.

10.   L. Wang, K.Z. Mah, and R. Ghosh, *Purification of human IgG using membrane based hybrid bioseparation technique and its variants: A comparative study.* Separation and Purification Technology, 2009. **66**(2): p. 242-247.

11.   E.J. Cohn, L.E. Strong, W. Hughes, D. Mulford, J. Ashworth, M.e. Melin, and H. Taylor, *Preparation and Properties of Serum and Plasma Proteins. IV. A System for the Separation into Fractions of the Protein and Lipoprotein Components of Biological Tissues and Fluids1a, b, c, d.* Journal of the American Chemical Society, 1946. **68**(3): p. 459-475.

12.   L. Wang, X. Sun, and R. Ghosh, *Purification of equine IgG using membrane based enhanced hybrid bioseparation technique: a potential method for manufacturing hyperimmune antibody.* Biotechnology and bioengineering, 2008. **99**(3): p. 625-633.

13.   G. Rojas, J. Jiménez, and J. Gutiérrez, *Caprylic acid fractionation of hyperimmune horse plasma: description of a simple procedure for antivenom production.* Toxicon, 1994. **32**(3): p. 351-363.

14.   W. Lebing, K. Remington, C. Schreiner, and H.I. Paul, *Properties of a new intravenous immunoglobulin (IGIV-C, 10%) produced by virus inactivation with caprylate and column chromatography.* Vox sanguinis, 2003. **84**(3): p. 193-201.

15.   D. Scheel-Toellner, K. Wang, N.V. Henriquez, P.R. Webb, R. Craddock, D. Pilling, A.N. Akbar, M. Salmon, and J.M. Lord, *Cytokine-mediated inhibition of apoptosis in non-transformed T cells and neutrophils can be dissociated from protein kinase B activation.* European Journal of Immunology, 2002. **32**(2): p. 486-493.

16.   Z. Du, S. Zhang, C. Zhou, M. Liu, and G. Li, *L-histidine functionalized multi-walled carbon nanotubes for on-line affinity separation and purification of immunoglobulin G in serum.* Talanta, 2012. **99**: p. 40-49.

17.   S. Burton and D. Harding, *Hydrophobic charge induction chromatography: salt independent protein adsorption and facile elution with aqueous buffers.* Journal of Chromatography a, 1998. **814**(1): p. 71-81.

18.   J. Yan, Q.L. Zhang, H.F. Tong, D.Q. Lin, and S.J. Yao, *Hydrophobic charge-induction resin with 5-aminobenzimidazol as the functional ligand: preparation, protein adsorption and immunoglobulin G purification.* Journal of separation science, 2015. **38**(14): p. 2387-2393.

19.   H. Adikane and G. Iyer, *Chemical modification of ethyl cellulose-based highly porous membrane for the purification of immunoglobulin G.* Applied biochemistry and biotechnology, 2013. **169**(3): p. 1026-1038.

20.   M.Y. Arıca, E. Yalçın, and G. Bayramoğlu, *Preparation and characterisation of surfaces properties of poly (hydroxyethylmethacrylate-co-methacrylolyamido-histidine) membranes: application for purification of human immunoglobulin G.* Journal of Chromatography B, 2004. **807**(2): p. 315-325.

21.   R.R. Prasanna and M.A. Vijayalakshmi, *Characterization of metal chelate methacrylate monolithic disk for purification of polyclonal and monoclonal immunoglobulin G.* Journal of Chromatography A, 2010. **1217**(23): p. 3660-3667.

22.   R. Hahn, R. Schlegel, and A. Jungbauer, *Comparison of protein A affinity sorbents.* Journal of Chromatography B, 2003. **790**(1): p. 35-51.

23.   Y. Liu, R. Zhao, D. Shangguan, H. Zhang, and G. Liu, *Novel sulfamethazine ligand used for one-step purification of immunoglobulin G from human plasma.* Journal of Chromatography B, 2003. **792**(2): p. 177-185.

24.   S. Menegatti, B.G. Bobay, K.L. Ward, T. Islam, W.S. Kish, A.D. Naik, and R.G. Carbonell, *Design of protease-resistant peptide ligands for the purification of antibodies from human plasma.* Journal of Chromatography A, 2016. **1445**: p. 93-104.

25.   W.-W. Zhao, Q.-H. Shi, and Y. Sun, *FYWHCLDE-based affinity chromatography of IgG: Effect of ligand density and purifications of human IgG and monoclonal antibody.* Journal of Chromatography A, 2014. **1355**: p. 107-114.

26.   R.R. Prasanna, A.S. Kamalanathan, and M.A. Vijayalakshmi, *Development of l-histidine immobilized CIM® monolithic disks for purification of immunoglobulin G.* Journal of Molecular Recognition, 2015. **28**(3): p. 129-141.

27.   M.G. Freire, A.F.M. Claudio, J.M.M. Araújo, J.A.P. Coutinho, I.M. Marrucho, J.N.C. Lopes, and L.P.N. Rebelo, *Aqueous biphasic systems: a boost brought about by using ionic liquids.* Chemical Society Reviews, 2012. **41**(14): p. 4966-4995.

28.   S.P.M. Ventura, F.A. e Silva, M.V. Quental, D. Mondal, M.G. Freire, and J.A.P. Coutinho, *Ionic-Liquid-Mediated Extraction and Separation Processes for Bioactive Compounds: Past, Present, and Future Trends.* Chemical Reviews, 2017.

29. M. Vargas, Á. Segura, M. Herrera, M. Villalta, Y. Angulo, J.M. Gutiérrez, G. León, and T. Burnouf, *Purification of IgG and albumin from human plasma by aqueous two phase system fractionation.* Biotechnology Progress, 2012. **28**(4): p. 1005-1011.

30. M. Rito-Palomares, C. Dale, and A. Lyddiatt, *Generic application of an aqueous two-phase process for protein recovery from animal blood.* Process Biochemistry, 2000. **35**(7): p. 665-673.

31. V.L. Dhadge, P.I. Morgado, F. Freitas, M.A. Reis, A. Azevedo, R. Aires-Barros, and A.C.A. Roque, *An extracellular polymer at the interface of magnetic bioseparations.* Journal of The Royal Society Interface, 2014. **11**(100): p. 20140743.

32. Q. Wu, D.-Q. Lin, and S.-J. Yao, *Evaluation of poly (ethylene glycol)/hydroxypropyl starch aqueous two-phase system for immunoglobulin G extraction.* Journal of Chromatography B, 2013. **928**: p. 106-112.

33. A.M. Ferreira, V.F. Faustino, D. Mondal, J.A.P. Coutinho, and M.G. Freire, *Improving the extraction and purification of immunoglobulin G by the use of ionic liquids as adjuvants in aqueous biphasic systems.* Journal of Biotechnology, 2016. **236**: p. 166-175.

34. J.F.B. Pereira, Á.S. Lima, M.G. Freire, and J.A.P. Coutinho, *Ionic liquids as adjuvants for the tailored extraction of biomolecules in aqueous biphasic systems.* Green Chemistry, 2010. **12**(9): p. 1661-1669.

35. D. Mondal, M. Sharma, M.V. Quental, A.P. Tavares, K. Prasad, and M.G. Freire, *Suitability of bio-based ionic liquids for the extraction and purification of IgG antibodies.* Green Chemistry, 2016. **18**(22): p. 6071-6081.

36. E.V. Capela, A.E. Santiago, A.F.C.S. Rufino, A.P.M. Tavares, M.M. Pereira, A. Mohamadou, M.R. Aires-Barros, J.A.P. Coutinho, A.M. Azevedo, and M.G. Freire, *Sustainable strategies based on glycine-betaine analogues ionic liquids for the recovery of monoclonal antibodies from cell culture supernatants.* Green Chemistry, 2019.

37. C.C. Ramalho, C.M.S.S. Neves, M.V. Quental, J.A.P. Coutinho, and M.G. Freire, *Separation of immunoglobulin G using aqueous biphasic systems composed of cholinium-based ionic liquids and poly (propylene glycol).* Journal of Chemical Technology & Biotechnology, 2018. **93**(7): p. 1931-1939.

38. B.Y. Zaslavsky, *Aqueous two-phase partitioning: physical chemistry and bioanalytical applications*. 1994: CRC Press.

39. P.-Å. Albertsson, *Partition of cell particles and macromolecules: separation and purification of biomolecules, cell organelles, membranes, and cells in aqueous polymer two-phase systems and their use in biochemical analysis and biotechnology*. Vol. 346. 1986: Wiley New York etc.

40. M.M. Bradford, *A rapid and sensitive method for the quantitation of microgram quantities of protein utilizing the principle of protein-dye binding.* Analytical biochemistry, 1976. **72**(1-2): p. 248-254.

41. A.F.M. Cláudio, L. Swift, J.P. Hallett, T. Welton, J.A.P. Coutinho, and M.G. Freire, *Extended scale for the hydrogen-bond basicity of ionic liquids.* Physical Chemistry Chemical Physics, 2014. **16**(14): p. 6593-6601.

42. P.A. Rosa, A.M. Azevedo, and M.R. Aires-Barros, *Application of central composite design to the optimisation of aqueous two-phase extraction of human antibodies.* Journal of Chromatography A, 2007. **1141**(1): p. 50-60.

43. M.F. Silva, A. Fernandes-Platzgummer, M.R. Aires-Barros, and A.M. Azevedo, *Integrated purification of monoclonal antibodies directly from cell culture medium with aqueous two-phase systems.* Separation and Purification Technology, 2014. **132**: p. 330-335.

44. P. Rosa, A. Azevedo, I. Ferreira, S. Sommerfeld, W. Bäcker, and M. Aires-Barros, *Downstream processing of antibodies: single-stage versus multi-stage aqueous two-phase extraction.* Journal of Chromatography A, 2009. **1216**(50): p. 8741-8749.

45. I. Campos-Pinto, E. Espitia-Saloma, S.A. Rosa, M. Rito-Palomares, O. Aguilar, M. Arévalo-Rodríguez, M.R. Aires-Barros, and A.M. Azevedo, *Integration of cell harvest with affinity-enhanced purification of monoclonal antibodies using aqueous two-phase systems with a dual tag ligand.* Separation and Purification Technology, 2017. **173**: p. 129-134.

46. I. Campos-Pinto, E.V. Capela, A.R. Silva-Santos, M.A. Rodríguez, P.R. Gavara, M. Fernandez-Lahore, M.R. Aires-Barros, and A.M. Azevedo, *LYTAG-driven purification strategies for monoclonal antibodies using quaternary amine ligands as affinity matrices.* Journal of Chemical Technology & Biotechnology, 2018. **93**(7): p. 1966-1974.

47. A.M. Azevedo, P.A. Rosa, I.F. Ferreira, J. De Vries, T. Visser, and M.R. Aires-Barros, *Downstream processing of human antibodies integrating an extraction capture step and cation exchange chromatography.* Journal of Chromatography B, 2009. **877**(1-2): p. 50-58.

2.2. Ionic-liquid-mediated extraction and purification of monoclonal antibodies from cell culture supernatants

This chapter is based on the manuscript under preparation with

Emanuel V. Capela, Sara A.S.L. Rosa, Virgínia Chu, João P. Conde, João A.P. Coutinho, M. Raquel Aires-Barros, Ana M. Azevedo, Mara G. Freire

2.2.1. Abstract

Monoclonal antibodies (mAbs) are the most prevalent class of recombinant protein therapeutics for the treatment of several diseases. Although the upstream processing of mAbs has improved considerably in the last years, the downstream processing has not evolved at the same pace, being considered the bottleneck in the manufacturing of therapeutic mAbs. In this work we propose the use of aqueous biphasic systems (ABS) constituted by two polymers, namely polyethylene glycol (PEG) and dextran, and ionic liquids (ILs) as adjuvants for mAbs capture and purification from serum-free and serum-containing Chinese Hamster Ovary (CHO) cell culture supernatants. At the best conditions, mAbs are mainly captured for the PEG-rich phase, allowing a recovery of 81.5 % and 85.4%, and a purity level of 69.3 % and of 92.4 %, obtained in a single-step, using the ABS containing the IL 1-butyl-3-methylimidazolium bromide ($[C_4mim]Br$) at 20 wt% for the anti-interleukin-8 (anti-IL-8) and anti-hepatitis C virus (anti-HCV) mAbs, respectively. The proteins profile of the ABS' phases was confirmed by SDS-PAGE and the maintenance of the isoelectric point of the mAbs was also proved. Finally, it is proposed a continuous microfluidic setting aiming to demonstrate the potential of the ABS to be operated in continuous mode and to be miniaturized for massive parallelization (scale-out). This work reports promising evidences on the possibility of introducing ILs for the simplification of mAbs downstream processing, allowing the integration of several steps (clarification, capture and polishing) in a single unit operation, ultimately contributing for their accessibility as recurrent therapies.

2.2.2. Introduction

Monoclonal antibodies (mAbs) are the leading family of biopharmaceuticals, valued in US$ 106.87 billion in 2020, and was expected to reach US$ 114.43 billion in 2021 at a compound annual growth rate (CAGR) of 7.1% (data from "Monoclonal Antibodies (MAbS) Global Market Report 2021" by The Business Research Company). Currently, these biomolecules are widely applied for therapeutic purposes, such as in the treatment of oncologic, autoimmune, cardiovascular, inflammatory and neurological diseases [1, 2]. By December 2020, 96 therapeutic mAbs had been approved by the US Food and Drug Administration (FDA) [3], and recently, in May 2021, the 100th mAb product was approved [4].

The efficiency of traditional drugs is decreasing and population is facing aging worldwide [5]; therefore, there is an increasing demand for large quantities of therapeutic mAbs [6]. Thus, the production of mAbs must meet high efficiency and safety standards, meaning that high yields and purity levels must be ultimately achieved [7]. In order to meet regulamentary requirements, mammalian cell lines became the predominant antibody expression system, in which Chinese Hamster Ovary (CHO) cells can be highlighted as the main choice [8]. The upstream processing of mAbs is nowadays well-established, while the high costs of the currently used downstream platform still is a critical bottleneck [9]. The downstream approach usually followed by most manufacturers consists in a multi-step platform, as follows: (i) one or two harvesting steps; (ii) one capture step performed by protein-A affinity chromatography; (iii) a low pH hold for virus inactivation; (iv) two polishing (chromatographic) steps; (v) a virus filtration step; and (vi) an ultrafiltration/diafiltration (UF/DF) step for the formulation buffer exchange, finally being ready for packaging and delivery to the patient [10]. Due to this multi-step approach, antibodies downstream costs can represent up to 80 % of their total production costs [11]. Therefore, the development of new purification and recovery platforms for antibodies is highly demanded.

Aqueous biphasic systems (ABS) can be used in liquid-liquid extraction processes and were first proposed by Albertsson [12], being conventionally created by two polymers, a polymer and a salt or two salts dissolved in aqueous media (ternary systems), that above given concentrations undergo phase separation. It is possible to manipulate the ABS' physicochemical features by changing the phase-forming components and their concentration, pH and temperature, so that the selective partitioning of a target compound can be achieved [2, 13]. Due to their water-rich nature, not requiring the use of volatile organic solvents, ABS provide a suitable environment to maintain biological activity and protein solubility [14], and represent a technique able to operate in continuous mode [13, 15]. Also, ABS exhibit a high advantage over other techniques commonly

applied to the recovery of mAbs, since the clarification, extraction, purification and concentration steps can be integrated in a single step [14, 16]. Hence, if properly designed, ABS can be efficient, sustainable and low-cost alternative strategies for mAbs downstream processing.

Conventional polymer-based ABS have been extensively investigated for the purification of IgG (including mAbs), in particular using polyethylene glycol (PEG)/dextran ABS [2]. However, these polymer-based systems present a restricted polarity range between the coexisting phases, limiting high recovery yields and purity factors to be achieved, and thus encouraging the development of other strategies to overcome this bottleneck, such as the addition of salts [17], affinity ligands [13, 15] and the use of modified phase-forming components [5]. In addition to these strategies, ionic liquids (ILs) can be used as adjuvants/additives to overcome the limited polarity range of traditional ABS. Due to their designer's solvent character, it is possible to manipulate the cation and anion that constitute the IL, ultimately allowing the tailoring of the ABS phases' polarities and affinities towards target biomolecules [18].

Despite the aforementioned advantages of ILs, few works are available on the use of IL-based ABS for IgG extraction/purification [7, 19-21], from which only one work [20] specifically refers to mAbs recovery and purification from CHO cell culture supernatants. This work [20] used ILs as primary phase-forming components. Another work by Ferreira et al. [7] reported the use of ILs as adjuvants in polymer-salt systems for IgG extraction and purification from rabbit serum, achieving a IgG purity level of *ca.* 26 %. To the best of our knowledge, there are no reports in the literature considering the mAbs extraction and purification from CHO cell culture supernatants using ILs as adjuvants in polymer-polymer ABS.

In the past few years, miniaturized techniques taking advantage of soft-lithography processes and microfluidics have emerged as efficient tools for ABS-based bioprocesses [22]. These miniaturized processes consist of parallel streams of immiscible phases that flow in continuous in a microchannel of the chip, under a laminar flow regime. These processes may be designed to be cost-effective due to the reduced amount of reagents and sample required to flow in the microchannels. Furthermore, several variables can be evaluated in parallel and allow similar results in a lab-scale as in the continuous large-scale processes [23]. These characteristics, allied to the possibility of adjusting the length and width of the microchannels and/or corresponding chip, the easiness in its operation and the absence of extensive manual preparation steps turns this technique as of high interest for the development of innovative downstream processes. Accordingly, they have been applied in the continuous extraction and purification of several

biomolecules, for instance BSA [24], membrane proteins [25], recombinant proteins [26], virus-like particles [23] and monoclonal antibodies [27].

In the work described in this chapter, the performance of two ILs used as adjuvants in conventional PEG-dextran ABS was evaluated towards the extraction and purification of anti-interleukin-8 (anti-IL-8) and anti-hepatitis C virus (anti-HCV) mAbs from serum-containing and serum-free CHO cell culture supernatants, respectively. Finally, a microfluidic chip was already designed, being suggested for the scale-out and operation of the ABS extraction/purification in continuous mode.

2.2.3. Experimental section

2.2.3.1. Materials

The ABS studied in this work were prepared using an aqueous solution of polyethylene glycol with a molecular weight of 3350 Da (PEG 3350), and an aqueous solution of dextran with a molecular weight of 500,000 Da (dextran 500k). Both polymers were obtained from Sigma-Aldrich (St. Louis, MO, USA) and used without any further purification. Two representative ILs, chosen according to the data obtained in Chapter 2.1, were used as adjuvants in the PEG-dextran ABS, namely cholinium acetate ([Ch][Ac], purity > 99 wt%) and 1-butyl-3-methylimidazolium bromide ([C_4mim]Br, purity of 99 wt%), both acquired from Iolitec (Heilbronn, Germany). Before use, both ILs were purified and dried for a minimum of 24 h, under constant agitation, at moderate temperature of ≈ 50˚C (± 1 °C) and under vacuum (to reduce their volatile impurities to negligible values). After this step, the purity of each IL was confirmed by ^{1}H and ^{13}C NMR spectra and found to be in accordance with the purity levels given by the suppliers. The chemical structures of the investigated ILs are depicted in **Figure 2.2.1**.

(i)   (ii)
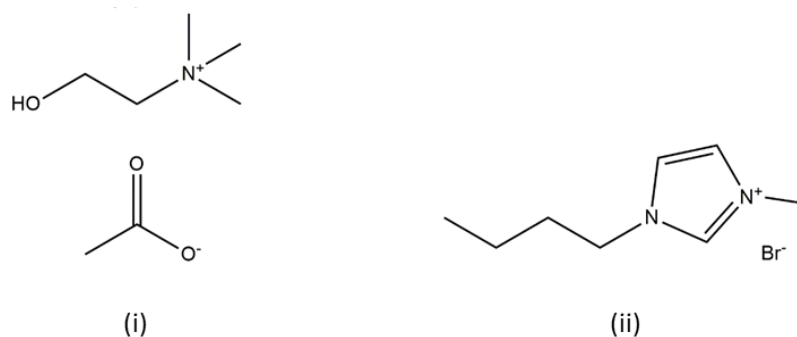
Figure 2.2.1. Chemical structures of the ILs investigated as adjuvants in ABS composed of PEG 3350 + dextran 500k + H$_2$O: (i) [Ch][Ac]; and (ii) [C$_4$mim]Br.

Serum-containing CHO cell culture supernatants containing anti-human interleukin-8 (anti-IL-8) monoclonal antibodies were produced in-house by a CHO DP-12 clone#1934 (ATCC CRL-12445) using DHFR minus/methotrexate selection system, obtained from the American Type Culture Collection (LGC Standards, Middlesex, UK). CHO DP-12 cells were grown in a mixture of 75 % (v/v) of serum-free media formulated with 0.1 % Pluronic® F-68 and without $_L$-glutamine, phenol red, hypoxanthine, or thymidine (ProCHO™5, Lonza Group Ltd, Belgium), and 25 % (v/v) of Dulbecco's modified Eagle's medium (DMEM), supplemented with 10 % (v/v) of ultra-low IgG fetal bovine serum (FBS). ProCHO™5 formulation contains 4 mmol·L^{-1} $_L$-glutamine (Gibco®, Carlsbad, CA), 2.1 g·L^{-1} NaHCO$_3$ (Sigma–Aldrich), 10 mg·L^{-1} recombinant human insulin (Lonza), 0.07 % (v/v) lipids (Lonza), 1 % (v/v) antibiotics (100 U·mL^{-1} penicillin and 100 μg·mL^{-1} streptomycin) (Gibco®) and 200 nmol·L^{-1} methotrexate (Sigma). DMEM was formulated to contain 4 mmol·L^{-1} of $_L$-glutamine, 4.5 g·L^{-1} of $_D$-glucose, 1 mmol·L^{-1} of sodium pyruvate, 1.5 g·L^{-1} of NaHCO$_3$, 2 mg·L^{-1} of recombinant human insulin, 35 mg·L^{-1} of $_L$-proline (all acquired at Sigma), 0.1 % (v/v) of a trace element A, 0.1 % (v/v) of a trace element B (both from Cellgro®, Manassas, VA, USA), and 1 % (v/v) of antibiotics (100 U·mL^{-1} of penicillin and 100 μg·mL^{-1} of streptomycin from Gibco®). The composition of trace element A includes 1.60 mg·L^{-1} of CuSO$_4$·5H$_2$O, 863.00 mg·L^{-1} of ZnSO$_4$·7H$_2$O, 17.30 mg·L^{-1} of selenite·2Na, and 1155.10 mg·L^{-1} of ferric citrate, while the trace element B is composed of 0.17 mg·L^{-1} of MnSO$_4$·H$_2$O, 140.00 mg·L^{-1} of Na$_2$SiO$_3$·9H$_2$O, 1.24 mg·L^{-1} of molybdic acid, ammonium salt, 0.65 mg·L^{-1} of NH$_4$VO$_3$, 0.13 mg·L^{-1} of NiSO$_4$·6H$_2$O, and 0.12 mg·L^{-1} of SnCl$_2$. Cultures were carried out in T-75 flasks (BD Falcon, Franklin Lakes, NJ) at 37 (±1) °C and 5 % CO$_2$ with an initial cell density of 2.1×10^6 cells·mL^{-1}. Cell passages were performed every 4 days in a laminar flow chamber. Cell supernatants were centrifuged in BD Falcon™ tubes at 175 × g for 7 min, collected and stored at -20 °C. This culture was maintained for several months, with the mAbs concentration varying between 82.5 and 102.8 mg·L^{-1}. The produced anti-IL-8 mAb has an isoelectric point (pI) of 9.3 [28].

Serum-free Chinese hamster ovary (CHO) cell culture supernatants were produced and delivered by Icosagen SA (Tartumaa, Estonia). These supernatants contain a humanized monoclonal antibody, from IgG1 class, derived from mouse anti-hepatitis C virus subtype 1b NS5B (non-structural protein 5B) monoclonal antibody 9A2 expressed in mouse hybridoma culture. cDNA of antibody variable regions was isolated and cloned into the human IgG1 constant region-containing antibody expression vector. CHO cells were grown in a mix of two serum-free growth media, the CD CHO Medium (Gibco®, Carlsbad, CA) and the 293 SFM II Medium (Gibco®). Final concentration of IgG is around 100 mg·L^{-1}.

The human immunoglobulin G (IgG) used as standard in this work was human IgG for therapeutic administration (trade name: Gammanorm®), obtained from Octapharma (Lachen, Switzerland), as a 165 mg·mL^{-1} solution containing 95 % of IgG (of which 59 % IgG1, 36 % IgG2, 4.9 % IgG3 and 0.5 % IgG4). Bovine serum albumin (BSA) standards (2 mg·mL^{-1}), used as model biomolecule for the calibration curve for Bradford protein assays, was purchased from Thermo Scientific Pierce. For total protein quantification by Bradford protein assay, Coomassie Plus (Bradford) Protein Assay was purchased from Thermo Scientific Pierce.

The required material for polyacrylamide gel electrophoresis (SDS-PAGE) includes: 40 % acrylamide/bis-acrylamide solution, 4x Laemmli Sample Buffer from Bio-Rad and Precision Plus Protein™ Dual Color Standards (Hercules, CA, USA); tris(hydroxymethyl)aminomethane, PA from Pronalab (Tlalnepantla, Mexico); sodium dodecyl sulfate, (SDS, purity > 98.5 wt%), glycine, ammonium persulfate (APS), *N,N,N',N'*-tetramethylethylenediamine (TEMED), $_{DL}$-dithiothreitol (DTT) solution 1 mol·L^{-1} in H$_2$O and Coomassie Brilliant Blue R in soluble tablets (commercial name: PhastGel® Blue R) from Sigma-Aldrich; ethanol from Thermo Scientific Pierce (Rockford, IL, USA); acetic acid (purity of 100 %) from Merck Millipore (Darmstadt, Germany).

For the fabrication of the microfluidic device, propylene glycol monomethyl ether acetate (PGMEA) 99.5 % was purchased from Sigma–Aldrich, SU-8 negative photoresist 2015 formulation was purchased from Microchem, and polydimethylsiloxane (PDMS) was purchased from Dow-Corning (Midland, MI, USA) as a Sylgard 184 silicon elastomer kit.

The water employed along this work was treated with a Milli-Q® Integral water purification apparatus from Merck Millipore. Other reagents used in this work were of analytical grade and used as acquired, without any further purification steps.

2.2.3.2. Methods

Extraction and purification of mAbs from cell cultures supernatants using ABS. In the studied ABS, the top phase corresponds to the PEG-rich aqueous phase while the bottom phase is mainly composed of dextran. The ternary mixture composition for the IgG extraction/partition was chosen based on the phase diagram already reported in the literature [29, 30], corresponding to 7 wt% PEG 3350 + 5 wt% dextran 500k + 88 wt% H$_2$O/CHO cell supernatant/IL. All partitioning studies of the quaternary systems (comprising the IL) were performed with the same extraction point, where the ILs were introduced as adjuvants in ABS at different concentrations, from 1 wt% to 25 wt%. The extraction/purification performance of PEG-dextran and PEG-dextran-IL two-phase systems for anti-IL-8 or anti-HCV mAbs from serum-containing or serum-free CHO cell culture

supernatants, respectively. In each system, the complex biological sample was loaded at 30 wt% to the phase-forming components to reach a total weight of the mixture of 2.0 g. The systems were mixed in a Vortex mixer (Ika, Staufen, Germany), centrifuged for 30 min in a fixed angle rotor bench centrifuge (Eppendorf, Hamburg, Germany) at 1372 × g, and to ensure total phase separation and chemical equilibrium they were settled for 30 min. After the required equilibrium conditions, both phases were carefully separated using a micropipette to extract the top phases and a 2.5 mL syringe to take the bottom phases, and their volumes were determined. Control systems without IL were also prepared to assess their effect in IgG partitioning, as well as blank systems without biological sample to consider the interference of the phase-forming compounds in the analytical methods.

IgG was quantified in the initial feeds and in each phase by affinity chromatography in ÄKTA™ 10 Purifier system from GE Healthcare (Uppsala, Sweden) using an analytical POROS Protein G affinity column (2.1 x 30 mm) from Applied Biosystems (Foster City, CA, USA). Adsorption of IgG to the column was performed in 50 mmol·L^{-1} sodium phosphate (NaH$_2$PO$_4$) buffer at pH 7.4 containing 150 mmol·L^{-1} sodium chloride (NaCl) for 1.8 min. Elution was triggered by decreasing the pH value of the buffer to 2–3, using 12 mmol·L^{-1} chloridric acid (HCl) with 150 mmol·L^{-1} NaCl during 2.5 min. Finally, the column was re-equilibrated with the adsorption buffer for 3.4 min. Samples from top and bottom phases containing IgG were diluted 20 times in the adsorption buffer and 0.5 mL were injected in the column using an Autosampler A-900 from GE Healthcare. Absorbance was monitored at 215 nm. IgG concentration was determined from a daily-fresh calibration curve obtained using Gammanorm IgG, in a concentration ranging between 0.2 to 20 mg·L^{-1}. In the end of each assay, the column was stored in 10 mmol·L^{-1} sodium phosphate (NaH$_2$PO$_4$) buffer at pH 7.4 containing 0.02 % sodium azide.

The total protein content (IgG + remaining proteins) of each phase was determined using the Bradford protein assay method with a Coomassie Plus kit from Pierce (Rockford, IL, USA) [31]. The assays were set up in 96 well polystyrene microplates and 200 μL of Coomassie reagent were added to 50 μL of samples, previously diluted 4 or 10 times, blanks and standard solutions. A calibration curve with bovine serum albumin (BSA) from 5 to 400 mg·L^{-1} was used as a standard biomolecule for protein calibration. Absorbance was read at 595 nm in a microplate reader from Molecular Devices (Sunnyvale, CA, USA). At least two individual experiments were performed to determine the average in performance parameters, as well as the respective standard deviations.

The IgG antibodies recovery yield for the PEG-rich phase, %Yield$_{IgG}$, is the percentage ratio between the amount of protein in the PEG-rich aqueous phase to that added in the initial mixture, and is defined according to Equation 1,

$$\%\text{Yield}_{\text{IgG}} = \frac{[\text{IgG}]_{\text{PEG}} \times V_{\text{PEG}}}{[\text{IgG}]_{\text{initial}} \times V_{\text{initial}}} \times 100 \tag{1}$$

where [IgG]$_{\text{PEG}}$ and [IgG]$_{\text{initial}}$ represents the total IgG concentration in the PEG-rich phase and in the initial solution, respectively, and the parameters V$_{\text{PEG}}$ and V$_{\text{initial}}$ represent the volume of the PEG-rich phase and the volume of the feed added to the ABS, respectively. The percentage purity of IgG was calculated dividing the IgG concentration by the total protein concentration at the PEG-rich phase, according to Equation 2,

$$\%\text{Purity}_{\text{IgG}} = \frac{[\text{IgG}]_{\text{PEG}}}{[\text{Total proteins}]_{\text{PEG}}} \tag{2}$$

where [IgG]$_{\text{PEG}}$ and [Total proteins]$_{\text{PEG}}$ represent the concentration of IgG and total proteins in the PEG-rich phase, respectively.

Proteins stability assessment. Sodium dodecyl sulfate polyacrylamide gel electrophoresis (SDS-PAGE) assays were performed to assess the proteins profile and infer the mAbs integrity. Samples were prepared and diluted in a sample buffer from Bio-Rad containing 62.5 mmol·L^{-1} Tris–HCl, pH 6.2, 2 % SDS, 0.01 % bromophenol blue and 10 % glycerol, under reducing conditions with 100 mmol·L^{-1} dithiothreitol (DTT) and then denaturated at 100°C for 10 min. A volume of 25 μL of these samples was applied in a 12 % acrylamide gel, prepared from a 40 % acrylamide/bis-acrylamide stock solution (29:1) from Bio-Rad, and ran at 90 mV using a running buffer containing 192 mmol·L^{-1} glycine, 25 mmol·L^{-1} Tris, and 0.1 % (w/v) SDS at pH 8.3. The molecular weight standard used was Precision Plus Protein™ Dual Color Standards from BioRad. Gels were stained with 0.1 % (w/v) Coomassie Brilliant Blue R-250 from Pharmacia AB Laboratory Separations® (Uppsala, Sweden), 30 % (v/v) ethanol, 10 % (v/v) acetic acid and water, in an orbital shaker at 40 °C and moderate velocity during 1 h. Gels were then distained using a solution containing 30 % (v/v) ethanol and 10 % (v/v) acetic acid, in an orbital shaker at 25 °C and moderate velocity, until background color disappeared. Finally, gels were stored in milli-Q water at room temperature, until digital images of the gels were acquired using a calibrated densitometer GS-800 from Bio-Rad and analyzed with the informatics tool Quantity One 4.6 also from Bio-Rad.

Isoelectric focusing (IEF) was performed to compare the initial CHO cell culture supernatant sample and the ABS' phases after bioprocessing. The IEF was performed in a Pharmacia PhastSystem™ separation module using PhastGel® IEF 3–9 with 50 mm × 46 mm × 0.45 mm (from GE Healthcare). Gels were ran at 2000 V for 500 Vh, after a 75 Vh prefocusing step at 2000 V and sample application at 200 V for 15 Vh. The isoelectric point standard used was broad pI kit (pH 3 – 10) calibration kit from GE Healthcare, containing the following components: amylglucosidase (pI =

3.50); methyl red (pI = 3.75); trypsin inhibitor (pI = 4.55); β-lactoglobulin A (pI = 5.20); carbonic anhydrase B bovine (pI = 5.85); carbonic anhydrase B human (pI = 6.55); myoglobin, acidic band (pI = 6.85); myoglobin, basic band (pI = 7.35); lentil lectin, acidic (pI = 8.15); lentil lectin, middle (pI = 8.45); lentil lectin, basic (pI = 8.65); trypsinogen (pI = 9.30). Afterwards the gels were stained with silver nitrate, and digital images of the gels were acquired using a calibrated densitometer GS-800 from Bio-Rad and analyzed with the informatics tool Quantity One 4.6, also from Bio-Rad.

Microfluidic chip fabrication. The microfluidic device was fabricated by us (INESC-MN authors). Briefly, the microchannel was designed in the AutoCAD 2013 software, and the pattern transferred to a hard mask by the photolithographic patterning and subsequent wet chemical etching of a 200 nm aluminium film deposited on a glass substrate using a Nordiko 7000 magnetron sputtering system. SU-8 2015 negative photoresist was spin-coated onto a clean silicon substrate to a final average thickness of 20 μm. The hard mask was placed over the SU-8 after 4 min of pre-exposure bake at 95 °C on a hotplate, and exposed to UV light. After exposure, a post-exposure bake at 95 °C for 5 min was performed. The SU-8 was developed by submerging the substrate in PGMEA for 2 min and subsequently rinsing with isopropanol. The substrate was then subjected to a final hard bake step at 150 °C for 15 min. PDMS, previously mixed at a ratio of 1:10 parts reticulating agent and degassed in a vacuum chamber, was poured over the SU-8 mold and left to reticulate in an oven at 70 °C for 75 − 90 min. PDMS membranes (500–1000 μm thick) were prepared by pouring PDMS over a silicon wafer and prepared under the same conditions as the PDMS structures. The structure was peeled off from the mold and holes were punched with a blunt 20-ga needle (Instech Solomon, Plymouth Meeting, PA, USA) through the inlets and outlets of the structure. To seal the channels, a PDMS membrane and the PDMS device containing the microfluidic structures were oxidized using a hand-held corona discharge device for 60 s, keeping about 0.5 cm between the device and the surfaces to be treated. After oxidation, the membrane was placed over the channel side of the PDMS and the structure was baked on hot plate at 130 °C for 5 min. The sealed channels were left undisturbed for at least 24 h before usage.

2.2.4. Results and discussion

2.2.4.1. Extraction and purification of anti-IL-8 mAbs from serum-containing CHO cell culture supernatants

The potential of PEG-dextran ABS containing ILs as adjuvants as extraction and purification routes for anti-IL-8 mAbs directly from serum-containing CHO cell culture supernatants was firstly addressed. A mixture composition of 7 wt% PEG 3350 + 5 wt% dextran 500k + 30 wt% CHO cell culture supernatant + IL ranging from 1 wt% to 25 wt% was selected, and two ILs chosen according to the data previously obtained (Chapter 2.1) were studied: [Ch][Ac] and [C$_4$mim]Br. These ILs contain different cations and anions structures, namely a highly hydrophobic cation combined with a low-hydrogen bond-basicity anion [32] ([C$_4$mim]Br) and a highly hydrophilic cation combined with a high hydrogen-bond basicity anion [32] ([Ch][Ac]), thus allowing to appraise the effect of two ILs with different chemical characteristics. The mixture composition was selected based on the phase diagrams already reported in the literature [29, 30], while trying to have a minimum concentration of both polymers and the maximum concentration of water (turning the process more economic and more biocompatible). The performance of all ABS was investigated in terms of mAbs recovery yield (%Yield$_{IgG}$) and purity level (%Purity$_{IgG}$), whose results for anti-IL-8 mAbs from serum-containing CHO cell culture supernatants are shown in **Figure 2.2.2**. The detailed data on the recovery yields and purity levels are given in the **Appendix B (Table B.1)**.

Based on the obtained results in **Figure 2.2.2**, it is clear that mAbs preferentially partition to the top (PEG-rich) phase, both in the control system (just PEG-dextran) and in the systems containing ILs as adjuvants, being this the phase in which the ILs under study are also enriched [%EE$_{IL}$ > 66 %, *cf.* **Appendix A (Table A.3)**]. Although the control system allows a recovery yield of 69.4 % of mAbs, higher recovery yields are achieved by using ILs as adjuvants, ranging between 73.3 % and 82.6 %. Overall, better recovery yields are obtained with the most hydrophobic IL, namely [C$_4$mim]Br. This phenomenon may be explained by the mAbs affinity and interactions established with ILs, e.g. van der Waals, hydrogen-bonding and electrostatic interactions [33-35]. The isoelectric point (pI) of anti-IL-8 is *ca.* 9.3 [28], and as the pH of the investigated systems is *ca.* 7.0, antibodies are positively charged and electrostatic interactions with the IL may play a role.

[Ch][Ac] was added to the PEG-dextran ABS at three different concentrations, namely 1 wt%, 5 wt% and 10 wt%, whose results are shown in **Figure 4.2.2 (A)**. Recovery yields of mAbs ranging from 73.3 % to 77.6 % were obtained in a single step, with purity levels ranging between 19.1 % and 26.8 %. With this IL, both parameters performance decreases as the concentration of IL increases

in the system, but still higher than that obtained with the control system with no IL added (69.4 %). However, the purity level is always lower than that obtained using the control system (29.3 %).

A

B
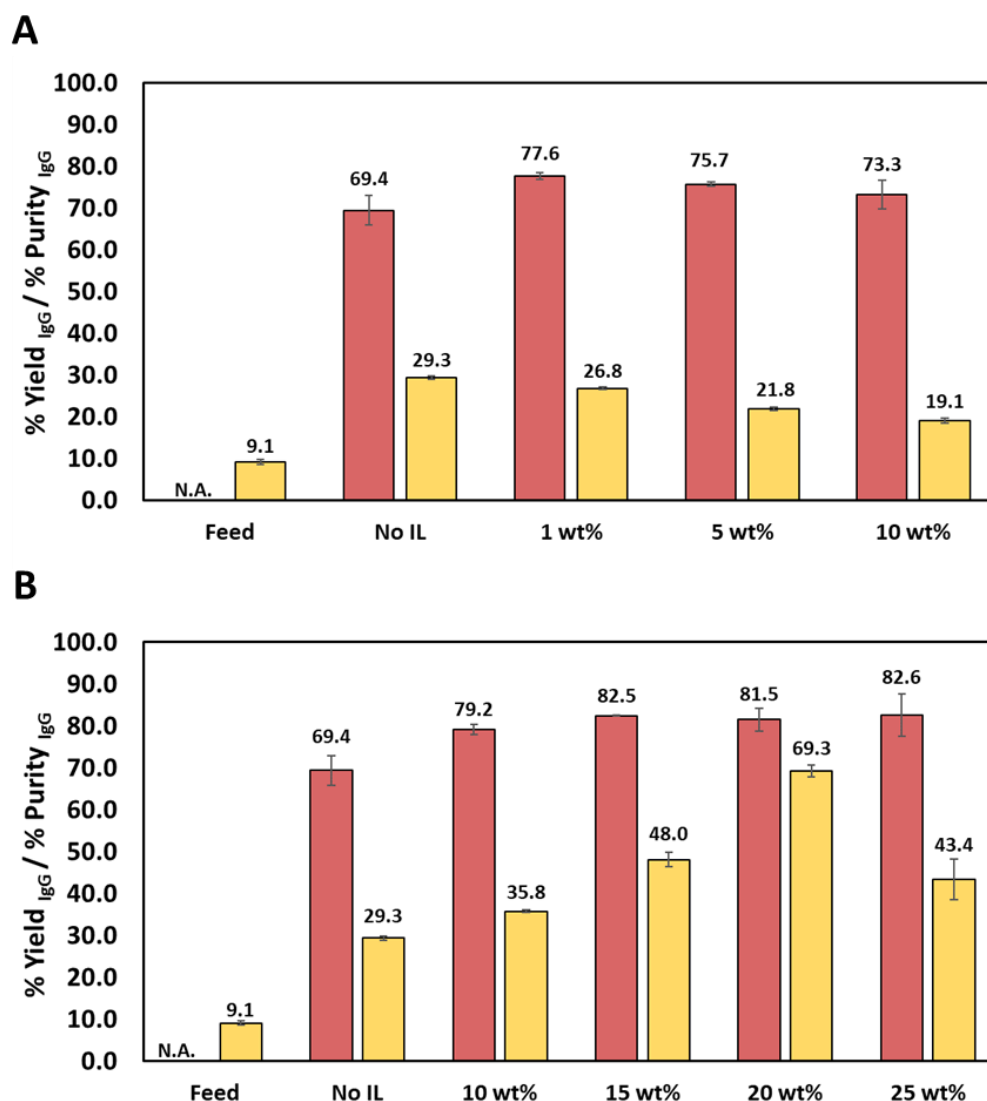
Figure 2.2.2. Percentage recovery yield (%Yield$_{IgG}$ – ■) and purity level (%Purity $_{IgG}$ – ■) of anti-IL-8 mAbs from serum-containing CHO cell culture supernatants using quaternary ABS formed by PEG 3350 + dextran 500 kDa + H$_2$O + ILs as adjuvants at different concentrations, at 25 °C – (A) [Ch][Ac]; (B) [C$_4$mim]Br. For the initial feed, the %Yield$_{IgG}$ is not applicable (N.A.).

These results show that the introduction of [Ch][Ac] is favorable to increase the extraction of proteins to the PEG-rich phase, in which the IL is enriched as well, due to the increase in the recovery yield. However, this IL leads to a lack of selectivity as observed by the decrease in the IgG purity. Still, it should be remarked that the mAbs purity levels achieved after (IL-based) ABS processing are higher than the purity of mAbs in the initial cell supernatant (9.1 %). Being in agreement with

Chapter 2.1, [Ch][Ac]-based ABS have low performance to improve the IgG purity, even from cell culture supernatants.

[C$_4$mim][Br] was then investigated as adjuvant in PEG-dextran ABS at different concentrations, namely 10 wt%, 15 wt%, 20 wt% and 25 wt%, whose results are shown in **Figure 4.2.2 (B)**. Recovery yields of mAbs ranging from 79.2 % to 82.6 % were obtained in a single step, with purity levels ranging between 35.8 % and 69.3 %. The performance shown by this IL clearly surpasses that of the [Ch][Ac]-based ABS, being also higher than the performance of the system without IL added (%Yield$_{IgG}$ = 69.4 % and %Purity$_{IgG}$ = 29.3 %). Although the increase in the IL concentration does not lead to relevant differences in the recovery yields, it has however a significant impact in the mAbs purity levels. The best performance was achieved by using 20 wt% of [C$_4$mim]Br, in which 81.5 % of mAbs were extracted to the top (PEG-rich) phase of the system, with a high purity level of 69.3 % obtained in one-step. This purity value represents an improvement of *ca.* 662 % (7.6-fold increase) in comparison with the initial cell supernatant purity (9.1 %). However, when increasing the IL concentration up to 25 wt%, the purification performance of the system is reduced, with only 43.4 % of purity being achieved, revealing that concentrations higher than 20 wt% of IL are not appropriate for mAbs downstream processing. Since the recovery yield is not compromised, these results show that the higher concentrations of IL allow as well the extraction of other proteins from the cell culture medium, being in agreement with the trend observed with [Ch][Ac].

Some mAbs characteristics were analyzed before and after the IL-ABS downstream process, such as integrity and proteins profile by SDS-PAGE, and isoelectric point (pI) determined by isoelectric focusing (**Figure 2.2.3**). In **Figure 2.2.3 (A)**, the SDS-PAGE gel results of the initial cell culture supernatant and recovered ABS phases are provided, allowing not only to infer the mAbs integrity, but also to corroborate the purification results previously discussed. The two bands corresponding to IgG (heavy chains, molecular weight of *ca.* 50 kDa; and light chains, molecular weight of *ca.* 25 kDa) are visible in the ABS top phase at the expected molecular weight, meaning that the integrity of mAbs was maintained after extraction process. Moreover, more bands are present in the lane of the bottom phase, corresponding to protein impurities that are retained in this phase; in particular, the band corresponding to BSA, the main protein impurity of serum-containing CHO cell culture supernatants, has a higher intensity in the bottom phase than in the top phase. These results show that the purity level of IgG increases due to the preferential retention of other proteins than IgG, and preferentially BSA, in the bottom phase. Regarding the pI, whose results are given in **Figure 2.2.3 (B)**, it is shown that anti-IL-8 mAbs recovered in the top phase of

the ABS maintain the same pI as in the initial serum-containing CHO cell culture supernatant, of *ca.* 9.3, in accordance with the value reported for this mAb in the literature [28]. Moreover, it is possible to observe some bands corresponding to acidic proteins in the ABS bottom phase, corresponding to protein impurities that are retained in this phase, corroborating the purification results previously discussed.
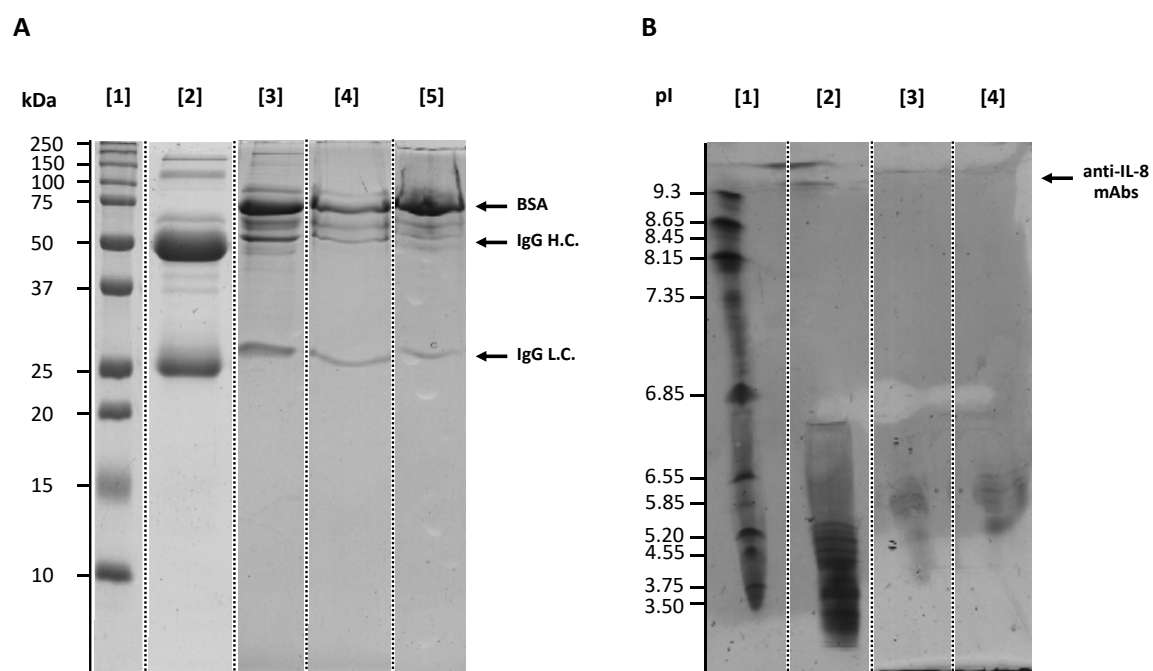
Figure 2.2.3. IgG characterization experiments after the downstream processing using the system composed of PEG 3350 + dextran 500 kDa + H$_2$O + 20 wt% [C$_4$mim]Br. (A) SDS-PAGE of the initial feed and ABS' phases: lane 1 – molecular weight marker (kDa); lane 2 – human IgG standard; lane 3 – serum-containing CHO cell culture supernatant; lane 4 – ABS top phase; lane 5 – ABS bottom phase. The bands corresponding to BSA, IgG heavy chain (H.C.) and IgG light chain (L.C.) are also labelled. (B) Silver stained IEF gel: lane 1 – isoelectric point standard; lane 2 – serum-containing CHO cell culture supernatant; lane 3 – ABS top phase; lane 4 – ABS bottom phase. The band corresponding to anti-IL-8 mAbs is also labelled.

Based on the aforementioned information, it can be concluded that [C$_4$mim]Br is the most promising IL under study, demonstrating a great potential to tailor the ABS' phases affinity for mAbs from serum-containing CHO cell culture supernatants, allowing to obtain an yield of 81.5 % with a purity level of 69.3 % in a single-step, and maintaining some characteristics of anti-IL-8 mAbs, as the integrity and pI.

2.2.4.2. Extraction and purification of anti-HCV mAbs from serum-free CHO cell culture supernatants

The best identified IL ([C$_4$mim]Br) was then studied as adjuvant in PEG-dextran ABS towards the extraction and purification of a different mAb – anti-HCV – directly from a distinct biological matrix, i.e. serum-free CHO cell culture supernatants. This study allowed to infer on the flexibility and robustness of the developed IL-based platform. An ABS with a mixture composition of 7 wt% PEG 3350 + 5 wt% dextran 500k + 30 wt% CHO cell culture supernatant + [C$_4$mim]Br ranging from 10 wt% to 25 wt% was selected, since high IL concentrations revealed better performance in the previous study. The performance of all ABS was investigated in terms of mAbs recovery yield (%Yield$_{IgG}$) and purity level (%Purity$_{IgG}$), whose results are shown in **Figure 2.2.4**. The detailed data on the recovery yields and purity levels are given in the **Appendix B (Table B.2)**.
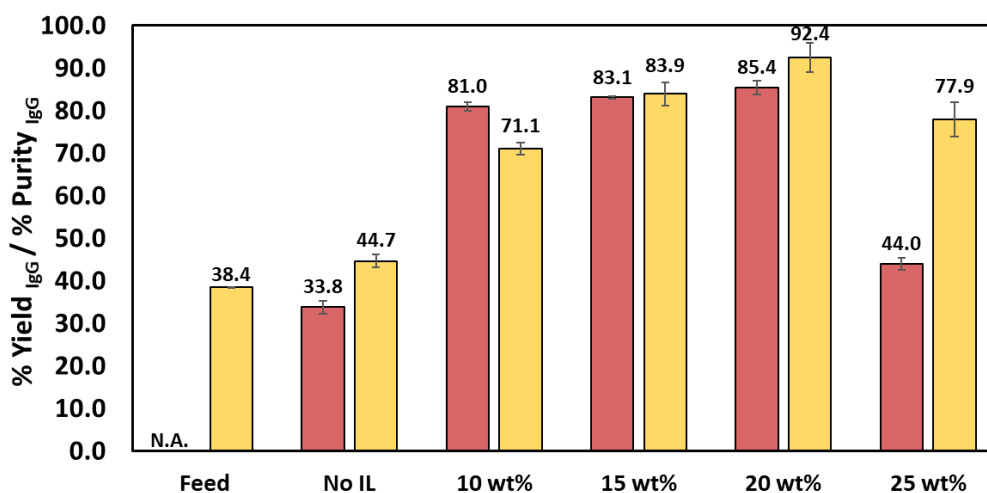
Figure 2.2.4. Percentage recovery yield (%Yield$_{IgG}$ – ■) and purity level (%Purity $_{IgG}$ – ■) of anti-HCV mAbs from serum-free CHO cell culture supernatants using quaternary ABS formed by PEG 3350 + dextran 500 kDa + H$_2$O + [C$_4$mim]Br as adjuvant at different concentrations, at 25 °C. For the initial feed, the %Yield$_{IgG}$ is not applicable (N.A.).

From the data shown in **Figure 2.2.4**, it is shown that when applying the conventional PEG-dextran ABS (no IL added) for bioprocessing the serum-free cell culture supernatant, mAbs preferentially partition to the bottom (dextran-rich) phase, with only 33.8 % of mAbs recovered in the top (PEG-rich) phase with 44.7 % of purity. However, with the addition of IL as adjuvant, the mAbs recovery in the top (PEG-rich) phase is promoted, the phase in which the IL is also enriched [for [C$_4$mim]Br – %EE$_{IL}$ > 72 %, *cf.* **Appendix A (Table A.3)**]. The extraction yields obtained with the IL from 10 to 20 wt% in the ABS range between 81.0 % and 85.4 %, with purity levels from 71.1 %

and 92.4 %. With higher IL concentrations (25 wt%), the selectivity towards IgG decreases, as previously observed for serum-containing CHO cell culture supernatants. These results suggest the establishment of specific and preferential interactions between IgG and [C$_4$mim]Br up to 20 wt% of IL, in which a maximum in recovery and purity is achieved.

The system with the best performance to recover and purify anti-HCV mAbs is also the ABS composed of 20 wt% of [C$_4$mim]Br, in which a recovery yield of 85.4 % and a purity level of 92.4 % was achieved in a single-step in the top (PEG-rich) phase. This value represents an improvement of *ca.* 140 % (2.4-fold increase) in comparison with the initial cell supernatant purity (38.4 %). Overall, the ABS constituted by 20 wt% of [C$_4$mim]Br is the one that best performs for the extraction and purification of mAbs from both serum-containing and serum-free cell culture supernatants; nevertheless, the purity level achieved for mAbs from serum-free cell culture supernatants is significantly higher than that obtained for mAbs from serum-containing cell culture supernatants (92.4 % vs. 69.3 %). Nevertheless, these results are extremely promising, since in comparison with the initial purity of mAbs in the cell supernatants, namely 9.1 % in serum-containing and 38.4 % in serum-free cell supernatants, both purity values represent an improvement of 662 % and 140 %. This trend is somehow expected since the serum-free cell supernatants do not contain some impurities prevenient from the serum (e.g. BSA), thus having an higher purity in the supernatant.

In the literature, conventional polymer-polymer ABS have been suggested as promising approaches for the extraction and purification of IgG antibodies, as reviewed by Capela *et al*. [2]. However, these kind of systems typically present a restricted polarity between the coexisting phases, encouraging the development of novel strategies to overcome that drawback, from which the addition of inorganic salts [17] and affinity ligands [13, 15], and the use of modified phase-forming components [5] can be highlighted. Concerning the use of IL-based ABS for the extraction/purification of IgG, few works were reported up to date in the literature [7, 19-21], with just one addressing the use of ILs as adjuvants in polymer-salt systems [7], being this work carried out with rabbit serum samples, and the work shown in Chapter 2.1 with polymer-polymer ABS and human serum samples. The current work consists in the first report on the use of ILs as adjuvants in polymer-polymer ABS for the extraction and purification of mAbs from CHO cell culture supernatants, and which results outperform those previously reported using IL-based ABS [7, 19-21]. This is probably a result of the tailoring ability of the ILs introduced in ABS composed of two polymers instead of a polymer and a salt, in which the effect of the salts commonly used as strong salting-out species may mask the IL effect.

Based on the findings reported by Ferreira *et al*. [7] using commercial ILs as adjuvants in polymer-salt ABS, IgG could be extracted from the rabbit serum with 26 % of purity, contrasting with the 92.4 % of purity achieved in this work with polymer-polymer ABS using ILs as adjuvants, again reinforcing the impact that ILs may exert in systems composed of two polymers (with no strong salting-out species present). The best results herein obtained (anti-IL-8 recovery yield of 81.5 % and purity level of 69.3 % from serum-containing CHO cell culture supernatants; anti-HCV recovery yield of 85.4 % and purity level of 92.4 % from serum-containing CHO cell culture supernatants) are also better than the results reported by Capela et al. [36], who used IL-based ABS for the purification and recovery of mAbs from cell cultures supernatants. The authors used glycine-betaine-based ILs as the main phase-forming compounds of ABS, reporting the complete recovery of mAbs (100 %) from serum-containing CHO cell culture supernatants with a purity level of 36 % (representing a 1.6-fold increase in purity) in the IL-rich phase. Overall, and in addition to the higher purity level achieved, the use of ILs as adjuvants in polymer-polymer ABS has the advantage of using the IL as adjuvant (in lower amounts), and ultimately, to decrease the overall cost of the process.

2.2.4.3. ABS miniaturization by microfluidics

Aiming to compare the performance of the developed IL-ABS process in batch and in continuous modes, microfluidics technique was selected and will be applied. For that purpose, a microfluidic chip was already designed, being its schematic representation shown in **Figure 2.2.5**.
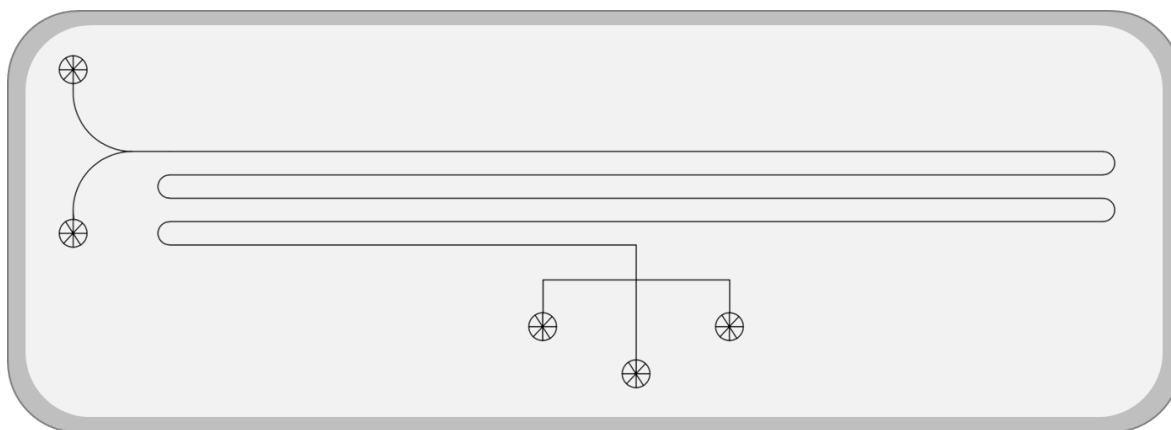
Figure 2.2.5. Schematic representation of the microfluidic chip fabricated for the miniaturized extraction and purification of mAbs using IL-based ABS. The height of the microchannel is 20 μm throughout the entire structure.

The miniaturized chip considered for this work was fabricated using PDMS soft lithography and presented a simple design, counting with two inlets (for feeding with the ABS phase-forming

components solutions and the complex biological matrix), a main separation channel and three outlets (allowing the separation of top phase, bottom phase and interphase – to guarantee no contaminations between the coexisting phases). Although the microfluidic assays were not yet performed, and aim to be in the near future, promising clues are given in the literature [23] regarding its feasibility for these types of systems. Therefore, it is suggested that a microfluidic chip will be useful to prove the possibility of operating the IL-ABS process in continuous mode, without losses in its efficacy (comparable to that of the lab scale), and ultimately proving the scale-out of the process for an increased scale.

2.2.5. Conclusions

This work focused on the use of ILs as adjuvants in polymer-polymer ABS as an alternative process for the extraction and purification of mAbs from CHO cell culture supernatants, namely anti-IL-8 and anti-HCV from serum-containing and serum-free supernatants, respectively. Initial assays were performed with mAbs from serum-containing cell supernatants, allowing to identify the best IL, which was then applied to purify mAbs from serum-free cell supernatants. In both cases, mAbs demonstrated a preferential partition towards the PEG-rich phase that is also the phase for which the ILs preferentially migrate. This is particularly relevant for serum-free cell culture supernatants, since an inversion on this trend occurs due to the presence of IL, i.e. in the system with no IL added, mAbs preferentially enrich in the dextran-rich phase.

The best ABS revealed to be 7 wt% PEG 3350 + 5 wt% dextran 500k + 30 wt% CHO cell culture supernatant + 20 wt% [C$_4$mim]Br, allowing an anti-IL-8 recovery yield of 81.5 % and purity level of 69.3 % from serum-containing CHO cell culture supernatants, and an anti-HCV recovery yield of 85.4 % and purity level of 92.4 % from serum-containing CHO cell culture supernatants. The developed platform revealed to be flexible and robust, allowing the downstream processing of two different mAbs from different cell culture supernatants, and surpassing the results reported in the literature up to date using ILs. Besides, the developed platform presents the potential to integrate the clarification, extraction, purification and concentration steps in a single step.

Overall, it was possible to conclude that a cost-effective strategy was herein developed, using ILs as adjuvants in traditional polymer-polymer ABS, allowing the recovery and purification of mAbs directly from the cell culture supernatants with high performance, representing a steppingstone for the widespread use of this type of biopharmaceuticals as a recurrent and accessible therapy. Further work in ongoing to prove the scale-out of the technology and operation of the ABS extraction/purification in continuous mode through microfluidics.

2.2.6. References

1.   P. Rosa, I. Ferreira, A. Azevedo, and M. Aires-Barros, *Aqueous two-phase systems: a viable platform in the manufacturing of biopharmaceuticals.* Journal of Chromatography A, 2010. **1217**(16): p. 2296-2305.

2.   E.V. Capela, M.R. Aires-Barros, M.G. Freire, and A.M. Azevedo, *Monoclonal Antibodies– Addressing the Challenges on the Manufacturing Processing of an Advanced Class of Therapeutic Agents.* Frontiers in Clinical Drug Research-Anti Infectives: Volume 4, 2017. **4**: p. 142.

3.   R.-M. Lu, Y.-C. Hwang, I.-J. Liu, C.-C. Lee, H.-Z. Tsai, H.-J. Li, and H.-C. Wu, *Development of therapeutic antibodies for the treatment of diseases.* Journal of Biomedical Science, 2020. **27**(1): p. 1-30.

4.   A.J.N.r.D.D. Mullard, *FDA approves 100th monoclonal antibody product.* Nature Reviews Drug Discovery, 2021. **20**: p. 491-495.

5.   A.M. Azevedo, P.A. Rosa, I.F. Ferreira, J. De Vries, T. Visser, and M.R. Aires-Barros, *Downstream processing of human antibodies integrating an extraction capture step and cation exchange chromatography.* Journal of Chromatography B, 2009. **877**(1-2): p. 50-58.

6.   A.M. Azevedo, P.A. Rosa, I.F. Ferreira, and M.R. Aires-Barros, *Chromatography-free recovery of biopharmaceuticals through aqueous two-phase processing.* Trends in Biotechnology, 2009. **27**(4): p. 240-247.

7.   A.M. Ferreira, V.F. Faustino, D. Mondal, J.A.P. Coutinho, and M.G. Freire, *Improving the extraction and purification of immunoglobulin G by the use of ionic liquids as adjuvants in aqueous biphasic systems.* Journal of Biotechnology, 2016. **236**: p. 166-175.

8.   J. Curling, *The development of antibody purification technologies*, in *Process Scale Purification of Antibodies*, U. Gottschalk, Editor. 2009. p. 23-54.

9.   P. Gronemeyer, R. Ditz, and J. Strube, *Trends in upstream and downstream process development for antibody manufacturing.* Bioengineering, 2014. **1**(4): p. 188-212.

10.   A.L. Grilo, M. Mateus, M.R. Aires-Barros, and A.M. Azevedo, *Monoclonal antibodies production platforms: an opportunity study of a non-protein-A chromatographic platform based on process economics.* Biotechnology Journal, 2017. **12**(12): p. 1700260.

11.   O. Yang, M. Qadan, and M. Ierapetritou, *Economic analysis of batch and continuous biopharmaceutical antibody production: a review.* Journal of Pharmaceutical Innovation, 2019. **15**: p. 182–200.

12.   P.-Å. Albertsson, *Partition of proteins in liquid polymer–polymer two-phase systems.* Nature, 1958. **182**(4637): p. 709.

13. I. Campos-Pinto, E.V. Capela, A.R. Silva-Santos, M.A. Rodríguez, P.R. Gavara, M. Fernandez-Lahore, M.R. Aires-Barros, and A.M. Azevedo, *LYTAG-driven purification strategies for monoclonal antibodies using quaternary amine ligands as affinity matrices.* Journal of Chemical Technology & Biotechnology, 2018. **93**(7): p. 1966-1974.

14. K. Schügerl and J. Hubbuch, *Integrated bioprocesses.* Current Opinion in Microbiology, 2005. **8**(3): p. 294-300.

15. I. Campos-Pinto, E. Espitia-Saloma, S.A. Rosa, M. Rito-Palomares, O. Aguilar, M. Arévalo-Rodríguez, M.R. Aires-Barros, and A.M. Azevedo, *Integration of cell harvest with affinity-enhanced purification of monoclonal antibodies using aqueous two-phase systems with a dual tag ligand.* Separation and Purification Technology, 2017. **173**: p. 129-134.

16. A.M. Azevedo, P.A. Rosa, I.F. Ferreira, and M.R. Aires-Barros, *Optimisation of aqueous two-phase extraction of human antibodies.* Journal of Biotechnology, 2007. **132**(2): p. 209-217.

17. P. Rosa, A. Azevedo, I. Ferreira, S. Sommerfeld, W. Bäcker, and M. Aires-Barros, *Downstream processing of antibodies: Single-stage versus multi-stage aqueous two-phase extraction.* Journal of Chromatography A, 2009. **1216**(50): p. 8741-8749.

18. J.F.B. Pereira, Á.S. Lima, M.G. Freire, and J.A.P. Coutinho, *Ionic liquids as adjuvants for the tailored extraction of biomolecules in aqueous biphasic systems.* Green Chemistry, 2010. **12**(9): p. 1661-1669.

19. D. Mondal, M. Sharma, M.V. Quental, A.P.M. Tavares, K. Prasad, and M.G. Freire, *Suitability of bio-based ionic liquids for the extraction and purification of IgG antibodies.* Green Chemistry, 2016. **18**(22): p. 6071-6081.

20. E.V. Capela, A.E. Santiago, A.F.C.S. Rufino, A.P.M. Tavares, M.M. Pereira, A. Mohamadou, M.R. Aires-Barros, J.A.P. Coutinho, A.M. Azevedo, and M.G. Freire, *Sustainable strategies based on glycine-betaine analogues ionic liquids for the recovery of monoclonal antibodies from cell culture supernatants.* Green Chemistry, 2019.

21. C.C. Ramalho, C.M.S.S. Neves, M.V. Quental, J.A.P. Coutinho, and M.G. Freire, *Separation of immunoglobulin G using aqueous biphasic systems composed of cholinium-based ionic liquids and poly (propylene glycol).* Journal of Chemical Technology & Biotechnology, 2018. **93**(7): p. 1931-1939.

22. S. Hardt and T. Hahn, *Microfluidics with aqueous two-phase systems.* Lab on a Chip, 2012. **12**(3): p. 434-442.

23. M. Jacinto, R. Soares, A. Azevedo, V. Chu, A. Tover, J. Conde, and M. Aires-Barros, *Optimization and miniaturization of aqueous two phase systems for the purification of recombinant*

human immunodeficiency virus-like particles from a CHO cell supernatant. Separation and Purification Technology, 2015. **154**: p. 27-35.

24.   U. Novak, A. Pohar, I. Plazl, and P. Žnidaršič-Plazl, *Ionic liquid-based aqueous two-phase extraction within a microchannel system.* Separation and Purification Technology, 2012. **97**: p. 172-178.

25.   R. Hu, X. Feng, P. Chen, M. Fu, H. Chen, L. Guo, and B.-F. Liu, *Rapid, highly efficient extraction and purification of membrane proteins using a microfluidic continuous-flow based aqueous two-phase system.* Journal of Chromatography A, 2011. **1218**(1): p. 171-177.

26.   R.J. Meagher, Y.K. Light, and A.K. Singh, *Rapid, continuous purification of proteins in a microfluidic device using genetically-engineered partition tags.* Lab on a Chip, 2008. **8**(4): p. 527-532.

27.   D. Silva, A. Azevedo, P. Fernandes, V. Chu, J. Conde, and M. Aires-Barros, *Design of a microfluidic platform for monoclonal antibody extraction using an aqueous two-phase system.* Journal of Chromatography A, 2012. **1249**: p. 1-7.

28.   R. dos Santos, S.A. Rosa, M.R. Aires-Barros, A. Tover, and A.M. Azevedo, *Phenylboronic acid as a multi-modal ligand for the capture of monoclonal antibodies: development and optimization of a washing step.* Journal of Chromatography A, 2014. **1355**: p. 115-124.

29.   B.Y. Zaslavsky, *Aqueous two-phase partitioning: physical chemistry and bioanalytical applications*. 1994: CRC Press.

30.   P.-Å. Albertsson, *Partition of cell particles and macromolecules: separation and purification of biomolecules, cell organelles, membranes, and cells in aqueous polymer two-phase systems and their use in biochemical analysis and biotechnology*. Vol. 346. 1986: Wiley New York etc.

31.   M.M. Bradford, *A rapid and sensitive method for the quantitation of microgram quantities of protein utilizing the principle of protein-dye binding.* Analytical biochemistry, 1976. **72**(1-2): p. 248-254.

32.   A.F.M. Cláudio, L. Swift, J.P. Hallett, T. Welton, J.A.P. Coutinho, and M.G. Freire, *Extended scale for the hydrogen-bond basicity of ionic liquids.* Physical Chemistry Chemical Physics, 2014. **16**(14): p. 6593-6601.

33.   M.M. Pereira, S.N. Pedro, M.V. Quental, Á.S. Lima, J.A.P. Coutinho, and M.G. Freire, *Enhanced extraction of bovine serum albumin with aqueous biphasic systems of phosphonium-and ammonium-based ionic liquids.* Journal of Biotechnology, 2015. **206**: p. 17-25.

34.   M. Taha, M.V. Quental, I. Correia, M.G. Freire, and J.A.P. Coutinho, *Extraction and stability of bovine serum albumin (BSA) using cholinium-based Good's buffers ionic liquids.* Process Biochemistry, 2015. **50**(7): p. 1158-1166.

35.   A.M. Ferreira, H. Passos, A. Okafuji, A.P.M. Tavares, H. Ohno, M.G. Freire, and J.A.P. Coutinho, *An integrated process for enzymatic catalysis allowing product recovery and enzyme reuse by applying thermoreversible aqueous biphasic systems.* Green Chemistry, 2018. **20**(6): p. 1218-1223.

36.   E.V. Capela, A.E. Santiago, A.F.C.S. Rufino, A.P.M. Tavares, M.M. Pereira, A. Mohamadou, M.R. Aires-Barros, J.A.P. Coutinho, A.M. Azevedo, and M.G. Freire, *Sustainable strategies based on glycine–betaine analogue ionic liquids for the recovery of monoclonal antibodies from cell culture supernatants.* Green Chemistry, 2019. **21**(20): p. 5671-5682.

2.3. Sustainable strategies based on glycine-betaine analogue ionic liquids for the recovery of monoclonal antibodies from cell culture supernatants

This chapter is based on the published manuscript

Emanuel V. Capela, Alexandre E. Santiago, Ana F.C.S. Rufino, Ana P.M. Tavares, Matheus M. Pereira, Aminou Mohamadou, M. Raquel Aires-Barros, João A.P. Coutinho, Ana M. Azevedo, Mara G. Freire; Green Chemistry 21 (2019) 5671-5682.

2.3.1. Abstract

Monoclonal antibodies (mAbs) are of crucial interest for therapeutic purposes, particularly in vaccination, immunization, and in the treatment of life-threatening diseases. However, their downstream processing from the complex cell culture media in which they are produced still requires multiple steps, rendering mAbs as extremely high-cost products. Therefore, the development of cost-effective, sustainable and biocompatible purification strategies for mAbs is in high demand to decrease the associated economic, environmental and health burdens. Herein, novel aqueous biphasic systems (ABS) composed of glycine-betaine analogues ionic liquids (AGB-ILs) and K_2HPO_4/KH_2PO_4 at pH 7.0, the respective three-phase partitioning (TPP) systems, and hybrid processes combining ultrafiltration, were investigated and compared in terms of performance as alternative strategies for the purification and recovery of anti-interleukin-8 (anti-IL-8) mAbs, which are specific therapeutics in the treatment of inflammatory diseases, from Chinese Hamster Ovary (CHO) cell culture supernatants. With the studied ABS, mAbs preferentially partition to the IL-rich phase, with recovery yields up to 100 % and purification factors up to 1.6. The best systems were optimized in what concerns the IL concentration, allowing to take advantage of IL-based three-phase partitioning approaches where a precipitate enriched in mAbs is obtained at the ABS interface, yielding 41.0 % of IgG with a purification factor of 2.7 (purity of 60.9 %). Hybrid processes combining the two previous techniques and an ultrafiltration step were finally applied, allowing the recovery of mAbs from the different fractions in an appropriate buffer solution for further biopharmaceuticals formulation, while allowing the simultaneous IL removal and reuse. The best

---

results were obtained with the hybrid process combining TPP and ultrafiltration, allowing to obtain mAbs with a purity greater than 60 %. The recyclability of the IL was additionally demonstrated, revealing no losses on the purification and recovery performance of these systems for mAbs. The biological activity of anti-IL-8 mAbs is maintained after the several purification and recovery steps, indicating that the novel ABS, three-phase partitioning and hybrid processes comprising AGB-ILs are promising and sustainable strategies in mAbs downstream processing.

2.3.2. Introduction

Despite all significant advances that have been accomplished in the development of effective therapies, biopharmaceuticals are in many cases the unique option in the treatment of particular diseases [1, 2]. Amongst biopharmaceuticals, monoclonal antibodies (mAbs) are widely applied for therapeutic purposes, namely in vaccination and immunization, but also in the treatment of oncologic, autoimmune, cardiovascular, inflammatory and neurological diseases [1, 3]. The first therapeutic monoclonal antibody approved, in 1986 by the US Food and Drug Administration (FDA), was Muromonab (Orthoclone OKT3), which is an *in vivo* produced mAb by hybridoma cells for the prevention of kidney transplant rejection [4]. By the end of 2017, 57 therapeutic mAbs were approved by FDA and the European Medicines Agency (EMA) for therapeutic purposes [5]. In 2017, the worldwide mAbs market exceeded US$ 98 billion in sales, aiming to reach US$ 137-200 billion in 2022 [4, 5]. Despite all advantages of mAbs, the high quantities of pure mAbs required and their extremely high manufacturing costs, mainly derived from the multiple downstream processing steps, are the most challenging features limiting their widespread use [6]. The bioprocessing of mAbs comprises 2 steps: (i) upstream processing, based on biological processes where mAbs production occurs through cell cultures derived from mammalian cells; and (ii) downstream processing, where the recovery, purification and isolation of mAbs from the complex medium takes place. The upstream processing suffered significant improvements in recent years and the main current bottleneck in mAbs production conveys in the downstream processing [7]. The current downstream platform includes several steps: (i) clarification of the supernatant, (ii) capture of mAbs, (iii) viral inactivation, (iv) mAbs polishing, (v) viral removal, and (vi) concentration/formulation of the final mAb-product [1, 8]. Protein A (ProA) affinity chromatography is the "gold standard" approach in the capture and purification steps since it is highly selective [9]. However, it presents several limitations, namely the low pH values necessary to elute mAb-products that can cause their aggregation, the presence of some impurities in the final formulation since the ProA ligand can be degraded by proteases present in the supernatants,

and the high cost of the resin (between US$ 5,000 and US$ 15,000/L; industrial columns require volumes up to 1000 L) [9, 10]. Accordingly, ProA affinity chromatography is the main center of costs of the mAbs manufacturing process, with the overall downstream processing contributing up to 80 % of the mAbs global production costs [1, 11]. Therefore, it is imperative to develop sustainable and cost-effective downstream processes for mAbs to decrease their cost and to allow their widespread use.

Aqueous biphasic systems (ABS) were first proposed as an extraction technique by Albertsson [12], being typically composed of two polymers, a polymer and a salt or two salts dissolved in aqueous media (ternary systems), which above given concentrations undergo phase separation. Their physicochemical characteristics can be tailored by changing the phase-forming components and their concentration, pH and temperature to profit the selective partitioning of a target compound [1, 13]. One of the major advantages of ABS over other techniques commonly applied to the recovery of mAbs is that the clarification, extraction, purification and concentration steps can be integrated in a single step. Furthermore, ABS are rich in water, do not require the use of volatile organic solvents, and represent a technique easy to scale up and able to operate in continuous mode [13, 14]. Thus, if properly designed, ABS are effective, sustainable and low-cost strategies when compared to the applied chromatographic methods. Traditional ABS formed by polymers have been largely investigated for the purification of IgG (including mAbs) [1]. However, the restricted polarity of the coexisting phases presented by this type of systems compromises enhanced recovery yields and purity factors to be achieved, thus encouraging the development of other strategies to overcome this bottleneck. The addition of salts [15], affinity ligands [13, 14] and the use of modified phase-forming components [16] are some examples in this field. In addition to more traditional polymer-based ABS, ionic-liquid-(IL)-based ABS emerged in more recent years with the pioneering work of Rogers and co-workers [17], and since then have been investigated as extraction/purification platforms for a plethora of (bio)molecules [18-23]. By using ILs as phase-forming components of ABS it is possible to tailor the phases' polarities and affinities to specific bioproducts, overcoming the limited polarity difference presented by traditional polymer-based systems [18, 24]. Given the designer solvents ability of ILs, they can be foreseen as promising phase-forming components to carry out the purification and recovery of mAbs. To the best of our knowledge, there are no reports in the literature considering the mAbs recovery from CHO cell culture supernatants using ILs as phase-forming components of ABS.

Within the field of IL-based ABS, ionic-liquid-based three-phase partitioning (ILTPP) have been investigated for the recovery of proteins [25, 26], yet never considered for the purification of

antibodies. Typically, three-phase partitioning (TPP) approaches involve the recovery of the target protein in an enriched precipitate at the interface of two liquid phases [27]. Alvarez *et al.* [25, 26] demonstrated the feasibility of this approach using IL-based ABS, proposing the concept of ionic-liquid-based TPP (ILTPP), but still only applied to food proteins and less complex matrices.

Even though ILs present interesting environmental features compared to volatile organic compounds, mainly due to their negligible vapor pressure at ambient conditions, their toxicity and biodegradability should be always considered [28, 29]. In order to overcome these drawbacks, glycine-betaine analogues ILs (AGB-ILs) were here synthesized and investigated as phase-forming components of ABS and TPP approaches. Glycine-betaine and its analogous are part of the mammalian diet, being present in fruits, vegetables, and coffee beans [30]. In particular, novel ABS and TPP systems formed by AGB-ILs and K_2HPO_4/K_2HPO_4 at pH 7.0 were investigated to purify and recover biopharmaceuticals, namely anti-human interleukin-8 (anti-IL-8) mAbs from Chinese Hamster Ovary (CHO) cell culture supernatants. These antibodies are potential therapeutics to treat inflammatory diseases [31-33]. Given their novelty, the ABS phase diagrams were determined to ascertain the compositions required to form two-phase and TPP systems able to act as separation techniques. Then, their potential in the extraction and purification of mAbs was evaluated and optimized, either as one-step platforms, as three-phase partitioning systems, or as hybrid processes combined with ultrafiltration, followed by the evaluation of the mAbs specific activity. The IL recyclability was additionally demonstrated.

2.3.3. Experimental section

2.3.3.1. Materials

AGB-ILs were synthesized by us according to previously reported protocols [34], corresponding to the following ILs: triethyl[4-ethoxy-4-oxobutyl]ammonium bromide ([Et$_3$NC$_4$]Br), tri(*n*-propyl)[4-ethoxy-4-oxobutyl]ammonium bromide ([Pr$_3$NC$_4$]Br), tri(*n*-butyl)[4-ethoxy-4-oxobutyl]ammonium bromide ([Bu$_3$NC$_4$]Br) and *N*-(1-methylpyrrolidyl-4-ethoxy-4-oxobutyl)ammonium bromide ([MepyrNC$_4$]Br). ILs with a common anion, Br⁻, were used since these correspond to ILs with low toxicity, as previously demonstrated [34]. Furthermore, bromide has a low hydrogen-bond basicity [35] when compared to other common IL anions, thus requiring lower amounts of salt to create ABS while contributing to the process sustainability. ILs were synthesized by the reaction of 4-bromobutyrate acid ethyl ester and triethylamine, tri(*n*-propyl)amine, tri(*n*-butyl)amine or 1-methylpyrrolidine, respectively. All ILs were dried under vacuum for at least 72 h at 45°C. After this procedure, the purity of each IL was checked by ^{1}H and ^{13}C nuclear magnetic

resonance (NMR), being > 97 %. All ILs synthesized are solid at room temperature, yet with melting points below 100 °C, and are water soluble at 25v°C [34]. The commercial ILs studied for comparison purposes are the following: tetra(*n*-butyl)ammonium bromide ([N$_{4444}$]Br, 98 % purity) and 1-butyl-3-methylimidazolium bromide ([C$_4$mim]Br, 99 % purity), acquired from Fluka and Iolitec, respectively. The chemical structures of the synthesized and commercial ILs are depicted in **Figure 2.3.1**.
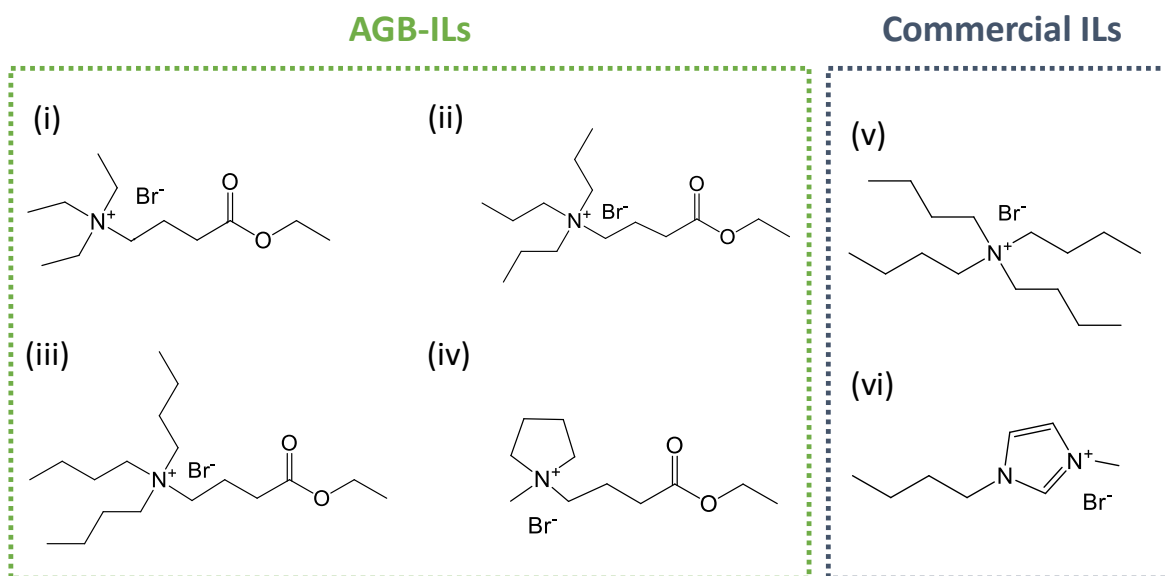
Figure 2.3.1. Chemical structures of the investigated ILs: (i) [Et$_3$NC$_4$]Br; (ii) [Pr$_3$NC$_4$]Br; (iii) [Bu$_3$NC$_4$]Br; (iv) [MepyrNC$_4$]Br; (v) [N$_{4444}$]Br; (vi) [C$_4$mim]Br.

A mixture of the salts K$_2$HPO$_4$ and KH$_2$PO$_4$ at pH 7.0 was used for the formation of ABS and TPP systems with AGB-ILs. K$_2$HPO$_4$·3H$_2$O extra pure was acquired from Scharlau, and KH$_2$PO$_4$ extra pure was acquired from Roic Farma, S.A. Phosphate buffered saline solution (PBS, pH ≈ 7.4) pellets were acquired from Sigma-Aldrich.

Human IL-8 (77aa) (CXCL8) standard (98 % purity) was acquired from Sigma-Aldrich. Commercial human immunoglobulin G (IgG) for therapeutic administration (trade name: Gammanorm®) was obtained from Octapharma (Lachen, Switzerland), as a 165 mg·mL^{-1} solution containing 95 % of IgG (of which 59 % correspond to IgG1, 36 % to IgG2, 4.9 % to IgG3 and 0.5 % to IgG4). Bovine serum albumin (BSA) standards (2 mg·mL^{-1}) were purchased from Thermo Scientific Pierce.

Anti-human interleukin-8 (anti-IL-8) monoclonal antibodies were produced in-house by a CHO DP-12 clone#1934 (ATCC CRL-12445) using DHFR minus/methotrexate selection system, obtained from the American Type Culture Collection (LGC Standards, Middlesex, UK). CHO DP-12

cells were grown in a mixture of 75 % (v/v) of serum-free media formulated with 0.1 % Pluronic® F-68 and without L-glutamine, phenol red, hypoxanthine, or thymidine (ProCHO™5, Lonza Group Ltd, Belgium), and 25 % (v/v) of Dulbecco's modified Eagle's medium (DMEM), supplemented with 10 % (v/v) of ultra-low IgG fetal bovine serum (FBS). ProCHO™5 formulation contains 4 mmol·L^{-1} L-glutamine (Gibco®, Carlsbad, CA), 2.1 g·L^{-1} NaHCO$_3$ (Sigma–Aldrich), 10 mg·L^{-1} recombinant human insulin (Lonza), 0.07 % (v/v) lipids (Lonza), 1 % (v/v) antibiotics (100 U·mL^{-1} penicillin and 100 µg·mL^{-1} streptomycin) (Gibco®) and 200 nmol·L^{-1} methotrexate (Sigma). DMEM was formulated to contain 4 mmol·L^{-1} of L-glutamine, 4.5 g·L^{-1} of D-glucose, 1 mmol·L^{-1} of sodium pyruvate, 1.5 g·L^{-1} of NaHCO$_3$, 2 mg·L^{-1} of recombinant human insulin, 35 mg·L^{-1} of L-proline (all acquired at Sigma), 0.1 % (v/v) of a trace element A, 0.1 % (v/v) of a trace element B (both from Cellgro®, Manassas, VA, USA), and 1 % (v/v) of antibiotics (100 U·mL^{-1} of penicillin and 100 µg·mL^{-1} of streptomycin from Gibco®). The composition of trace element A includes 1.60 mg·L^{-1} of CuSO$_4$·5H$_2$O, 863.00 mg·L^{-1} of ZnSO$_4$·7H$_2$O, 17.30 mg·L^{-1} of selenite·2Na, and 1155.10 mg·L^{-1} of ferric citrate, while the trace element B is composed of 0.17 mg·L^{-1} of MnSO$_4$·H$_2$O, 140.00 mg·L^{-1} of Na$_2$SiO$_3$·9H$_2$O, 1.24 mg·L^{-1} of molybdic acid, ammonium salt, 0.65 mg·L^{-1} of NH$_4$VO$_3$, 0.13 mg·L^{-1} of NiSO$_4$·6H$_2$O, and 0.12 mg·L^{-1} of SnCl$_2$. Cultures were carried out in T-75 flasks (BD Falcon, Franklin Lakes, NJ) at 37 (±1) °C and 5 % CO$_2$ with an initial cell density of 2.1×10^6 cells·mL^{-1}. Cell passages were performed every 4 days in a laminar flow chamber. Cell supernatants were centrifuged in BD Falcon™ tubes at 175 × g for 7 min, collected and stored at -20 °C. This culture was maintained for several months, with the mAbs concentration varying between 40.5 and 99.4 mg·L^{-1}. The produced anti-IL-8 mAb has an isoelectric point (pI) of 9.3 [36].

2.3.3.2. Methods

Determination of ABS phase diagrams, tie-lines and tie-line lengths. The ternary phase diagrams of the investigated ABS were initially determined to identify the mixture compositions where two phases can be formed, so that the extraction conditions could be defined for the recovery of mAbs. The determination of the binodal curves was performed using the cloud point titration method at 25 (± 1) °C and atmospheric pressure, where the mixture compositions were gravimetrically determined [37]. IL aqueous solutions with concentrations ranging between 60 wt% and 80 wt% were prepared. To these solutions, a 40 wt% K$_2$HPO$_4$/KH$_2$PO$_4$ aqueous solution at pH 7.0 was added, allowing the identification of a cloud point corresponding to the biphasic system, followed by the addition of water up to the identification of clear solutions, which correspond to

Sustainable strategies based on glycine-betaine analogue ionic liquids for the recovery of monoclonal antibodies from cell culture supernatants

2

the monophasic region. The experimental binodal curves were adjusted by the equation proposed by Merchuk *et al.* [38],

$$[IL] = A . e^{B.[salt]^{0.5} - C.[salt]^3}$$ (1)

where [IL] and [salt] correspond the IL and phosphate salt weight fraction percentages, respectively, and the coefficients A, B and C are fitting parameters determined using the SigmaPlot 11.0 software.

The tie-lines (TLs), which give the coexisting phases compositions for a given mixture point, and respective lengths (tie-line lengths, TLLs), were determined according to lever-arm rule originally proposed by Merchuk *et al.* [38]. The TLs were determined by the resolution of the following equations (2 − 5), allowing to obtain the concentrations of IL and salt in both top and bottom phases:

$$[IL]_{TOP} = A \times \exp[B[salt]_{TOP}^{0.5} - C[salt]_{TOP}^3]$$ (2)

$$[IL]_{BOT} = A \times \exp[B[salt]_{BOT}^{0.5} - C[salt]_{BOT}^3]$$ (3)

$$[IL]_{TOP} = \frac{[IL]_M}{VR} - \left(\frac{1-VR}{VR}\right)[IL]_{BOT}$$ (4)

$$[salt]_{TOP} = \frac{[salt]_M}{VR} - \left(\frac{1-VR}{VR}\right)[salt]_{BOT}$$ (5)

where the terms TOP, BOT, and M represents the top phase, bottom phase and the mixture point, respectively. The VR parameter represents the ratio between the top phase weight and the total system weight. Tie-line lengths (TLLs), which give indication on the coexisting phases compositions difference, were calculated according to Equation S6:

$$TLL = \sqrt{([IL]_{TOP} - [IL]_{BOT})^2 + ([salt]_{TOP} - [salt]_{BOT})^2}$$ (6)

For each ternary phase diagram, 3 TLs were determined, including the mixture compositions at which the extractions of IgG were carried out. In all studied systems, the top phase is majorly enriched in the IL, whereas the bottom phase is mainly composed of the salt and water.

Recovery of anti-IL-8 mAbs from CHO cell culture supernatants. For the recovery of anti-IL-8 mAbs directly from CHO cell culture supernatants, ABS and TPP systems with 2.0 g of total weight were prepared with a fixed concentration of phosphate salt (15 wt%), combined with (i) 25 wt%, (ii) 30 wt% and (iii) 40 wt% of IL. CHO cell culture supernatant was loaded at 37.5 wt% in all systems, with the remaining amount to complete each composition corresponding to water. Each ABS and TPP was prepared at least in duplicate. Each mixture was stirred, centrifuged for 3 min at 112 × g, and left to equilibrate for 30 min at 25°C in order to achieve the separation of mAbs from the remaining proteins. The volume and weight of the phases and the macroscopic aspect of each extraction system were registered, and both phases were carefully separated. In the cases in which

a precipitate was observed in the ABS interface, i.e. for the TPP systems, the precipitate was completely isolated from the remaining phases and resuspended in PBS aqueous solutions for further analysis. The pH values of each phase at 25 (± 1) °C were determined using a Mettler Toledo U402-M3-S7/200 micro electrode, showing that a pH 7.0 ± 0.2 was maintained in all systems.

The best identified systems to purify mAbs from the cell culture supernatant were exposed to an additional ultrafiltration step aiming at recovering mAbs in PBS aqueous solution, while allowing the IL removal and recycling. The IL-rich phase and the precipitate of the ABS composed of 40 wt% of [Bu$_3$NC$_4$]Br + 15 wt% of K$_2$HPO$_4$/KH$_2$PO$_4$ (pH 7) + 37.5 wt% of CHO cell culture supernatant + 7.5 wt% of water were placed in a microcentrifuge tube with an Amicon® Ultra-0.5 device containing a cut-off filter of 100 kDa (aiming the simultaneous IL recovery, buffer exchange, and to improve the purification factor by separating lower molecular weight proteins), and centrifuged at 14000 × g for 15 min. The filtrated solution was collected and phosphate buffer aqueous solution was added. This procedure was repeated for two times to assure the maximum removal of the IL. To recover the retentate concentrated solution, the Amicon® Ultra-0.5 filter device was placed upside down in a clean microcentrifuge tube and centrifuged at 1000 × g for 2 min, and then PBS aqueous solution was added. Both the retentate and the filtrate were analyzed.

IgG and protein impurities were quantified in all feeds and in each ABS phase by size-exclusion high-performance liquid chromatography (SE-HPLC). Samples were diluted at a 1:2 (v:v) ratio in an aqueous potassium phosphate buffer solution (50 mmol·L^{-1}, pH 7.0, with NaCl 0.3 mol·L^{-1}) used as the mobile phase. The equipment used was a Chromaster HPLC system (VWR Hitachi) equipped with a binary pump, column oven (operating at 40 °C), temperature controlled auto-sampler (operating at 10 °C), DAD detector and a column Shodex Protein KW-802.5 (8 mm × 300 mm). The mobile phase was run isocratically with a flow rate of 0.5 mL·min^{-1} and the injection volume was 25 µL. The wavelength was set at 280 nm. The calibration curve was established with commercial human IgG, from 5 to 200 mg·L^{-1}. Blank systems without biological sample were also prepared to address the interference of the ABS phase-forming compounds.

The ABS performance was evaluated by the recovery yield and purification factor or purity level for IgG. The recovery yield (%Yield$_{IgG}$) in the top (IL-rich) phase was determined according to the following equation:

$$\%\text{Yield}_{\text{IgG}} = \frac{[\text{IgG}]_{\text{TOP}} \times V_{\text{TOP}}}{[\text{IgG}]_{\text{initial}} \times V_{\text{initial}}} \times 100 \tag{7}$$

where [IgG]$_{TOP}$ and [IgG]$_{initial}$ represent the IgG concentration in the top phase and the initial concentration of IgG in the CHO cell culture supernatant, respectively, and V$_{TOP}$ and V$_{initial}$

correspond to the volumes of the top phase and cell culture supernatant loaded in the system, respectively.

In the cases where a precipitate of proteins at the ABS interface occurs, corresponding to the ILTPP approach, the %Yield$_{IgG}$ in the precipitate was determined according to the following equation:

$$\%\text{Yield}_{IgG} = \frac{[IgG]_{PP} \times V_{final}}{[IgG]_{initial} \times V_{initial}} \times 100 \qquad (8)$$

where [IgG]$_{PP}$ and V$_{final}$ represent the IgG concentration and the final volume of the solution after resuspension, respectively.

The percentage purity level of IgG (%Purity$_{IgG}$) was calculated by dividing the HPLC peak area of IgG (A$_{IgG}$) by the total area of the peaks corresponding to all proteins present in the respective sample (A$_{Total}$):

$$\%\text{Purity}_{IgG} = \frac{A_{IgG}}{A_{Total}} \times 100 \qquad (9)$$

The purification factor of IgG (PF$_{IgG}$) was calculated according to Equation 10:

$$\text{PF}_{IgG} = \frac{\%\text{Purity}_{IgG \text{ phase/precipitate}}}{\%\text{Purity}_{IgG \text{ initial}}} \qquad (10)$$

where %Purity$_{IgG\ phase/precipitate}$ and %Purity$_{IgG\ inital}$ correspond to the purity level of IgG in the top phase of each system or in the precipitate (when the ILTPP studies are being carried out) and the purity level of IgG in the cell culture supernatant, respectively.

The same type of analysis, comprising the determination of the recovery yield, purity level and purification factor, was performed after the ultrafiltration step (hybrid process). The overall yield of the two-step process was calculated according to Equation 11:

$$\%\text{Yield}_{overall} = \frac{\%\text{Yield}_{ABS/TPP} \times \%\text{Yield}_{UF}}{100} \qquad (11)$$

where %Yield$_{ABS/TPP}$ and %Yield$_{UF}$ represent the recovery yield of IgG in the ABS or in the TPP approach and ultrafiltration step, respectively.

IL recycling. The IL recycling possibility was investigated in the best identified system, composed of 40 wt% of [Bu$_3$NC$_4$]Br + 15 wt% of K$_2$HPO$_4$/KH$_2$PO$_4$ (pH 7) + 37.5 wt% of CHO cell culture supernatant + 7.5 wt% of water, in which the first separation step was performed according to the procedure previously described. After the IL recovery in the ultrafiltration filtrate fraction of the top phase, biological contaminants present in the sample were precipitated with cold ethanol, and removed after centrifugation. Ethanol was chosen due to its greener credentials compared to other organic solvents that can be used for the same purpose [39]. The ethanol present in the IL-rich sample was removed and recovered using a rotary evaporator. However, in order to assure the

minimal presence of volatile solvents (including water) aiming the preparation of accurate mixture compositions to address the process performance using the recycled IL, the IL sample was further subjected to high vacuum (0.1 Pa) at 60 °C for 72h. It should be however remarked that when foreseeing the process scale-up, less energetic-intensive conditions need to be optimized and applied. Prior to the IL reuse in a new ABS and TPP system, the water content (< 200 ppm) of the dried IL sample was determined using a Metrohm 831 Karl Fischer coulometer, with the analyte Hydranal® – Coulomat AG from Riedel-de Haën, and considered in the mixture composition. This procedure was repeated for 2 times. The IL stability was confirmed by ^{1}H and ^{13}C NMR, showing no evidences of degradation.

Proteins profile and anti-IL-8 mAbs integrity and activity. Sodium dodecyl sulfate polyacrylamide gel electrophoresis (SDS-PAGE) assays were performed to infer the proteins profile of each fraction, and to address the anti-IL-8 mAbs integrity/stability after the downstream processing. Samples were prepared and diluted in a sample buffer from Bio-Rad containing 62.5 mmol·L^{-1} Tris–HCl, pH 6.2, 2 % SDS, 0.01 % bromophenol blue and 10 % glycerol, under reducing conditions with 100 mmol·L^{-1} dithiothreitol (DTT) and then denatured at 100°C for 10 min. A volume of 25 µL of each prepared sample was applied in a 12 % acrylamide gel, prepared from a 40 % acrylamide/bis-acrylamide stock solution (29:1) from Bio-Rad, and ran at 90 mV using a running buffer containing 192 mmol·L^{-1} glycine, 25 mmol·L^{-1} Tris, and 0.1 % (w/v) SDS at pH 8.3. The molecular weight standard used was Precision Plus Protein™ Dual Color Standards from BioRad. Gels were stained with 0.1 % (w/v) Coomassie Brilliant Blue R-250 from Pharmacia AB Laboratory Separations® (Uppsala, Sweden), 30 % (v/v) ethanol, 10 % (v/v) acetic acid and water, in an orbital shaker at 40 °C and moderate velocity during 1 h. Gels were then distained using a solution containing 30 % (v/v) ethanol and 10 % (v/v) acetic acid, in an orbital shaker at 25 °C and moderate velocity, until background color disappeared. Finally, gels were stored in milli-Q water at room temperature, until digital images of the gels were acquired using a calibrated densitometer GS-800 from Bio-Rad and analyzed with the informatics tool Quantity One 4.6 also from Bio-Rad.

Competitive enzyme linked immunosorbent assays (ELISA) were performed for the CHO cell culture supernatant and for the top (IL-rich) phase and retentate after the ultrafiltration step to evaluate the activity of anti-human IL-8 mAbs after the studied recovery processes. The assay was conducted using a 96-well ELISA plate from a Quantikine® Human IL-8/CXCL8 kit from R&D systems (Minnneapolis, MN, USA). The plate was coated with 100 µL assay diluent followed by the addition of 50 µL of 1 mg·L^{-1} of human IL-8 standard from Sigma-Aldrich. The plate was left for incubating

Sustainable strategies based on glycine-betaine analogue ionic liquids for the recovery of monoclonal antibodies from cell culture supernatants

2

for 2 h at room temperature. After this period, each well was aspirated and washed for four consecutive times with wash buffer. Then, 100 μL of each sample containing anti-IL-8 mAbs was added to the wells, and were left to incubate for 1 h at room temperature, being further washed as previously described. 100 μL of anti-IL-8 conjugate was added to all wells and incubated for 1 h at room temperature, and after washed again as previously described. 200 μL of substrate solution was then added to the wells and incubated for 30 min at room temperature (protected from the light with a plate sealer). Finally, 50 μL of stop solution was added to end the reaction, and the absorbance was measured at 450 nm and 540 nm in a BioTek SYNERGY|HT microplate reader. Final results were calculated based on the subtraction of the absorbance at 450 nm for the obtained at 570 nm, to correct optical deviations from the plate.

2.3.4. Results and discussion

2.3.4.1. Characterization of ABS and TPP systems

Novel ABS and TPP systems composed of ILs + KH_2PO_4/K_2HPO_4 (pH 7.0) + H_2O were studied as alternative purification and recovery routes for proteins using anti-IL-8 mAbs from CHO cell culture supernatants. AGB-ILs were chosen due to their biocompatible features, whereas the potassium phosphate buffer salt was used to maintain the pH of the overall ABS at physiological conditions, providing thus an appropriate environment for proteins and simultaneously being able to be used in IgG formulations when envisaging their therapeutic application. ILs comprising the common bromide anion were used since it is a halogen, generating lower cost and less toxic ILs. Furthermore, aiming the creation and evaluation of the separation performance of TPP systems, ILs must be designed to be more hydrophobic, what is here achieved by combining tetraalkylammonium cations and the low hydrogen-bond basicity anion Br^-. This property also contributes to the process sustainability since lower amounts of salt and IL are required to create ABS and TPP systems, as shown and discussed below.

The ABS phase diagrams, and respective tie-lines and length, were initially determined at 25°C and atmospheric pressure to characterize the systems and assess the minimum amounts required of each phase-forming component to be used in the investigated separation processes. The AGB-ILs studied correspond to $[Et_3NC_4]Br$, $[Pr_3NC_4]Br$, $[Bu_3NC_4]Br$ and $[MepyrNC_4]Br$, whereas the commercially available ILs studied for comparison purposes are $[C_4mim]Br$ and $[N_{4444}]Br$ - *cf.* **Figure 2.3.1** with the ILs chemical structures. **Figure 2.3.2** depicts the binodal curves of the different ternary systems formed by AGB-ILs and potassium phosphate buffer at pH 7.0, in an orthogonal

representation. The experimental weight fraction data are given in the **Appendix C (Tables C.1 – C.6).** The values of the fitting parameters and equation, as well the experimental TLs, TLLs, and volume ratio (VR), are provided in the **Appendix C (Tables C.7 and C.8)**. TLs give the composition of each phase for a given mixture composition.
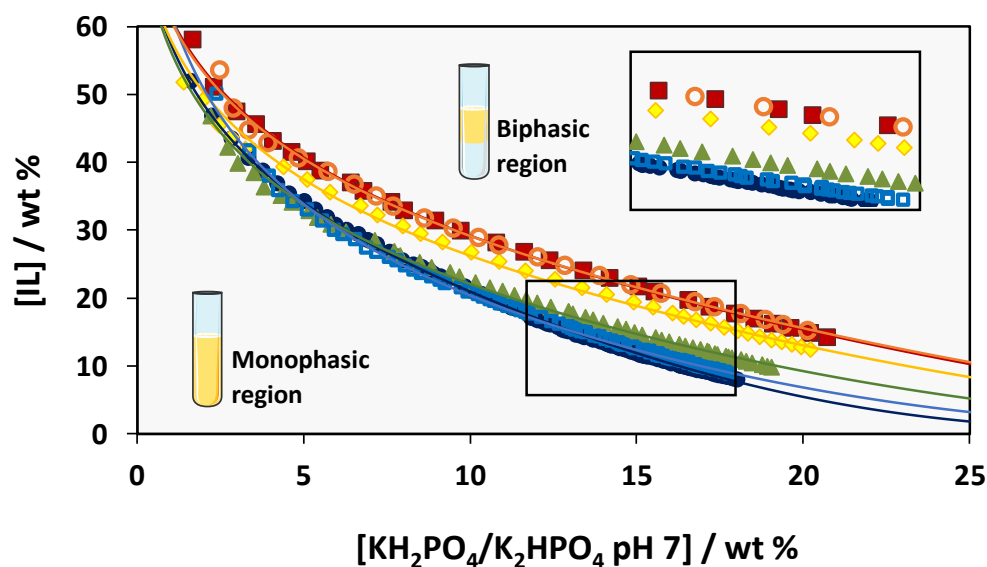
Figure 2.3.2. Phase diagrams of the ABS composed of IL + KH$_2$PO$_4$/K$_2$HPO$_4$ + H$_2$O at pH 7.0 in weight fraction percentage: [Et$_3$NC$_4$]Br (♦); [Bu$_3$NC$_4$]Br (●); [Pr$_3$NC$_4$]Br (▲); [MepyrNC$_4$]Br (■); [N$_{4444}$]Br (□); [C$_4$mim]Br (○).

All ILs investigated are able to form ABS with the phosphate buffer salt at pH 7.0, with all compositions above the respective binodal curve resulting in ABS or TPP systems that can be used in separation processes, as in the current work for the purification and recovery of mAbs. The amount required to reach 100 wt% corresponds to the content of water or supernatant that needs to be added to each system.

A larger biphasic region indicates a higher ability of the IL to form two immiscible phases (biphasic system); e.g. at 15 wt% of salt, the following trend for ABS formation was found: [C$_4$mim]Br ≈ [MepyrNC$_4$]Br < [Et$_3$NC$_4$]Br < [Pr$_3$NC$_4$]Br < [N$_{4444}$]Br < [Bu$_3$NC$_4$]Br. All ILs share the same anion, being this trend a direct result of the IL cation chemical structure and its affinity for water. IL cations with lower affinity for water, *i.e.* with longer aliphatic chains or with no aromatic groups, are more prone to form ABS.

The trend obtained indicates the preferential formation of hydration complexes of the salt ions, leading to the IL salting-out, and in agreement with literature [18]. Furthermore, compared to the widely investigated IL [C$_4$mim]Br, it is here shown that AGB-ILs require lower amounts of IL and/or salt to create ABS and consequently TPP systems, which is beneficial when envisioning the

Sustainable strategies based on glycine-betaine analogue ionic liquids for the recovery of monoclonal antibodies from cell culture supernatants

2

development of low-cost and sustainable separation processes. It should be remarked that these AGB-ILs have been previously described as harmless or practically harmless toward the marine bacteria *Allvibrio fischeri* [34]. Even when compared to a more hydrophobic and commercial IL, such as [N$_{4444}$]Br, the AGB-IL [Bu$_3$NC$_4$]Br performs better, requiring lower amounts to undergo liquid-liquid demixing.

2.3.4.2. Purification and recovery of anti-IL-8 mAbs by ABS and TPP strategies

The qualitative and quantitative characterization of the CHO cell culture supernatants was initially performed to appraise the complexity of the medium from which anti-IL-8 mAbs aimed to be purified. The SDS-PAGE under reducing conditions and SE-HPLC characterization results of the CHO cell culture supernatant are provided in **Figure 2.3.3**.
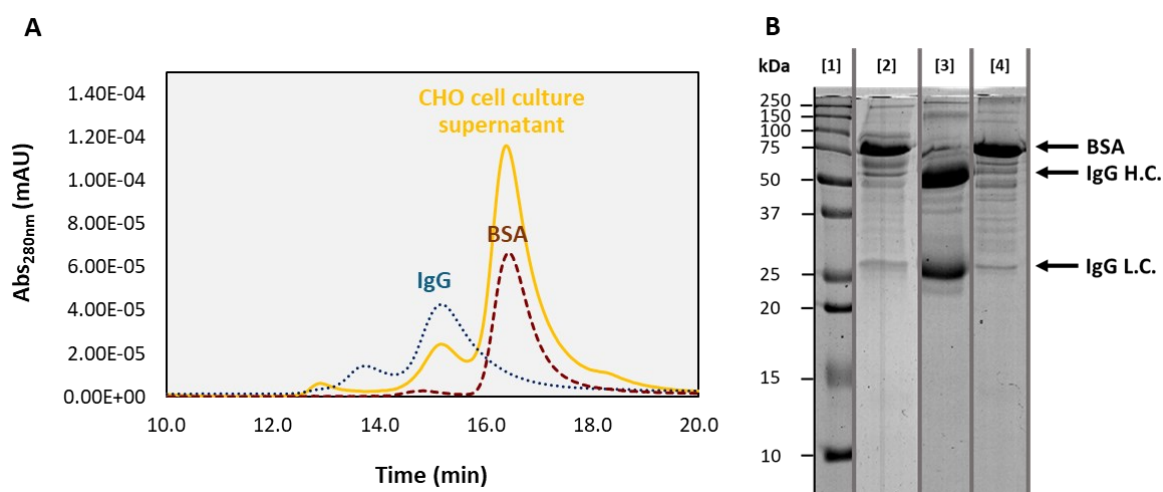
Figure 2.3.3. Characterization of the CHO cell culture supernatant: (A) SE-HPLC chromatograms of the CHO cell culture supernatant (−), pure IgG solution 100 mg·L^{-1} (··), and pure BSA solution 200 mg·L^{-1} (--); (B) SDS-PAGE gel: lane 1 – molecular weight marker; lane 2 – CHO cell culture supernatant; lane 3 – pure IgG solution 1 g·L^{-1}; lane 4 – pure BSA solution 1 g·L^{-1}. BSA and IgG heavy (H.C.) and light (L.C.) chains are identified.

Under the chromatographic conditions used, pure IgG samples present 2 chromatographic peaks: one corresponding to the IgG monomer and the other to IgG aggregates, with a retention time of *ca.* 15.0 min and 13.8 min, respectively. IgG is composed of 2 heavy chains with a molecular weight of 50 kDa, and 2 light chains with a molecular weight of 25 kDa, visible in the reduced SDS-PAGE results (**Figure 2.3.3 (B)**). The major protein impurity in the feed is bovine serum albumin (BSA), with a retention time of *ca.* 16.8 min and a molecular weight of 66.5 kDa. Apart from IgG and BSA, CHO cell culture supernatants also present other protein impurities resulting from the medium

used in the cell proliferation and growth, and also from their metabolism (*e.g.* insulin, transferrin and other CHO host cell proteins), which may correspond to the lighter protein corresponding bands in **Figure 2.3.3**.

The cell culture was maintained for several months, resulting in a natural variation of the proteins content between each feedstock. The anti-IL-8 mAbs concentration varied between 40.5 and 99.4 mg·L^{-1}, with an average content of 67.7 ± 23.7 mg·L^{-1} and an average purity of 16.9 ± 3.8 %. However, in all cases where ABS and TPP systems were applied, the original feedstock was always analyzed to infer the improvements achieved in respect to the original feedstock.

After the characterization of the phase diagrams and of the mAbs-containing feedstock, the potential of IL-based ABS as purification routes for anti-IL-8 directly from CHO cell culture supernatants was addressed for three mixture compositions (15 wt% KH_2PO_4/K_2HPO_4 pH 7.0 + 22.5 wt% H_2O + 37.5 wt% CHO cell culture supernatant + IL ranging from 25 wt% to 40 wt%). The performance of all ABS was investigated in terms of recovery yield (%Yield$_{IgG}$) and purification factor (PF$_{IgG}$), whose results are shown in **Figure 2.3.4**. The use of the purification factor allows to reduce discrepancies in the results derived from the variability of the biological matrix, and is valuable to carry out a first screening of the several AGB-IL-based systems performance. The composition of each phase for the mixture points used in the separation studies, i.e. the respective TLs, and detailed data on the recovery yields and purification factors are given in the **Appendix C (Table C.9)**.

For the mixture composition with a lower IL content (25 wt%), a preferential partition of all proteins to the top (IL-rich) phase was observed with all ILs (**Figure 2.3.4 (A)**). This phenomenon may be explained by the salting-out effect induced by the phosphate-based salt, promoting the exclusion of proteins into the opposite phase. Nevertheless, biomolecules affinity and interactions with ILs play a significant role since this behavior does not commonly occur in polymer-salt ABS [40], where the salt also acts as a salting-out agent. In IL-based ABS, a multitude of specific interactions (van der Waals, hydrogen-bonding and electrostatic interactions) occurring between the amino acids residues at the proteins surface and ILs seem to govern their partitioning to the IL-rich phase, as previously reported with other proteins [41-43]. The isoelectric point (pI) of anti-IL-8 is *ca.* 9.3 [36], and as the pH of the investigated IL-based systems is 7.0, antibodies are positively charged and electrostatic interactions may play a role. Nevertheless, if they were the most relevant type of interactions, IgG should preferentially partition to the salt-rich phase, as typically observed in polymer-salt ABS [40, 44]. In this work, the partition of IgG is triggered to the top phase of ABS using ILs instead of polymers, which may be due to preferential hydrogen-bonding and dispersive forces between the target protein and ILs.

Sustainable strategies based on glycine-betaine analogue ionic liquids for the recovery of monoclonal antibodies from cell culture supernatants

2
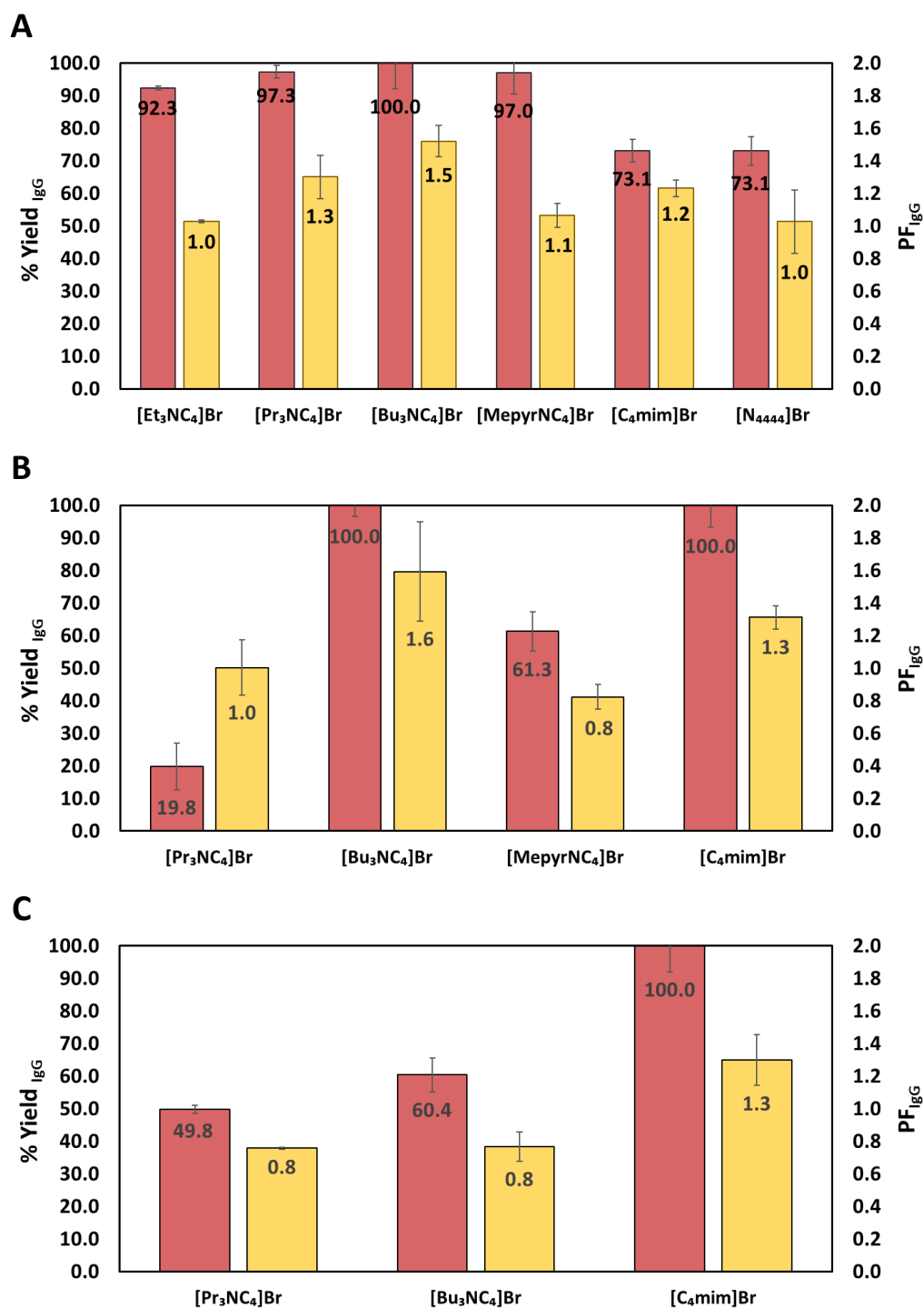
Figure 2.3.4. Recovery yields (%Yield$_{IgG}$ – ■) and purification factors (PF$_{IgG}$ – ■) of anti-IL-8 mAbs in the IL-rich phase using ABS composed of IL + 15 wt% KH$_2$PO$_4$/K$_2$HPO$_4$ pH 7 + 22.5 wt% H$_2$O + 37.5 wt% CHO cell culture supernatant: (A) 25 wt% IL; (B) 30 wt% IL; and (C) 40 wt% IL.

When using 25 wt% of IL in the ABS composition, recovery yields of mAbs ranging from 73.1 % up to 100.0 % (for [Bu$_3$NC$_4$]Br) are obtained in a single step, with purification factors ranging from

1.0 to 1.5. Moreover, all AGB-IL-based ABS composed of 25 wt% of IL allow a high recovery of mAbs (> 92 %), performing better than the commercial ILs that lead to a maximum recovery yield of 73.1 %. mAbs losses with these ILs are probably associated to precipitation since some turbidity was detected in these systems. Overall, the best results were obtained using the ABS composed of [Bu$_3$NC$_4$]Br, allowing the complete recovery of the antibodies in a single-step, with a purification factor of 1.5 ± 0.1. According to the recovery yields achieved, it is clear that the IL cation core and the respective alkyl side chain length have a significant influence on the mAbs partitioning between the phases and in the maintenance of their structure.

The separation of biomolecules from a complex mixture in ABS can be manipulated by various factors, e.g. by the nature of the phase-forming components and their concentrations. This last possibility was taken into account, and conducted by increasing the concentration of the IL from 25 wt% to 30 wt% and 40 wt% while maintaining the composition of the salt at 15 wt%. The goal was to optimize the purification process with the four ILs that led to the most promising results in the first screening ([Pr$_3$NC$_4$]Br, [Bu$_3$NC$_4$]Br, [MepyrNC$_4$]Br and [C$_4$mim]Br). The results obtained are depicted in **Figure 2.3.4 (B)** and **(C)**.

The recovery yields for IgG of the systems composed of 30 wt% of IL range from 19.8 % to 100 %; however, when 40 wt% of IL is used (**Figure 2.3.4 (C)**), recovery yields ranging from 49.8 % to 100 % are obtained at the IL-rich phase. In general, ABS formed by [Pr$_3$NC$_4$]Br present the lowest performance regarding the IgG recovery in the top phase. Similarly, ABS composed of 30 wt% of [MepyrNC$_4$]Br lead to a decrease in the anti-IL-8 recovery and purification factor (61.3 ± 6.1 % and 0.8 ± 0.1, respectively), being these two ILs discarded for the evaluation with 40 wt% of IL. For comparison purposes, the systems composed of the commercial IL [C$_4$mim]Br were studied. These systems allow the complete recovery of anti-IL-8 mAbs with the increase of the IL concentration up to 40 wt%, with a purification factor of 1.3 in both cases. Regarding AGB-ILs, ABS composed of [Pr$_3$NC$_4$]Br and [MepyrNC$_4$]Br are not suitable to purify the target biomolecule from the complex medium under any concentration of IL (from 25 wt% to 40 wt%). The most promising ABS is constituted by [Bu$_3$NC$_4$]Br at 30 wt%, where a recovery yield of 100 % and purification factors of 1.6 are achieved in one-step. Overall, the most hydrophilic ILs, which present smaller biphasic regions in their phase diagrams and shorter TLs, are the ones that lead to the less promising results (*e.g.* [Pr$_3$NC$_4$]Br and [MepyrNC$_4$]Br). On the other hand, more hydrophobic ILs (*e.g.* [Bu$_3$NC$_4$]Br, but still miscible in water), with larger biphasic regions and longer TLs, are more efficient options to recover and purify mAbs.

Sustainable strategies based on glycine-betaine analogue ionic liquids for the recovery of monoclonal antibodies from cell culture supernatants

2

In addition to the IgG recovered at the IL-rich phase, the best identified ABS composed of [Bu$_3$NC$_4$]Br also leads to the creation of a protein-rich interface precipitate [*cf.* **Appendix C (Figure C.1)**], particularly visible at the higher IL concentrations (40 wt%) and responsible for the lower recovery yields shown in **Figure 2.3.4 (C)**. This phenomenon is related with the water content in the top phase, which decreases as the IL concentration increases [data given in the **Appendix C (Table C.10)**], thus not allowing the complete solubilization of proteins and resulting in the formation of ILTPP systems. Mixture compositions comprising higher concentrations of IL, corresponding to longer tie-lines, imply higher concentrations of salt in the bottom phase. Due to the salt ions preferential solvation, less water will be available for the proteins solvation, resulting in the exposure of hydrophobic patches which promotes protein-protein interactions that ultimately lead to the proteins precipitation. This salting-out phenomenon has been reported for the precipitation of food proteins at the interface of IL-salt ABS, defined as ILTPP, although no complex mixtures have been addressed [25, 26].

The antibodies precipitation in ABS has been systematically considered as a "bad feature" in the literature and, consequently, ABS promoting IgG precipitation are usually discarded due to their "low performance" [44-49]. Nevertheless, if precipitation is selective and does not compromise the antibodies stability and activity, this approach should be considered as an alternative and effective IgG downstream strategy. Accordingly, the presence of a significant amount of precipitate in ABS composed of higher amounts (40 wt%) of [Bu$_3$NC$_4$]Br encouraged the investigation of the ILTPP approach as a potential strategy to purify and recover mAbs.

The proteins precipitate formed between the two coexisting phases in the ABS was recovered, resuspended in an aqueous solution of PBS (pH 7.4, 10 mmol·L^{-1}) and further analyzed. Through this approach and at the conditions under discussion, there is the selective (one-step) precipitation of IgG directly from the CHO cell culture supernatant, with a recovery yield of 41.0 ± 2.6 % and a purification factor of 2.7 ± 0.1 (%Purity$_{IgG}$ = 60.9 ± 2.0 %). Overall, with the ABS formed by 40 wt % of [Bu$_3$NC$_4$]Br, 60.4 ± 5.2 % of IgG with a purification factor of 0.8 ± 0.1 is recovered in the IL-rich phase, whereas the remaining antibody is recovered at the ABS interface with a recovery yield of 41.0 ± 2.6 % and a purification factor of 2.7 ± 0.1. In **Figure 2.3.5**, the SDS-PAGE gel of all the recovered fractions is provided, allowing not only to infer the mAbs integrity, but also to corroborate the discussed purification results. It should be remarked that although promising results were obtained with higher concentrations of IL, higher concentrations of IL (> 40 wt%) are not experimentally feasible given the amount of feedstock that needs to be loaded to create ABS.
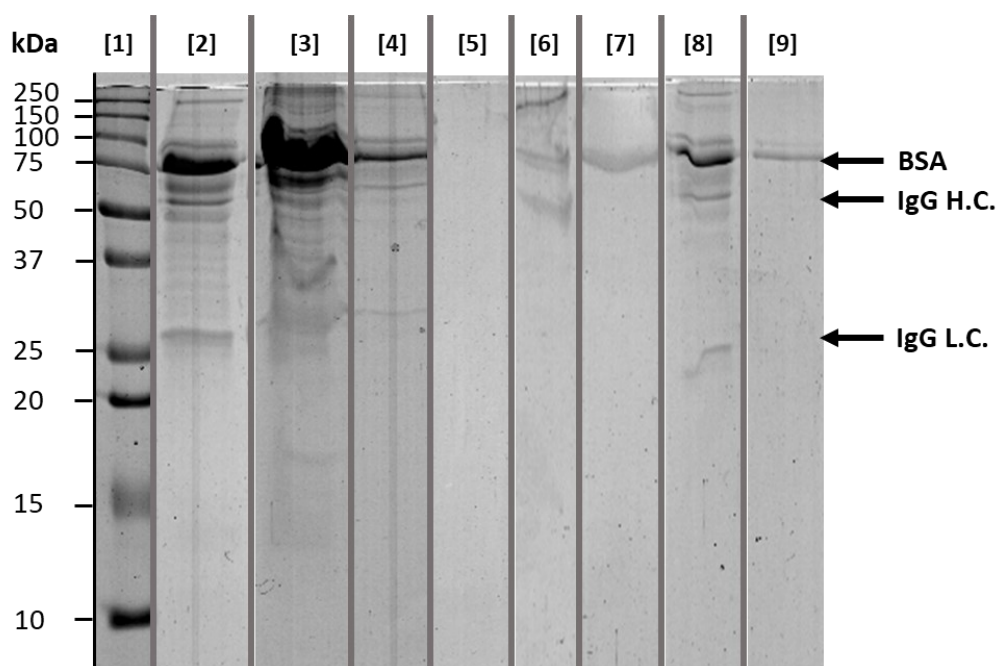
Figure 2.3.5. SDS-PAGE of the recovered fractions using the system composed of 40 wt% [Bu$_3$NC$_4$]Br + 15 wt% KH$_2$PO$_4$/K$_2$HPO$_4$ pH 7.0 + 22.5 wt% H$_2$O + 37.5 wt% CHO cell culture supernatant (ABS fractions + UF fractions). Lane 1 – molecular weight marker (kDa); lane 2 – CHO cell culture supernatant; lane 3 – ABS top phase; lane 4 – ABS precipitate; lane 5 – ABS bottom phase; lane 6 – UF retentate of top phase; lane 7 – UF filtrate of top phase; lane 8 – UF retentate of precipitate; lane 9 – UF filtrate of precipitate. The bands corresponding to BSA, IgG heavy chain (H.C.) and IgG light chain (L.C.) are also labelled.

To fully characterize the potential of ABS and TPP as IgG one-step purification platforms, we evaluated the biological activity of the anti-IL-8 mAbs in the IL-rich phase and in the precipitate by competitive ELISA, which was found to be 90.5 ± 2.0 % and 74.7 ± 3.2, respectively. The detailed mAbs activity results are given in the **Appendix C (Table C.11)**. The mAbs activity in the IL-rich phase is similar to that presented by the antibodies in the CHO cell culture supernatant before the purification process (90.6 ± 1.3 %), meaning that the extraction using the IL-based approach does not affect or decrease the anti-IL-8 biological activity. Despite the remarkable results obtained with ILTPP, the anti-IL-8 activity slightly decreases in the precipitate fraction, probably due to structural changes induced by precipitation, but still in the order of that reported for anti-IL-8 purification using ProA affinity chromatography (79 ± 9 %) [36]. Since the biological activity of proteins is closely related with their 3D structure, these observations allowed us to infer that minimal conformational changes occur with IL-based ABS and TPP systems.

Albeit large efforts have been carried out with more traditional polymer-based ABS to purify antibodies, as reviewed by Capela et al. [1], the IgG recovery and purification results gathered in

Sustainable strategies based on glycine-betaine analogue ionic liquids for the recovery of monoclonal antibodies from cell culture supernatants

2

this work outstand those reported up to date using IL-based ABS [37, 50, 51]. For instance, Ferreira et al. [37] using commercial ILs as adjuvants in polymer-salt ABS achieved 26 % of IgG purity, whereas Mondal et al. [50] recovered 85 % of IgG from rabbit serum with a purity level of 25 %. Ramalho et al. [51] reached the best results, being able to recover all the IgG from rabbit serum with a purity level up to 49 %. Considering the best results found in the literature with ABS comprising ILs, it can be concluded that the systems herein developed allow higher purification levels. Furthermore, the previous works were carried out with mammal's serum samples, where in this work the use of IL-based ABS for mAbs recovery/purification from CHO cell culture supernatants was considered for the first time. In the same line, for the first time ILTPP approaches were considered to recover IgG.

2.3.4.3. Hybrid processes and IgG recovery

Aiming the IgG recovery from the IL-rich phase and the IL removal from the antibodies' fractions, ultrafiltration (UF) was finally applied, allowing to propose the use of hybrid processes to purify IgG by combining ABS + UF and TPP + UF steps. UF also allows to recover antibodies in a biological buffer, viable for the envisioned IgG therapeutic applications, and to recover the IL for further use. As a proof of concept, an ultrafiltration step was applied to the IL-rich phase and precipitate containing IgG of the most promising identified ABS (composed of 40 wt% of $[Bu_3NC_4]Br$ + 15 wt% of KH_2PO_4/K_2HPO_4 pH 7.0 + 7.5 wt% of H_2O + 37.5 wt% of CHO cell culture supernatant). The performance of this additional step was investigated in terms of IgG concentration ([IgG]), recovery yield (%$Yield_{IgG}$), purity level (%$Purity_{IgG}$) and purification factor (PF). These parameters were determined for the different strategies that could be combined: (i) TOP phase + UF retentate; (ii) TOP phase + UF filtrate; (iii) Precipitate + UF retentate; and (iv) Precipitate + UF filtrate. Detailed data are given in the **Appendix C (Table C.11)**. A summary of the results, while highlighting the developed integrated processes in which the purification, recovery and final formulation of mAbs in phosphate-based solutions can be performed, is given in **Figure 2.3.6**.

The UF step of the top IL-rich phase allows to recover 47.3 ± 13.5 % of IgG in the retentate, with an increase of 88.5 % in the purity level, up to 32.8 ± 1.5 % vs. 17.4 ± 2.0 % before UF, and with an overall IgG recovery yield of 28.6 ± 18.7 % in route (i). The IgG recovery yield in the filtrate is 45.1 ± 16.1 %, presenting an IgG purity of 29.8 ± 5.7 %, and with an overall yield of the two-step process (route (ii)) of 27.2 ± 21.3 %, with the anti-IL-8 mAbs biological activity of 66.4 ± 2.4 %. Nevertheless, it should be remarked that the filtrate is the fraction where the IL is also present, and therefore the

choice of using this fraction for IgG formulation or for IL recovery for further reuse should be made based on the final desired application.
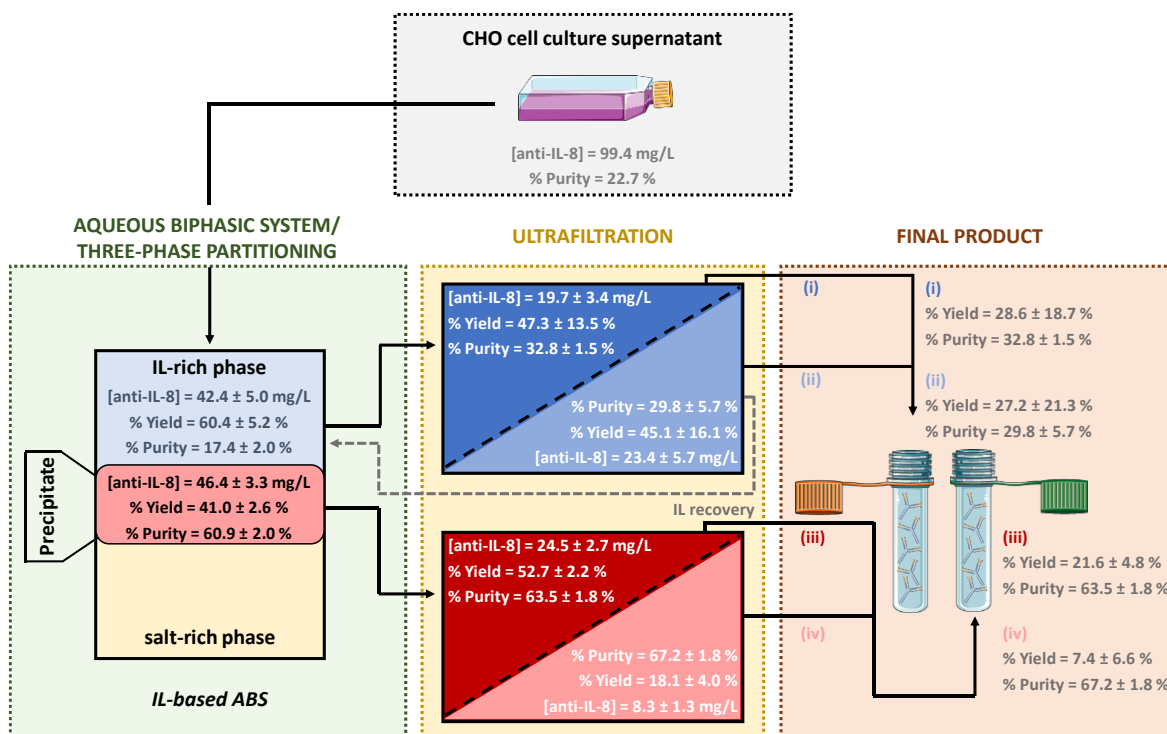
Figure 2.3.6. Schematic representation of the integrated and hybrid processes developed for mAbs downstream processing; routes to recover IgG with different purity levels and allowing the IL recover and reuse are identified.

Despite the good results accomplished using the ABS IL-rich phase, an even better performance was achieved with the ILTPP approach combined with ultrafiltration. The IgG recovery yield in the retentate is 52.7 ± 2.2 %, with a purity level of 63.5 ± 1.8 %, whereas the overall recovery yield of the two steps is 21.6 ± 4.8 % (overall process/route (iii)). The UF step in the filtrate results in a low IgG recovery yield of 18.1 ± 4.0 % (that only results in an overall yield of the two-step process of 7.4 ± 6.6 %); however, this approach leads to an increase in the purity level up to 67.2 ± 1.8 % (route (iv)).

The proteins profile of each UF fraction is provided in **Figure 2.3.5**, in which is possible to identify that IgG is mainly retained in the retentate fractions. It is important to remark that IgG is present in all fractions evaluated, as shown in the SE-HPLC chromatograms [given in the **Appendix C (Figure C.2)**], even though in lower concentrations. After UF the peak corresponding to low molecular weight protein impurities is only present in the filtrate, meaning that with this step we completely remove one class of protein impurities, representing the basis for the increment of 88.5

Sustainable strategies based on glycine-betaine analogue ionic liquids for the recovery of monoclonal antibodies from cell culture supernatants

2

% in the purity level of IgG in the retentate fraction (comparing to the top IL-rich phase fraction). The precipitate fraction after UF does not contain protein impurities with lower molecular weights (that are only retained in the top phase of the system), supporting the high purity level achieved with this fraction (up to 67.2 %). Although a membrane with a 100 kDa cut-off was used, some 3D conformation of the antibodies allow, in some extension, their passage through the membrane, thus leading to some losses in the IgG recovery yield. This step is however of high relevance since the IL can be recovered and reused, and IgG can be recovered in a phosphate aqueous solutions viable to proceed to biotechnological and health related applications.

Since the previously described processes allow the IL recovery, the IL recyclability was finally demonstrated. The respective experimental details are given in the Experimental Section. After the first separation step with "fresh" IL, the IL recycling and its use in the formation of a new system was investigated for two more times. The results obtained for the 3 cycles of separation in terms of mAbs recovery/purification are provided in **Figure 2.3.7** [detailed values are given in the **Appendix C (Table C.12)**].
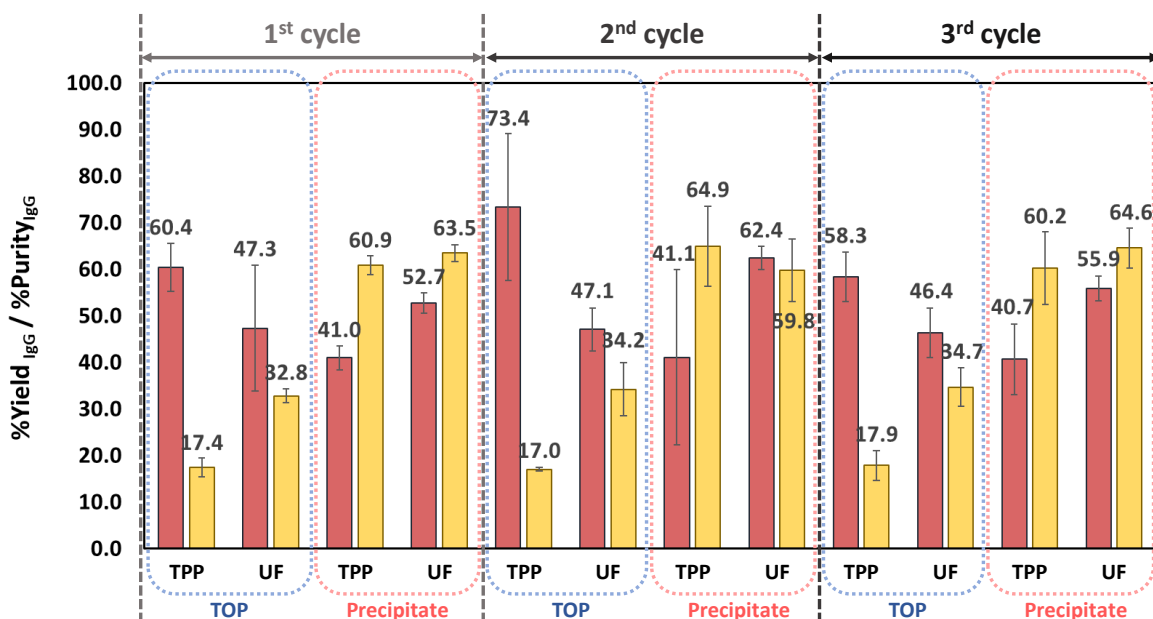
Figure 2.3.7. Recovery yields (%Yield$_{IgG}$ – ■) and purity levels (%Purity$_{IgG}$ – ■) of anti-IL-8 mAbs in three separation cycles, where the last two correspond to the use of recycled IL.

Overall, similar results in the recovery yield and purity level of IgG were obtained in the 3 separation cycles, both in the IL-rich phase and precipitate fractions, meaning that the proposed processes keep their separation performance even using recycled IL, while contributing to these processes sustainability. Through the tie-line data corresponding to the mixture compositions used

in the separation of IgG [*cf.* **Appendix C (Table C.8)**], the concentration of IL in the bottom salt-rich phase is significantly low (0.0003460 wt%). Accordingly, ILs are mainly lost during the recovery and recycling steps and transference between vials. The IL loss in each recycling step is below 3 wt%. However, it should be remarked that this loss corresponds to a lab-scale procedure, being expected that it can be reduced by properly optimizing the IL transference and by scaling-up the process.

Based on the overall results obtained, an hybrid and integrated purification platform is proposed to purify mAbs from CHO cell culture supernatants, comprising the following steps: (1) IL-based ABS and TPP for mAbs recovery and purification; (2) UF for mAbs polishing and IL removal/salt exchange; and (3) a final product formulation through two routes, according to the IgG desired purity. Based on the combination of the fractions with similar purity levels summarized in **Figure 2.3.6**, such as routes (i) + (ii) and (iii) + (iv), two fractions of anti-IL-8 mAbs can be recovered with purity levels higher than 29 % and 63 %, respectively. Although further optimization studies can be carried out aiming at achieving the complete precipitation of mAbs at the ABS interface, as well as the testing of other membrane cut-offs, the developed platforms reveal a high potential and provide new directions in the design of more sustainable IL-based strategies for the purification and recovery of biopharmaceuticals such as mAbs.

2.3.5. Conclusions

The use of IL-based purification and recovery strategies for mAbs directly from CHO cell culture supernatants was here proposed and evaluated for the first time. To this end, novel ABS composed of glycine-betaine analogues ILs and K_2HPO_4/KH_2PO_4 at pH 7.0, the respective three-phase partitioning systems, and hybrid processes combined with ultrafiltration, were investigated. With the studied ABS, mAbs preferentially partition to the IL-rich phase, with recovery yields up to 100 % and purification factors up to 1.6. With IL-based three-phase partitioning approaches a precipitate enriched in mAbs is obtained at the ABS interface, yielding 41.0 % of IgG with a purification factor of 2.7 (purity of 60.9 % achieved in a single-step). The biological activity of anti-IL-8 mAbs is maintained after the several purification and recovery steps, being superior and competitive with the activity of mAbs purified by ProA chromatography. Hybrid processes combining the two previous techniques and an ultrafiltration step were finally applied and evaluated, allowing the recovery of mAbs from the different fractions in an appropriate buffer solution for biopharmaceuticals formulation, while allowing the simultaneous IL removal and reuse. The IL recyclability was demonstrated, with no losses on the separation performance. The best

results were obtained with the hybrid process combining ILTPP and ultrafiltration, where IgG with a purity greater than 60 % is obtained.

2.3.6. References

1.   E.V. Capela, M.R. Aires-Barros, M.G. Freire, and A.M. Azevedo, *Monoclonal Antibodies– Addressing the Challenges on the Manufacturing Processing of an Advanced Class of Therapeutic Agents.* Frontiers in Clinical Drug Research-Anti Infectives: Volume 4, 2017. **4**: p. 142.

2.   A. Hey, *History and practice: antibodies in infectious diseases.* Microbiology Spectrum, 2015. **3**: p. AID-0026-2014.

3.   P. Rosa, I. Ferreira, A. Azevedo, and M. Aires-Barros, *Aqueous two-phase systems: a viable platform in the manufacturing of biopharmaceuticals.* Journal of Chromatography A, 2010. **1217**(16): p. 2296-2305.

4.   D.M. Ecker, S.D. Jones, and H.L. Levine. *The therapeutic monoclonal antibody market*. in *MAbs*. 2015. Taylor & Francis.

5.   A.L. Grilo and A. Mantalaris, *The increasingly human and profitable monoclonal antibody market.* Trends in biotechnology, 2019. **37**(1): p. 9-16.

6.   M.F. Silva, A. Fernandes-Platzgummer, M.R. Aires-Barros, and A.M. Azevedo, *Integrated purification of monoclonal antibodies directly from cell culture medium with aqueous two-phase systems.* Separation and Purification Technology, 2014. **132**: p. 330-335.

7.   U. Gottschalk, *Bioseparation in antibody manufacturing: the good, the bad and the ugly.* Biotechnology progress, 2008. **24**(3): p. 496-503.

8.   H.F. Liu, J. Ma, C. Winter, and R. Bayer. *Recovery and purification process development for monoclonal antibody production*. in *MAbs*. 2010. Taylor & Francis.

9.   A.A. Shukla, B. Hubbard, T. Tressel, S. Guhan, and D. Low, *Downstream processing of monoclonal antibodies—application of platform approaches.* Journal of Chromatography B, 2007. **848**(1): p. 28-39.

10.   J. Weinberg, S. Zhang, A. Kirkby, E. Shachar, G. Carta, and T. Przybycien, *Chemical modification of protein a chromatography ligands with polyethylene glycol. II: Effects on resin robustness and process selectivity.* Journal of Chromatography A, 2018. **1546**: p. 89-96.

11.   S. Sommerfeld and J. Strube, *Challenges in biotechnology production—generic processes and process optimization for monoclonal antibodies.* Chemical Engineering and Processing: Process Intensification, 2005. **44**(10): p. 1123-1137.

12.   P.-Å. Albertsson, *Partition of proteins in liquid polymer–polymer two-phase systems.* Nature, 1958. **182**(4637): p. 709.

13.   I. Campos-Pinto, E.V. Capela, A.R. Silva-Santos, M.A. Rodríguez, P.R. Gavara, M. Fernandez-Lahore, M.R. Aires-Barros, and A.M. Azevedo, *LYTAG-driven purification strategies for monoclonal antibodies using quaternary amine ligands as affinity matrices.* Journal of Chemical Technology & Biotechnology, 2018. **93**(7): p. 1966-1974.

14.   I. Campos-Pinto, E. Espitia-Saloma, S.A. Rosa, M. Rito-Palomares, O. Aguilar, M. Arévalo-Rodríguez, M.R. Aires-Barros, and A.M. Azevedo, *Integration of cell harvest with affinity-enhanced purification of monoclonal antibodies using aqueous two-phase systems with a dual tag ligand.* Separation and Purification Technology, 2017. **173**: p. 129-134.

15.   P. Rosa, A. Azevedo, I. Ferreira, S. Sommerfeld, W. Bäcker, and M. Aires-Barros, *Downstream processing of antibodies: Single-stage versus multi-stage aqueous two-phase extraction.* Journal of Chromatography A, 2009. **1216**(50): p. 8741-8749.

16.   A.M. Azevedo, P.A. Rosa, I.F. Ferreira, J. De Vries, T. Visser, and M.R. Aires-Barros, *Downstream processing of human antibodies integrating an extraction capture step and cation exchange chromatography.* Journal of Chromatography B, 2009. **877**(1-2): p. 50-58.

17.   K.E. Gutowski, G.A. Broker, H.D. Willauer, J.G. Huddleston, R.P. Swatloski, J.D. Holbrey, and R.D. Rogers, *Controlling the aqueous miscibility of ionic liquids: aqueous biphasic systems of water-miscible ionic liquids and water-structuring salts for recycle, metathesis, and separations.* Journal of the American Chemical Society, 2003. **125**(22): p. 6632-6633.

18.   M.G. Freire, A.F.M. Claudio, J.M.M. Araújo, J.A.P. Coutinho, I.M. Marrucho, J.N.C. Lopes, and L.P.N. Rebelo, *Aqueous biphasic systems: a boost brought about by using ionic liquids.* Chemical Society Reviews, 2012. **41**(14): p. 4966-4995.

19.   S.P.M. Ventura, F.A. e Silva, M.V. Quental, D. Mondal, M.G. Freire, and J.A.P. Coutinho, *Ionic-liquid-mediated extraction and separation processes for bioactive compounds: past, present, and future trends.* Chemical reviews, 2017. **117**(10): p. 6984-7052.

20.   E.V. Capela, M.V. Quental, P. Domingues, J.A.P. Coutinho, and M.G. Freire, *Effective separation of aromatic and aliphatic amino acid mixtures using ionic-liquid-based aqueous biphasic systems.* Green Chemistry, 2017. **19**(8): p. 1850-1854.

21.   M. Taha, M.V. Quental, F.A. e Silva, E.V. Capela, M.G. Freire, S.P.M. Ventura, and J.A.P. Coutinho, *Good's buffer ionic liquids as relevant phase-forming components of self-buffered aqueous biphasic systems.* Journal of Chemical Technology & Biotechnology, 2017. **92**(9): p. 2287-2299.

22.   Z. Li, X. Liu, Y. Pei, J. Wang, and M. He, *Design of environmentally friendly ionic liquid aqueous two-phase systems for the efficient and high activity extraction of proteins.* Green Chemistry, 2012. **14**(10): p. 2941-2950.

23.   M.V. Quental, M.M. Pereira, A.M. Ferreira, S.N. Pedro, S. Shahriari, A. Mohamadou, J.A.P. Coutinho, and M.G. Freire, *Enhanced separation performance of aqueous biphasic systems formed by carbohydrates and tetraalkylphosphonium-or tetraalkylammonium-based ionic liquids.* Green Chemistry, 2018. **20**(13): p. 2978-2983.

24.   H. Passos, T.B. Dinis, E.V. Capela, M.V. Quental, J. Gomes, J. Resende, P.P. Madeira, M.G. Freire, and J.A.P Coutinho, *Mechanisms ruling the partition of solutes in ionic-liquid-based aqueous biphasic systems–the multiple effects of ionic liquids.* Physical Chemistry Chemical Physics, 2018. **20**(13): p. 8411-8422.

25.   E. Alvarez-Guerra and A. Irabien, *Ionic liquid-based three phase partitioning (ILTPP) for lactoferrin recovery.* Separation Science and Technology, 2014. **49**(7): p. 957-965.

26.   E. Alvarez-Guerra and A. Irabien, *Ionic liquid-based three phase partitioning (ILTPP) systems for whey protein recovery: ionic liquid selection.* Journal of Chemical Technology & Biotechnology, 2015. **90**(5): p. 939-946.

27.   C. Dennison and R. Lovrien, *Three phase partitioning: concentration and purification of proteins.* Protein expression and purification, 1997. **11**(2): p. 149-161.

28.   M. Petkovic, K.R. Seddon, L.P.N. Rebelo, and C.S. Pereira, *Ionic liquids: a pathway to environmental acceptability.* Chemical Society Reviews, 2011. **40**(3): p. 1383-1403.

29.   R.A. Sheldon, *The E factor 25 years on: the rise of green chemistry and sustainability.* Green Chemistry, 2017. **19**(1): p. 18-43.

30.   F. De Zwart, S. Slow, R. Payne, M. Lever, P. George, J. Gerrard, and S. Chambers, *Glycine betaine and glycine betaine analogues in common foods.* Food chemistry, 2003. **83**(2): p. 197-204.

31.   S. Huang, L. Mills, B. Mian, C. Tellez, M. McCarty, X.-D. Yang, J.M. Gudas, and M. Bar-Eli, *Fully humanized neutralizing antibodies to interleukin-8 (ABX-IL8) inhibit angiogenesis, tumor growth, and metastasis of human melanoma.* The American Journal of Pathology, 2002. **161**(1): p. 125-134.

32.   L. Skov, F.J. Beurskens, C.O. Zachariae, S. Reitamo, J. Teeling, D. Satijn, K.M. Knudsen, E.P. Boot, D. Hudson, and O. Baadsgaard, *IL-8 as antibody therapeutic target in inflammatory diseases: reduction of clinical activity in palmoplantar pustulosis.* The Journal of Immunology, 2008. **181**(1): p. 669-679.

33.   A. Harada, N. Sekido, T. Akahoshi, T. Wada, N. Mukaida, and K. Matsushima, *Essential involvement of interleukin-8 (IL-8) in acute inflammation.* Journal of Leukocyte Biology, 1994. **56**(5): p. 559-564.

34.   M.M. Pereira, S.N. Pedro, J. Gomes, T.E. Sintra, S.P.M. Ventura, J.A.P. Coutinho, M.G. Freire, and A. Mohamadou, *Synthesis and characterization of analogues of glycine-betaine ionic liquids and their use in the formation of aqueous biphasic systems.* Fluid Phase Equilibria, 2019. **494**: p. 239-245.

35.   A.F.M. Cláudio, L. Swift, J.P. Hallett, T. Welton, J.A.P. Coutinho, and M.G. Freire, *Extended scale for the hydrogen-bond basicity of ionic liquids.* Physical Chemistry Chemical Physics, 2014. **16**(14): p. 6593-6601.

36.   R. dos Santos, S.A. Rosa, M.R. Aires-Barros, A. Tover, and A.M. Azevedo, *Phenylboronic acid as a multi-modal ligand for the capture of monoclonal antibodies: development and optimization of a washing step.* Journal of Chromatography A, 2014. **1355**: p. 115-124.

37.   A.M. Ferreira, V.F. Faustino, D. Mondal, J.A.P. Coutinho, and M.G. Freire, *Improving the extraction and purification of immunoglobulin G by the use of ionic liquids as adjuvants in aqueous biphasic systems.* Journal of biotechnology, 2016. **236**: p. 166-175.

38.   J.C. Merchuk, B.A. Andrews, and J.A. Asenjo, *Aqueous two-phase systems for protein separation: studies on phase inversion.* Journal of Chromatography B: Biomedical Sciences and Applications, 1998. **711**(1-2): p. 285-293.

39.   C. Capello, U. Fischer, and K. Hungerbühler, *What is a green solvent? A comprehensive framework for the environmental assessment of solvents.* Green Chemistry, 2007. **9**(9): p. 927-934.

40.   P.A. Rosa, A.M. Azevedo, and M.R. Aires-Barros, *Application of central composite design to the optimisation of aqueous two-phase extraction of human antibodies.* Journal of Chromatography A, 2007. **1141**(1): p. 50-60.

41.   M.M. Pereira, S.N. Pedro, M.V. Quental, Á.S. Lima, J.A.P. Coutinho, and M.G. Freire, *Enhanced extraction of bovine serum albumin with aqueous biphasic systems of phosphonium-and ammonium-based ionic liquids.* Journal of Biotechnology, 2015. **206**: p. 17-25.

42.   M. Taha, M.V. Quental, I. Correia, M.G. Freire, and J.A.P. Coutinho, *Extraction and stability of bovine serum albumin (BSA) using cholinium-based Good's buffers ionic liquids.* Process Biochemistry, 2015. **50**(7): p. 1158-1166.

43.   A.M. Ferreira, H. Passos, A. Okafuji, A.P. Tavares, H. Ohno, M.G. Freire, and J.A.P. Coutinho, *An integrated process for enzymatic catalysis allowing product recovery and enzyme reuse by applying thermoreversible aqueous biphasic systems.* Green Chemistry, 2018. **20**(6): p. 1218-1223.

Sustainable strategies based on glycine-betaine analogue ionic liquids for the recovery of monoclonal antibodies from cell culture supernatants

2

44.   A.M. Azevedo, P.A. Rosa, I.F. Ferreira, and M.R. Aires-Barros, *Optimisation of aqueous two-phase extraction of human antibodies.* Journal of Biotechnology, 2007. **132**(2): p. 209-217.

45.   A.M. Azevedo, A.G. Gomes, P.A. Rosa, I.F. Ferreira, A.M. Pisco, and M.R. Aires-Barros, *Partitioning of human antibodies in polyethylene glycol–sodium citrate aqueous two-phase systems.* Separation and Purification Technology, 2009. **65**(1): p. 14-21.

46.   A. Azevedo, P. Rosa, I. Ferreira, and M. Aires-Barros, *Integrated process for the purification of antibodies combining aqueous two-phase extraction, hydrophobic interaction chromatography and size-exclusion chromatography.* Journal of Chromatography A, 2008. **1213**(2): p. 154-161.

47.   P. Rosa, A. Azevedo, S. Sommerfeld, M. Mutter, M. Aires-Barros, and W. Bäcker, *Application of aqueous two-phase systems to antibody purification: a multi-stage approach.* Journal of biotechnology, 2009. **139**(4): p. 306-313.

48.   B. Andrews, S. Nielsen, and J. Asenjo, *Partitioning and purification of monoclonal antibodies in aqueous two-phase systems.* Bioseparation, 1996. **6**(5): p. 303-313.

49.   F. Hachem, B. Andrews, and J. Asenjo, *Hydrophobic partitioning of proteins in aqueous two-phase systems.* Enzyme and Microbial Technology, 1996. **19**(7): p. 507-517.

50.   D. Mondal, M. Sharma, M.V. Quental, A.P. Tavares, K. Prasad, and M.G. Freire, *Suitability of bio-based ionic liquids for the extraction and purification of IgG antibodies.* Green Chemistry, 2016. **18**(22): p. 6071-6081.

51.   C.C. Ramalho, C.M.S.S. Neves, M.V. Quental, J.A.P. Coutinho, and M.G. Freire, *Separation of immunoglobulin G using aqueous biphasic systems composed of cholinium-based ionic liquids and poly (propylene glycol).* Journal of Chemical Technology & Biotechnology, 2018.

Purification of Antibodies using Three-Phase Partitioning Systems

3

3.1. Three-phase partitioning systems based on aqueous biphasic systems with ionic liquids as novel strategies for the purification and recovery of antibodies

This chapter is based on the manuscript under preparation with

Emanuel V. Capela, Ilaria Magnis, Ana F.C.S. Rufino, M. Raquel Aires-Barros, João A.P. Coutinho,

Ana M. Azevedo, Francisca A. e Silva, Mara G. Freire

3.1.1. Abstract

Antibodies, in particular immunoglobulin G (IgG), are one of the driving forces of the biopharmaceutical industry, with high relevance for the treatment of several diseases. Despite their wide potential, the recovery of these biomolecules from their complex biological media with high quality and purity is complex, based on multi-step approaches and being of high cost. Herein, we propose a novel and cost-effective approach using three-phase partitioning (TPP) systems based on aqueous biphasic systems (ABS) comprising ionic liquids (ILs) for IgG antibodies (pAbs) recovery purification. The process was first optimized by addressing the human IgG recovery yield and purification level from human serum samples by playing with the molecular weight of the polymer in TPP systems composed of polyethylene glycol (PEG) and citrate buffer ($K_3C_6H_5O_7/C_6H_8O_7$) at pH 7. Then, the use of ionic liquids (ILs) as adjuvants was studied to tailor the efficiency and selectivity of the PEG-salt TPP, in which the IL chemical structure and concentration were optimized. The most promising conditions obtained with polyclonal IgG from human serum were then applied for the recovery and purification of monoclonal antibodies (mAbs) directly from different cell culture supernatants (serum-containing and serum-free) to prove the robustness and flexibility of the developed process. Based on the obtained results, it was verified that IgG could be preferentially recovered either in the interphase of the TPP or in the top phase depending on the molecular weight of the ABS polymer. The system composed of PEG 1000 g·mol^{-1} is the most efficient, leading to a recovery yield of human polyclonal IgG of 65.8 % with 80.7 % of purity; by using the ILs tetra(n-butyl)ammonium bromide ($[N_{4444}]$Br) and 1-butyl-3-methylimidazolium chloride ($[C_4mim]$Cl) at 1 wt%, it is possible to improve the recovery yield to 80.5 % and the purity level to 82.6 %, respectively. Finally, the optimized conditions were applied in the processing of mAbs from cell

---

culture supernatants. Only the system composed of 1 wt% of [N$_{4444}$]Br was able to create a TPP with serum-containing cell culture supernatants, while all the systems were able to create TPP with serum-free cell culture supernatants, with the best performance achieved using 1 wt% of [C$_4$mim]Cl, in which 74.4 % of mAbs were recovered in the precipitate layer with 89.2 % purity and an impressive reduction of 100 % in the host cell proteins (HCPs) content. Overall, TPP systems based on ABS comprising ILs as adjuvants display high performance to recover and purify IgG from complex biological matrices, such as human serum, serum-containing and serum-free cell culture supernatants.

3.1.2. Introduction

Although relevant advances have been accomplished in the last years regarding the development of effective therapies, biopharmaceuticals are one of the most important therapeutics, being in many cases the only available option in the treatment of particular diseases [1, 2]. Amongst biopharmaceuticals, antibodies are widely applied for therapeutic purposes. Monoclonal antibodies (mAbs) present and important role in vaccination, immunization and in the treatment of oncologic, autoimmune, cardiovascular, inflammatory and neurological diseases [1, 3], whilst polyclonal antibodies (pAbs) derived from human serum are usually applied for the prevention and treatment of infections in immunodeficient patients, and also for the treatment of autoimmune and inflammatory diseases [4, 5].

The production of therapeutic antibodies must met high efficiency and safety standards, meaning that high recovery yields and purity levels must be achieved [6]. Even though their upstream processing is well-established, the high cost of the currently used downstream technologies represents a critical challenge which has been preventing the widespread use of antibodies as recurrent therapies. The purification of antibodies usually followed by most (if not all) manufacturers reccurs to a complex multi-step platform constituted by high resolution technologies such as chromatographic steps, including affinity chromatography (with biological ligands – protein A) [7]. Therefore, antibodies downstream costs can represent up to 80 % of their total production costs [8]. So, the development of new, simpler and cost-effective purification platforms for antibodies is required.

To overcome these issues, the extraction and purification of antibodies using aqueous biphasic systems (ABS) represents a promising alternative [9]. ABS are liquid-liquid extraction systems that consist of two immiscible aqueous-rich phases based on polymer-polymer, polymer-salt, or salt-salt combinations [10]. More recently, other phase-forming components, such as ionic

liquids (ILs) [11], surfactants [12], amino acids [13] and carbohydrates [14], have been disclosed. When dissolved in aqueous media above certain concentrations and under specific conditions, there is phase separation. In an ABS, each phase is enriched in each of the solutes and has a high water content, which means that they can offer a biocompatible medium for biologically active molecules if properly designed. Due to this advantage, ABS have been successfully used for the recovery of biological products, such as proteins/enzymes, antibiotics, antibodies, among others [6, 9, 15].

Three-phase partitioning (TPP) is a type of extraction technique that usually uses a water-miscible aliphatic alcohol (usually *t*-butanol) and an aqueous solution of ammonium sulfate ($(NH_4)_2SO_4$) to promote the recovery of target products, mainly proteins, in an enriched precipitate at the interface of two liquid phases [16]. In this way, an easy, direct and simple recovery of the final product is allowed, with no need for additional polishing steps, simultaneously allowing the recycling of solvents. In fact, TPP has been successfully reported in the literature regarding the purification of several biomolecules, including proteins [17-27]. When properly designed, ABS can be used to develop TPP systems, in which both phases are water-rich. By combining both ABS and TPP concepts, simpler and more bio- and eco-friendly extraction techniques can be created. For instance, Belchior *et al.* [28] recently investigated the performance of ABS-TPP systems composed of polyethylene glycol (PEG) of different molecular weights and potassium phosphate buffer at pH 7 for the fractionation of three main proteins of the egg white samples, namely ovalbumin, lysozyme and ovoinhibitor, by their partition between the three phases of the system. Also, the use of ionic liquids (ILs) has contributed to develop high performance ABS and TPP, as these are considered "designer solvents" and can be easily customized to meet the needs of a given application [11]. Ionic-liquid-based TPP (ILTPP) systems have been firstly proposed by Alvarez-Guerra *et al.* [29, 30] for the extraction of food proteins (for instance, lactoferrin). More recently, they were also proposed by Castro *et al.* [31] as viable candidates for recombinant proteins (interferon alpha-2b) purification from *E. coli* BL21 (DE3) inclusion bodies using PEG/poly(propylene) glycol (PPG) ABS-TPP with ILs as adjuvants (at 5 wt%), being possible its purification at the PEG-rich phase with the simultaneous precipitation of the remaining proteins at the ABS interface. To the best of our knowledge, there are currently no reports in the literature concerning the use of conventional ABS as TPP systems for antibodies purification, and only one work [32] reports the viability of ILTPP for monoclonal antibodies' purification directly from cell culture supernatants, using systems composed of glycine-betaine analogues ionic liquids (AGB-ILs

and potassium phosphate buffer at pH 7 [32]. Thus, regardless of their undeniable advantages, TPP based on ABS remains underexplored as compared to other techniques.

This work aims to combine the concepts of ABS and TPP to create cost-effective and biocompatible platforms for the purification of antibodies. The types of TPP available up to date are herein expanded by the development of systems formed by polymer-salt combinations, namely PEG with different molecular weights (600, 1000, 1500 and 2000 g·mol^{-1}) and citrate buffer ($K_3C_6H_5O_7/C_6H_8O_7$) at pH 7. The applicability of these systems was evaluated through the evaluation of their ability to selectively precipitate IgG antibodies from human serum at the interphase of the ABS. Distinct ILs were further added as adjuvants as an attempt to tune the selectivity of the polymer-salt ABS-TPP towards IgG, and their chemical structure and concentration were optimized. Finally, the most promising TPP systems were applied to other complex biological matrices, such as serum-containing and serum-free Chinese hamster ovary (CHO) cell culture supernatants, to prove the robustness and flexibility of the developed platform.

3.1.3. Experimental section

3.1.3.1. Materials

The TPP systems studied in this work were initially established using PEG of different molecular weights, namely 600, 1000, 1500 and 2000 g·mol^{-1} (hereafter abbreviated as PEG 600, PEG 1000, PEG 1500 and PEG 2000, respectively), purchased from Alfa Aesar, with the exception of PEG 1500 and PEG 2000 that were supplied by Acros Organics and Sigma Aldrich, respectively. Concerning the citrate buffer components, potassium citrate tribasic monohydrate ($K_3C_6H_5O_7 \cdot H_2O$, ≥ 99 wt% purity) was acquired from Acros Organics, and citric acid ($C_6H_8O_7$, ≥ 99.5 wt% purity) was supplied by Panreac. Phosphate buffered saline solution (PBS, pH ≈ 7.4) pellets were acquired from Sigma-Aldrich, and prepared according to the indications of the supplier, by solubilizing each pellet in 200 mL of distilled water. Distilled water was employed in all the experiments of this work, unless otherwise specified.

The ILs studied in this work are the following: 1-butyl-3-methylimidazolium bromide ([C$_4$mim]Br, 98 % purity), 1-butyl-3-methylimidazolium chloride ([C$_4$mim]Cl, 99 % purity), tetra(*n*-butyl)ammonium bromide ([N$_{4444}$]Br, 98 % purity), tetra(*n*-butyl)ammonium chloride ([N$_{4444}$]Cl, 97 % purity), tetra(*n*-butyl)phosphonium bromide ([P$_{4444}$]Br, 95 % purity), and tetra(*n*-butyl)phosphonium chloride ([P$_{4444}$]Cl, 95 % purity). All the ILs were acquired from Iolitec, with the exception of [N$_{4444}$]Br and [N$_{4444}$]Cl that were supplied from Fluka and Sigma Aldrich, respectively. The chemical structures of the studied ILs are depicted in **Figure 3.1.1**.
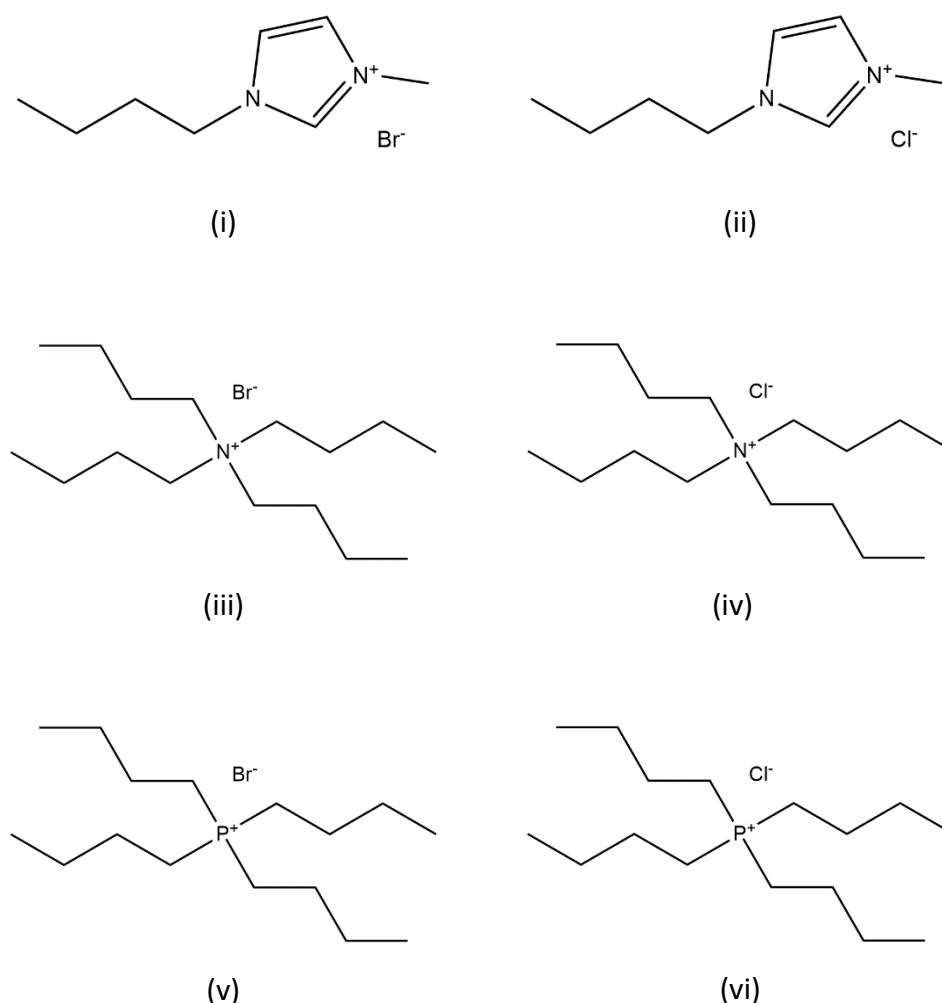
Figure 3.1.1. Chemical structures of the investigated ILs: (i) [C₄mim]Br; (ii) [C₄mim]Cl; (iii) [N₄₄₄₄]Br; iv) [N₄₄₄₄]Cl; (v) [P₄₄₄₄]Br; (vi) [P₄₄₄₄]Cl.

For the preparation of the HPLC buffer, di-sodium hydrogen phosphate 7-hydrate (Na₂HPO₄.H₂O) and di-sodium hydrogen phosphate anhydrous (NaHPO₄) were purchased from Panreac, while sodium chloride (NaCl) was obtained by Fisher Scientific. The water employed was double distilled, passed across a reverse osmosis system and further treated with a Milli-Q plus 185 water purification apparatus. The membrane filters (Whatman, 0.45µm, diameter 47mm) used for the mobile phase filtration was made of regenerated cellulose R55 and were provided by GE Healthcare Life Science. The disposable syringes (5 mL) used for phase's separation were purchased from Injekt.

The model proteins used as standards were: immunoglobulin G (IgG) for therapeutic administration (trade name: Gammanorm®), obtained from Octapharma (Lachen, Switzerland), as

a 165 mg·mL^{-1} solution containing 95 % of IgG (of which 59 % IgG1, 36 % IgG2, 4.9 % IgG3 and 0.5 % IgG4), human serum albumin (HSA, > 97 % purity) acquired from Sigma-Aldrich, and bovine serum albumin (BSA) standards (2 mg·mL^{-1}) purchased from Thermo Scientific Pierce.

The human serum used in this study was from human male AB plasma, USA origin, sterile-filtered, obtained from Sigma Aldrich (H4522 Sigma), with a total protein content ranging between 40-90 mg·mL^{-1}. This product was provided as a liquid and was stored at -20 °C. Human serum was previously diluted to its use on each assay using PBS solution. Serum-free Chinese hamster ovary (CHO) cell culture supernatants were produced and delivered by Icosagen SA (Tartumaa, Estonia). These supernatants contain a humanized monoclonal antibody, from IgG1 class, derived from mouse anti-hepatitis C virus subtype 1b NS5B (non-structural protein 5B) monoclonal antibody 9A2 expressed in mouse hybridoma culture. cDNA of antibody variable regions was isolated and cloned into the human IgG1 constant region-containing antibody expression vector. CHO cells were grown in a mix of two serum-free growth media, the CD CHO Medium (Gibco®, Carlsbad, CA) and the 293 SFM II Medium (Gibco®). Final concentration of IgG is around 100 mg·L^{-1}. Serum-containing CHO cell culture supernatants containing anti-human interleukin-8 (anti-IL-8) monoclonal antibodies were produced in-house by a CHO DP-12 clone#1934 (ATCC CRL-12445) using DHFR minus/methotrexate selection system, obtained from the American Type Culture Collection (LGC Standards, Middlesex, UK). CHO DP-12 cells were grown in a mixture of 75 % (v/v) of serum-free media formulated with 0.1 % Pluronic® F-68 and without L-glutamine, phenol red, hypoxanthine, or thymidine (ProCHO™5, Lonza Group Ltd, Belgium), and 25 % (v/v) of Dulbecco's modified Eagle's medium (DMEM), supplemented with 10 % (v/v) of ultra-low IgG fetal bovine serum (FBS). ProCHO™5 formulation contains 4 mmol·L^{-1} L-glutamine (Gibco®, Carlsbad, CA), 2.1 g·L^{-1} NaHCO$_3$ (Sigma–Aldrich), 10 mg·L^{-1} recombinant human insulin (Lonza), 0.07 % (v/v) lipids (Lonza), 1 % (v/v) antibiotics (100 U·mL^{-1} penicillin and 100 μg·mL^{-1} streptomycin) (Gibco®) and 200 nmol·L^{-1} methotrexate (Sigma). DMEM was formulated to contain 4 mmol·L^{-1} of L-glutamine, 4.5 g·L^{-1} of D-glucose, 1 mmol·L^{-1} of sodium pyruvate, 1.5 g·L^{-1} of NaHCO$_3$, 2 mg·L^{-1} of recombinant human insulin, 35 mg·L^{-1} of L-proline (all acquired at Sigma), 0.1 % (v/v) of a trace element A, 0.1 % (v/v) of a trace element B (both from Cellgro®, Manassas, VA, USA), and 1 % (v/v) of antibiotics (100 U·mL^{-1} of penicillin and 100 μg·mL^{-1} of streptomycin from Gibco®). The composition of trace element A includes 1.60 mg·L^{-1} of CuSO$_4$·5H$_2$O, 863.00 mg·L^{-1} of ZnSO$_4$·7H$_2$O, 17.30 mg·L^{-1} of selenite·2Na, and 1155.10 mg·L^{-1} of ferric citrate, while the trace element B is composed of 0.17 mg·L^{-1} of MnSO$_4$·H$_2$O, 140.00 mg·L^{-1} of Na$_2$SiO$_3$·9H$_2$O, 1.24 mg·L^{-1} of molybdic acid, ammonium salt, 0.65 mg·L^{-1} of NH$_4$VO$_3$, 0.13 mg·L^{-1} of NiSO$_4$·6H$_2$O, and 0.12 mg·L^{-1} of SnCl$_2$. Cultures were carried out in T-75 flasks (BD

Three-phase partitioning systems based on aqueous biphasic systems with ionic liquids as novel strategies for the purification and recovery of antibodies

3

Falcon, Franklin Lakes, NJ) at 37 (±1) °C and 5 % CO_2 with an initial cell density of $2.1×10^6$ cells·mL^{-1}. Cell passages were performed every 4 days in a laminar flow chamber. Cell supernatants were centrifuged in BD Falcon™ tubes at 175 × g for 7 min, collected and stored at -20 °C. This culture was maintained for several months, with the mAbs concentration varying between 40.5 and 99.4 mg·L^{-1}. The produced anti-IL-8 mAb has an isoelectric point (pI) of 9.3 [33].

Other reagents used in this work were of analytical grade and used as acquired, without any further purification steps.

3.1.3.2. Methods

ABS-TPP preparation. In this work, ABS composed of PEG and $K_3C_6H_5O_7$/$C_6H_8O_7$ at pH 7 were studied, in which the top phase corresponds to the PEG-rich aqueous phase while the bottom phase is mainly composed of salt. The ternary mixture composition for the IgG recovery/purification was chosen based on the phase diagrams already reported in the literature [6]. In order to have the minimal concentration of phase-forming compounds and the maximum concentration of water (more economic and more biocompatible process), but simultaneously being in the biphasic region of the diagrams of all the polymers under study, the following mixture composition was investigated: 20 wt% PEG + 25 wt% $K_3C_6H_5O_7$/$C_6H_8O_7$ + 40 wt% human serum/cell culture supernatant + 15 wt% H_2O/IL. All partitioning studies of the quaternary systems (comprising the IL) were performed with the same extraction point, where the ILs were introduced as adjuvants at 5 wt%; for $[C_4mim]Br$, $[C_4mim]Cl$, and $[N_{4444}]Br$, concentrations of 1, 2, 10 and 15 wt% were also tested. The recovery/purification performance of human IgG in aqueous polymer-salt and polymer-salt-IL ABS-TPP was investigated using human serum 20-fold diluted in PBS (phosphate buffered saline at 10 mmol·L^{-1}, pH ≈ 7.4, at 25°C) or CHO cell culture supernatants (serum-free or serum-containing). In each system, the biological sample (human serum diluted at 1:20 (v:v) or cell culture supernatants) was loaded at 40 wt% to the phase-forming components to reach a total weight of the mixture of 2.0 g. The systems were mixed in a Vortex mixer (Ika, Staufen, Germany), centrifuged for 15 min in a fixed angle rotor bench centrifuge (Eppendorf, Hamburg, Germany) at 1372 × g, and to ensure total phase separation and interphase formation and chemical equilibrium they were settled for 30 min. After equilibrium, both phases were carefully separated using syringes to extract the top and bottom phases and their volumes were determined and also their pH values at 25 °C (± 1 °C) using a Mettler Toledo U402-M3-S7/200 micro electrode, showing that a pH of 7.0 ± 0.2 was maintained in all systems. In the cases in which an interphase precipitate was observed, i.e., for the TPP systems, the precipitate was completely isolated from the remaining phases by being

centrifugated again for a short time and high rotation (for 2 min at 12000 × g) for a facilitated removal of the remaining residues of the phases, and then resuspended in 1.0 mL of PBS. Blank systems without biological sample were also prepared to discount the interference of the phase-forming compounds in the analytical methods.

Recovery and purification of human antibodies using ABS-TPP. IgG and protein impurities were quantified in all feeds and in each ABS-TPP phase by size-exclusion high-performance liquid chromatography (SE-HPLC). Samples were diluted at a 1:2 (v:v) ratio in an aqueous potassium phosphate buffer solution (50 mmol·L^{-1}, pH 7.0, with NaCl 0.3 mol·L^{-1}) used as the mobile phase. The equipment used was a Chromaster HPLC system (VWR Hitachi) equipped with a binary pump, column oven (operating at 40 °C), temperature controlled auto-sampler (operating at 10 °C), DAD detector and a column Shodex Protein KW-802.5 (8 mm × 300 mm). The mobile phase was run isocratically with a flow rate of 0.5 mL·min^{-1} and the injection volume was 25 μL. The wavelength was set at 280 nm. The calibration curve was established with commercial human IgG, ranging from 5 to 200 mg·L^{-1}. Blank systems without biological sample were also injected to address the possible interference of the ABS phase-forming compounds.

The ABS performance was evaluated by the recovery yield and purity level for IgG. For each sample, the peaks areas were estimated using PeakFit® software, and the remaining data was treated on Excel. The recovery yield (%Yield$_{IgG}$) in the ABS top and bottom phases were determined according to the following equation:

$$\%\text{Yield}_{\text{IgG}} = \frac{[\text{IgG}]_{\text{TOP/BOT}} \times V_{\text{TOP/BOT}}}{[\text{IgG}]_{\text{initial}} \times V_{\text{initial}}} \times 100 \tag{1}$$

where [IgG]$_{TOP/BOT}$ and [IgG]$_{initial}$ represent the IgG concentration in the top or bottom phases and the initial concentration of IgG in the biological matrix (human serum or CHO cell culture supernatants), respectively, and V$_{TOP/BOT}$ and V$_{initial}$ correspond to the volumes of the top or bottom phases and biological matrix (human serum or CHO cell culture supernatants) loaded in the system, respectively.

In the cases where a precipitate of proteins at the ABS interface occurs, corresponding to the TPP approach, the %Yield$_{IgG}$ in the precipitate was determined according to the following equation:

$$\%\text{Yield}_{\text{IgG}} = \frac{[\text{IgG}]_{\text{PP}} \times V_{\text{final}}}{[\text{IgG}]_{\text{initial}} \times V_{\text{initial}}} \times 100 \tag{2}$$

where [IgG]$_{PP}$ and V$_{final}$ represent the IgG concentration and the final volume of the solution after resuspension, respectively.

Three-phase partitioning systems based on aqueous biphasic systems with ionic liquids as novel strategies for the purification and recovery of antibodies

3

The percentage purity level of IgG (%Purity$_{IgG}$) was calculated by dividing the HPLC peak area of IgG (A$_{IgG}$) by the total area of the peaks corresponding to all proteins present in the respective sample (A$_{Total}$):

$$\%\text{Purity}_{IgG} = \frac{A_{IgG}}{A_{Total}} \times 100 \tag{3}$$

A calibration curve was also established for HSA with the commercial protein, ranging from 50 to 1800 mg·L^{-1}, since HSA is the main impurity of IgG in human serum. The same performance parameters were also determined (%Yield$_{HSA}$ and %Purity$_{HSA}$) whenever indicated.

At least two individual experiments were performed to determine the average in performance parameters, as well as the respective standard deviations.

Proteins stability assessment. Circular dichroism (CD) experiments were performed to infer the stability of the secondary structure of the purified samples, using a Jasco J-1500 CD spectrophotometer. CD spectra of aqueous solutions containing 0.25 g·L^{-1} of commercial IgG, HSA and BSA in PBS (pH ≈ 7.4), human serum 400-fold diluted, cell culture supernatants and precipitates from selected TPP systems were acquired at a constant temperature of 25 °C using a scanning speed of 100 nm·min^{-1}, with a response time of 4 s over wavelengths ranging from 190 nm to 260 nm. The CD spectra of PBS (pH ≈ 7.4) was firstly taken as a blank. The recording bandwidth was of 1 nm with a step size of 0.5 nm using a quartz cell with an optical path length of 1 mm. Three scans were averaged *per* spectrum to improve the signal-to-noise ratio. Measurements were performed under a constant nitrogen flow, which was used to purge the ozone generated by the light source of the instrument. This process was carried out in triplicate to ascertain the associated standard deviations.

Host cell proteins quantification. Host cell proteins (HCP) were quantified in the precipitates (IgG-rich samples) of the TPP systems applied for the processing of serum-free CHO cell culture supernatants. The quantification was made using a CHO Host Cell Proteins 3rd Generation ELISA kit from Cygnus Technologies (Southport, NC, USA), and according with the suppliers' procedures. Briefly, both the standards (0 − 75 ng·mL^{-1}), controls and samples (50 μL) were pipetted into the well of the ELISA microplate, as well as 200 μL of anti-CHO:alkaline phosphatase, and then covered and left to incubate at 400 − 600 rpm for 120 min at room temperature. Following, the content of each well was discarded and each well was cleaned with diluted wash solution. Then, 200 μL of PNPP substrate was pipetted to each well, and the microplate was covered again and left to

incubate for 90 min at room temperature. The absorbance was finally measured at 405 and 492 nm in a BioTek SYNERGY|HT microplate reader.

3.1.4. Results and discussion

3.1.4.1. Characterization of biological media

The qualitative and quantitative characterization of the feedstocks used in this work (human serum 20-fold diluted, serum-containing and serum-free CHO cell culture supernatants) was initially performed to appraise the complexity and composition of the media from which human antibodies aimed to be purified. The SE-HPLC chromatographic profiles of IgG, BSA and biological complex media are provided in **Figure 3.1.2**.

Under the chromatographic conditions used, pure IgG samples present 2 chromatographic peaks: one corresponding to the IgG monomer and the other to IgG aggregates, with a retention time of *ca.* 15.0 min and 13.8 min, respectively, being in accordance with previous reports in the literature [32, 34]. In human serum, the major protein impurity is human serum albumin (HSA), with a retention time of *ca.* 16.8 min. The IgG content in the human serum samples was ascertained before each assay, and it was found that its average concentration was 760.3 ± 80.1 mg·L^{-1}, with an average purity of 45.2 ± 0.9 %, while for HSA, the average concentration was found to be 2723.7 ± 211.2 mg·L^{-1}, with an average purity of 54.8 ± 0.9 %.

The serum-containing cell culture supernatant presents a similar chromatographic profile to human serum – two peaks of IgG (corresponding to mAbs) are found, one corresponding to the IgG monomer and the other to IgG aggregates, at similar retention times. However, these peaks present a smaller area than the respective peaks on human serum, which is closely related with the lower concentration of IgG in the supernatant. The major protein impurity in the feed is bovine serum albumin (BSA), the closest analogue of HSA, also presenting a similar retention time. The mAbs content in the serum-containing supernatant was found to be 85.8 ± 1.2 mg·L^{-1} in average concentration, with an average purity of 21.0 ± 1.0 %.

Interestingly, serum-free cell culture supernatant presents a different chromatographic profile: in this matrix, IgG, in its monomeric form, is the main protein present, and, as expected, no peak corresponding to BSA is present (since the supernatant is serum-free, and so, free of albumin). By the chromatographic profile, it is possible to observe the presence of high molecular weight (HMW) impurities, with retention times below 15.0 min, and also some low molecular weight (LMW) impurities with retention times above 17.0 min. The mAbs content in serum-free

Three-phase partitioning systems based on aqueous biphasic systems with ionic liquids as novel strategies for the purification and recovery of antibodies

3

supernatants was determined before each assay, revealing an average concentration of 274.9 ± 2.1 mg·L^{-1}, with an average purity of 36.5 ± 0.1 %.
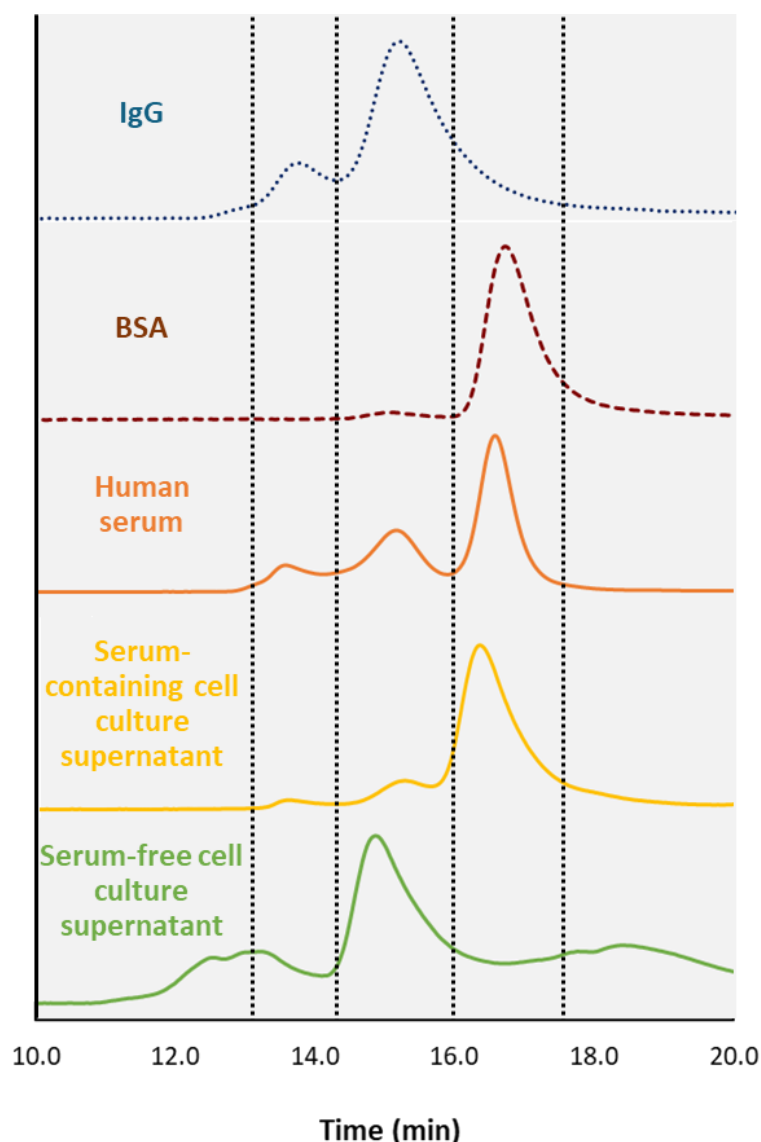
Figure 3.1.2. Characterization of the cell culture supernatants: SE-HPLC chromatograms of pure IgG solution 100 mg·L^{-1} (··), pure BSA solution 200 mg·L^{-1} (--), human serum (—), serum-containing cell culture supernatant (—), and serum-free cell culture supernatant (—).

3.1.4.2. Purification of antibodies from human serum samples

After the characterization of the IgG-containing feedstocks, the potential of TPP systems based on ABS as purification routes for human antibodies from human serum samples was addressed, and several optimizations were performed, namely through the study of three different effects: (i) PEG molecular weight, (ii) addition of ILs as adjuvants, and (iii) ILs concentration. For sake

of discussion clarity, the yields and purity levels of IgG referring to the interphase (as the final objective of a TPP system is to precipitate target molecules at the interphase) will be considered along this section; still, whenever relevant, yield and purity level at the top or bottom phases will be mentioned. Additionally, the partitioning of HSA (major protein impurity of IgG in human serum) in the systems was evaluated to provide more detailed information on the TPP selectivity.

Effect of polymer molecular weight

Firstly, the effect of the molecular weight of the phase-forming polymer was evaluated using four different PEGs, namely PEG 600, PEG 1000, PEG 1500 and PEG 2000. Based on the relative position of the binodal curves taken from the literature [6], a common mixture point was chosen in the biphasic region of all systems: 20 wt% PEG + 25 wt% $K_3C_6H_5O_7/C_6H_8O_7$ + 40 wt% human serum 20-fold diluted + 15 wt% H_2O. The performance of the ABS-TPP was investigated in terms of recovery yield (%$Yield_{IgG}$) and purity level (%$Purity_{IgG}$), whose results are shown in **Figure 3.1.3**. The detailed data on the recovery yields and purity levels are given in the **Appendix D (Table D.1)**.
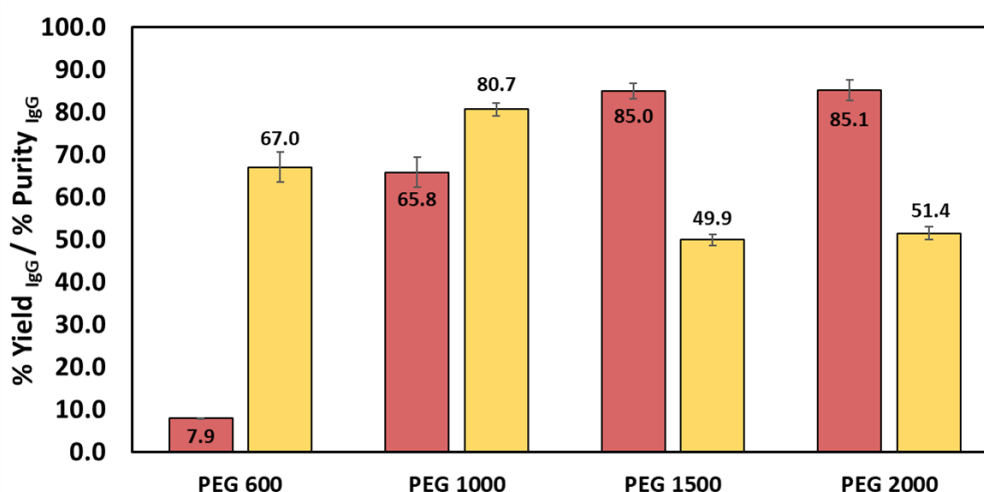
Figure 3.1.3. Recovery yields (%$Yield_{IgG}$ – ■) and purity levels (%$Purity_{IgG}$ – ■) of human IgG at the interphase of ABS-TPP composed of 20 wt% PEG + 25 wt% $K_3C_6H_5O_7/C_6H_8O_7$ + 40 wt% human serum 20-fold diluted + 15 wt% H_2O.

The results obtained for the IgG recovery indicate that, with the exception of PEG 600, there is a preferential precipitation of IgG at the interphase with yields ranging from 65.8 % and 85.1 % with PEG 1000, PEG 1500 and PEG 2000. PEGs with higher molecular weight are more hydrophobic, promoting a higher precipitation of IgG at the interphase, and following a similar molecular-level phenomenon induced by butanol in conventional TPP. In turn, PEG 600 is not a proper candidate to

Three-phase partitioning systems based on aqueous biphasic systems with ionic liquids as novel strategies for the purification and recovery of antibodies

3

develop TPP systems based on ABS for the purification of IgG from serum; instead, a preferential migration of IgG to the top phase with a yield of 85.2 % was obtained. As previously reported in literature, the basis of a given protein two-phase partitioning is dependent on hydrophobicity, electrostatic forces, molecular size, solubility, and affinity for both phases, and their magnitudes further depend on the phase compositions and on the nature of the phase-forming components [35]. If traditional ABS formed by polymers have been extensively investigated for the purification of IgG [36], the majority of TPP systems studied so far are made up with *t*-butanol and ammonium sulfate, and at the current moment there are not present studies on polymer-based TPP systems for the purification of IgG. Overall, better results are achieved with strong salting-out salts, being this a common trend in all systems investigated, and more hydrophobic polymers, i.e. of higher molecular weight, lead to a lower solubility of IgG in the PEG-rich phase and thus inducing its precipitation. According to our results, it seems that there is a balance between solubility/saturation at the PEG-rich phase and a "salting-out" effect caused by the citrate buffer to induce protein-protein interactions and respective precipitation.

Regarding the IgG purification achieved, all TPP systems provide satisfactory results ranging from 49.9 % to 80.7 %. It is interesting to notice that both PEG 1500 and PEG 2000 showed similar performance, and although allowing to obtain the best recovery yields (85.0 % and 85.1 %, respectively), both lead to the lowest purity among all polymers under study (49.9 % and 51.4 %, respectively). This observation suggests that by increasing the molecular weight of PEG, not only more IgG but also other protein are precipitated due to a reduced solubility in the PEG-rich phase, thus reducing the systems selectivity towards. On the other hand, the application of PEG 600, although allowing 67.0 % of IgG purity, is limited by very low yields of IgG at the interphase (only 7.9 %). Overall, the TPP system composed of PEG 1000 provides the best balance between IgG recovery and purification in the precipitate fraction (yield of 65.8 % with 80.7 % purity), representing an improvement of 78.5% in purity when comparing with the initial human serum sample, while HSA is mainly retained in the top (HSA yield of 70.0 %) and bottom (HSA yield of 17.7 %) phases [*cf.* **Appendix D (Table D.1)**], being thus used for further studies.

Effect of ILs as adjuvants

It has been shown that the application of ILs as adjuvants in ABS makes possible to tune the phases' polarities and affinities to target molecules, improving the limited polarity difference between phases and, thus, enhancing selectivity [6, 37]. Based on these previous findings, it has

been hypothesized that the use of ILs as adjuvants might also tune the phases' properties and improve the performance of polymer-salt TPP, particularly to purify human IgG.

To this end, six structurally different ILs were added as adjuvants at 5 wt%, namely [C$_4$mim]Br, [C$_4$mim]Cl, [N$_{4444}$]Br, [N$_{4444}$]Cl, [P$_{4444}$]Br and [P$_{4444}$]Cl, using the following mixture point: 20 wt% PEG 1000 + 25 wt% K$_3$C$_6$H$_5$O$_7$/C$_6$H$_8$O$_7$ + 40 wt% human serum 20-fold diluted + 10 wt% H$_2$O + 5 wt% IL. The ILs were chosen in order to contain different cations structures (different ILs families – imidazolium, quaternary ammonium and phosphonium-based) to cover a large hydrophobic/hydrophilic range and different types of interactions, such as dispersive forces, van der Waals, electrostatic and π ⋯ π interactions, combined with anions at extremes of hydrogen-bond basicity [38], namely bromide and chloride.

The performance of all ABS was investigated in terms of IgG recovery yield (%Yield$_{IgG}$) and purity level (%Purity$_{IgG}$) at the interphase, whose results are shown in **Figure 3.1.4**. The detailed data on the recovery yields and purity levels are given in the **Appendix D (Table D.2)**.

It is important to highlight that, although the addition of [P$_{4444}$]Br to the system resulted in the formation of a TPP with a third solid layer in its macroscopic appearance, no proteins could be detected in the SE-HPLC chromatogram, not allowing the determination of the performance parameters. This observation is in accordance with the literature, since [P$_{4444}$]Br has been reported to induce the precipitation of several proteins [39, 40], however in this work the gathered data suggests a negative impact of this IL on the proteins structure and it is not adequate to design TPP systems for human IgG (and/or other serum components, such as HSA).
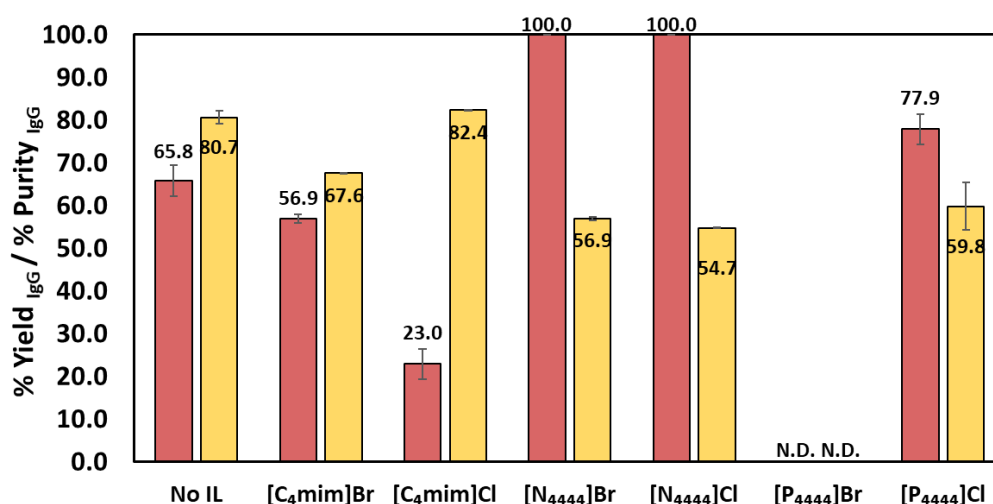
Figure 3.1.4. Recovery yields (%Yield$_{IgG}$ – ■) and purity levels (%Purity$_{IgG}$ – ■) of human IgG at the interphase of ABS-TPP composed of 20 wt% PEG 1000 + 25 wt% K$_3$C$_6$H$_5$O$_7$/C$_6$H$_8$O$_7$ + 40 wt% human serum 20-fold diluted + 10 wt% H$_2$O + 5 wt% IL. N.D. means not determined.

With the exception of [P$_{4444}$]Br and [C$_4$mim]Cl, in all the remaining ILs introduced in the system, IgG is preferentially precipitated at the interphase, with yields higher than 56.9 % and up to 100 % achieved in one-step. In fact, the introduction of a properly designed IL as adjuvant, if compared to the conventional TPP formed by polymer-salt, allowed to maximize the precipitation yield of IgG, being possible its complete recovery in the presence of 5 wt% of ammonium-based ILs (both [N$_{4444}$]Br and [N$_{4444}$]Cl). Still, [N$_{4444}$]Br allowed a slightly higher purity value to be achieved (56.9 %) than that obtained with [N$_{4444}$]Cl (purity of 54.7 %). On the other hand, when employing [C$_4$mim]Cl, it is possible to slightly increase the purity level of IgG to 82.4 %, yet compromising the recovery yield (only 23.0 %). [C$_4$mim]Br allowed an IgG recovery yield of 56.9 % and purity of 67.6 % of purity, that although being lower performance parameters than those obtained with the system without any IL, was the one among all the ILs that allowed a better balance between the yield an purity. Also, and similarly to what happens with the system in which no IL is added, 68.3 % of HSA is retained in the top phase of the system composed of [C$_4$mim]Br, with 80.4 % of purity [*cf.* **Appendix D (Table D.2)**], opening the door to the possibility to simultaneously recover and purify two different value-added proteins in a single step, i.e. IgG at the interphase and HSA at the top phase. This result is in line with the literature, where [C$_4$mim]Br exhibited remarkable selectivities in the extraction of proteins both using ABS [6] and TPP [32].

Analogously to what observed with higher molecular weight PEGs, the impact of the IL in the precipitation of IgG follows the same trend. In general, the more hydrophobic the IL, the more extensive the precipitation. [N$_{4444}$]Br, [N$_{4444}$]Cl and [P$_{4444}$]Cl possess larger cations with four butyl chains attached to the central heteroatom than [C$_4$mim]Br and [C$_4$mim]Cl, being more hydrophobic ILs and promoting an higher degree of protein-protein interactions and, thus, better precipitations at the interphase. Also, [C$_4$mim]Br allows a more extensive precipitation than [C$_4$mim]Cl, being in accordance with the hydrophobicity of these two ILs as well, once the bromide (Br$^-$) anion presents a lower hydrogen-bond basicity (β) than the chloride (Cl$^-$) anion (β (Br-) = 0.87 < β (Cl-) = 0.95 [38]), and consequently being more hydrophobic. These results show that a similar molecular-level phenomenon to conventional TPP occurs, in which a highly hydrophobic phase is required to induce a higher precipitation of proteins. In fact, Ferreira et al. [6] previously reported that ILs preferentially migrate to the PEG-rich phase in PEG + K$_3$C$_6$H$_5$O$_7$/C$_6$H$_8$O$_7$ ABS, thus justifying the increase of its hydrophobicity, and subsequent more extensive protein precipitation in the TPP systems herein studied. Nevertheless, a careful balance is required since selectivity is needed, and as such the ILs that lead to a higher precipitation extent are not the best ones since other proteins

are precipitated as well. Based on the aforementioned results and discussion, [C$_4$mim]Br, [C$_4$mim]Cl and [N$_{4444}$]Br were considered for further optimization.

The effect of the concentration of the three selected ILs was then addressed. To this end, [C$_4$mim]Br, [C$_4$mim]Cl and [N$_{4444}$]Br were added as adjuvants at 1, 2, 5, 10 and 15 wt% in systems with the following composition: 20 wt% PEG 1000 + 25 wt% K$_3$C$_6$H$_5$O$_7$/C$_6$H$_8$O$_7$ + 40 wt% human serum 20-fold diluted + 15 wt% H$_2$O/IL. The performance of all ABS was investigated in terms of IgG recovery yield (%Yield$_{IgG}$) and purity level (%Purity$_{IgG}$) at the interphase, whose results are shown in **Figure 3.1.5**. The detailed data on the recovery yields and purity levels are given in the **Appendix D (Table D.3)**.

Based on the results obtained, it was found that by changing the concentration of [C$_4$mim]Br (**Figure 3.1.5 (A)**) from 1 wt% to 10 wt%, recovery yields ranging from 56.9 % and 77.7 % and purity levels ranging between 67.6 % and 70.0 % are obtained at the interphase of the ABS-TPP. On the other hand, at high [C$_4$mim]Br concentrations (i.e., 15 wt%), a negative effect over antibodies is observed, since no peaks were found in the corresponding SE-HPLC chromatograms, thus not allowing the determination of the performance parameters. The obtained results at the interphase suggest that the most efficient concentration of [C$_4$mim]Br is the lowest under investigation (i.e., 1 wt%), yielding 77.7 % of IgG with 69.1 % of purity. Under these conditions, it should be remarked that it is to simultaneously recover HSA, the major protein impurity of IgG in human serum and that is also an added-value protein, in the top phase of the ABS, with 49.7 % yield and 89.1 % purity [*cf.* **Appendix D (Table D.3)**], and with improved purity level when compared to that obtained using the system without IL (HSA purity of 81.9 % in the ABS top phase).

Regarding the results obtained with the IL [C$_4$mim]Cl (**Figure 3.1.5 (B)**), a continuous decrease in the recovery yields of IgG as the concentration of the IL increases occurs, ranging between 6.9 % and 50.2 %; however, no significant variation in the purity levels is seen (from 79.4 % to 86.5 %). On the other hand, it is interesting to notice that the recovery yield of IgG in the top phase of the ABS increases by using higher IL concentrations. This observation suggests that [C$_4$mim]Cl possibly improves the proteins solubility in the ABS top phase and/or establish non-covalent interactions with the target protein promoting its partition to the polymer-rich top phase (the phase where the IL is also enriched), thus hampering its precipitation in the interphase. The use of 15 wt% of this IL also seems to be not appropriate for the processing of human serum proteins since a deleterious effect was found, abruptly decreasing the performance of the system.

Three-phase partitioning systems based on aqueous biphasic systems with ionic liquids as novel strategies for the purification and recovery of antibodies

3
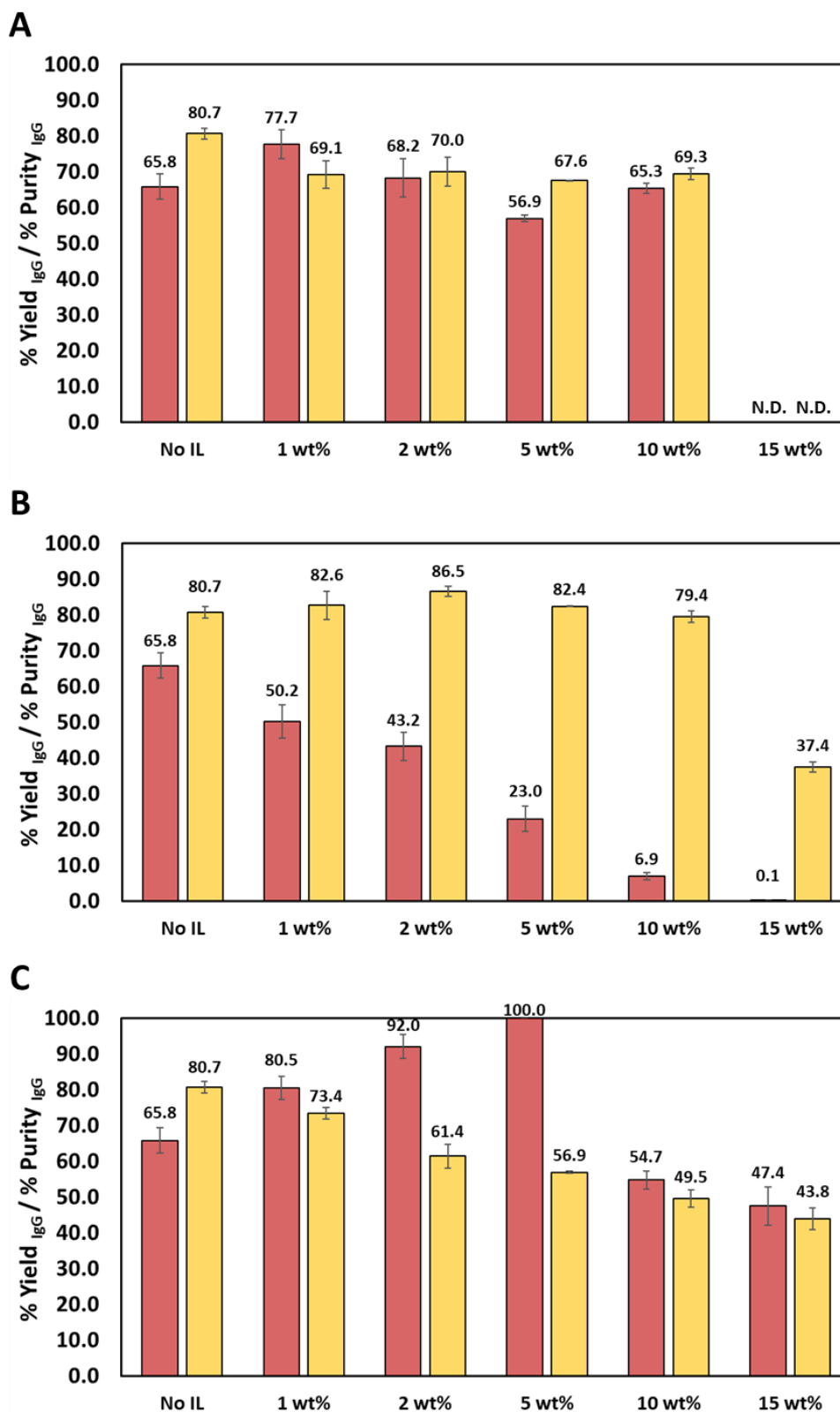
Figure 3.1.5. Recovery yields (%Yield$_{IgG}$ – ■) and purity levels (%Purity$_{IgG}$ – ■) of human IgG at the interphase of ABS/TPP composed of 20 wt% PEG 1000 + 25 wt% K$_3$C$_6$H$_5$O$_7$/C$_6$H$_8$O$_7$ + 40 wt% human serum 20-fold diluted + 15 wt% H$_2$O/IL: (A) [C$_4$mim]Br; (B) [C$_4$mim]Cl; and (C) [N$_{4444}$]Br. N.D. means not determined.

Besides this, by using 2 wt% of this IL, it was possible to recover 43.2 % of IgG with an increase in the purity level up to 86.5 %; still, just by using 1 wt% of IL, it is possible to improve the purity level up to 82.6 % with a recovery yield of 50.2 %.

Regarding the results obtained with [N$_{4444}$]Br (**Figure 3.1.5 (C)**), it is observed that using lower concentrations of IL (1, 2 and 5 wt%) allows to maximize the recovery yield of IgG in the precipitate layer from 80.5 % to 100 %, in a single-step. Higher concentrations (i.e., 10 and 15 wt%) of IL lead to a decrease in the recovery yields (54.7 % and 47.4 %, respectively), meaning that the maximum recovery performance of this system is achieved using 5 wt% of IL. In what concerns the purification performance, it was found a continuous decrease in the purity levels of IgG in the precipitate layer, ranging between 43.8 % and 73.4 %. This fact suggests that by increasing the amount of IL in the system, other proteins besides IgG start to precipitate as well, thus decreasing the system selectivity. For this reason, the best condition that allows a better compromise between yield and purity was achieved using 1 wt% of [N$_{4444}$]Br, in which 80.5 % of IgG was recovered with 73.4 % of purity.

The results herein discussed show the role of ILs as adjuvants in polymer-salt ABS acting as TPP approaches. By simply changing the IL content it is possible to maximize the yield of extraction or purity of the recovered IgG. Unfortunately, it was not possible to found any condition allowing to maximize both the recovery yield and purity level, but providing, nevertheless, some clues for high-performance ABS/TPP development. It was found that IL increasing concentrations have a negative impact on the percentage yield and purity of IgG in the interphase. The systems containing the highest amount of IL tested, i.e., 15 wt%, led to the complete loss of native IgG in the interphase or to a high decrease on its recovery yield. Therefore, it should be remarked that for ILs to be efficient adjuvants for IgG purification, not only their chemical structure, but also their concentration in TPP systems must be carefully optimized for any desired target compound. Nevertheless, it should be highlighted that lower amounts of IL are beneficial not only to the performance and selectivity of the system, but also to decrease the economic cost of the whole process.

Based on all the aforementioned information and discussed topics, the systems composed of 1 wt% of [C$_4$mim]Cl and 1 wt% of [N$_{4444}$]Br were selected as the best ILTPP platforms, allowing the best compromise between both yield and purity of IgG in the IgG-rich precipitate layer. Therefore, these systems were further studied towards the recovery and purification of monoclonal antibodies from cell cultures supernatants to infer their robustness and flexibility.

3.1.4.3. Purification of antibodies from cell culture supernatants

The best identified TPP-ABS were applied towards the recovery and purification of mAbs directly from cell culture supernatants. For that purpose, two different matrices were considered: (i) a serum-containing CHO cell culture supernatant with anti-interleukin-8 (anti-IL-8) mAbs; and (ii) a serum-free CHO cell culture supernatant with anti-hepatitis C virus (anti-HCV) mAbs. The following mixture ABS-TPP compositions were evaluated: (i) 20 wt% PEG 1000 + 25 wt% $K_3C_6H_5O_7/C_6H_8O_7$ + 40 wt% (serum-containing or serum-free) CHO cell culture supernatant + 15 wt% H_2O; (ii) 20 wt% PEG 1000 + 25 wt% $K_3C_6H_5O_7/C_6H_8O_7$ + 40 wt% (serum-containing or serum-free) CHO cell culture supernatant + 14 wt% H_2O + 1 wt% [C_4mim]Cl; and 20 wt% PEG 1000 + 25 wt% $K_3C_6H_5O_7/C_6H_8O_7$ + 40 wt% (serum-containing or serum-free) CHO cell culture supernatant + 14 wt% H_2O + 1 wt% [N_{4444}]Br.

In what concerns TPP formation, it was observed that by using serum-containing cell supernatants in the systems without IL and with 1 wt% [C_4mim]Cl, although some small particles could be found at the interphase of the ABS, the precipitation did not occur in an extension to allow a proper recovery of a third solid layer for subsequent analysis [*cf.* macroscopic aspect in **Appendix D (Figure D.1)**]. A TPP system could only be formed when using 1 wt% of [N_{4444}]Br, thus allowing to evaluate its performance. Through this TPP system, 46.2 ± 2.6 % of anti-IL-8 mAbs could be directly recovered in the precipitate layer, with a purity of 64.4 ± 4.2 %. Even though these results revealed to be lower than those obtained with the same system for human IgG from serum samples (yield of 80.5 % of IgG with 73.4 % of purity; improvement of 62.4 % in purity in comparison with the initial serum sample), they still represent a large improvement when comparing with the initial purity of the feedstock (purity of 64.4 % *vs.* 21.0 % in the initial supernatant; improvement of 206.7 % in purity in comparison with the initial supernatant). When bioprocessing human serum, the TPP composed of [N_{4444}]Br revealed an higher aptitude to precipitate proteins (leading to the highest recovery yields), being probably due to this reason that the system composed of 1 wt% of [N_{4444}]Br was the only capable to create a TPP system with serum-containing cell supernatants. These results highlight the importance of the introduction of ILs in the process, since it was only possible to create TPP system in the presence of an IL (and not in the system without IL).

On the opposite, all the systems under study were capable to create TPP systems with serum-free CHO cell culture supernatants [*cf.* macroscopic aspect in **Appendix D (Figure D.1)**]. It is interesting to notice that the serum-containing cell supernatant that presented similar chromatographic profile to that of human serum was not able to create TPP systems in all the selected conditions, but the serum-free cell supernatant that presents a completely different

protein profile was able to create TPPs in all the conditions under study. These observations suggest that the biological matrix composition plays a role in TPP system formation, i.e. depending on the effect that each protein exerts to the others in specific macromolecular crowded pools, that in this case leads to TPP systems formation only with the less complex medium. However, a higher mAbs concentration is present in the serum-free cell supernatants (274.9 mg·L^{-1} *vs.* 85.8 mg·L^{-1} in the serum-containing), suggesting that high concentrations of proteins are required to induce the formation of TPP, being in agreement with the molecular-level mechanisms of TPP formation previously discussed.

Precipitate layers enriched in anti-HCV mAbs were obtained in all systems. The performance of these systems was also investigated in terms of IgG recovery yield (%Yield$_{IgG}$) and purity level (%Purity$_{IgG}$) at the interphase, whose results are shown in **Figure 3.1.6**. The detailed data on the recovery yields and purity levels are given in the **Appendix D (Table D.4)**. These results show a very interesting performance of the TPP systems under study, with mAbs recovery yields ranging from 55.3 % to 79.7 %, and purity levels between 82.8 % and 89.2 %, being these levels much higher than the initial purity level of the cell supernant of 36.5 %.
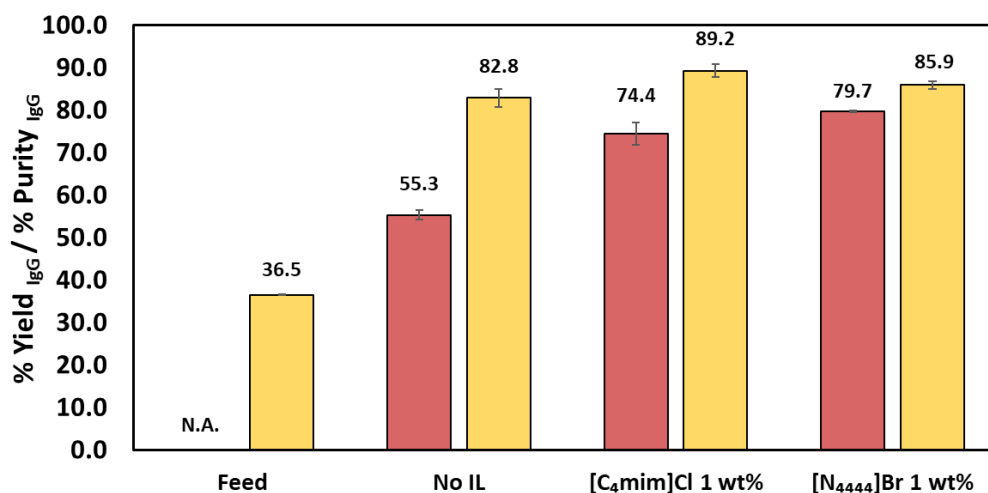
Figure 3.1.6. Recovery yields (%Yield$_{IgG}$ – ■) and purity levels (%Purity$_{IgG}$ – ■) of human IgG at the interphase of ABS/TPP composed of 20 wt% PEG 1000 + 25 wt% $K_3C_6H_5O_7/C_6H_8O_7$ + 40 wt% serum-free CHO cell culture supernatant + 15 wt% H_2O/IL. For the feed, the %Yield$_{IgG}$ is not applicable (N.A.).

The conventional ternary TPP system presents the lowest performance, yielding 55.3 % of anti-HCV mAbs with 82.8 % of purity. The purified sample was also analyzed by ELISA towards the host cell proteins (HCP) content, revealing HCP removal values of 94.7 % from the original feed. Yet, by using ILs as adjuvants, better performances of the TPP systems were obtained. By using 1 wt%

of [N$_{4444}$]Br, an increase in the recovery yield to 79.7 % with 85.9 % of purity was achieved, with 93.3 % of HCP removal comparing to the original cell supernatant. Still, the best results were obtained for the system composed of 1 wt% of [C$_4$mim]Cl, allowing to recover 74.4 % of anti-HCV mAbs with the best purity level – 89.2 %. Also, this system proved to be an efficient TPP to deplete HCPs (100 % HCP removal), since the results obtained were below the limit of detection of the method.

The SE-HPLC chromatograms of the precipitates of the systems discussed are presented in **Appendix D (Figure D.2 (A) to (C))**, as well as the representative chromatograms of the coexisting phases of the best TPP system containing 1 wt% of [C$_4$mim]Cl in **Appendix D (Figure D.2 (D))**. The analysis of the SE-HPLC chromatograms shows the high purities allowed by the TPP systems under study, since the main peak present corresponds to mAbs (retention time of *ca.* 15.0 min); only a small peak is noticed, corresponding to HMW impurities (or IgG aggregates). It is also interesting to notice that the remaining IgG that is not recovered in the precipitate fraction seems to partition to the polymer PEG-rich phase with the majority of the LMW protein impurities. On the other hand, HMW protein impurities seems to be preferentially retained in the opposite layer, the salt-rich phase.

Finally, circular dichroism (CD) spectroscopy was used to analyze the secondary structure of mAbs after recovery and purification using TPP systems. The spectrum of a standard solution of IgG 250 mg·L^{-1} was also measured and included for comparison purposes. The CD spectra depicted in **Figure 3.1.7** clearly shows that the secondary structure of mAbs after the recovery procedure, and for all systems, is similar to the one of the freshly prepared solution of IgG. All spectra exhibit typical shape of a β-sheet protein as IgG, with a characteristic maximum of negative ellipticity at *ca.* 216 nm [41]. Thus, it is possible to conclude that after the recovery of mAbs with the investigated ABS-TPP, the conformation is not affected, and the recovered proteins maintain their secondary structure.

The available literature on TPP based on ABS for the recovery and purification of antibodies is scarce. Indeed, to the best of our knowledge, one report refers to the use of this technique towards the recovery of avian antibodies (IgY) from chicken egg yolk [42], and another work refers to the recovery and purification of human mAbs [32], but using an IL-based TPP. Capela et al. [32] showed that ABS-TPP composed of glycine-betaine analogues ILs and K$_2$HPO$_4$/KH$_2$PO$_4$ at pH 7.0 allow a recovery of 41.0 % with 60.9 % purity. In this work, the results obtained surpass those previously reported in the literature, since a mAbs recovery yield of 74.4 % with 89.2 % purity was

achieved, using the IL as adjuvant (and not as phase-forming component), which brings additional advantages regarding the reduction of the costs of the process.
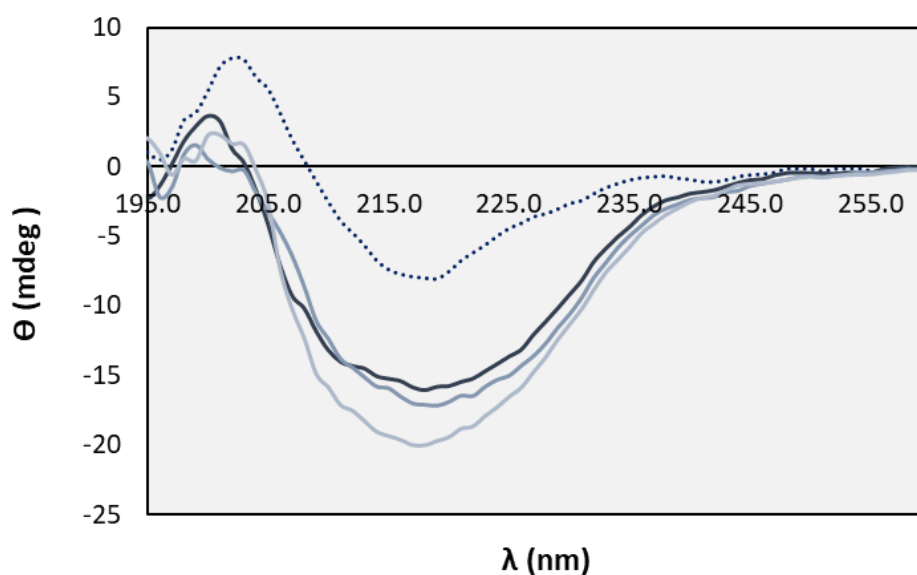
Figure 3.1.7. Circular dichroism (CD) spectra (ellipticity, θ, in mdeg) for the recovered mAbs-rich precipitate fractions of the TPP/ABS composed of 20 wt% PEG 1000 + 25 wt% $K_3C_6H_5O_7/C_6H_8O_7$ + 40 wt% serum-free CHO cell culture supernatant + 15 wt% H_2O/IL: pure IgG solution 250 mg·L^{-1} in PBS (··), TPP with no IL (—), TPP with 1 wt% [N_{4444}]Br (—), TPP with 1 wt% [C_4mim]Cl (—).

Besides the works reporting TPP approaches based on ABS, it is also interesting to understand how the results obtained in this work compare with those obtained with their parent ABS (not TPP). Indeed, large efforts have been carried out with more traditional polymer-based ABS to purify antibodies, as previously reviewed by us [1]; yet, the IgG recovery and purification results gathered in this work with TPP/ABS are better than those reported up to date using conventional ABS. In the field of IL-based ABS, Ferreira et al. [6] studied polymer-salt ABS composed of commercial ILs as adjuvants, achieving the complete IgG extraction to the polymer-rich phase, but with a lower purity (26 %); in this work, although the complete recovery of IgG was not achieved, IgG could be recovered with purity values of up to 89.2 %. Also, the previous work was carried out with mammal's serum samples, where in this work the use of ILs as adjuvants in polymer-salt ABS allowed the creation of TPP systems for human antibodies recovery/purification from both human serum and CHO cell culture supernatants. The developed TPP strategy is robust, since different antibodies (pAbs, anti-IL-8 mAbs and anti-HCV mAbs) could be successfully recovered and purified from different matrices (human serum and serum-containing and serum-free CHO cell cultures supernatants).

Three-phase partitioning systems based on aqueous biphasic systems with ionic liquids as novel strategies for the purification and recovery of antibodies

3

Although there is still room for improvement and a path to follow to fully explore the potential of TPP based on ABS, it is here shown that this combination is highly advantageous to the recovery and purification of proteins from real and complex biological matrices, particularly for antibodies. The addition of ILs to TPP-ABS also brings advantages to the process in terms of selectivity and performance parameters improvement due to their designer solvent feature. Thus, high yields of proteins with high purity can be easily collected at the interface of the system, and further conditioned in an adequate buffered aqueous solution for storage.

3.1.5. Conclusions

The present work aimed to develop an alternative and cost-efficient approach for the recovery and purification of human antibodies from biological complex matrices using TPP based in ABS. ABS-TPP composed of PEG 1000 + $K_3C_6H_5O_7/C_6H_8O_7$ pH 7 + H_2O were studied for the recovery and purification of IgG from human serum samples, being optimized by: (i) the effect of the polymer molecular weight; (ii) the introduction of ILs with different chemical structures; and (iii) the effect of the concentration of IL. All the investigated systems allowed the formation of an IgG-rich precipitate layer, with the best performance being achieved with systems composed of intermediate PEG molecular weight (PEG 1000) and also by using low amounts (just 1 wt%) of [C_4mim]Cl and [N_{4444}]Br ILs. Under the optimal conditions, recovery yields of IgG from human serum could be maximized to 80.5 % and purity levels of 82.6 % could be achieved.

The best systems were investigated for the recovery and purification of mAbs directly from cell culture supernatants. It was observed an influence of the molecular crowding effect of the matrices and of the effect of the chemical structure of the IL. For the serum-containing CHO cell culture supernatant with anti-IL-8 mAbs, only the system composed of 1 wt% of [N_{4444}]Br was able to create a TPP system, yielding 46.2 % of mAbs with a purity of 64.4 %. For serum-free CHO cell culture supernatant with anti-HCV mAbs, that also presented higher IgG concentration, all the systems under study were able to create TPP systems. The best results were achieved with the system composed of 1 wt% of [C_4mim]Cl, in which a recovery yield of 74.4 % of mAbs was observed with 89.2 % of purity, and exceptional HCP removal – 100 %. The stability of the recovered antibodies was proved by CD spectroscopy.

Overall, it is herein shown that ABS-TPP is a promising combination of techniques to recover and purify proteins from real complex biological matrices, particularly antibodies, in a single-step approach. The developed process proved to be robust for the successful recovery and purification of different antibodies (pAbs, anti-IL-8 and anti-HCV mAbs) from different matrices (human serum

samples, serum-containing and serum-free CHO cell cultures supernatants), allowing high recovery yields and purity levels to be achieved, being easy to recover the protein of interest and resuspend it in an appropriate final buffered formulation for storage and further commercialization.

3.1.6. References

1.   E.V. Capela, M.R. Aires-Barros, M.G. Freire, and A.M. Azevedo, *Monoclonal Antibodies– Addressing the Challenges on the Manufacturing Processing of an Advanced Class of Therapeutic Agents.* Frontiers in Clinical Drug Research-Anti Infectives: Volume 4, 2017. **4**: p. 142.

2.   A. Hey, *History and practice: antibodies in infectious diseases.* Microbiology Spectrum, 2015. **3**: p. AID-0026-2014.

3.   P. Rosa, I. Ferreira, A. Azevedo, and M. Aires-Barros, *Aqueous two-phase systems: a viable platform in the manufacturing of biopharmaceuticals.* Journal of Chromatography A, 2010. **1217**(16): p. 2296-2305.

4.   H.B. Dickler and E.W. Gelfand, *Current perspectives on the use of intravenous immunoglobulin.* Advances in internal medicine, 1996. **41**: p. 641.

5.   U. Katz, A. Achiron, Y. Sherer, and Y. Shoenfeld, *Safety of intravenous immunoglobulin (IVIG) therapy.* Autoimmunity reviews, 2007. **6**(4): p. 257-259.

6.   A.M. Ferreira, V.F. Faustino, D. Mondal, J.A.P. Coutinho, and M.G. Freire, *Improving the extraction and purification of immunoglobulin G by the use of ionic liquids as adjuvants in aqueous biphasic systems.* Journal of Biotechnology, 2016. **236**: p. 166-175.

7.   A.L. Grilo, M. Mateus, M.R. Aires-Barros, and A.M. Azevedo, *Monoclonal antibodies production platforms: an opportunity study of a non-protein-A chromatographic platform based on process economics.* Biotechnology Journal, 2017. **12**(12): p. 1700260.

8.   O. Yang, M. Qadan, and M. Ierapetritou, *Economic analysis of batch and continuous biopharmaceutical antibody production: a review.* Journal of Pharmaceutical Innovation, 2019. **15**: p. 182–200.

9.   M. Iqbal, Y. Tao, S. Xie, Y. Zhu, D. Chen, X. Wang, L. Huang, D. Peng, A. Sattar, and M.A.B. Shabbir, *Aqueous two-phase system (ATPS): an overview and advances in its applications.* Biological Procedures Online, 2016. **18**(1): p. 1-18.

10.   E.V. Capela, J.H. Santos, I. Boal-Palheiros, J.A.P. Coutinho, S.P. Ventura, and M.G. Freire, *A simple approach for the determination and characterization of ternary phase diagrams of aqueous two-phase systems composed of water, polyethylene glycol and sodium carbonate.* Chemical Engineering Education, 2019. **53**(2): p. 112.

Three-phase partitioning systems based on aqueous biphasic systems with ionic liquids as novel strategies for the purification and recovery of antibodies

3

11.   M.G. Freire, A.F.M. Claudio, J.M.M. Araújo, J.A.P. Coutinho, I.M. Marrucho, J.N.C. Lopes, and L.P.N. Rebelo, *Aqueous biphasic systems: a boost brought about by using ionic liquids.* Chemical Society Reviews, 2012. **41**(14): p. 4966-4995.

12.   T. Lu, Z. Li, J. Huang, and H. Fu, *Aqueous surfactant two-phase systems in a mixture of cationic gemini and anionic surfactants.* Langmuir, 2008. **24**(19): p. 10723-10728.

13.   E.V. Capela, M.V. Quental, P. Domingues, J.A.P. Coutinho, and M.G. Freire, *Effective separation of aromatic and aliphatic amino acid mixtures using ionic-liquid-based aqueous biphasic systems.* Green Chemistry, 2017. **19**(8): p. 1850-1854.

14.   M.V. Quental, M.M. Pereira, A.M. Ferreira, S.N. Pedro, S. Shahriari, A. Mohamadou, J.A.P. Coutinho, and M.G. Freire, *Enhanced separation performance of aqueous biphasic systems formed by carbohydrates and tetraalkylphosphonium-or tetraalkylammonium-based ionic liquids.* Green Chemistry, 2018. **20**(13): p. 2978-2983.

15.   E.V. Capela, A.I. Valente, J.C. Nunes, F.F. Magalhães, O. Rodríguez, A. Soto, M.G. Freire, and A.P. Tavares, *Insights on the laccase extraction and activity in ionic-liquid-based aqueous biphasic systems.* Separation and Purification Technology, 2020. **248**: p. 117052.

16.   K.W. Chew, T.C. Ling, and P.L. Show, *Recent developments and applications of three-phase partitioning for the recovery of proteins.* Separation & Purification Reviews, 2019. **48**(1): p. 52-64.

17.   V. Dobreva, B. Zhekova, and G. Dobrev, *Use of aqueous two-phase and three-phase partitioning systems for purification of lipase obtained in solid-state fermentation by Rhizopus arrhizus.* The Open Biotechnology Journal, 2019. **13**(1): p. 27-36.

18.   H. Bayraktar and S. Önal, *Concentration and purification of α-galactosidase from watermelon (Citrullus vulgaris) by three phase partitioning.* Separation and Purification Technology, 2013. **118**: p. 835-841.

19.   S. Rawdkuen, A. Vanabun, and S. Benjakul, *Recovery of proteases from the viscera of farmed giant catfish (Pangasianodon gigas) by three-phase partitioning.* Process Biochemistry, 2012. **47**(12): p. 2566-2569.

20.   S. Gautam, P. Dubey, P. Singh, R. Varadarajan, and M.N. Gupta, *Simultaneous refolding and purification of recombinant proteins by macro-(affinity ligand) facilitated three-phase partitioning.* Analytical Biochemistry, 2012. **430**(1): p. 56-64.

21.   R. Borbás, B.S. Murray, and É. Kiss, *Interfacial shear rheological behaviour of proteins in three-phase partitioning systems.* Colloids and Surfaces A: Physicochemical and Engineering Aspects, 2003. **213**(1): p. 93-103.

22.   S. Ketnawa, S. Benjakul, O. Martínez-Alvarez, and S. Rawdkuen, *Three-phase partitioning and proteins hydrolysis patterns of alkaline proteases derived from fish viscera.* Separation and Purification Technology, 2014. **132**: p. 174-181.

23.   T. Senphan and S. Benjakul, *Use of the combined phase partitioning systems for recovery of proteases from hepatopancreas of Pacific white shrimp.* Separation and Purification Technology, 2014. **129**: p. 57-63.

24.   R. Borbás, É. Kiss, and M. Nagy, *Elastic properties of protein gels obtained by three-phase partitioning*, in *Adsorption and Nanostructure*. 2001, Springer. p. 189-194.

25.   S. Sharma and M. Gupta, *Purification of phospholipase D from Dacus carota by three-phase partitioning and its characterization.* Protein Expression and Purification, 2001. **21**(2): p. 310-316.

26.   H.S. Choonia and S. Lele, *Three phase partitioning of β-galactosidase produced by an indigenous Lactobacillus acidophilus isolate.* Separation and Purification Technology, 2013. **110**: p. 44-50.

27.   J. Simental-Martínez, M. Rito-Palomares, and J. Benavides, *Potential application of aqueous two-phase systems and three-phase partitioning for the recovery of superoxide dismutase from a clarified homogenate of K luyveromyces marxianus.* Biotechnology Progress, 2014. **30**(6): p. 1326-1334.

28.   D.C. Belchior and M.G. Freire, *Simultaneous separation of egg white proteins using aqueous three-phase partitioning systems.* Journal of Molecular Liquids, 2021. **336**: p. 116245.

29.   E. Alvarez-Guerra and A. Irabien, *Ionic liquid-based three phase partitioning (ILTPP) for lactoferrin recovery.* Separation Science and Technology, 2014. **49**(7): p. 957-965.

30.   E. Alvarez-Guerra and A. Irabien, *Ionic liquid-based three phase partitioning (ILTPP) systems for whey protein recovery: ionic liquid selection.* Journal of Chemical Technology & Biotechnology, 2015. **90**(5): p. 939-946.

31.   L.S. Castro, P. Pereira, L.A. Passarinha, M.G. Freire, and A.Q. Pedro, *Enhanced performance of polymer-polymer aqueous two-phase systems using ionic liquids as adjuvants towards the purification of recombinant proteins.* Separation and Purification Technology, 2020. **248**: p. 117051.

32.   E.V. Capela, A.E. Santiago, A.F.C.S. Rufino, A.P.M. Tavares, M.M. Pereira, A. Mohamadou, M.R. Aires-Barros, J.A.P. Coutinho, A.M. Azevedo, and M.G. Freire, *Sustainable strategies based on glycine–betaine analogue ionic liquids for the recovery of monoclonal antibodies from cell culture supernatants.* Green Chemistry, 2019. **21**(20): p. 5671-5682.

Three-phase partitioning systems based on aqueous biphasic systems with ionic liquids as novel strategies for the purification and recovery of antibodies

3

33.   R. dos Santos, S.A.L.S. Rosa, M.R. Aires-Barros, A. Tover, and A.M. Azevedo, *Phenylboronic acid as a multi-modal ligand for the capture of monoclonal antibodies: development and optimization of a washing step.* Journal of Chromatography A, 2014. **1355**: p. 115-124.

34.   C.C. Ramalho, C.M.S.S. Neves, M.V. Quental, J.A.P. Coutinho, and M.G. Freire, *Separation of immunoglobulin G using aqueous biphasic systems composed of cholinium-based ionic liquids and poly (propylene glycol).* Journal of Chemical Technology & Biotechnology, 2018. **93**(7): p. 1931-1939.

35.   J.F.B. Pereira and J.A.P. Coutinho, *Aqueous two-phase systems*, in *Liquid-Phase Extraction*. 2020, Elsevier. p. 157-182.

36.   E.V. Capela, M.R. Aires-Barros, M.G. Freire, and A.M. Azevedo, *Monoclonal antibodies — addressing the challenges on the manufacturing processing of an advanced class of therapeutic agents*, in *Frontiers in Clinical Drug Research - Anti-Infectives*, Atta-ur-Rahman, Editor. 2017, Bentham Science p. 142-203.

37.   M.R. Almeida, H. Passos, M.M. Pereira, Á.S. Lima, J.A.P. Coutinho, and M.G. Freire, *Ionic liquids as additives to enhance the extraction of antioxidants in aqueous two-phase systems.* Separation and Purification Technology, 2014. **128**: p. 1-10.

38.   A.F.M. Cláudio, L. Swift, J.P. Hallett, T. Welton, J.A.P. Coutinho, and M.G. Freire, *Extended scale for the hydrogen-bond basicity of ionic liquids.* Physical Chemistry Chemical Physics, 2014. **16**(14): p. 6593-6601.

39.   J.F.B. Pereira, Á.S. Lima, M.G. Freire, and J.A.P. Coutinho, *Ionic liquids as adjuvants for the tailored extraction of biomolecules in aqueous biphasic systems.* Green Chemistry, 2010. **12**(9): p. 1661-1669.

40.   M.M. Pereira, S.N. Pedro, M.V. Quental, Á.S. Lima, J.A.P. Coutinho, and M.G. Freire, *Enhanced extraction of bovine serum albumin with aqueous biphasic systems of phosphonium-and ammonium-based ionic liquids.* Journal of Biotechnology, 2015. **206**: p. 17-25.

41.   L. Borlido, A.M. Azevedo, and M.R. Aires-Barros, *Extraction of human IgG in thermo-responsive aqueous two-phase systems: assessment of structural stability by circular dichroism.* Separation Science and Technology, 2010. **45**(15): p. 2171-2179.

42.   B. Priyanka, K. Abhijith, N.K. Rastogi, K. Raghavarao, and M. Thakur, *Integrated approach for the extraction and purification of IgY from chicken egg yolk.* Separation Science and Technology, 2014. **49**(4): p. 562-568.

Purification of Antibodies using Supported Ionic Liquid Materials

4

4.1. Novel downstream routes for the purification of antibodies using supported ionic liquid materials

This chapter is based on the manuscript under preparation with

<u>*Emanuel V. Capela*</u>, *Jéssica Bairos, Márcia C. Neves, M. Raquel Aires-Barros, João A.P. Coutinho,*

Ana M. Azevedo, Ana P.M. Tavares, Mara G. Freire

4.1.1. Abstract

Over the past few years, antibodies such as immunoglobulin G, IgG, have gained high interest as promising alternative therapeutics. Despite their large potential, their production with high quality and purity levels is still costly due to the absence of a cost-effective extraction-purification platform for the recovery of these biopharmaceuticals from the complex biological media in which they are present. The downstream processing of IgG is being considered the limiting and most costly step in the production of these biopharmaceuticals. The "gold standard" platform adopted by the biopharmaceutical industry counts with multiple steps, mostly recurring to chromatography. In particular, a primary antibody capture step by protein A affinity chromatography is used, being extremely costly due to the required biological affinity ligand (ProA). This work investigated novel materials employing ionic liquids (ILs) as chemical ligands, leading to the creation of ionic liquid materials as alternative matrices for the capture and/or purification of antibodies from complex biological matrices. The operating conditions of the process were optimized towards the extraction/purification of human IgG from serum samples, in terms of the solid:liquid ratio (S:L ratio), pH and contact time (t), in order to maximize the process performance parameters. The best results allowed to obtain 59 % and 76 % IgG yields with 84 % and 100 % purity levels, respectively. These results are obtained with different IL chemical structures, acting in a "flowthrough-like mode" or "bind-and-elute-like mode", further demonstrating the chemical versatility of ILs as chemical ligands and flexibility of the developed materials. The best conditions were finally applied to other IgG-containing matrices, namely rabbit serum and Chinese hamster ovary cell culture supernatants, proving the robustness of the developed strategy. Two new cost-effective strategies for antibodies

---

downstream processing have been developed, representing a steppingstone towards the use of ILs as potential cheaper chemical ligands for chromatography-based platforms used in the biopharmaceutical field.

4.1.2. Introduction

In a time where the efficacy of conventional drugs is decreasing and population is aging, the biopharmaceuticals market is currently one of the fastest growing segments of the pharmaceutical industry [1]. In recent decades, technological advances in bioprocess engineering have been made in the field of biopharmaceuticals due to their high sensitivity, specificity and low risk and low adverse effects to the patient [2]. In this context, therapies based on polyclonal (pAbs) and monoclonal (mAbs) antibodies have emerged. Plasma-derived human IgG (e.g. polyvalent intravenous immunoglobulins, IVIGs) are increasingly used for the treatment of genetic and acquired immunodeficiencies and for several inflammatory and autoimmune disorders (e.g. thrombocytopenic purpura, Kawasaki disease, polymyositis/dermatomyositis, Guillain-Barré syndrome, among others) [3, 4]. Regarding mAbs, in May 2021 the US Food and Drug Administration approved the 100th mAb product [5], 35 years after the first mAbs approval, accounting nowadays for almost a fifth of the FDA's new drug approvals each year. mAbs present a high potential for different applications, such as immunotherapy and, in particular, for the treatment of several diseases such as cancer, transplant rejection, inflammatory and autoimmune diseases [6]. In order to be used in these applications, antibodies must be produced under harsh conditions, and must meet standards of safety, efficacy, potency and purity [7].

Several advances were registered in the past years regarding the upstream processing of antibodies improving its productivity; however, improvements in the downstream processing have been neglected since the biopharmaceuticals industries are unwilling to replace well-established processes [8]. Thus, the downstream processing is now considered the bottleneck in antibodies production, accounting for up to 80 % of the total production costs [9]. The traditional downstream scheme used by the biopharmaceutical industry usually includes multiple steps for the recovery, isolation, purification and polishing, including several chromatographic unit operations [10]. Particularly, the selective capture and purification steps, largely dominated by chromatography, accounts with more of 70 % of the downstream total costs [8]. Among these chromatographic steps, affinity chromatography using protein A (proA) as an affinity biological ligand is the "gold standard" of the pharmaceutical industry for the capture and purification of antibodies, representing the largest fraction of the costs of the chromatographic steps required.

Besides the non-chromatographic methods that could be valuable alternatives for the downstream processing of antibodies [6], several chromatographic platforms have been proposed during the last years, including cation exchange chromatography [11, 12], anion exchange chromatography [13], hydrophobic interaction chromatography [14], multimodal chromatography [15, 16], immobilized metal affinity chromatography [17], expanded bed adsorption chromatography [18], continuous annular chromatography [19] and affinity chromatography [20, 21]. Also, mimetic resins can also be considered as potential alternatives to proA chromatography, for instance matrices that specifically bind IgG such as protein G and L, synthetic ligands, proA-like porous polymeric monoliths or bioengineered peptides [22-25], in which the research group of Roque and collaborators have highly contributed [26-38]. Nevertheless, the development of simpler and cost-efficient techniques capable to separate, extract and purify antibodies and other proteins with relevance for the peoples' health is still of upmost importance.

Based on the exposed, supported ionic liquids (SILs) can be seen as a potential alternative class of materials to be employed in capture/purification processes [39-42]. Ionic liquids (ILs) are salts, usually composed of a large organic cation and by a smaller organic or inorganic anion [43]. Most neat ILs present interesting features, such as low vapour pressure, negligible volatility, high thermal stability and high polarity [39, 43]; still, their main advantage in the field of separation is their "designer solvent" ability and consequent possibility of manipulating their cation/anion combination to improve extraction performance and selectivity. This important property is also featured in SILs, since ILs are the functional groups of a matrix (in which they are covalently bound), allowing different interactions to be established between the target compounds and the solid support, ultimately leading to increased selectivity when processing complex biological matrices.

The vast majority of SILs investigated up to date have been applied as enzymatic supports [44] or in the capture of gases [45]. In addition to these applications, SILs have been reported for the separation of various molecules, such as inorganic/organic anions [46-48], metals [42, 49, 50] and small organic molecules [51, 52]. Despite their relevance in bioprocessing, few works are still found in the extraction/separation of biomolecules, such as proteins [53-55]. Shu et al. [53] reported an ionic liquid–polyvinyl chloride based on *N*-methylimidazole capable to successfully adsorb lysozyme, cytochrome c and haemoglobin, with yields of 97 %, 98 % and 94 %, respectively, while the adsorption capacity for acidic proteins such as IgG, BSA and transferrin was negligible. All these studies were carried out with model protein solutions. Even though the material was finally applied to the extraction of haemoglobin from human whole blood, the authors did not provide the purity levels obtained [53]. In the same line, Zhao et al. [54] successfully demonstrated the use of

imidazolium-modified polystyrene (*N*-methylimidazole and crosslinked chloromethyl polystyrene resin) for the extraction of cytochrome c from horse heart and bovine haemoglobin with yields of 93 % and 91 %, respectively, while the retention of other proteins (IgG, BSA and transferrin) was negligible. Also, the material was applied to the extraction of haemoglobin from human whole blood; however, no purity levels were provided [54]. More recently, Song et al. [55] used an imidazolium hydrogen sulfate modified silica gel for the extraction/purification of BSA from cow's blood, achieving 28 % of yield and a purity of 91 %. The mentioned works highlight the potential of SILs to recover proteins [53-55]. Nevertheless, only one work [55] gives indication regarding the selectivity/performance of the studied materials when applied to real and complex matrices, in which a large number of proteins and other metabolites are present.

Despite the success of SILs in the processing of (bio)molecules, to the best of our knowledge, their application in the development of downstream processes for antibodies was never reported in the literature up to date. In this work, silica material was functionalized with three ILs, the materials were chemically and morphologically characterized, and finally evaluated as alternative adsorbents for the capture and purification of human antibodies from serum samples. The process was optimized in terms of solid: liquid ratio, pH and contact time in order to develop cost-effective strategies. Finally, the best conditions were also applied to other different IgG-containing matrices (rabbit serum and Chinese hamster ovary cell culture supernatants) to demonstrate the feasibility of the developed SIL-based platforms to bioprocess other matrices.

4.1.3. Experimental section

4.1.3.1. Materials

The chemicals used for the activation of silica (used as supporting material) were silica gel (60 Å) with a particle size of 0.2-0.5 nm (35-70 mesh ASTM) from Merck and hydrochloric acid (HCl, purity 37 wt%) from Sigma-Aldrich. The solvents used to prepare the IL-functionalized silica were toluene (99.98 % purity) and ethanol (99.99 % purity) both from Fisher Scientific; methanol (99.99 % purity) from Fisher Chemical; (3-chloropropyl)trimethoxysilane (98 % purity), *N*-methylimidazole (99 % purity), tributylamine (99 % purity) provided by Acros Organics; and trioctylamine (> 98 % purity) acquired from Fluka.

For the HPLC mobile phase, the following salts were used: anhydrous monobasic sodium phosphate (99 - 100.5 % purity), sodium phosphate dibasic heptahydrate (98 - 102 % purity), and sodium chloride (99.5 % purity), all provided by Panreac.

The biologicals used in this work were human IgG for therapeutic administration (trade name: Gammanorm®), obtained from Octapharma (Lachen, Switzerland), as a 165 mg·mL^{-1} solution; HSA (96 % purity) provided by Alfa Aesar; human serum from human male AB plasma, USA origin, sterile-filtered, obtained from Sigma-Aldrich (H4522 Sigma) (≥ 95.0 % purity); rabbit serum (containing 0.01 % of thimerosal) unconjugated and pooled from a normal donor population, also purchased from Sigma-Aldrich. The CHO cell culture supernatant containing anti-human interleukin-8 (anti-IL-8) monoclonal antibodies were produced in-house by a CHO DP-12 clone#1934 (ATCC CRL-12445) using DHFR minus/methotrexate selection system, obtained from the American Type Culture Collection (LGC Standards, Middlesex, UK). CHO DP-12 cells were grown in a mixture of 75 % (v/v) of serum-free media formulated with 0.1 % Pluronic® F-68 and without L-glutamine, phenol red, hypoxanthine, or thymidine (ProCHO™5, Lonza Group Ltd, Belgium), and 25 % (v/v) of Dulbecco's modified Eagle's medium (DMEM), supplemented with 10 % (v/v) of ultra-low IgG fetal bovine serum (FBS). ProCHO™5 formulation contains 4 mmol·L^{-1} L-glutamine (Gibco®, Carlsbad, CA), 2.1 g·L^{-1} NaHCO$_3$ (Sigma–Aldrich), 10 mg·L^{-1} recombinant human insulin (Lonza), 0.07 % (v/v) lipids (Lonza), 1 % (v/v) antibiotics (100 U·mL^{-1} penicillin and 100 μg·mL^{-1} streptomycin) (Gibco®) and 200 nmol·L^{-1} methotrexate (Sigma). DMEM was formulated to contain 4 mmol·L^{-1} of L-glutamine, 4.5 g·L^{-1} of D-glucose, 1 mmol·L^{-1} of sodium pyruvate, 1.5 g·L^{-1} of NaHCO$_3$, 2 mg·L^{-1} of recombinant human insulin, 35 mg·L^{-1} of L-proline (all acquired at Sigma), 0.1 % (v/v) of a trace element A, 0.1 % (v/v) of a trace element B (both from Cellgro®, Manassas, VA, USA), and 1 % (v/v) of antibiotics (100 U·mL^{-1} of penicillin and 100 μg·mL^{-1} of streptomycin from Gibco®). The composition of trace element A includes 1.60 mg·L^{-1} of CuSO$_4$·5H$_2$O, 863.00 mg·L^{-1} of ZnSO$_4$·7H$_2$O, 17.30 mg·L^{-1} of selenite·2Na, and 1155.10 mg·L^{-1} of ferric citrate, while the trace element B is composed of 0.17 mg·L^{-1} of MnSO$_4$·H$_2$O, 140.00 mg·L^{-1} of Na$_2$SiO$_3$·9H$_2$O, 1.24 mg·L^{-1} of molybdic acid, ammonium salt, 0.65 mg·L^{-1} of NH$_4$VO$_3$, 0.13 mg·L^{-1} of NiSO$_4$·6H$_2$O, and 0.12 mg·L^{-1} of SnCl$_2$. Cultures were carried out in T-75 flasks (BD Falcon, Franklin Lakes, NJ) at 37 (±1) °C and 5 % CO$_2$ with an initial cell density of 2.1×10^6 cells·mL^{-1}. Cell passages were performed every 4 days in a laminar flow chamber. Cell supernatants were centrifuged in BD Falcon™ tubes at 175 × g for 7 min, collected and stored at -20 °C. This culture was maintained for several months, with the mAbs concentration varying between 40.5 and 99.4 mg·L^{-1}. The produced anti-IL-8 mAb has an isoelectric point (pI) of 9.3 [56].

Other reagents used in this work were of analytical grade and used as acquired, without any further purification steps.

4.1.3.2. Methods

Synthesis of SIL materials. Three different SIL materials were herein synthesized, namely a 1-methyl-3-propylimidazolium-based supported silica with chloride as the counter ion ([Si][C$_3$mim]Cl), a propyltributylammonium-based supported silica with chloride as the counter ion ([Si][N$_{3444}$]Cl) and a propyltrioctylammonium-based supported silica with chloride as the counter ion ([Si][N$_{3888}$]Cl). The initial step for the synthesis of the SIL materials consists in the activation of the silica gel (pore size of 60Å) with a solution of hydrochloric acid (37 wt%) for 24 h to increase the content of silanol groups on the silica surface. Subsequently, the activated silica was washed with *ca.* 2 L of distilled water, until the washing water achieves a neutral pH (pH ≈ 7), and then placed in the kiln for 24 h at 60 °C. The second step of the synthesis of SILs consists in the functionalization of the activated silica by the addition of 60 mL of toluene and 5 mL of 3-chloropropyl-trimethoxysilane to 5.0 g of activated silica. Then, the mixture was refluxed under magnetic stirring for 24 h to obtain the intermediate 3-chloropropylsilane ([Si][C$_3$]Cl). Afterwards, the obtained material was filtered and washed with 100 mL of toluene, 200 mL of 1:1 mixture of ethanol:water, 500 mL of distilled water and 100 mL of methanol, and finally dried for 24 h at 60 °C. The third step in the SILs synthesis consisted in the functionalization of the [Si][C$_3$]Cl, by mixing 5.0 g of the material with 50 mL of toluene and 5 mL of the respective cation source (*N*-methylimidazole, tributylamine or trioctylamine; *cf.* **Figure 4.1.1**). The suspension was magnetically stirred under reflux for 24 h. Finally, the obtained materials were filtered and washed with 100 mL of toluene, 350 mL of methanol, 300 mL of distilled water and 150 mL of methanol, and once again dried for 24 h at 60 °C. In **Figure 4.1.1**, a schematic representation of the synthesis protocol used for the preparation of the SILs under study is provided.

Characterization of SILs materials. The synthesized materials were characterized through several techniques, namely elemental analysis, solid-state ^{13}C nuclear magnetic resonance (NMR) spectroscopy, attenuated total reflectance Fourier-transform infrared (ATR-FTIR) spectroscopy, point zero charge (PZC), specific surface area (S$_{BET}$) and scanning electron microscopy (SEM).

The elemental analysis technique is based on the high temperature oxidation of organic compounds, converting the elements of interest into gaseous molecules. In this method, the content of carbon, hydrogen and nitrogen of the three SILs ([Si][C$_3$mim]Cl, [Si][N$_{3444}$]Cl and [Si][N$_{3888}$]Cl) were determined using the TruSpec LECO-CHNS 630-200-200 analyser. A small amount of solid sample (approximately 2 mg) was placed and analyzed at a combustion furnace temperature of 1075 °C and an afterburner temperature of 850 °C. Infrared absorption was used to

determine the carbon and hydrogen contents whereas thermal conductivity was used for nitrogen quantification. The gases required are the following: combustion - oxygen; carrier - helium; pneumatic - compressed air.
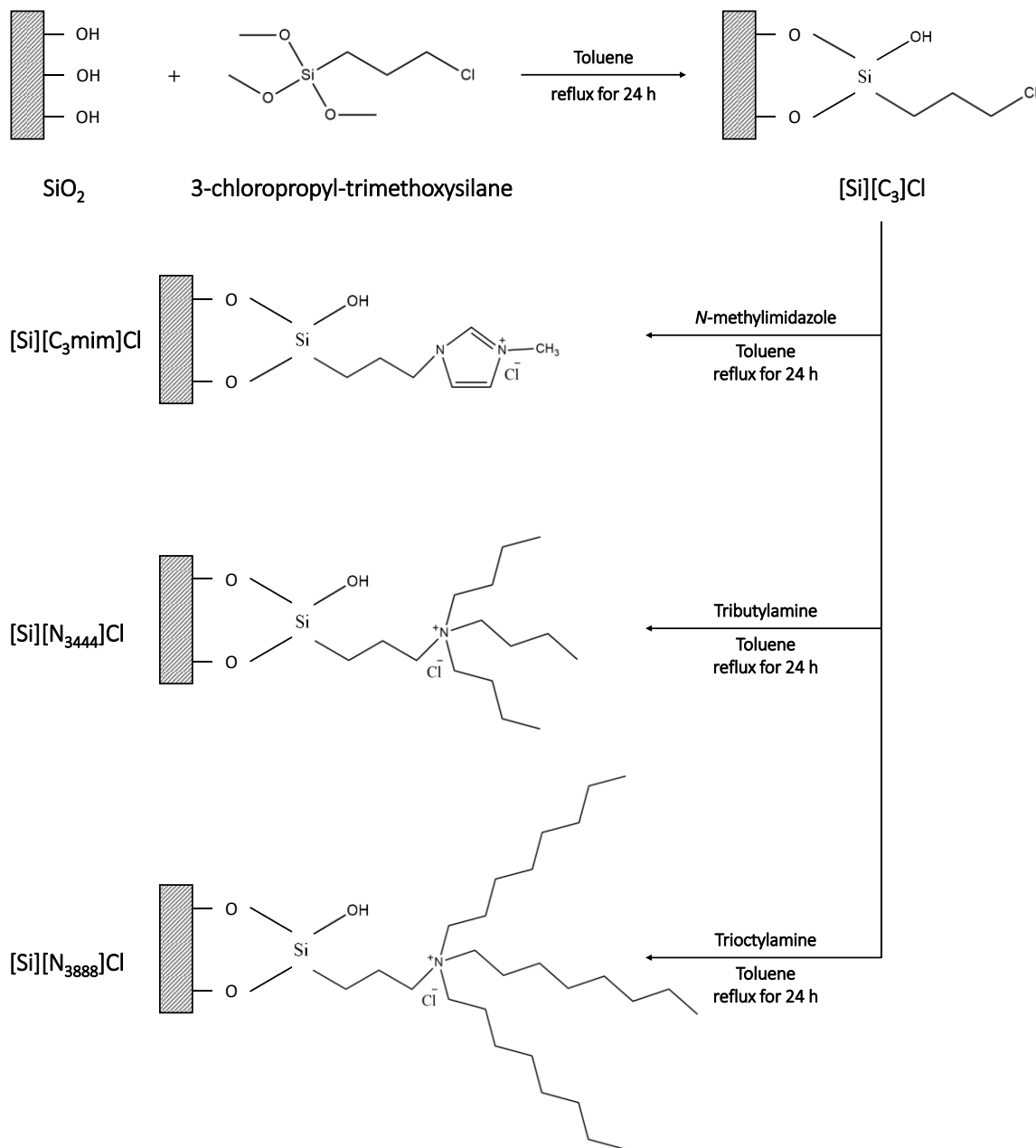
Figure 4.1.1. Schematic representation of the preparation of SILs, their chemical structures and respective abbreviations – [Si][C$_3$mim]Cl, [Si][N$_{3444}$]Cl and [Si][N$_{3888}$]Cl. 3-chloropropylsilane ([Si][C$_3$]Cl), the intermediate of the two-step reaction, is also represented.

Solid-state carbon-13 Nuclear Magnetic Resonance (^{13}C NMR) spectroscopy was used to confirm the SILs preparation. The spectra of the three SIL materials were recorded at 9.4 T, on a spectrometer BRUKER AVANCE III (wide-bore), at room temperature, on a 4 mm BL cross-polarization magic-angle spinning (CPMAS) VTN probe at 100.62 MHz.

Fourier-Transform infrared spectroscopy (FTIR) uses interferometry to record information about the materials; the synthesized SILs were analyzed in a spectrophotometer of FTIR (Perkin Elmer FT-IRSystem Spectrum BX), between 4000 - 400 cm^{-1}. For recording the FTIR spectra, each material was deposited in the instrument and then the analysis started at a temperature of 25 °C, working at a maximum resolution of 2 cm^{-1} and averaging 256 scans per sample.

The point of zero charge (PZC), that describes when the surface charge density is zero, was also determined for the three prepared SILs through zeta potential measurements, at 25 °C, using a folded capillary cell in the Malvern Zetasizer Nano ZS equipment (Malvern Instruments Ltd. Malvern). Zeta potential values were recorded for suspensions of materials in water at different pH values, which were adjusted with NaOH (0.01 M) and HCl (0.01 M) solutions, and using a suitable cell for this purpose.

Brunauer-Emmett-Teller (BET) allows the measurement of the specific surface area of the sample, including the pore size distribution, which permits to predict the bioavailability and evaluation of product performance. The surface area (S_{BET}) of SiO_2, $[Si][C_3]Cl$ and SILs was estimated by the BET method, the pore surface area (A) and pore volume (V) were determined by the BJH (Barrett-Joyner-Halenda) model, and the mean pore diameter (Dp) was calculated from Dp= (4V)/A) [57]. The specific surface area of SILs was assessed by nitrogen adsorption BET measurements performed with a Gemini V2.0 surface analyser from Micromeritics Instrument Corp. Norcross, GA, USA, at -196 °C. Prior to BET measurements, the samples were degassed at -80 °C under nitrogen flow overnight.

Scanning electron microscopy (SEM) runs an electron beam fixed on a surface to produce an image, allowing to obtain information about the materials surface composition. SEM assays were performed using a high-resolution Hitachi SU-70 Schottky emission instrument, equipped with EDS Bruker (model Quantax 400). The material was deposited on an aluminium sample holder followed by carbon coating using an Emitech K950X carbon evaporator. Afterwards, the sample was analyzed.

Determination of the SIL-based processes performance. IgG and protein impurities were quantified in all feeds and in each sample by size-exclusion high-performance liquid

chromatography (SE-HPLC). Samples were diluted at a 1:2 (v:v) ratio in an aqueous potassium phosphate buffer solution (50 mmol·L^{-1}, pH 7.0, with NaCl 0.3 mol·L^{-1}) used as the mobile phase. The equipment used was a Chromaster HPLC system (VWR Hitachi) equipped with a binary pump, column oven (operating at 40 °C), temperature controlled auto-sampler (operating at 10 °C), DAD detector and a column Shodex Protein KW-802.5 (8 mm × 300 mm). The mobile phase was run isocratically with a flow rate of 0.5 mL·min^{-1} and the injection volume was 25 µL. The wavelength was set at 280 nm. The calibration curve was established with commercial human IgG, ranging from 5 to 200 mg·L^{-1}.

The process performance was evaluated by the recovery yield and purity level for IgG. In addition, both the IgG concentration and aggregation percentage were also determined for a full characterization of the process outputs. For each sample, the peaks areas were estimated using PeakFit® software, and the remaining data was treated on Excel.

The recovery yield (%Yield$_{IgG}$) of IgG retained in solution was determined according to the following equation:

$$\%\text{Yield}_{IgG} = \frac{[IgG]_{final} \times V_{final}}{[IgG]_{initial} \times V_{initial}} \times 100 \tag{1}$$

where [IgG]$_{initial}$ and [IgG]$_{final}$ correspond to the concentration of IgG in the initial complex media (before being in contact with the material) and of aqueous solutions after contact with the material, respectively. V$_{initial}$ and V$_{final}$ corresponds to initial and final volumes, which is the same for both cases, 0.5 mL.

The percentage purity level of IgG was determined according to the following equation:

$$\%\text{Purity}_{IgG} = \frac{A_{IgG}}{A_{Total}} \times 100 \tag{2}$$

where A$_{IgG}$ corresponds to the SE-HPLC peak area of IgG and A$_{Total}$ corresponds to the total area of the peaks corresponding to all proteins present in the respective sample.

The aggregation percentage of IgG was determined according to the equation:

$$\%\text{Aggregation}_{IgG} = \frac{A_{IgG\ aggregates}}{A_{IgG}} \times 100 \tag{3}$$

where A$_{IgG\ aggregates}$ corresponds to the SE-HPLC peak area of IgG aggregates.

In the cases where IgG was adsorbed on the supported materials, the %Yield$_{IgG}$ in the material was determined according to the following equation:

$$\%\ \text{Yield}_{IgG} = \frac{([IgG]_{initial} \times V_{initial}) - ([IgG]_{final} \times V_{final})}{[IgG]_{initial} \times V_{initial}} \times 100 \tag{4}$$

while the purity level of IgG being determined according to equation given below:

$$\% \ \text{Purity}_{\text{IgG}} = \frac{A_{\text{initial IgG}} - A_{\text{final IgG}}}{\left(A_{\text{initial IgG}} - A_{\text{final IgG}}\right) + \left(A_{\text{initial imp.}} - A_{\text{final imp.}}\right)} \times 100 \qquad (5)$$

where the $A_{\text{initial IgG}}$ and $A_{\text{final IgG}}$ correspond to the SE-HPLC peak area of IgG of the initial complex media (before being in contact with the material) and aqueous solutions (after contact with the material), respectively. $A_{\text{initial imp.}}$ and $A_{\text{final imp.}}$ represent the SE-HPLC area of the peak of protein impurities in the initial complex media (before being in contact with the material), respectively.

In these cases, the aggregation percentage of IgG was determined according to the following equation:

$$\% \ \text{Aggregation}_{\text{IgG}} = \frac{A_{\text{initial aggregates}} - A_{\text{final aggregates}}}{\left(A_{\text{initial aggregates}} - A_{\text{final aggregates}}\right) + \left(A_{\text{initial IgG}} - A_{\text{final IgG}}\right)} \times 100 \qquad (6)$$

where $A_{\text{initial aggregates}}$ and $A_{\text{final aggregates}}$ correspond to the SE-HPLC peak area of IgG aggregates of the initial complex media (before being in contact with the material) and aqueous solutions (after contact with the material), respectively.

At least two individual experiments were performed to determine the average in performance parameters, as well as the respective standard deviations.

Screening of the SIL materials for the downstream processing of IgG from human serum. An initial screening was performed with all the synthesized materials to purify IgG. Activated silica was used as a control for comparison purposes. Each SIL/activated silica was added to 2 mL microtubes under the following operating conditions: S:L ratio (S:L ratio) of 100 mg·mL^{-1} (50 mg of supported material (SILs) and 500 μL of human serum 20-fold diluted); pH value of 3, 5, 7 and 9; and contact time of 60 min. The samples were stirred on a programmable rotator-mixer from PTR-30 Grant-bio. Finally, the samples were centrifuged in a VRW MICRO STAR 17 at 13000 rpm during 20 min to separate the aqueous solution from the material, that remained in the bottom of the microtube. All aqueous solutions were diluted at a 1:1 (v:v) ratio with the HPLC mobile phase, and then analyzed by SE-HPLC.

Optimization of the purification process by factorial design experiments. After the first screening performed, factorial design was used to maximize human antibodies recovery and purification. A 2^k factorial planning was carried out, in which there are k factors that can contribute to a different response regarding the final IgG recovery yield or purity in just one step. The experimental data was treated according to the second order polynomial equation described as follows:

$$y = \beta_0 + \beta_i X_i + \beta_j X_j + \beta_{ii} X_i^2 + \beta_{jj} X_j^2 + \beta_{ij} X_i X_j \qquad (7)$$

where y is the dependent variable, namely the IgG yield or purity, and β_0, β_i, β_j, β_{ii}, β_{jj} and β_{ij} are the regression coefficients used respectively, to the intersection, linear, quadratic, and interaction of the terms. X_i and X_j represent the independent variables in the 2^k factorial planning. The experimental design involves the combination of three factors (independent variables) at two-levels. The number of runs (N) of each experiment is given by Equation 8:

$$N = 2^k + 2k + Cx \tag{8}$$

where 2^k is the number of factorial readings, $2k$ the number of axial readings and Cx a random number of repetitions of the central point which is expected to be closer to the best process operation conditions. It is very important to have several readings for the central point, to know the residual graph and, consequently, the standard deviation and the reproducibility quality of the experiment. On the other hand, the axial points are added to adjust the experience. Given the conditions and the number of independent variables to be studied, a Central Composite Rotatable Design was chosen, and the axial points calculated according to the value of α through Equation 9:

$$\alpha = (2^k)^{\frac{1}{4}} \tag{9}$$

where ± α is the distance between the central and axial points.

In this work, a 2^3 factorial planning was used aiming at the optimization of three independent variables (inputs), namely i) solid:liquid ratio (mg of material per mL of aqueous solution of biological media); ii) pH value; and iii) contact time (min), both for the maximization of the IgG yield or purity. The inputs were studied at three levels: the central point (zero level), factorial points (1 and -1, level one), and axial points (level α), being the 2^3 factorial planning is provided in **Appendix E (Table E.1)**. Based on Equation 8, a total of 17 experiments were performed for the development of the proposed factorial design. Also, for k = 3 and considering Equation 9, α adopts a value of 1.68. The range was defined according to preliminary results, and the chosen central point was 100 mg·mL^{-1} for S:L ratio, pH 5 and 60 min of contact time. The detailed list of experiments performed with the coded and uncoded coefficients is provided in **Appendix E (Table E.2)**.

The results obtained were statistically analyzed using Statsoft$^©$ STATISTICA 10.0 software, and considering a confidence level of 95 %. Three-dimensional surface response plots were originated by changing two variables within the experimental range and maintaining the remaining factors at the central point. Each factorial planning developed used a central point experimentally obtained at least three times. The response surfaces and contour plots were also obtained using Statsoft$^©$ STATISTICA 10.0 software.

Optimization of the IgG downstream processes. In order to further optimize the processes based on the information given by the design of experiments, a set of new conditions regarding the pH value and S:L ratio were considered for the IgG capture and/or purification using the three SILs under study ([Si][C$_3$mim]Cl, [Si][N$_{3444}$]Cl and [Si][N$_{3888}$]Cl). For the optimization of the process pH, a S:L ratio of 100 mg·mL^{-1} (50 mg of SILs and 500 µL of human serum 20-fold diluted) and an intermediate contact time of 60 min were fixed, while pH values of 10, 11 and 12 were studied (values higher than the pI of the protein of interest, pI$_{IgG}$ = 9 [7]). Further optimization of the S:L ratio was performed for [Si][C$_3$mim]Cl, also using the three pH values (10, 11 and 12) and 60 min of contact time, and at two different S:L ratio – 150 and 200 mg·mL^{-1} (75 and 100 mg of material with 500 µL of human serum 20-fold diluted, respectively). All the assays were prepared following the procedure given above**.**

Evaluation of the robustness of the processes. The two best conditions identified were finally investigated to prove the robustness of the IgG downstream processes developed. The materials were set in contact with two new biological complex matrices, namely rabbit serum and CHO cell culture supernatants. For [Si][C$_3$mim]Cl, the operating conditions were a S:L ratio of 150 mg.mL^{-1}, pH 12 and 60 min, while for [Si][N$_{3888}$]Cl the selected operating conditions were a S:L ratio of 100 mg·mL^{-1}, pH 11 and 60 min. The experimental procedure adopted followed the one mentioned above.

4.1.4. Results and discussion

4.1.4.1. Synthesis and characterization of SIL materials

In **Figure 4.1.1** is presented a schematic overview of the SILs synthesis procedure adopted in this work, by which three different SILs were obtained: [Si][C$_3$mim]Cl, [Si][N$_{3444}$]Cl and [Si][N$_{3888}$]Cl. Although different cation sources have been investigated, chloride was kept as the counterion in all SILs, avoiding the use of more complex anions, allowing to lower the costs of the materials and reduce their eco- and cytotoxicity [51]. All SILs were prepared by a two-step reaction process, as shown in **Figure 4.1.1**, where activated silica react with a silane-coupling agent (3-chloropropyltrimethoxysilane) and the obtained chloropropylsilica reacts with *N*-methylimidazole or other tertiary ammines (as cation sources).

Elemental analysis was carried out to quantitatively determine the carbon, hydrogen, and nitrogen contents of the prepared SILs, whose results are provided in **Table 4.1.1**.

Table 4.1.1. Elemental analysis (in percentage) of the functionalized part of the synthesized SILs.

Material	C (%)	H (%)	N (%)
[Si][C$_3$]Cl	76.9	23.1	0.1
[Si][C$_3$mim]Cl	62.8	15.9	21.3
[Si][N$_{3444}$]Cl	79.5	18.5	2.1
[Si][N$_{3888}$]Cl	83.1	16.1	0.9

The intermediate [Si][C$_3$]Cl, shows carbon (C) and hydrogen (H), but as expected does not contain nitrogen (N), indicating the absence of the cation source. The carbon and nitrogen percentage of the remaining supported materials ranges from 62.8 % to 83.1 % and from 0.9 % to 21.3 %, respectively. For carbon, its percentage increases as the length of the alkyl chain increases, as follows: [Si][C$_3$mim]Cl < [Si][N$_{3444}$]Cl < [Si][N$_{3888}$]Cl. For nitrogen, this percentage is higher in the [Si][C$_3$mim]Cl, related with the presence of the imidazolium aromatic ring, being lower in [Si][N$_{3888}$]Cl, due to the steric effect promoted by its long alkyl chain.

The successful preparation of SILs was additionally confirmed through solid-state [13]C Nuclear magnetic resonance (NMR), whose spectra are shown in **Appendix E (Figure E.1)**. Concerning the intermediate [Si][C$_3$]Cl spectrum, three peaks at 10, 27 and 47 ppm are assigned to the three carbons of the propyl alkyl chain. For [Si][C$_3$mim]Cl, the presence of the six peaks was noticed: the three carbon atoms of the alkyl side chain of the aromatic ring (C2, C1 and C6) corresponds to the peaks at 10, 25 and 38 ppm, respectively. The signals between 120 - 140 ppm correspond to the aromatic carbons of the imidazolium ring (C5 and C4), respectively. The last carbon of the alkyl chain (C3), corresponds to the peak at 53 ppm. Regarding the solid-state ^{13}C NMR spectra of [Si][N$_{3444}$]Cl and [Si][N$_{3888}$]Cl are similar to the spectrum of the intermediate material ([Si][C$_3$]Cl), which is due to the low functionalization degree of these materials, being in agreement with the elemental analysis results and a previous report in the literature [51]. Nevertheless, it should be remarked that the remaining characterizations of SILs, by means of elemental analysis, FTIR, PZC determination, BET surface characterization and SEM, allowed to successfully confirm the functionalization of these materials.

The attenuated total reflectance Fourier-Transform infrared spectroscopy (ATR-FTIR) spectra of activated silica, chloropropyl silica, and prepared SILs were also recorded between the range of 400 and 4000 cm^{-1}. All were obtained using silica as background, being represented in **Appendix E (Figure E.2)**. At around 3400-3900 cm^{-1} it was observed a band corresponding to Si-OH stretching,

which corresponds to the first step of reaction with the 3-chloropropyltrimethoxysilane. The relatively weaker bands occurring at 2900-3200 cm^{-1} are the stretching vibrations of CH_3 and CH_2 and the band at 1100 cm^{-1} represents the aliphatic chain C-N from all the SILs after their reaction with the corresponding cation source. Finally, the peaks at 400-900 cm^{-1} are related with the OH bending from the first reaction of the active silica with the anion, and to the chloride anion, also from the first reaction. Thus, ATR-FTIR also allowed to confirm the silica functionalization by ILs.

Zeta potential measurements were performed to study the surface charge of the functionalized silica-based materials. Data of the zeta potential as a function of pH for [Si][C$_3$]Cl and the synthesized SILs are provided in **Figure 4.1.2**. From these data, it was possible to determine the point of zero charge (PZC), which is the pH value at which a solid particle in suspension exhibits zero net electrical charge on its surface. In **Table 4.1.2** the PZC values of the different materials studied in this work are presented.

Table 4.1.2. Point zero charge (PZC) values of activated silica, [Si][C$_3$]Cl and remaining synthesized SILs ([Si][C$_3$mim]Cl, [Si][N$_{3444}$]Cl and [Si][N$_{3888}$]Cl).

Material	PZC
Activated silica	3.0
[Si][C$_3$]Cl	4.1
[Si][C$_3$mim]Cl	8.9
[Si][N$_{3444}$]Cl	5.7
[Si][N$_{3888}$]Cl	5.8

All the studied materials presented different PZC values. Activated Silica presents the lowest PZC value (3.0), while all the other materials have higher PZC values, ranging from 4.1 (intermediate material, [Si][C$_3$]Cl) to 8.9 ([Si][C$_3$mim]Cl). These results suggest that the surface of [Si][C$_3$mim]Cl, [Si][N$_{3444}$]Cl and [Si][N$_{3888}$]Cl is more positively charged when compared to the activated silica and to the intermediate material, therefore confirming the successful functionalization of the synthesized SILs, since they are more positively charged due to the addition of the cation of the ILs to the silica surface during their synthesis.
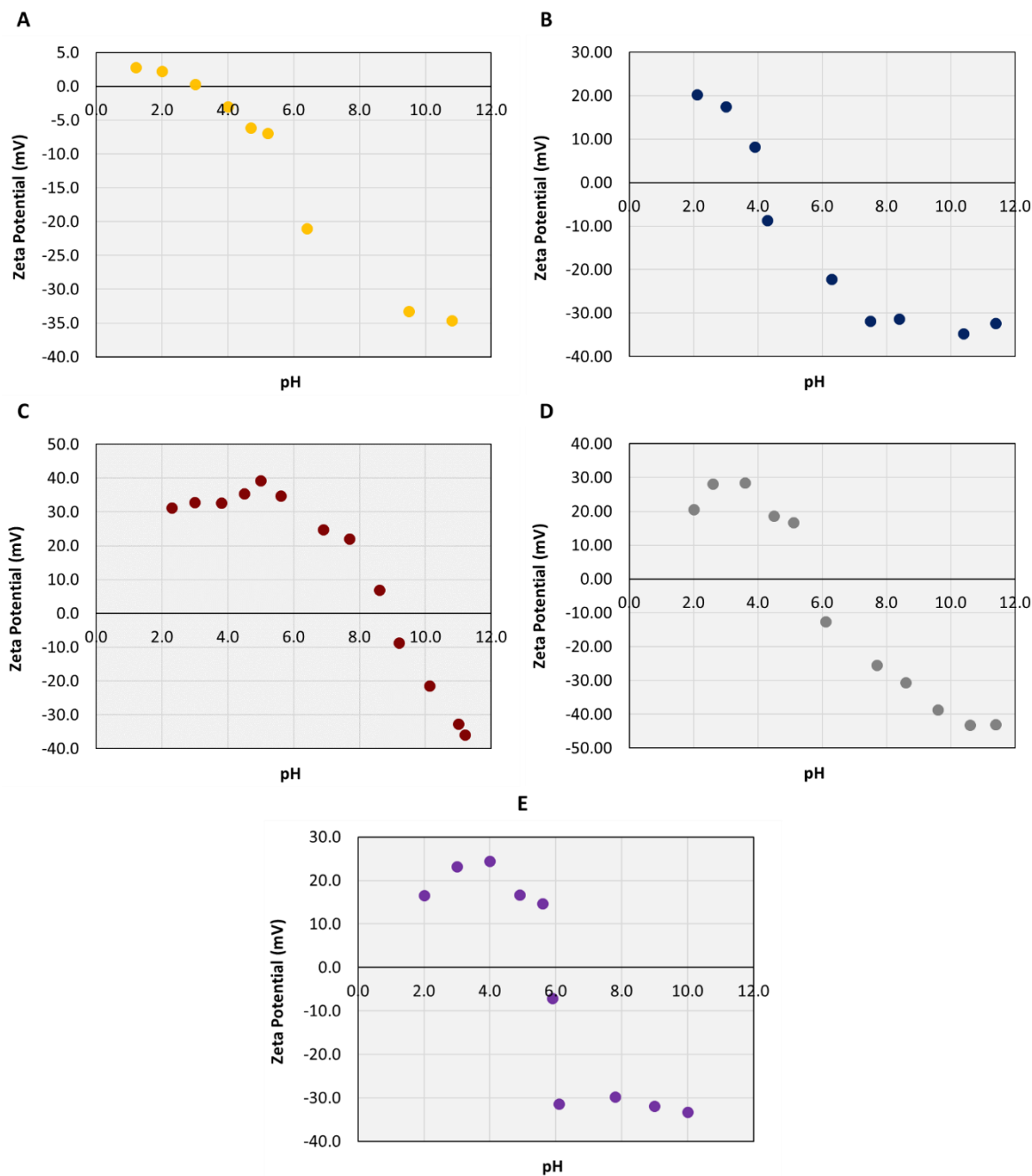
Figure 4.1.2. Representation of the zeta potential as a function of the pH for: (A) activated silica; (B) $[Si][C_3]Cl$; (C) $[Si][C_3mim]Cl$; (D) $[Si][N_{3444}]Cl$; and (E) $[Si][N_{3888}]Cl$.

The specific surface area and pore structure characterization of the materials under study were appraised using the BET method [57], and can be found in **Table 4.1.3**. According to the data shown, the material with lower PZC (3.0, correspondent to activated silica) is the one with the highest pore diameter (49.5 Å), whereas $[Si][C_3]Cl$ has the lowest value (38.8 Å). The synthetized SILs show a pore diameter ranging between 42.2 Å and 45.2 Å. In fact, the pore size diameter (D_p)

values decrease in the following order: activated silica (D_p = 49.5 Å) > [Si][C$_3$mim]Cl (D_p = 45.2 Å) > [Si][N$_{3888}$]Cl (D_p = 43.6 Å) > [Si][N$_{3444}$]Cl (D_p = 42.2 Å) > [Si][C$_3$]Cl (D_p = 38.8 Å). On the other hand, the BET surface areas decrease in the following order: activated Silica (S_{BET} = 434.5 m$^2 \cdot$g^{-1}) > [Si][C$_3$]Cl (S_{BET} = 322.9 m$^2 \cdot$g^{-1}) > [Si][N$_{3444}$]Cl (S_{BET} = 322.4 m$^2 \cdot$g^{-1}) > [Si][N$_{3888}$]Cl (S_{BET} = 319.3 m$^2 \cdot$g^{-1}) > [Si][C$_3$mim]Cl (S_{BET} = 185.3 m$^2 \cdot$g^{-1}). It can be concluded that activated silica presents the highest S_{BET}, meaning that it presents a more accessible pore available for adsorption. In general, the materials with the smallest diameter present the highest BET surface area.

Table 4.1.3. Summary of the characterization of activated silica, [Si][C$_3$]Cl and synthesized SILs ([Si][C$_3$mim]Cl, [Si][N$_{3444}$]Cl and [Si][N$_{3888}$]Cl): BET surface area (S_{BET}), Barrett-Joyner-Halenda (BJH) pore surface area (A), BJH pore volume (V), pore size diameter (Dp) and point of zero charge (PZC).

Material	S_{BET} (m$^2 \cdot$g^{-1})	A (m$^2 \cdot$g^{-1})	V (cm$^3 \cdot$g^{-1})	D_p (Å)	PZC
Activated silica	434.5	569.5	0.7	49.5	3.0
[Si][C$_3$]Cl	322.9	327.0	0.3	38.8	4.1
[Si][C$_3$mim]Cl	185.3	256.1	0.3	45.2	8.9
[Si][N$_{3444}$]Cl	322.4	311.9	0.3	42.2	5.7
[Si][N$_{3888}$]Cl	319.3	301.5	0.3	43.6	5.8

Finally, Scanning Electron Microscopy (SEM) was used to morphologically characterize the synthesized materials. The SEM images of activated silica and the synthesized SILs can be found in the **Appendix E (Figure E.3)**. Overall, no significant differences in the materials morphology is observed between the prepared SILs and the non-functionalized silica, meaning that the intermediate step and remaining steps required for silica functionalization with ILs do not change the material morphology.

4.1.4.2. Characterization of the complex biological matrices

Aqueous solutions of commercially available pure IgG, pure albumin and the complex biological matrices used in this work (human serum 20-fold diluted, CHO cell culture supernatants and rabbit serum 20-fold diluted) were analyzed by SE-HPLC for the characterization of their chromatographic profiles. The results obtained are presented in **Figure 4.1.3**.

Under the chromatographic conditions used, pure IgG samples present 2 chromatographic peaks: one corresponding to the IgG monomer and the other to IgG aggregates, with a retention time of *ca.* 15.0 min and 13.8 min, respectively, being in accordance with previous reports [58, 59].

The major protein impurity in the feed is human serum albumin (HSA), with a retention time of *ca.* 16.8 min. Both rabbit serum and CHO cell culture supernatant also exhibit a similar chromatographic profile as mentioned for human serum; nevertheless, it should be highlighted that in the cell culture supernatant, the main protein impurity is bovine serum albumin (BSA), whereas in the rabbit serum it corresponds to rabbit albumin.
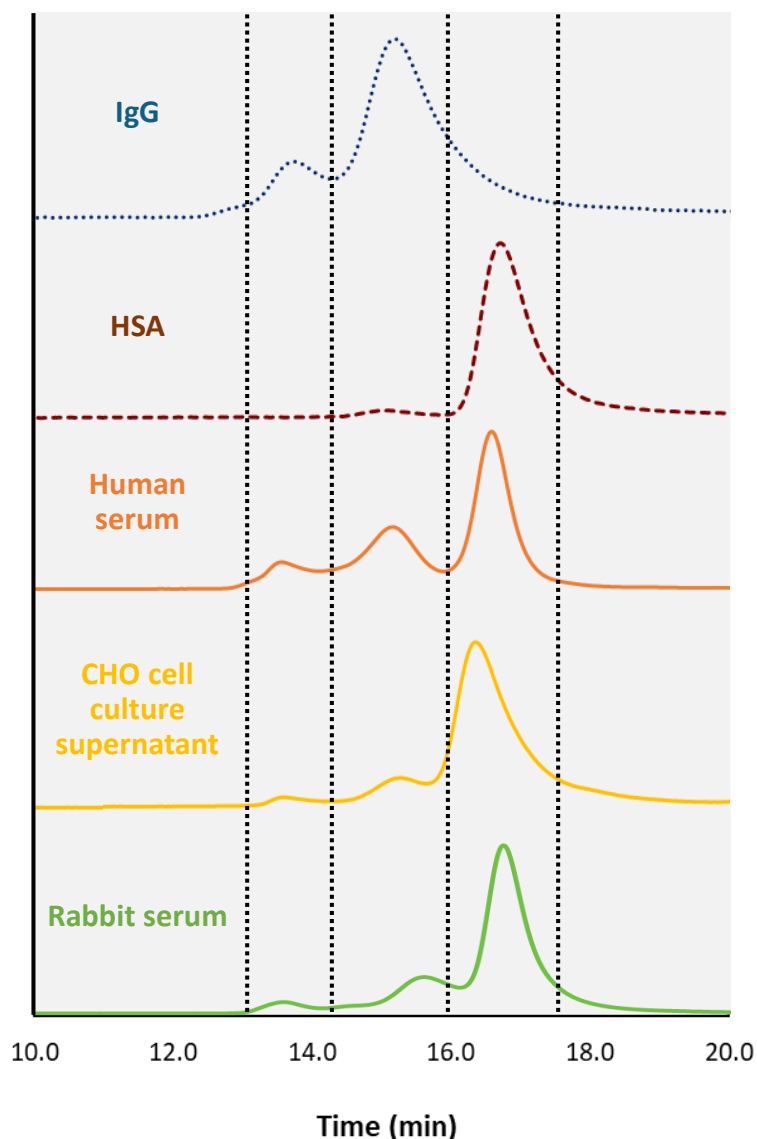
Figure 4.1.3. Characterization of the complex biological matrices studied in this work: SE-HPLC chromatograms of pure IgG solution 100 mg·L^{-1} (··), pure HSA solution 200 mg·L^{-1} (--), human serum (—), CHO cell culture supernatant (—), and rabbit serum (—).

The IgG content in the human serum samples was ascertained before each assay, and it was found that its average concentration was 470.1 ± 12.5 mg·L^{-1}, with a purity of 47.0 ± 1.6 %; in CHO

cell culture supernatants it was found an average concentration of IgG of 46.0 ± 5.8 mg·L^{-1} with a purity of 19.90 ± 4.5 %; finally, for rabbit serum, the IgG average concentration was found to be 297.2 ± 22.0 mg·L^{-1}, with an average purity of 24.6 ± 0.3 %.

In this work, all the assays were initially conducted using human serum, since it is a consistent and homogenous biological complex medium, containing high concentrations of value-added antibodies of great interest for the (bio)pharmaceutical industry, and also presenting similar composition between samples, allowing consistent and comparable results along the work and avoiding discrepancies arising from the use of different batches. Nevertheless, CHO cell culture supernatants and rabbit serum were later investigated to evaluate the possible applicability of the developed IgG downstream processes in the bioprocessing of different biological matrices.

4.1.4.3. Screening of SIL materials for IgG downstream processing

An initial screening was performed to understand the behaviour of the IgG antibodies of human serum samples in the presence of activated silica (without any functionalization) and the SIL materials under study ([Si][C$_3$mim]Cl, [Si][N$_{3444}$]Cl and [Si][N$_{3888}$]Cl). For that, activated silica and SILs were placed in contact with human serum samples at different pH values (ranging from 3 to 9) to evaluate the influence of the pH in the (selective) adsorption of proteins from human serum.

The same operational conditions were applied for all materials: a S:L ratio of 100 mg.mL^{-1} and 60 min of contact time, while the pH value was changed (3, 5, 7 and 9). After the contact of the human serum sample with the materials, the chromatograms of the aqueous solutions were acquired and compared with the initial chromatogram of the human serum (before contact with the material), allowing to evaluate the ability of these materials to (selectively) adsorb proteins present in the biological complex medium. All the chromatograms acquired are presented in **Figure 4.1.4**.

Based on the obtained results, for all the pH values studied, activated silica presents no selectivity for any of the biomolecules present in human serum, since similar SE-HPLC chromatograms were obtained for the aqueous solutions after contact with activated silica and the initial human serum sample. At pH 3, similar chromatographic profiles between the initial and final samples were also found for all the SILs under study, meaning that no IgG nor albumin preferentially adsorb into the materials under these conditions. This behaviour seems to be related with the fact that, at pH 3 both IgG and HSA are positively charged (pI$_{IgG}$ = 9.0 and pI$_{HSA}$ = 4.9). As the studied SILs are also positively charged (PZC$_{[Si][C_3mim]Cl}$ = 8.9; PZC$_{[Si][N_{3444}]Cl}$ = 5.7 and PZC$_{[Si][N_{3888}]Cl}$ = 5.8), there is

electrostatic repulsion of the proteins, not allowing their adsorption to the material *via* electrostatic interactions.
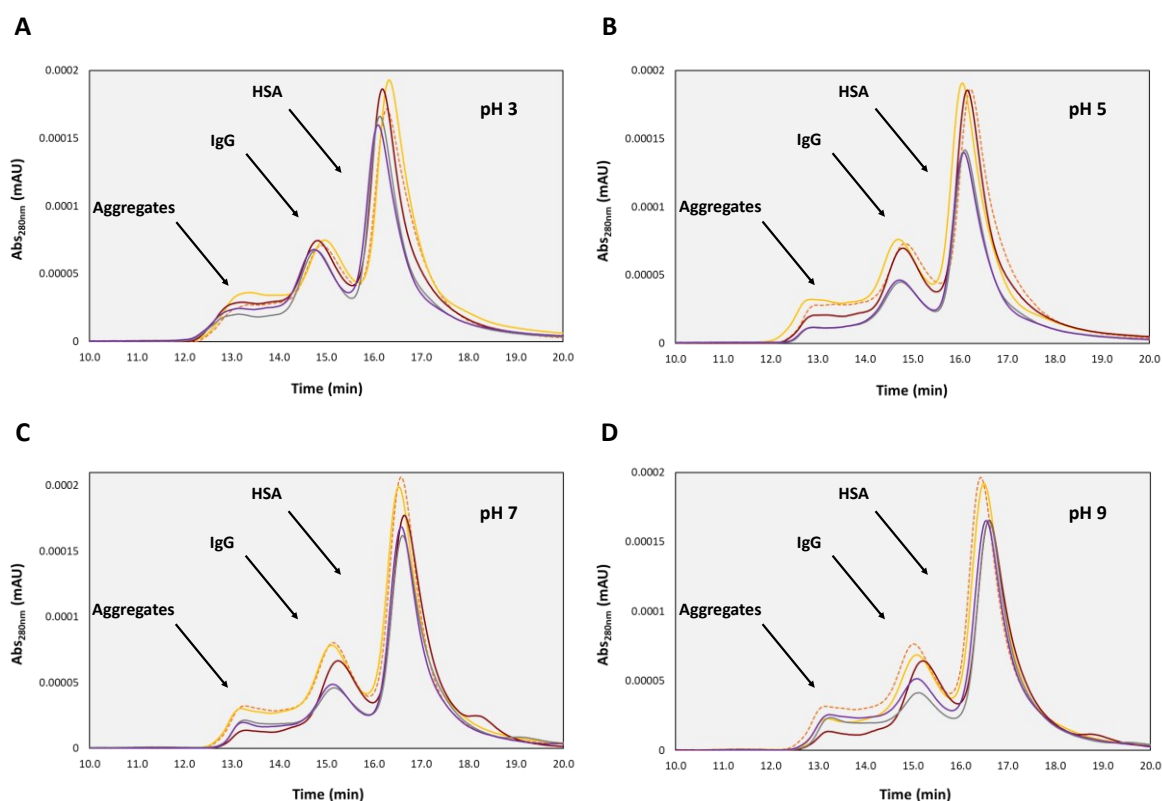
Figure 4.1.4. SE-HPLC chromatograms of the human serum samples 20-fold diluted after contact with the supported materials under study at: (A) pH 3; (B) pH 5; (C) pH 7; and (D) pH 9. For each graph, the chromatographic profiles of human serum (⋅⋅), and human serum after contact with activated silica (—), [Si][C₃mim]Cl (—), [Si][N₃₄₄₄]Cl (—), and [Si][N₃₈₈₈]Cl (—) are presented.

When increasing the pH up to 5, it is noticed that IgG and albumin start to adsorb into [Si][N$_{3444}$]Cl and [Si][N$_{3888}$]Cl; however, there is no significant adsorption of proteins into [Si][C$_3$mim]Cl, since it consist in the material with most positive charges (and higher PZC). At pH 7, a preferential adsorption of IgG onto [Si][N$_{3444}$]Cl and [Si][N$_{3888}$]Cl occurs, in accordance with the pI of the proteins and the PZC of the materials: at pH 7, both [Si][N$_{3444}$]Cl and [Si][N$_{3888}$]Cl are negatively charged, while IgG is positively charged, promoting its adsorption by electrostatic interactions. However, as albumin is also negatively charged, its adsorption into the materials does not occur in a high extent. Curiously, [Si][C$_3$mim]Cl that is positively charged at the work pH, lead to the less promising results, adsorbing less IgG and albumin than the quaternary ammonium-based SILs. The adsorption of IgG (also positively charged) was unexpected taking into account the establishment of electrostatic interaction, thus meaning that other type of interactions are playing

a role in the process (e.g. $\pi \cdots \pi$ and anion $\cdots \pi$ interactions between the aromatic residues of the proteins and the aromatic ring of the imidazolium cation attached in the material, hydrogen bonding and hydrophobic interactions). Finally, at pH 9, both IgG and albumin were adsorbed into the three SILs, however, less than at pH 7. Once again, the lower adsorption was found for [Si][C$_3$mim]Cl, revealing that the pH seems to be a no significant parameter for the adsorption onto this SIL.

In conclusion, the gathered data allowed to conclude that the functionalization of activated silica with ILs is fundamental to introduce selectivity in the materials (SILs); by using activated silica, no adsorption of proteins was observed in the pH range herein studied. Although for pH 3 no significant proteins adsorption could be noticed, for pH 5 it was observed a preferential IgG adsorption into two SILs, [Si][N$_{3444}$]Cl and [Si][N$_{3888}$]Cl, whereas for [Si][C$_3$mim]Cl it only occurs at pH 7. Thus, less acidic pH values seem to favour the adsorption phenomenon. The [Si][C$_3$mim]Cl was the SIL with lower ability for proteins adsorption.

4.1.4.4. Optimization of the adsorption process and selectivity by factorial design experiments

Based on the most promising conditions obtained in the initial screening of the three SILs, a 2^3 factorial planning was performed aiming at optimizing the operation conditions (S:L ratio, pH and contact time) in the SIL-based process for the capture/recovery and purification of IgG antibodies from human serum. The performance parameters (%Yield$_{IgG}$ and %Purity$_{IgG}$) were experimentally obtained for each assay using the three SILs. For [Si][C$_3$mim]Cl, the performance parameters were determined in the aqueous solution after contact with the supported material (since IgG is preferentially maintained in solution using this SIL), and for [Si][N$_{3444}$]Cl and [Si][N$_{3888}$]Cl the performance parameters refers to the material after contact with the supported material (due to the preferential adsorption of IgG onto these materials). The quantitative results obtained are presented in **Table 4.1.4**, while the comparison between the experimental and theoretical results, as well as the statistical analyses performed (regression coefficients and ANOVA), are presented in the **Appendix E (Tables E.3 – E.20** and **Figures E.4 – E.9)**.

After the analysis of the results presented in **Table 4.1.4**, it was found that for each SIL material there are optimal conditions that provide good purity levels without impairing the IgG recovery yield (highlighted in bold). For [Si][C$_3$mim]Cl, the IgG was completely retained in solution with a purity of 46.9 ± 0.7 % using a S:L ratio of 50 mg·mL^{-1}, pH 3 and a contact time of 90 min.

Table 4.1.4. Performance parameters (%Yield$_{IgG}$ and %Purity$_{IgG}$) regarding IgG antibodies recovery and purification from human serum, after contact with [Si][C$_3$mim]Cl (results in the aqueous medium), [Si][N$_{3444}$]Cl and [Si][N$_{3888}$]Cl (results in the materials). The best condition for each SIL is highlighted in grey/bold.

	[Si][C$_3$mim]Cl		[Si][N$_{3444}$]Cl		[Si][N$_{3888}$]Cl	
System	%Yield$_{IgG}$	%Purity$_{IgG}$	%Yield$_{IgG}$	%Purity$_{IgG}$	%Yield$_{IgG}$	%Purity$_{IgG}$
1	100.0	45.8	10.0	53.2	0.0	0.0
2	**100.0**	**46.9**	0.0	0.0	0.0	0.0
3	63.3	42.2	24.5	80.5	35.3	66.7
4	68.3	42.7	13.8	72.5	**42.8**	**81.1**
5	100.0	43.6	45.1	55.3	25.7	24.8
6	97.2	42.8	0.0	0.0	26.2	28.7
7	58.7	46.4	**57.0**	**65.0**	67.3	59.9
8	58.7	45.0	52.0	55.8	65.5	57.7
9	84.9	40.4	33.5	57.4	34.4	45.5
10	86.8	40.8	30.6	53.8	47.2	42.7
11	100.0	42.6	0.0	0.0	16.8	22.4
12	70.5	37.6	26.4	93.3	48.2	52.7
13	86.4	42.1	12.6	85.8	22.8	43.5
14	80.0	39.4	12.5	97.8	47.6	39.3
15	88.6	42.2	15.9	98.3	48.0	43.7
16	84.0	40.4	10.4	97.4	45.3	42.4
17	86.5	41.2	15.2	98.2	36.2	46.0

On the other hand, by using [Si][N$_{3444}$]Cl, IgG was preferentially adsorbed in the SIL material with a yield of 57.0 ± 7.5 % and a purity level of 65.0 ± 5.9 %, using a S:L ratio of 150 mg·mL^{-1}, pH 7 and a contact time of 30 min. Finally, for [Si][N$_{3888}$]Cl, the IgG was also adsorbed into the material with a yield of 42.8 ± 0.7 % and a purity of 81.1 ± 8.9 %, using a S:L ratio of 50 mg·mL^{-1}, pH 7 and a contact time of 90 min. These results are in agreement with what expected and reveal a high influence of electrostatic, π ··· π, and hydrophobic interactions in the adsorption phenomenon and selectivity of the materials. At pH 3, [Si][C$_3$mim]Cl and IgG are positively charged, thus promoting a preferential capture of the protein impurities in the SIL and allowing IgG to be recovered in a simple and quick way directly in the aqueous solution that contacted with the material. Also, [Si][C$_3$mim]Cl presents an aromatic ring on its structure, and thus π ··· π interactions between the aromatic ring of the SIL and the aromatic residues of protein impurities may be playing a role in the process. On

the other hand, by using [Si][N$_{3444}$]Cl and [Si][N$_{3888}$]Cl at pH 7, IgG is positively charged, while both SILs are negatively charged, being observed in this case a preferential adsorption of IgG onto the material. Also, hydrophobic interactions may be playing a role, since [Si][N$_{3444}$]Cl and [Si][N$_{3888}$]Cl are composed of long alkyl chains and are, consequently, the most hydrophobic SILs under study, and IgG is the most hydrophobic protein in the biological matrix (i.e. the protein composed of higher number of surface hydrophobic residues [7]).

The experimental data obtained in the 2^3 factorial plannings (response surface and contour plots) regarding the optimization of IgG recovery yield and purity are depicted in **Figure 4.1.5** and **Figure 4.1.6**, respectively. Based on the results presented in these figures, it was found that the best conditions abovementioned for [Si][C$_3$mim]Cl are close to the optimum zone (dark red), whereas for [Si][N$_{3444}$]Cl and [Si][N$_{3888}$]Cl they fit within the optimum zone obtained in the response surface and contour plots. Still, based on response surface plots it is possible to predict the optimal conditions of S:L ratio, pH and contact time that allow to maximize IgG recovery yield and purity. For [Si][C$_3$mim]Cl (**Figure 4.1.5 (A) and (B)**; **Figure 4.1.6 (A) and (B)**), the optimum conditions for IgG recovery yield (> 86 %) are using a S:L ratio of 70 mg·mL^{-1}, pH 5 and a contact time of 70 min, while for IgG purity (> 47 %) are a S:L ratio of 100 mg·mL^{-1}, a pH below 1 and a contact time of 60 min. For [Si][N$_{3444}$]Cl (**Figure 4.1.5 (C) and (D)**; **Figure 4.1.6 (C) and (D)**), the optimum conditions for IgG yield (> 70 %) are a S:L ratio of 100 mg·mL^{-1}, a pH higher than 9 and a contact time of 60 min and for IgG purity (< 100 %) are a S:L ratio of 100 mg·mL^{-1}, a pH of 6 and a contact time of 60 min. Finally, for [Si][N$_{3888}$]Cl (**Figure 4.1.5 (E) and (F)**; **Figure 4.1.6 (E) and (F)**), the optimum conditions for IgG yield (> 50 %) are a S:L ratio of 100 mg·mL^{-1}, a pH higher than 8 and a contact time of 90 min, and for IgG purity (> 70 %) are a S:L ratio of 100 mg·mL^{-1}, a pH higher than 9 and a contact time of 60 min. Thus, there is a close agreement between the optimum conditions for both the IgG recovery yield and IgG purity for [Si][N$_{3444}$]Cl and [Si][N$_{3888}$]Cl, while a pH discrepancy was observed for [Si][C$_3$mim]Cl. By the analysis of the pareto charts from [Si][C$_3$mim]Cl [*cf.* **Appendix E (Figure E.10 (A)** and **Figure E.11 (A))**] it is shown that individual pH displays a significant influence upon the IgG recovery yield, and that no parameters appears to affect IgG purity. For [Si][N$_{3444}$]Cl [*cf.* **Appendix E (Figure E.10 (B)** and **Figure E.11 (B))**], it was observed that pH significantly affects IgG recovery yield, and not only the pH, but also its quadratic function and the quadratic function of contact time are also statistically relevant for IgG purity. Finally, for [Si][N$_{3888}$]Cl [*cf.* **Appendix E (Figure E.10 (C)** and **Figure E.11 (C))**] it was found that both pH and S:L ratio display a significant influence in IgG recovery yield, whereas only the pH significantly affects the IgG purity.

(A)

(B)

(C)

(D)

(E)

(F)
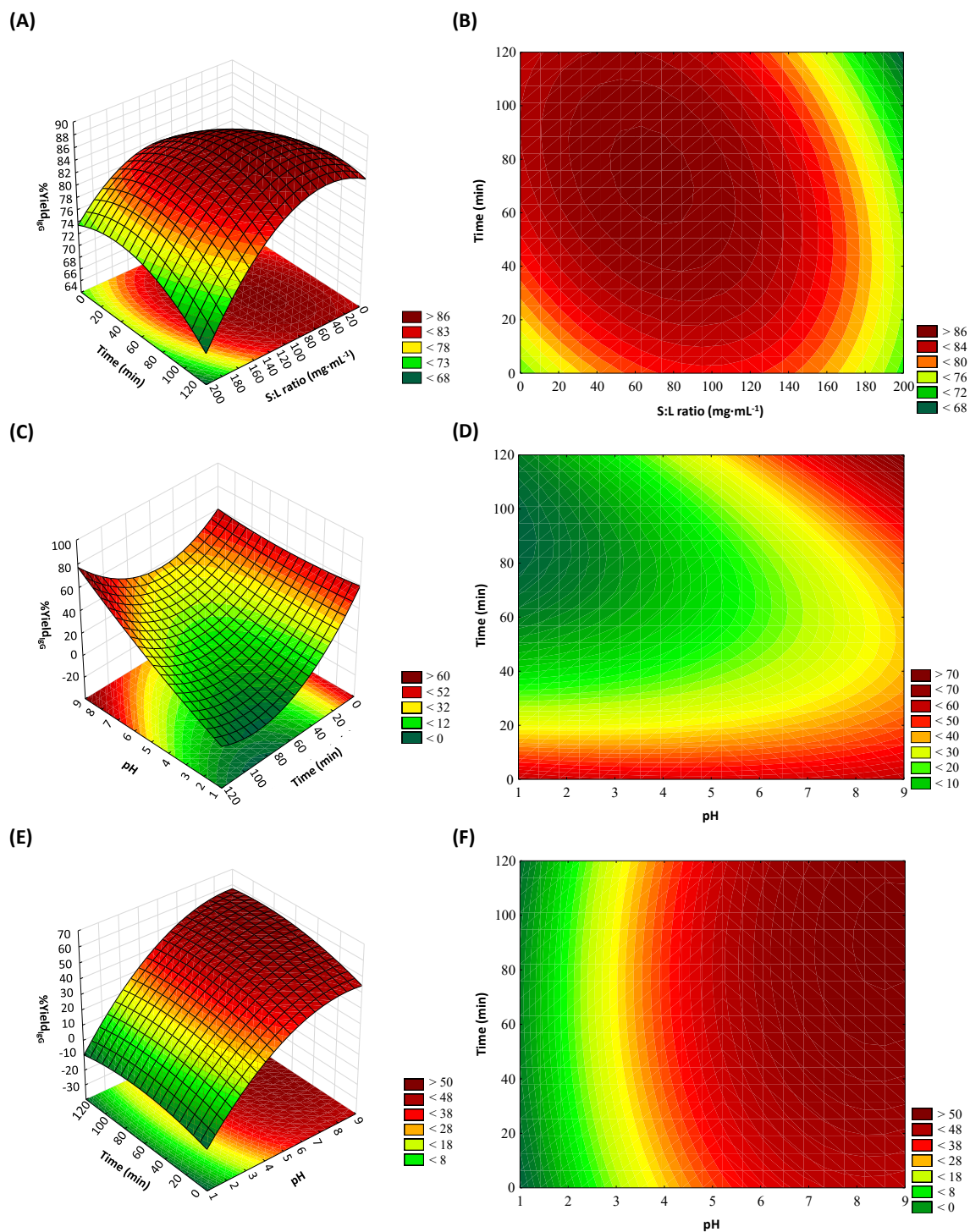
Figure 4.1.5. Response surface plots (left) and contour plots (right) on the IgG recovery yield (%Yield$_{IgG}$) using: (A) and (B) [Si][C$_3$mim]Cl (focused on pH 5); (C) and (D) [Si][N$_{3444}$]Cl (focused on S:L ratio of 100 mg·mL^{-1}); and (E) and (F) [Si][N$_{3888}$]Cl (focused on S:L ratio of 100 mg·mL^{-1}).

(A)

(B)

(C)

(D)

(E)

(F)
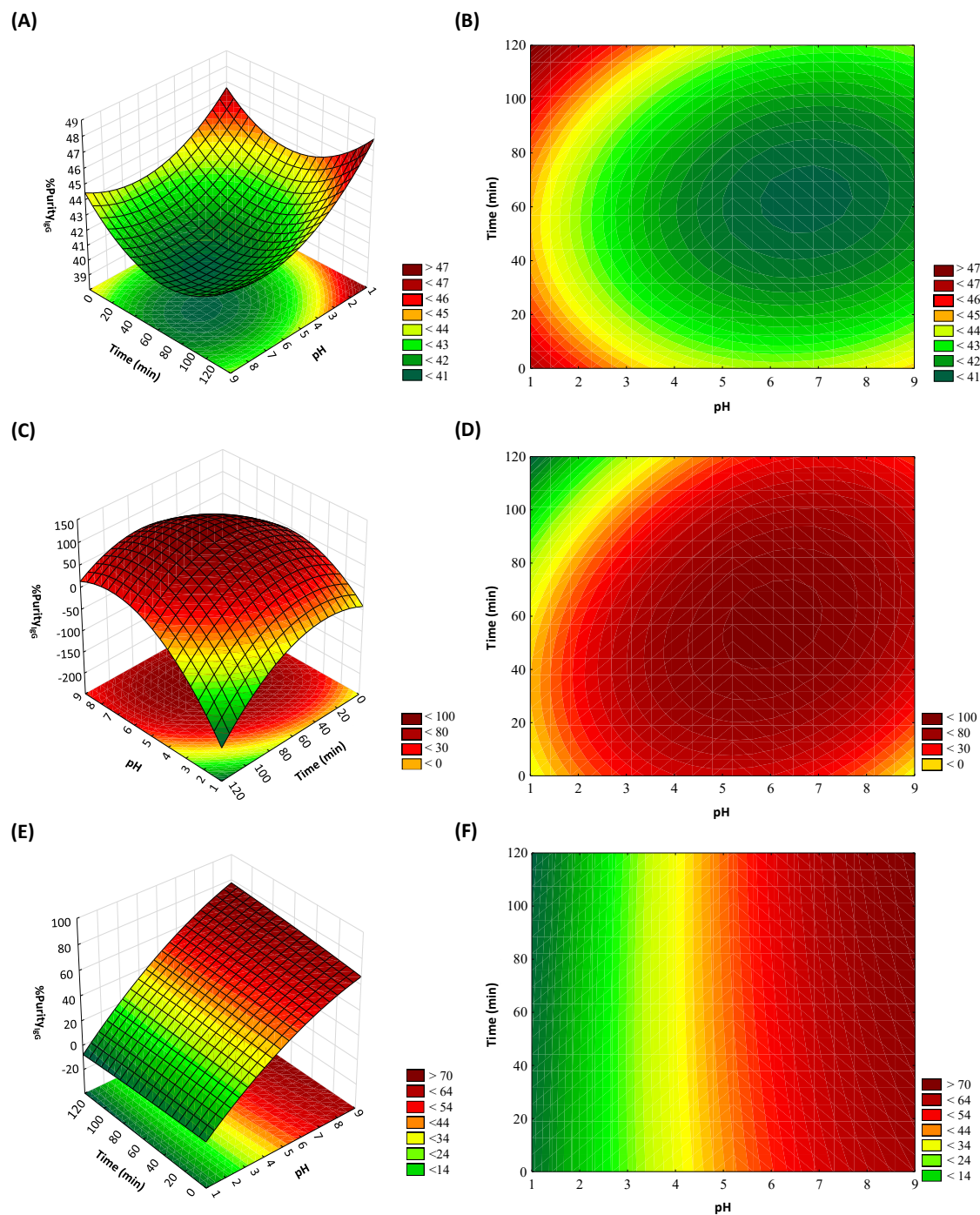
Figure 4.1.6. Response surface plots (left) and contour plots (right) on the IgG purity level (%Purity$_{IgG}$) using: (A) and (B) [Si][C$_3$mim]Cl (focused on pH 5); (C) and (D) [Si][N$_{3444}$]Cl (focused on S:L ratio of 100 mg·mL^{-1}); and (E) and (F) [Si][N$_{3888}$]Cl (focused on S:L ratio of 100 mg·mL^{-1}).

From all these observations, it was possible to conclude that the pH is the most important and statistically relevant variable ruling the IgG recovery/purification process. Moreover, it was possible to conclude that the central point was appropriate for the optimization of the IgG recovery

yield using [Si][C$_3$mim]Cl, since the area of maximum yield is included in the defined intervals; however, the factorial planning using the same materials for the optimization of IgG purity only allowed to define a region in which the IgG purification seems to be maximized (but with an undefined optimum point). Only slight discrepancies were identified between the predicted and experimental values [*cf.* **Appendix E (Figure E.4** and **Figure E.5)**], assuring the accuracy and precision of the factorial design, allowing to define as the optimum conditions for this material a S:L ratio of 50 mg·mL^{-1}, pH 3 and a contact time of 90 min. For the remaining SILs, [Si][N$_{3444}$]Cl and [Si][N$_{3888}$]Cl, some discrepancies were also identified between the predicted and experimental values [*cf.* **Appendix E (Figure E.6**, **Figure E.7**, **Figure E.8** and **Figure E.9)**], but it is still possible to clearly identify the most promising conditions for the recovery and purification of IgG from human serum samples.

Therefore, the results obtained through these factorial plannings allowed to get some new insights and directions on the conditions that improved the developed process, allowing to achieve its maximum performance. In general, S:L ratios of 100 mg·mL^{-1}, more alkaline pH values (> 8), and contact times above 60 min proved to be beneficial for the process improvement.

4.1.4.5. Experimental optimization of the IgG downstream process

Based on the results obtained from the factorial planning, the best conditions in terms of S:L ratio and contact time were fixed (100 mg·mL^{-1} and 60 min of contact time, in order to reduce the energetic input and the economic cost of the process), while the pH value, a parameter that was proven to be statistically significant, was then optimized to maximize the yield/purity of IgG from human serum samples. Since the factorial planning showed that alkaline pH values were more favourable for the processes under development, a pH study was carried out for all SILs, considering pH 10, 11 and 12. The data was analyzed in terms of performance parameters (%Yield$_{IgG}$ and %Purity$_{IgG}$) for each material after contact with human serum samples at the three pH values under study, whose results are presented in **Figure 4.1.7**. The detailed obtained data ([IgG], %Yield$_{IgG}$, %Purity$_{IgG}$ and %Purity$_{IgG}$) can be found in the **Appendix E (Table E.21)**.

It should be highlighted that, as previously described, using [Si][C$_3$mim]Cl there is a preferential adsorption of the protein impurities onto the material while human IgG remains in solution, and using [Si][N$_{3444}$]Cl and [Si][N$_{3888}$]Cl the opposite behavior was observed – there is a preferential adsorption of IgG onto the material, while the protein impurities remained in solution. These different behaviors could be explained by the differences in the chemical structures of the SILs under study and the interactions they are capable to establish: for [Si][C$_3$mim]Cl, electrostatic interactions and π ⋯ π interactions between the aromatic ring of the SIL and the aromatic residues

of protein impurities appear to be more relevant for the adsorption phenomenon; in the case of [Si][N₃₄₄₄]Cl and [Si][N₃₈₈₈]Cl, the most hydrophobic SILs under study, both electrostatic and hydrophobic interactions seem to play a role in the selective adsorption of proteins.

Due to the different behaviors of the materials, the results shown in **Figure 4.1.7** reflect the performance parameters obtained in the aqueous medium for [Si][C₃mim]Cl and in the SIL material for [Si][N₃₄₄₄]Cl and [Si][N₃₈₈₈]Cl.
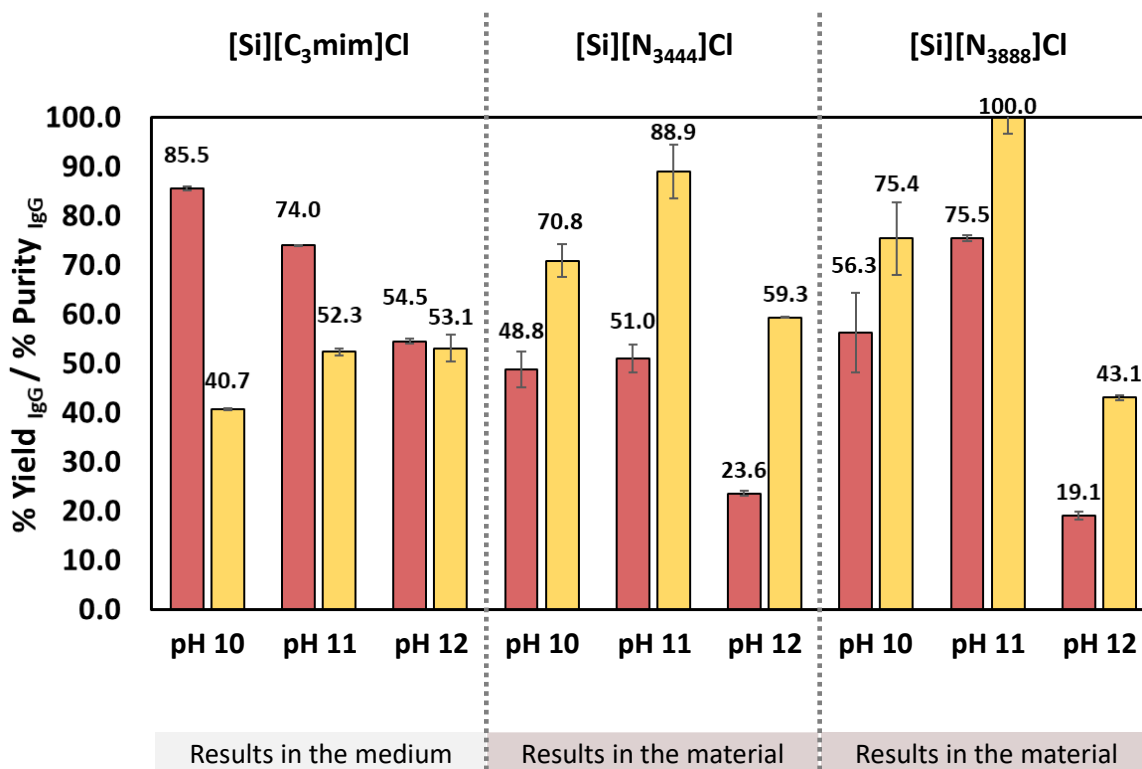
Figure 4.1.7. Recovery yields (%Yield$_{IgG}$ – ■) and purity levels (%Purity$_{IgG}$ – ■) of human IgG from serum samples after contact with SILs materials ([Si][C₃mim]Cl, [Si][N₃₄₄₄]Cl and [Si][N₃₈₈₈]Cl), using the following operation conditions: S:L ratio of 100 mg·mL^{-1}, three different pH values (pH 10, 11 and 12) and 60 min of contact time.

In general, good recovery yields were achieved, ranging between a low value of 19.1 % and up to 85.5 %, as well as promising purity levels, ranging from 40.7 % and up to 100 %. It was found that pH 11 leads to the best compromise between recovery yield and purity level for all the three SILs studied. For instance, for [Si][C₃mim]Cl, an IgG recovery yield of 74.0 % and a purity level of 52.3 % were obtained in the aqueous medium, with a full removal of aggregates [%Aggregation$_{IgG}$ = 0.0 %, *cf.* **Appendix E (Table E.21)**]. Regarding [Si][N₃₄₄₄]Cl, an extraction yield of 51.0 % was obtained with a purity level of 88.9 %, and with low aggregates content (%Aggregation$_{IgG}$ = 15.7 %

vs. 30.0 % in the initial human serum sample). Remarkably, the complete purification of IgG was achieved (100.0 %) in a single step by using [Si][N$_{3888}$]Cl, with a recovery yield of 75.5 %, and also with low content in aggregates (%Aggregation$_{IgG}$ = 15.9 % vs. 30.0 % in the initial human serum sample).

Based on the aforementioned information, the most hydrophobic SIL, [Si][N$_{3888}$]Cl, performs better than [Si][N$_{3444}$]Cl, since a good IgG recovery and complete purification (%Yield$_{IgG}$ = 75.5 %; %Purity$_{IgG}$ = 100.0 %) was achieved under the operation conditions studied – S:L ratio of 100 mg·mL^{-1}, pH 11, contact time of 60 min. Using [Si][C$_3$mim]Cl, a good recovery of IgG was obtained (74.0 %), however, with a purity of only 52.3 %; therefore, this material was selected to proceed with an optimization of the S:L ratio, aiming to maximize the performance parameters achieved using the present SIL.

The process based on [Si][C$_3$mim]Cl, that allowed a simple and direct recovery of IgG in the aqueous media without requiring any elution step, was optimized concerning the S:L ratio (100, 150 and 200 mg·mL^{-1}), at different pH values (pH 10, 11 and 12) and at a fixed contact time of 60 min. The results obtained (%Yield$_{IgG}$ and %Purity$_{IgG}$) are shown in **Figure 4.1.8**, whereas the detailed obtained data ([IgG], %Yield$_{IgG}$, %Purity$_{IgG}$ and %Purity$_{IgG}$) can be found in the **Appendix E (Table E.22)**.

In general, recovery yields ranging between 54.5 % and 88.2 % with purity levels comprised between 31.3 % and up to 84.2 % were achieved in a single step. Moreover, independently of the S:L ratio used, higher recovery yields were obtained for the lowest pH value (%Yield$_{IgG}$ ranging between 79.3 % and 88.2 %), while lower recovery yields for the highest pH value (%Yield$_{IgG}$ ranging between 54.5 % and 59.2 %). Nevertheless, it is interesting to notice that an opposite trend was observed regarding the purity of IgG, which increases with the pH value, allowing purity levels up to 84.2 % to be achieved at pH 12. It is important to highlight that the increase of the S:L ratio from 100 up to 200 mg·mL^{-1} for pH 10 and 11 leads to a decrease on the purity levels of IgG (from 40.7 % to 32.6 %, and from 52.3 % to 42.6 %, respectively), thus revealing not to favour the IgG purification process. However, at pH 12, the increase on the S:L ratio revealed to have an important role on the purification process, since an increase of the IgG purity level was observed for higher S:L ratios. The best results in terms of compromise between recovery yield and purity were obtained at pH 12 and using a S:L ratio of 150 mg·mL^{-1}, allowing to recover 59.1 % of IgG from human serum with a purity level of 84.2 % in a single-step.

Based on the exposed, it was possible to optimize the SIL-mediated process with [Si][C$_3$mim]Cl in order to show a good performance towards IgG recovery and purification, having

the advantage that IgG can be simply and directly recovered in the aqueous medium after contact with the SIL material.
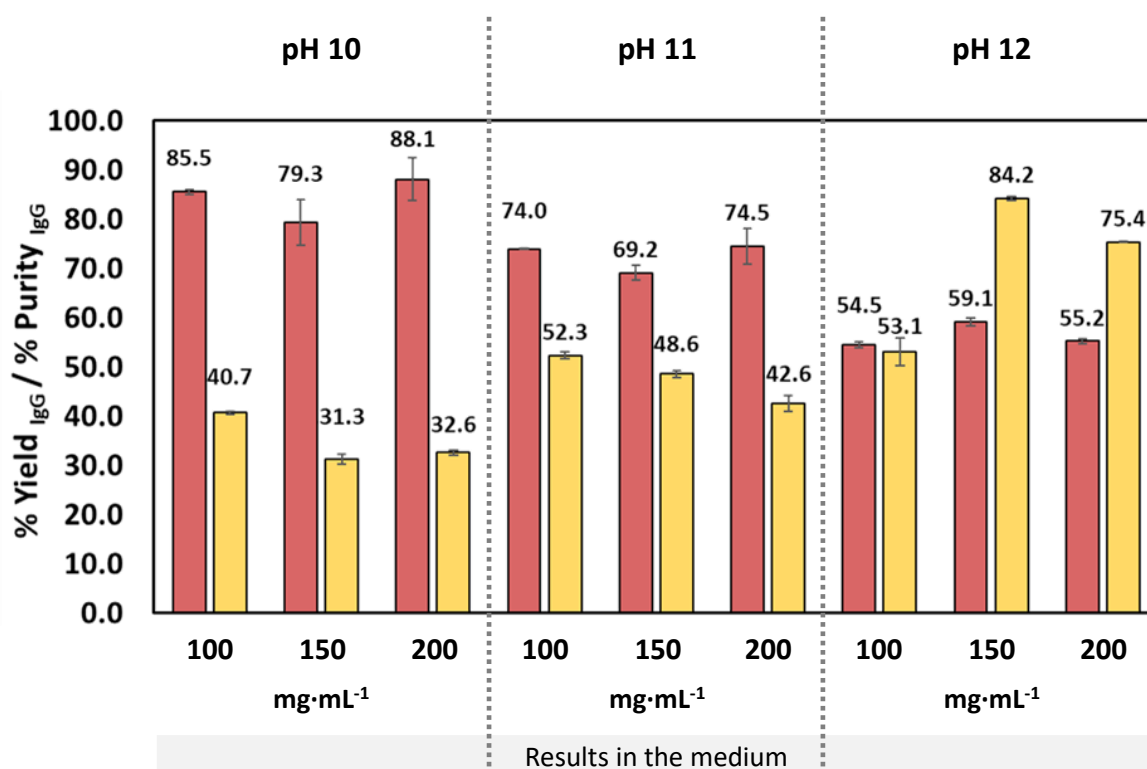
Figure 4.1.8. Recovery yields (%Yield$_{IgG}$ – ▪) and purity levels (%Purity$_{IgG}$ – ▪) of human IgG from serum samples after contact with [Si][C$_3$mim]Cl, using the following operation conditions: S:L ratio of 100, 150 and 200 mg·mL^{-1}, three different pH values (pH 10, 11 and 12) and 60 min of contact time.

4.1.4.6. SILs as chromatographic matrices for IgG downstream processing

Based on the aforementioned results, two different IgG recovery/purification mechanisms can be applied, depending on the chemical structure of the IL supported in the silica material. These results confirm that SILs may act as innovative and flexible chromatographic matrices. The two different strategies are schematically presented in **Figure 4.1.9**.

We showed that IgG can be purified and recovered in a very simple and direct way in the aqueous medium after contact with [Si][C$_3$mim]Cl, under specific operation conditions (S:L ratio of 150 mg·mL^{-1}, pH 12, and contact time of 60 min). In this case, it is possible to adsorb the protein impurities onto the SIL material, in particular albumin, as well as high molecular weight protein aggregates, while IgG remain in the aqueous media. Therefore, these features seem to be appropriate for the use of [Si][C$_3$mim]Cl as a chemically-modified chromatographic matrix for the

downstream processing of IgG antibodies in a flowthrough-like mode, as represented in **Figure 4.1.9 (A)**.
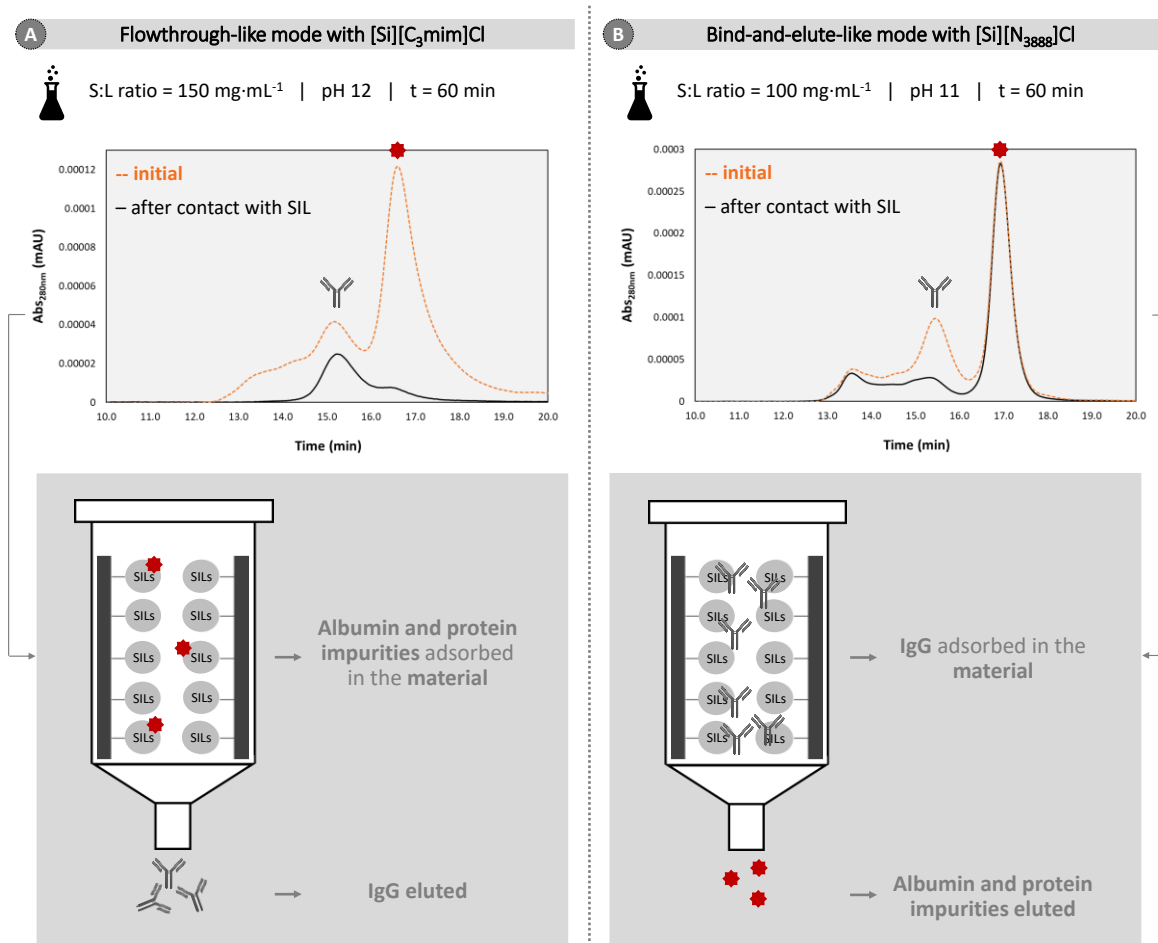
Figure 4.1.9. Schematic overview on the proposed IgG recovery and purification processes mediated by SILs: (A) a flowthrough-like mode with [Si][C$_3$mim]Cl, in which albumin and other protein impurities are adsorbed onto the material and IgG can ideally be eluted; and (B) a bind-and-elute-like mode with [Si][N$_{3888}$]Cl), in which IgG is adsorbed onto the material, while albumin and other protein impurities are ideally eluted from the column.

Through the SE-HPLC chromatogram presented in **Figure 4.1.9 (A)**, it is noticeable the predominance of the IgG peak in the sample after contact with the SIL material, confirming its presence with a high purity level in the aqueous solution (recovery yield of 59.2 and purity level of 84.2 %), and free of protein aggregates. Regarding the molecular mechanisms underlying the adsorption process, besides the electrostatic interactions and π ⋯ π interactions that were previously discussed, the molecular crowding phenomenon may also be playing a role, since

albumin is the most abundant protein, and it can potentially adsorb onto the material at a larger extent, saturating the SIL and avoiding IgG to be adsorbed as well.

Even though SILs were never explored in the literature for the recovery/purification of antibodies, imidazolium-based SILs were reported by Song et al. [55] for the extraction and purification of a biomolecule (BSA) from cow blood, reporting slightly higher purities than those achieved herein (91 % vs. 84 % in this work), although with lower recovery yield (28 % vs 59.2 % in this work). Imidazolium-based ILs already proved to improve the results achieved for the downstream processing of antibodies with other techniques, namely as adjuvants in aqueous biphasic systems [60], where an IgG extraction yield of 46 % and a purity level of 26 % were obtained by the authors. Still, the results obtained in this work using the imidazolium-based SIL seems to be very promising with a better performance than that previously reported in the literature.

In the opposite approach, IgG could be adsorbed onto $[Si][N_{3888}]Cl$, leading to the protein impurities to be retained in the aqueous media, under specific operation conditions (S:L ratio of 100 $mg \cdot mL^{-1}$, pH 11, and contact time of 60 min). This observation allows to propose $[Si][N_{3888}]Cl$ as chemically-modified matrix for the downstream processing of IgG antibodies in a bind-and-elute-like mode, as shown in **Figure 4.1.9 (B)**. Under the mentioned operation conditions, 75.5 % of IgG could be recovered with a purity of 100 %, in a single-step, and with a reduction of the protein aggregates to 15.9 % (*cf.* the SE-HPLC chromatogram in **Figure 4.1.9 (B)**). In fact, this particular SIL is composed of long alkyl chains, assuring to this material a hydrophobic nature (hydrophobicity value of 10.5, data from PubChem; CID for trioctylamine – 14227). Curiously, IgG is the only protein being adsorbed into the material, which is probably related with the fact that IgG is the most hydrophobic protein in the complex medium (*ca.* 14 % of surface hydrophobic residues [7]), hence being preferentially retained in the material through hydrophobic interactions.

It is interesting to notice that, similarly to the results achieved with the imidazolium-based SIL, the results obtained with the quaternary ammonium-based SIL also outstands those results reported by Song et al. [55] on the extraction and purification of BSA using SILs. Also, the results herein reported are better than those obtained with the corresponding ionic liquids (quaternary ammonium-based ILs) in other relevant techniques, such as aqueous micellar two-phase systems (AMTPS) [61], concerning the purification of IgG from human plasma. Vicente et al. [61] reported a slightly higher recovery yield of 82 % (vs. 76 % obtained in this work using $[Si][N_{3888}]Cl$), however with a lower purification factor of 1.08.

Overall, SILs appear as promising candidates for the development of cost-effective and green alternatives for the downstream processing of therapeutic antibodies, that can easily be adapted

into chromatographic matrices, potentially working in flowthrough or bind-and-elute modes, depending on the choice of the IL chemical structure attached to the silica.

4.1.4.7. Reproducibility and robustness of the developed processes

To evaluate the reproducibility and robustness of the proposed SILs for processing other complex biological matrices, additional studies were carried out using CHO cell culture supernatants and rabbit serum samples (20-fold diluted). The studies were carried out under the best operation conditions identified for the two most promising SILs: [Si][C$_3$mim]Cl (S:L ratio of 150 mg·mL^{-1}, pH 12, and contact time of 60 min) and [Si][N$_{3888}$]Cl (S:L ratio of 100 mg·mL^{-1}, pH 11, and contact time of 60 min). The results obtained (%Yield$_{IgG}$ and %Purity$_{IgG}$) are shown in **Figure 4.1.10**, whereas the detailed obtained data ([IgG], %Yield$_{IgG}$, %Purity$_{IgG}$ and %Purity$_{IgG}$) can be found in the **Appendix E (Table E.23)**.
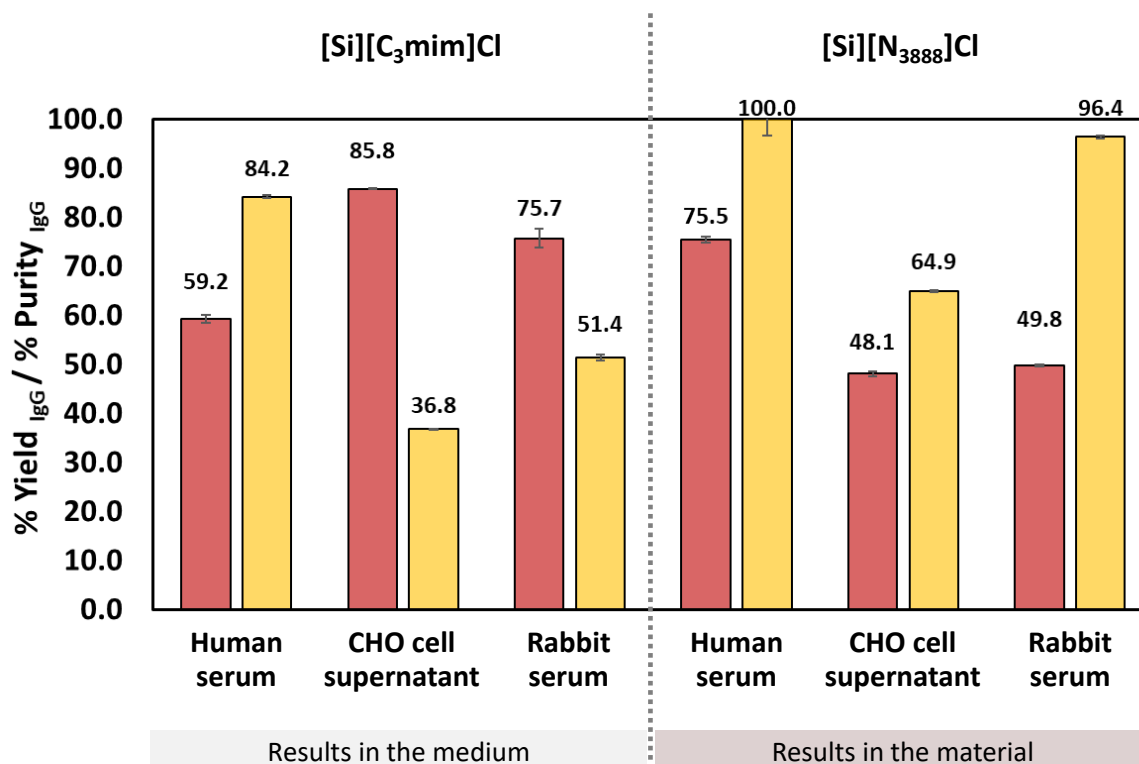
Figure 4.1.10. Recovery yields (%Yield$_{IgG}$ – ■) and purity levels (%Purity$_{IgG}$ – ■) of IgG from different complex biological matrices (human serum, CHO cell culture supernatants and rabbit serum) after contact with [Si][C$_3$mim]Cl (operation conditions: S:L ratio of 150 mg·mL^{-1}, pH 12 and 60 min of contact time) and [Si][N$_{3888}$]Cl (operation conditions: S:L ratio of 100 mg·mL^{-1}, pH 11 and 60 min of contact time).

Although dealing with different biological samples, that inherently display different compositions, the obtained results show that, in general, the similar trends are obtained. For [Si][C$_3$mim]Cl, independently of the biological matrix, the IgG remains in solution after contact with the SIL adsorbent. When bioprocessing the two new biological matrices, it was found that higher IgG recovery yields are obtained (> 75 %) in comparison with human serum (59.2 %); however, with lower purity values (< 52 %). In particular, for the rabbit serum samples, 75.7 % of IgG could be recovered with a purity level of 51.4 %, and when bioprocessing CHO cell culture supernatants, a higher recovery yield is achieved (85.8 %) even though with a lower purity (36.8 %). Regarding the bioprocess mediated by [Si][N$_{3888}$]Cl, and for the new matrices, IgG was evenly distributed between the SIL and the aqueous media, since a recovery yield of around 50% was achieved in both cases. Particularly, a recovery yield of 49.8 % with a purity of 96.4 % was achieved in the material for rabbit serum, and a recovery yield of 48.1 % with a purity of 64.9 % was achieved in the material for the CHO cell culture supernatant.

Although in general, lower performance parameters were obtained for the new matrices than those achieved for human serum samples, it should be remarked that a similar yield/purity level was observed for rabbit serum – a matrix with higher similarity to human serum than cell culture supernatants. In the CHO cell culture supernatant, the major protein impurity is bovine serum albumin (BSA) whereas other protein impurities are also present resulting from the medium used in the cell proliferation, growth, and also from their metabolism (e.g. insulin, transferrin and other CHO host cell proteins) [58]. Therefore, it can be concluded that the same adsorption mechanisms were present in each SIL, independently of the matrix under study. Although lower performance was found when bioprocessing other matrices than human serum, good results for the recovery yield/purity have been found for one-step approaches. Still, there is room for improvements in the performance of SILs-mediated downstream processes for other complex biological matrices such as rabbit serum or CHO cell culture supernatants, namely through optimization of the operational parameters, specifically for each matrix.

4.1.5. Conclusions

Aiming to develop new recovery/purification platforms for therapeutic IgG antibodies from complex biological media, in this work, the potential of SIL materials was ascertained. Three SILs ([Si][C$_3$mim]Cl, [Si][N$_{3444}$]Cl and [Si][N$_{3888}$]Cl) were synthesized, characterized and studied for the first time towards the recovery and purification of IgG antibodies from biological matrices.

Firstly, an initial screening of several pH values (from 3.0 to 9.0) was performed to evaluate the effect of the pH in the (selective) adsorption of proteins from human serum, being possible to conclude that a pH equal to 5 or higher is required for proteins adsorption, being at the most alkaline pH values that the adsorption occurs more extensively. Then, a factorial planning was implemented in order to get some insights regarding the optimum conditions at which the processes under development occur, namely in term of S:L ratio, pH and contact time. Based on the results obtained, a S:L ratio of 100 mg·mL^{-1}, a pH higher than 9, and a contact time of 60 min were identified as the optimum conditions for the best performance of the SIL-mediated processes. The performance parameters were then optimized through the optimization of the pH value and S:L ratio.

Two different IgG recovery/purification mechanisms were identified, being highly dependent on the IL chemical structure: (i) by using [Si][C$_3$mim]Cl, IgG could be simply and directly recovered in the aqueous solution after contact with the material under a specific set of operation conditions, namely an S:L ratio of 150 mg·mL^{-1}, pH 12, and a contact time of 60 min, yielding 59 % of IgG with a purity level of 84 %; and (ii) by using [Si][N$_{3888}$]Cl, IgG is mainly adsorbed onto the material, using as operation conditions an S:L ratio of 100 mg·mL^{-1}, pH 11 and contact time of 60 min, yielding 76 % of IgG with a purity level of 100 %.

The developed platforms were applied for the downstream processing of IgG antibodies from other complex biological matrices, namely CHO cell culture supernatants and rabbit serum, revealing the same recovery/purification mechanisms. Still, lower performance parameters were achieved with such matrices (in comparison with those obtained with human serum samples), thus indicating that an optimization of the operation conditions may be required, in order to improve the SILs-based process performance for each specific matrix.

In conclusion, novel, high-efficient and low-cost platforms were successfully developed for the recovery and purification of IgG antibodies from complex biological media based on the use of SILs nanomaterials, and capable of being adopted by the pharmaceutical industry as novel chromatographic matrices.

4.1.6. References

1.   A.M. Azevedo, P.A. Rosa, I.F. Ferreira, J. De Vries, T. Visser, and M.R. Aires-Barros, *Downstream processing of human antibodies integrating an extraction capture step and cation exchange chromatography.* Journal of Chromatography B, 2009. **877**(1-2): p. 50-58.

2.   S. Fekete, A. Goyon, J.-L. Veuthey, and D. Guillarme, *Size exclusion chromatography of protein biopharmaceuticals: past, present and future.* American Pharmaceutical Review, 2018: p. 1-4.

3.   M. Vargas, Á. Segura, M. Herrera, M. Villalta, Y. Angulo, J.M. Gutiérrez, G. León, and T. Burnouf, *Purification of IgG and albumin from human plasma by aqueous two phase system fractionation.* Biotechnology Progress, 2012. **28**(4): p. 1005-1011.

4.   J. Dwyer, *Intravenous therapy with gamma globulin.* Advances in Internal Medicine, 1987. **32**: p. 111-135.

5.   A.J.N.r.D.D. Mullard, *FDA approves 100th monoclonal antibody product.* Nature Reviews Drug Discovery, 2021. **20**: p. 491-495.

6.   E.V. Capela, M.R. Aires-Barros, M.G. Freire, and A.M. Azevedo, *Monoclonal antibodies — addressing the challenges on the manufacturing processing of an advanced class of therapeutic agents*, in *Frontiers in Clinical Drug Research - Anti-Infectives*, Atta-ur-Rahman, Editor. 2017, Bentham Science p. 142-203.

7.   P.A. Rosa, A.M. Azevedo, and M.R. Aires-Barros, *Application of central composite design to the optimisation of aqueous two-phase extraction of human antibodies.* Journal of Chromatography A, 2007. **1141**(1): p. 50-60.

8.   A.M. Azevedo, P.A. Rosa, I.F. Ferreira, and M.R. Aires-Barros, *Chromatography-free recovery of biopharmaceuticals through aqueous two-phase processing.* Trends in Biotechnology, 2009. **27**(4): p. 240-247.

9.   A.C.A. Roque, C.R. Lowe, and M.Â. Taipa, *Antibodies and genetically engineered related molecules: production and purification.* Biotechnology Progress, 2004. **20**(3): p. 639-654.

10.   A.L. Grilo, M. Mateus, M.R. Aires-Barros, and A.M. Azevedo, *Monoclonal antibodies production platforms: an opportunity study of a non-protein-A chromatographic platform based on process economics.* Biotechnology Journal, 2017. **12**(12): p. 1700260.

11.   A.M. Clausen, A. Subramanian, and P.W. Carr, *Purification of monoclonal antibodies from cell culture supernatants using a modified zirconia based cation-exchange support.* Journal of Chromatography A, 1999. **831**(1): p. 63-72.

12.   G. Joucla, C. Le Senechal, M. Begorre, B. Garbay, X. Santarelli, and C. Cabanne, *Cation exchange versus multimodal cation exchange resins for antibody capture from CHO supernatants: identification of contaminating Host Cell Proteins by mass spectrometry.* Journal of Chromatography B, 2013. **942**: p. 126-133.

13.   Y. Hou, M. Brower, D. Pollard, D. Kanani, R. Jacquemart, B. Kachuik, and J. Stout, *Advective hydrogel membrane chromatography for monoclonal antibody purification in bioprocessing.* Biotechnology Progress, 2015. **31**(4): p. 974-982.

14.   R. Ghosh and L. Wang, *Purification of humanized monoclonal antibody by hydrophobic interaction membrane chromatography.* Journal of Chromatography A, 2006. **1107**(1-2): p. 104-109.

15.   L. Guerrier, I. Flayeux, and E. Boschetti, *A dual-mode approach to the selective separation of antibodies and their fragments.* Journal of Chromatography B: Biomedical Sciences and Applications, 2001. **755**(1-2): p. 37-46.

16.   S.A. Rosa, R. dos Santos, M.R. Aires-Barros, and A.M. Azevedo, *Phenylboronic acid chromatography provides a rapid, reproducible and easy scalable multimodal process for the capture of monoclonal antibodies.* Separation and Purification Technology, 2016. **160**: p. 43-50.

17.   S. Vançan, E.A. Miranda, and S.M.A. Bueno, *IMAC of human IgG: studies with IDA-immobilized copper, nickel, zinc, and cobalt ions and different buffer systems.* Process Biochemistry, 2002. **37**(6): p. 573-579.

18.   Y. González, N. Ibarra, H. Gómez, M. Gonzalez, L. Dorta, S. Padilla, and R. Valdés, *Expanded bed adsorption processing of mammalian cell culture fluid: comparison with packed bed affinity chromatography.* Journal of Chromatography B, 2003. **784**(1): p. 183-187.

19.   R. Giovannini and R. Freitag, *Isolation of a recombinant antibody from cell culture supernatant: continuous annular versus batch and expanded-bed chromatography.* Biotechnology and Bioengineering, 2001. **73**(6): p. 522-529.

20.   S. Schwark, W. Sun, J. Stute, D. Lütkemeyer, M. Ulbricht, and B. Sellergren, *Monoclonal antibody capture from cell culture supernatants using epitope imprinted macroporous membranes.* RSC Advances, 2016. **6**(58): p. 53162-53169.

21.   L.R. Castilho, F.B. Anspach, and W.-D. Deckwer, *Comparison of affinity membranes for the purification of immunoglobulins.* Journal of Membrane Science, 2002. **207**(2): p. 253-264.

22.   S. Ghose, B. Hubbard, and S.M. Cramer, *Evaluation and comparison of alternatives to Protein A chromatography: mimetic and hydrophobic charge induction chromatographic stationary phases.* Journal of Chromatography A, 2006. **1122**(1-2): p. 144-152.

23.   G. El Khoury and C.R. Lowe, *A biomimetic Protein G affinity adsorbent: an Ugi ligand for immunoglobulins and Fab fragments based on the third IgG-binding domain of Protein G.* Journal of Molecular Recognition, 2013. **26**(4): p. 190-200.

24.   T. Arakawa, Y. Kita, H. Sato, and D. Ejima, *MEP chromatography of antibody and Fc-fusion protein using aqueous arginine solution.* Protein Expression and Purification, 2009. **63**(2): p. 158-163.

25.   Y. Liu, Y. Lu, and Z. Liu, *Restricted access boronate affinity porous monolith as a protein A mimetic for the specific capture of immunoglobulin G.* Chemical Science, 2012. **3**(5): p. 1467-1471.

26.   C.S. Fernandes, R. Dos Santos, S. Ottengy, A.C. Viecinski, G. Béhar, B. Mouratou, F. Pecorari, and A.C.A. Roque, *Affitins for protein purification by affinity magnetic fishing.* Journal of Chromatography A, 2016. **1457**: p. 50-58.

27.   B.M. Alves, L. Borlido, S.A. Rosa, M.F. Silva, M.R. Aires-Barros, A.C. Roque, and A.M. Azevedo, *Purification of human antibodies from animal cell cultures using gum arabic coated magnetic particles.* Journal of Chemical Technology & Biotechnology, 2015. **90**(5): p. 838-846.

28.   V.L. Dhadge, A. Hussain, A.M. Azevedo, R. Aires-Barros, and A.C. Roque, *Boronic acid-modified magnetic materials for antibody purification.* Journal of The Royal Society Interface, 2014. **11**(91): p. 20130875.

29.   T. Barroso, R.J. Branco, A. Aguiar-Ricardo, and A.C. Roque, *Structural evaluation of an alternative Protein A biomimetic ligand for antibody purification.* Journal of Computer-aided Molecular Design, 2014. **28**(1): p. 25-34.

30.   T. Barroso, A. Lourenço, M. Araújo, V.D. Bonifácio, A.C. Roque, and A. Aguiar-Ricardo, *A green approach toward antibody purification: a sustainable biomimetic ligand for direct immobilization on (bio) polymeric supports.* Journal of Molecular Recognition, 2013. **26**(12): p. 662-671.

31.   S.D. Santana, V.L. Dhadge, and A.C. Roque, *Dextran-coated magnetic supports modified with a biomimetic ligand for IgG purification.* ACS Applied Materials & Interfaces, 2012. **4**(11): p. 5907-5914.

32.   L. Borlido, A. Azevedo, A. Roque, and M. Aires-Barros, *Potential of boronic acid functionalized magnetic particles in the adsorption of human antibodies under mammalian cell culture conditions.* Journal of Chromatography A, 2011. **1218**(43): p. 7821-7827.

33.   I.L. Batalha, A. Hussain, and A. Roque, *Gum Arabic coated magnetic nanoparticles with affinity ligands specific for antibodies.* Journal of Molecular Recognition, 2010. **23**(5): p. 462-471.

34.   T. Barroso, M. Temtem, A. Hussain, A. Aguiar-Ricardo, and A.C. Roque, *Preparation and characterization of a cellulose affinity membrane for human immunoglobulin G (IgG) purification.* Journal of Membrane Science, 2010. **348**(1-2): p. 224-230.

35.   A. Roque, S. Bispo, A. Pinheiro, J. Antunes, D. Gonçalves, and H. Ferreira, *Antibody immobilization on magnetic particles.* Journal of Molecular Recognition, 2009. **22**(2): p. 77-82.

36.   A.C.A. Roque, M.Â. Taipa, and C.R. Lowe, *Synthesis and screening of a rationally designed combinatorial library of affinity ligands mimicking protein L from Peptostreptococcus magnus.* Journal of Molecular Recognition, 2005. **18**(3): p. 213-224.

37.   A.C.A. Roque, M.Â. Taipa, and C.R. Lowe, *An artificial protein L for the purification of immunoglobulins and Fab fragments by affinity chromatography.* Journal of Chromatography A, 2005. **1064**(2): p. 157-167.

38.   A.C.A. Roque, M.Â. Taipa, and C.R. Lowe, *A new method for the screening of solid-phase combinatorial libraries for affinity chromatography.* Journal of Molecular Recognition, 2004. **17**(3): p. 262-267.

39.   N. Fontanals, S. Ronka, F. Borrull, A.W. Trochimczuk, and R.M. Marcé, *Supported imidazolium ionic liquid phases: a new material for solid-phase extraction.* Talanta, 2009. **80**(1): p. 250-256.

40.   T.D. Ho, A.J. Canestraro, and J.L. Anderson, *Ionic liquids in solid-phase microextraction: a review.* Analytica Chimica Acta, 2011. **695**(1-2): p. 18-43.

41.   L. Vidal, M.-L. Riekkola, and A. Canals, *Ionic liquid-modified materials for solid-phase extraction and separation: a review.* Analytica Chimica Acta, 2012. **715**: p. 19-41.

42.   N. Fontanals, F. Borrull, and R.M. Marcé, *Ionic liquids in solid-phase extraction.* TrAC Trends in Analytical Chemistry, 2012. **41**: p. 15-26.

43.   S.K. Singh and A.W. Savoy, *Ionic liquids synthesis and applications: an overview.* Journal of Molecular Liquids, 2020. **297**: p. 112038.

44.   P. Du, S. Liu, P. Wu, and C. Cai, *Preparation and characterization of room temperature ionic liquid/single-walled carbon nanotube nanocomposites and their application to the direct electrochemistry of heme-containing proteins/enzymes.* Electrochimica Acta, 2007. **52**(23): p. 6534-6547.

45.   Y.-Y. Jiang, Z. Zhou, Z. Jiao, L. Li, Y.-T. Wu, and Z.-B. Zhang, *SO2 gas separation using supported ionic liquid membranes.* The Journal of Physical Chemistry B, 2007. **111**(19): p. 5058-5061.

46.   H. Qiu, S. Jiang, X. Liu, and L. Zhao, *Novel imidazolium stationary phase for high-performance liquid chromatography.* Journal of Chromatography A, 2006. **1116**(1-2): p. 46-50.

47.   H. Qiu, S. Jiang, and X. Liu, *N-Methylimidazolium anion-exchange stationary phase for high-performance liquid chromatography.* Journal of Chromatography A, 2006. **1103**(2): p. 265-270.

48.   Q. Wang, G.A. Baker, S.N. Baker, and L.A. Colón, *Surface confined ionic liquid as a stationary phase for HPLC.* Analyst, 2006. **131**(9): p. 1000-1005.

49.   J.C. Moreira and Y. Gushikem, *Preconcentration of metal ions on silica gel modified with 3 (1-imidazolyl) propyl groups.* Analytica Chimica Acta, 1985. **176**: p. 263-267.

50.   M. Van de Voorde, K. Van Hecke, K. Binnemans, and T. Cardinaels, *Supported ionic liquid phases for the separation of samarium and europium in nitrate media: towards purification of medical samarium-153.* Separation and Purification Technology, 2020. **232**: p. 115939.

51.   S.C. Bernardo, B.R. Araújo, A.C. Sousa, R.A. Barros, A.C. Cristovão, M.C. Neves, and M.G. Freire, *Supported ionic liquids for the efficient removal of acetylsalicylic acid from aqueous solutions.* European Journal of Inorganic Chemistry, 2020. **2020**(24): p. 2380-2389.

52.   H.F. Almeida, M.C. Neves, T. Trindade, I.M. Marrucho, and M.G. Freire, *Supported ionic liquids as efficient materials to remove non-steroidal anti-inflammatory drugs from aqueous media.* Chemical Engineering Journal, 2020. **381**: p. 122616.

53.   Y. Shu, X.-W. Chen, and J.-H. Wang, *Ionic liquid–polyvinyl chloride ionomer for highly selective isolation of basic proteins.* Talanta, 2010. **81**(1-2): p. 637-642.

54.   G. Zhao, S. Chen, X.-W. Chen, and R.-H. He, *Selective isolation of hemoglobin by use of imidazolium-modified polystyrene as extractant.* Analytical and Bioanalytical Chemistry, 2013. **405**(15): p. 5353-5358.

55.   H. Song, C. Yang, A. Yohannes, and S. Yao, *Acidic ionic liquid modified silica gel for adsorption and separation of bovine serum albumin (BSA).* RSC Advances, 2016. **6**(109): p. 107452-107462.

56.   R. dos Santos, S.A. Rosa, M.R. Aires-Barros, A. Tover, and A.M. Azevedo, *Phenylboronic acid as a multi-modal ligand for the capture of monoclonal antibodies: development and optimization of a washing step.* Journal of Chromatography A, 2014. **1355**: p. 115-124.

57.   J.B. Costa, M.J. Lima, M.J. Sampaio, M.C. Neves, J.L. Faria, S. Morales-Torres, A.P. Tavares, and C.G. Silva, *Enhanced biocatalytic sustainability of laccase by immobilization on functionalized carbon nanotubes/polysulfone membranes.* Chemical Engineering Journal, 2019. **355**: p. 974-985.

58.   E.V. Capela, A.E. Santiago, A.F.C.S. Rufino, A.P.M. Tavares, M.M. Pereira, A. Mohamadou, M.R. Aires-Barros, J.A.P. Coutinho, A.M. Azevedo, and M.G. Freire, *Sustainable strategies based on glycine–betaine analogue ionic liquids for the recovery of monoclonal antibodies from cell culture supernatants.* Green Chemistry, 2019. **21**(20): p. 5671-5682.

59.   C.C. Ramalho, C.M. Neves, M.V. Quental, J.A.P. Coutinho, and M.G. Freire, *Separation of immunoglobulin G using aqueous biphasic systems composed of cholinium-based ionic liquids and poly (propylene glycol).* Journal of Chemical Technology & Biotechnology, 2018. **93**(7): p. 1931-1939.

60.   A.M. Ferreira, V.F. Faustino, D. Mondal, J.A.P. Coutinho, and M.G. Freire, *Improving the extraction and purification of immunoglobulin G by the use of ionic liquids as adjuvants in aqueous biphasic systems.* Journal of Biotechnology, 2016. **236**: p. 166-175.

61.   F.A. Vicente, J. Bairos, M. Roque, J.A.P. Coutinho, S.P.M. Ventura, and M.G. Freire, *Use of ionic liquids as cosurfactants in mixed aqueous micellar two-phase systems to improve the simultaneous separation of immunoglobulin G and human serum albumin from expired human plasma.* ACS Sustainable Chemistry & Engineering, 2019. **7**(17): p. 15102-15113.

Final Remarks and Future Work 5

This thesis started by saying that all lives are important. However, and particularly in the healthcare field, it is known that some lives are often compromised since not all therapies are accessible to all the people. Indeed, antibody-based therapies have already shown a great potential throughout the years for the treatment of several diseases, including 21st century diseases such as cancer and autoimmune and inflammatory diseases. Sometimes, they are even the only available therapy for some specific disorders. Nevertheless, these biopharmaceuticals are not yet widely applied as recurrent therapies due to the absence of cost-effective downstream platforms, making the final product of high price and thus, not accessible as a conventional therapy. And this fact was what motivated the development of this PhD thesis, i.e. trying to develop novel cost-effective process that could afford IgG therapeutics at lower cost while allowing their widespread use by population.

The 2015 Nobel Prize in Physiology or Medicine, Tu Youyou, said that "every scientist dreams of doing something that can help the world", and that is a completely realistic vision of the scientists' motivation. That was my motivation. When I first started this PhD thesis, I was not conscious about the roller coaster it was going to be, but I was focused in just one aim – to do something relevant that could help the world. If the set of works composing this thesis contribute with knowledge and insights for future improvements in the biopharmaceuticals field, and could help somehow improving the worldwide society healthcare, then I achieved the biggest success I could aspire, and it was all worth it.

Following on from this idea, this PhD thesis started by a comprehensive literature review on the current state of the art of the biopharmaceuticals market, the importance of mAbs for therapeutic purposes, and the current bottlenecks associated with the production and widespread use of this type of biopharmaceuticals. Also, a literature review about inflammatory diseases was introduced, allowing to highlight the remarkable potential of mAbs in the prevention and treatment of this particular group of diseases. Then, a set of five works were developed towards the downstream processing of therapeutic human antibodies using ionic liquids (ILs) using three different approaches: aqueous biphasic systems (ABS), three-phase partitioning (TPP) systems and supported ionic liquid (SIL) materials.

Concerning the set of works referring to ABS, it was interesting to conclude that it is possible to tailor the phases' polarities and affinities by the addition of ILs as adjuvants, which ultimately allow a high performance to be achieved for the extraction and purification of human antibodies (polyclonal – pAbs and monoclonal – mAbs) from different complex biological media. Moreover, it was also shown that it is possible to properly design ILs to present more biocompatible and

sustainable features, such as glycine-betaine analogue ILs, and successfully use them as phase-forming components of ABS. These ABS were optimized and allowed good results in terms of extraction/purification to be achieved, both in a single-step, and in a two-step (hybrid) approach combined with an ultrafiltration step for buffer exchange and final formulation of the antibodies for commercialization. Also, it is important to highlight that herein, we reported that the ABS step do not affect the biological activity of mAbs. In a subsequent chapter, TPP approaches based on ABS were investigated towards the purification and recovery of human antibodies (pAbs and mAbs), showing an enhanced performance under the optimized conditions. Moreover, the addition of ILs to the process was found to be advantageous, since it enables the maximization of the performance parameters, and in some cases allowing the complete depletion of the host cell proteins present in cell supernatants. Finally, having already in mind the potential of ILs in the development of bioprocesses for human antibodies due to their designer solvent character, that allow a multitude of interactions to be established with (bio)molecules, in the last experimental chapter we developed new IL-based materials to be potentially used as chromatographic matrices in antibodies downstream processing. Silica was modified with different ILs chemical structures, giving rise to SILs materials, that were further evaluated towards their ability to selectively adsorb antibodies or other protein impurities. Remarkably, two promising SIL materials were identified, allowing the purification of antibodies (pAbs and mAbs) through two different approaches: a flowthrough-like mode or a bind-and-elute-like mode.

Before this whole PhD started, the only thing I knew was that it consisted in a very attractive, pioneer and ambitious project – indeed, this is the first work bringing together the manufacture of mAbs and the use of ILs, and joining two relevant institutions (University of Aveiro and Instituto Superior Técnico – University of Lisbon) in the field to cooperate. The road so far reveals a promising future for ILs, and it was possible to demonstrate along this thesis that ILs may also have space in biopharmaceutical applications. Nevertheless, this is still far from the end and much more work is still required in the future.

In what concerns ABS, it is still important to study other biocompatible ILs, from natural sources, to increase the number of more sustainable ABS processes available, and ultimately allowing to maximize the performance of these kind of ABS (in terms of recovery yields and purification levels). Microfluidics assays are also crucial to be performed to prove the possibility of operating the IL-ABS processes in continuous mode, without losses in their efficacy (comparable to that of the lab scale), and also proving the scale-out of the process for an increased scale. For the TPP approaches, that were herein explored using (IL-based-)ABS and conventional ILs, it is expected

that, in the future, more biocompatible and sustainable ILs can be considered for the development of novel (high efficient) TPP systems. Regarding the SIL-based processes, it is of upmost importance to study different elution strategies for IgG recovery from the IgG-containing SILs, as well as to prove the best results and optimize the elution step directly through preparative chromatography since the introduction of flow can lead to a different behavior. Finally, it is crucial that partnerships with the (bio)pharmaceutical industry are established, so that these processes can reach the right place in which they can make the difference, and start to be applied and optimized in the bioprocessing of other relevant matrices from those partners.

The achievements herein reported consisted in a steppingstone in the antibodies downstream processing/manufacture, allowing to fight some stigmas from the pharmaceutical industry, for instance: (i) the use of ILs – ILs are versatile candidates to integrate different processes, allowing cost-effective platforms to be developed; (ii) the use of non-chromatographic approaches – ABS and/or TPP can be as effective as chromatographic techniques, allowing easier recoveries of the antibodies and a lower number of unit operations required; and (iii) there is life beyond protein A – SILs can act as efficient and highly-selective chromatographic matrices and of lower price (since they are based on chemical ligands, and not biological ligands, as protein A), capable to be integrated in the chromatographic equipments already available/acquired by the industry.

The journey on this roller coaster is now ending, and all I know is that this PhD was life-changing and shaped my way of being and thinking, making me realize the power that science holds to change and improve peoples' lives. I do not know if I will have a new ticket to go on further turns, but I sincerely hope that all efforts could be made so that the progresses made so far can have a happy ending and that people worldwide could benefit from that.

"Whatever you do in life will be insignificant, but it is very important that you do it because nobody else will."

- Mahatma Gandhi

List of Publications 6

6.1. Publications within the current thesis

6.1.1. Book chapters

1. Jéssica Bairos[§], <u>Emanuel V. Capela</u>[§*], Ana P.M. Tavares, Mara G. Freire; "Monoclonal antibodies as therapeutic agents for inflammatory diseases", Chapter 1 in Frontiers in Clinical Drug Research – Anti Infectives (FCDR-AI), Volume 8, Edited by Atta-ur-Rahman, Bentham Science Publishers (2021) 1-54. DOI: 10.2174/9789815039412121080003. [§]Equal contribution. [*]Corresponding author;

2. <u>Emanuel V. Capela</u>, M. Raquel Aires-Barros, Mara G. Freire, Ana M. Azevedo; "Monoclonal Antibodies – Addressing the Challenges on the Manufacturing Processing of an Advanced Class of Therapeutic Agents", Chapter 5 in Frontiers in Clinical Drug Research – Anti Infectives (FCDR-AI), Volume 4, Edited by Atta-ur-Rahman, Bentham Science Publishers (2017) 142-203. DOI: 10.2174/9781681084879117040.

6.1.2. Papers in international scientific periodicals with referees

1. <u>Emanuel V. Capela</u>, Alexandre E. Santiago, Ana F.C.S. Rufino, Ana P.M. Tavares, Matheus M. Pereira, Aminou Mohamadou, M. Raquel Aires-Barros, João A.P. Coutinho, Ana M. Azevedo, Mara G. Freire; "Sustainable strategies based on glycine–betaine analogue ionic liquids for the recovery of monoclonal antibodies from cell culture supernatants", Green Chemistry 21 (2019) 5671-5682. DOI: 10.1039/C9GC02733E;

2. <u>Emanuel V. Capela</u>, Alexandra Wagner, João A.P. Coutinho, M. Raquel Aires-Barros, Ana M. Azevedo, Mara G. Freire; "Purification of human antibodies from serum samples using aqueous biphasic systems comprising ionic liquids as adjuvants" [under preparation];

3. <u>Emanuel V. Capela</u>, Sara A.S.L. Rosa, Virgínia Chu, João P. Conde, João A.P. Coutinho, M. Raquel Aires-Barros, Ana M. Azevedo, Mara G. Freire; "Ionic-liquid mediated extraction and purification of monoclonal antibodies from cell culture supernatants" [under preparation];

4. <u>Emanuel V. Capela</u>, Ilaria Magnis, Ana F.C.S. Rufino, M. Raquel Aires-Barros, João A.P. Coutinho, Ana M. Azevedo, Francisca A. e Silva, Mara G. Freire; "Three-phase partitioning systems based on aqueous biphasic systems with ionic liquids as novel strategies for the purification and recovery of antibodies" [under preparation];

5. <u>Emanuel V. Capela</u>, Jéssica Bairos, Márcia C. Neves, M. Raquel Aires-Barros, João A.P. Coutinho, Ana M. Azevedo, Ana P.M. Tavares, Mara G. Freire; "*Novel downstream routes*

for the purification of antibodies using supported ionic liquid materials" [under preparation].

6.1.3. Oral communications in international and national conferences

1. <u>Emanuel V. Capela</u>, Mara G. Freire, João A.P. Coutinho, Ana M. Azevedo; "Towards the development of cost-effective downstream processes for monoclonal antibodies". RS 2020, Research Summit 2020, Aveiro, Portugal, June 2020;

2. <u>Emanuel V. Capela</u>, Jéssica Bairos, Márcia C. Neves, João A.P. Coutinho, M. Raquel Aires-Barros, Ana M. Azevedo, Ana P.M. Tavares, Mara G. Freire; "Capture and purification of monoclonal antibodies using supported ionic liquid phase materials". ILSEPT 2019, 4th International Conference on Ionic Liquids in Separation and Purification Technology, Sitges, Spain, September 2019;

3. <u>Emanuel V. Capela</u>; "Towards the development of effective downstream processes for monoclonal antibodies". Research Summit 2019, Aveiro, Portugal, June 2019;

4. <u>Emanuel V. Capela</u>, João A.P. Coutinho, M. Raquel Aires-Barros, Ana M. Azevedo, Mara G. Freire; "Extraction of antibodies from human serum using ionic-liquid-based approaches". DCE 19, 3rd Doctoral Congress in Engineering, Oporto, Portugal, June 2019;

5. Ana F.C.S. Rufino, Alexandre E. Santiago, <u>Emanuel V. Capela</u>, Ana P.M. Tavares, Matheus M. Pereira, Aminou Mohamadou, João A.P. Coutinho, M. Raquel Aires-Barros, Ana M. Azevedo, Mara G. Freire; "Recovery of monoclonal antibodies using aqueous biphasic systems formed by ionic liquids". DCE 19, 3rd Doctoral Congress in Engineering, Oporto, Portugal, June 2019;

6. <u>Emanuel V. Capela</u>, João A.P. Coutinho, Mara G. Freire; "Biocompatible ionic-liquid-mediated recovery and purification of monoclonal antibodies from CHO cell culture supernatants". V IMFAHE International Conference – International Innovation Camp, San Cristobal de La Laguna, Santa Cruz de Tenerife, Canary Islands, Spain, March 2019;

7. Ana F.C.S. Rufino, Alexandre E. Santiago, <u>Emanuel V. Capela</u>, Ana P.M. Tavares, Matheus M. Pereira, Aminou Mohamadou, João A.P. Coutinho, M. Raquel Aires-Barros, Ana M. Azevedo, Mara G. Freire; "Purification platform for monoclonal antibodies based on aqueous biphasic systems formed by glycine-betaine ionic liquids". XXIV ELGQ, XXIV Encontro Luso-Galego de Química, Oporto, Portugal, November 2018;

8. Emanuel V. Capela, João A.P. Coutinho, M. Raquel Aires-Barros, Ana M. Azevedo, Mara G. Freire; "Recovery of value-added antibodies from serum samples". CHEMPOR 2018, 13th International Chemical and Biological Engineering Conference, Aveiro, Portugal, October 2018;

9. Emanuel V. Capela, João A.P. Coutinho, M. Raquel Aires-Barros, Ana M. Azevedo, Mara G. Freire; "Recovery of immunoglobulin G from human serum using ionic-liquid-based aqueous biphasic systems". ESBES2018, 12th European Symposium on Biochemical Engineering Sciences, Lisbon, Portugal, September 2018;

10. Emanuel V. Capela, Sara A.S.L. Rosa, João A.P. Coutinho, M. Raquel Aires-Barros, Mara G. Freire, Ana M. Azevedo; "Ionic-liquid mediated extraction and purification of monoclonal antibodies from cell culture supernatants". ABC^2, Anything But Conventional Chromatography, Lisbon, Portugal, November 2017;

11. Emanuel V. Capela, Sara A.S.L. Rosa, João A.P. Coutinho, M. Raquel Aires-Barros, Mara G. Freire, Ana M. Azevedo; "Ionic-liquid-based strategies for monoclonal antibodies downstream processing". Bioprocess Engineering Session, UBI-HSR 2017, II International Congress in Health Sciences Research: Towards Innovation and Entrepreneurship - Trends in Biotechnology for Biomedical Applications, Covilhã, Portugal, May 2017.

12. Emanuel V. Capela, Sara A.S.L. Rosa, João A.P. Coutinho, M. Raquel Aires-Barros, Ana M. Azevedo, Mara G. Freire; "Integration of capture and polishing of monoclonal antibodies from cell culture supernatants using ionic-liquids-based approaches". V ENEQUI, V National Meeting of Chemistry Students, Coimbra, Portugal, April 2017 [Prize under the best scientific poster presented in IV ENEQUI].

6.1.4. Posters in international and national conferences

1. Emanuel V. Capela, Alexandre E. Santiago, Ana F.C.S. Rufino, Ana P.M Tavares, Matheus M. Pereira, Aminou Mohamadou, João A.P. Coutinho, M. Raquel Aires-Barros, Ana M. Azevedo, Mara G. Freire; "Applying ionic-liquid-based strategies in cell culture supernatants bioprocessing for monoclonal antibodies recovery". Jornadas CICECO 2020, Aveiro, Portugal, November 2020;

2. Emanuel V. Capela, João A.P. Coutinho, M. Raquel Aires-Barros, Ana M. Azevedo, Mara G. Freire; "Purification of immunoglobulin G from human serum using ionic-liquid-based

aqueous biphasic systems". ILSEPT 2019, 4th International Conference on Ionic Liquids in Separation and Purification Technology, Sitges, Spain, September 2019;

3. <u>Emanuel V. Capela</u>, Alexandre E. Santiago, Ana F.C.S. Rufino, Ana P.M. Tavares, Matheus M. Pereira, Aminou Mohamadou, João A.P. Coutinho, M. Raquel Aires-Barros, Ana M. Azevedo, Mara G. Freire; "Recovery of monoclonal antibodies using novel glycine-betaine analogues ionic liquids". ILSEPT 2019, 4th International Conference on Ionic Liquids in Separation and Purification Technology, Sitges, Spain, September 2019;

4. <u>Emanuel V. Capela</u>, João A.P. Coutinho, M. Raquel Aires-Barros, Ana M. Azevedo, Mara G. Freire; "Human serum bioprocessing – towards the recovery of antibodies applying ionic liquids". Jornadas CICECO 2019, Aveiro, Portugal, June 2019;

5. Alexandre E. Santiago, <u>Emanuel V. Capela</u>, Ana F.C.S. Rufino, Ana P.M Tavares, Matheus M. Pereira, Aminou Mohamadou, João A.P. Coutinho, M. Raquel Aires-Barros, Ana M. Azevedo, Mara G. Freire; "Three-phase partitioning systems as a viable strategy for the recovery of monoclonal antibodies". Jornadas CICECO 2019, Aveiro, Portugal, June 2019;

6. Jéssica Bairos, <u>Emanuel V. Capela</u>, Márcia C. Neves, João A. P. Coutinho, Ana P.M. Tavares, Mara G. Freire; "Purification of antibodies using supported ionic liquid materials". Jornadas CICECO 2019, Aveiro, Portugal, June 2019;

7. Ana F.C.S. Rufino, Alexandre E. Santiago, <u>Emanuel V. Capela</u>, Ana P.M. Tavares, Matheus M. Pereira, Aminou Mohamadou, João A.P. Coutinho, M. Raquel Aires-Barros, Ana M. Azevedo, Mara G. Freire; "Ionic-liquid-based aqueous biphasic systems for the recovery of monoclonal antibodies". MMB 2019, 4th Meeting of Medicinal Biotechnology, Oporto, Portugal, May 2019;

8. Jéssica Bairos, Maria Santos, <u>Emanuel V. Capela</u>, Márcia C. Neves, Ana P.M. Tavares, Mara G. Freire; "The two sides of the use of supported ionic liquid (SIL) materials". MMB 2019, 4th Meeting of Medicinal Biotechnology, Oporto, Portugal, May 2019;

9. Jéssica Bairos, Maria Santos, <u>Emanuel V. Capela</u>, Márcia C. Neves, Ana P.M. Tavares, Mara G. Freire; "The two sides of the use of supported ionic liquid (SIL) materials". XI Biochemistry Day at University of Aveiro, Aveiro, Portugal, May 2019;

10. Alexandre E. Santiago, <u>Emanuel V. Capela</u>, Ana P.M. Tavares, Matheus M. Pereira, Aminou Mohamadou, João A.P. Coutinho, M. Raquel Aires-Barros, Ana M. Azevedo, Mara G. Freire; "Development of an alternative bio-based process for the extraction and purification of

monoclonal antibodies". CHEMPOR 2018, 13th International Chemical and Biological Engineering Conference, Aveiro, Portugal, October 2018;

11. Emanuel V. Capela, Alexandre E. Santiago, Ana P.M. Tavares, Aminou Mohamadou, João A.P. Coutinho, M. Raquel Aires-Barros, Ana M. Azevedo, Mara G. Freire; "Innovative purification platform of monoclonal antibodies using biocompatible ionic liquids". ESBES2018, 12th European Symposium on Biochemical Engineering Sciences, Lisbon, Portugal, September 2018;

12. Emanuel V. Capela, João A.P. Coutinho, M. Raquel Aires-Barros, Ana M. Azevedo, Mara G. Freire; "Monoclonal antibodies downstream processing: an alternative ionic-liquid-based approach". Jornadas CICECO 2018, Aveiro, Portugal, June 2018;

13. Alexandre E. Santiago, Emanuel V. Capela, Ana P.M. Tavares, João A.P. Coutinho, M. Raquel Aires-Barros, Ana M. Azevedo, Mara G. Freire; "Innovative bio-based purification process for monoclonal antibodies". Jornadas CICECO 2018, Aveiro, Portugal, June 2018;

14. Alexandre E. Santiago, Emanuel V. Capela, Ana P.M. Tavares, Ana M. Azevedo, Mara G. Freire; "Bio-based downstream process development for therapeutic monoclonal antibodies from Chinese Hamster Ovary cell culture supernatant". X Biochemistry Day at University of Aveiro, Aveiro, Portugal, April 2018;

15. Emanuel V. Capela, Sara A.S.L. Rosa, João A.P. Coutinho, M. Raquel Aires-Barros, Ana M. Azevedo, Mara G. Freire; "Novel ionic-liquid-based strategies for the downstream processing of monoclonal antibodies". Engineering and Technology Sciences Scientific Area, Encontro Ciência 2017 - Encontro com a Ciência e Tecnologia em Portugal, Lisbon, Portugal, July 2017 [Selected poster to represent CICECO research unit];

16. Emanuel V. Capela, Sara A.S.L. Rosa, João A.P. Coutinho, M. Raquel Aires-Barros, Ana M. Azevedo, Mara G. Freire; "Novel ionic-liquid-based strategies for the downstream processing of monoclonal antibodies". RD 2017, University of Aveiro (UA) Research Day 2017, Aveiro, Portugal, June 2017 [Selected poster to represent G5 - Biomedical and Biomimetic Materials research group from CICECO];

17. Emanuel V. Capela, Sara A.S.L. Rosa, João A.P. Coutinho, M. Raquel Aires-Barros, Ana M. Azevedo, Mara G. Freire; "Exploring the use of ionic liquids in the extraction and purification of monoclonal antibodies directly from CHO cell culture supernatants". IMIL2017, Iberoamerican Meeting on Ionic Liquids, Santos, São Paulo, Brazil, April 2017;

18. <u>Emanuel V. Capela</u>, Sara A.S.L. Rosa, João A.P. Coutinho, M. Raquel Aires-Barros, Mara G. Freire, Ana M. Azevedo; "Purification of monoclonal antibodies from cell culture supernatants using aqueous biphasic systems constituted by ionic liquids". III ENEBT, III National Meeting of Biotechnology Students, Aveiro, Portugal, March 2017.

6.2. Other publications

6.2.1. Encyclopedia entries

1. <u>Emanuel V. Capela</u>, João A.P. Coutinho, Mara G. Freire; "Application of Ionic Liquids in Separation and Fractionation Processes", in Encyclopedia of Sustainability Science and Technology, Second Edition, Edited by Robert A. Meyers, Springer Nature, New York, NY, United States of America, USA (2018) 1-29. ISBN: 978-1-4939-2493-6. DOI: 10.1007/978-1-4939-2493-6_1005-1.

6.2.2. Book chapters

1. <u>Emanuel V. Capela</u>, João A.P. Coutinho, Mara G. Freire; "Application of Ionic Liquids in Separation and Fractionation Processes", in Green Chemistry and Chemical Engineering, Encyclopedia of Sustainability Science and Technology Series, Edited by Buxing Han and Tianbin Wu, Springer Nature, New York, NY, United States of America, USA (2019) 637-665. ISBN: 978-1-4939-9059-7. DOI: 10.1007/978-1-4939-9060-3_1005.

6.2.3. Papers in international scientific periodicals with referees

1. Sandra C. Bernardo, <u>Emanuel V. Capela</u>, Jorge F.B. Pereira, Sónia P.M. Ventura, Mara G. Freire, João A.P. Coutinho; "Opposite effects induced by cholinium-based ionic liquid electrolytes in the formation of aqueous biphasic systems comprising polyethylene glycol and sodium polyacrylate", Molecules (2021). [accepted];

2. <u>Emanuel V. Capela</u>, Ana I. Valente, João C.F. Nunes, Flávia F. Magalhães, Oscar Rodríguez, Ana Soto, Mara G. Freire, Ana P.M. Tavares; "Insights on the laccase extraction and activity in ionic-liquid-based aqueous biphasic systems", Separation and Purification Technology (2020) 117052. DOI: 10.1016/j.seppur.2020.117052;

3. <u>Emanuel V. Capela</u>, João H.P.M. Santos, Isabel Boal-Palheiros, Pedro J. Carvalho, João A.P. Coutinho, Sónia P.M. Ventura, Mara G. Freire; "A simple approach for the determination and characterization of ternary phase diagrams of aqueous two-phase systems composed

of water, polyethylene glycol and sodium carbonate", Chemical Engineering Education 53 (2019) 112-120. ISSN: 2165-6428;

4. João H.P.M. Santos, <u>Emanuel V. Capela</u>, Isabel Boal-Palheiros, João A.P. Coutinho, Mara G. Freire, Sónia P.M. Ventura; "Aqueous Biphasic Systems in the Separation of Food Colorants", Biochemistry and Molecular Biology Education 46 (2018) 390-397. DOI: 10.1002/bmb.21125;

5. Helena Passos, Teresa B.V. Dinis, <u>Emanuel V. Capela</u>, Maria V. Quental, Joana Gomes, Judite Resende, Pedro P. Madeira, Mara G. Freire, João A.P. Coutinho; "Mechanisms ruling the partition of solutes in ionic-liquid-based aqueous biphasic systems – the multiple effects of ionic liquids", Physical Chemistry Chemical Physics 20 (2018) 8411-8422. DOI: 10.1039/C8CP00383A. [Featured as a content highlight in the PCCP promotional flyer □ Part of themed collection "2018 PCCP HOT Articles" and "PCCP Perspectives"];

6. Isabel Campos-Pinto[§], <u>Emanuel V. Capela</u>[§], Ana Rita Silva-Santos[§], Miguel Arévalo Rodríguez, Poondi Rajesh Gavara, Marcelo Fernandez-Lahore, M. Raquel Aires-Barros, Ana M. Azevedo; "LYTAG-driven purification strategies for monoclonal antibodies using quaternary amine ligands as affinity matrices", Journal of Chemical Technology & Biotechnology 93 (2018) 1966-1974. DOI: 10.1002/jctb.5460. [§]Equal contribution;

7. Ana Rita R. Teles, <u>Emanuel V. Capela</u>, Rafael S. Carmo, João A.P. Coutinho, Armando J.D. Silvestre, Mara G. Freire; "Solvatochromic parameters of deep eutectic solvents formed by ammonium-based salts and carboxylic acids", Fluid Phase Equilibria 448 (2017) 15-21. DOI: 10.1016/j.fluid.2017.04.020. [Most Downloaded Fluid Phase Equilibria Articles];

8. Mohamed Taha[§], Maria V. Quental[§], Francisca A. e Silva, <u>Emanuel V. Capela</u>, Mara G. Freire, Sónia P.M. Ventura, João A.P. Coutinho; "Good's Buffer Ionic Liquids as Relevant Phase-Forming Components of Self-Buffered Aqueous Biphasic Systems", Journal of Chemical Technology & Biotechnology 92 (2017) 2287–2299. DOI: 10.1002/jctb.5222. [§]Equal contribution;

9. <u>Emanuel V. Capela</u>[§], Maria V. Quental[§], Pedro Domingues, João A.P. Coutinho, Mara G. Freire; "Effective separation of aromatic and aliphatic amino acid mixtures using ionic-liquid-based aqueous biphasic systems", Green Chemistry 19 (2017) 1850-1854. DOI: 10.1039/C6GC03060B. [§]Equal contribution. [Part of themed collection "2017 Green

Chemistry Hot Articles" and "Celebrating Excellence in Research: 100 Women of Chemistry" □ Green Chemistry Issue 8 (2017) Back Cover];

10. Ana Rita R. Teles, Teresa B.V. Dinis, <u>Emanuel V. Capela</u>, Luís M.N.B.F. Santos, Simão P. Pinho, Mara G. Freire, João A.P. Coutinho; "Solubility and solvation of monosaccharides in ionic liquids", Physical Chemistry Chemical Physics 18 (2016) 19722-19730. DOI: 10.1039/C6CP03495K.

6.2.4. Oral communications in international and national conferences

1. Ana F.C.S. Rufino, Joana M. Bola, <u>Emanuel V. Capela</u>, Maria V. Quental, João A.P. Coutinho, Mara G. Freire; "Development of double-reversible aqueous biphasic systems based in protic and aprotic ionic liquids". 14 ENQF, 14th Meeting of Physical Chemistry, March 2021;

2. Bojan Kopilović, <u>Emanuel V. Capela</u>, Aleksandar Marić, Catarina M.S.S. Neves, João A.P. Coutinho, Slobodan Gadžurić, Mara G. Freire; "Ion Exchange in Aqueous Biphasic Systems". 14 ENQF, 14th Meeting of Physical Chemistry, March 2021;

3. Jéssica S. Almeida, <u>Emanuel V. Capela</u>, Ana F.C.S. Rufino, Mara G. Freire, Ana P.M. Tavares; "Stabilization and activation of laccase from Trametes versicolor in aqueous solutions of glycine-betaine analogue ionic liquids". Symbio Wired, XI Symposium on Bioengineering, Oporto, Portugal, April 2020 [1 out of 4 selected pitches for presentation at Science Under '5 contest];

4. <u>Emanuel V. Capela</u>, Maria V. Quental, Pedro Domingues, João A.P. Coutinho, Mara G. Freire; "Effective separation of amino acids mixtures using ionic-liquid-based approaches". DCE 19, 3rd Doctoral Congress in Engineering, Oporto, Portugal, June 2019;

5. <u>Emanuel V. Capela</u>; "Avian antibodies – he(gg)roes that can save lives". Jornadas CICECO 2019, Aveiro, Portugal, June 2019;

6. Bojan Kopilović, <u>Emanuel V. Capela</u>, Aleksandar Marić, João A.P. Coutinho, Slobodan Gadžurić, Mara G. Freire; "Thermoreversible aqueous biphasic systems composed of protic ionic liquids for biotechnological applications". MMB 2019, 4th Meeting of Medicinal Biotechnology, Oporto, Portugal, May 2019 [1 out of 5 selected oral communications];

7. <u>Emanuel V. Capela</u>; "Antibodies from egg yolk in tablets against the flu". At a "Science Coffee" of XII ENEBIOQ, XII National Meeting of Biochemistry Students, Aveiro, Portugal, April 2019;

8. <u>Emanuel V. Capela</u>, A. Rita Silva-Santos, Isabel Campos-Pinto, Miguel Arévalo Rodríguez, Poondi Rajesh Gavara, Marcelo Fernandez-Lahore, M. Raquel Aires-Barros, Ana M. Azevedo; "LYTAG-driven purification strategies for monoclonal antibodies using quaternary amine ligands as affinity matrices". At PATh Group/CICECO – University of Aveiro, Aveiro, Portugal, April 2019;

9. <u>Emanuel V. Capela</u>, Ana Rita R. Teles, Ana Filipa M. Cláudio, João A.P. Coutinho, Mara G. Freire; "Solvatochromic parameters of mixtures of ionic liquids: experimental studies and COSMO-RS prediction". EuCheMSIL 2018, 27th EuCheMS Conference on Molten Salts and Ionic Liquids, Lisbon, Portugal, October 2018;

10. <u>Emanuel V. Capela</u>, Maria V. Quental, Pedro Domingues, João A.P. Coutinho, Mara G. Freire; "Remarkable platform for the separation of aromatic and aliphatic amino acid mixtures using ionic-liquid-based processes". ABC^2, Anything But Conventional Chromatography, Lisbon, Portugal, November 2017;

11. Helena Passos, Teresa B.V. Dinis, <u>Emanuel V. Capela</u>, Maria V. Quental, Joana M. Gomes, Judite Resende, Pedro P. Madeira, Mara G. Freire, João A.P. Coutinho; "Factors driving solute partition in ionic-liquid-based aqueous biphasic systems". BPP2017, Biopartitioning and Purification Conference 2017, Copenhagen, Denmark, September 2017;

12. Ana Rita R. Teles, <u>Emanuel V. Capela</u>, Rafael S. Carmo, João A.P. Coutinho, Armando J.D. Silvestre, Mara G. Freire; "Solvatochromic parameters of deep eutectic solvents formed by ammonium-based salts and carboxylic acids". PATh Spring Workshop 2017 – 2nd edition – Deep Eutectis Solvents (DES), Aveiro, Portugal, June 2017;

13. <u>Emanuel V. Capela</u>, Mafalda R. Almeida, João A.P. Coutinho, Mara G. Freire; "Exploring ionic liquids for the development of a purification platform for therapeutic immunoglobulin Y (IgY) from egg yolk". XXII ELGQ, XXII Encontro Luso-Galego de Química, Bragança, Portugal, November 2016;

14. <u>Emanuel V. Capela</u>, Isabel Campos-Pinto, Sara A.S.L. Rosa, João A.P. Coutinho, M. Raquel Aires-Barros, Ana M. Azevedo, Mara G. Freire; "Novel Systems for the Extraction and Purification of Monoclonal Antibodies directly from CHO Cell Cultures Supernatants using Aqueous Biphasic Systems comprising Ionic Liquids". ISPPP2016, International Symposium on the Separation of Proteins, Peptides and Polynucleotides 2016, Salzburg, Austria, November 2016;

15. Emanuel V. Capela, Maria V. Quental, João A.P. Coutinho, Mara G. Freire; "Selective separation of amino acids using aqueous biphasic systems composed of ionic liquids". PATh Spring Workshop 2016 – 1st edition – Aqueous Biphasic Systems (ABS), Ílhavo, Aveiro, Portugal, May 2016;

16. Helena Passos, Teresa B. V. Dinis, Emanuel V. Capela, Pedro P. Madeira, Mara G. Freire, João A.P. Coutinho; "New Insights into the Physicochemical Behaviour of Ionic-Liquid-based Aqueous Biphasic Systems". PATh Spring Workshop 2016 – 1st edition – Aqueous Biphasic Systems (ABS), Ílhavo, Aveiro, Portugal, May 2016;

17. Emanuel V. Capela, Isabel Campos-Pinto, Sara A.S.L. Rosa, João A.P. Coutinho, M. Raquel Aires-Barros, Ana M. Azevedo, Mara G. Freire; "Development of Integrated Systems for Extraction and Purification of Monoclonal Antibodies directly from CHO Cell Cultures Supernatants using Aqueous Biphasic Systems composed of Ionic Liquids as Adjuvants". Medicinal Chemistry Session, 5th PYCheM & 1st EYCheM, 5th Portuguese Young Chemists Meeting and 1st European Young Chemists Meeting, Guimarães, Portugal, April 2016;

18. Emanuel Capela, Maria V. Quental, João A.P. Coutinho, Mara G. Freire; "Aqueous biphasic systems composed of ionic liquids and amino acids as remarkable selective extraction approaches". III ENEQUI, III National Meeting of Chemistry Students, Aveiro, Portugal, March 2015 [1 out of 5 selected oral communications].

6.2.5. Posters in international and national conferences

1. Joana M. Bola, Ana F.C.S. Rufino, Emanuel V. Capela, João A.P. Coutinho, Mara G. Freire; "Development of double-reversible aqueous biphasic systems envisioning their application in biochemical applications". XII Biochemistry Day at University of Aveiro, April 2021;

2. Ana F.C.S. Rufino, Emanuel V. Capela, Maria V. Quental, João A.P. Coutinho, Mara G. Freire; "Switchable aqueous biphasic systems formed with protic ionic liquids". Jornadas CICECO 2020, Aveiro, Portugal, November 2020;

3. Ana F.C.S. Rufino, Emanuel V. Capela, Maria V. Quental, João A.P. Coutinho, Mara G. Freire; "Reversible aqueous biphasic systems for biotechnology applications". Microbiotec'19, Congress of Microbiology and Biotechnology 2019, Oporto, Portugal, December 2019;

4. Helena Passos, Teresa B. V. Dinis, Emanuel V. Capela, Maria V. Quental, Joana M. Gomes, Judite Resende, Pedro P. Madeira, Mara G. Freire, João A.P. Coutinho; "Mechanisms ruling

the partition of solutes in ionic-liquid-based aqueous biphasic systems – multiple effects of ionic liquids". BPP2019, Biopartitioning and Purification Conference 2019, Guarujá, SP, Brazil, November 2019;

5. Ana F.C.S. Rufino, <u>Emanuel V. Capela</u>, Maria V. Quental, João A.P. Coutinho, Mara G. Freire; "Aqueous biphasic systems formed by protic ionic liquids and polymers". DCE 19, 3rd Doctoral Congress in Engineering, Oporto, Portugal, June 2019;

6. <u>Emanuel V. Capela</u>, Ana Rita R. Teles, Ana Filipa M. Cláudio, João A.P. Coutinho, Mara G. Freire; "Mixtures of ionic liquids: addressing their polarity by solvatochromic parameters and COSMO-RS predictions". Jornadas CICECO 2019, Aveiro, Portugal, June 2019;

7. <u>Emanuel V. Capela</u>, Ana I. Valente, Oscar Rodriguez, João A.P. Coutinho, Ana Soto, Mara G. Freire, Ana P.M. Tavares; "Ionic-liquid-based strategies for the extraction and laccase activity enhancement". Jornadas CICECO 2019, Aveiro, Portugal, June 2019;

8. Ana Fonseca, <u>Emanuel V. Capela</u>, João A.P. Coutinho, Kumud Malika Tripathi, Ana P.M. Tavares, Mara G. Freire; "Sustainable pear graphene aerogels as novel materials for the purification of human antibodies". Jornadas CICECO 2019, Aveiro, Portugal, June 2019;

9. Ana F.C.S. Rufino, <u>Emanuel V. Capela</u>, Maria V. Quental, João A.P. Coutinho, Mara G. Freire; "Reversible pH-dependent aqueous biphasic systems formed by protic ionic liquids and polymers". Jornadas CICECO 2019, Aveiro, Portugal, June 2019;

10. Bojan Kopilović, <u>Emanuel V. Capela</u>, Aleksandar Marić, João A.P. Coutinho, Slobodan Gadžurić, Mara G. Freire; "Novel thermoreversible platforms based on protic ionic liquids for biotechnological applications". Jornadas CICECO 2019, Aveiro, Portugal, June 2019;

11. Bruno J. Carvalho, <u>Emanuel V. Capela</u>, Cláudia G. Silva, Sónia Carabineiro, João A.P. Coutinho, Mara G. Freire and Ana P.M. Tavares; "Carbon xerogels as efficient nanomaterials for human antibodies purification from serum samples". Jornadas CICECO 2019, Aveiro, Portugal, June 2019;

12. <u>Emanuel V. Capela</u>, Ana I. Valente, Oscar Rodriguez, João A.P. Coutinho, Ana Soto, Mara G. Freire, Ana P.M. Tavares; "Laccase extraction and activity enhancement using ionic-liquid-based strategies – toward its application in the medicinal field". MMB 2019, 4th Meeting of Medicinal Biotechnology, Oporto, Portugal, May 2019;

13. Ana Fonseca, <u>Emanuel V. Capela</u>, João A.P. Coutinho, Kumud Malika Tripathi, Ana P.M. Tavares, Mara G. Freire; "Sustainable pear graphene aerogels as novel materials for the

purification of antibodies". XI Biochemistry Day at University of Aveiro, Aveiro, Portugal, May 2019;

14. Bruno J. Carvalho, <u>Emanuel V. Capela</u>, Cláudia G. Silva, Mara G. Freire, Ana P.M. Tavares; "Novel purification strategies for human antibodies based on carbon xerogels". XI Biochemistry Day at University of Aveiro, Aveiro, Portugal, May 2019;

15. Ana Fonseca, <u>Emanuel V. Capela</u>, João A.P. Coutinho, Kumud Malika Tripathi, Ana P.M. Tavares, Mara G. Freire; "Capture and purification of human antibodies using sustainable pear graphene aerogels". XII ENEBIOQ, XII National Meeting of Biochemistry Students, Aveiro, Portugal, April 2019;

16. Ana F.C.S. Rufino, <u>Emanuel V. Capela</u>, Maria V. Quental, João A.P. Coutinho, Mara G. Freire; "Reversible aqueous biphasic systems formed by ionic liquids and polymers". XXIV ELGQ, XXIV Encontro Luso-Galego de Química, Oporto, Portugal, November 2018;

17. <u>Emanuel V. Capela</u>, Ana Rita R. Teles, Ana Filipa M. Cláudio, João A.P. Coutinho, Mara G. Freire; "Solvatochromic parameters of mixtures of ionic liquids: experimental studies and COSMO-RS prediction". EuCheMSIL 2018, 27th EuCheMS Conference on Molten Salts and Ionic Liquids, Lisbon, Portugal, October 2018;

18. <u>Emanuel V. Capela</u>, Maria V. Quental, Pedro Domingues, João A.P. Coutinho, Mara G. Freire; "One-step separation of aromatic and aliphatic amino acids using aqueous biphasic systems". EuCheMSIL 2018, 27th EuCheMS Conference on Molten Salts and Ionic Liquids, Lisbon, Portugal, October 2018;

19. <u>Emanuel V. Capela</u>, João H.P.M. Santos, Isabel Boal-Palheiros, João A.P. Coutinho, Sónia P.M. Ventura, Mara G. Freire; "A simple laboratory approach for the determination and characterization of ternary phase diagrams for Chemical Engineering undergraduate students". CHEMPOR 2018, 13th International Chemical and Biological Engineering Conference, Aveiro, Portugal, October 2018;

20. Ana Rita R. Teles, <u>Emanuel V. Capela</u>, Ana Filipa M. Cláudio, João A.P. Coutinho, Mara G. Freire; "Solvatochromic parameters of mixtures of ionic liquids: experimental studies and COSMO-RS predictions". Jornadas CICECO 2018, Aveiro, Portugal, June 2018;

21. <u>Emanuel V. Capela</u>, A. Rita Silva-Santos, Isabel Campos-Pinto, Miguel Arévalo Rodríguez, Poondi Rajesh Gavara, Marcelo Fernandez-Lahore, M. Raquel Aires-Barros, Ana M. Azevedo; "LYTAG-driven purification strategies as a key to integrate and intensify the

downstream processing of monoclonal antibodies". Bioprocess Engineering Symposium, Microbiotec'17, Congress of Microbiology and Biotechnology 2017, Oporto, Portugal, December 2017;

22. <u>Emanuel V. Capela</u>, Maria V. Quental, Pedro Domingues, João A.P. Coutinho, Mara G. Freire; "Development of a novel ionic-liquid-based platform for the separation of aromatic and aliphatic amino acid mixtures". Bioprocess Engineering Symposium, Microbiotec'17, Congress of Microbiology and Biotechnology 2017, Oporto, Portugal, December 2017;

23. <u>Emanuel V. Capela</u>, Maria V. Quental, João A.P. Coutinho, Mara G. Freire; "One-step separation of aromatic and aliphatic amino acids using ionic-liquid-based strategies". BPP2017, Biopartitioning and Purification Conference 2017, Copenhagen, Denmark, September 2017;

24. Helena Passos, Teresa B. V. Dinis, <u>Emanuel V. Capela</u>, Maria V. Quental, Joana M. Gomes, Judite Resende, Pedro P. Madeira, Mara G. Freire, João A.P. Coutinho; "Factors driving solute partition in ionic-liquid-based aqueous biphasic systems". BPP2017, Biopartitioning and Purification Conference 2017, Copenhagen, Denmark, September 2017;

25. <u>Emanuel V. Capela</u>, Maria V. Quental, João A.P. Coutinho, Mara G. Freire; "Remarkable platforms for the selective separation of amino acids based on the use of aqueous biphasic systems composed of ionic liquids". IMIL2017, Iberoamerican Meeting on Ionic Liquids, Santos, São Paulo, Brazil, April 2017;

26. <u>Emanuel V. Capela</u>, Maria V. Quental, Pedro Domingues, João A.P. Coutinho, Mara G. Freire; "Efficient separation of aromatic and aliphatic amino acid mixtures using ionic-liquid-based processes". III ENEBT, III National Meeting of Biotechnology Students, Aveiro, Portugal, March 2017;

27. <u>Emanuel V. Capela</u>, Ana Rita R. Teles, Ana Filipa M. Cláudio, João A.P. Coutinho, Mara G. Freire; "Characterization of the solvatochromic parameters of binary mixtures of ionic liquids: experimental and COSMO-RS approaches". ILWS2017, Ionic Liquids Winter School, Oporto, Portugal, February 2017;

28. <u>Emanuel V. Capela</u>, Maria V. Quental, João A.P. Coutinho, Mara G. Freire; "High-efficient approach for the selective separation of amino acids based on the use of aqueous biphasic systems composed of ionic liquids". ISPPP2016, International Symposium on the Separation of Proteins, Peptides and Polynucleotides 2016, Salzburg, Austria, November 2016;

29. Emanuel V. Capela, Mafalda R. Almeida, João A.P. Coutinho, Mara G. Freire; "Exploring ionic liquids for the development of a purification platform for therapeutic immunoglobulin Y (IgY) from egg yolk". ISPPP2016, International Symposium on the Separation of Proteins, Peptides and Polynucleotides 2016, Salzburg, Austria, November 2016;

30. Emanuel V. Capela, Isabel Campos-Pinto, Sara A.S.L. Rosa, M. Raquel Aires-Barros, Ana M. Azevedo, Mara G. Freire; "Purification Of Monoclonal Antibodies From Cell Cultures Supernatants Using Aqueous Biphasic Systems With Ionic Liquids". ESBES2016, European Symposium on Biochemical Engineering Sciences 2016, Dublin, Ireland, September 2016;

31. Emanuel V. Capela, João H.P.M. Santos, Isabel Boal-Palheiros, João A.P. Coutinho, Sónia P.M. Ventura, Mara G. Freire; "Aqueous Biphasic Systems For The Extraction Of Food Colorants: A Laboratory Experiment". ESBES2016, European Symposium on Biochemical Engineering Sciences 2016, Dublin, Ireland, September 2016;

32. Emanuel V. Capela, Mafalda R. Almeida, João A.P. Coutinho, Mara G. Freire; "Platform For The Purification Of Immunoglobulin Y (IgY) From Egg Yolk Using Aqueous Biphasic Systems". ESBES2016, European Symposium on Biochemical Engineering Sciences 2016, Dublin, Ireland, September 2016;

33. Maria V. Quental, Emanuel V. Capela, João A.P. Coutinho, Mara G. Freire; "Selective Separation Of Amino Acids Using Aqueous Biphasic Systems Composed Of Ionic Liquids". ESBES2016, European Symposium on Biochemical Engineering Sciences 2016, Dublin, Ireland, September 2016;

34. Emanuel V. Capela, Ana Rita R. Teles, Ana Filipa M. Cláudio, João A.P. Coutinho, Mara G. Freire; "Binary Mixtures of Ionic Liquids: Characterization of their Solvatochromic Parameters". XII ENQF, 12th Portuguese Meeting on Physical Chemistry/1st Symposium on Computational Chemistry, Évora, Portugal, June 2016;

35. Emanuel V. Capela, Ana Rita R. Teles, Ana Filipa M. Cláudio, Kiki A. Kurnia, João A.P. Coutinho, Mara G. Freire; "Hydrogen-bond Acidity and Basicity of Mixtures of Ionic Liquids: Experimental and COSMO-RS Approaches". Jornadas CICECO 2016, Aveiro, Portugal, June 2016;

36. Emanuel V. Capela, Maria V. Quental, João A.P. Coutinho, Mara G. Freire; "Aqueous Biphasic Systems Composed of Ionic Liquids for the Selective Separation of Amino Acids".

Green Chemistry Session, 5th PYCheM & 1st EYCheM, 5th Portuguese Young Chemists Meeting and 1st European Young Chemists Meeting, Guimarães, Portugal, April 2016;

37. Emanuel V. Capela, Mafalda R. Almeida, João A.P. Coutinho, Mara G. Freire; "Purification of therapeutic Immunoglobulin Y (IgY) from egg yolk using Aqueous Biphasic Systems". IV ENEQUI, IV National Meeting of Chemistry Students, Oporto, Portugal, March 2016;

38. Emanuel V. Capela, Maria V. Quental, João A.P. Coutinho, Mara G. Freire; "Selective extraction of amino acids by aqueous biphasic systems composed of ionic liquids". IV ENEQUI, IV National Meeting of Chemistry Students, Oporto, Portugal, March 2016;

39. Emanuel V. Capela, Ana Filipa M. Cláudio, João A.P. Coutinho, Mara G. Freire; "Hydrogen-bond Acidity and Basicity of Mixtures of Ionic Liquids: Experimental and COSMO-RS Approaches". IV ENEQUI, IV National Meeting of Chemistry Students, Oporto, Portugal, March 2016;

40. Emanuel V. Capela, Ana Filipa M. Cláudio, João A.P. Coutinho, Mara G. Freire; "Characterization of Mixtures of Ionic Liquids by their Solvatochromic Parameters". 2nd EuGSC, 2nd EuCheMS Congress on Green and Sustainable Chemistry, Lisbon, Portugal, October 2015;

41. Emanuel V. Capela, Maria V. Quental, João A.P. Coutinho, Mara G. Freire; "Aqueous biphasic systems composed of ionic liquids: enhanced platforms for the selective separation of amino acids". 2nd EuGSC, 2nd EuCheMS Congress on Green and Sustainable Chemistry, Lisbon, Portugal, October 2015;

42. Emanuel V. Capela, Mafalda R. Almeida, João A.P. Coutinho, Mara G. Freire; "Purification of Immunoglobulin Y (IgY) using Aqueous Biphasic Systems". 2nd EuGSC, 2nd EuCheMS Congress on Green and Sustainable Chemistry, Lisbon, Portugal, October 2015;

43. Emanuel Capela, Ana Filipa M. Cláudio, João A.P. Coutinho, Mara G. Freire; "Hydrogen-bond Acidity and Basicity of Mixtures of Ionic Liquids: Experimental and COSMO-RS Approaches". IMIL2015, Iberoamerican Meeting on Ionic Liquids, Madrid, Spain, July 2015;

44. Emanuel Capela, Maria V. Quental, João A.P. Coutinho, Mara G. Freire; "Aqueous biphasic systems composed of ionic liquids and amino acids as remarkable selective extraction approaches". IMIL2015, Iberoamerican Meeting on Ionic Liquids, Madrid, Spain, July 2015;

45. Emanuel Capela, João H.P.M. Santos, Sónia P.M. Ventura, Isabel Boal-Palheiros, Mara G. Freire; "Characterization of Aqueous Biphasic Systems Composed of Poly(ethyleneglycol)

and Sodium Carbonate". BPP2015, Biopartitioning & Purification Conference 2015, Vienna, Austria, June 2015;

46. Emanuel Capela, Maria V. Quental, João A.P. Coutinho, Mara G. Freire; "Selective extraction of amino acids by aqueous biphasic systems composed of ionic liquids". BPP2015, Biopartitioning & Purification Conference 2015, Vienna, Austria, June 2015;

47. Mafalda R. Almeida, Emanuel Capela, Helena Passos, João A.P. Coutinho, Mara G. Freire; "Addition of ionic liquids to tune the phases' polarities of polymer-salt aqueous biphasic systems". ECTP2014, 20th European Conference on Thermophysical Properties, Oporto, Portugal, August - September 2014;

48. Mafalda R. Almeida, Emanuel Capela, Helena Passos, João A.P. Coutinho, Mara G. Freire; "Tailoring the phases' polarities of polymer-salt aqueous biphasic systems by the addition of ionic liquids". ILSEPT 2014, 2nd International Conference on Ionic Liquids in Separation and Purification Technology, Toronto, Canada, June - July 2014.

Appendix A

This appendix contains supplementary data of subchapter 2.1: "Purification of human antibodies from serum samples using aqueous biphasic systems comprising ionic liquids as adjuvants".

A.1. ABS formation

Table A.1. Two-phase formation ability of the studied ABS composed of 7 wt% PEG 3350 + 5 wt% dextran 500k + H_2O + IL, with the corresponding phases' volume ratio (bottom:top).

IL	IL concentration	ABS formation	Volume ratio (bottom:top)
No IL	-	✓	1:1.92
[N$_{1111}$]Cl	1 wt%	✓	1:2.20
	5 wt%	✓	1:2.25
	10 wt%	✓	1:1.87
[N$_{4444}$]Cl	1 wt%	✓	1:2.63
	5 wt%	✓	1:2.73
	10 wt%	✓	1:2.80
[C$_4$-4mpy]Cl	1 wt%	✓	1:2.44
	5 wt%	✓	1:2.63
	10 wt%	✓	1:2.63
[Ch]Cl	1 wt%	✓	1:2.22
	5 wt%	✓	1:2.17
	10 wt%	✓	1:2.15
[Ch][Ac]	1 wt%	✓	1:2.26
	5 wt%	✓	1:2.02
	10 wt%	✓	1:1.64
[C$_4$mim]Cl	1 wt%	✓	1:2.24
	5 wt%	✓	1:2.33
	10 wt%	✓	1:2.69
[C$_4$mim][HSO$_4$]	1 wt%	✓	1:2.17
	5 wt%	✓	1:2.42
	10 wt%	✓	1:2.22
[C$_4$mim]Br	1 wt%	✓	1:2.61
	5 wt%	✓	1:2.73
	10 wt%	✓	1:2.78
	15 wt%	✓	1:2.98
	20 wt%	✓	1:3.26
	35 wt%	✓	1:4.38

A.2. Performance parameters determination

Table A.2. Evaluation of the effect of the IL ions on the extraction of commercial IgG, using quaternary ABS composed of 7 wt% PEG 3350 + 5 wt% dextran 500k + H_2O/IgG solution + 1 wt% IL, and corresponding recovery yield (%Yield$_{IgG}$) and partition coefficient (K_{IgG}).

IL	%Yield$_{IgG}$	K_{IgG}
No IL	70.8 ± 2.3	0.9 ± 0.0
Effect of the IL cation		
[Ch]Cl	76.8 ± 1.3	1.0 ± 0.0
[C$_4$mim]Cl	82.0 ± 1.4	1.0 ± 0.0
[C$_4$-4mpy]Cl	86.7 ± 1.1	1.0 ± 0.0
[N$_{1111}$]Cl	82.3 ± 3.9	1.0 ± 0.1
[N$_{4444}$]Cl	82.4 ± 0.1	1.2 ± 0.0
Effect of the IL anion		
[Ch]Cl	76.8 ± 1.3	1.0 ± 0.0
[Ch][Ac]	86.7 ± 0.2	1.1 ± 0.1
[C$_4$mim]Cl	82.0 ± 1.4	1.1 ± 0.0
[C$_4$mim]Br	77.7 ± 1.2	1.0 ± 0.0
[C$_4$mim][HSO$_4$]	18.9 ± 2.4	2.1 ± 0.2

Table A.3. Evaluation of the effect of the IL concentration on the extraction of commercial IgG, using quaternary ABS composed of 7 wt% PEG 3350 + 5 wt% dextran 500k + H_2O/IgG solution + IL, and corresponding IgG recovery yield (%Yield$_{IgG}$), IgG partition coefficient (K_{IgG}), IL extraction efficiency (%EE$_{IL}$) and extraction pH value.

IL	IL concentration	%Yield$_{IgG}$	K_{IgG}	pH	%EE$_{IL}$
No IL	-	70.8 ± 2.3	0.9 ± 0.0	7.75	-
[N$_{4444}$]Cl	1 wt%	82.4 ± 0.1	1.2 ± 0.0	-	-
	5 wt%	85.3 ± 0.5	1.9 ± 0.2	-	-
	10 wt%	80.8 ± 0.1	3.4 ± 0.3	-	-
[C$_4$-4mpy]Cl	1 wt%	86.7 ± 1.1	1.0 ± 0.0	-	-
	5 wt%	92.4 ± 1.1	1.2 ± 0.0	-	-
	10 wt%	91.4 ± 5.2	1.2 ± 0.2	-	-
[Ch][Ac]	1 wt%	86.7 ± 0.2	1.1 ± 0.1	7.46	-
	5 wt%	88.6 ± 3.8	1.1 ± 0.0	7.07	-
	10 wt%	97.2 ± 1.1	1.1 ± 0.2	6.90	-
[C$_4$mim][HSO$_4$]	1 wt%	18.9 ± 2.4	2.1 ± 0.2	1.63	70.7 ± 0.7
	5 wt%	8.1 ± 0.4	1.3 ± 0.1	1.12	69.5 ± 1.8
	10 wt%	5.9 ± 0.4	1.0 ± 0.1	0.93	71.0 ± 1.7
[Ch]Cl	1 wt%	76.8 ± 1.3	1.0 ± 0.0	-	66.9 ± 2.9
	5 wt%	81.2 ± 0.5	1.2 ± 0.0	-	70.2 ± 1.0
	10 wt%	82.9 ± 1.6	1.1 ± 0.1	-	69.8 ± 0.8
[N$_{1111}$]Cl	1 wt%	82.3 ± 3.9	1.0 ± 0.1	-	77.2 ± 0.7
	5 wt%	88.6 ± 1.4	1.1 ± 0.0	-	75.1 ± 0.4
	10 wt%	84.7 ± 2.9	1.1 ± 0.0	-	71.8 ± 1.4
[C$_4$mim]Cl	1 wt%	82.0 ± 1.4	1.1 ± 0.0	5.72	71.4 ± 1.1
	5 wt%	84.3 ± 0.5	1.1 ± 0.0	6.01	71.7 ± 0.5
	10 wt%	83.2 ± 0.4	1.1 ± 0.0	5.97	72.7 ± 1.4
[C$_4$mim]Br	1 wt%	77.7 ± 1.2	1.0 ± 0.0	6.83	72.2 ± 0.7
	5 wt%	90.1 ± 1.1	1.4 ± 0.0	6.57	75.6 ± 0.6
	10 wt%	95.4 ± 1.9	1.7 ± 0.1	6.57	75.9 ± 2.3
	15 wt%	100.0 ± 0.0	1.5 ± 0.7	6.54	78.2 ± 1.2
	20 wt%	100.0 ± 0.0	2.4 ± 0.2	6.55	77.2 ± 1.9
	35 wt%	79.6 ± 0.5	10.7 ± 0.3	6.55	85.2 ± 0.7

Table A.4. Bioprocess performance of quaternary ABS composed of 7 wt% PEG 3350 + 5 wt% dextran 500k + H_2O/serum + IL for the extraction and purification of IgG antibodies from human serum, and corresponding recovery yield (%$Yield_{IgG}$), partition coefficient (K_{IgG}), purity level (%$Purity_{IgG}$) and extraction pH value.

IL	IL concentration	%$Yield_{IgG}$	K_{IgG}	%$Purity_{IgG}$	pH
Human Serum	-	-	-	5.8 ± 0.1	7.40
No IL	-	68.0 ± 1.6	0.8 ± 0.0	9.5 ± 0.2	7.39
[Ch][Ac]	1 wt%	72.2 ± 0.6	1.1 ± 0.0	12.5 ± 0.7	6.61
	5 wt%	73.3 ± 0.3	1.1 ± 0.0	11.7 ± 0.7	6.31
	10 wt%	73.1 ± 1.3	1.2 ± 0.0	11.4 ± 0.6	6.44
[C₄mim]Br	10 wt%	80.2 ± 0.3	1.4 ± 0.0	13.7 ± 0.9	7.15
	15 wt%	82.8 ± 1.2	1.6 ± 0.1	16.3 ± 1.5	7.05
	20 wt%	87.8 ± 0.3	2.1 ± 0.1	22.0 ± 1.1	7.02
	25 wt%	90.9 ± 0.8	2.9 ± 0.3	42.1 ± 1.8	7.04
	30 wt%	93.6 ± 0.2	3.8 ± 0.2	75.3 ± 5.0	6.91
	32.5 wt%	93.5 ± 1.6	3.7 ± 0.5	85.3 ± 8.4	6.98
	35 wt%	93.0 ± 0.3	2.8 ± 0.7	93.2 ± 6.4	6.89
	37.5 wt%	92.7 ± 1.4	3.1 ± 0.1	80.5 ± 3.9	6.82
	40 wt%	98.8 ± 0.1	18.1 ± 3.8	81.8 ± 6.6	6.89

Purification of human antibodies from serum samples using aqueous biphasic systems comprising ionic liquids as adjuvants

A

A.3. Proteins profile and ABS macroscopic aspect
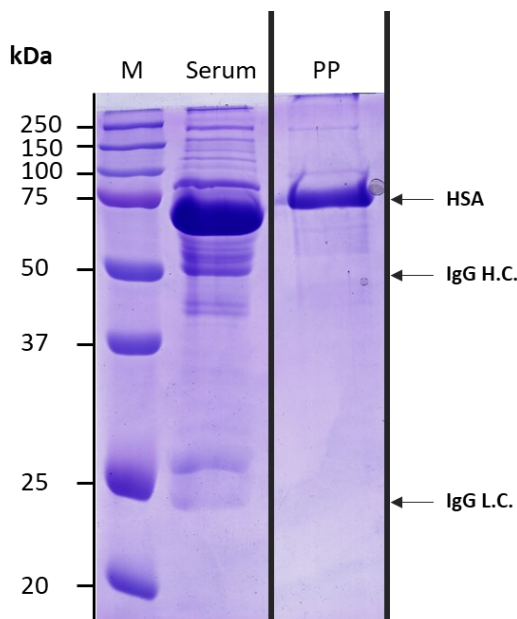
Figure A.1. SDS-PAGE gel of human serum and precipitated layer pre-conditioned in PBS (PP), of the quaternary ABS formed by PEG 3350 + dextran 500 kDa + H_2O + 35 wt% of [C_4mim]Br, at 25 °C. Lane 1 – M – represents the molecular weight marker (kDa) and lane 2 – Serum – correspond to the protein profile of the human serum diluted 1:400 (v:v). The bands corresponding to HSA, IgG heavy chain (H.C.) and IgG light chain (L.C.) are also labelled in the figure.
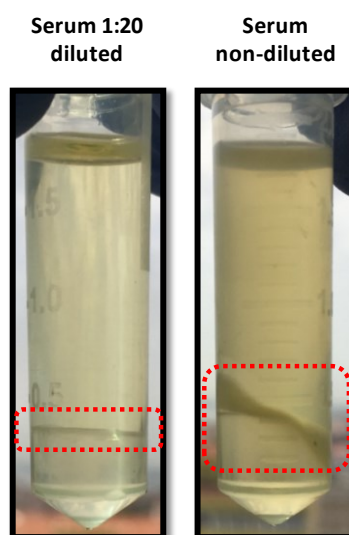
Figure A.2. Macroscopic aspect of the systems after human serum processing using quaternary ABS formed by PEG 3350 + dextran 500 kDa + H_2O + 35 wt% of [C_4mim]Br + 30 wt% human serum diluted 1:20 (v:v) and non-diluted, with the precipitated layer highlighted in the red box.

Appendix **B**

This appendix contains supplementary data of subchapter 2.2: "Ionic-liquid mediated extraction and purification of monoclonal antibodies from cell culture supernatants".

B.1. Performance parameters determination

Table B.1. Bioprocess performance of quaternary ABS composed of 7 wt% PEG 3350 + 5 wt% dextran 500k + H_2O/serum + IL for the extraction and purification of anti-IL-8 mAbs from serum-containing CHO cell culture supernatants, in terms of recovery yield (%$Yield_{IgG}$) and purity level (%$Purity_{IgG}$).

IL	IL concentration	%$Yield_{IgG}$	%$Purity_{IgG}$
CHO cell supernatant	-	-	9.1 ± 0.6
No IL	-	69.4 ± 3.6	29.3 ± 0.5
[Ch][Ac]	1 wt%	77.6 ± 0.8	26.8 ± 0.3
	5 wt%	75.7 ± 0.5	21.8 ± 0.4
	10 wt%	73.3 ± 3.4	19.1 ± 0.6
[C$_4$mim]Br	10 wt%	79.2 ± 1.2	35.8 ± 0.3
	15 wt%	82.5 ± 0.2	48.0 ± 1.7
	20 wt%	81.5 ± 2.7	69.3 ± 1.4
	25 wt%	82.6 ± 5.1	43.4 ± 4.8

Table B.2. Bioprocess performance of quaternary ABS composed of 7 wt% PEG 3350 + 5 wt% dextran 500k + H_2O/serum + IL for the extraction and purification of anti-HCV mAbs from serum-free CHO cell culture supernatants, in terms of recovery yield (%$Yield_{IgG}$) and purity level (%$Purity_{IgG}$).

IL	IL concentration	%$Yield_{IgG}$	%$Purity_{IgG}$
CHO cell supernatant	-	-	38.4 ± 0.1
No IL	-	33.8 ± 1.5	44.7 ± 1.6
[C$_4$mim]Br	10 wt%	81.0 ± 0.9	71.1 ± 1.4
	15 wt%	83.1 ± 0.3	83.9 ± 2.8
	20 wt%	85.4 ± 1.6	92.4 ± 3.4
	25 wt%	44.0 ± 1.4	77.9 ± 4.1

Appendix C

This appendix contains supplementary data of subchapter 2.3: "Sustainable strategies based on glycine-betaine analogue ionic liquids for the recovery of monoclonal antibodies from cell culture supernatants".

C.1. Experimental data of binodal curves and characterization

Table C.1. Experimental binodal weight fraction data for the system composed of $[Et_3NC_4]Br$ + K_2HPO_4/KH_2PO_4 (pH = 7) + H_2O at 25°C and atmospheric pressure.

w_{IL}	$w_{K_2HPO_4/KH_2PO_4}$	w_{H_2O}	w_{IL}	$w_{K_2HPO_4/KH_2PO_4}$	w_{H_2O}
51.7158	1.3968	46.8874	21.4961	13.3615	65.1424
49.1841	2.0115	48.8044	20.4072	14.1098	65.4829
45.3876	2.4604	52.1519	19.3642	14.9166	65.7192
43.6260	2.8236	53.5503	18.5393	15.4864	65.9743
41.8363	3.2445	54.9192	17.6821	16.0854	66.2325
39.2609	4.4043	56.3348	17.2613	16.4102	66.3285
37.3440	5.1186	57.5374	16.7545	16.7801	66.4654
35.5340	5.7994	58.6666	16.1590	17.2296	66.6114
33.5615	6.7174	59.7211	15.6074	17.6410	66.7516
32.1482	7.2128	60.6389	15.0983	18.0283	66.8734
30.5871	7.9867	61.4262	14.6943	18.3353	66.9703
29.4386	8.5074	62.0540	14.2288	18.6864	67.0849
28.1514	9.1755	62.6732	13.7727	19.0652	67.1622
26.6557	10.0327	63.3115	13.4202	19.3552	67.2246
25.2733	10.8654	63.8613	13.0383	19.6609	67.3007
23.9932	11.6712	64.3356	12.6732	19.9368	67.3900
22.7115	12.5375	64.7510	12.3236	20.2188	67.4576

Table C.2. Experimental binodal weight fraction data for the system composed of [Pr$_3$NC$_4$]Br + K$_2$HPO$_4$/KH$_2$PO$_4$ (pH = 7) + H$_2$O at 25°C and atmospheric pressure.

w_{IL}	$w_{K_2HPO_4/KH_2PO_4}$	w_{H_2O}	w_{IL}	$w_{K_2HPO_4/KH_2PO_4}$	w_{H_2O}
46.7054	2.1985	51.0961	17.0550	13.4711	69.4740
42.1058	2.7180	55.1762	16.6708	13.6951	69.6341
39.7763	3.0260	57.1977	16.2161	14.0025	69.7814
38.3309	3.5038	58.1653	15.7029	14.4182	69.8789
36.3250	3.8135	59.8615	15.2808	14.6902	70.0290
35.0851	4.3104	60.6045	14.8764	14.9377	70.1859
34.0362	4.6568	61.3069	14.5101	15.1736	70.3164
32.8430	5.1607	61.9963	14.0598	15.5842	70.3559
31.7858	5.4230	62.7912	13.7562	15.7541	70.4897
30.7993	5.8231	63.3776	13.4437	15.9700	70.5863
29.7088	6.2842	64.0070	13.1126	16.2745	70.6129
28.4249	7.1453	64.4298	12.8116	16.4715	70.7169
26.8219	7.7220	65.4561	12.5339	16.6910	70.7750
26.1978	7.8928	65.9095	12.3199	16.9234	70.7567
25.1770	8.4974	66.3256	12.0934	17.1225	70.7841
24.4584	8.8353	66.7063	11.9741	17.1840	70.8419
23.6273	9.4027	66.9701	11.7659	17.3459	70.8882
23.0131	9.6684	67.3185	11.6193	17.4225	70.9582
22.2044	10.1700	67.6256	11.3859	17.6797	70.9344
21.4931	10.6041	67.9028	11.2426	17.7580	70.9994
20.8855	10.9855	68.1289	11.0875	17.8563	71.0562
20.2877	11.3269	68.3854	10.8142	18.1385	71.0472
19.6855	11.6886	68.6259	10.5802	18.3009	71.1189
19.1518	12.0150	68.8332	10.3550	18.4575	71.1875
18.5498	12.4290	69.0212	10.0686	18.7651	71.1663
17.9196	12.9447	69.1357	9.8677	18.9253	71.2070
17.5541	13.0904	69.3555	9.6748	19.0543	71.2710

Sustainable strategies based on glycine-betaine analogue ionic liquids for the recovery of monoclonal antibodies from cell culture supernatants

C

Table C.3. Experimental binodal weight fraction data for the system composed of $[Bu_3NC_4]Br$ + K_2HPO_4/KH_2PO_4 (pH = 7) + H_2O at 25°C and atmospheric pressure.

w_{IL}	$w_{K_2HPO_4/KH_2PO_4}$	w_{H_2O}	w_{IL}	$w_{K_2HPO_4/KH_2PO_4}$	w_{H_2O}
51.9191	1.5923	46.4886	19.1145	10.9999	69.8857
46.9127	2.2425	50.8448	18.8703	11.1478	69.9819
43.5194	2.8259	53.6547	18.6285	11.2366	70.1349
40.6580	3.3347	56.0073	18.3906	11.3605	70.2489
38.7496	3.7627	57.4877	18.0247	11.6521	70.3232
36.9253	4.1905	58.8841	17.7833	11.7297	70.4870
35.3648	4.5575	60.0777	17.5645	11.8503	70.5852
34.3087	4.9972	60.6941	17.4554	11.7549	70.7897
33.0009	5.3309	61.6682	17.1115	11.8054	71.0831
31.9095	5.6870	62.4036	16.8963	11.9177	71.1860
30.8285	5.9424	63.2291	16.7101	12.0118	71.2781
29.9970	6.2751	63.7279	16.4733	12.1863	71.3404
29.3602	6.6332	64.0066	16.2437	12.3013	71.4550
28.5857	6.8980	64.5163	16.0542	12.3871	71.5587
27.8617	7.1895	64.9489	15.7384	12.6363	71.6253
26.7656	7.5591	65.6753	15.5206	12.7421	71.7373
26.2042	7.7500	66.0458	15.3861	12.7600	71.8539
25.6010	7.9565	66.4425	15.2391	12.8375	71.9233
24.9938	8.2821	66.7241	15.0648	12.9345	72.0007
24.5268	8.5354	66.9378	14.8445	13.1257	72.0298
24.0878	8.7532	67.1590	14.6358	13.1686	72.1956
23.5363	8.8867	67.5770	14.4703	13.2813	72.2484
23.1539	9.0881	67.7581	14.2562	13.4088	72.3350
22.7397	9.3094	67.9509	14.0149	13.6488	72.3362
21.7278	9.8415	68.4306	13.8367	13.6957	72.4676
21.3484	9.8776	68.7740	13.5768	13.8901	72.5331
21.0914	10.0179	68.8906	13.4128	14.0051	72.5821
20.8433	10.1843	68.9724	13.2620	14.1119	72.6261
20.5244	10.3452	69.1304	13.1412	14.1659	72.6929
20.2125	10.4667	69.3208	12.9857	14.2291	72.7852
19.9229	10.6083	69.4688	12.8099	14.3801	72.8099
19.6559	10.7165	69.6276	12.6944	14.4451	72.8605
19.3711	10.8592	69.7697	12.5847	14.4919	72.9235

w_{IL}	$w_{K_2HPO_4/KH_2PO_4}$	w_{H_2O}	w_{IL}	$w_{K_2HPO_4/KH_2PO_4}$	w_{H_2O}
12.4572	14.6170	72.9258	10.0124	16.3119	73.6757
12.3302	14.6830	72.9868	9.8769	16.4291	73.6940
12.1484	14.8117	73.0398	9.7809	16.5342	73.6849
12.0215	14.9158	73.0627	9.6936	16.5702	73.7362
11.9090	14.9821	73.1089	9.5839	16.6483	73.7678
11.7858	15.0514	73.1628	9.4728	16.7449	73.7824
11.6448	15.0975	73.2577	9.3885	16.8200	73.7915
11.5268	15.1950	73.2783	9.3028	16.8918	73.8054
11.4269	15.2454	73.3276	9.1908	16.9694	73.8399
11.3341	15.3180	73.3479	9.0704	17.0956	73.8340
11.1809	15.4807	73.3384	8.9516	17.2253	73.8231
10.9538	15.6209	73.4253	8.8276	17.2695	73.9029
10.8184	15.7586	73.4230	8.7369	17.3473	73.9158
10.7250	15.8024	73.4726	8.6171	17.4598	73.9230
10.6031	15.9322	73.4647	8.5204	17.5681	73.9114
10.4472	16.0085	73.5443	8.3911	17.7123	73.8965
10.3766	16.0386	73.5849	8.2205	17.8465	73.9330
10.1812	16.2248	73.5940	8.1151	17.9201	73.9647
10.0949	16.2673	73.6377			

Sustainable strategies based on glycine-betaine analogue ionic liquids for the recovery of monoclonal antibodies from cell culture supernatants

C

Table C.4. Experimental binodal weight fraction data for the system composed of [MepyrNC$_4$]Br + K$_2$HPO$_4$/KH$_2$PO$_4$ (pH = 7) + H$_2$O at 25°C and atmospheric pressure.

w_{IL}	$w_{K_2HPO_4/KH_2PO_4}$	w_{H_2O}
58.1075	1.6606	40.2319
51.1023	2.2806	46.6171
47.4332	2.9757	49.5912
45.6564	3.5523	50.7913
43.1322	4.0567	52.8111
41.4770	4.6154	53.9075
40.1201	5.0927	54.7873
38.8002	5.4909	55.7089
37.0268	6.3923	56.5809
35.7334	6.7845	57.4821
34.0957	7.6148	58.2894
32.9499	8.0007	59.0495
31.4460	8.9373	59.6166
29.9522	9.6941	60.3537
28.2156	10.7641	61.0203
26.8084	11.5994	61.5922
25.5219	12.3816	62.0965
24.0855	13.3985	62.5160
22.9392	14.1729	62.8879
21.7332	15.0486	63.2182
20.9443	15.5108	63.5448
19.6848	16.5412	63.7739
18.7191	17.1825	64.0984
17.7646	17.9354	64.3000
16.9757	18.5246	64.4997
16.2394	19.0688	64.6917
15.5946	19.6120	64.7933
14.8761	20.1964	64.9275
14.2163	20.7115	65.0722

Table C.5. Experimental binodal weight fraction data for the system composed of [C$_4$mim]Br + K$_2$HPO$_4$/KH$_2$PO$_4$ (pH = 7) + H$_2$O at 25°C and atmospheric pressure.

w_{IL}	$w_{K_2HPO_4/KH_2PO_4}$	w_{H_2O}
47.8896	2.8782	49.2322
44.6709	3.3364	51.9927
42.7620	3.9148	53.3232
40.6202	4.8294	54.5504
38.5897	5.7409	55.6694
36.6716	6.5095	56.8190
34.9949	7.1748	57.8303
33.4899	7.6854	58.8248
31.7325	8.6182	59.6493
30.2865	9.5007	60.2128
28.8790	10.2398	60.8811
27.6987	10.8714	61.4299
26.0237	12.0395	61.9367
24.7303	12.8324	62.4373
23.2340	13.8948	62.8711
21.9085	14.8360	63.2554
20.6594	15.7425	63.5981
19.4208	16.7565	63.8227
18.6038	17.3371	64.0591
17.6196	18.1176	64.2628
16.7150	18.8506	64.4344
16.0224	19.3893	64.5883
15.1673	20.1299	64.7028

Sustainable strategies based on glycine-betaine analogue ionic liquids for the recovery of monoclonal antibodies from cell culture supernatants

C

Table C.6. Experimental binodal weight fraction data for the system composed of $[N_{4444}]Br + K_2HPO_4/KH_2PO_4$ (pH = 7) + H_2O at 25°C and atmospheric pressure.

w_{IL}	$w_{K_2HPO_4/KH_2PO_4}$	w_{H_2O}	w_{IL}	$w_{K_2HPO_4/KH_2PO_4}$	w_{H_2O}
49.9689	2.4034	47.6277	16.9962	12.1610	70.8428
44.1506	2.6017	53.2478	16.4493	12.4598	71.0909
41.5556	3.4015	55.0429	16.0400	12.6959	71.2640
37.8742	3.9722	58.1536	15.6227	12.9768	71.4005
35.7664	4.2466	59.9870	15.3555	13.0590	71.5854
34.0903	4.6862	61.2235	15.1463	13.1795	71.6742
32.7900	5.1248	62.0852	14.9276	13.3432	71.7292
31.2127	5.5757	63.2117	14.7185	13.5051	71.7764
29.8797	5.9235	64.1968	14.2949	13.7538	71.9514
29.1839	6.1756	64.6405	14.0990	13.9120	71.9891
28.5238	6.5591	64.9171	13.7383	14.0869	72.1748
27.2931	6.9072	65.7997	13.5464	14.2548	72.1988
26.6248	7.1952	66.1800	13.2829	14.4597	72.2574
25.9214	7.5842	66.4944	13.0889	14.5421	72.3690
25.3178	7.8177	66.8645	12.9008	14.6227	72.4765
24.6583	8.0711	67.2706	12.6184	14.8947	72.4869
24.0394	8.3259	67.6347	12.4582	14.9839	72.5579
23.5126	8.5586	67.9288	12.1939	15.2358	72.5703
22.9492	8.8461	68.2046	11.9768	15.4133	72.6099
22.4423	9.0995	68.4582	11.8414	15.4239	72.7347
22.0426	9.2601	68.6973	11.6420	15.6514	72.7066
21.3796	9.7366	68.8838	11.4691	15.6472	72.8837
20.8133	9.9356	69.2511	11.3481	15.7390	72.9130
20.3810	10.2482	69.3708	11.2308	15.8197	72.9495
20.0379	10.4119	69.5502	11.0741	15.9457	72.9802
19.6974	10.5982	69.7044	10.9616	16.0328	73.0056
19.3656	10.7446	69.8898	10.8320	16.1466	73.0214
18.9979	10.9113	70.0907	10.6485	16.3437	73.0078
18.6544	11.1490	70.1967	10.5295	16.4137	73.0568
18.3464	11.3659	70.2877	10.3581	16.5640	73.0779
18.0533	11.5277	70.4189	10.2351	16.5659	73.1990
17.7389	11.6696	70.5915	10.0696	16.7696	73.1608
17.4655	11.7658	70.7687	9.9792	16.7621	73.2587

w_{IL}	$w_{K_2HPO_4/KH_2PO_4}$	w_{H_2O}	w_{IL}	$w_{K_2HPO_4/KH_2PO_4}$	w_{H_2O}
9.8453	16.8889	73.2658	9.1144	17.5130	73.3726
9.7277	16.9738	73.2985	8.9721	17.6519	73.3760
9.5551	17.1341	73.3108	8.8628	17.6816	73.4556
9.3807	17.3017	73.3176	8.7199	17.8158	73.4643
9.2694	17.3650	73.3656			

Sustainable strategies based on glycine-betaine analogue ionic liquids for the recovery of monoclonal antibodies from cell culture supernatants

C

Table C.7. Correlation parameters used to describe the experimental binodal curve of the ternary system composed of IL + K_2HPO_4/KH_2PO_4 pH 7 + H_2O through Merchuk equation.

IL	$A \pm \sigma$	$B \pm \sigma$	$C \pm \sigma \, (\times 10^{-4})$	R^2
[Et$_3$NC$_4$]Br	82.968 ± 2.194	-0.353 ± 0.014	0.338 ± 0.078	0.9892
[Pr$_3$NC$_4$]Br	85.806 ± 1.860	-0.415 ± 0.010	0.475 ± 0.057	0.9944
[Bu$_3$NC$_4$]Br	87.536 ± 0.418	-0.415 ± 0.002	1.141 ± 0.001	0.9996
[MepyrNC$_4$]Br	85.693 ± 1.246	-0.331 ± 0.007	0.297 ± 0.033	0.9979
[C$_4$mim]Br	84.974 ± 2.374	-0.330 ± 0.013	0.281 ± 0.060	0.9945
[N$_{4444}$]Br	101.442 ± 1.689	-0.486 ± 0.007	0.649 ± 0.039	0.9975

Table C.8. Experimental data of TLs and TLLs for the ternary systems composed of IL + K_2HPO_4/KH_2PO_4 pH 7 + H_2O. [IL] and [salt] correspond to the compositions of IL and salt, respectively, while content of water corresponds to the amount required to reach 100 wt%. The subscripts TOP, M and BOT refers to the top (IL-rich) phase, mixture point and bottom (salt-rich) phase, respectively. The ratio (VR) between the top and bottom phases weight is also denoted.

IL	Mass fraction composition (wt%)						TLL	VR
	$[IL]_{TOP}$	$[salt]_{TOP}$	$[IL]_M$	$[salt]_M$	$[IL]_{BOT}$	$[salt]_{BOT}$		
[Et₃NC₄]Br	37.427	5.023	24.989	15.103	3.434	32.572	44.851	0.634
	38.959	4.540	27.350	15.141	1.231	28.992	51.091	0.692
	43.016	3.442	30.196	14.897	0.816	41.147	56.590	0.696
[Pr₃NC₄]Br	34.655	4.723	19.840	15.172	4.494	25.996	36.908	0.509
	39.272	3.530	22.023	15.402	3.186	28.367	43.808	0.522
	40.731	3.212	24.978	14.992	1.584	32.487	48.883	0.598
	44.985	2.417	29.910	17.730	0.025	48.086	64.086	0.665
	55.047	1.144	40.190	17.480	4.828×10^{-5}	61.669	81.814	0.730
[Bu₃NC₄]Br	34.048	5.022	14.974	14.941	5.778	19.723	31.864	0.325
	43.734	2.778	20.034	14.923	2.387	23.967	46.460	0.427
	49.522	1.880	25.312	14.941	0.878	27.679	55.062	0.491
	53.548	1.401	29.790	17.750	0.014	37.811	64.742	0.556
	65.722	0.477	39.900	17.560	3.460×10^{-4}	43.956	78.802	0.607
[MepyrNC₄]Br	36.792	6.398	24.961	14.978	8.764	26.711	34.599	0.578
	37.478	6.132	27.014	15.346	2.597	36.845	46.475	0.700
	42.197	4.539	29.944	14.898	2.010	38.513	52.623	0.695
[C₄mim]Br	32.578	8.190	25.046	14.998	4.198	33.842	38.255	0.735
	35.532	6.853	27.357	15.010	1.540	40.769	48.018	0.760
	39.931	5.195	29.673	15.407	0.853	44.098	55.140	0.738
	54.397	1.830	38.850	17.410	0.015	60.073	79.685	0.732
[N₄₄₄₄]Br	25.441	7.752	14.775	15.032	5.963	21.046	23.582	0.452
	32.537	5.380	19.950	15.022	1.466	29.182	39.140	0.595
	44.451	2.873	25.058	15.180	1.134	30.363	51.303	0.552

Sustainable strategies based on glycine-betaine analogue ionic liquids for the recovery of monoclonal antibodies from cell culture supernatants

C

C.2. Performance parameters determination

Table C.9. Performance of ABS composed of IL + K_2HPO_4/KH_2PO_4 pH 7 + H_2O for the purification of anti-IL-8 mAbs directly from CHO cell culture supernatant given by the recovery yield (%Yield$_{IgG}$) and purification factor (%Purity$_{IgG}$).

25 wt% IL + 15 wt% K2HPO4/KH2PO4 pH 7 + 22.5 wt% H2O + 37.5 wt% CHO cell culture supernatant		
IL	%Yield$_{IgG}$ ± σ	PF ± σ
[Et$_3$NC$_4$]Br	92.3 ± 0.6	1.0 ± 0.0
[Pr$_3$NC$_4$]Br	97.3 ± 1.9	1.3 ± 0.1
[Bu$_3$NC$_4$]Br	100.0 ± 8.0	1.5 ± 0.1
[MepyrNC$_4$]Br	97.0 ± 6.5	1.1 ± 0.1
[C$_4$mim]Br	73.1 ± 3.4	1.2 ± 0.1
[N$_{4444}$]Br	73.1 ± 4.4	1.0 ± 0.2
30 wt% IL + 15 wt% K$_2$HPO$_4$/KH$_2$PO$_4$ pH 7 + 17.5 wt% H$_2$O + 37.5 wt% CHO cell culture supernatant		
IL	%Yield$_{IgG}$ ± σ	PF ± σ
[Pr$_3$NC$_4$]Br	19.8 ± 1.9	1.0 ± 0.2
[Bu$_3$NC$_4$]Br	100.0 ± 3.4	1.6 ± 0.3
[MepyrNC$_4$]Br	61.3 ± 6.1	0.8 ± 0.1
[C$_4$mim]Br	100.0 ± 6.8	1.3 ± 0.1
40 wt% IL + 15 wt% K$_2$HPO$_4$/KH$_2$PO$_4$ pH 7 + 7.5 wt% H$_2$O + 37.5 wt% CHO cell culture supernatant		
IL	%Yield$_{IgG}$ ± σ	PF ± σ
[Pr$_3$NC$_4$]Br	49.8 ± 1.1	0.8 ± 0.0
[Bu$_3$NC$_4$]Br	60.4 ± 5.2	0.8 ± 0.1
[C$_4$mim]Br	100.0 ± 8.1	1.3 ± 0.2

Table C.10. Water content (in weight fraction percentage; determined by the TL data) in the top (IL-rich) phase of the systems evaluated for the extraction and purification of anti-IL-8 mAbs directly from CHO cell culture supernatant using ABS composed of 25, 30 and 40 wt% IL + 15 wt% K_2HPO_4/KH_2PO_4 pH 7 + H_2O.

IL	25 wt% IL	30 wt% IL	40 wt% IL
[Et$_3$NC$_4$]Br	57.550	-	-
[Pr$_3$NC$_4$]Br	56.057	52.598	43.810
[Bu$_3$NC$_4$]Br	48.598	45.050	33.801
[MepyrNC$_4$]Br	56.810	53.260	-
[C$_4$mim]Br	59.232	54.870	43.773
[N$_{4444}$]Br	52.676	-	-

Sustainable strategies based on glycine-betaine analogue ionic liquids for the recovery of monoclonal antibodies from cell culture supernatants

C

Table C.11. Performance parameters of the mAbs purification two-step process based on: (a) an ABS step using a system composed of 40 wt% [Bu$_3$NC$_4$]Br + 15 wt% K$_2$HPO$_4$/KH$_2$PO$_4$ pH 7 + 7.5 wt% H$_2$O + 37.5 wt% CHO cell culture supernatant and (b) an ultrafiltration (UF) step. Parameters evaluated: mAbs concentration ([IgG]), recovery yield (%Yield$_{IgG}$), purity level (%Purity$_{IgG}$), purification factor (PF), and activity of mAbs (%Activity$_{anti-IL-8}$) (whenever applicable). Overall processes refers to the final product obtained by the two-step platforms based on the following unit operations: (i) TPP (TOP phase) + UF (retentate); (ii) TPP (TOP phase) + UF (filtrate); (iii) TPP (Precipitate) + UF (retentate); (iv) TPP (Precipitate) + UF (filtrate).

		[IgG] ± σ (mg·L^{-1})	%Yield$_{IgG}$ ± σ	%Purity$_{IgG}$ ± σ	PF ± σ	%Activity$_{anti-IL-8}$
Supernatant		99.4	-	22.7	-	90.6 ± 1.3
ABS	TOP phase	42.4 ± 5.0	60.4 ± 5.2	17.4 ± 2.0	0.8 ± 0.1	90.5 ± 2.0
UF	Retentate	19.7 ± 3.4	47.3 ± 13.5	32.8 ± 1.5	1.4 ± 0.1	66.4 ± 2.4
	Filtrate	23.4 ± 5.7	45.1 ± 16.1	29.8 ± 5.7	1.3 ± 0.1	
ABS	Precipitate	46.4 ± 3.3	41.0 ± 2.6	60.9 ± 2.0	2.7 ± 0.1	74.7 ± 3.2
UF	Retentate	24.5 ± 2.7	52.7 ± 2.2	63.5 ± 1.8	2.8 ± 0.1	52.7 ± 3.7
	Filtrate	8.3 ± 1.3	18.1 ± 4.0	67.2 ± 1.8	3.0 ± 0.1	
Overall process (i)		19.7 ± 3.4	28.6 ± 18.7	32.8 ± 1.5	1.4 ± 0.1	-
Overall process (ii)		23.4 ± 5.7	27.2 ± 21.3	29.8 ± 5.7	1.3 ± 0.1	-
Overall process (iii)		24.5 ± 2.7	21.6 ± 4.8	63.5 ± 1.8	2.8 ± 0.1	-
Overall process (iv)		8.3 ± 1.3	7.4 ± 6.6	67.2 ± 1.8	3.0 ± 0.1	-

Table C.12. Performance parameters of the mAbs purification two-step process after the IL recycling. Recovery yields (%Yield$_{IgG}$) and purity levels (%Purity$_{IgG}$) determined in the three cycles, for the top phase and precipitate in the TPP and UF steps.

			%Yield$_{IgG}$ ± σ	%Purity$_{IgG}$ ± σ
1st cycle	TOP phase	TPP	60.4 ± 5.2	17.4 ± 2.0
		UF	47.3 ± 13.5	32.8 ± 1.5
	Precipitate	TPP	41.0 ± 2.6	60.9 ± 2.0
		UF	52.7 ± 2.2	63.5 ± 1.8
2nd cycle	TOP phase	TPP	73.4 ± 15.8	17.0 ± 0.4
		UF	47.1 ± 4.6	34.2 ± 5.7
	Precipitate	TPP	41.1 ± 18.8	64.9 ± 8.6
		UF	62.4 ± 2.5	59.8 ± 6.7
3rd cycle	TOP phase	TPP	58.3 ± 5.3	17.9 ± 3.2
		UF	46.4 ± 5.3	34.7 ± 4.2
	Precipitate	TPP	40.7 ± 7.6	60.2 ± 7.8
		UF	55.9 ± 2.7	64.6 ± 4.3

Sustainable strategies based on glycine-betaine analogue ionic liquids for the recovery of monoclonal antibodies from cell culture supernatants

C

C.3. ABS macroscopic aspect and chromatographic profiles
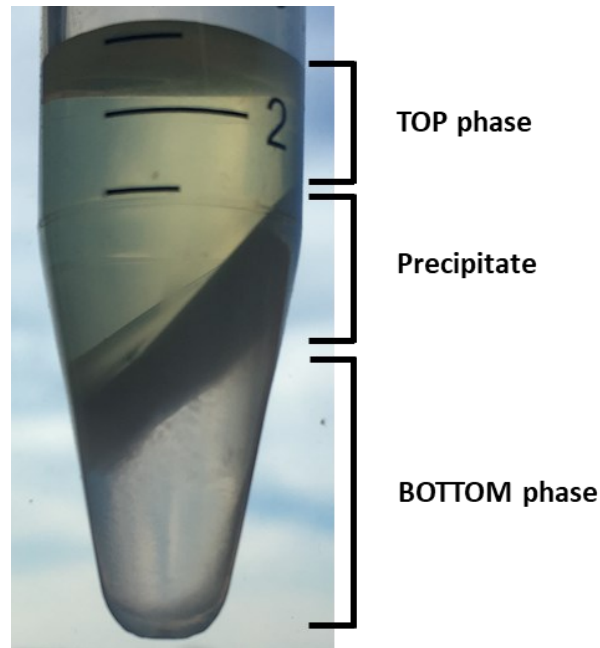
Figure C.1. Macroscopic aspect of the ABS composed of 40 wt% [Bu$_3$NC$_4$]Br + 15 wt% KH$_2$PO$_4$/K$_2$HPO$_4$ pH 7 + 22.5 wt% H$_2$O + 37.5 wt% CHO cell culture supernatant, where the top phase corresponds to the IL-rich phase and the bottom phase to the salt-rich phase. The precipitate rich in proteins is at the interface.
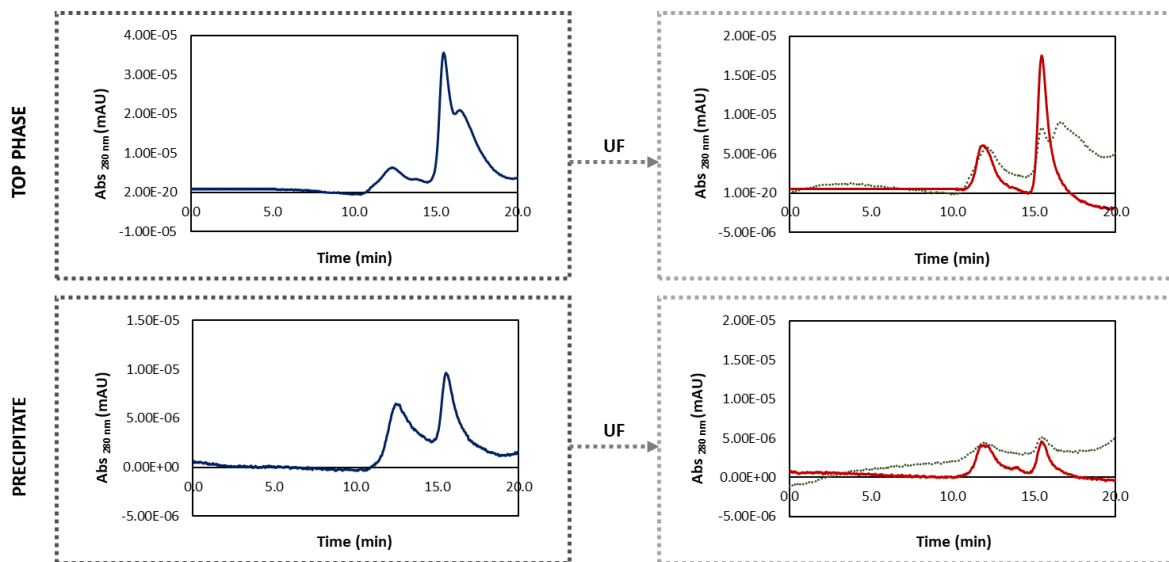
Figure C.2. SE-HPLC chromatographic profiles of mAbs purification in the top phase/precipitate of ABS composed of 40 wt% [Bu$_3$NC$_4$]Br + 15 wt% KH$_2$PO$_4$/K$_2$HPO$_4$ pH 7 + 7.5 wt% H$_2$O + 37.5 wt% CHO cell culture supernatant (–), and after an ultrafiltration step of both samples: retentate (–) and filtrate (··).

Appendix D

This appendix contains supplementary data of subchapter 3.1: "Three-phase partitioning systems based on aqueous biphasic systems with ionic liquids as novel strategies for the purification and recovery of antibodies".

D.1. Performance parameters determination – human serum

Table D.1. Evaluation of the effect of the polymer molecular weight on the recovery and purification of human IgG in the top PEG-rich phase (TOP), precipitate layer (PP) and bottom salt-rich phase (BOT), using ABS composed of 20 wt% PEG + 25 wt% $K_3C_6H_5O_7/C_6H_8O_7 + H_2O$/serum, and corresponding IgG recovery yield (%Yield$_{IgG}$), purity level (%Purity$_{IgG}$), and HSA recovery yield (%Yield$_{HSA}$) and purity level (%Purity$_{HSA}$).

IL		%Yield$_{IgG}$	%Purity$_{IgG}$	%Yield$_{HSA}$	%Purity$_{HSA}$
PEG 600	TOP	85.2 ± 5.1	46.9 ± 0.0	89.7 ± 5.3	53.1 ± 0.0
	PP	7.9 ± 0.0	67.0 ± 3.5	5.4 ± 0.6	33.0 ± 3.5
	BOT	1.8 ± 0.9	22.0 ± 2.8	9.7 ± 1.4	78.0 ± 2.8
PEG 1000	TOP	19.0 ± 7.6	18.1 ± 5.2	70.0 ± 2.8	81.9 ± 5.2
	PP	65.8 ± 3.6	80.7 ± 1.6	14.2 ± 1.9	19.3 ± 1.6
	BOT	1.2 ± 0.0	9.0 ± 0.5	17.7 ± 0.5	91.0 ± 0.5
PEG 1500	TOP	9.0 ± 2.8	45.2 ± 7.9	10.0 ± 0.1	54.8 ± 7.9
	PP	85.0 ± 1.7	49.9 ± 1.3	70.1 ± 2.2	50.1 ± 1.3
	BOT	0.0 ± 0.0	0.0 ± 0.0	8.0 ± 0.7	96.5 ± 0.2
PEG 2000	TOP	2.1 ± 0.5	27.4 ± 2.8	6.6 ± 0.4	72.6 ± 2.8
	PP	85.1 ± 2.4	51.4 ± 1.5	69.9 ± 2.1	48.6 ± 1.5
	BOT	1.8 ± 0.2	11.8 ± 1.6	16.7 ± 0.9	88.2 ± 1.6

Table D.2. Evaluation of the effect of the IL ions on the recovery and purification of human IgG in the top PEG-rich phase (TOP), precipitate layer (PP) and bottom salt-rich phase (BOT), using ABS composed of 20 wt% PEG + 25 wt% $K_3C_6H_5O_7/C_6H_8O_7$ + H_2O/serum + 5 wt% IL, and corresponding IgG recovery yield (%$Yield_{IgG}$), purity level (%$Purity_{IgG}$), and HSA recovery yield (%$Yield_{HSA}$) and purity level (%$Purity_{HSA}$).

IL		%$Yield_{IgG}$	%$Purity_{IgG}$	%$Yield_{HSA}$	%$Purity_{HSA}$
No IL	TOP	19.0 ± 7.6	18.1 ± 5.2	70.0 ± 2.8	81.9 ± 5.2
	PP	65.8 ± 3.6	80.7 ± 1.6	14.2 ± 1.9	19.3 ± 1.6
	BOT	1.2 ± 0.0	9.0 ± 0.5	17.7 ± 0.5	91.0 ± 0.5
[C₄mim]Br	TOP	22.7 ± 7.4	19.6 ± 2.2	68.3 ± 12.6	80.4 ± 2.2
	PP	56.9 ± 0.9	67.6 ± 0.0	21.2 ± 0.3	32.4 ± 0.0
	BOT	0.0 ± 0.0	0.0 ± 0.0	0.0 ± 0.0	0.0 ± 0.0
[C₄mim]Cl	TOP	46.7 ± 4.7	31.3 ± 2.0	80.0 ± 0.4	68.7 ± 2.0
	PP	23.0 ± 3.5	82.4 ± 0.1	5.5 ± 0.6	17.6 ± 0.1
	BOT	6.5 ± 1.5	30.7 ± 1.1	13.9 ± 3.1	69.3 ± 1.1
[N₄₄₄₄]Br	TOP	1.9 ± 0.0	42.8 ± 1.2	3.8 ± 0.3	57.2 ± 1.2
	PP	100.0 ± 0.0	56.9 ± 0.3	72.2 ± 3.6	43.1 ± 0.3
	BOT	0.0 ± 0.0	0.0 ± 0.0	2.3 ± 0.3	100.0 ± 0.0
[P₄₄₄₄]Br	TOP	0.0 ± 0.0	0.0 ± 0.0	0.0 ± 0.0	0.0 ± 0.0
	PP	0.0 ± 0.0	0.0 ± 0.0	0.0 ± 0.0	0.0 ± 0.0
	BOT	0.0 ± 0.0	0.0 ± 0.0	0.0 ± 0.0	0.0 ± 0.0
[N₄₄₄₄]Cl	TOP	0.0 ± 0.0	0.0 ± 0.0	4.9 ± 0.6	100.0 ± 0.0
	PP	100.0 ± 0.0	54.7 ± 0.1	52.9 ± 1.1	45.3 ± 0.1
	BOT	0.0 ± 0.0	0.0 ± 0.0	0.0 ± 0.0	0.0 ± 0.0
[P₄₄₄₄]Cl	TOP	0.0 ± 0.0	0.0 ± 0.0	0.0 ± 0.0	0.0 ± 0.0
	PP	77.9 ± 3.6	59.8 ± 5.6	42.7 ± 11.4	40.2 ± 5.6
	BOT	0.0 ± 0.0	0.0 ± 0.0	0.0 ± 0.0	0.0 ± 0.0

Three-phase partitioning systems based on aqueous biphasic systems with ionic liquids as novel strategies for the purification and recovery of antibodies

D

Table D.3. Evaluation of the effect of the IL concentration on the recovery and purification of human IgG in the top PEG-rich phase (TOP), precipitate layer (PP) and bottom salt-rich phase (BOT), using ABS composed of 20 wt% PEG + 25 wt% $K_3C_6H_5O_7/C_6H_8O_7$ + H_2O/IL/serum, and corresponding IgG recovery yield (%Yield$_{IgG}$), purity level (%Purity$_{IgG}$), and HSA recovery yield (%Yield$_{HSA}$) and purity level (%Purity$_{HSA}$).

IL / %			%Yield$_{IgG}$	%Purity$_{IgG}$	%Yield$_{HSA}$	%Purity$_{HSA}$
No IL		TOP	19.0 ± 7.6	18.1 ± 5.2	70.0 ± 2.8	81.9 ± 5.2
		PP	65.8 ± 3.6	80.7 ± 1.6	14.2 ± 1.9	19.3 ± 1.6
		BOT	1.2 ± 0.0	9.0 ± 0.5	17.7 ± 0.5	91.0 ± 0.5
[C$_4$mim]Br	1 wt%	TOP	7.2 ± 3.7	10.9 ± 2.8	49.7 ± 10.2	89.1 ± 2.8
		PP	77.7 ± 4.1	69.1 ± 3.8	29.7 ± 6.5	30.9 3.8±
		BOT	1.4 ± 0.4	10.0 ± 0.2	15.7 ± 2.2	90.0 ± 0.2
	2 wt%	TOP	27.7 ± 0.3	19.5 ± 1.1	82.3 ± 5.0	80.5 ± 1.1
		PP	68.2 ± 5.4	70.0 ± 4.1	21.9 ± 6.3	30.0 ± 8.1
		BOT	4.5 ± 0.1	12.5 ± 0.2	26.7 ± 0.4	87.5 ± 0.2
	5 wt%	TOP	22.7 ± 7.4	19.6 ± 2.2	68.3 ± 12.6	80.4 ± 2.2
		PP	56.9 ± 0.9	67.6 ± 0.0	21.2 ± 0.3	32.4 ± 0.0
		BOT	0.0 ± 0.0	0.0 ± 0.0	0.0 ± 0.0	0.0 ± 0.0
	10 wt%	TOP	7.7 ± 4.7	12.7 ± 6.3	45.7 ± 0.7	87.3 ± 6.3
		PP	65.3 ± 1.4	69.3 ± 1.6	24.7 ± 1.2	30.7 ± 1.6
		BOT	1.5 ± 0.1	25.3 ± 0.4	5.4 ± 0.1	74.7 ± 0.4
	15 wt%	TOP	8.5 ± 1.4	8.1 ± 1.6	69.6 ± 4.8	91.9 ± 1.6
		PP	0.0 ± 0.0	0.0 ± 0.0	0.0 ± 0.0	0.0 ± 0.0
		BOT	0.0 ± 0.0	0.0 ± 0.0	0.0 ± 0.0	0.0 ± 0.0
[C$_4$mim]Cl	1 wt%	TOP	29.8 ± 1.3	24.2 ± 0.3	73.4 ± 1.8	75.8 ± 0.3
		PP	50.2 ± 4.6	82.6 ± 4.0	10.0 ± 3.9	17.4 ± 4.0
		BOT	3.9 ± 1.1	17.9 ± 0.9	18.1 ± 3.0	82.1 ± 0.9
	2 wt%	TOP	37.5 ± 2.8	28.9 ± 1.3	72.0 ± 0.8	71.1 ± 1.3
		PP	43.2 ± 3.9	86.5 ± 1.4	6.8 ± 0.4	13.5 ± 1.4
		BOT	4.5 ± 3.2	16.2 ± 11.5	22.5 ± 15.9	83.8 ± 9.2
	5 wt%	TOP	46.7 ± 4.7	31.3 ± 2.0	80.0 ± 0.4	68.7 ± 2.0
		PP	23.0 ± 3.5	82.4 ± 0.1	5.5 ± 0.6	17.6 ± 0.1
		BOT	6.5 ± 1.5	30.7 ± 1.1	13.9 ± 3.1	69.3 ± 1.1
	10 wt%	TOP	42.1 ± 7.9	28.7 ± 4.0	85.0 ± 0.9	71.3 ± 4.0
		PP	6.9 ± 1.0	79.4 ± 1.6	3.1 ± 0.4	20.6 ± 1.6
		BOT	2.6 ± 1.3	37.8 ± 8.9	4.3 ± 1.4	81.1 ± 26.7
	15 wt%	TOP	12.2 ± 1.3	14.3 ± 1.2	63.4 ± 0.0	85.7 ± 1.2

		PP	0.1 ± 0.0	37.4 ± 1.5	2.8 ± 0.0	62.6 ± 1.5
		BOT	0.0 ± 0.0	0.0 ± 0.0	0.0 ± 0.0	0.0 ± 0.0
[N₄₄₄₄]Br	1 wt%	TOP	10.8 ± 0.4	17.1 ± 3.3	47.7 ± 12.5	82.9 ± 3.3
		PP	80.5 ± 3.2	73.4 ± 1.6	25.7 ± 1.0	26.6 ± 1.6
		BOT	0.0 ± 0.0	0.0 ± 0.0	5.3 ± 0.2	100.0 ± 0.0
	2 wt%	TOP	7.2 ± 1.1	14.8 ± 0.4	37.8 ± 4.4	85.2 ± 0.4
		PP	92.0 ± 3.3	61.4 ± 3.3	50.3 ± 12.7	38.6 ± 3.3
		BOT	0.6 ± 0.3	26.7 ± 3.3	3.9 ± 0.1	86.7 ± 18.9
	5 wt%	TOP	1.9 ± 0.0	42.8 ± 1.2	3.8 ± 0.3	57.2 ± 1.2
		PP	100.0 ± 0.0	56.9 ± 0.3	72.2 ± 3.6	43.1 ± 0.3
		BOT	0.0 ± 0.0	0.0 ± 0.0	2.3 ± 0.3	100.0 ± 0.0
	10 wt%	TOP	0.0 ± 0.0	0.0 ± 0.0	0.0 ± 0.0	0.0 ± 0.0
		PP	54.7 ± 2.6	49.5 ± 2.5	49.2 ± 2.5	50.5 ± 2.5
		BOT	0.0 ± 0.0	0.0 ± 0.0	0.0 ± 0.0	0.0 ± 0.0
	15 wt%	TOP	0.0 ± 0.0	0.0 ± 0.0	0.0 ± 0.0	0.0 ± 0.0
		PP	47.4 ± 5.4	43.8 ± 3.0	53.5 ± 0.6	56.2 ± 3.0
		BOT	0.0 ± 0.0	0.0 ± 0.0	0.0 ± 0.0	0.0 ± 0.0

Three-phase partitioning systems based on aqueous biphasic systems with ionic liquids as novel strategies for the purification and recovery of antibodies

D

D.2. TPP/ABS macroscopic aspect

PEG 1000 ABS/TPP (without IL)
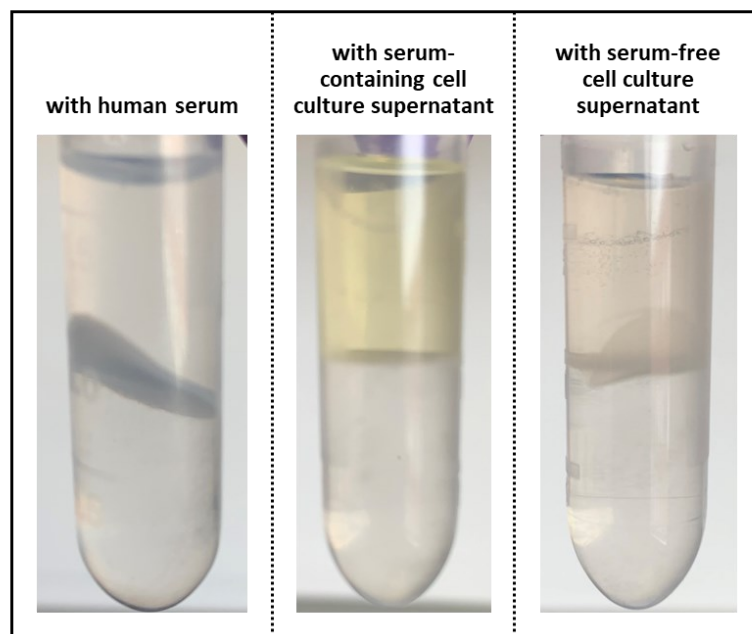
Figure D.1. Example of the macroscopic aspect of the TPP/ABS composed of 20 wt% PEG + 25 wt% $K_3C_6H_5O_7/C_6H_8O_7$ + H_2O/biological matrix, where the top phase corresponds to the polymer-rich phase and the bottom phase to the salt-rich phase. The precipitate rich in proteins is located at the interface (except in the system with serum-containing cell culture supernatant, in which no precipitate was created).

D.3. Performance parameters determination – cell culture supernatants

Table D.4. Performance evaluation of the ABS/TPP composed of 20 wt% PEG 1000 + 25 wt% $K_3C_6H_5O_7/C_6H_8O_7$ + 40 wt% serum-free CHO cell culture supernatant + 15 wt% H_2O/IL towards the recovery and purification of anti-HCV mAbs from serum-free CHO cell culture supernatants in the top PEG-rich phase (TOP), precipitate layer (PP) and bottom salt-rich phase (BOT), and corresponding recovery yield (%Yield$_{IgG}$) and purity level (%Purity$_{IgG}$).

IL		%Yield$_{IgG}$	%Purity$_{IgG}$
	TOP	41.0 ± 5.1	41.8 ± 5.6
No IL	PP	55.3 ± 1.1	82.8 ± 2.0
	BOT	0.0 ± 0.0	0.0 ± 0.0
	TOP	26.9 ± 1.7	31.9 ± 4.5
[C$_4$mim]Cl 1 wt%	PP	74.4 ± 2.6	89.2 ± 1.5
	BOT	0.0 ± 0.0	0.0 ± 0.0
	TOP	13.5 ± 1.5	23.4 ± 1.0
[N$_{4444}$]Br 1 wt%	PP	79.7 ± 0.2	85.9 ± 0.9
	BOT	0.0 ± 0.0	0.0 ± 0.0

Three-phase partitioning systems based on aqueous biphasic systems with ionic liquids as novel strategies for the purification and recovery of antibodies

D
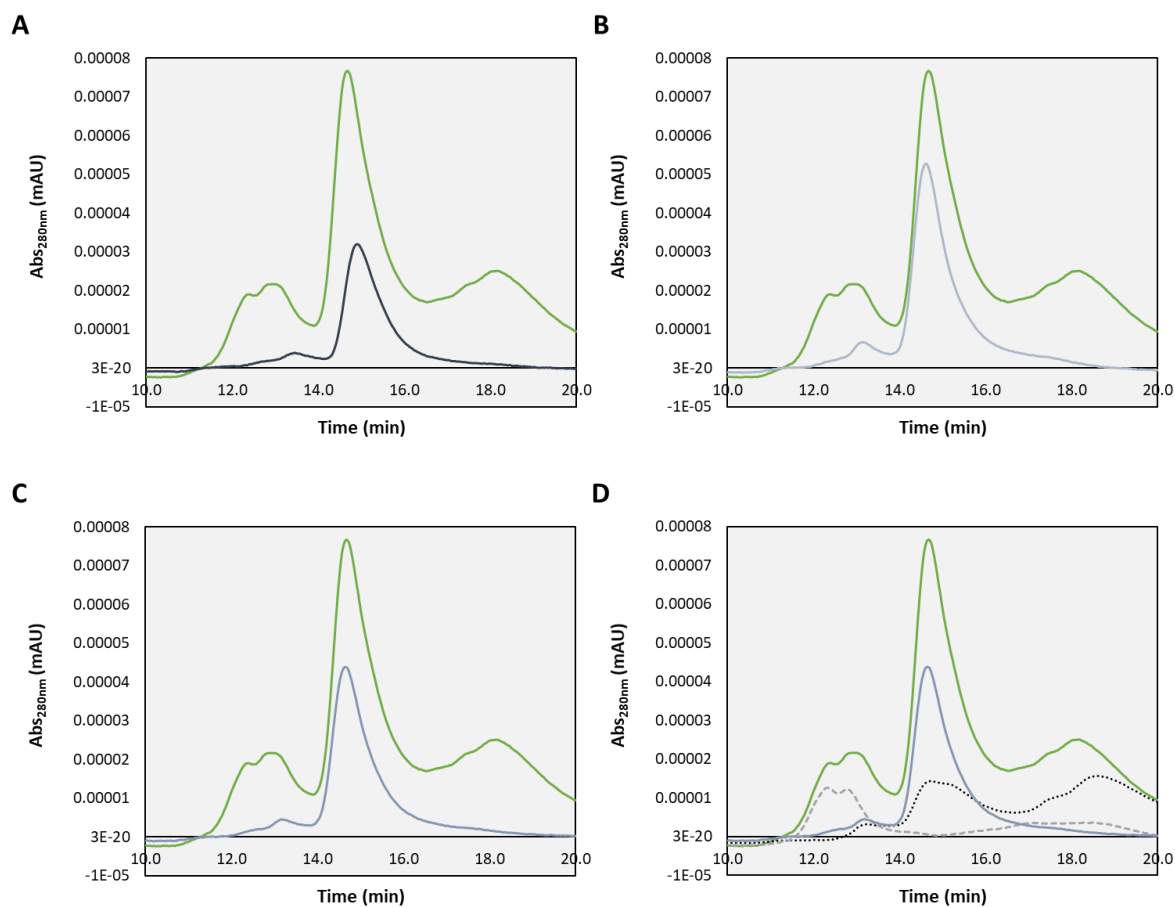
Figure D.2. SE-HPLC chromatograms of serum-free cell culture supernatant (—) and phases of the TPP systems composed of 20 wt% PEG 1000 + 25 wt% $K_3C_6H_5O_7/C_6H_8O_7$ + 40 wt% serum-free CHO cell culture supernatant + 15 wt% H_2O/IL: (A) precipitate fraction of the TPP with no IL (—); (B) precipitate fraction of the TPP with 1 wt% [N_{4444}]Br (—); (C) precipitate fraction of the TPP with 1 wt% [C_4mim]Cl (—); (D) phases of the TPP with 1 wt% [C_4mim]Cl – top (··), bottom (--) and precipitate (—).

Appendix E

This appendix contains supplementary data of subchapter 4.1: "Novel downstream routes for the purification of antibodies using supported ionic liquids materials".

E.1. Factorial planning

Table E.1. Factors tested and experimental Central Composite Rotatable Design levels.

	Axial Point	Factorial Point	Central Point	Factorial Point	Axial Point
	-1.68	**-1**	**0**	**1**	**1.68**
Contact time (min)	9.6	30.0	60.0	90.0	110.4
pH	1.6	3.0	5.0	7.0	8.4
S:L ratio (mg·mL^{-1})	16.0	50.0	100.0	150.0	184.0

Table E.2. Factors tested and experimental Central Composite Rotatable Design levels for each system (coded and uncoded).

System	Coded coefficients			Uncoded coefficients		
	Contact time (min)	pH	S:L ratio (mg·mL^{-1})	Contact time (min)	pH	S:L ratio (mg·mL^{-1})
1	-1	-1	-1	30.0	3	50.0
2	1	-1	-1	90.0	3	50.0
3	-1	1	-1	30.0	7	50.0
4	1	1	-1	90.0	7	50.0
5	-1	-1	1	30.0	3	150.0
6	1	-1	1	90.0	3	150.0
7	-1	1	1	30.0	7	150.0
8	1	1	1	90.0	7	150.0
9	-1.68	0	0	9.6	5	100.0
10	1.68	0	0	110.4	5	100.0
11	0	-1.68	0	60.0	1.64	100.0
12	0	1.68	0	60.0	8.36	100.0
13	0	0	-1.68	60.0	5	16.0
14	0	0	1.68	60.0	5	184.0
15	0	0	0	60.0	5	100.0
16	0	0	0	60.0	5	100.0
17	0	0	0	60.0	5	100.0

E.2. SILs characterization
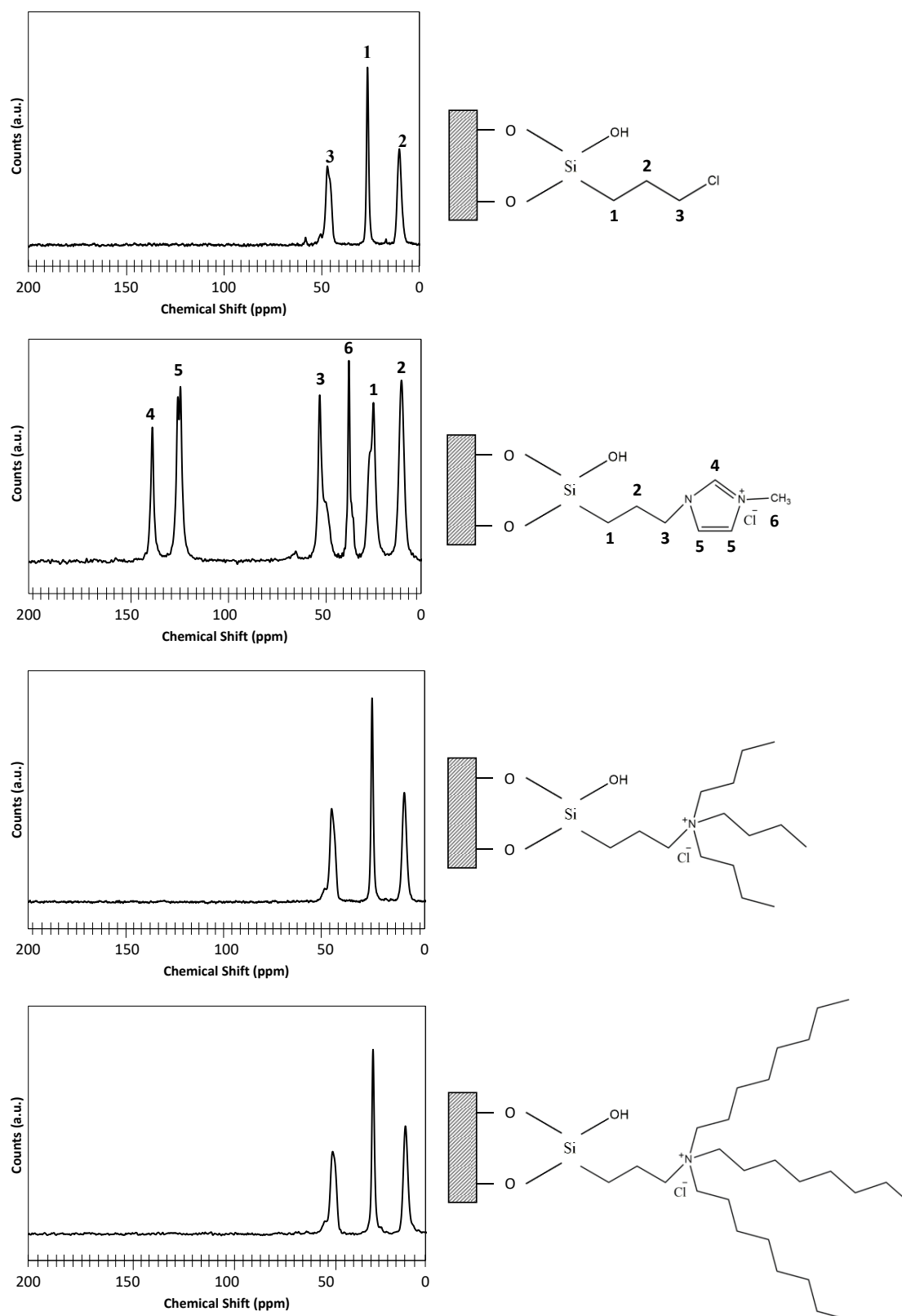
Figure E.1. Solid-state ^{13}C NMR spectra of [Si][C$_3$]Cl and SILs ([Si][C$_3$mim]Cl, [Si][N$_{3444}$]Cl and [Si][N$_{3888}$]Cl).
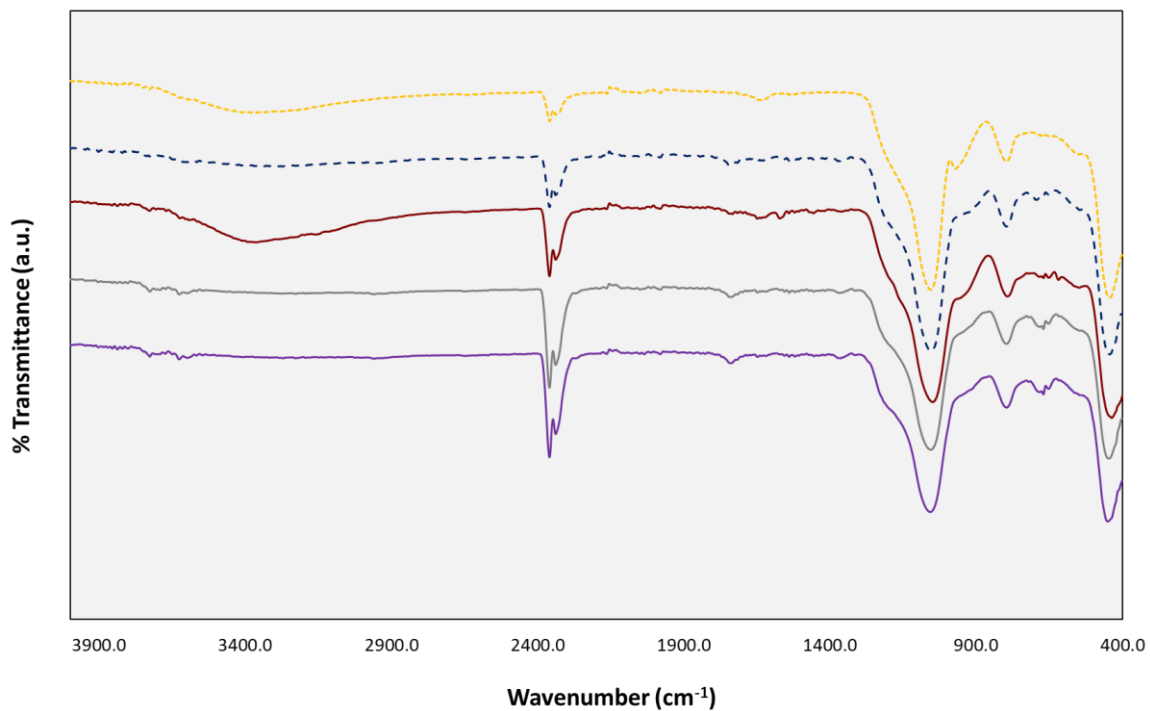
Figure E.2. ATR-FTIR spectra of the different materials under study: activated silica ($\cdots$); [Si][C$_3$]Cl (--);

[Si][C$_3$mim]Cl (—); [Si][N$_{3444}$]Cl (—); and [Si][N$_{3888}$]Cl (—).
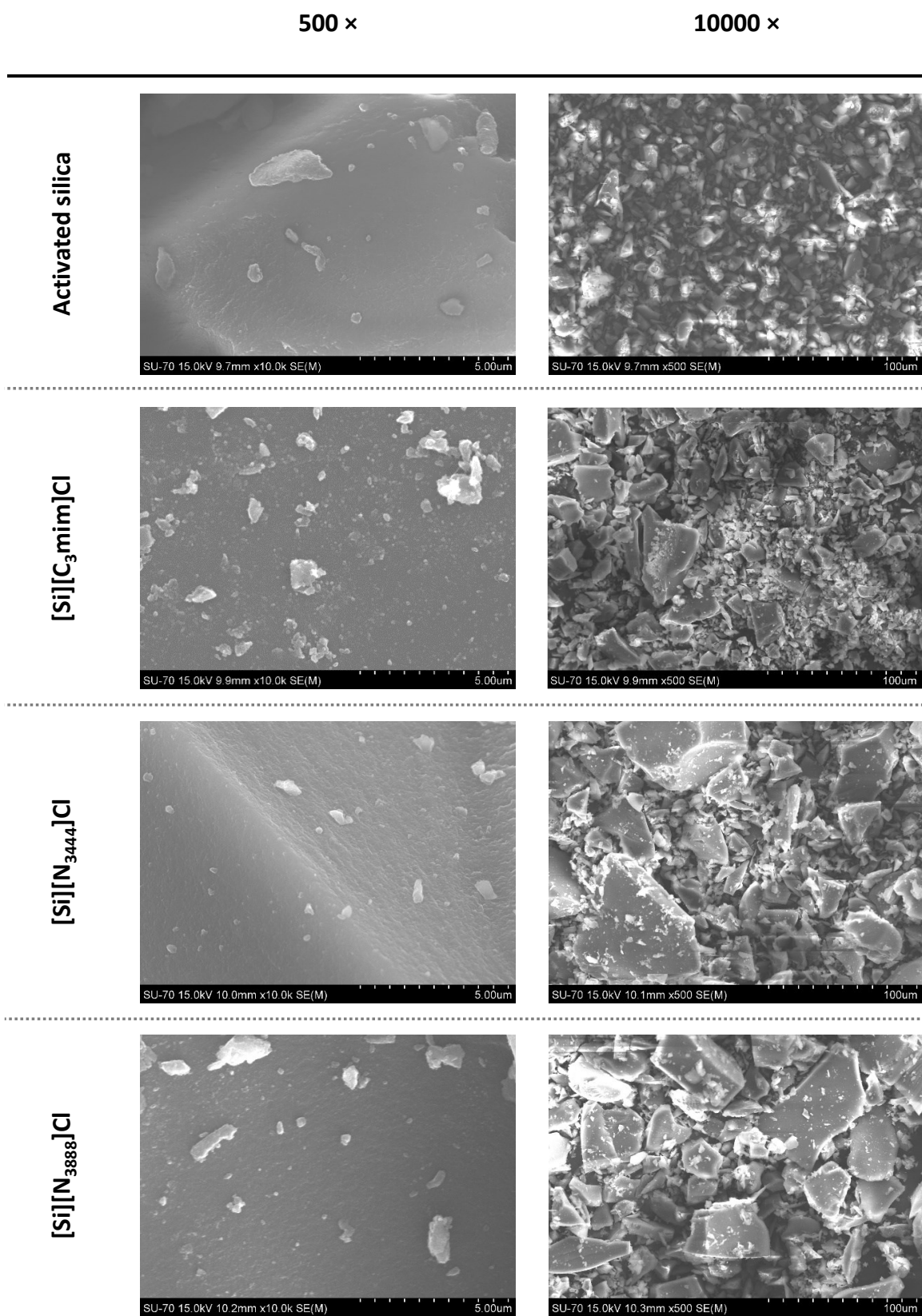
Figure E.3. SEM images of the activated silica and synthesized SILs ([Si][C$_3$mim]Cl, [Si][N$_{3444}$]Cl and [Si][N$_{3888}$]Cl) at two different magnifications (500 × and 10000 ×).

E.3. Factorial planning using [Si][C₃mim]Cl

Table E.3. Data attributed to the independent variables (S:L ratio, pH and contact time) to define the 2^3 factorial planning and respective experimental results of recovery yield of IgG using [Si][C₃mim]Cl, theoretical results of the developed mathematical model and respective relative deviation.

System	S:L ratio (mg·mL^{-1})	pH	Contact time (min)	%Yield$_{IgG}$ experimental	%Yield$_{IgG}$ theoretical	Residues
1	50.0	3	30.0	100.0	97.0	3.0
2	50.0	3	90.0	100.0	97.8	2.2
3	50.0	7	30.0	63.3	69.0	-5.6
4	50.0	7	90.0	68.3	73.6	-5.3
5	150.0	3	30.0	100.0	97.8	2.3
6	150.0	3	90.0	97.2	94.6	2.5
7	150.0	7	30.0	58.7	64.0	-5.3
8	150.0	7	90.0	58.7	64.7	-6.1
9	100.0	5	9.6	84.9	83.0	1.9
10	100.0	5	110.4	86.7	84.3	2.5
11	100.0	1.64	60.0	100.0	107.4	-7.4
12	100.0	8.36	60.0	70.5	58.7	11.8
13	16.0	5	60.0	86.4	84.4	2.0
14	184.0	5	60.0	80.0	77.6	2.4
15	100.0	5	60.0	88.6	86.6	2.0
16	100.0	5	60.0	84.0	86.6	-2.6
17	100.0	5	60.0	86.5	86.6	-0.2

Table E.4. Regression coefficients of the predicted second-order polynomial model for the recovery yield of IgG with [Si][C$_3$mim]Cl.

	Regression coefficients	Standard deviation	t-student (7)	p - value
Interception	99.8	29.4	3.4	0.0
S:L ratio	0.2	0.2	0.9	0.4
S:L ratio²	0.0	0.0	-0.9	0.4
pH	-3.6	6.6	-0.6	0.6
pH²	-0.3	0.5	-0.6	0.6
Time	0.1	0.4	0.3	0.7
Time²	0.0	0.0	-0.5	0.6
S:L ratio × pH	-0.0	0.0	-0.6	0.6
S:L ratio × Time	0.0	0.0	-0.4	0.7
pH × Time	0.0	0.0	0.4	0.7

Table E.5. ANOVA data for the recovery yield of IgG, obtained from the factorial planning carried with [Si][C$_3$mim]Cl.

	Sum Squares (SS)	Degrees of Freedom	Mean Square	Fcal	p - value
S:L ratio	57.0	1.0	57.0	1.1	0.3
S:L ratio²	44.8	1.0	44.8	0.8	0.4
pH	2865.6	1.0	2865.6	53.7	0.0
pH²	18.0	1.0	18.0	0.3	0.6
Time	2.1	1.0	2.1	0.0	0.9
Time²	12.9	1.0	12.9	0.2	0.6
S:L ratio × pH	16.4	1.0	16.4	0.3	0.6
S:L ratio × Time	7.6	1.0	7.6	0.1	0.7
pH × Time	7.6	1.0	7.6	0.1	0.7
Error	373.7	7.0	53.4		
Total SS	3381.8	16.0			
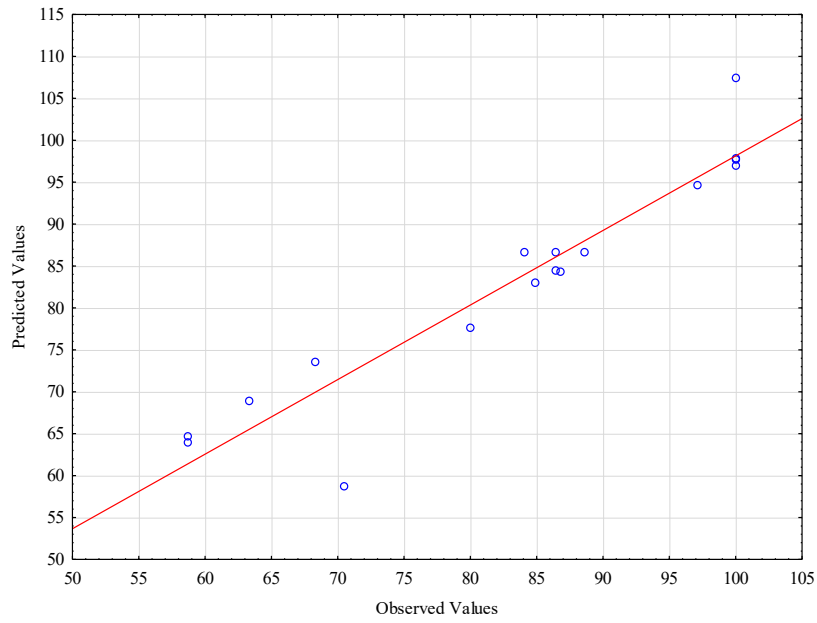
Figure E.4. Predicted *versus* observed values for the recovery yield of IgG from human serum using [Si][C$_3$mim]Cl.

Table E.6. Data attributed to the independent variables (S:L ratio, pH and contact time) to define the 2^3 factorial planning and respective experimental results of purity of IgG using [Si][C$_3$mim]Cl, theoretical results of the developed mathematical model and respective relative deviation.

System	S:L ratio (mg·mL^{-1})	pH	Contact time (min)	%Purity$_{IgG}$ experimental	%Purity$_{IgG}$ theoretical	Residues
1	50.0	3	30.0	45.8	45.0	0.9
2	50.0	3	90.0	46.9	46.2	0.7
3	50.0	7	30.0	42.2	40.4	1.8
4	50.0	7	90.0	42.7	41.1	1.6
5	150.0	3	30.0	43.6	42.1	1.6
6	150.0	3	90.0	42.8	41.4	1.4
7	150.0	7	30.0	46.4	43.9	2.5
8	150.0	7	90.0	45.0	42.7	2.3
9	100.0	5	9.6	40.4	42.8	-2.4
10	100.0	5	110.4	40.8	42.8	-2.1
11	100.0	1.64	60.0	42.6	43.7	-1.1
12	100.0	8.36	60.0	37.6	41.0	-3.4
13	16.0	5	60.0	42.1	43.5	-1.4
14	184.0	5	60.0	39.4	42.5	-3.1
15	100.0	5	60.0	42.2	41.0	1.2
16	100.0	5	60.0	40.4	41.0	-0.6
17	100.0	5	60.0	41.2	41.0	0.2

Table E.7. Regression coefficients of the predicted second-order polynomial model for the purity of IgG with [Si][C$_3$mim]Cl.

	Regression coefficients	Standard deviation	t-student (7)	p - value
Interception	57.6	11.7	4.9	0.0
S:L ratio	-0.1	0.1	-1.3	0.2
S:L ratio²	0.0	0.0	0.8	0.4
pH	-3.1	2.6	-1.2	0.3
pH²	0.1	0.2	0.6	0.6
Time	-0.0	0.2	-0.3	0.8
Time²	0.0	0.0	0.8	0.5
S:L ratio × pH	0.0	0.0	1.6	0.2
S:L ratio × Time	0.0	0.0	-0.5	0.7
pH × Time	0.0	0.0	-0.1	0.9

Table E.8. ANOVA data for the purity of IgG, obtained from the factorial planning carried with [Si][C$_3$mim]Cl.

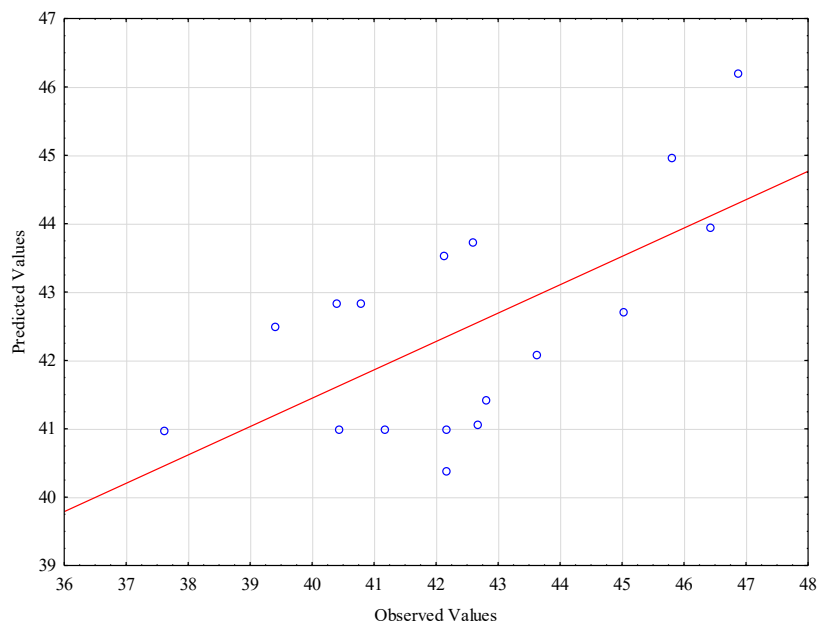|	Sum Squares (SS)	Degrees of Freedom	Mean Square	Fcal	p - value
S:L ratio	1.3	1.0	1.3	0.2	0.7
S:L ratio²	5.8	1.0	5.8	0.7	0.4
pH	9.2	1.0	9.2	1.1	0.3
pH²	2.6	1.0	2.6	0.3	0.6
Time	0.0	1.0	0.0	0.0	1.0
Time²	4.8	1.0	4.8	0.6	0.5
S:L ratio × pH	20.7	1.0	20.7	2.5	0.2
S:L ratio × Time	1.8	1.0	1.8	0.2	0.7
pH × Time	0.2	1.0	0.2	0.0	0.9
Error	58.8	7.0	8.4		
Total SS	100.4	16.0			

Figure E.5. Predicted *versus* observed values for the purity of IgG from human serum using [Si][C$_3$mim]Cl.

E.4. Factorial planning using [Si][N$_{3444}$]Cl

Table E.9. Data attributed to the independent variables (S:L ratio, pH and contact time) to define the 2^3 factorial planning and respective experimental results of recovery yield of IgG using [Si][N$_{3444}$]Cl, theoretical results of the developed mathematical model and respective relative deviation.

System	S:L ratio (mg·mL^{-1})	pH	Contact time (min)	%Yield$_{IgG}$ experimental	%Yield$_{IgG}$ theoretical	Residues
1	50.0	3	30.0	10.0	16.6	-6.5
2	50.0	3	90.0	0.0	2.9	-2.9
3	50.0	7	30.0	24.5	17.8	6.7
4	50.0	7	90.0	13.8	23.9	-10.1
5	150.0	3	30.0	45.1	30.5	14.6
6	150.0	3	90.0	0.0	2.2	-2.2
7	150.0	7	30.0	57.0	49.5	7.5
8	150.0	7	90.0	52.0	41.0	11.1
9	100.0	5	9.6	33.5	44.5	-11.1
10	100.0	5	110.4	30.6	25.9	4.7
11	100.0	1.64	60.0	0.0	-0.4	0.4
12	100.0	8.36	60.0	26.4	33.2	-6.8
13	16.0	5	60.0	12.6	2.8	9.8
14	184.0	5	60.0	12.5	28.8	-16.3
15	100.0	5	60.0	15.9	13.4	2.4
16	100.0	5	60.0	10.4	13.4	-3.1
17	100.0	5	60.0	15.2	13.4	1.8

Table E.10. Regression coefficients of the predicted second-order polynomial model for the recovery yield of IgG with [Si][N$_{3444}$]Cl.

	Regression coefficients	Standard deviation	t-student (7)	p - value
Interception	57.1	51.9	1.1	0.3
S:L ratio	0.0	0.4	0.0	1.0
S:L ratio²	0.0	0.0	0.2	0.8
pH	-7.0	11.7	-0.6	0.6
pH²	0.3	1.0	0.3	0.8
Time	-1.4	0.7	-1.9	0.1
Time²	0.0	0.0	2.0	0.1
S:L ratio × pH	0.0	0.1	1.0	0.4
S:L ratio × Time	0.0	0.0	-0.8	0.5
pH × Time	0.1	0.1	1.1	0.3

Table E.11. ANOVA data for the recovery yield of IgG, obtained from the factorial planning carried with [Si][N$_{3444}$]Cl.

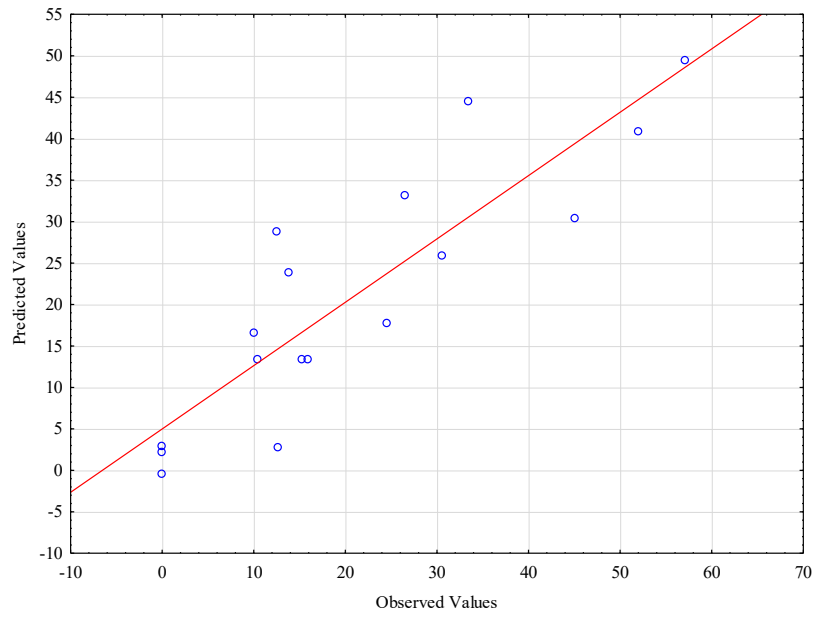|	Sum Squares (SS)	Degrees of Freedom	Mean Square	Fcal	p - value
S:L ratio	816.7	1.0	816.7	4.9	0.1
S:L ratio²	7.7	1.0	7.7	0.1	0.8
pH	1368.2	1.0	1368.2	8.2	0.0
pH²	12.5	1.0	12.5	0.1	0.8
Time	419.5	1.0	419.5	2.5	0.2
Time²	669.0	1.0	669.0	4.0	0.1
S:L ratio × pH	159.0	1.0	159.0	1.0	0.4
S:L ratio × Time	107.7	1.0	107.7	0.7	0.5
pH × Time	194.3	1.0	194.3	1.2	0.3
Error	1165.1	7.0	166.4		
Total SS	4935.4	16.0			

Figure E.6. Predicted *versus* observed values for the recovery yield of IgG from human serum using [Si][N$_{3444}$]Cl.

Table E.12. Data attributed to the independent variables (S:L ratio, pH and contact time) to define the 2^3 factorial planning and respective experimental results of purity of IgG using [Si][N$_{3444}$]Cl, theoretical results of the developed mathematical model and respective relative deviation.

System	S:L ratio (mg·mL^{-1})	pH	Contact time (min)	%Purity$_{IgG}$ experimental	%Purity$_{IgG}$ theoretical	Residues
1	50.0	3	30.0	53.2	47.2	6.1
2	50.0	3	90.0	0.0	5.8	-5.8
3	50.0	7	30.0	80.5	80.1	0.4
4	50.0	7	90.0	72.5	84.5	-11.9
5	150.0	3	30.0	55.3	55.1	0.2
6	150.0	3	90.0	0.0	12.1	-12.1
7	150.0	7	30.0	65.0	70.9	-5.9
8	150.0	7	90.0	55.8	73.6	-17.8
9	100.0	5	9.6	57.4	63.5	-6.1
10	100.0	5	110.4	53.8	31.0	22.7
11	100.0	1.64	60.0	0.0	-1.3	1.3
12	100.0	8.36	60.0	93.3	78.0	15.4
13	16.0	5	60.0	85.8	84.7	1.1
14	184.0	5	60.0	97.8	82.2	15.6
15	100.0	5	60.0	98.3	98.9	-0.7
16	100.0	5	60.0	97.4	98.9	-1.6
17	100.0	5	60.0	98.2	98.9	-0.7

Table E.13. Regression coefficients of the predicted second-order polynomial model for the purity of IgG with [Si][N$_{3444}$]Cl.

	Regression coefficients	Standard deviation	t-student (7)	p - value
Interception	-134.7	63.6	-2.1	0.1
S:L ratio	0.7	0.5	1.2	0.3
S:L ratio²	0.0	0.0	-1.2	0.3
pH	58.4	14.4	4.1	0.0
pH²	-5.4	1.2	-4.6	0.0
Time	1.2	0.9	1.4	0.2
Time²	-0.0	0.0	-3.9	0.0
S:L ratio × pH	-0.0	0.1	-0.8	0.5
S:L ratio × Time	0.0	0.0	-0.1	0.9
pH × Time	0.2	0.01	2.0	0.1

Table E.14. ANOVA data for the purity of IgG, obtained from the factorial planning carried with [Si][N$_{3444}$]Cl.

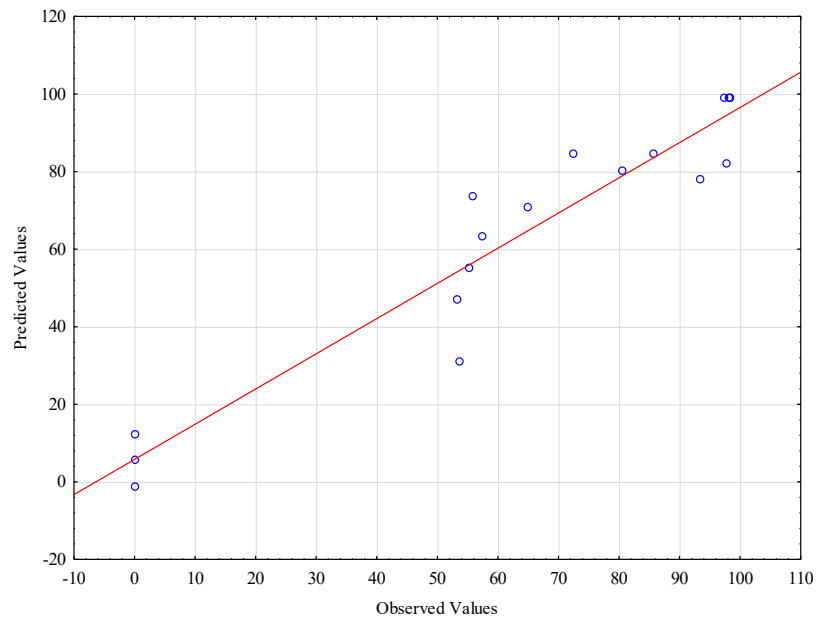|	Sum Squares (SS)	Degrees of Freedom	Mean Square	Fcal	p - value
S:L ratio	7.3	1.0	7.3	0.0	0.9
S:L ratio²	337.3	1.0	337.3	1.4	0.3
pH	7601.4	1.0	7601.4	30.4	0.0
pH²	5183.7	1.0	5183.7	20.7	0.0
Time	1274.5	1.0	1274.5	5.1	0.1
Time²	3768.6	1.0	3768.6	15.1	0.0
S:L ratio × pH	147.6	1.0	147.6	0.6	0.5
S:L ratio × Time	1.4	1.0	1.4	0.0	0.9
pH × Time	1043.8	1.0	1043.8	4.2	0.1
Error	1751.9	7.0	250.3		
Total SS	18945.9	16.0			

Figure E.7. Predicted *versus* observed values for the purity of IgG from human serum using [Si][N$_{3444}$]Cl.

E.5. Factorial planning using [Si][N$_{3888}$]Cl

Table E.15. Data attributed to the independent variables (S:L ratio, pH and contact time) to define the 2^3 factorial planning and respective experimental results of recovery yield of IgG using [Si][N$_{3888}$]Cl, theoretical results of the developed mathematical model and respective relative deviation.

System	S:L ratio (mg·mL^{-1})	pH	Contact time (min)	%Yield$_{IgG}$ experimental	%Yield$_{IgG}$ theoretical	Residues
1	50.0	3	30.0	0.0	5.5	-5.5
2	50.0	3	90.0	0.0	10.4	-10.4
3	50.0	7	30.0	35.3	34.5	0.8
4	50.0	7	90.0	42.8	42.0	0.7
5	150.0	3	30.0	25.7	28.7	-3.0
6	150.0	3	90.0	26.2	29.3	-3.1
7	150.0	7	30.0	67.3	59.1	8.1
8	150.0	7	90.0	65.5	62.3	3.2
9	100.0	5	9.6	34.4	35.8	-1.4
10	100.0	5	110.4	47.2	42.6	4.6
11	100.0	1.64	60.0	16.8	4.8	12.0
12	100.0	8.36	60.0	48.2	56.9	-8.8
13	16.0	5	60.0	22.8	15.3	7.5
14	184.0	5	60.0	47.6	51.8	-4.2
15	100.0	5	60.0	48.0	43.4	4.7
16	100.0	5	60.0	45.3	43.4	2.0
17	100.0	5	60.0	36.2	43.4	-7.2

Table E.16. Regression coefficients of the predicted second-order polynomial model for the recovery yield of IgG with [Si][N$_{3888}$]Cl.

	Regression coefficients	Standard deviation	t-student (7)	p - value
Interception	-68.1	38.1	-1.8	0.1
S:L ratio	0.5	0.3	1.7	0.1
S:L ratio²	0.0	0.0	-1.2	0.3
pH	17.8	8.6	2.1	0.1
pH²	-1.1	0.7	-1.6	0.2
Time	0.3	0.5	0.5	0.6
Time²	0.0	0.0	-0.5	0.6
S:L ratio × pH	0.0	0.0	0.1	0.9
S:L ratio × Time	0.0	0.0	-0.3	0.8
pH × Time	0.0	0.1	0.2	0.9

Table E.17. ANOVA data for the recovery yield of IgG, obtained from the factorial planning carried with [Si][N$_{3888}$]Cl.

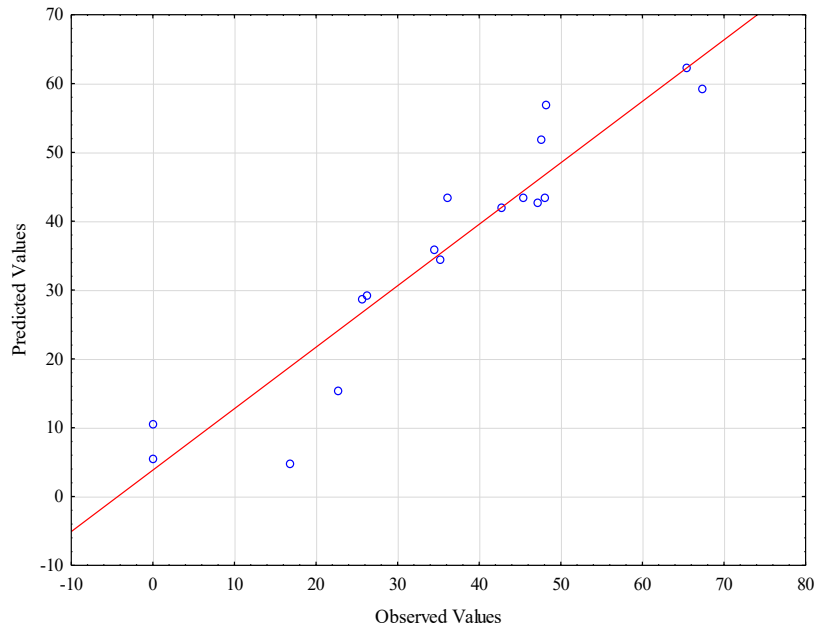|	Sum Squares (SS)	Degrees of Freedom	Mean Square	Fcal	p - value
S:L ratio	1612.3	1.0	1612.3	17.9	0.004
S:L ratio²	135.7	1.0	135.7	1.5	0.3
pH	3280.2	1.0	3280.2	36.5	0.0005
pH²	220.1	1.0	220.1	2.5	0.2
Time	56.2	1.0	56.2	0.6	0.5
Time²	24.6	1.0	24.6	0.3	0.6
S:L ratio × pH	01.0	1.0	1.0	0.0	0.9
S:L ratio × Time	9.6	1.0	9.6	0.1	0.8
pH × Time	3.3	1.0	3.3	0.0	0.9
Error	629.8	7.0	90.0		
Total SS	5871.9	16.0			

Figure E.8. Predicted *versus* observed values for the recovery yield of IgG from human serum using [Si][N$_{3888}$]Cl.

Table E.18. Data attributed to the independent variables (S:L ratio, pH and contact time) to define the 2^3 factorial planning and respective experimental results of purity of IgG using [Si][N$_{3888}$]Cl, theoretical results of the developed mathematical model and respective relative deviation.

System	S:L ratio (mg·mL⁻¹)	pH	Contact time (min)	%Purity$_{IgG}$ experimental	%Purity$_{IgG}$ theoretical	Residues
1	50.0	3	30.0	0.0	7.9	-7.9
2	50.0	3	90.0	0.0	10.7	-10.7
3	50.0	7	30.0	66.7	65.3	1.4
4	50.0	7	90.0	81.1	72.2	8.9
5	150.0	3	30.0	24.8	34.4	-9.7
6	150.0	3	90.0	28.7	30.8	-2.1
7	150.0	7	30.0	59.9	50.0	10.0
8	150.0	7	90.0	57.7	50.5	7.2
9	100.0	5	9.6	45.5	42.2	3.4
10	100.0	5	110.4	42.7	45.0	-2.3
11	100.0	1.64	60.0	22.4	4.6	17.8
12	100.0	8.36	60.0	52.7	69.4	-16.7
13	16.0	5	60.0	43.5	38.9	4.6
14	184.0	5	60.0	39.3	42.8	-3.6
15	100.0	5	60.0	43.7	44.1	-0.4
16	100.0	5	60.0	42.4	44.1	-1.7
17	100.0	5	60.0	46.0	44.1	1.9

Table E.19. Regression coefficients of the predicted second-order polynomial model for the purity of IgG with [Si][N$_{3888}$]Cl.

	Regression coefficients	Standard deviation	t-student (7)	p - value
Interception	-82.7	51.7	-1.6	0.2
S:L ratio	0.7	0.4	1.6	0.2
S:L ratio²	0.0	0.0	-0.3	0.8
pH	25.4	11.7	2.2	0.1
pH²	-0.6	1.0	-0.7	0.5
Time	0.1	0.7	0.1	0.9
Time²	0.0	0.0	-0.1	1.0
S:L ratio × pH	-0.1	0.1	-2.3	0.1
S:L ratio × Time	0.0	0.0	-0.4	0.7
pH × Time	0.0	0.1	0.2	0.8

Table E.20. ANOVA data for the purity of IgG, obtained from the factorial planning carried with [Si][N$_{3888}$]Cl.

	Sum Squares (SS)	Degrees of Freedom	Mean Square	Fcal	p - value
S:L ratio	19.0	1.0	19.0	0.1	0.7
S:L ratio²	14.7	1.0	14.7	0.09	0.8
pH	5063.0	1.0	5063.0	30.6	0.0009
pH²	71.0	1.0	71.0	0.4	0.5
Time	9.4	1.0	9.4	0.06	0.8
Time²	0.4	1.0	0.4	0.002	1.0
S:L ratio × pH	875.5	1.0	875.5	5.3	0.06
S:L ratio × Time	20.4	1.0	20.4	0.1	0.7
pH × Time	8.4	1.0	8.4	0.05	0.8
Error	1158.8	7.0	165.6		
Total SS	7232.9	16.0			
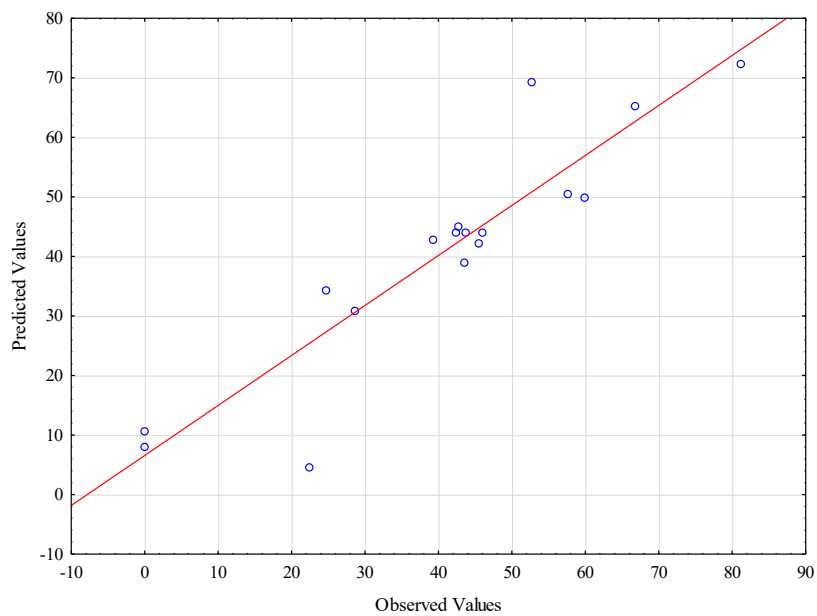
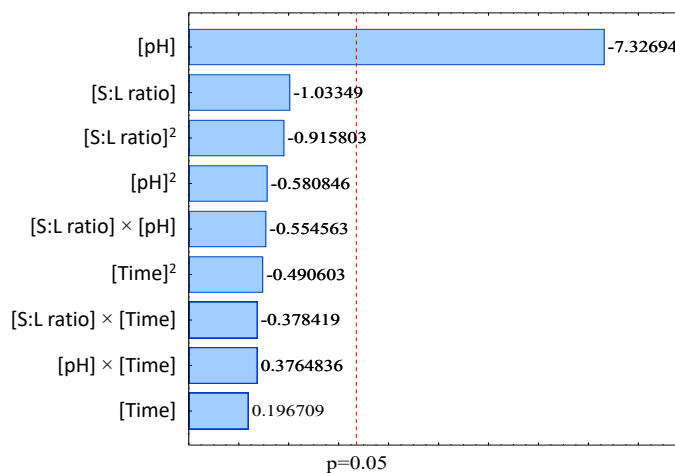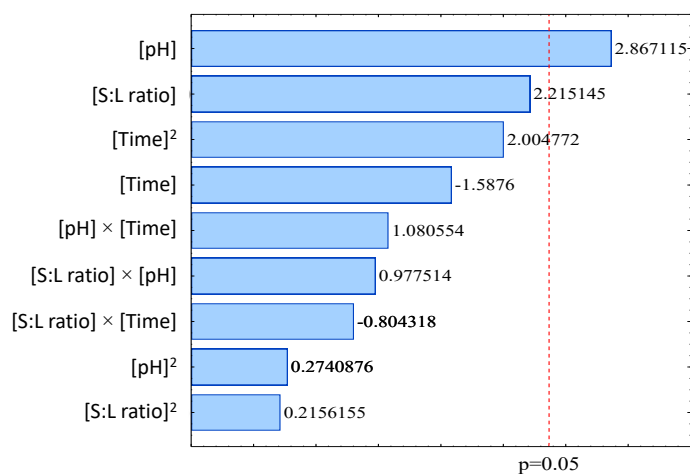**Figure E.9.** Predicted *versus* observed values for the purity of IgG from human serum using [Si][N$_{3888}$]Cl.

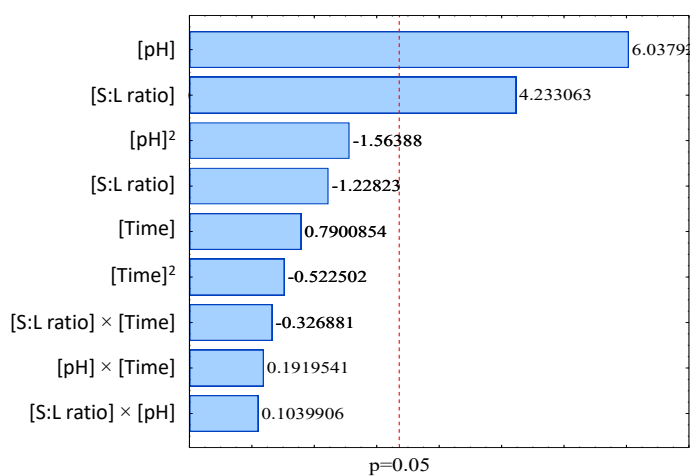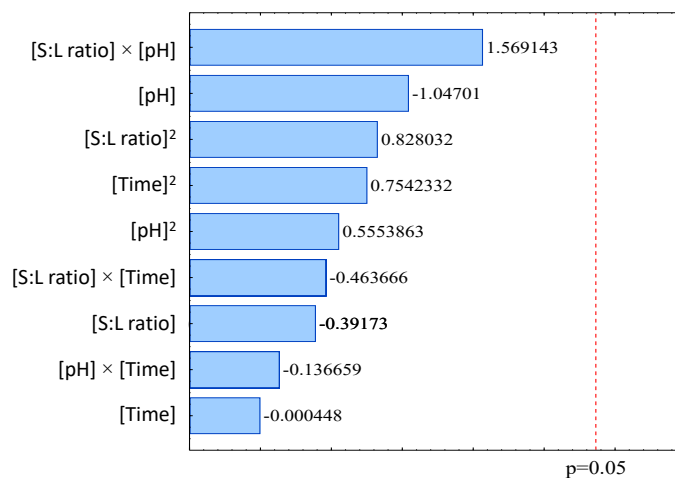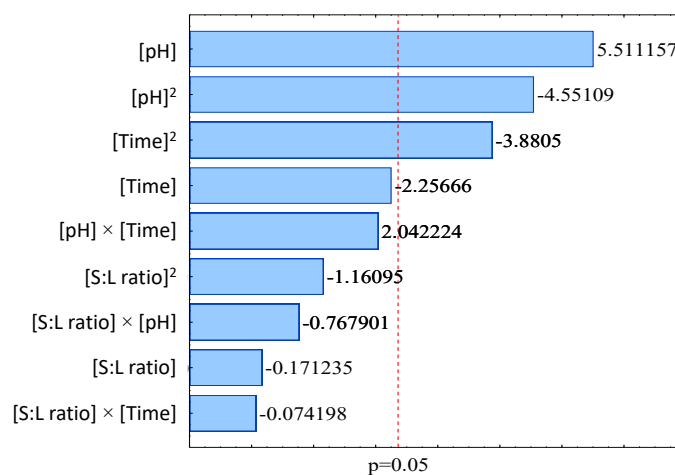## E.6. Pareto charts

(A)

(B)

(C)

Figure E.10. Pareto charts obtained for the 2^3 factorial planning regarding the study of the IgG recovery yield using: (A) [Si][C$_3$mim]Cl; (B) [Si][N$_{3444}$]Cl; and (C) [Si][N$_{3888}$]Cl.
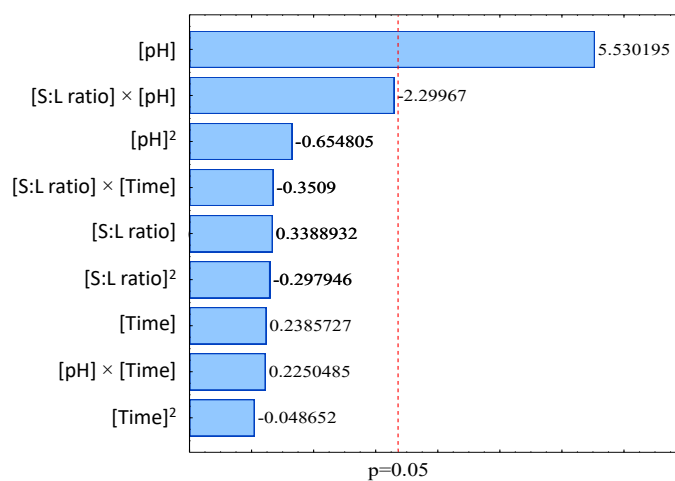
(A)

(B)

(C)

Figure E.11. Pareto charts obtained for the 2^3 factorial planning regarding the study of the IgG purity using: (A) [Si][C$_3$mim]Cl; (B) [Si][N$_{3444}$]Cl; and (C) [Si][N$_{3888}$]Cl.

E.7. Experimental optimization of the IgG downstream processes

Table E.21. Performance parameters ([IgG], %Yield$_{IgG}$, %Purity$_{IgG}$ and %Aggregation$_{IgG}$) regarding IgG antibodies recovery and purification from human serum, after contact with [Si][C$_3$mim]Cl (results in the aqueous medium), [Si][N$_{3444}$]Cl and [Si][N$_{3888}$]Cl (results in the materials), using a S:L ratio of 100 mg·mL^{-1}, three different pH values (pH 10, 11 and 12), and a contact time of 60 min.

	[IgG] ± σ (mg·L^{-1})	%Yield$_{IgG}$ ± σ	%Purity$_{IgG}$ ± σ	%Aggregation$_{IgG}$
[Si][C$_3$mim]Cl				
pH 10	252.3 ± 1.3	85.5 ± 0.4	40.7 ± 0.3	15.2 ± 1.7
pH 11	217.2 ± 0.3	74.0 ± 0.1	52.3 ± 0.7	0.0 ± 0.0
pH 12	77.2 ± 0.8	54.5 ± 0.5	53.1 ± 2.8	0.0 ± 0.0
[Si][N$_{3444}$]Cl				
pH 10	151.0 ± 40.1	48.8 ± 3.6	70.8 ± 3.3	16.1 ± 2.1
pH 11	144.0 ± 8.2	51.0 ± 2.8	88.9 ± 5.5	15.7 ± 3.0
pH 12	210.0 ± 1.3	23.6 ± 0.5	59.3 ± 0.1	35.3 ± 3.4
[Si][N$_{3888}$]Cl				
pH 10	129.0 ± 53.2	56.3 ± 8.0	75.4 ± 7.4	16.2 ± 0.2
pH 11	71.9 ± 1.7	75.5 ± 0.6	100 ± 3.3	15.9 ± 6.1
pH 12	222.4 ± 2.3	19.1 ± 0.8	43.1 ± 0.5	31.3 ± 0.9

Table E.22. Performance parameters ([IgG], %Yield$_{IgG}$, %Purity$_{IgG}$ and %Aggregation$_{IgG}$) regarding IgG antibodies recovery and purification from human serum, after contact with [Si][C$_3$mim]Cl (results in the aqueous medium), using three different S:L ratios (100 mg·mL^{-1}, 150 mg·mL^{-1} and 200 mg·mL^{-1}) and pH values (pH 10, 11 and 12), and a contact time of 60 min.

	[IgG] ± σ (mg·L^{-1})	%Yield$_{IgG}$ ± σ	%Purity$_{IgG}$ ± σ	%Aggregation$_{IgG}$
pH 10				
100 mg·mL^{-1}	252.3 ± 1.3	85.5 ± 0.4	40.7 ± 0.3	15.2 ± 1.7
150 mg·mL^{-1}	214.4 ± 12.4	79.3 ± 4.6	31.3 ± 1.0	13.1 ± 0.1
200 mg·mL^{-1}	238.2 ± 11.5	88.1 ± 4.3	32.6 ± 0.5	12.3 ± 0.4
pH 11				
100 mg·mL^{-1}	217.2 ± 0.3	74.0 ± 0.1	52.3 ± 0.7	0.0 ± 0.0
150 mg·mL^{-1}	191.8 ± 4.2	69.2 ± 1.5	48.6 ± 0.7	5.9 ± 0.1
200 mg·mL^{-1}	206.8 ± 10.0	74.5 ± 3.6	42.6 ± 1.6	0.0 ± 0.0
pH 12				
100 mg·mL^{-1}	77.2 ± 0.8	54.5 ± 0.5	53.1 ± 2.8	0.0 ± 0.0
150 mg·mL^{-1}	83.8 ± 1.1	59.1 ± 0.8	84.2 ± 0.4	0.0 ± 0.0
200 mg·mL^{-1}	78.3 ± 0.6	55.2 ± 0.4	75.4 ± 0.1	0.0 ± 0.0

	[IgG] ± σ (mg·L^{-1})	%Yield$_{IgG}$ ± σ	%Purity$_{IgG}$ ± σ	%Aggregation$_{IgG}$
[Si][C$_3$mim]Cl				
Human serum	83.8 ± 1.1	59.1 ± 0.8	84.2 ± 0.4	0.0 ± 0.0
CHO cell supernatant	35.9 ± 0.1	85.8 ± 0.2	36.8 ± 0.1	0.0 ± 0.0
Rabbit serum	213.1 ± 5.5	75.7 ± 1.9	51.4 ± 0.6	0.0 ± 0.0
[Si][N$_{3888}$]Cl				
Human serum	71.9 ± 1.7	75.5 ± 0.6	100.0 ± 3.3	15.9 ± 6.1
CHO cell supernatant	21.7 ± 0.2	48.1 ± 0.5	64.9 ± 0.2	4.4 ± 0.2
Rabbit serum	157.1 ± 0.7	49.8 ± 0.2	96.4 ± 0.3	3.4 ± 0.5

E.8. Reproducibility and robustness of the developed processes

Table E.23. Performance parameters ([IgG], %Yield$_{IgG}$, %Purity$_{IgG}$ and %Aggregation$_{IgG}$) regarding IgG antibodies recovery and purification from different complex biological matrices (human serum, CHO cell culture supernatants and rabbit serum), after contact with [Si][C$_3$mim]Cl (results in the aqueous medium; operation conditions: S:L ratio of 150 mg·mL^{-1}, pH 12 and 60 min of contact time) and [Si][N$_{3888}$]Cl (results in the material; S:L ratio of 100 mg·mL^{-1}, pH 11 and 60 min of contact time).

	[IgG] ± σ (mg·L^{-1})	%Yield$_{IgG}$ ± σ	%Purity$_{IgG}$ ± σ	%Aggregation$_{IgG}$
[Si][C$_3$mim]Cl				
Human serum	83.8 ± 1.1	59.1 ± 0.8	84.2 ± 0.4	0.0 ± 0.0
CHO cell supernatant	35.9 ± 0.1	85.8 ± 0.2	36.8 ± 0.1	0.0 ± 0.0
Rabbit serum	213.1 ± 5.5	75.7 ± 1.9	51.4 ± 0.6	0.0 ± 0.0
[Si][N$_{3888}$]Cl				
Human serum	71.9 ± 1.7	75.5 ± 0.6	100.0 ± 3.3	15.9 ± 6.1
CHO cell supernatant	21.7 ± 0.2	48.1 ± 0.5	64.9 ± 0.2	4.4 ± 0.2
Rabbit serum	157.1 ± 0.7	49.8 ± 0.2	96.4 ± 0.3	3.4 ± 0.5